Universitat de Girona

SOLID-PHASE SYNTHESIS OF CELL-PENETRATING γ-PEPTIDE/ANTIMICROBIAL PEPTIDE CONJUGATES AND OF CYCLIC LIPODEPSIPEPTIDES DERIVED FROM FENGYCINS

Cristina Rosés Subirós

Per citar o enllaçar aquest document:
Para citar o enlazar este documento:
Use this url to cite or link to this publication:

http://hdl.handle.net/10803/393895

ADVERTIMENT. L'accés als continguts d'aquesta tesi doctoral i la seva utilització ha de respectar els drets de la persona autora. Pot ser utilitzada per a consulta o estudi personal, així com en activitats o materials d'investigació i docència en els termes establerts a l'art. 32 del Text Refós de la Llei de Propietat Intel·lectual (RDL 1/1996). Per altres utilitzacions es requereix l'autorització prèvia i expressa de la persona autora. En qualsevol cas, en la utilització dels seus continguts caldrà indicar de forma clara el nom i cognoms de la persona autora i el títol de la tesi doctoral. No s'autoritza la seva reproducció o altres formes d'explotació efectuades amb finalitats de lucre ni la seva comunicació pública des d'un lloc aliè al servei TDX. Tampoc s'autoritza la presentació del seu contingut en una finestra o marc aliè a TDX (framing). Aquesta reserva de drets afecta tant als continguts de la tesi com als seus resums i índexs.

ADVERTENCIA. El acceso a los contenidos de esta tesis doctoral y su utilización debe respetar los derechos de la persona autora. Puede ser utilizada para consulta o estudio personal, así como en actividades o materiales de investigación y docencia en los términos establecidos en el art. 32 del Texto Refundido de la Ley de Propiedad Intelectual (RDL 1/1996). Para otros usos se requiere la autorización previa y expresa de la persona autora. En cualquier caso, en la utilización de sus contenidos se deberá indicar de forma clara el nombre y apellidos de la persona autora y el título de la tesis doctoral. No se autoriza su reproducción u otras formas de explotación efectuadas con fines lucrativos ni su comunicación pública desde un sitio ajeno al servicio TDR. Tampoco se autoriza la presentación de su contenido en una ventana o marco ajeno a TDR (framing). Esta reserva de derechos afecta tanto al contenido de la tesis como a sus resúmenes e índices.

WARNING. Access to the contents of this doctoral thesis and its use must respect the rights of the author. It can be used for reference or private study, as well as research and learning activities or materials in the terms established by the 32nd article of the Spanish Consolidated Copyright Act (RDL 1/1996). Express and previous authorization of the author is required for any other uses. In any case, when using its content, full name of the author and title of the thesis must be clearly indicated. Reproduction or other forms of for profit use or public communication from outside TDX service is not allowed. Presentation of its content in a window or frame external to TDX (framing) is not authorized either. These rights affect both the content of the thesis and its abstracts and indexes.

Universitat de Girona

DOCTORAL THESIS

Solid-phase synthesis of cell-penetrating γ-peptide/antimicrobial peptide conjugates and of cyclic lipodepsipeptides derived from fengycins

CRISTINA ROSÉS SUBIRÓS

2015

Doctoral Programme in Experimental Sciences and Sustainability

Supervised by: Dr. Lidia Feliu Soley
Dr. Marta Planas Grabuleda

This manuscript has been presented to opt for the **Doctoral Degree** from the
University of Girona

Dr. Lidia Feliu Soley and Dr. Marta Planas Grabuleda, of the University of Girona,

WE DECLARE:

That the thesis entitled “Solid-phase synthesis of cell-penetrating γ-peptide/antimicrobial peptide conjugates and of cyclic lipodepsipeptides derived from fengycins”, presented by Cristina Rosés Subirós to obtain a doctoral degree, has been completed under our supervision and meets the requirements to opt for an International Doctorate.

For all intents and purposes, we hereby sign this document.

Dr. Lidia Feliu Soley

Dr. Marta Planas Grabuleda

Girona, September 16th 2015

A la meva família,

Full list of publications:

Publications derived from this thesis:

- **Chapter 3:** Rosés, C.; Carbajo, D.; Sanclimens, G.; Farrera-Sinfreu, J.; Blancafort, A.; Oliveras, G.; Cirac, A.D.; Bardají, E.; Puig, T.; Planas, M.; Feliu, L.; Albericio, F.; Royo, M. Cell-penetrating γ-peptide/antimicrobial undecapeptide conjugates with anticancer activity. *Tetrahedron* **2012**, *68*, 4406-4412.

Manuscripts in preparation derived from this thesis:

- **Chapter 4:** Rosés, C.; Camó, C.; Planas, M.; Feliu, L. Solid-phase synthesis of cyclic depsipeptides containing a phenyl ester bond. *In preparation*.

- **Chapter 5:** Rosés, C.; López, N.; Oliveras, A.; Feliu, L.; Planas, M. Total solid-phase synthesis of dehydroxy fengycin derivatives. *In preparation*.

List of abbreviations

AMP	Antimicrobial peptide
Aa	Amino acid
Ac	Acetyl
AHDMHA	(2*R*,3*R*,4*R*)-2-Amino-3-hydroxy-4,5-dimethylhexanoic acid
All	Allyl
Alloc	Allyloxycarbonyl
Aq	Aqueous
Bn	Benzyl
Boc	*tert*-Butyloxycarbonyl
^{t}Bu	*tert*-Butyl
Bz	Benzoyl
Cat	Catalytic
COMU	1-[(1-Cyano-2-ethoxy-2-oxoethylideneaminooxy)-dimethylamino-morpholinomethylene)]methanaminium hexafluorophosphate
CPP	Cell penetrating peptide
DCC	*N,N’*-Dicyclohexylcarbodiimide
DEPBT	3-(Diethoxyphosphoryloxy)-1,2,3-benzotriazin-4(3*H*)-one
DHB	2,5-Dihydroxybenzoic acid
DIAD	Diisopropylazodicarboxylate
DIEA	*N*,*N′*-Diisopropylethylamine
DIPCDI	*N,N’*-Diisopropylcarbodiimide
DMAP	*N,N’*-Dimethylaminopyridine
DMEM	Dulbecco’s modified Eagle’s medium
DMF	*N,N’*-Dimethylformamide
DMSO	Dimethyl sulfoxide
DOE	Design of experiments
Equiv	Equivalent
ESI-MS	Electrospray Ionization Mass Spectrometry
Et	Ethyl
FBS	Fetal bovine serum
Fmoc	9-Fluorenylmethyloxycarbonyl
HATU	*N*-[(Dimethylamino)-1*H*-1,2,3-triazolo-[4,5-*b*]pyridin-1-yl-methylene]-*N*-methylmethanaminium hexafluorophosphate *N*-oxide
HBTU	*N*-[(1*H*-Benzotriazol-1-yl)-(dimethylamino)methylene]-*N*-methylmethanaminium hexafluorophosphate *N*-oxide

HMPA	4-Hydroxymethylphenoxyacetic acid
HOBt	1-Hydroxybenzotriazole
HPLC	High Pressure Liquid Chromatography
IC_{50}	Concentration that causes 50% growth inhibition
MALDI-TOF	Matrix-Assisted Laser Desorption Ionization with Time-Of-Flight
MBHA	4-Methylbenzhydrylamine resin
MIC	Minimum inhibitory concentration
MTT	3-(4,5-Dimethylthiazol-2-yl)-2,5-diphenyltetrazolium bromide
NMM	*N*-Methylmorpholine
NMP	*N*-Methylpyrrolidinone
OD	Optical density
Oxyma	Ethyl 2-cyano-2-(hydroxyimino)acetate
PBS	Phosphate Saline Buffer
PEG	Polyethylenglycol or 8-amino-3,6-dioxaoctanoic acid
*p*NZ	*p*-Nitrobenzyloxycarbonyl
PyBOP	Benzotriazol-1-yl-*N*-oxy-tris(pyrrolidino)phosphonium hexafluorophosphate
PyBrOP	Bromo-tris(pyrrolidino)phosphonium hexafluorophosphate
PyOxim	[Ethyl cyano(hydroxyimino)acetato-O^2]tri-(1-pyrrolidinyl)-phosphonium hexafluorophosphate
Rink amide	4-(2’,4’-Dimethoxyphenylaminomethyl) phenoxyacetic acid
RP-HPLC	Reverse Phase High Pressure Liquid Cromathography
SPPS	Solid-phase peptide synthesis
TFA	Trifluoroacetic acid
TFE	Trifluoroethanol
THF	Tetrahydrofuran
TIS	Triisopropylsilane
TLC	Thin Layer Chromatography
TMBE	*tert*-Butyl methyl ether
TMSOTf	Trimethylsilyl trifluoromethanesulfonate
Tr	Trityl
t_R	Retention time
p-Ts	*p*-Toluenesulfonyl

Amino acids

Name	Three letter code	One letter code
Alanine	Ala	A
Arginine	Arg	R
Asparagine	Asn	N
Aspartic Acid	Asp	D
Cysteine	Cys	C
Glutamic Acid	Glu	E
Glutamine	Gln	Q
Glycine	Gly	G
Histidine	His	H
Isoleucine	Ile	I
Leucine	Leu	L
Lysine	Lys	K
Methionine	Met	M
Ornitine	Orn	O
Phenylalanine	Phe	F
Proline	Pro	P
Sarcosine	Sar	-
Serine	Ser	S
Threonine	Thr	T
Tryptophan	Trp	W
Tyrosine	Tyr	Y
Valine	Val	V

List of Figures

Figure 1.1. *Secondary structure of antimicrobial peptides: (A) α-helical; (B) extended; (C) β-sheet; and (D) looped. Disulfide bonds are represented in green (adapted from Powers and Hancock, 2003).* 36

Figure 1.2. *Structure of the non-ribosomal peptide daptomycin.* 40

Figure 1.3. *Mechanisms of membrane cell disruption mediated by antimicrobial peptides:* ***A)*** *barrel-stave;* ***B)*** *toroidal-pore;* ***C)*** *disordered toroidal-pore; and* ***D)*** *carpet-like models (adapted from Melo et al., 2009).* 41

Figure 1.4. *Mode of action of antimicrobial peptides. The bacterial membrane is represented as a yellow lipid bilayer. The cylinders are peptides, where the hydrophilic regions are colored red and the hydrophobic regions are in blue. Mechanisms of membrane permeabilization are indicated in panels* ***A*** *to* ***D****, while mechanisms of action of peptides which do not act by permeabilizing the bacterial membrane are indicated by panels* ***E*** *to* ***I*** *(adapted from Jenssen et al., 2006).* 42

Figure 1.5. *Molecular basis for membrane selectivity by antimicrobial peptides (extracted from Matsuzaki, 2009).* 43

Figure 1.6. *Graphic of estimate incidence of cancer disease in males (****a****) and in females (****b****) during 2012 (Globocan2012, IARC).* 46

Figure 1.7. *Examples of antimetabolites.* 47

Figure 1.8. *Examples of DNA-interactive drugs.* 47

Figure 1.9. *Examples of antitubulin agents.* 48

Figure 1.10. *Peptide sequence of r7-kla.* 53

Figure 1.11. *Edmunson wheel projection of the 125-member peptide library CECMEL11. Hydrophilic amino acids (Lys) are represented in black background while hydrophobic residues (Leu, Phe, Ile) are in white.* X^1 *and* X^{10} *are represented in grey (*X^1*= Lys, Leu, Trp, Tyr or Phe;* X^{10}*= Lys, Val, Trp, Tyr or Phe). R represents the N-terminus derivatization (H, Ac, Ts, Bz or Bn) (Badosa et al., 2007).* 56

Figure 1.12. *Structure of surfactins. The β-hydroxy fatty acid can contain iso or anteiso branches.* 60

Figure 1.13. *Structure of iturins. The β-hydroxy fatty acid can contain iso or anteiso branches.* 61

Figure 1.14. *Structure of fengycin A and B.* 62

Figure 1.15. *Structure of fengycin S according to Sang-Cheol et al., 2010.* 62

Figure 1.16. *Two different structures of fengycin C described by Villegas-Escobar et al. (****A****) and Pathak et al. (****B****). The amino acid configuration was not described for compound* ***A****.* 63

Figure 1.17. *Structural differences between fengycins and plipastatins. The "&" symbol indicates the ester bond between the phenol group of Tyr^3 and the α-carboxylic group of Ile^{10}.* *64*

Figure 1.18. *Structure of some representative coupling reagents and additives.* *71*

Figure 3.1. *Structures of the peptide conjugates.* *104*

Figure 4.1. *Structure of fengycins A, B and S.* *129*

Figure 4.2. *General structure of fengycin analogues* ***I***, ***II*** *and* ***III***. *130*

Figure 4.3. *Structure of cyclic depsipeptides* ***IIb*** *and* ***III***. *142*

Figure 5.1. *Structure of fengycins A, B and S.* *177*

Figure 5.2. *General structure of dehydroxy fengycin derivatives* ***I***. *178*

Figure 5.3. *Structure of cyclic lipodepsipeptides* ***BPC840***, ***BPC842*** *and* ***BPC844***. *183*

Figure 5.4. *Structure of cyclic lipodepsipeptides* ***BPC846***, ***BPC848***, ***BPC850***, ***BPC852***, ***BPC858*** *and* ***BPC860***. *183*

Figure 6.1. *Structure of the conjugate* ***BP100-PEG-1***. *215*

Figure 6.2. *Structure of the peptide conjugates.* *216*

Figure 6.3. *Structure of fengycins A, B and S.* *218*

Figure 6.4. *General structure of the cyclic octapeptides. Bonds involved in the cyclization step in routes A and B are highlighted.* *219*

List of Tables

Table 1.1. *Examples of natural antimicrobial peptides categorized according to their secondary structure. 38*

Table 1.2. *Examples of antimicrobial peptides with anticancer activity. 51*

Table 1.3. *Sequences of DPT-sh1, C9, C9h and of the peptide conjugates DPT-C9 and DPT-C9h. 53*

Table 1.4. *Sequence of cecropin A, melittin and two synthetic analogues. 55*

Table 1.5. *Antibacterial and hemolytic activity of several peptides selected from the CECMEL11 library. 57*

Table 1.6. *Antibacterial and hemolytic activity of selected cyclic decapeptides. 58*

Table 1.7. *Examples of solid supports used in SPPS. 68*

Table 1.8. *Examples of commonly used linkers. 68*

Table 1.9. *Protecting groups used in this thesis. 70*

Table 3.1. *Characterization of peptide conjugates. 108*

Table 3.2. *Cytotoxicity against MDA-MB-231 cells and non-malignan fibroblast (N1). .. 110*

Table 6.1. *Structure of the dehydroxy fengycin derivatives. 224*

List of Schemes

Scheme 1.1. *General strategy for SPPS.* *66*

Scheme 1.2. *Intramolecular O→N acyl shift in depsipeptides.* *72*

Scheme 1.3. *Synthetic strategy for the synthesis of Kahalalide F (López-Macià et al., 2001; López et al., 2005).* *74*

Scheme 1.4. *Synthetic strategy for the synthesis of lysobactin proposed by Hall et al., 2012.* *75*

Scheme 1.5. *Total solid-phase synthesis of the cyclic lipodepsipeptide* ***9*** *(Stawikowski and Cudic, 2006).* *76*

Scheme 1.6. *Synthesis of halicylindramide A (Seo and Lim, 2009).* *77*

Scheme 1.7. *Synthesis of pipecolidepsin A (Pelay-Gimeno et al., 2013).* *78*

Scheme 1.8. *Solid-phase synthesis of surfactin and analogues described by Pagadoy et al., 2005.* *79*

Scheme 1.9. *Solid-phase synthesis of iturin-A2 (Bland, 1996).* *80*

Scheme 1.10. *Synthesis of a fengycin analogue through chemoenzymatic cyclization (Samel et al., 2006).* *81*

Scheme 3.1. *Solid phase synthesis of* ***PEG-1-MBHA****.* *106*

Scheme 3.2. *Solid-phase synthesis of peptide conjugates.* *107*

Scheme 4.1. *Retrosynthetic analysis of cyclic peptides* ***I-III****.* *132*

Scheme 4.2. *Structure and general synthetic strategy of cyclic octapeptides* ***Ia*** *and* ***IIa*** *(route A).* *134*

Scheme 4.3. *Synthetic approaches for the synthesis of cyclic depsipeptide* ***2*** *(routes A1 and A2).* *137*

Scheme 4.4. *Structure and general synthetic strategy of cyclic depsipeptides* ***2****,* ***7****,* ***8*** *and* ***BPC822*** *(route B).* *139*

Scheme 4.5*.* *Hydrolysis of the ester bond of cyclic depsipeptide* ***8****.* *140*

Scheme 5.1. *Retrosynthetic analysis of* ***I****.* *179*

Scheme 5.2. *Structure and general synthetic approach of cyclic lipodepsipeptides* ***BPC838****,* ***BPC854*** *and* ***BPC856****.* *181*

Scheme 5.3. *Hydrolysis reaction of the crude reaction mixtures from the synthesis of the cyclic lipodepsipeptides.* ***A****. Hydrolysis of the linear precursors.* ***B****. Hydrolysis of the cyclic lipodepsipeptides.* *185*

Scheme 6.1. *Synthesis of cyclic octapeptides following route A.* *220*

Scheme 6.2. *Synthesis of cyclic octadepsipeptides following the route B.* *221*

Scheme 6.3. *Synthesis of the dehydroxy fengycin derivative* ***BPC838****.* *223*

Acknowlegments

No podria començar aquestes línees sense agrair a les meves directores de tesi, la Lidia i la Marta. Sense el seu suport i la seva confiança aquest projecte no hagués estat possible. Moltes gràcies per tots aquests anys. També vull fer extensiu aquest agraïment als altres membres del grup. A la Montse, per tots els seus bons consells i les seves paraules de suport i a l'Eduard, per oferir un bon consell sempre que l'he necessitat. Moltes gràcies.

Amb aquestes línees també voldria agrair als Serveis Tècnics de Recerca de la Universitat de Girona per tots els serveis prestats. En especial a la Lluïsa, a l'Anna, a la Laura i en Vicenç, que m'han obert les portes als seus laboratoris i m'han ofert la seva ajuda en tot moment. Gràcies.

També vull fer extensiu aquest agraïment al grup IdibGi de la Universitat de Girona. En especial a la Teresa, a la Glòria i a la Adriana que em van acollir com un membre més del grup i em van ensenyar tots els secrets dels cultius cel·lulars. Guardo un molt bon record d'aquells dies. Gràcies per tot.

Tampoc em voldria oblidar de la Unitat de Química Combinatòria de la Universitat de Barcelona. En especial a la Míriam i en Daniel, gràcies per fer possible aquesta col·laboració i oferir-me en tot moment l'ajuda necessària per dur a bon port aquest projecte. Moltes gràcies.

Aquestes paraules d'agraïment també les vull fer extensives a totes les altres persones que han format part d'aquesta aventura i que d'una manera o altra l'han convertit en una història inoblidable. En primer lloc voldria agrair al Dr. Miguel Castanho del Instituto de Medicina Molecular de la Universidade de Lisboa i a tot el seu grup. Thank you for give me the opportunity to stay in your lab and discover the world of molecular biology. Specially, I would like to thank Diana, for help me unconditionally and guide me through this new world. Thanks so much for all your good advices. I also would like to thank Gabri for open the doors of her home and for all the good moments we shared. And I would like to thank all the lab members. I really met a nice people there. Muito obrigado por tudo ea grande recepçao. Eu só tenho boas lembranças daqueles dias.

També vull donar les gràcies a la Dra. M^{a} Àngeles Jimenez del CSIC. Muchas gracias por acogerme en su laboratorio y abrirme las puertas del RMN y los análisis conformacionales. Fue una experiencia muy gratificante.

Tampoc em puc oblidar tots els meus companys, molts d'ells ja grans amics, que han fet d'aquest viatge una aventura molt especial i amb els quals he compartit molts bons moments.

Per suposat tots els meus companys de laboratori. Des dels inicis, amb l'Ana A., l'Anna D., la Gemma, la Vane, l'Imma i en Tyffa, els quals van ser, en gran part, els culpables que m'iniciés al món de la recerca. Però també de les Lippsianes amb les que hem compartit pràcticament tota aquesta aventura. Iteng, Silvia i Marta, vam fer un gran Team, "y lo sabes!". Tinc molt bons records d'aquells dies de laboratori i de totes les nostres sortides. També vull recordar tots els nous companys que van anar arribant i ampliant aquesta gran família lippsiana. En especial, vull agrair a la Cristina, la Nerea i l'Àngel amb els que he treballat colze amb colze i dels que estic orgullosa d'haver conegut i compartit experiències. I també de l'Eduard, per suposat, amb el que he compartit molts bons moments en el lab. Sou tots uns cracks!

Tampoc em voldria oblidar de la resta de amics i companys del departament de Química. Els sopars de Nadal, barbacoes, cremats a la platja o jornades Jodete... heu fet que aquests anys hagin passat volant i hem format un gran grup. En especial vull donar un gràcies enorme a els meus "cuquis". Pep i Íngrid sou genials. Per tots els moments compartits en els passadissos de la facultat i pels nostres dinars. Aquests anys no haurien estat igual sense vosaltres. I també als meus "tigers", Marc i Eloy. No crec que pugui oblidar mai les nostres sortides de desconnexió i sobretot els vostres bailoteos. Gràcies a tots per aquests moments i pels que ben segur que vindran.

Amb aquestes paraules també vull donar les gràcies a una persona molt especial i amb la qual he compartit molts bons moments dins i fora de la facultat. Aida, gràcies per tot. Aquest viatge el vam iniciar ara fa 11 anys, de sobte i sense saber ben bé on ens portaria, i mira fins on hem arribat! Tampoc em vull oblidar de la Mònica, la meva alacantina, que m'ha animat en tot moment i m'ha donat una paraula de suport sempre que l'he necessitada. Moltes gràcies Mònica! I també a tots els meus amics de fora del món científic i que molt pacientment han escoltat les meves explicacions i preocupacions sobre la tesi. En especial a l'Anna, que ha estat allà sempre i de la qual només en puc dir bones paraules. Gràcies per tot floreta! Així com a tota la resta d'amics, dels quals no escriuré noms perquè no em vull oblidar de ningú. Simplement us diré que si sabeu què és un pèptid aquestes paraules van dedicades a vosaltres! Gràcies pel vostre "aguante" durant les meves xerrades sobre frikades científiques. No sé què hagués fet sense vosaltres.

Per últim, vull dedicar unes paraules a la meva família. Gràcies per tota la paciència i suport que m'heu donat tots aquests anys. Sé que a hores d'ara encara no teniu molt clar què és un doctorat i molt menys què és un pèptid, però m'heu animat a continuar en tot moment i sense adonar-nos-en hem arribat fins aquí. Sense el vostre suport tot això no hagués estat possible. Per això us dedico aquesta tesi, moltes gràcies per tot.

The development of this doctoral thesis has been funded by the following research projects from the Spanish government (MICINN and MINECO):

"Control biotecnológico del fuego bacteriano. Utilización de péptidos antimicrobianos sintéticos derivados de bacteriocinas y de ciclolipopéptidos" (AGL2009-13255-C02-02/AGR).

"Nuevas estrategias de control del fuego bacteriano. Péptidos sintéticos estimuladores de defensa en el huésped" (AGL2012-39880-C02-02).

Cristina Rosés Subirós gratefully acknowledges the financial support from Generalitat de Catalunya (AGAUR) (2010FI_B 00379) and Spanish government (MICINN) (AP2009-2821).

Table of contents

General Abstract 27
Resum General 29
Resumen General 31

CHAPTER 1. General Introduction 33
1.1. ANTIMICROBIAL PEPTIDES 35
1.1.1. Classification of antimicrobial peptides 36
1.1.1.1. Classification of antimicrobial peptides according to their secondary structure 36
1.1.1.2. Classification of antimicrobial peptides according to their biosynthetic pathway 38
1.1.2. Mechanism of action of antimicrobial peptides 40
1.1.3. Selectivity of antimicrobial peptides 43
1.2. ANTIMICROBIAL PEPTIDES AS ANTICANCER AGENTS 45
1.2.1. The disease of cancer 45
1.2.2. Antimicrobial peptides with anticancer activity 49
1.3. ANTIMICROBIAL PEPTIDES FOR PLANT PROTECTION 54
1.3.1. Cecropin A-melittin hybrid linear undecapeptides 55
1.3.2. *De novo* designed cyclic decapeptides 57
1.4. BIOACTIVE LIPOPEPTIDES FROM *BACILLUS SUBTILIS* FOR PLANT PROTECTION 59
1.4.1. Surfactins 60
1.4.2. Iturins 60
1.4.3. Fengycins 61
1.5. SYNTHESIS OF PEPTIDES 65
1.5.1. Solid-phase peptide synthesis 65
1.5.1.1. Solid support 67
1.5.1.2. Linker 68
1.5.1.3. Protecting groups 69
1.5.1.4. Coupling reagents 70
1.5.2. Solid phase synthesis of cyclic depsipeptides 72
1.5.3. Obtention of *Bacillus* cyclic lipopeptides 79
1.6. REFERENCES 81

CHAPTER 2. Main Objectives.. 95

CHAPTER 3. Cell-penetrating γ-peptide/antimicrobial undecapeptide conjugates with anticancer activity.. 99

3.1. INTRODUCTION.. 101
3.2. RESULTS AND DISCUSSION... 105
  3.2.1. Design and synthesis.. 105
  3.2.2. Cytotoxicity... 108
3.3. CONCLUSIONS... 111
3.4. EXPERIMENTAL SECTION.. 111
  3.4.1. General methods... 111
    3.4.1.1. General method for solid-phase synthesis of CECMEL11 undecapeptides.. 112
    3.4.1.2. PEG-1-MBHA resin synthesis.. 114
    3.4.1.3. General method for solid-phase synthesis of peptide conjugates........... 115
  3.4.2. Cell lines and cell culture... 117
  3.4.3. Cell growth inhibition assay... 118
3.5. REFERENCES.. 118

CHAPTER 4. Solid-phase synthesis of cyclic depsipeptides containing a phenyl ester bond... 125

4.1. INTRODUCTION.. 127
4.2. RESULTS AND DISCUSSION... 131
  4.2.1. Retrosynthetic analysis.. 131
  4.2.2. Synthesis of cyclic octapeptides (route A)... 132
  4.2.3. Synthesis of cyclic octadepsipeptides (routes A and B)........................... 135
4.3. CONCLUSIONS... 142
4.4. EXPERIMENTAL SECTION.. 142
  4.4.1. General methods... 142
  4.4.2. Synthesis of Amino Acids.. 144
  4.4.3. Solid-Phase Synthesis of cyclic octapeptides... 149
    4.4.3.1. General method for the synthesis of linear peptidyl resins.................... 149
    4.4.3.2. General method for the allyl and Fmoc group removal from linear peptidyl resins.. 151
    4.4.3.3. General method for the synthesis of cyclic peptides............................ 152
  4.4.4. Solid-Phase Synthesis of cyclic octadepsipeptides.................................. 154

4.4.4.1. Synthesis of Fmoc-L-Tyr(Wang)-OAll or Fmoc-D-Tyr(Wang)-OAll 154
4.4.4.2. Synthesis of the linear peptidyl resins 155
4.4.4.3. General method for the solid-phase synthesis of the linear depsipeptidyl resins 157
4.4.4.4. General method for the allyl and Alloc group removal from linear depsipeptidyl resins 160
4.4.4.5. Synthesis of cyclic depsipeptides 163
4.4.4.6. General method for the hydrolysis of cyclic depsipeptides 166
4.5. REFERENCES 167

CHAPTER 5. Total solid-phase synthesis of dehydroxy fengycin derivatives ... 173
5.1. INTRODUCTION 175
5.2. RESULTS AND DISCUSSION 178
5.2.1. Synthetic approach for the preparation of cyclic lipodepsipeptides with general structure **I** 178
5.2.2. Synthesis of cyclic lipodepsipeptides bearing a L-Tyr^3/D-Tyr^9 179
5.2.3. Synthesis of cyclic lipodepsipeptides bearing D-Tyr^3/L-Tyr^9 183
5.3. CONCLUSIONS 185
5.4. EXPERIMENTAL SECTION 186
5.4.1. General methods 186
5.4.2. Synthesis of Amino Acids 188
5.4.3. Solid-Phase Synthesis of Cyclic Lipodepsipeptides 189
5.4.3.1. Synthesis of linear lipopeptidyl resins 189
5.4.3.2. Synthesis of linear depsipeptidyl resins containing a phenyl ester 193
5.4.3.3. General method for allyl/Alloc removal 197
5.4.3.4. Synthesis of the cyclic lipodepsipeptides 200
5.4.3.5. General method for the hydrolysis of cyclic lipodepsipeptides 204
5.5. REFERENCES 207

CHAPTER 6. General Discussion 211
6.1. SYNTHESIS OF CELL-PENETRATING γ-PEPTIDE/ANTIMICROBIAL UNDECAPEPTIDE CONJUGATES WITH ANTICANCER ACTIVITY 214
6.2. SYNTHESIS OF ANTIMICROBIAL CYCLIC LIPODEPSIPEPTIDES DERIVED FROM FENGYCINS 217
6.2.1. Synthesis of cyclic octadepsipeptides containing a phenyl ester bond 218
6.2.2. Synthesis of dehydroxy fengycin derivatives 222
6.3. REFERENCES 225

CHAPTER 7. General Conclusions 229

Supplementary Digital Information

- PhD thesis (pdf file)
- APPENDIX: Electronic supporting information for Chapters 3, 4, 5 (pdf file)

General Abstract

Bioactive peptides have become an important reference in the drug discovery process in recent years. They can be found in a wide range of organisms, from vertebrate to bacteria, playing a key role in countless biological processes. Among them, antimicrobial peptides are one of the most studied. Their activity is not only restricted to bacteria, but are active against many other different pathogens, such as fungi, viruses or even cancer cells. Their mechanism of action mainly involves the interaction with negatively charged membranes which decreases the probability that microorganisms develop resistance to them. These features have prompted antimicrobial peptides to be considered as a resourceful strategy for the discovery of new therapeutic drugs. However, there are hurdles which must be overcome before their *in vivo* use can be implemented, such as their poor bioavaibility or their high susceptibility to enzymatic degradation. Chemical modification of the peptide backbone, cyclization or introduction of non-natural amino acids can prevent protease recognition resulting in an enhancement of the peptide stability. These structural modifications require new versatile strategies suitable for the preparation of a large range of analogues. Towards this aim, this PhD thesis is focused on the development of new synthetic approaches to obtain new bioactive peptides.

In the first part of this thesis (Chapter 3) peptide conjugates incorporating an antimicrobial peptide and a cell-penetrating peptide (CPP) were synthesized and evaluated for their antitumoral activity. In particular, in collaboration with the *Combinatorial Chemistry Unit* of the *Institute for Research in Biomedicine* from Barcelona, selected peptides from the CECMEL11 library of antimicrobial peptides were conjugated to the cell-penetrating γ-peptide **PEG-1**. This CPP prompted the cellular uptake of the antimicrobial peptides improving their activity against cancer cells. The best conjugate produced a high growth inhibition percentage of MDA-MB-231 cells and it was low toxic against non-malignant fibroblasts.

In the second part of this thesis (Chapter 4 and 5) a feasible strategy for the synthesis of bioactive cyclic lipodepsipeptides produced by *Bacillus* strains, useful for plant protection, was envisaged. In Chapter 4 an efficient solid-phase methodology for the preparation of the macrolactone of eight amino acids present in fengycins was developed. In this regard, two synthetic routes were designed and evaluated. The key

steps of these strategies were the formation of the ester bond and the on-resin cyclization. The best approach allowed the preparation of cyclic octadepsipeptides derived from fengycins A, B and S. In Chapter 5, this methodology was extended to the preparation of dehydroxy fengycin analogues which differ on the amino acid composition. This study represents, to the best of our knowledge, the first approach towards the solid-phase synthesis of this family of cyclic lipodepsipeptides and it can be easily adapted to the preparation of a wide variety of analogues.

Resum General

En els últims anys, els pèptids bioactius s'han convertit en una referència important en el procés de desenvolupament de nous fàrmacs. Aquests compostos es poden trobar en una gran varietat d'organismes, des de vertebrats fins a bactèries, i tenen un paper important en nombrosos processos biològics. Entre ells, els pèptids antimicrobians són uns dels més estudiats. La seva activitat no es limita únicament a les bactèries, sinó que també són actius en front molts altres patògens com fongs, virus o inclús cèl·lules cancerígenes. A més, el seu mecanisme d'acció es basa principalment en la interacció amb les membranes carregades negativament, cosa que redueix la probabilitat que el microorganisme desenvolupi mecanismes de resistència. Aquestes característiques han convertit als pèptids antimicrobians en una estratègia prometedora per al descobriment de nous agents terapèutics. No obstant això, hi ha certs obstacles que s'han de solucionar abans de poder implementar el seu ús *in vivo*, com per exemple la seva biodisponibilitat baixa o la seva susceptibilitat elevada a la degradació enzimàtica. La modificació química de l'esquelet peptídic, la ciclació o la introducció d'aminoàcids no naturals són estratègies que eviten el reconeixement per proteases augmentant la estabilitat del pèptid. Aquestes modificacions estructurals requereixen de noves tècniques sintètiques més versàtils i que permetin la preparació d'una gran varietat d'anàlegs. En aquest sentit, aquesta tesi doctoral s'ha centrat en el desenvolupament de noves estratègies sintètiques per a l'obtenció de nous pèptids bioactius.

En la primera part d'aquesta tesi (Capítol 3) s'han sintetitzat nous pèptids conjugats incorporant un pèptid antimicrobià i un pèptid amb capacitat de penetrar la membrana cel·lular (CPP), i s'ha avaluat la seva activitat antitumoral. Concretament, en col·laboració amb la *Unitat de Química Combinatòria* de l'*Institut d'Investigació Biomèdica* de Barcelona, seqüències seleccionades de la quimioteca de pèptids antimicrobians CECMEL11 s'han unit al CPP **PEG-1**. Aquest CPP ha facilitat la internalització cel·lular dels pèptids antimicrobians augmentant la seva activitat antitumoral. El pèptid conjugat amb un millor perfil biològic ha mostrat un percentatge elevat d'inhibició del creixement de les cèl·lules cancerígenes MDA-MB-231 i una toxicitat baixa enfront fibroblasts no malignes.

En la segona part d’aquesta tesi (Capítols 4 i 5) s’ha desenvolupat una estratègia útil per a la preparació de lipodepsipèptids cíclics produïts per soques de *Bacillus*, utilitzats en la protecció de plantes. En el Capítol 4 s’ha establert una metodologia en fase sòlida eficaç per a la preparació de la macrolactona de vuit aminoàcids present en la estructura de les fengicines. Amb aquesta finalitat, s’han dissenyat i avaluat dues rutes sintètiques. Les etapes clau d’aquestes estratègies han estat la formació de l’enllaç èster i la ciclació en fase sòlida. La ruta millor ha permès la preparació d’octadepsipèptids cíclics derivats de les fengicines A, B i S. En el Capítol 5, aquesta metodologia ha estat estesa a la preparació de dehidroxi anàlegs de fengicina que difereixen en la seqüència d’aminoàcids que presenten. Aquest estudi representa la primera estratègia sintètica dissenyada per a la preparació en fase sòlida d’aquesta família de lipodepsipèptids cíclics i pot ser fàcilment adaptada per a l’obtenció d’una gran varietat d’anàlegs.

Resumen General

En los últimos años, los péptidos bioactivos se han convertido en una referencia importante en el proceso de desarrollo de nuevos fármacos. Estos compuestos se pueden encontrar en una gran variedad de organismos, desde vertebrados hasta bacterias, y poseen un papel importante en numerosos procesos biológicos. Entre ellos, los péptidos antimicrobianos son unos de los más estudiados. Su actividad no se limita sólo a bacterias, sino que también son activos frente a muchos otros patógenos, como hongos, virus o incluso células cancerígenas. Además, su mecanismo de acción se basa principalmente en la interacción con las membranas cargadas negativamente, lo que reduce la probabilidad que el microorganismo desarrolle mecanismos de resistencia. Estas características han convertido a los péptidos antimicrobianos en una estrategia prometedora para el descubrimiento de nuevos agentes terapéuticos. Sin embargo, hay algunos obstáculos que deben ser superados antes de poder implementar su uso *in vivo*, como por ejemplo su biodisponibilidad baja o su susceptibilidad elevada a la degradación enzimática. La modificación química del esqueleto peptídico, la ciclación o la introducción de aminoácidos no naturales son estrategias que evitan el reconocimiento por proteasas aumentando la estabilidad del péptido. Estas modificaciones estructurales requieren nuevas técnicas sintéticas más versátiles y que permitan la preparación de una amplia variedad de análogos. En este sentido, esta tesis doctoral se ha centrado en el desarrollo de nuevas estrategias sintéticas para la obtención de nuevos péptidos bioactivos.

En la primera parte de esta tesis (Capítulo 3) se han sintetizado nuevos péptidos conjugados incorporando un péptido antimicrobiano y un péptido con capacidad de penetrar la membrana celular (CPP), y se ha evaluado su actividad antitumoral. Concretamente, en colaboración con la *Unidad de Química Combinatoria* del *Instituto de Investigación Biomédica* de Barcelona, secuencias seleccionadas de la quimioteca de péptidos antimicrobianos CECMEL11 se han unido al CPP **PEG-1**. Este CPP ha facilitado la internalización celular de los péptidos antimicrobianos aumentando su actividad antitumoral. El péptido conjugado con un mejor perfil biológico ha mostrado un porcentaje elevado de inhibición del crecimiento de las células cancerígenas MDA-MB-231 y una toxicidad baja frente a fibroblastos no malignos.

En la segunda parte de esta tesis (Capítulos 4 y 5) se ha desarrollado una estrategia útil para la preparación de lipodepsipéptidos cíclicos bioactivos producidos por cepas de *Bacillus*, utilizados en la protección de plantas. En el Capítulo 4 se ha establecido una metodología en fase sólida eficaz para la preparación de la macrolactona de ocho aminoácidos presente en la estructura de las fengicinas. Con esta finalidad, se han diseñado y evaluado dos rutas sintéticas. Los etapas clave de estas estrategias han sido la formación del enlace éster y la ciclación en fase sólida. La ruta mejor ha permitido la preparación de octadepsipéptidos cíclicos derivados de las fengicinas A, B y S. En el Capítulo 5, esta metodología ha sido extendida a la preparación de dehidroxi análogos de fengicina que difieren en la secuencia de aminoácidos que presentan. Este estudio representa la primera estrategia sintética diseñada para la preparación en fase sólida de esta familia de lipodepsipéptidos cíclicos y puede ser fácilmente adaptada para la obtención de una gran variedad de análogos.

CHAPTER 1.

General Introduction

1.1 ANTIMICROBIAL PEPTIDES

Natural products have been considered as an interesting reference in the drug discovery process. It is no wonder that they play a crucial role in the discovery of leads and most of the pharmaceutical companies' efforts have been focused not only on their discovery, but also on the design of analogues to improve their biological profile (Newman and Cragg, 2012; Butler et al., 2013). Among them, antimicrobial peptides (AMPs) have been the focus of numerous research projects, because of their key role in biological processes as well as for their high efficacy and low toxicity.

Antimicrobial peptides are an assorted group of molecules produced by virtually all forms of life. They can be found in organisms ranging from bacteria to plants as well as mammals (Zasloff, 2002; Jenssen et al., 2006; Li et al., 2012; Costa et al., 2015). Moreover, they are involved in the nonspecific innate immune system of these organisms and show a broad spectrum of activities towards a wide range of pathogens, such as bacteria, fungi, virus and even cancer cells (Hancock, 2001; Jenssen et al., 2006; Li et al., 2012; Pasupuleti et al., 2012). Regarding their structure, antimicrobial peptides are typically polypeptides of low molecular weight, composed of less than 100 amino acids. Although the length and composition are both variable, their sequence contains cationic and hydrophobic residues, having an amphiphilic structure.

1.1.1 Classification of antimicrobial peptides

The increasing interest in antimicrobial peptides has not only prompted the isolation and characterization of many natural peptides, but also the *de novo* design and synthesis of analogues. Up to now, more than 2000 different antimicrobial peptides have been reported (APD database: Wang et al., 2009 http://aps.unmc.edu/AP/main.php; CAMP database: Waghu et al., 2014 http://www.camp.bicnirrh.res.in/index.php; peptaibol database: Whitmore and Wallace, 2004 http://www.cryst.bbk.ac.uk/peptaibol). Due to their structural diversity, their classification is difficult. Several criterions have been proposed in order to sort out this wide variety of compounds, some of which are detailed below.

1.1.1.1 Classification of antimicrobial peptides according to their secondary structure

Although antimicrobial peptides are typically unstructured in solution, most of them can adopt a defined conformation in presence of lipid membranes. According to their secondary structure, antimicrobial peptides can be classified into four major groups: α-helical, β-sheet, loop and extended peptides, with the first two classes being the most common in nature (*Figure 1.1*) (Hancock, 2001; Powers and Hancock, 2003; Jenssen et al., 2006; Giuliani et al., 2007; Peters et al., 2010; Baltzer and Brown, 2011).

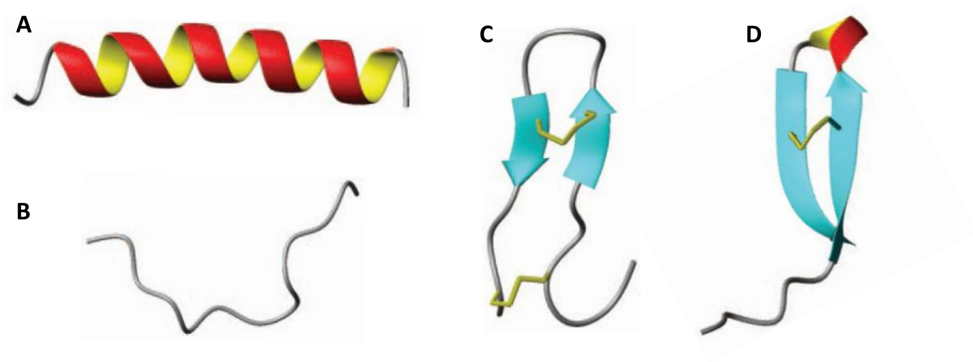

Figure 1.1. *Secondary structure of antimicrobial peptides: (**A**) α-helical; (**B**) extended; (**C**) β-sheet; and (**D**) looped. Disulfide bonds are represented in green (adapted from Powers and Hancock, 2003).*

α-Helical peptides are one of the most widely distributed and studied families (Tossi et al., 2000). These peptides are usually unstructured in an aqueous environment. Nevertheless, it has been shown that they are able to adopt a secondary helical conformation upon encountering lipid membranes (Tossi et al., 2000; Zasloff, 2002; Pasupuleti et al., 2012). Moreover, many of these peptides also display distinct amphiphilic characteristics that enable their insertion into the lipid membrane. Some examples of α-helical peptides are cecropins, melittin and magainins (*Table 1.1*). Cecropins are a well-known family of cationic linear peptides isolated from the giant silk moth *Hyalophora cecropia* (Steiner et al., 1981; Andreu et al., 1983). They are mainly active against Gram-negative bacteria, but they also show activity towards some Gram-positive bacteria and fungi. These peptides are 35-40 residues long and their structure contains a basic *N*-terminal amphipathic α-helical domain connected to a hydrophobic *C*-terminal α-helical stretch by a flexible hinge (Tossi et al., 2000; Li et al., 2012). Melittin is another family of well-known α-helical peptides. This 26-residue peptide, which was found in the venom of the European honey bee *Apis mellifera*, contains in its structure two well-defined α-helical regions with different polarities (Terwilliger and Eisenberg, 1982a, 1982b; Terwilliger et al., 1982). The *N*-terminal region, predominantly hydrophobic, contains nonpolar, hydrophobic and neutral amino acids; whereas the *C*-terminal region is mainly rich in hydrophilic and basic residues. Melittin induces membrane permeabilization and lyses prokaryotic as well as eukaryotic cells in a non-selective manner, which is responsible for its antibacterial and its highly hemolytic activity (Terwilliger et al., 1982; Tossi et al., 2000; Raghuraman and Chattopadhyay, 2007; Lee et al., 2013). Finally, other examples of well-known cationic α-helical peptides are magainins. These 20-25-residue peptides have been isolated from the skin and stomach of the frog *Xenopus laevis*, and are able to adopt a single rod-like helix structure in presence of lipid bilayers (Zasloff, 1987; Tossi et al., 2000). Magainins also exhibit activity towards a broad-spectrum of pathogens, such as bacteria, fungi, protozoa, cancer cells and even viruses.

In contrast to α-helical peptides, β-sheet sequences are in general cyclic structures constrained by intramolecular bridges, usually disulfide bonds. Some of the best studied peptides in this group are defensins and protegrins (*Table 1.1*). The first family includes cysteine-rich peptides of 18-45 amino acids which contain several disulfide bonds in their structure (Nissen-Meyer and Nes, 1997; Ganz, 2003; Li et al., 2012; Pasupuleti et al., 2012). Defensins have been isolated mainly from mammals, although they have also been found in insects and plants, and they show a broad spectrum of activity towards bacteria and fungi. On the other hand, protegrins are a family of arginine-rich peptides with 16-18 amino acids isolated from porcine leukocytes. They contain two intramolecular cysteine disulfide bonds which provide them with a defined anti-parallel β-hairpirin secondary structure (Kokryakov et al., 1993; Pasupuleti et al., 2012).

Table 1.1. *Examples of natural antimicrobial peptides categorized according to their secondary structure.*

Secondary structure	**Peptide**	**Sequence**	**References**
α-Helical peptides	**Cecropin A**	KWKLFKKIEKVGQNIRDGIIKAGPAVAVVGQATQIAK-NH_2	Steiner et al., 1981
	Melittin	GIGAVLKVLTTGLPALISWIKRKRQQ-NH_2	Terwilliger and Eisenberg 1982b
	Magainin 1	GIGKFLHSAGKFGKAFVGEIMKS-OH	Zasloff, 1987
	Magainin 2	GIGKFLHSAKKFGKAFVGEIMNS-OH	Zasloff, 1987
β-Sheet peptides	**α-Defensin (HNP-3)**	$C_1YC_2RIPAC_3IAGERRYGTC_3IYQGRLWAFC_2C_1$-OH[a]	Ganz, 2003
	β-Defensin (HBD-2)	$GGIGDPVTC_1LKSGAIC_2HPVFC_3PRRYK$- -$QIGTC_3GLPGTKC_1C_2KKP$-OH[a]	Ganz, 2003
	Protegrin-1	$RGGRLC_1YC_2RRRFC_2VC_1VGR$-$NH_2$[a]	Kokryakov et al., 1993

[a] Subscript numbers represent amino acids joined by a disulfide bridge.

1.1.1.2 Classification of antimicrobial peptides according to their biosynthetic pathway

Regardless their structure, natural antimicrobial peptides can also be classified into two major groups according to their biosynthetic pathway as ribosomal and non-ribosomal peptides.

Ribosomal peptides are widely distributed in nature, being produced by mammals, insects, plants and microorganisms (Nissen-Meyer and Nes, 1997). These gene-encode peptides are synthesized in the ribosome through a transcription and translation pathway. Therefore, ribosomal peptides only contain the 20 proteinogenic amino acids in their sequence. Nevertheless, it has been demonstrated that most of them are post-translationally modified leading to products with a more complex structure (McIntosh et al., 2009). Most of the isolated antimicrobial peptides are ribosomally synthesized and some examples are the aforementioned cecropins and defensins (*Table 1.1*).

On the other hand, non-ribosomal peptides comprise *β*-lactams, glycopeptides, lipopeptides and peptaibols (Baltz, 2006; Leitgeb et al., 2007; Duclohier, 2007; Zakeri and Lu, 2013). These peptides are produced in a nucleic acid-independent way through large multienzyme complexes, so-called non-ribosomal peptide synthetases, which are able to catalyze stepwise peptide condensations. Unlike ribosomal synthesis, the substrates of these multienzymes are not restricted to the 20 natural amino acids but also include non-proteinogenic ones, such as D-isomers or *N*-methylated residues, and even heterocyclic rings and fatty acids (Mankelow and Neilan, 2000; Sieber and Marahiel, 2003; McIntosh et al., 2009). Another common feature of many non-ribosomal peptides is their constrained structure, usually resulting from cyclization or oxidative cross-linking (Sieber and Marahiel, 2003). As a result, they show a more diverse chemical space than ribosomal peptides. One example of these peptides is the antibiotic daptomycin (*Figure 1.2*). This lipopeptide contains a cyclic peptide linked to a fatty chain. It shows interesting bactericidal activity against Gram-positive bacteria and is used to treat skin infections as well as other infections caused by multi-drug resistant microorganisms (Micklefield, 2004; Zakeri and Lu, 2013).

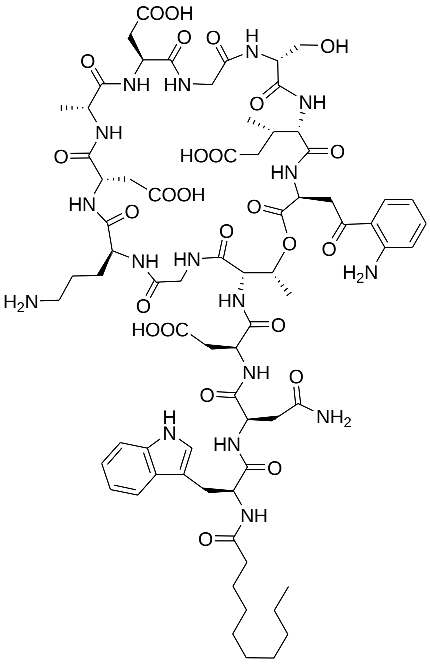

Figure 1.2. *Structure of the non-ribosomal peptide daptomycin.*

1.1.2 Mechanism of action of antimicrobial peptides

The main mode of action of antibiotics involves their interaction with specific cellular targets. In contrast, most antimicrobial peptides act through a nonreceptor-mediated mechanism, being the cell membrane their main target (Shai, 2002; Pasupuleti et al., 2012; Galdiero et al., 2013; Henderson and Lee, 2013; Costa et al., 2015). The negative nature of the cell membrane enables the electrostatic interaction with antimicrobial peptides, which are mainly cationic (Tossi et al., 2000; Hancock, 2001; Shai, 2002; Zasloff, 2002; Powers and Hancock, 2003; Brogden, 2005; Huang, 2006; Jenssen et al., 2006; Baltzer and Brown, 2011). Depending on both the peptide and bilayer composition, different permeabilization models have been proposed, such as the barrel stave, the carpet, the toroidal pore and the disordered toroidal pore models (*Figure 1.3*) (Brogden, 2005; Melo et al., 2009). In the barrel-stave model, peptides aggregate and insert perpendicularly into the bilayer forming a pore. The hydrophobic peptide region aligns with the lipid core of the bilayer while the hydrophilic region forms the lumen of the pore. This peptide orientation allows the phospholipid chains of the pore to remain perpendicular to the bilayer plane. In the toroidal-pore model, peptides also aggregate and insert perpendicularly into the bilayer, but unlike the barrel-stave model, they induce a membrane curvature. This model suggests that the two lipid monolayers, the inner and the outer one, continuously bend through the pore. Thus, the hydrophilic pore is formed by both peptides and phospholipid head groups. A modification of this model has been reported, called the disordered toroidal pore model. The latter proposes the same mechanism as the toroidal pore one, but it involves pore formation through peptides in a more disordered orientation. The carpet-like model describes a different mechanism. In this case, peptides accumulate parallel to the bilayer until they reach a high surface coverage. At this point, they start to disrupt the membrane in a detergent-like manner, even causing the formation of micelles.

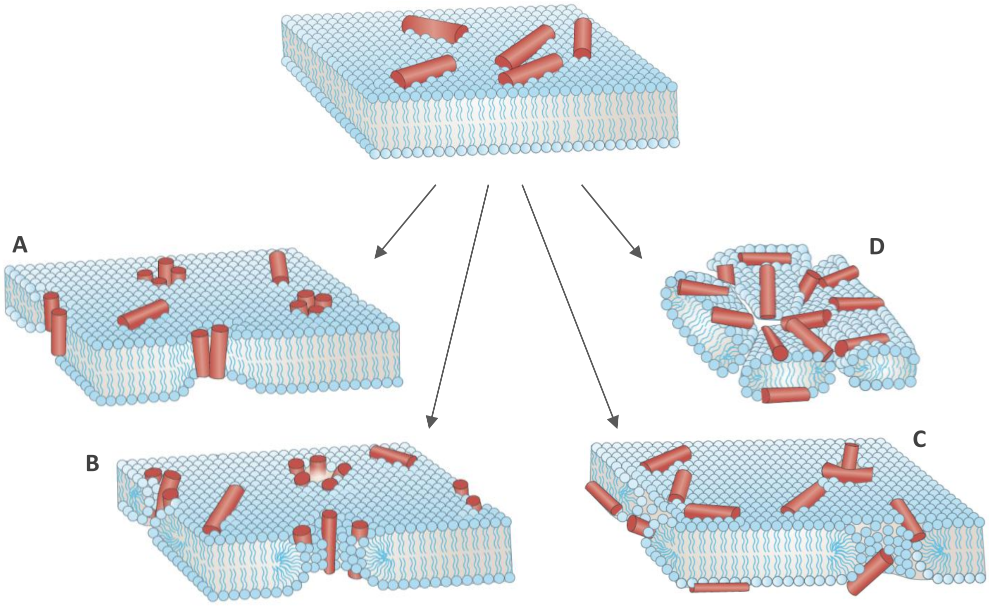

Figure 1.3. *Mechanisms of membrane cell disruption mediated by antimicrobial peptides:* ***A)*** *barrel-stave;* ***B)*** *toroidal-pore;* ***C)*** *disordered toroidal-pore; and* ***D)*** *carpet-like models (adapted from Melo et al., 2009).*

Besides their ability to interact with membranes, it has been described that antimicrobial peptides may also interact with intracellular targets (Shai, 2002; Powers and Hancock, 2003; Giuliani et al., 2007; Costa et al., 2015). There is increasing evidence that antimicrobial peptides are able to translocate the membrane, block essential cellular processes and kill the bacteria without extensively damaging the membrane (*Figure 1.4*). For instance, translocated peptides can inhibit the cell-wall synthesis (I), the nucleic acid synthesis (E), the protein synthesis (F), and even the enzymatic activity of the cell (G-H) (Brogden, 2005; Jenssen et al., 2006; Li et al., 2012; Pasupuleti et al., 2012). These mechanisms of action may occur independently or synergistically with membrane permeabilization (Giuliani et al., 2007). However, the interaction with the bacterial membrane appears to be the main mechanism of action for the vast majority of antimicrobial peptides (Shai, 2002; Powers and Hancock, 2003; Brogden, 2005; Jenssen et al., 2006; Pasupuleti et al., 2012).

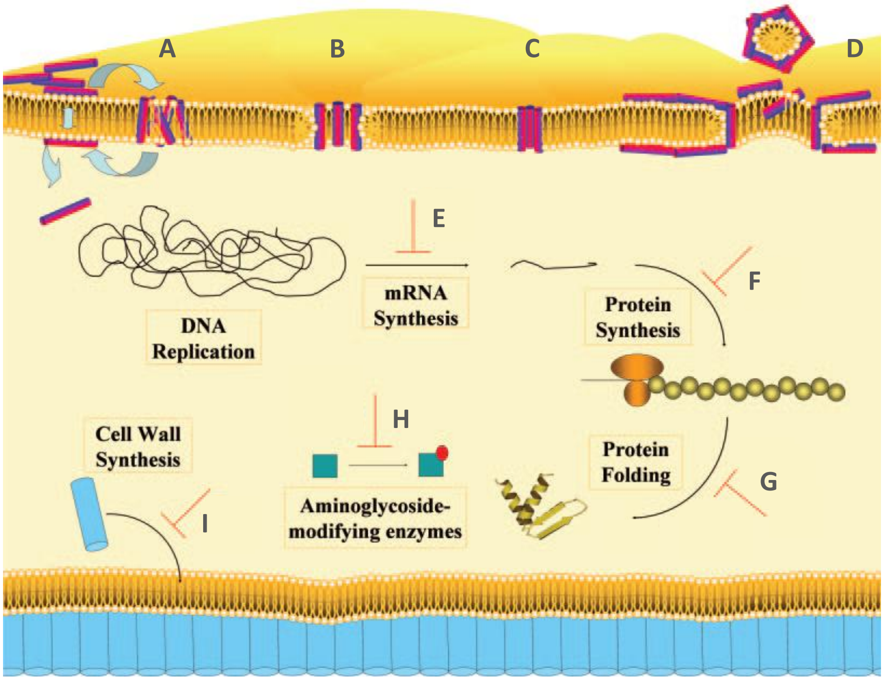
A
B
C
D
E
mRNA Synthesis
DNA Replication
Protein Synthesis
F
H
Cell Wall Synthesis
Aminoglycoside-modifying enzymes
Protein Folding
G
I

Figure 1.4. *Mode of action of antimicrobial peptides. The bacterial membrane is represented as a yellow lipid bilayer. The cylinders are peptides, where the hydrophilic regions are colored red and the hydrophobic regions are in blue. Mechanisms of membrane permeabilization are indicated in panels* ***A*** *to* ***D****, while mechanisms of action of peptides which do not act by permeabilizing the bacterial membrane are indicated by panels* ***E*** *to* ***I*** *(adapted from Jenssen et al., 2006).*

1.1.3 Selectivity of antimicrobial peptides

One of the most important characteristics of antimicrobial peptides is their ability to selectively interact with microbial membranes over that of host cells (Matsuzaki, 1999; Henderson and Lee, 2013). Although the negative nature of the microbial membrane seems to be the main factor for the selectivity of antimicrobial peptides, other elements are also involved. Membrane fluidity, lipid head groups identity and lipid acyl chain length may further explain how the behaviour of antimicrobial peptides is tuned to selectively disrupt bacterial membranes over those of mammals (Pasupuleti et al., 2012; Henderson and Lee, 2013).

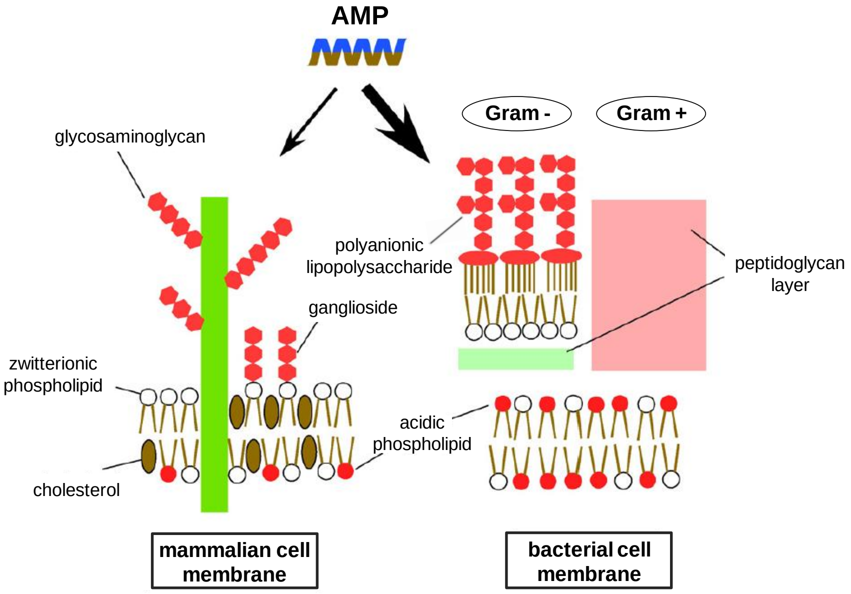
AMP
Gram -
Gram +
glycosaminoglycan
polyanionic lipopolysaccharide
peptidoglycan layer
ganglioside
zwitterionic phospholipid
acidic phospholipid
cholesterol
mammalian cell membrane
bacterial cell membrane

Figure 1.5. *Molecular basis for membrane selectivity by antimicrobial peptides (extracted from Matsuzaki, 2009).*

Lipid composition of prokaryotic and eukaryotic cell membranes is significantly different and seems to be the cause for the preferential binding of antimicrobial peptides to the former cell membranes (*Figure 1.5*) (Matsuzaki, 1999; Zasloff, 2002). Bacteria outer membranes contain large amounts of negatively charged phospholipids, such as phosphatidylglycerol and cardiolipin (Brogden, 2005; Giuliani et al., 2007; Matsuzaki, 2009; Pasupuleti et al., 2012; Galdiero et al., 2013). In addition, the outer membrane of

Gram-negative bacteria is covered with a layer of polyanionic lipopolysaccharides that raise its negative character. In the same way, Gram-positive bacteria contains some acidic polysaccharides on their outer surface, such as teichoic acids, that also increase the negative charge of the membrane (Tossi et al., 2000; Shai, 2002; Brogden, 2005; Matsuzaki, 2009; Galdiero et al., 2013). All these anionic components provide a high negative charge on the outer leaflet of the bacteria enabling their interaction with antimicrobial peptides.

In contrast, mammalian membranes are rich in zwitterionic phospholipids, including phosphatidylethanolamine, phosphatidylcholine and sphingomyelin, which are neutrally charged at physiological pH (Giuliani et al., 2007; Hoskin and Ramamoorthy, 2008; Matsuzaki, 2009; Pasupuleti et al., 2012; Galdiero et al., 2013; Henderson and Lee, 2013). Another important difference between bacterial and mammalian cell membranes is the presence of cholesterol. While it is absent in bacterial membranes, cholesterol is an important constituent of mammalian cell membranes, influencing the selectivity of antimicrobial peptides (Matsuzaki, 1999; Zasloff, 2002; Galdiero et al., 2013). Cholesterol reduces the membrane fluidicity difficulting the insertion of antimicrobial peptides and the subsequent membrane deformation (Hoskin and Ramamoorthy, 2008; Henderson and Lee, 2013).

It is also interesting to note that tumor cells are more susceptible to antimicrobial peptides than non-malignan eukaryotic cells. The membrane of tumor cells is rich in anionic molecules such as phosphatydilserine, *O*-glycosylated mucins, sialylated gangliosides and heparin sulphates (Hoskin and Ramamoorthy, 2008; Schweizer, 2009). This composition is responsible for the partial loss of lipid symmetry and architecture, which in turn leads to an increase of negative membrane potential that enables the binding of antimicrobial peptides to these membranes (Pasupuleti et al., 2012). Apart from the differences in cell membrane composition, other factors that have also been proposed for the antitumor activity of antimicrobial peptides are fluidicity and the glycosylation pattern of membrane–associated proteins (Hoskin and Ramamoorthy, 2008).

1.2 ANTIMICROBIAL PEPTIDES AS ANTICANCER AGENTS

It is well-know that antimicrobial peptides are cytotoxic not only against bacteria, but also towards different types of human cancer cells, such as breast, bladder, ovarian and lung cells (Mader and Hoskin, 2006; Hoskin and Ramamoorthy, 2008; Li et al., 2012; Gaspar et al., 2013; Wu et al., 2014). Due to their physicochemical properties and their mode of action, antimicrobial peptides are expected to display higher selectivity and lower toxicity than conventional chemotherapy treatments.

1.2.1 The disease of cancer

Cancer remains a major cause of death affecting millions of people around the world. The International Agency for Research on Cancer (IARC) estimates that 14.1 millions of new cancer cases and 8.2 millions of cancer deaths occurred worldwide during 2012 (Globocan2012. IARC http://globocan.iarc.fr/Pages/fact_sheets_population.aspx). The international statistics also reveals that among the male population the five more frequently detected cancers are lung, prostate, colorectum, stomach and liver (*Figure 1.6a*); whereas breast, colorectum, lung, cervix uteri and stomach ones are the most common among women (*Figure 1.6b*).

Although there are more than 100 distinct types of cancer that can affect different organs and tissues, all of them are characterized by the growth and spreading of abnormal cells in an uncontrolled manner (Hanahan and Weinberg, 2000). This disease is initiated by a series of accumulative genetic and epigenetic changes that occur in normal cells (Harris et al., 2013). As a result, cancer cells acquire unique traits that alter their physiology, such as the creation of their own growth signals; the capacity to ignore antiproliferative signals; the resistance to programmed cell death (apoptosis); the ability to replicate without limits; the development of new blood vessels allowing the tumor growth; and the ability to invade tissues, at first locally and later through metastasis (Hanahan and Weinberg, 2000). Recently, other hallmarks have been added to this list, such as the ability to reconfigure the energy metabolism of cells as well as to evade the immune system of the organism (Hanahan and Weinberg, 2011).

a) Male cancer incidence

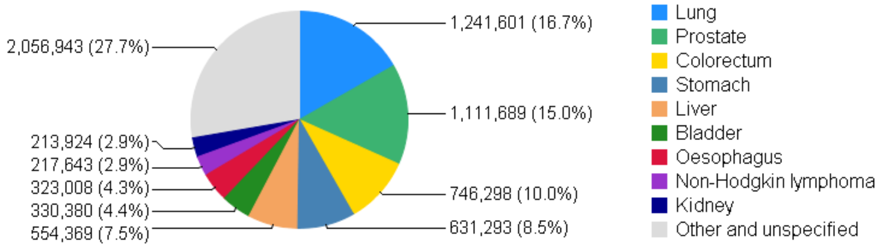

b) Female cancer incidence

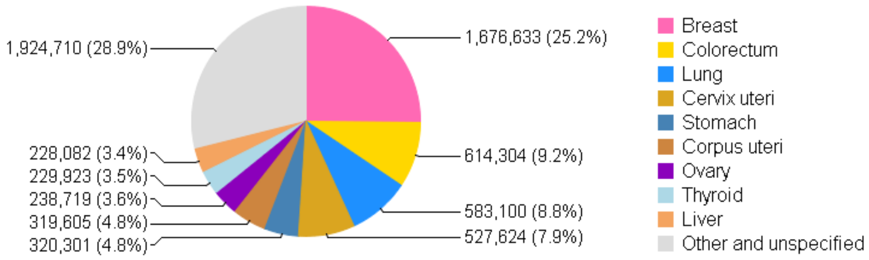

Figure 1.6. *Graphic of estimate incidence of cancer disease in males (**a**) and in females (**b**) during 2012 (Globocan2012, IARC).*

The conventional cytotoxic treatments for cancer management mainly involve radiotherapy and chemotherapy (Bhutia and Maiti, 2008; Nussbaumer et al., 2011; Riedl et al., 2011; Harris et al., 2013). Both treatments are used against a broad array of cancer diseases. Radiotherapy is a relatively precise treatment and is used to achieve a local control; whereas chemotherapy exerts a more systemic effect on the organism. Chemotherapy involves the use of low-molecular-weight drugs that can be classified according to their mechanism of action (Nussbaumer et al., 2011). Some examples are detailed below:

(i) **Antimetabolites**. The mechanism of these anticancer drugs is based on their interaction with essential biosynthetic pathways. Some examples are 5-fluorouracil and mercaptopurine (*Figure 1.7*). They are structural analogues of pyrimidine and purine, respectively, and are able to disrupt the nucleic acid synthesis. 5-Fluorouracil is widely used for the treatment of breast tumor, gastrointestinal tract cancers, including colorectal one, and certain skin cancers. Mercaptopurine is mainly used as maintenance therapy for acute leukemia. Another example of antimetabolite is methotrexate (*Figure 1.7*). It is able to interfere enzymatic processes of the cell metabolism and is used as maintenance therapy for acute lymphoblastic leukemia, non-Hodgkin's lymphoma and several solid tumors.

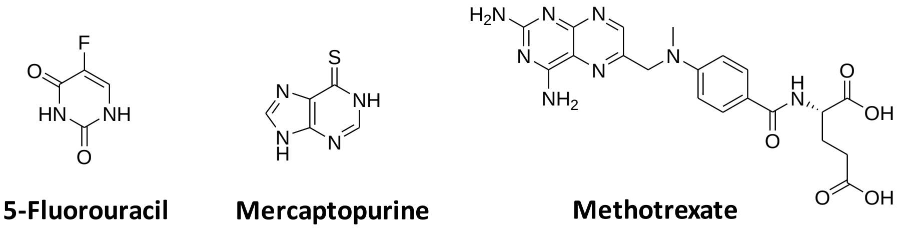

5-Fluorouracil **Mercaptopurine** **Methotrexate**

Figure 1.7. *Examples of antimetabolites.*

(ii) **DNA-interactive agents**. They constitute one of the largest and most important anticancer drug families which includes alkylating, cross-linking and intercalating agents as well as topoisomerase inhibitors and DNA-cleaving agents. Some examples are doxorubicin, cyclophosphamide and cisplatin (*Figure 1.8*). Doxorubicin is a natural product extracted from *Streptomyces peucetiusor* or *S. galilaeus*. This intercalating agent is widely used to treat leukemia, lymphomas and a variety of solid tumors. Cyclophosphamide is a member of the nitrogen mustard family which displays a broad spectrum of activity in solid tumors, lymphocytic leukemia and lymphomas. Cisplatin was the first platinum complex used for anticancer treatment and shows a pronounced activity against testicular and ovarian cancers.

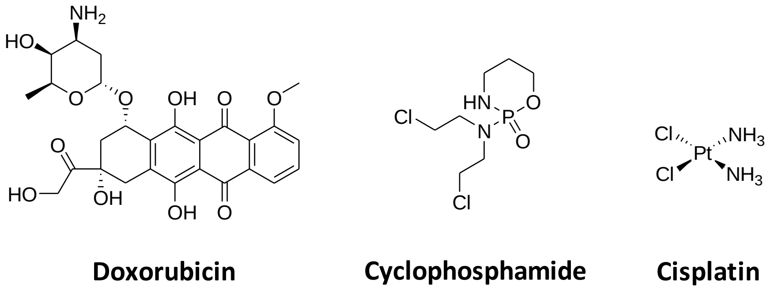

Doxorubicin **Cyclophosphamide** **Cisplatin**

Figure 1.8. *Examples of DNA-interactive drugs.*

(iii) **Antitubulin agents**. These compounds are characterized to interfere the division of the nucleus leading to cell death. The main members of this family are taxanes and the vinca alkaloids, such as paclitaxel and vincristine, respectively (*Figure 1.9*). Paclitaxel is a compound isolated from the Pacific yew tree *Taxus brevifolia* and is used for advanced or metastatic lung and breast cancers. In combination with cisplatin, paclitaxel is also used for the treatment of ovarian cancer. Vincristine is a natural alkaloid isolated from the Madagascar periwinkle *Vinca rosea*. It is used to treat solid tumors, mainly of lung and breast, as well as lymphomas and acute leukemia.

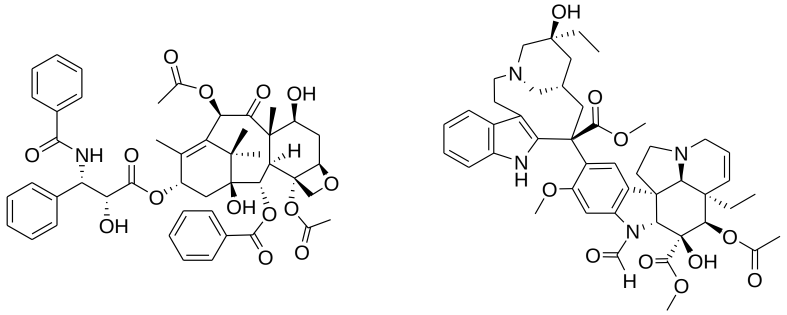

Paclitaxel **Vincristine**

Figure 1.9. *Examples of antitubulin agents.*

Although these treatments are extensively used, they suffer from low therapeutic indices and a broad spectrum of side effects, which are mainly due to the low or no selectivity of drugs for cancer cells over healthy ones (Mader et al., 2005; Mader and Hoskin, 2006; Riedl et al., 2011; Harris et al., 2013). In addition, there are malignant cells that are inactive or have a slow proliferating rate and, therefore, they respond poorly to these chemotherapeutic agents (Mader and Hoskin, 2006; Hoskin and Ramamoorthy, 2008). It has also been observed that cancer cells can develop multiple drug resistance to anticancer drugs, which makes them not only resistant to the drug being used in the treatment, but also to a variety of other unrelated compounds, reducing their therapeutic usefulness (Pérez-Tomás, 2006; Harris et al., 2013).

Based on the above considerations, there is a clear urgent need to develop new therapies that overcome chemoresistance and that have a higher selectivity for malignant cells than drugs currently used, being less harmful for patients. In this context, antimicrobial peptides are considered as a promising alternative to the conventional chemotherapies.

1.2.2 Antimicrobial peptides with anticancer activity

Antimicrobial peptides are potential candidates for cancer therapy due to the advantages that they offer over the traditional chemotherapeutic drugs. The so-called anticancer peptides show a broad spectrum of activity and are able to kill cancer cells rapidly, destroy primary tumors, prevent metastasis and do not harm vital organs (Leuschner and Hansel, 2004; Papo and Shai, 2005; Wu et al., 2014). Moreover, they are unlikely to cause rapid emergence of resistance and can have the ability to synergize with current anticancer treatments (Leuschner and Hansel, 2004; Papo and Shai, 2005; Schweizer, 2009; Feliu et al., 2010).

Based on their spectrum of activity, anticancer peptides can be sorted out into two categories (Papo and Shai, 2005; Harris et al., 2013). The first one includes peptides that are active against both bacteria and cancer cells, but not against normal mammalian cells, such as cecropin B1, magainin 2, lactoferricin, *Bacillus* lipopeptides or synthetic peptides (e.g. P18, **BPC96**). Their structures and activities are summarized in *Table 1.2*. As an example, the antimicrobial peptide cecropin B1, an analogue of the natural peptide cecropin B, not only shows an interesting antimicrobial activity against different bacteria, such as *Escherichia coli* or *Pseudomonas aeruginosa*, but it also displays cytotoxicity against different leukemia cancer cell lines (IC_{50} from 2.4 to 10.2 µM), whereas it is not cytotoxic against fibroblast cells (Chen et al., 1997). Other examples are the lipopeptides surfactin and fengycin produced by the marine microorganism *Bacillus circulans*. These natural lipopeptides display a selective antiproliferative activity towards two human colon cancer cell lines (IC_{50} from 80 to 120 µg ml^{-1}), and show a low cytotoxicity against non-malignant ones (Sivapathasekaran et al., 2010). One example of synthetic peptide is P18, a derivative of the hybrid peptide cecropin A(1-8)-magainin 2(1-12). This peptide not only shows good antimicrobial activity, but also displays anticancer activity against human tumor cells exhibiting low cytolytic effect against non-malignant fibroblasts (Shin et al., 2001). Another example of synthetic peptide is the *de novo* designed cyclic peptide **BPC96**, previously described in the LIPPSO group as antimicrobial agent (see *section 1.3.2*). Along with other cyclic peptides, the anticancer activity of **BPC96** was tested against a panel of cancer cell lines, being the candidate with the best biological activity profile. **BPC96** shows an interesting inhibitory activity against HeLa cervix carcinoma cells, and it is low hemolytic and low cytotoxic against non-malignant fibroblasts. Further studies also demonstrated that, at low doses, **BPC96** is able to synergize with the cytotoxic anticancer drug cisplatin, improving its activity (Feliu et al., 2010).

The second group of anticancer peptides contains peptides that are cytotoxic against the three types of cells, bacteria, cancer and non-malignant mammalian cells. Members of this class are melittin, tachyplesin, the human neutrophil defensin HNP-1 and the human peptide LL-37. In *Table 1.2*, there is a summary of their structures and anticancer activities. Melittin shows a broad spectrum of activity against different cell lines, such as leukemia, lung or ovarian carcinoma cells. However, this peptide also shows an important lytic activity against normal cells which decreases its therapeutic potential as a new anticancer agent (Hoskin and Ramamoorthy, 2008; Gajski and Garaj-Vrhovac, 2013). LL-37 is a member of the cathelicidin family and it is involved in the tumor growth modulation of various types of cancer. It can enhance the proliferation and the metastatic capacity of ovarian, breast and lung cancers, and it has been demonstrated that LL-37 can inhibit the cell proliferation in gastric cancer. Moreover, LL-37 has also been used as immunostimulant to promote the elimination of cancer cells by the host immune system (Wu et al., 2010).

Table 1.2. *Examples of antimicrobial peptides with anticancer activity.*

Peptide	**Sequence**	**Cancer cells**	**Selectivity**	**References**
Cecropin B1	KWKVFKKIEKMGRNIRNGIVKAGPKWKVFKKIEK-NH$_2$	Leukemia cells	Yes	Chen et al., 1997
Magainin 2	GIGKFLHSAKKFGKAFVGEIMNS-OH	Bladder, lung and breast cancer cells, human melanomas and leukemia	Yes	Lehmann et al., 2006; Mader and Hoskin, 2006
Bovine lactoferricin	FKCRRWQWRMKKLGAPSITCVRRAF-OH	Leukemia, breast, colon and ovarian carcinoma cells	Yes	Mader et al., 2005; Mader and Hoskin, 2006
Surfactin	Fatty acid(&)-ELLVDLL(&)[a]	Colon cancer cells	Yes	Sivapathasekaran et al., 2010
Fengycin	Fatty acid-EOY(&)TEAPQYI(&)[b]	Colon cancer cells	Yes	Sivapathasekaran et al., 2010
P18	KWKLFKKIPKFLHLAKKF-NH$_2$	Human myelogenous leukemia, T-cell leukemia and breast adenocarcinoma cells	Yes	Shin et al., 2001
BPC96	c(LKLKKFKKLQ)	Human cervical carcinoma cells	Yes	Feliu et al., 2010
Melittin	GIGAVLKVLTTGLPALISWIKRKRQQ-NH$_2$	Leukemia, ovarian carcinoma, osteosarcoma, lung, prostate and renal cancer cells	No	Gajski and Garaj-Vrhovac, 2013
Tachyplesin	KWC$_1$FRVC$_2$YRGIC$_2$YRRC$_1$R-NH$_2$[c]	Human gastric carcinoma, hepatocarcinoma and prostate carcinoma cells	No	Nakamura et al., 1988; Li et al., 2000; Ouyang et al., 2002; Hoskin and Ramamoorthy, 2008
α-Defensin HNP-1	AC$_1$YC$_2$RIPAC$_3$IAGERRYGTC$_2$IYQGRLWAFC$_3$C$_1$-OH[c]	Human oral squamous carcinoma, renal and prostate carcinoma cells	No	McKeown et al., 2006; Hoskin and Ramamoorthy, 2008; Gaspar et al., 2015
LL-37	LLGDFFRKSKEKIGKEFKRIVQRIKDFLRNLVPRTES-OH	Gastric carcinoma cells. Also used in cancer immunotherapy	No	Wu et al., 2010

[a] The β-carboxyl group of the fatty acid chain forms an ester bond (&) with the carboxylic group of a Leu. [b] Ester bond (&) between the phenol group of Tyr and the α-carboxylic group of Ile.
[c] Subscript numbers represent amino acids joined by a disulfide bridge.

The mechanism of action by which anticancer peptides kill cancer cells is still controversial. However, it has been suggested that they target the cell membrane and cause the cell death through similar membrane permeabilization/disruption models described for antimicrobial peptides (see *section 1.1.2*). Anticancer peptides are able to preferentially interact with the membrane of malignant cells and insert into it due to its higher fluidicity and net negative charge compared to those of normal cells (Leuschner and Hansel, 2004; Mader and Hoskin, 2006; Hoskin and Ramamoorthy, 2008; Riedl et al., 2011; Gaspar et al., 2013; Harris et al., 2013; Gaspar et al., 2015). Once peptides are inside the cells, they can also perturb the integrity of the negatively charged mitochondrial membrane, resulting in the release of the cytochrome *c* and the consequent activation of the apoptosis mechanism (Papo and Shai, 2005; Bhutia and Maiti, 2008). The disruption of the plasma or mitochondrial membrane is not the only mode of action of anticancer peptides. Other mechanisms involving mediated immunity, hormonal receptors, DNA synthesis inhibition or anti-angiogenic effects have also been described (Papo and Shai, 2005; Schweizer, 2009; Gaspar et al., 2013; Wu et al., 2014; Gaspar et al., 2015).

One potential method to increase peptide activity is its conjugation to a drug delivery system able to enhance its internalization (Stewart et al., 2008; Fonseca et al., 2009). The use of cell-penetrating peptides (CPPs) is a promising strategy to promote the cellular uptake of numerous types of drugs, including small molecules, imaging agents, oligonuleotides, proteins and other peptides (Mäe and Langel, 2006; Stewart et al., 2008; Fonseca et al., 2009; Koren and Torchilin, 2012; Zhang et al., 2012). They are usually short cationic sequences that may derive from natural peptides or proteins, e.g. TAT peptide (RKKRRQRRR) or penetratin (RQIKIWFQNRRMKWKK), or be *de novo* designed peptides, as trasportant (GWTLNSAGYLLGKINLKALAALAKKIL) or polyarginines (e.g. R_9 (RRRRRRRRR))(Stewart et al., 2008; Fonseca et al., 2009; Milletti, 2012). The use of CPPs for the intracellular delivery represents an interesting strategy to enhance the bioactivity of the anticancer peptides and several examples have been reported (Mäe and Langel, 2006; Stewart et al., 2008; Fonseca et al., 2009). This strategy is particularly straightforward because the drug and carrier share a similar structure and their total synthesis can be performed completely via solid-phase peptide synthesis (Stewart et al., 2008).

An example of this strategy is the cytotoxic peptide r7-kla which was obtained by conjugating the linear antimicrobial peptide kla to the cell-penetrating domain r7 (*Figure 1.10*) (Law et al., 2006). Whereas the antimicrobial peptide is not active, the peptide conjugate r7-kla shows low IC_{50} values against different tumor cell lines, being more cytotoxic than other clinically used anticancer agents such as doxorubicin, paclitaxel or methotrexate. It has been observed that once the antimicrobial peptide is internalized it can disrupt the mitochondrial membrane inducing apoptosis. Moreover, r7-kla shows a rapid kinetic of cell killing and also induces apoptosis *in vivo* (Law et al., 2006).

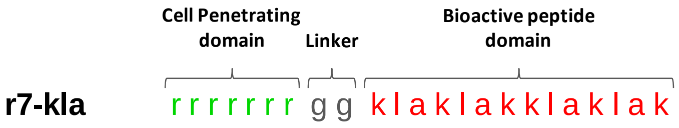

Figure 1.10. *Peptide sequence of r7-kla.*

Another example of this strategy is the conjugation of peptides C9h and C9 to the CPP DPT-sh1. C9h and C9 are involved in the modulation of the caspase-9/PP2A interaction and, consequently, in the cell death regulation process (*Table 1.3*) (Arrouss et al., 2013). Whereas DPT-sh1, C9 and C9h do not induce apoptotic effects in any cell line, the peptide conjugates DPT-C9h and DPT-C9 show apoptotic effects in several human and mouse cancer cell lines. These conjugates specifically target caspase-9/PP2A interaction, leading to mitochondrial membrane permeabilization, cytochrome *c* release and induction of the cell death mechanism. They also inhibit tumor growth both in mouse and in primary human breast cancer models. In addition, DPT-C9h and DPT-C9 do not affect healthy cells (Arrouss et al., 2013).

Table 1.3. *Sequences of DPT-sh1, C9, C9h and of the peptide conjugates DPT-C9 and DPT-C9h.*

Peptide	Sequence
DPT-sh1	VKKKKIKREIKI
C9	YIETLDGILEQWARSEDL
C9h	YVETLDDIFEQWAHSEDL
DPT-C9	VKKKKIKREIKI-YIETLDGILEQWARSEDL
DPT-C9h	VKKKKIKREIKI-YVETLDDIFEQWAHSEDL

1.3 ANTIMICROBIAL PEPTIDES FOR PLANT PROTECTION

One of the current biggest challenges in agroscience is the development of environmentally friendly alternatives to the extensive use of chemical pesticides for combating crop diseases (Montesinos, 2007; Ongena and Jacques, 2008). Phytopathogenic bacteria are responsible for great losses in economically important crops, such as vegetables and fruits, but their control mainly relays on chemical pesticides. The most common pesticides are copper derivatives and antibiotics. Although these compounds are effective, they are regarded as environmental contaminants. In addition, an inappropriate use of antibiotics induces the emergence of multidrug resistant microorganisms. Due to these limitations, antibiotics are not authorized in some countries of the European Union prompting the necessity to develop new agents to control plant diseases.

In particular, the LIPPSO group, in collaboration with the Plant Pathology group of the University of Girona, is currently studying the development of antimicrobial peptides active against the phytopathogenic bacteria *Erwinia amylovora*, *Xanthomonas vesicatoria* and *Pseudomonas syringae*, and the fungi *Fusarium oxysporum* and *Penicillium expansum*, which are responsible for plant diseases of economic importance (Ferre et al., 2006; Monroc et al., 2006a, 2006b; Badosa et al., 2007, 2009; Ng-Choi et al., 2014). The bacteria *E. amylovora* is the causal agent of fire blight in rosaceous plants, *X. vesicatoria* is responsible for the bacterial spot of tomato and pepper plants, and *P. syringae* causes several blight diseases. The fungus *F. oxysporum* is the causal agent of vascular wilt disease in a wide variety of economically important crops and *P. expansum* is the main causal agent of blue mould in stored apples.

The main objective of the LIPPSO group is to find peptides with high antimicrobial activity against these pathogens and, at the same time, with low toxicity against eukaryotic cells and high stability towards protease degradation. Two families of peptides, including linear undecapeptides and cyclic decapeptides, have been studied.

1.3.1 Cecropin A-melittin hybrid linear undecapeptides

Although natural antimicrobial peptides, such as cecropins and melittin, display an interesting activity against plant pathogens, their use in plant protection is not suitable because of the high production cost of their long sequences and their susceptibility to protease degradation. For this reason, several studies have been focused on the development of shorter and more stable synthetic analogues which retain the antimicrobial activity of the parent peptides. One example is **Pep3**, derived from the well-known hybrid cecropin A(1-7)-melittin(2-9) (Andreu et al., 1992; Giacometti et al., 2004). **Pep3** is an 11-residue sequence which shows a good biological activity profile against phytopathogenic bacteria and fungi (*Table 1.4*) (Cavallarin et al., 1998; Ali and Reddy, 2000).

Table 1.4. *Sequence of cecropin A, melittin and two synthetic analogues.*

Peptide	**Sequence**
Cecropin A	KWKLFKKIEKVGQNIRDGIIKAGPAVAVVGQATQIAK-NH_2
Melittin	GIGAVLKVLTTGLPALISWIKRKRQQ-NH_2
Cecropin A(1-7)-melittin(2-9)	KWKLFKKIGAVLKVL-NH_2
Pep3	WKLFKKILKVL-NH_2

Based on the structure of **Pep3**, the LIPPSO group designed and synthesized a library of 125 linear undecapeptides (CECMEL11) with general structure R-X^1-Lys-Leu-Phe-Lys-Lys-Ile-Leu-Lys-X^{10}-Leu-NH_2 (R= H, Ac, Ts, Bz or Bn; X^1, X^{10}= Leu, Lys, Phe, Trp, Tyr or Val) (*Figure 1.11*) (Ferre et al., 2006; Badosa et al., 2007). This library was tested against the bacteria *E. amylovora*, *X. vesicatoria* and *P. syringae*, and the fungus *P. expansum*. The hemolytic activity was also evaluated (Ferre et al., 2006; Badosa et al., 2007, 2009).

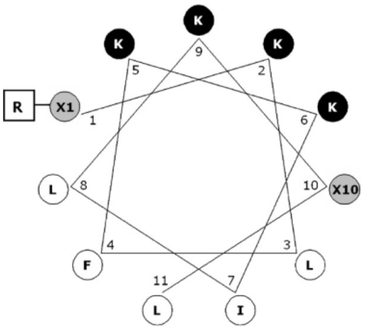

Figure 1.11. *Edmunson wheel projection of the 125-member peptide library CECMEL11. Hydrophilic amino acids (Lys) are represented in black background while hydrophobic residues (Leu, Phe, Ile) are in white.* X^1 *and* X^{10} *are represented in grey (*X^1*= Lys, Leu, Trp, Tyr or Phe;* X^{10}*= Lys, Val, Trp, Tyr or Phe). R represents the N-terminus derivatization (H, Ac, Ts, Bz or Bn) (Badosa et al., 2007).*

The results obtained demonstrated the importance of the peptide charge on the activity. In general terms, the most active peptides are those with a net charge of +5 or +6, a basic *N*-terminus and an aromatic residue at X^{10}. Several sequences show a better biological profile than the parent peptide **Pep3**. In particular, peptides **BP15**, **BP33**, **BP76**, **BP77**, **BP100**, **BP125** and **BP126** display an optimal balance between antimicrobial and hemolytic activities (*Table 1.5*) (Ferre et al., 2006; Badosa et al., 2007). Moreover, **BP21** exhibits a high activity against *P. expansum* (Badosa et al., 2009). These peptides show a good stability towards protease degradation. Moreover, **BP100** exhibits preventive inhibition of *E. amylovora* infection in detached apple and pear flowers, being only less effective than streptomycin, antibiotic currently used for fire blight control (Badosa et al., 2007).

Table 1.5. *Antibacterial and hemolytic activity of several peptides selected from the CECMEL11 library.*

Peptide	Sequence	MIC (μM)[a]				H (%)[c]
		Ea[b]	Ps[b]	Xv[b]	Pe[b]	
BP15	H-Lys-Lys-Leu-Phe-Lys-Lys-Ile-Leu-Lys-Val-Leu-NH_2	5.0-7.5	2.5-5.0	>7.5	12.5-25.0	16±2.9
BP33	H-Leu-Lys-Leu-Phe-Lys-Lys-Ile-Leu-Lys-Val-Leu-NH_2	5.0-7.5	5.0-7.5	>7.5	>25.0	37±2.7
BP21	Ac-Phe-Lys-Leu-Phe-Lys-Lys-Ile-Leu-Lys-Val-Leu-NH_2	>7.5	>7.5	2.5-5.0	<6.2	85±1.4
BP76	H-Lys-Lys-Leu-Phe-Lys-Lys-Ile-Leu-Lys-Phe-Leu-NH_2	2.5-5.0	2.5-5.0	2.5-5.0	>25.0	34±2.1
BP77	Ac-Lys-Lys-Leu-Phe-Lys-Lys-Ile-Leu-Lys-Phe-Leu-NH_2	5.0-7.5	5.0-7.5	<2.5	6.2-12.5	40±3.8
BP100	H-Lys-Lys-Leu-Phe-Lys-Lys-Ile-Leu-Lys-Tyr-Leu-NH_2	2.5-5.0	2.5-5.0	5.0-7.5	>25.0	22±2.8
BP125	Ts-Lys-Lys-Leu-Phe-Lys-Lys-Ile-Leu-Lys-Lys-Leu-NH_2	>7.5	2.5-5.0	2.5-5.0	>25.0	8±1.6
BP126	Bz-Lys-Lys-Leu-Phe-Lys-Lys-Ile-Leu-Lys-Lys-Leu-NH_2	5.0-7.5	2.5-5.0	2.5-5.0	>25.0	14±2.9

[a] Minimum inhibitory concentration. [b] Ea stands for *E. amylovora;* Ps for *P. syringae*; Xv for X. *Vesicatoria*; Pe for *P. expansum*. [c] Percent hemolysis at 150 μM plus confidence interval (α = 0.05).

1.3.2 *De novo* designed cyclic decapeptides

Although linear peptides are the most explored antimicrobial peptides, their practical use has not been completely satisfactory. The conformational flexibility of their primary structure seems to be associated with a low target selectivity, poor bioavailability as well as low stability towards protease degradation. Backbone cyclization is an interesting method to introduce conformational constraints on peptide secondary structures which generally improves the metabolic stability and can also increase the activity as well as the selectivity towards specific targets (Gilon et al., 1991; Fung and Hruby, 2005; Monroc et al., 2006a; Werle and Bernkop-Schnürch, 2006; Ong et al., 2014).

The LIPPSO group focused its attention on the *de novo* design and synthesis of cyclic antimicrobial peptides. During the last years, *head-to-tail* amphipathic cyclic peptides ranging from 4 to 10 residues have been *de novo* designed and prepared (Monroc et al., 2006a, 2006b). These peptides consist of alternating hydrophilic (Lys) and hydrophobic (Leu and Phe) amino acids with the general formula c(X_n-Y-X_m-Gln) (X= Lys or Leu, Y= L- or D-Phe, m=n=1 or m=3 and n=0-5). The antimicrobial activity of these peptides was evaluated against the economically important plant pathogenic bacteria *X. vesicatoria*, *P. syringae* and *E. amylovora.* Their hemolytic activity as well as their proteolytic susceptibility were also evaluated. Among them, the most active sequence was the cyclic decapeptide **BPC16**, which exhibits minimum inhibitory concentration (MIC) values raging from 6.2 to 12.5 µM against *X. vesicatoria* and 12.5 to 25 µM against *P. syringae*. However, **BPC16** is not active against *E. amylovora* and shows a significant hemolytic activity (Monroc et al., 2006a).

In order to improve the biological profile of the lead peptide **BPC16**, a first library of 56 cyclic decapeptides based on its structure was synthesized (Library I). Analysis of the antimicrobial activity against the aforementioned bacteria suggested that the substructure Lys^{5}PheLysLysLeuGln^{10} constitutes a structural requirement for the activity. In fact, peptides of Library I containing this moiety exhibit low MIC values against the three plant pathogenic bacteria. Therefore, a second library based on the structure c(X^{1}X^{2}X^{3}X^{4}LysPheLysLysLeuGln) was prepared using a design of experiments (DOE) methodology (Library II). It comprised 16 cyclic decapeptides with all possible combinations of Leu and Lys at positions X^1 to X^4. Evaluation of the antibacterial activity and hemolysis led to the identification of sequences with a better biological profile than the parent peptide **BPC16** (*Table 1.6*). In particular, **BPC96**, **BPC98**, **BPC194** and **BPC198** display a high antimicrobial activity against the three pathogenic bacteria (MIC values from 1.6 to 25 µM) while maintaining a low hemolysis. Moreover, DOE analysis showed that all of them fulfill the substitution rule $X^2 \neq X^3$ and include Lys at position 4 (Monroc et al., 2006b).

Table 1.6. *Antibacterial and hemolytic activity of selected cyclic decapeptides.*

Peptide	**Sequence**	**MIC (µM)[a]**			**H (%)[c]**
		Ea[b]	**Ps[b]**	**Xv[b]**	
BPC16	c(Lys-Leu-Lys-Leu-Lys-Phe-Lys-Leu-Lys-Gln)	>100	12.5-25	6.2-12.5	84±6.9
BPC96	c(Leu-Lys-Leu-Lys-Lys-Phe-Lys-Lys-Leu-Gln)	12.5-25	6.2-12.5	3.1-6.2	32±7.2
BPC98	c(Leu-Leu-Lys-Lys-Lys-Phe-Lys-Lys-Leu-Gln)	12.5-25	6.2-12.5	1.6-3.1	36±3.7
BP194	c(Lys-Lys-Leu-Lys-Lys-Phe-Lys-Lys-Leu-Gln)	6.2-12.5	3.1-6.2	3.1-6.2	17±1.7
BP198	c(Lys-Leu-Lys-Lys-Lys-Phe-Lys-Lys-Leu-Gln)	12.5-25	3.1-6.2	3.1-6.2	14±1.4

[a] Minimum inhibitory concentration. [b] Ea stands for *E. amylovora;* Ps for *P. syringae*; Xv for X. *vesicatoria*.
[c] Percent hemolysis at 375 µM plus confidence interval (α = 0.05).

1.4 BIOACTIVE LIPOPEPTIDES FROM *BACILLUS SUBTILIS* FOR PLANT PROTECTION

The use of microorganisms as biocontrol agents is considered as a rational and safe crop-management method against plant pathogens (Emmert and Handelsman, 1999; Touré et al., 2004; Ongena and Jacques, 2008). Members of *Bacillus* genus, and particularly *Bacillus subtilis* species, are among the most exploited and studied beneficial bacteria as biopesticides to control plant diseases (Emmert and Handelsman, 1999; Touré et al., 2004; Stein, 2005; Montesinos, 2007; Ongena et al., 2007; Ongena and Jacques, 2008; Mora et al., 2015). *Bacillus* species are mostly isolated from the plant rhizosphere, although they can also be found in deep-sea sediments, fermented food or animal gastrointestinal tracts (Raaijmakers et al., 2010). These species are of particular interest since they are able to survive adverse conditions due to the development of spores, and to produce compounds that are beneficial for agronomical purposes (Emmert and Handelsman, 1999; Montesinos, 2007; Ongena and Jacques, 2008; Pueyo et al., 2009). These compounds mainly include ribosomal and non-ribosomal peptides, as well as non-peptidic compounds, such as polyketides, aminosugars or phospholipids (Stein, 2005).

Non-ribosomal peptides comprise cyclic lipopeptides of the surfactin, iturin and fengycin families (Jacques et al., 1999; Stein, 2005; Ongena and Jacques, 2008; Raaijmakers et al., 2010; Mora et al., 2015). They are amphiphilic structures composed of a hydrophilic peptide portion and a hydrophobic fatty acid part, which can be either a β-hydroxy or a β-amino fatty acid. They differ in the length and branching of the fatty acid chain as well as in the amino acid sequence (Akpa et al., 2001; Ongena and Jacques, 2008; Raaijmakers et al., 2010; Inès and Dhouha, 2015). These cyclic lipopeptides have well-recognized application in biotechnology and biopharmaceutical fields, because of their surfactant and bio-active properties. Moreover, it has also been demonstrated that these cyclic lipopeptides are also able to stimulate plant defence responses against pathogens, a phenomenon termed induced systemic resistance (Ongena et al., 2007; Ongena and Jacques, 2008; Raaijmakers et al., 2010). For example, it has been reported that surfactins and fengycins can stimulate the defence responses of bean and tomato plants (Ongena et al., 2005, 2007).

1.4.1 Surfactins

Surfactins are cyclic lipodepsipeptides composed of seven *α*-amino acids and a *β*-hydroxy fatty acid. Apart from surfactins, this family encompasses esperin, lichenysin and pumilacidin derivates, which are represented in *Figure 1.12* (Peypoux et al., 1999; Seydlová and Svobodová, 2008; Raaijmakers et al., 2010). They are powerful biosurfactants with exceptional emulsifying and foaming properties (Peypoux et al., 1999; Stein, 2005; Ongena and Jacques, 2008). Surfactins display a detergent-like action on biological membranes and are distinguished by their hemolytic, antiviral, antimycoplasma and antibacterial activities (Peypoux et al., 1999; Stein, 2005; Ongena and Jacques, 2008; Seydlová and Svobodová, 2008; Raaijmakers et al., 2010). Unlike other *Bacillus* lipopeptides, surfactins do not show a remarkable fungitoxicity. On the other hand, surfactins are a key factor in the formation of stable biofilms by *B. subtilis* strains. Moreover, these cyclic lipopeptides may inhibit the formation of biofilms by other bacteria, contributing to the protective action of *Bacillus* strains (Bais et al., 2004).

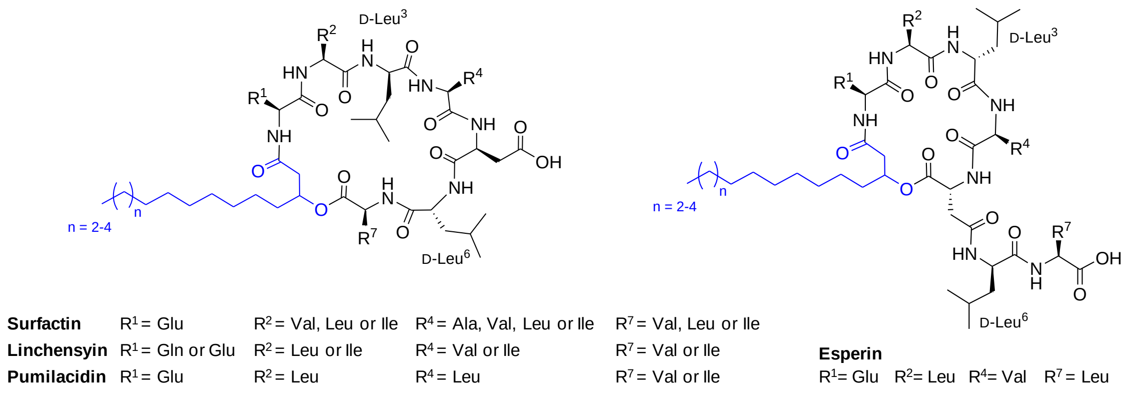
D-Leu3
R2
R1
R4
R7
D-Leu6
n = 2-4
n
OH
Surfactin R1 = Glu R2 = Val, Leu or Ile R4 = Ala, Val, Leu or Ile R7 = Val, Leu or Ile
Linchensyin R1 = Gln or Glu R2 = Leu or Ile R4 = Val or Ile R7 = Val or Ile
Pumilacidin R1 = Glu R2 = Leu R4 = Leu R7 = Val or Ile
Esperin
R1= Glu R2= Leu R4= Val R7 = Leu

Figure 1.12. *Structure of surfactins. The β-hydroxy fatty acid can contain iso or anteiso branches.*

1.4.2 Iturins

Iturin A and C, bacillomycin D, F, L and LC, and mycosubtilin are the main peptide variants that encompass the iturin family (Besson et al., 1978; Besson and Michel, 1987; Ongena and Jacques, 2008; Raaijmakers et al., 2010). They are composed of a heptapeptide cyclised by a *β*-amino acid (iturinic acid), which has a variety of chain lengths (C_{14}-C_{17}) (*Figure 1.13*). Unlike surfactins, iturins are mainly antifungal, showing a strong *in vitro* activity against a wide variety of yeast and fungi (Ongena and Jacques, 2008; Raaijmakers et al., 2010). However, they display a high hemolytic activity against human erythrocytes (Aranda et al., 2005).

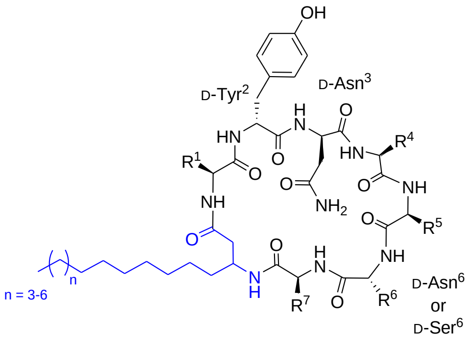

Iturin A	R^1 = Asn	R^4 = Gln	R^5 = Pro	R^6 = D-Asn	R^7 = Ser
Iturin C	R^1 = Asp	R^4 = Gln	R^5 = Pro	R^6 = D-Asn	R^7 = Ser
Bacillomycin D	R^1 = Asn	R^4 = Pro	R^5 = Glu	R^6 = D-Ser	R^7 = Thr
Bacillomycin F	R^1 = Asn	R^4 = Gln	R^5 = Pro	R^6 = D-Asn	R^7 = Thr
Bacillomycin L	R^1 = Asp	R^4 = Ser	R^5 = Gln	R^6 = D-Ser	R^7 = Thr
Bacillomycin LC	R^1 = Asn	R^4 = Ser	R^5 = Glu	R^6 = D-Ser	R^7 = Thr
Mycosubtilin	R^1 = Asn	R^4 = Gln	R^5 = Pro	R^6 = D-Ser	R^7 = Asn

Figure 1.13. *Structure of iturins. The β-hydroxy fatty acid can contain iso or anteiso branches.*

1.4.3 Fengycins

The fengycin family, isolated from several *Bacillus* strains, comprises closely related lipopeptides which share a common cyclic structure with several exceptional features (Vanittanakom et al., 1986; Wang et al., 2004; Stein, 2005; Chen et al., 2008; Deleu et al., 2008; Ongena and Jacques, 2008; Bie et al., 2009; Pueyo et al., 2009; Pecci et al., 2010; Raaijmakers et al., 2010; Sang-Cheol et al., 2010; Pathak et al., 2012; Villegas-Escobar et al., 2013). They consist on a *β*-hydroxy fatty acid chain connected to the *N*-terminus of a decapeptide moiety. Eight of these amino acids form a macrocycle containing an ester bond between the phenol group of Tyr^3 and the *α*-carboxylic group of Ile^{10} (*Figure 1.14*). According to their sequence, fengycins can be divided into two major groups, fengycin A and B. Fengycin A has a D-Ala at position 6, whereas fengycin B has a D-Val at this position. The length of the *β*-hydroxy fatty acid ranges from 14 to 18 carbons and it can be saturated or unsaturated, and it can contain iso or anteiso branches (Vanittanakom et al., 1986; Wang et al., 2004; Chen et al., 2008;

Ongena and Jacques, 2008; Bie et al., 2009; Pueyo et al., 2009; Pecci et al., 2010; Faria et al., 2011; Pathak et al., 2012).

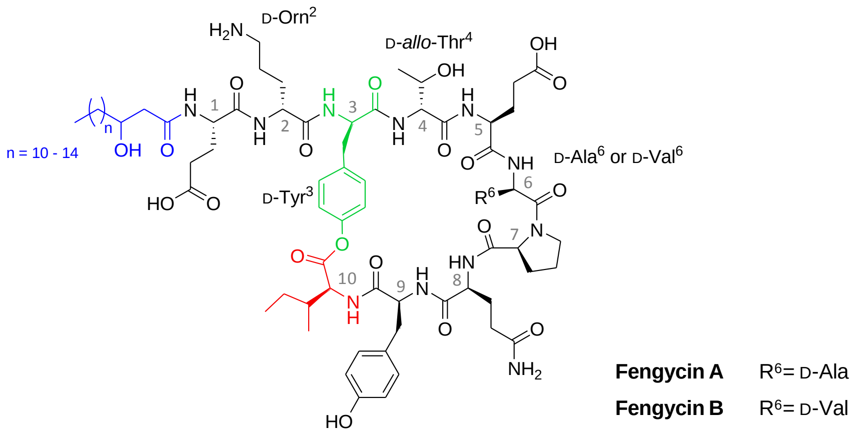

D-Orn2
H2N
D-allo-Thr4
OH
n = 10 - 14
D-Ala6 or D-Val6
D-Tyr3
R6
HO
NH2
Fengycin A R6= D-Ala
Fengycin B R6= D-Val

Figure 1.14. *Structure of fengycin A and B.*

Although fengycin A and B are the most common isoforms, other fengycin isoforms have also been isolated. For example, Sang-Cheol and collaborators isolated fengycin S from a *Bacillus amyloliquefaciens* culture. The analysis of this compound demonstrated that it differed from fengycin B on the amino acid at position 4, containing a Ser instead of an *allo*-Thr (*Figure 1.15*) (Sang-Cheol et al., 2010).

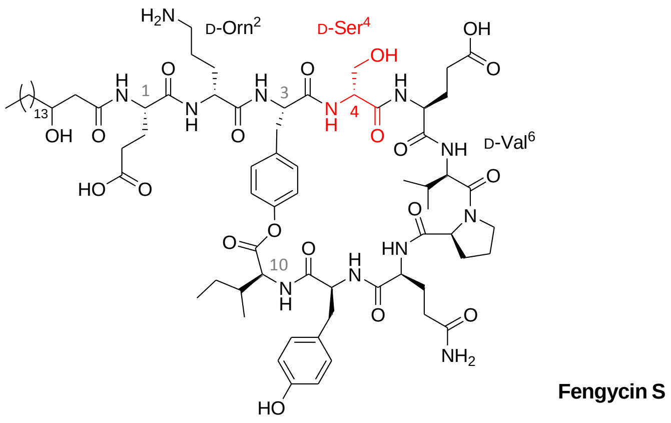

H2N
D-Orn2
D-Ser4
OH
D-Val6
HO
NH2
Fengycin S

Figure 1.15. *Structure of fengycin S according to Sang-Cheol et al., 2010.*

Another recent example of a fengycin isoform is fengycin C described by Villegas-Escobar and co-workers (Villegas-Escobar et al., 2013). It was isolated from the supernatant culture of *Bacillus subtilis* EA-CB0015, along with some surfactin analogues. This lipopeptide contains an *allo*-Thr at position 9 instead of the Tyr usually present in the structure of fengycins (*Figure 1.16A*) (Villegas-Escobar et al., 2013). Nevertheless, it has to be pointed out that one year before Pathak and collaborators had described a new compound, also called fengycin C, isolated from a culture of *Bacillus subtilis* K1 (Pathak et al., 2012). Unlike the fengycin C described by Villegas-Escobar et al., this compound contains a Leu or an Ile at position 6 instead of the Ala or Val present in fengycin A and B, respectively (*Figure 1.16B*). In this study, other isoforms of fengycin A and B were also isolated. They differ on the length and the saturation of the *β*-hydroxy fatty acid tail as well as on the amino acid composition. They incorporate a Val at position 10 and a Glu at position 8 instead of an Ile and a Gln, respectively (Pathak et al., 2012).

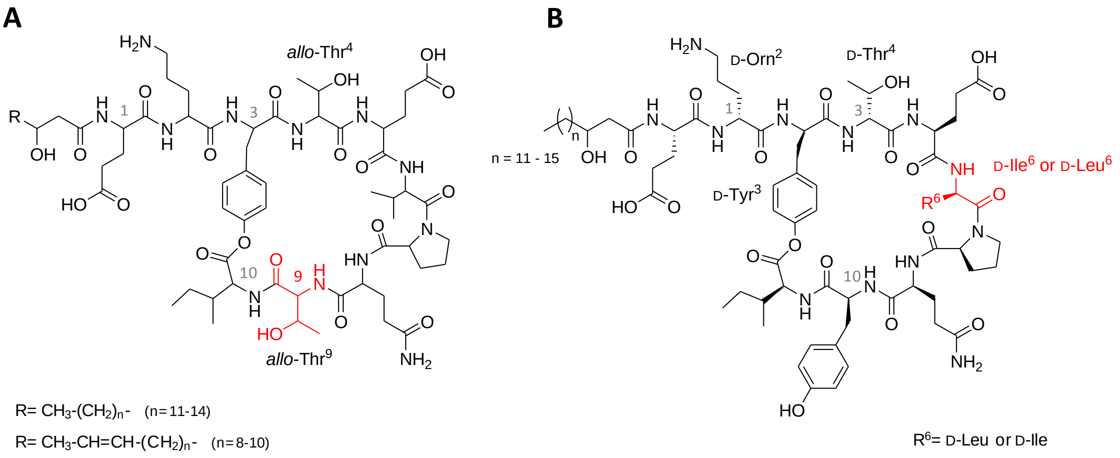

Figure 1.16. *Two different structures of fengycin C described by Villegas-Escobar et al. (**A**) and Pathak et al. (**B**). The amino acid configuration was not described for compound **A**.*

Plipastatins are other well-known analogues of the fengycin family. However, there has been certain confusion between the terms fengycin and plipastatin in the literature. Although sometimes they are considered as synonyms (Stein, 2005), most of the reports refer to plipastatins as diastereoisomers of fengycins differing in the L- and D- configurations of the Tyr at positions 3 and 9 (Ongena and Jacques, 2008;

Raaijmakers et al., 2010). Specifically, fengycins contain a D-Tyr^3 and an L-Tyr^9 while plipastatins have the reversed configuration, an L-Tyr^3 and a D-Tyr^9 (*Figure 1.17*) (Nishikiori et al., 1986a, 1986b; Schneider et al., 1999; Volpon et al., 2000). However, recent studies show that fengycins and plipastatins could have the same primary structure, being L-Tyr^3 and D-Tyr^9 the unique amino acid configuration (Honma et al., 2012; Nasir et al., 2013). According to these studies, plipastatins could be the potassium salt of the peptide whereas fengycins could be the trifluoroacetate salt (Honma et al., 2012).

Fengycin A	Fatty acid-L-Glu^1-D-Orn^2- **D-Tyr^3(&)** -D-*allo*Thr^4-L-Glu^5-D-Ala^6-L-Pro^7-L-Gln^8- **L-Tyr^9** -L-Ile^{10}(&)
Plipaspatin A	Fatty acid-L-Glu^1-D-Orn^2- **L-Tyr^3(&)** -D-*allo*Thr^4-L-Glu^5-D-Ala^6-L-Pro^7-L-Gln^8- **D-Tyr^9** -L-Ile^{10}(&)

Figure 1.17. *Structural differences between fengycins and plipastatins. The "&" symbol indicates the ester bond between the phenol group of Tyr^3 and the α-carboxylic group of Ile^{10}.*

Fengycin lipopeptides are known to be specifically active against filamentous fungi (Vanittanakom et al., 1986; Deleu et al., 2008; Ongena and Jacques, 2008; Raaijmakers et al., 2010). They are active against *Fusarium verticillioides*, also known as *F. moniliforme*, a toxigenic fungal strain in maize (Hu et al., 2007, 2009), against the blight disease caused by the fungus *Fusarium graminearum* (Wang et al., 2007; Chan et al., 2009), against fungal strains responsible for the grey mould disease of apples, such as *Botrytis cinerea* (Touré et al., 2004; Ongena et al., 2005), or against the powdery mildew of melon caused by *Podosphaera fusca* (Romero et al., 2007). In contrast to the other lipopeptides produced by *Bacillus* species, they are low hemolytic (a 40-fold less that surfactins) (Vanittanakom et al., 1986; Deleu et al., 2008)

1.5 SYNTHESIS OF PEPTIDES

The amount of peptide that can be generally extracted from natural sources, such as plants, animals or microorganisms, is usually very low and complex purification and characterization methodologies are required. For this reason, several alternative methods for the obtention of these compounds have been developed. In particular, peptide synthesis is a widely spread methodology that can be carried out both in solution and on solid-phase (Costa et al., 2015). Nevertheless, in recent years, solid-phase peptide synthesis (SPPS) has become one of the most used methodologies for the preparation of peptides (Kates and Albericio, 2000; Pires et al., 2014).

1.5.1 Solid-phase peptide synthesis

Solid-phase peptide synthesis (SPPS) was introduced in 1963 by Robert Bruce Merrifield (Merrifield, 1963, 1986). It allows the preparation of different sequences through fast and feasible reactions. This method offers important advantages over the synthesis in solution, such as fewer by-products, easier and less time-consuming work-up procedures, and the possibility to be automated (Coin et al., 2007; Pires et al., 2014). For the discovery of this efficient methodology, R.B. Merrifield was awarded the Nobel Prize in 1984.

SPPS is based on the sequential incorporation of conveniently protected amino acids onto a solid support. As shown in *Scheme 1.1*, the main steps involved in SPPS are: (i) the attachment to the solid support of the first amino acid, conveniently protected, through its α-carboxylic acid group; the solid matrix usually incorporates a linker or spacer to facilitate both the anchoring of the amino acid and the cleavage of the final peptide; (ii) the selective removal of the N^{α}-amino protecting group of the amino acid previously incorporated; (iii) the coupling of the next amino acid through its α-carboxyl group; (iv) sequential cycles of removal and coupling steps until completion of the desired peptide sequence and (v) cleavage and simultaneous removal of the side-chain protecting groups to obtain the deprotected peptide (Kates and Albericio, 2000).

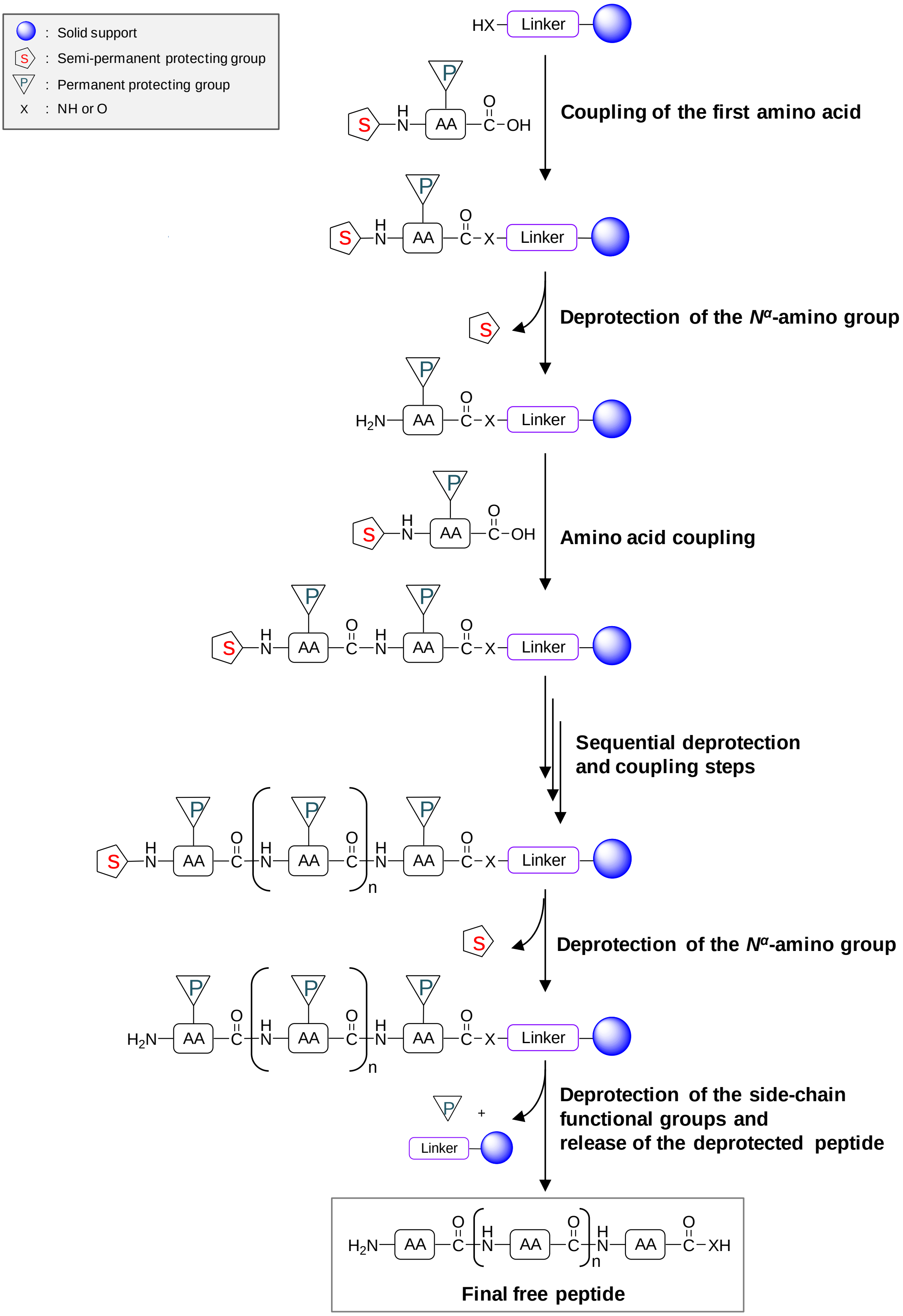
Solid support
Semi-permanent protecting group
Permanent protecting group
X : NH or O
HX
Linker
S
P
H
N
AA
O
C
OH
X
H2N
n
XH
Coupling of the first amino acid
Deprotection of the Nα-amino group
Amino acid coupling
Sequential deprotection and coupling steps
Deprotection of the Nα-amino group
Deprotection of the side-chain functional groups and release of the deprotected peptide
+
Final free peptide

Scheme 1.1. *General strategy for SPPS.*

Due to its high efficiency and its feasibility to prepare a large variety of products, the use of solid-phase synthesis on combinatorial chemistry has been rising in recent years and, nowadays, its use is not only limited to peptide synthesis, but also to the preparation of nucleotides, oligosaccharides, oligonucleotides and a wide range of other organic and pharmaceutical compounds (Kates and Albericio, 2000).

1.5.1.1 Solid support

The term solid support refers to the insoluble matrix onto which the reactions are carried out when following solid-phase methodologies. An efficient solid support must contain functional groups that enable the attachment of the first compound, allowing the beginning of the synthesis. Moreover, there are other features that a solid support must fulfill to be considered suitable for SPPS. In particular, it must (i) be made of uniform particles with an appropriate size and shape to perform the reactions; (ii) allow the rapid filtration of the solvents; (iii) be stable to changes of the temperature; (iv) be inert and insoluble to all the reagents and chemical conditions used; (v) swell extensively in a broad range of solvents allowing the access of the reagents to all the reactive sites; and (vi) also have a good mechanical and physical stability (Martin and Albericio, 2008).

Nowadays, there are available a wide range of solid supports suitable for SPPS. However, the most typical ones are resin beads made of cross-linked polystyrene with 1% divinylbenzene, polyacrylamide, or polyethyleneglycol grafted onto cross-linked polystyrene. Some of them are represented in *Table 1.7* (Coin et al., 2007; Martin and Albericio, 2008).

Table 1.7. *Examples of solid supports used in SPPS.*

Structure	Name
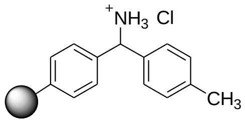	4-Methylbenzhydrylamine (MBHA) resin (Kates and Albericio, 2000)
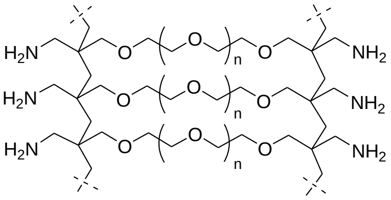	Aminomethyl ChemMatrix resin (García-Ramos et al., 2010)
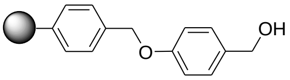	4-Benzyloxybenzyl alcohol resin (Wang resin) (Wang, 1973, Kates and Albericio, 2000)

1.5.1.2 Linker

A linker is a bifunctional spacer which, on the one hand, allows the binding of the peptide sequence to the solid support and, on the other hand, facilitates its cleavage. Therefore, a suitable linker must be irreversibly anchored to the solid support whereas its linkage with the peptide sequence must be stable along the synthesis, but labile to the cleavage conditions (Kates and Albericio, 2000).

Nowadays, a wide range of commercial linkers are available. They are commonly categorized according to their cleavage conditions and their *C*-terminus functionality. Some representative examples are shown in *Table 1.8*.

Table 1.8. *Examples of commonly used linkers.*

Structure	Linker	Cleavage conditions	*C*-terminus functionality
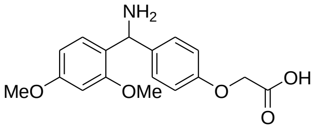	4-(2',4'-Dimethoxyphenylaminomethyl) phenoxyacetic acid (Rink amide)	95% Trifluoroacetic acid (TFA)	Amide
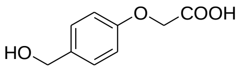	4-Hydroxymethylphenoxyacetic acid (HMPA)	95% TFA	Carboxylic acid

1.5.1.3 Protecting groups

The use of protecting groups is essential to avoid non-desired reactions along the peptide synthesis. The protecting groups used in SPPS are divided into two categories, permanent and semi-permanent. The former are employed to protect the side-chain groups of trifunctional amino acids while the latter are used to protect the N^{α}-amino group. Ideally, these two categories of groups should be orthogonal, hence they can be removed in any order and in the presence of the other category (Isidro-Llobet et al., 2009).

One of the most used SPPS protecting group strategies is the 9-fluorenylmethyloxycarbonyl (Fmoc)/ *tert*-butyl (^{t}Bu) (Coin et al., 2007; Pires et al., 2014). In this strategy, the base-labile Fmoc group is employed as semi-permanent group to protect the N^{α}-amino group of amino acids. On the other hand, the ^{t}Bu or their derivatives, such as the *tert*-butyloxycarbonyl (Boc), which are acid-labile, are used as permanent protecting groups of the amino acid side-chains. Apart from this, other feasible orthogonal strategies have been described based on protecting groups that are removed under more specific conditions, such as metal-catalyzed reactions, reductions, hydrogenolysis or even photolysis (Isidro-Llobet et al., 2009). In fact, the synthesis of complex peptide sequences generally requires the combination of more than two orthogonal protecting groups. For example, cyclic peptides are commonly synthesized following the three-dimensional orthogonal strategy Fmoc/^{t}Bu/allyl. The most representative protecting groups used along this thesis are described in *Table 1.9*.

***Table 1.9.** Protecting groups used in this thesis.*

Structure	Name	General removal conditions
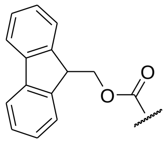	9-Fluorenylmethyloxycarbonyl (Fmoc)	20% Piperidine- *N,N'*-dimethylformamide (DMF)
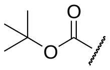	*tert*-Butyloxycarbonyl (Boc)	25-50% TFA-CH_2Cl_2 Scavenger: Triisopropylsilane (TIS)
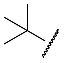	*tert*-Butyl (^{t}Bu)	90% TFA-CH_2Cl_2 Scavenger: TIS
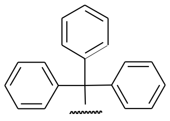	Trityl (Tr)	1% TFA-CH_2Cl_2 Scavenger: TIS
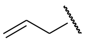	Allyl (All)	$Pd(Ph_3)_4$ (0.1 eq) Scavengers: H_2O/TIS
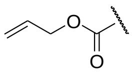	Allyloxycarbonyl (Alloc)	$Pd(Ph_3)_4$ cat. Scavenger: $PhSiH_3$ in CH_2Cl_2
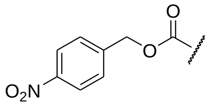	*p*-Nitrobenzyloxycarbonyl (*p*NZ)	6 M $SnCl_2$, 1.6 mM HCl/dioxane in DMF

1.5.1.4 Coupling reagents

The formation of the peptide bond between the *α*-carboxylic group of one amino acid and the N^{α}-amino group of another amino acid is performed in presence of coupling reagents, which allow the *in situ* activation of the *α*-carboxylic group under mild conditions.

The most common coupling reagent families used in SPPS are carbodiimides, and aminium and phosphonium salts (*Figure 1.18*). The carbodiimide approach for the formation of the peptide bond has been used in combination with benzotriazoles, such as 1-hydroxybenzotriazole (HOBt), as additives to avoid racemisation (Kates and Albericio, 2000; Subirós-Funosas et al., 2009; Pires et al., 2014). Common carbodiimides are *N,N'*-diisopropylcarbodiimide (DIPCDI) and *N,N'*-dicyclohexylcarbodiimide (DCC).

Other coupling strategies involve the use of the aminium salts *N*-[(dimethylamino)-1*H*-1,2,3-triazolo-[4,5-*b*]pyridin-1-yl-methylene]-*N*-methylmethanaminium hexafluorophosphate *N*-oxide (HATU) or *N*-[(1*H*-benzotriazol-1-yl)-(dimethylamino)methylene]-*N*-methylmethanaminium hexafluorophosphate *N*-oxide (HBTU), and of the phosphonium salts benzotriazol-1-yl-*N*-oxy-tris(pyrrolidino)phosphonium hexafluorophosphate (PyBOP) or bromo-tris(pyrrolidino)phosphonium hexafluorophosphate (PyBrOP). The use of these reagents is also enhanced by the presence of benzotriazoles as additives.

Despite their efficiency, these strategies have some drawbacks. It has been observed that benzotriazole derivatives can be explosive and can induce chemical sensitive dermatitis and asthma (Wehrstedt et al., 2005). To overcome these problems, recently, a family of coupling reagents and additives based on ethyl 2-cyano-2-(hydroxyimino)acetate has been described as a safer alternative. These coupling reagents include 1-[(1-cyano-2-ethoxy-2-oxoethylideneaminooxy)-dimethylamino-morpholinomethylene)]methanaminium hexafluorophosphate (COMU) or [ethyl cyano(hydroxyimino)acetato-O^2]tri-(1-pyrrolidinyl)-phosphonium hexafluorophosphate (PyOxim), which are used in presence of ethyl 2-cyano-2-(hydroxyimino)acetate (Oxyma) as additive (*Figure 1.18*) (El-Faham et al., 2009; Subirós-Funosas et al., 2009; El-Faham and Albericio, 2010).

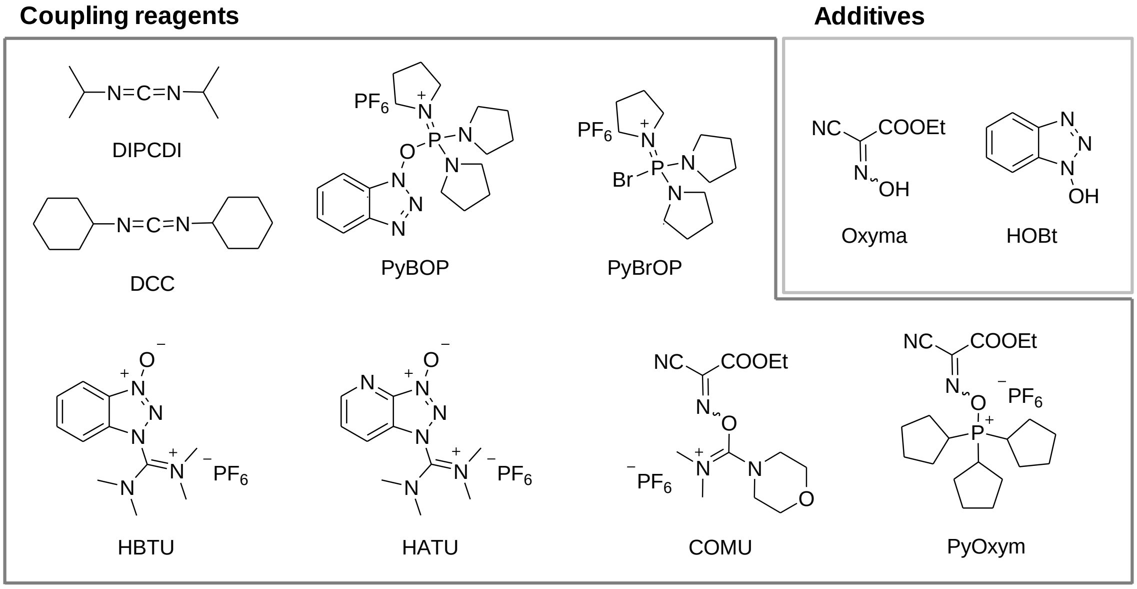

Figure 1.18. *Structure of some representative coupling reagents and additives.*

1.5.2 Solid phase synthesis of cyclic depsipeptides

Although peptides mostly contain amide bonds, some natural cyclic peptides can incorporate other types of linkages in their structure. In particular, cyclic depsipeptides are characterized by the occurrence of at least one ester bond, which is in the backbone, or is formed between the hydroxyl group of an amino acid side-chain, usually a Ser or Thr residue, and the α-carboxyl group of another residue (Davies, 2003; Filip and Cavelier, 2004). The formation of the ester bond is always a synthetic challenge (Davies, 2003; Coin, 2010; Pelay-Gimeno et al., 2013). A well-known side reaction that may take place due to the presence of the ester bond, especially if basic conditions are used, is the intramolecular *O*→ *N* acyl shift of *β*-aminoalcohols, such as Ser or Thr residues (*Scheme 1.2*) (Mouls et al., 2004; Stawikowski and Cudic, 2006; Seo and Lim, 2009; Coin, 2010). However, several examples of solid-phase synthesis of cyclic depsipeptides are found in the literature.

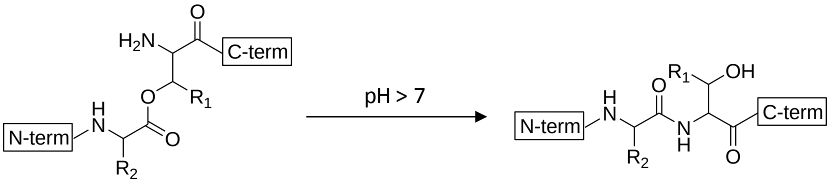

Scheme 1.2. *Intramolecular O→ N acyl shift in depsipeptides.*

Traditionally, the preparation of cyclic peptides or depsipeptides involves the solid-phase synthesis of the protected linear precursor followed by its cyclization in solution under high dilution conditions (Stawikowski and Cudic, 2006). In the case of cyclic depsipeptides, the ester bond is usually formed in the linear precursor prior to the peptide cyclization through an amide bond (Davies, 2003). One example of this strategy is the synthesis of the antitumoral peptide Kahalalide F and its analogues (López-Macià et al., 2001; López et al., 2005; Gracia et al., 2006). Kahalalide F is a cyclic lipodepsipeptide isolated from *Elysia rufescens,* a Hawaiian herbivorous marine species of mollusk, and from the green alga *Bryopsis* sp. (López-Macià et al., 2001; Gracia et al., 2006). The synthesis of Kahalalide F involved the elongation of the peptide chain on the solid support, including the ester bond formation, followed by the cleavage, the cyclization in solution and the final deprotection of the product (*Scheme 1.3*). The synthesis of Kahalalide F was performed on a 2-chlorotrityl chloride (TrCl) resin using the Fmoc/^{t}Bu strategy (López-Macià et al., 2001; López et al., 2005) and started with the preparation of the tetrapeptidyl resin **1**, containing a D-*allo*-Thr with the side chain deprotected. Next, an ester bond between the hydroxyl group of the D-*allo*-Thr and the *α*-carboxyl group of Alloc-Val-OH was formed using DIPCDI (7 equiv) in presence of 4-(*N,N'*-dimethylamino)pyridine (DMAP) (0.7 equiv) (López-Macià et al., 2001). Then, the peptide sequence was elongated and the *N*-terminal amino acid was acylated with 5-methylhexanoic acid affording the peptidyl resin **3**. The Alloc group of **3** was removed and the dipeptide Alloc-Phe-Z-Dhb-OH (Z-Dhb: (Z)-didehydro-*α*-aminobutyric acid) was coupled leading to **4** (López-Macià et al., 2001; López et al., 2005). After Alloc group removal, the protected peptide was cleaved from the resin. The resulting sequence **5** was cyclized in solution through the formation of an amide bond using PyBOP and *N,N'*-diisopropylethylamine (DIEA) for 1h. Finally, the side-chain protecting groups were removed yielding Kahalalide F (López-Macià et al., 2001).

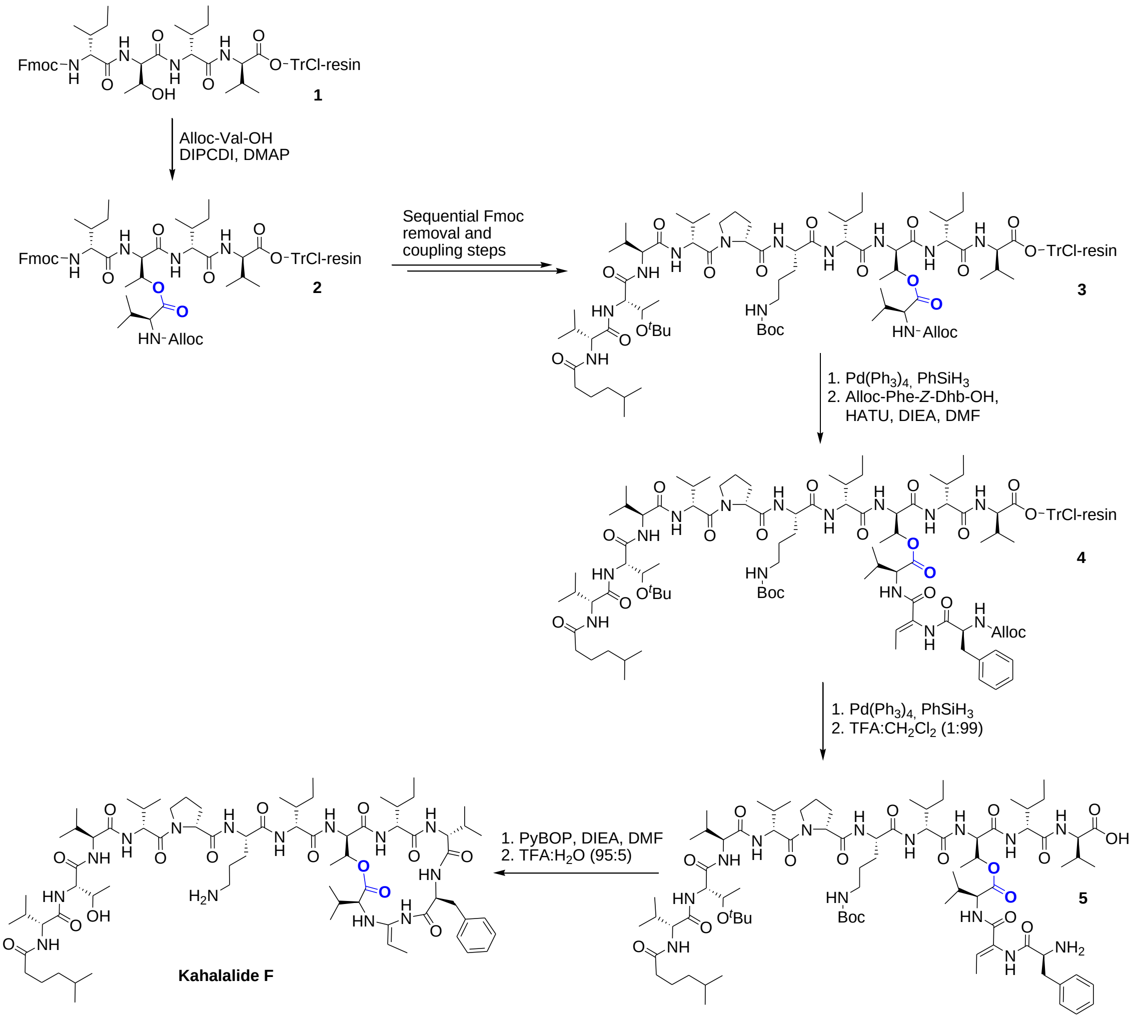
Fmoc
O-TrCl-resin
1
Alloc-Val-OH
DIPCDI, DMAP
2
HN-Alloc
Sequential Fmoc removal and coupling steps
3
O^{t}Bu
Boc
1. Pd(Ph$_3$)$_4$, PhSiH$_3$
2. Alloc-Phe-*Z*-Dhb-OH, HATU, DIEA, DMF
4
Alloc
1. Pd(Ph$_3$)$_4$, PhSiH$_3$
2. TFA:CH$_2$Cl$_2$ (1:99)
5
OH
NH$_2$
1. PyBOP, DIEA, DMF
2. TFA:H$_2$O (95:5)
H$_2$N
Kahalalide F

Scheme 1.3. *Synthetic strategy for the synthesis of Kahalalide F (López-Macià et al., 2001; López et al., 2005).*

Following a similar strategy, in 2012, Hall and co-workers prepared the cyclic depsipeptide lysobactin and an analogue (*Scheme 1.4*) (Hall et al., 2012). Lysobactin is an 11-amino acid cyclic lipopeptide which shows antibacterial activity against a wide range of Gram-positive bacteria. Using a 2-chlorotrityl resin and following conventional Fmoc chemistry, the linear peptidyl resin **6** was prepared using 3-(diethoxyphosphoryloxy)-1,2,3-benzotriazin-4(3*H*)-one (DEPBT) and DIEA as coupling reagents. Next, the hydroxyl group of the *threo*-phenylserine residue in **6** was esterified with Alloc-Ser(^{t}Bu)-OH in presence of DIPCDI and DMAP. After Alloc removal, a Fmoc-*β*-HyAsn-OH residue was incorporated and the Fmoc group was cleaved providing the peptidyl resin **7**. The linear peptide **8** was released from the solid support and cyclised in solution using DEPBT and DIEA. Treatment with TFA/H_2O yielded lysobactin in 8% overall yield (Hall et al., 2012).

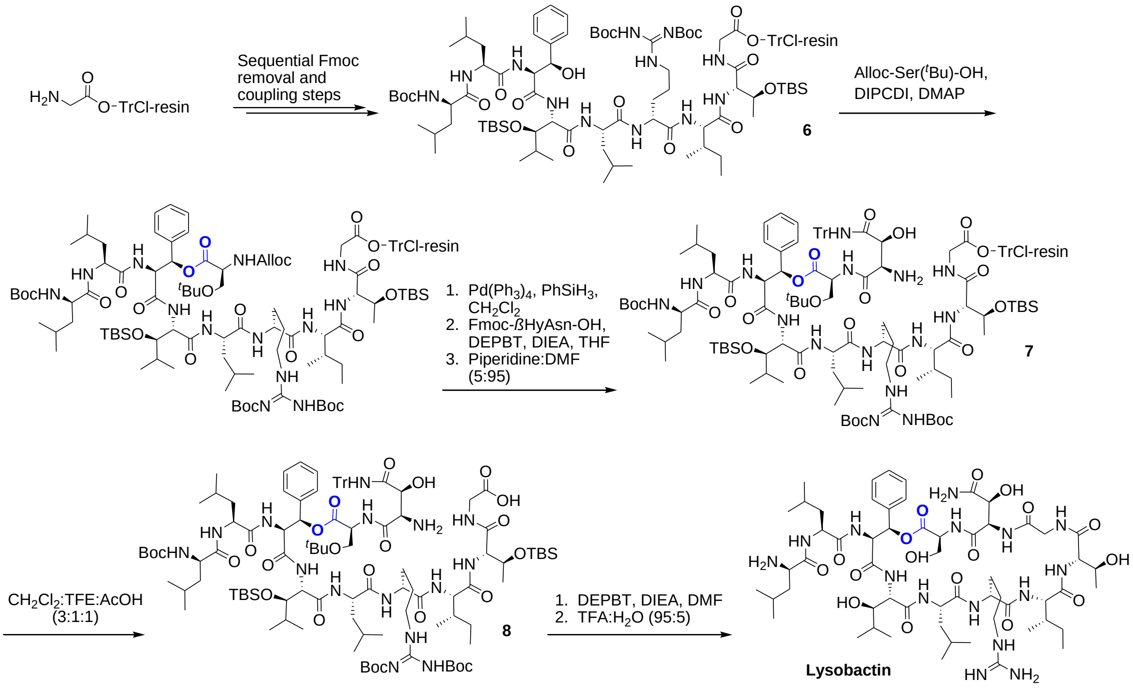
H2N O-TrCl-resin
Sequential Fmoc removal and coupling steps
6
Alloc-Ser(tBu)-OH, DIPCDI, DMAP
1. Pd(Ph3)4, PhSiH3, CH2Cl2
2. Fmoc-ßHyAsn-OH, DEPBT, DIEA, THF
3. Piperidine:DMF (5:95)
7
CH2Cl2:TFE:AcOH (3:1:1)
8
1. DEPBT, DIEA, DMF
2. TFA:H2O (95:5)
Lysobactin

Scheme 1.4. *Synthetic strategy for the synthesis of lysobactin proposed by Hall et al., 2012.*

Unlike the previous examples, other cyclic depsipeptides have been prepared through cyclization on solid phase. Following this approach, in 2006, Stawikowski and Cudic synthesized the depsipeptide **9**, an analogue of the antimicrobial peptide fusaricidin A (*Scheme 1.5*) (Stawikowski and Cudic, 2006). The preparation of **9** included the side-chain anchoring of a conveniently protected Asp residue, the stepwise Fmoc solid-phase synthesis of the linear peptide precursor followed by attachment of Fmoc-protected 12-aminododecanoic acid as pentafluorophenyl ester. Next, the hydroxyl group of a Thr residue in the resulting linear lipopetidyl resin **10** was esterified with Alloc-D-Ala-OH using DIPCDI and DMAP. After the selective removal of Alloc and allyl, the linear peptidyl resin was cyclised in presence of PyBOP, HOBt and DIEA providing resin **11**. The Fmoc group of **11** was removed and the amino group was guanylated by treatment with *N,N'*-bis(*tert*-butoxycarbonyl)thiourea and the Mukaiyama's reagent. Final deprotection and cleavage from the solid support afforded the desired cyclic lipodepsipeptide **9** in 60% yield based on the HPLC analysis of the crude (Stawikowski and Cudic, 2006).

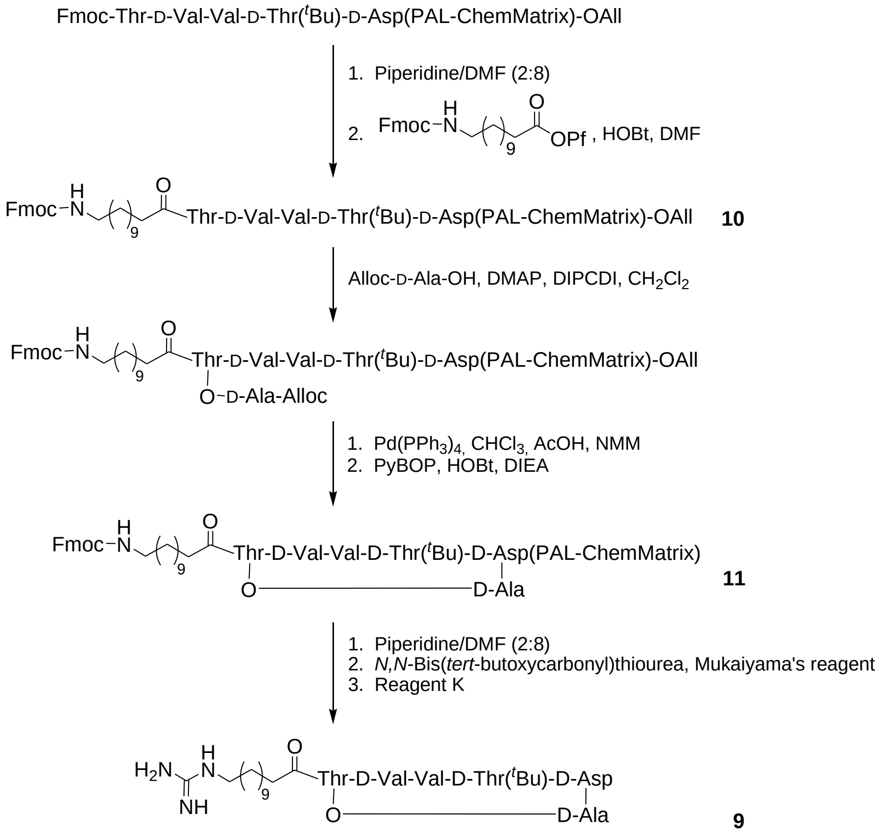

Fmoc-Thr-D-Val-Val-D-Thr(tBu)-D-Asp(PAL-ChemMatrix)-OAll
1. Piperidine/DMF (2:8)
2. Fmoc-N(H)-(CH2)9-C(O)-OPf, HOBt, DMF
10
Alloc-D-Ala-OH, DMAP, DIPCDI, CH2Cl2
O-D-Ala-Alloc
1. Pd(PPh3)4, CHCl3, AcOH, NMM
2. PyBOP, HOBt, DIEA
11
1. Piperidine/DMF (2:8)
2. N,N-Bis(tert-butoxycarbonyl)thiourea, Mukaiyama's reagent
3. Reagent K
9

Scheme 1.5. *Total solid-phase synthesis of the cyclic lipodepsipeptide* ***9*** *(Stawikowski and Cudic, 2006).*

Similarly, in 2009, Seo and Lim described the total synthesis of the cyclic depsipeptide halicylindramide A, which contains an ester bond between the hydroxyl group of a Thr and the carboxyl group of a sarcosine residue (*Scheme 1.6*) (Seo and Lim, 2009). The strategy began with the attachment of Fmoc-Asp-OAll via its side chain to a Rink amide resin followed by stepwise solid-phase synthesis of the linear peptidyl resin **12** using standard Fmoc chemistry. Next, Alloc-Sar-OH was coupled to the hydroxyl group of a Thr through an ester bond using DIPCDI and DMAP. The Alloc and allyl protecting groups of the resulting peptidyl resin **13** were selectively removed and the deprotected peptide was on-resin cyclized yielding **14**. Afterwards, the remaining amino acids were stepwise coupled following the standard SPPS conditions providing resin **15**. The last steps included the oxidation of the Cys residue to cysteic acid, the cleavage of the peptide from the support, and the formylation in solution of the *N*-terminal Ala affording halicylindramide A (Seo and Lim, 2009).

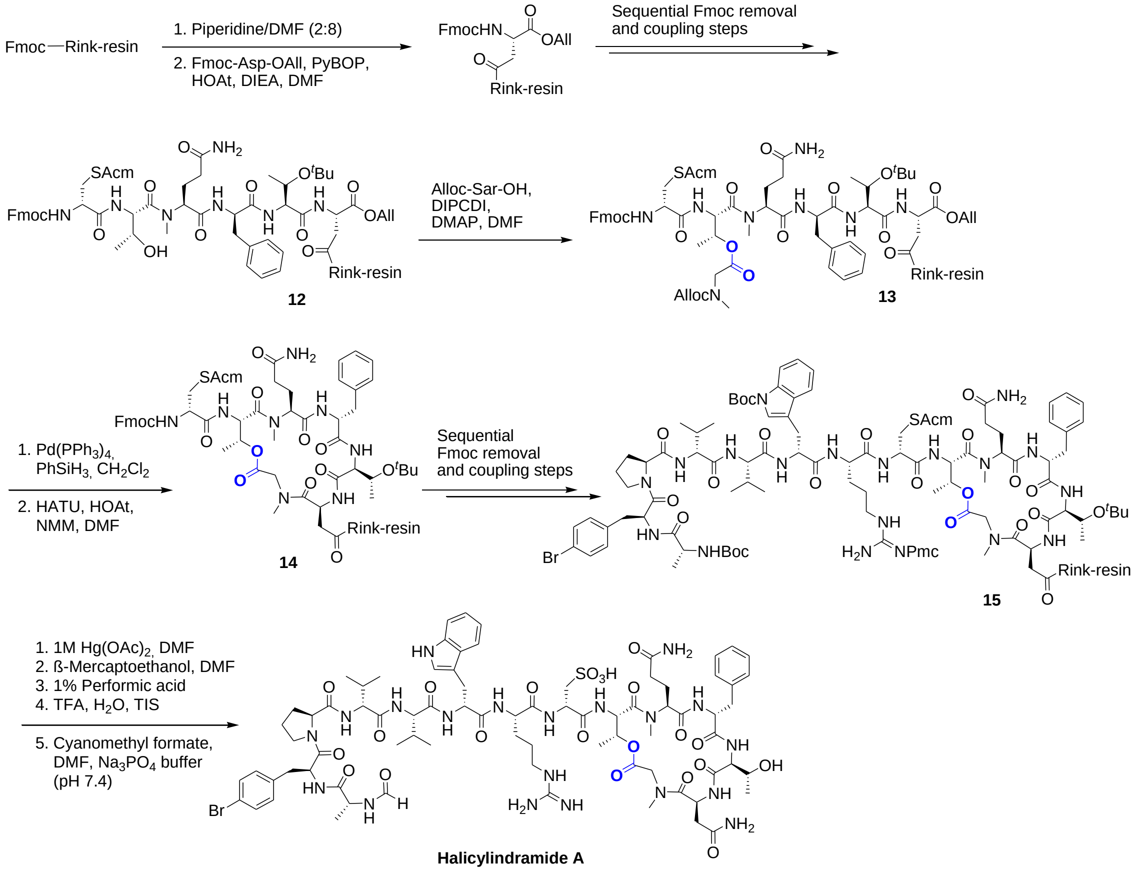
Fmoc—Rink-resin
1. Piperidine/DMF (2:8)
2. Fmoc-Asp-OAll, PyBOP, HOAt, DIEA, DMF
FmocHN
OAll
Rink-resin
Sequential Fmoc removal and coupling steps
12
Alloc-Sar-OH, DIPCDI, DMAP, DMF
13
AllocN
1. Pd(PPh3)4, PhSiH3, CH2Cl2
2. HATU, HOAt, NMM, DMF
14
Sequential Fmoc removal and coupling steps
15
BocN
NHBoc
H2N
NPmc
SAcm
OtBu
1. 1M Hg(OAc)2, DMF
2. ß-Mercaptoethanol, DMF
3. 1% Performic acid
4. TFA, H2O, TIS
5. Cyanomethyl formate, DMF, Na3PO4 buffer (pH 7.4)
SO3H
Br
Halicylindramide A

Scheme 1.6. *Synthesis of halicylindramide A (Seo and Lim, 2009).*

Another recent example is the total synthesis of the cyclic depsipeptide pipecolidepsin A described by Pelay-Gimeno and collaborators in 2013 (*Scheme 1.7*) (Pelay-Gimeno et al., 2013). Pipecolidepsin A shows anticancer activity against lung, colon and breast human tumor cells, and presents a complex structure with an ester linkage between the hydroxyl group of a D-*allo*-(2*R*,3*R*,4*R*)-2-amino-3-hydroxy-4,5-dimethylhexanoic acid (AHDMHA) and the carboxyl group of an L-pipecolic acid. This depsipeptide was prepared on solid phase following Fmoc chemistry and using a low-functionalized aminomethyl Wang resin derivatizated with a 3-(4-hydroxymethylphenoxy)propionic acid linker. The synthesis of the linear precursor started by the side-chain anchoring of Fmoc-D-Asp-OAll followed by elongation of the peptide sequence to obtain the octapeptidyl resin **16**, which contains an Fmoc-diMeGln-

OH residue. Its introduction before ester bond formation was important to avoid the *O*-to-*N* transacylation that can occur during the Fmoc deprotection of the D-*allo*-AHDMHA residue. Next, the ester bond was constructed using Alloc-pipecolic-OH, DIPCDI and DMAP for 2.3 h at 45ºC. Stepwise incorporation of the last three residues, the two later as a pseudodipeptide, resulted on the linear peptidyl resin **17**. Allyl and Alloc groups were then simultaneously removed and peptide cyclization was carried out on solid phase providing pipecolidepsin A in >95% purity.

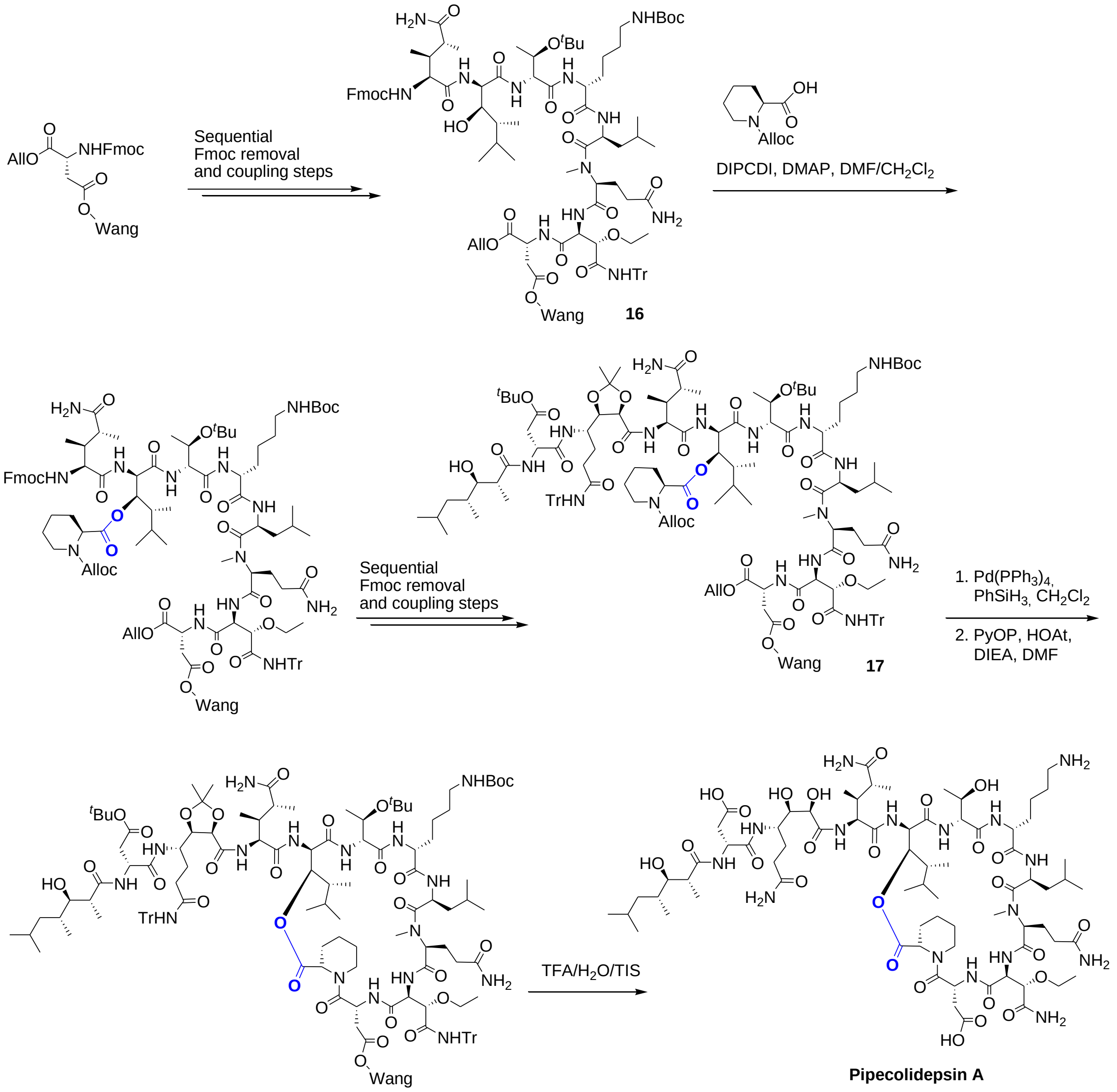
AllO
NHFmoc
Wang
Sequential
Fmoc removal
and coupling steps
16
Alloc
DIPCDI, DMAP, DMF/CH2Cl2
Sequential
Fmoc removal
and coupling steps
17
1. Pd(PPh3)4,
PhSiH3, CH2Cl2
2. PyOP, HOAt,
DIEA, DMF
TFA/H2O/TIS
Pipecolidepsin A

Scheme 1.7. *Synthesis of pipecolidepsin A (Pelay-Gimeno et al., 2013).*

It is noteworthy to mention that all these examples describe the formation of an ester bond involving a primary or a secondary aliphatic hydroxyl group. However, examples of ester bond formation involving an aromatic hydroxyl group, such as the phenol of a Tyr residue, are rare to find.

1.5.3 Obtention of *Bacillus* cyclic lipopeptides

Cyclic lipopeptides produced by *Bacillus spp.* are mainly obtained by fermentation followed by extraction (Jacques et al., 1999; Akpa et al., 2001; Inès and Dhouha, 2015). However, it has been observed that the *Bacillus* strain as well as the nutritional and culture conditions can influence the production of the different lipopeptide homologous (Akpa et al., 2001; Rangarajan et al., 2015).

Although fermentation is the most extended procedure, some cyclic lipopeptides have also been chemically synthesized. For instance, surfactin was first prepared in solution in 1996 (Nagai et al., 1996) and, few years later, Pagadoy and co-workers developed a more feasible methodology using solid-phase peptide synthesis (Pagadoy et al., 2005). Their methodology consisted on synthesizing the corresponding linear lipopeptide precursor on a Sasrin resin, using an Fmoc strategy, which was then cyclized in solution (*Scheme 1.8*). Following a similar methodology, the cyclic lipopeptide iturin-A2 was also chemically synthesized (*Scheme 1.9*) (Bland, 1996).

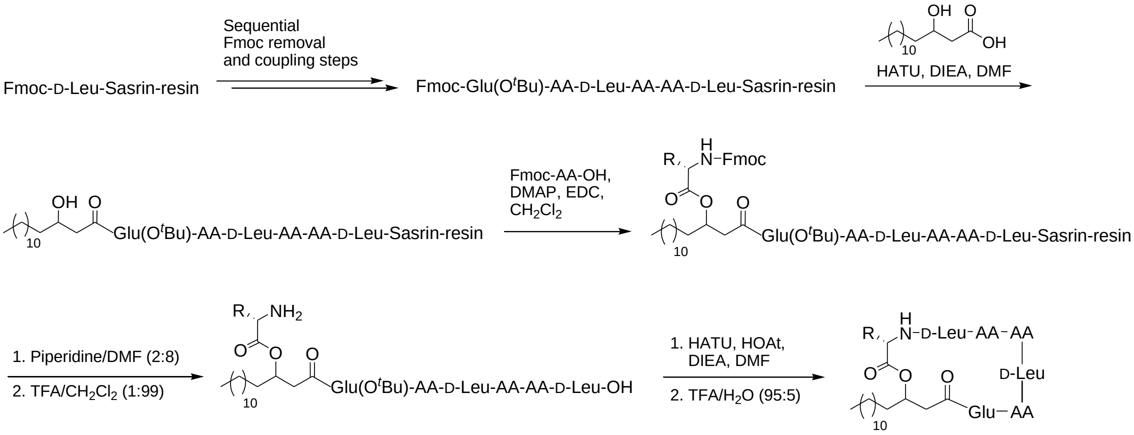
Fmoc-D-Leu-Sasrin-resin
Sequential Fmoc removal and coupling steps
Fmoc-Glu(O^{t}Bu)-AA-D-Leu-AA-AA-D-Leu-Sasrin-resin
OH O
10
OH
HATU, DIEA, DMF
Glu(O^{t}Bu)-AA-D-Leu-AA-AA-D-Leu-Sasrin-resin
Fmoc-AA-OH, DMAP, EDC, CH_2Cl_2
R
H
N-Fmoc
1. Piperidine/DMF (2:8)
2. TFA/CH_2Cl_2 (1:99)
NH_2
Glu(O^{t}Bu)-AA-D-Leu-AA-AA-D-Leu-OH
1. HATU, HOAt, DIEA, DMF
2. TFA/H_2O (95:5)
N-D-Leu-AA-AA
D-Leu
Glu-AA

Scheme 1.8. *Solid-phase synthesis of surfactin and analogues described by Pagadoy et al., 2005.*

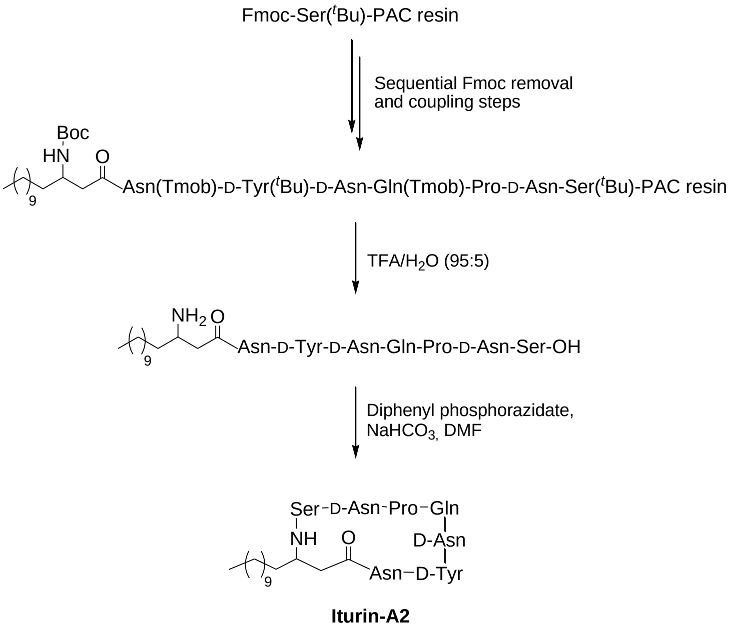

Scheme 1.9. *Solid-phase synthesis of iturin-A2 (Bland, 1996).*

In contrast, the total synthesis of fengycins has not yet been reported. However, it has been described the preparation of analogues through chemoenzymatic cyclization of the corresponding linear peptide (*Scheme 1.10*) (Sieber et al., 2003, 2004; Samel et al., 2006). These linear sequences were synthesized on solid phase using a 2-chlorotrityl resin derivatized with L-Leu. The synthesis was carried out following an Fmoc/^{t}Bu strategy (Kohli et al., 2001). The linear peptides were cleaved from the solid support under mild acid conditions avoiding the removal of the side-chain protecting groups. In order to enable their insertion into the enzyme complex, the *C*-terminus of these linear sequences was derivatizated with a thiophenol group using DCC and HOBt (Samel et al., 2006). Afterwards, all the side-chain protecting groups were removed and the resulting deprotected peptidyl thiophenols were purified and cyclized using the enzyme Fen PCP-TE. This enzyme consisted on a peptidyl carrier protein, onto which the linear peptide can be bound through a thioester linkage, and a thioesterase domain (TE), which catalyzes the cyclization and the consequent release of the final product. Using this methodology Samel and co-workers obtained the desired cyclic lipopeptide together with other by-products, such as the hydrolyzed peptide (Samel et al., 2006).

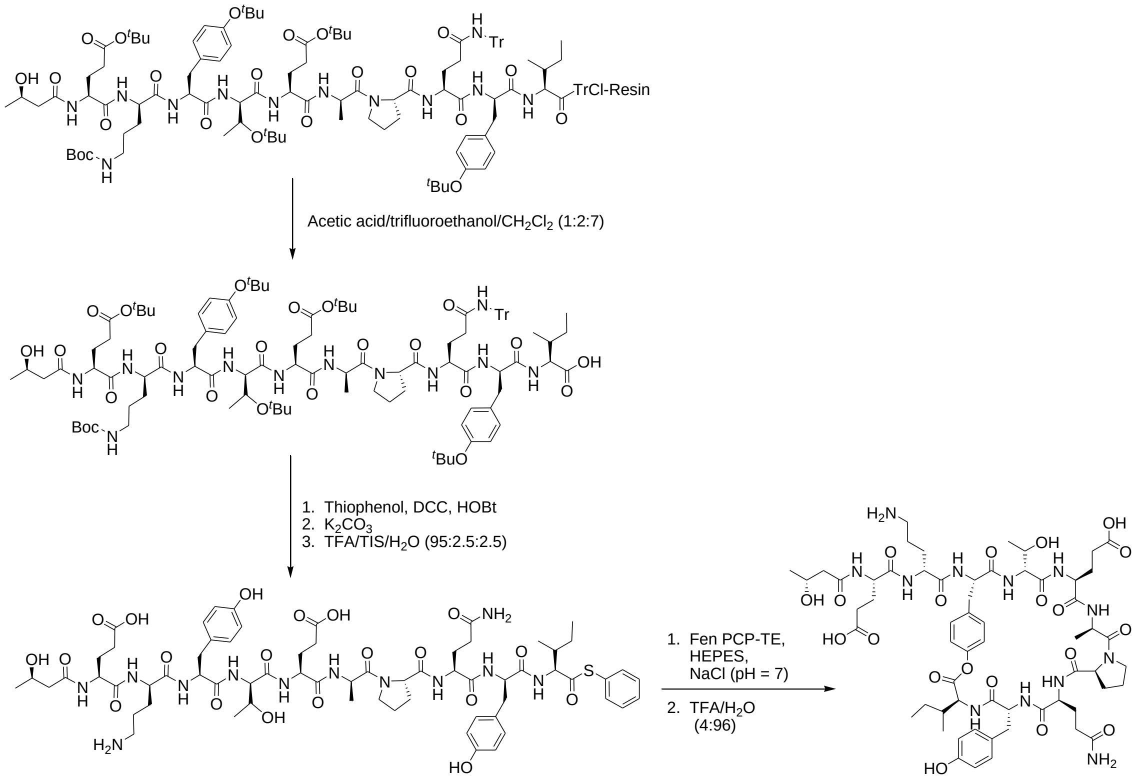
Acetic acid/trifluoroethanol/CH_2Cl_2 (1:2:7)
1. Thiophenol, DCC, HOBt
2. K_2CO_3
3. TFA/TIS/H_2O (95:2.5:2.5)
1. Fen PCP-TE, HEPES, NaCl (pH = 7)
2. TFA/H_2O (4:96)
TrCl-Resin

Scheme 1.10. *Synthesis of a fengycin analogue through chemoenzymatic cyclization (Samel et al., 2006).*

1.6 REFERENCES

Akpa, E.; Jacques, P.; Wathelet, B.; Paquot, M.; Fuchs, R.; Budzikiewicz, H, Thonart, P. Influence of culture conditions on lipopeptide production by *Bacillus subtilis*. *Appl. Biochem. Biotechnol.* **2001**, *91-93,* 551-561.

Ali, G.S.; Reddy, A.S.N. Inhibition of Fungal and Bacterial Plant Pathogens by Synthetic Peptides: In Vitro Growth Inhibition, Interaction Between Peptides and Inhibition of Disease Progression. *MPMI* **2000**, *13(8)*, 847-859.

Andreu, D.; Merrifield, R.B.; Steiner, H.; Boman, H.G. Solid-phase synthesis of cecropin A and related peptides. *Proc. Natl. Acad. Sci.* **1983**, *80*, 6475-6479.

Andreu, D.; Ubach, J.; Boman, A.; Wahlin, B.; Wade, D.; Merrifield, R.B.; Boman, H.G. Shortened cecropin A-Melittin hybrids. Significant size reduction retains potent antibiotic activity *FEBS* **1992**, *296(2)*, 190-194.

Aranda, F.J.; Teruel, J.A.; Ortiz, A. Further aspects on the hemolytic activity of the antibiotic lipopeptide iturin A. *Biochim. Biophys. Acta* **2005**, *1713*, 51-56.

Arrouss, I.; Nemati, F.; Roncal, F.; Wislez, M.; Dorgham, K.; Vallerand, D.; Rabbe, N.; Karboul, N.; Carlotti, F.; Bravo, J.; Mazier, D.; Decaudin, D.; Rebollo, A. Specific targeting of Caspase-9/PP2A interaction as potential new anti-cancer therapy. *Plos One*, **2013**, *4*, e60816.

Badosa, E.; Ferre, R.; Francés, J.; Bardají, E.; Feliu, L.; Planas, M.; Montesinos, E. Sporicidal activity of synthetic antifungal undecapeptides and control of *Penicillium* Rot of Apples. *Appl. Environ. Microbiol.* **2009**, *75(17)*, 5563-5569.

Badosa, E.; Ferre, R.; Planas, M.; Feliu, L.; Besalú, E.; Cabrefiga, J.; Bardají, E.; Montesinos, E. A library of linear undecapeptides with bactericidal activity against phytopathogenic bacteria. *Peptides* **2007**, *28*, 2276-2285.

Bais, H.P.; Fall, R.; Vivanco, J.M. Biocontrol of *Bacillus subtilis* against infection of Arabidopsis roots by *Pseudomonas syringae* is facilitated by biofilm formation and surfactin production. *Plant Physiol.* **2004**, *134*, 307-319.

Baltz, R. H. Molecular engineering approaches to peptide, polyketide and other antibiotics. *Nat. Biotechnol.* **2006**, *24*, 1533-1540.

Baltzer, S.A.; Brown, M.H. Antimicrobial peptides – Promising alternatives to conventional antibiotics. *J. Mol. Microbiol. Biotechnol.* **2011**, *20(4)*, 228-235.

Besson, F.; Michel, G. Isolation and characterization of new iturins: Iturin D and iturin E. *J. Antibiot.* **1987**, *40(4)*, 437-442.

Besson, F.; Peypoux, F.; Michel, G.; Delcambe, L. Identification of antibiotics of iturin group in various strains of *Bacillus subtilis*. *J. Antibiot.* **1978**, *31(4)*, 284-288.

Bhutia, S.K.; Maiti, T.K. Targeting tumors with peptides from natural sources. *Trends Biotechnol.* **2008**, *26(4)*, 210-217.

Bie, X.; Lu, Z.; Lu, F. Identification of fengycin homologues from *Bacillus subtilis* with ESI-MS/CID. *J. Microbiol. Methods* **2009**, *79*, 272-278.

Bland, J.M. The first synthesis of a member of the Iturin family, the antifungal cyclic lipopeptide, Iturin-A2. *J. Org. Chem.* **1996**, *61*, 5663-5664.

Brogden, K.A. Antimicrobial peptides: Pore formers or metabolic inhibitors in bacteria? *Nat. Rev. Microbiol.* **2005**, *3*, 238-250.

Butler, M. S.; Blaskovich, M. A.; Cooper, M. A. Antibiotics in the clinical pipeline in 2013. *J. Antibiot.* **2013**, *66(10)*, 571-591.

Cavallarin, L.; Andreu, D.; San Segundo, B. Cecropin A-Derived peptides are pontent inhibitors of fungal plant pathogens. *MPMI* **1998**, *11(3)*, 218-227.

Chan, Y.K.; Savard, M.E.; Reid, L.M.; Cyr, T.; McCormick, W.A., Seguin, C. Identification of lipopeptide antibiotics of a *Bacillus subtilis* isolate and their control of *Fusarium graminearum* diseases in maize and wheat. *BioControl* **2009**, *54*, 567-574.

Chen H.; Wang, L.; Su, C.X.; Gong, G.H.; Wang, P.; Yu, Z.L. Isolation and characterization of lipopeptide antibiotics produced by *Bacillus subtilis*. *Lett. Appl. Microbiol.* **2008**, *47*, 180-186.

Chen, H.M.; Wang, W.; Smith, D.; Chan, S.C. Effects of the anti-bacterial peptide cecropin B and its analogs, cecropins B-1 and B-2, on liposomes, bacteria, and cancer cells. *Biochim. Biophys. Acta* **1997**, *1336*, 171-179.

Coin, I. The depsipeptide method for solid-phase synthesis of difficult peptides. *J. Pept. Sci.* **2010**, *16*, 223-230.

Coin, I.; Beyermann, M.; Bienert, M. Solid-phase peptide synthesis: from standard procedures to the synthesis of difficult sequences. *Nature Protocols* **2007**, *2(12)*, 3247-3256.

Costa, J.P.; Cova, M.; Ferreira, R.; Vitorino, R. Antimicrobial peptides: an alternative for innovative medicines? *Appl. Microbiol. Biotechnol.* **2015**, *99*, 2023-2040.

Davies, J.S. The Cyclization of Peptides and Depsipeptides. *J. Peptide Sci.* **2003**, *9*, 471-501.

Deleu, M.; Paquot, M.; Nylander, T. Effect of Fengycin, a lipopeptide produced by *Bacillus subtilis,* on model biomembranes. *Biophys. J.* **2008**, *94*, 2667-2679.

Duclohier, H. Peptaibiotics and Peptaibols: An alternative to classical antibiotics? *Chem. Biodivers.* **2007**, *4*, 1023-1026.

El-Faham, A.; Albericio, F. COMU: A third generation of uronium-type coupling reagents. *J. Pept. Sci.* **2010**, *16*, 6-9.

El-Faham, A.; Subirós-Funosas, R.; Prohens, R.; Albericio, F. COMU: A safer and more effective replacement for benzotriazole-based uronium coupling reagents. *Chem. Eur. J.* **2009**, *15*, 9404-9416.

Emmert, E.A.B.; Handelsman, J. Biocontrol of plant disease: a (Gram-) positive perspective. *FEMS Microbiol. Letters* **1999**, *171*, 1-9.

Faria, A.F.; Stéfani, D.; Vaz, B.G.; Silva, I.S.; Garcia, J.S.; Eberlin, M.N.; Grossman, M.J.; Alves, O.L.; Durrant, L.R. Purification and structural characterization of fengycin homologues produced by *Bacillus subtilis* LSFM-05 grown on raw glycerol. *J. Ind. Microbiol. Biotechnol.* **2011**, *38,* 863-871.

Feliu, L.; Oliveras, G.; Cirac, A.D.; Besalú, E.; Rosés, C.; Colomer, R.; Bardají, E.; Planas, M.; Puig, T. Antimicrobial cyclic decapeptides with anticancer activity. *Peptides,* **2010***, 31*, 2017-2026.

Ferre, R.; Badosa, E.; Feliu, L.; Planas, M.; Montesinos, E.; Bardají, E. Inhibition of Plant-Pathogenic Bacteria by Short Synthetic Cecropin A-Melittin Hybrid Peptides. *Appl. Environ. Microbiol.* **2006**, *72(5)*, 3302-3308.

Filip, S.V.; Cavelier, F. A contribution to the nomenclature of depsipeptides. *J. Peptide Sci.* **2004**, *10*, 115-118.

Fonseca, S.B.; Pereira, M.P.; Kelley, S.O. Recent advances in the use of cell-penetrating peptides for medical and biological applications. *Adv. Drug Deliv. Rev.* **2009**, *61*, 953-964.

Fung, S.; Hruby, V.J. Design of cyclic and other templates for potent and selective peptide α-MSH analogues. *Curr. Opin. Chem. Biol.* **2005**, *9*, 352-358.

Gajski, G.; Garaj-Vrhovac, V. Melittin: A lytic peptide with anticancer properties. *Environ. Toxicol. Pharmacol.* **2013**, *36,* 697-705.

Galdiero, S.; Falanga, A.; Cantisani, M.; Vitiello, M.; Morelli, G.; Galdiero, M. Peptide-lipid interactions: Experiments and applications. *Int. J. Mol. Sci.* **2013**, *14*, 18758-18789.

Ganz, T. Defensins: Antimicrobial peptides of innate immunity. *Nat. Rev. Immunol.* **2003**, *3(9)*, 710-720.

García-Ramos, Y.; Paradís-Bas, M.; Tulla-Puche, J.; Albericio, F. ChemMatrix® for complex peptides and combinatorial chemistry. *J. Pept. Sci.* **2010**, *16*, 675-678.

Gaspar, D.; Veiga, A.S.; Castanho, M.A.R.B. From antimicrobial to anticancer peptides. A review. *Front. Microbiol.* **2013**, *4*:294.

Gaspar, D.; Freire, J.M.; Pacheco, T.R.; Barata, J.T.; Castanho, M.A.R.B. Apoptotic human neutrophil peptide-1 anti-tumor activity revealed by cellular biomechanics. *Biochim. Biophys. Acta* **2015**, *1853*, 308-316.

Giacometti, A.; Cirioni, O.; Kamysz, W.; Amato, G.; Silvestri, C.; Prete, M.S.; Lukasiak, J.; Scalise, G. In vitro activity and killing effect of the synthetic hybrid cecropin A-melittin peptide CA(1-7)M(2.9)NH_2 on methicinllin-resistant nosocomial isolates of *Staphylococcus aureus* and interactions with clinically used antibiotics. *Diagnostic Microbiology and Infectious Disease* **2004**, *49*, 197-200.

Gilon, C.; Halle, D.; Chorev, M.; Selinger, Z.; Byk, G. Backbone cyclization: A new method for conferring conformational constraint on peptides. *Biopolymers* **1991**, *31*, 745-750.

Giuliani, A.; Pirri, G.; Nicoletto, S.F. Antimicrobial peptides: an overview of a promising class of therapeutics. *Cent. Eur. J. Biol.* **2007**, *2(1)*, 1-33.

Gracia, C.; Isidro-Llobet, A.; Cruz, L.J.; Acosta, G.A.; Álvarez, M.; Cuevas, C.; Giralt, E.; Albericio, F. Convergent approaches for the synthesis of the antitumoral peptide, Kahalalide F. Study of orthogonal proctecting groups. *J. Org. Chem.* **2006**, *71*, 7196-7204.

Hall, E.A.; Kuru, E.; VanNieuwenhze, M.S. Solid-phase synthesis of Lysobactin (Katanosin B): insights into structure and function. *Org. Lett.* **2012**, *14(11)*, 2730-2733.

Hanahan, D.; Weinberg, R.A. Hallmarks of Cancer: The next generation. *Cell*, **2011**, *144*, 646-674.

Hanahan, D.; Weinberg, R.A. The hallmarks of cancer. *Cell*, **2000**, *100*, 57-70.

Hancock, R.E.W. Cationic peptides: effectors in innate immunity and novel antimicrobials. *Lancet: Infect. Dis.* **2001**, *1*, 156-164.

Harris, F.; Dennison, S.R.; Singh, J.; Phoenix, D.A. On the selectivity and efficacy of defense peptides with respect to cancer cells *Med. Res. Rev.* **2013**, *33(1)*, 190-234.

Henderson, J.M.; Lee, K.Y.C. Promising antimicrobial agents designed from natural peptide templates. *Curr. Opin. Solid State Mater. Sci.* **2013**, *17*, 175-192.

Honma, M.; Tanaka, K.; Konno, K.; Tsuge, K.; Okuno, T.; Hashimoto, M. Termination of the structural confusion between plipastatin A1 and fengycin IX. *Bioorg. Med. Chem.* **2012**, *20*, 3793-3798.

Hoskin, D.W.; Ramamoorthy, A. Studies on anticancer activities of antimicrobial peptides. *Biochim. Biophys. Acta* **2008**, *1778*, 357-375.

Hu, L.B.; Shi, Z.Q.; Zhang, T.; Yang, Z.M. Fengycin antibiotics isolated from B-FS01 culture inhibit the growth of *Fusarium moniliforme* Sheldon ATCC38932. FEMS Microbiol. Lett. **2007**, *272*, 91-98.

Hu, L.B.; Zhang, T.; Yang, Z.M.; Zhou, W.; Shi, Z.Q. Inhibition of fengycins on the production of fumonisin B_1 from *Fusarium verticillioides. Lett. Appl. Microbiol.* **2009**, *48*, 84-89.

Huang, H.W. Molecular mechanism of antimicrobial peptides: The origin of cooperativity. *Biochim. Biophys. Acta* **2006**, *1458*, 1292-1302.

Inès, M.; Dhouha, G. Lipopeptide surfactants: Production, recovery and pore forming capacity. *Peptides,* **2015**, *71*, 100-112.

Isidro-Llobet, A.; Álvarez, M.; Albericio, F. Amino Acid-Protecting Groups. *Chem. Rev.* **2009**, *109,* 2455-2504.

Jacques, P.; Hbid, C.; Destain, J.; Razafindralambo, H.; Paquot, M.; Pauw, E.; Thonart, P. Optimization of biosurfactant lipopeptide production from *Bacillus subtilis* S499 by Plackett-Burman design. *Appl. Biochem. Biotechnol.* **1999**, *77-79*, 223-233.

Jenssen, H.; Hamill, P.; Hancock, R. E. W. Peptide antimicrobial agents. *Clin. Microbiol. Rev.* **2006**, *19(3),* 491-511.

Kates, S.A.; Albericio, F. Solid-Phase Synthesis: A Practical Guide. *Marcel Dekker Inc.*: New York, **2000**.

Kohli, R.M.; Trauger, J.W.; Schwarzer, D.; Marahiel, M.A.; Walsh, C.T. Generality of peptide cyclization catalyzed by isolated thioesterase domains of nonribosomal peptide synthetases. *Biochemistry* **2001**, *40*, 7099-7108.

Kokryakov, V. N.; Harwig, S.S.L.; Panyutich, E.A.; Shevchenko, A.A.; Aleshina, G.M.; Shamova, O.V.; Korneva, H.A.; Lehrer, R.I. Protegrins: leukocyte antimicrobial peptides that combine features of corticostatic defensins and tachyplesins. *FEBS Letters* **1993**, *327(2),* 231-236.

Koren, E.; Torchilin, V.P. Cell-penetrating peptides: breaking through to the other side. *Trends Mol. Med.* **2012**, *18(7)*, 385-393.

Law, B.; Quinti, L.; Choi, Y.; Weissleder, R.; Tung, C.H. A mitochondrial targeted fusion peptide exhibits remarkable cytotoxicity. *Mol. Cancer Ther.* **2006**, *5(8)*, 1944-1949.

Lee, M.T.; Sun, T.L.; Hung, W.C.; Huang, H.W. Process of inducing pores in membranes by melittin. *PNAS*, **2013**, *10(35)*, 14243-14248.

Lehmann, J.; Retz, M.; Sidhu, S.S.; Suttmann, H.; Sell, M.; Paulsen, F.; Harder, J.; Unteregger, G.; Stöckle, M. Antitumor activity of the antimicrobial peptide Magainin II against bladder cancer cell lines. *Eur. Urol.* **2006,** *50*, 141-147.

Leitgeb, B.; Szekeres, A.; Manczinger, L.; Vágvölgyi, C.; Kredics, L. The history of Alamethicin: A review of the most extensively studied peptaibol. *Chem. Biodivers.* **2007**, *4*, 1027-1051.

Leuschner, C.; Hansel, W. Membrane disrupting lytic peptides for cancer treatments. *Curr. Pharm. Design* **2004**, *10*, 2299-2310.

Li, Q.F.; Ou-Yang, G.L.; Li, C.Y.; Hong, S.G. Effects of tachyplesin on the morphology and ultrastructure of human gastric carcinoma cell line BGC-823. *World J. Gastroentero.* **2000**, *6(5)*, 676-680.

Li, Y.; Xiang, Q.; Zhang, Q.; Huang, Y.; Su, Z. Overview on the recent study of antimicrobial peptides: Origins, functions, relative mechanisms and application. *Peptides* **2012**, *37(2)*, 207-215.

López, P.E.; Isidro-Llobet, A.; Gracia, C.; Cruz, L.J.; García-Granados, A.; Parra, A.; Álvarez, M.; Albericio, F. Use of *p*-nitrobenzyloxycarbonyl (*p*NZ) as a permanent protecting group in the synthesis of Kahalalide F Analogs. *Tetrahedron Lett.* **2005**, *46*, 7737-7741.

López-Macià, A.; Jiménez, J.C.; Royo, M.; Giralt, E.; Albericio, F. Synthesis and Structure Determination of Kahalalide F. *J. Am. Chem. Soc.* **2001,** *123,* 11398-11401.

Mader, J.S.; Hoskin, D.W. Cationic antimicrobial peptides as novel cytotoxic agents for cancer treatment. *Expert Opin. Investig. Drugs* **2006**, *15(8)*, 933-946.

Mader, J.S.; Salsman, J.; Conrad, D.M.; Hoskin, D.W. Bovine lactoferricin selectively induces apoptosis in human leukemia and carcinoma cell lines. *Mol. Cancer Ther.* **2005**, *4*, 612-624.

Mäe, M.; Langel, Ü. Cell-penetrating peptides as vectors for peptide, protein and oligonucleotide delivery. *Curr. Opin. Pharmacol.* **2006**, *6*, 509-514.

Mankelow, D.P.; Neilan, B.A. Non-ribosomal peptide antibiotics. *Exp. Opin. Ther. Patents* **2000**, *10(10)*, 1583-1591.

Martin, F. G.; Albericio, F. Solid supports for the synthesis of peptides: from the first resin used to the most sophisticated in the market. *Chimica Oggi./Chem. Today* **2008**, *26(4)*, 29-34.

Matsuzaki, K Control of cell selectivity of antimicrobial peptides. *Biochim. Biophys. Acta* **2009**, *1788*, 1687-1692.

Matsuzaki, K. Why and how are peptide-lipid interactions utilized for self-defense? Magainins and tachyplesins as archetypes. *Biochim. Biophys. Acta* **1999**, *1462*, 1-10.

McIntosh, J. A.; Donia, M. S.; Schmidt, E.W. Ribosomal peptide natural products: bridging the ribosomal and nonribosomal worlds. *Nat. Prod. Rep.* **2009**, *26*, 537-559.

McKeown, S.T.W.; Lundy, F.T.; Nelson, J.; Lockhart, D.; Irwin, C.R.; Cowan, C.G.; Marley, J.J. The cytotoxic effects of human neutrophil peptide-1 (HNP1) and lactoferrin on oral squamous cell carcinoma (OSCC) in vitro. *Oral Oncol.* **2006**, *42*, 685-690.

Melo, M.N; Ferre, R.; Castanho, M.A.R.B. Antimicrobial peptides: linking partition, activity and high membrane-bound concentrations. *Nat. Rev. Microbiol.* **2009**, *7*, 245-250.

Merrifield, R.B. Solid Phase peptide synthesis 1. Synthesis of a tetrapeptide. *J. Am. Chem. Soc.* **1963**, *85(14)*, 2149-2154.

Merrifield, R.B. Solid-Phase Synthesis. *Science* **1986**, *232* (4748), 341-347.

Micklefield, J. Daptomycin structure and mechanism of action revealed. *Chem. Biol.* **2004**, *11*, 887-895.

Milletti, F. Cell-penetrating peptides: classes, origin, and current landscape. *Drug Discov. Today* **2012**, *17 (15/16),* 850-860.

Monroc, S.; Badosa, E.; Feliu, L.; Planas, M.; Montesinos, E.; Bardají, E. De novo designed cyclic cationic peptides as inhibitors of plant pathogenic bacteria. *Peptides*, **2006a**, *27*, 2567-2574.

Monroc, S.; Badosa, E.; Besalú, E.; Planas, M.; Bardají, E.; Montesinos, E.; Feliu, L. Improvement of cyclic decapeptides against plant pathogenic bacteria using a combinatorial chemistry approach. *Peptides*, **2006b**, *27*, 2575-2584.

Montesinos, E. Antimicrobial peptides and plant disease control. *FEMS Microbiol. Lett.* **2007**, *270*, 1-11.

Mora, I.; Cabrefiga, J.; Montesinos, E. Cyclic lipopeptide biosynthetic genes and products, and inhibitory activity of plant-associated *Bacillus* against phytopathogenic bacteria. *PLoS ONE,* **2015**, *10(5)*: e0127738.

Mouls, L.; Subra, G.; Enjalbal, C.; Martinez, J.; Aubagnac, J.L. O-N-Acyl migration in *N*-terminal serine-containing peptides: mass spectrometric elucidation and subsequent development of site-directed acylation protocols. *Tetrahedron Lett.* **2004**, *45*, 1173-1178.

Nagai, S.; Okimura, K.; Kaizawa, N.; Ohki, K.; Kanatomo, S. Study on surfactin, a cyclic depsipeptide. II. Synthesis of surfactin B_2 produced by *Bacillus natto* KMD 2311. *Chem. Pharm. Bull.* **1996**, *44(1)*, 5-10.

Nakamura, T.; Furunaka, H.; Miyata, T.; Tokunaga, F.; Muta, T.; Iwanaga, S. Tachyplesin, a class of antimicrobial peptide from the hemocytes of the Horseshoe Crab (*Tachypleus tridentatus*). *J. Biol. Chem.* **1988**, *236(32)*, 16709-16713.

Nasir, M.N.; Laurent, P.; Flore, C.; Lins, L.; Ongena, M.; Deleu, M. Analysis of calcium-induced effects on the conformation of fengycin. *Spectrochim. Acta A.* **2013**, *110*, 450-457.

Newman, D. J.; Cragg, G.M. Natural products as sources of New Drugs over the 30 years from 1981 to 2010. *J. Nat. Prod.* **2012**, *75(3)*, 311-335.

Ng-Choi, I.; Soler, M.; Güell, I.; Badosa, E.; Cabrefiga, J.; Bardají, E.; Montesinos, E.; Planas, M.; Feliu, L. Antimicrobial peptides incorporating Non-natural Amino Acids as Agents for plant protection. *Protein Pept. Lett*. **2014**, *21(4)*, 357-367.

Nishikiori, T.; Naganawa, H.; Muraoka, Y.; Aoyagi, T.; Umezawa, H. Plipastatins: New inhibitors of phospholipase A_2, produced by *Bacillus cereus* BMG302-fF67. II. Structure of fatty acid residue and amino acid sequence. *J. Antibiot.* **1986a**, *39(6)*, 745-754.

Nishikiori, T.; Naganawa, H.; Muraoka, Y.; Aoyagi, T.; Umezawa, H. Plipastatins: New inhibitors of phospholipase A_2, produced by *Bacillus cereus* BMG302-fF67. III. Structural elucidation of plipastatins. *J. Antibiot.* **1986b**, *39(6)*, 755-761.

Nissen-Meyer, J.; Nes, I.F. Ribosomally synthesized antimicrobial peptides: their function, structure, biogenesis, and mechanism of action. *Arch. Microbiol.* **1997**, *167*, 67-77.

Nussbaumer, S.; Bonnabry, P.; Veuthey, J.L.; Fleury-Souverain, S. Analysis of anticancer drugs: A review. *Talanta* **2011**, *85*, 2265-2289.

Ong, Z.Y.; Wiradharma, N.; Yang, Y.Y. Strategies employed in the design and optimitzation of synthetic antimicrobial peptide amphiphiles with enhanced therapeutic potentials. *Adv. Drug Deliv. Rev.* **2014**, *78*, 28-45.

Ongena, M.; Jacques, P. *Bacillus* lipopeptides: versatile weapons for plant disease biocontrol *Trends Microbiol.* **2008**, *16(3)*, 115-125.

Ongena, M.; Jacques, P.; Touré, Y.; Destain, J.; Jabrane, A.; Thonart, P. Involvement of fengycin-type lipopeptides in the multifaceted biocontrol potential of *Bacillus subtilis*. *Appl. Microbiol. Biotechnol.* **2005**, *69*, 29-38.

Ongena, M.; Jourdan, E.; Adam, A.; Paquot, M.; Brans, A.; Joris, B.; Arpigny, J.L.; Thonart, P. Surfactin and fengycin lipopeptides of *Bacillus subtilis* as elicitors of induced systemic resistance in plants. *Environ. Microbiol.* **2007**, *9(4)*, 1084-1090.

Ouyang, G.L.; Li, Q.F.; Peng, X.X.; Liu, Q.R.; Hong, S.G. Effects of tachyplesin on proliferation and differentiation of human hepatocellular carcinoma SMMC-7721 cells. *World J. Gastroenterol.* **2002**, *8(6)*, 1053-1058.

Pagadoy, M.; Peypoux, F.; Wallach, J. Solid-Phase synthesis of Surfactin, a powerful biosurfactant produced by *Bacillus subtilis*, and of four analogues. *Int. J. Pept. Res. Ther.* **2005**, *11(3)*, 195-202.

Papo, N.; Shai, Y. Host defense peptides as new weapons in cancer treatment. *Cell. Mol. Life. Sci.* **2005**, *62*, 784-790.

Pasupuleti, M.; Schmidtchen, A.; Malmsten, M. Antimicrobial peptides: key components of the innate immune system. *Crit. Rev. Biotechnol.* **2012**, *32(2)*, 142-171.

Pathak, K.V.; Keharia, H.; Gupta, K.; Thakur, S.S.; Balaram, P. Lipopeptides from the Banyan Endophyte, *Bacillus subtilis* K1: Mass spectrometric characterization of a library of Fengycins. *J. Am. Soc. Mass. Spectrom.* **2012**, *23*, 1716-1728.

Pecci, Y.; Rivardo, F.; Martinotti, M.G.; Allegrone, G. LC/ESI-MS/MS characterization of lipopeptide biosurfactants produced by the *Bacillus licheniformis* V9T14 strain. *J. Mass. Spectrom.* **2010**, *45*, 722-778.

Pelay-Gimeno, M.; García-Ramos, Y.; Martin, M.J.; Spengler, J.; Molina-Guijarro, J.M.; Munt, S.; Francesch, A.M.; Cuevas, C.; Tulla-Puche, J.; Albericio, F. The first total synthesis of the cyclodepispeptide pipecolidepsin A. *Nature Comm.* **2013**, *4*, 2352.

Pérez-Tomás, R. Multidrug resistance: Retrospect and prospects in Anti-cancer drug treatment. *Curr. Med. Chem.* **2006**, *13*, 1859-1876.

Peters, B.M.; Shirtliff, M.E.; Jabra-Rizk, M.A. Antimicrobial Peptides: Primeval molecules or future drugs? *PLoS Pathog.* **2010**, *6(10)*, e1001067.

Peypoux, F.; Bonmatin, J.M.; Wallach, J. Recent trends in the biochemistry of surfactin. *Appl. Microbiol. Biotechnol.* **1999**, *51*, 553-563.

Pires, D.A.T.; Bemquerer, M.P.; Nascimento, C.J. Some mechanistic aspects on Fmoc Solid Phase Peptide Synthesis. *Int. J. Pept. Res. Ther.* **2014**, *20*, 53-69.

Powers, J.P.S; Hancock, R.E.W The relationship between peptide structure and antibacterial activity. *Peptides* **2003**, *24*, 1681-1691.

Pueyo, M.T.; Bloch C.; Carmona-Ribeiro, A.M.; Mascio, P. Lipopeptides produced by a soil *Bacillus magaterium* strain. *Microb. Ecol.* **2009**, *57*, 367-378.

Raaijmakers, J.M.; Brujin, I.; Nybroe, O.; Ongena, M. Natural functions of lipopeptides from *Bacillus* and *Pseudomonas*: more than surfactants and antibiotics. *FEMS Microbiol. Rev.* **2010**, *34*, 1037-1062.

Raghuraman, H.; Chattopadhyay, A. Melittin: a membrane-active peptide with diverse functions. *Biosci. Rep.* **2007**, *27*, 189-223.

Rangarajan, V.; Dhanarajan, G.; Sen, R. Bioprocess design for selective enhancement of fengycin production by a marine isolate *Bacillus megaterium*. *Biochem. Eng. J.* **2015**, *99*, 147-155.

Riedl, S.; Zweytick, D.; Lohner, K. Membrane-active host defense peptides- Challenges and perspectives for the development of novel anticancer drugs. *Chem. Phys. Lipids* **2011,** *164*, 766-781.

Romero, D.; Vicente, A.; Rakotoaly, R.H.; Dufour, S.E.; Veening, J.W.; Arrebola, E.; Cazorla, F.M.; Kuipers, O.P.; Paquot, M.; Pérez-García, A. The iturin and fengycin families of lipopeptides are key factors in antagonism of *Bacillus subtilis* toward *Podosphaera fusca*. *MPMI* **2007**, *20(4)*, 430-440.

Samel, S.A.; Wagner, B.; Marahiel, M.A.; Essen, L.O. The thioesterase domain of the fengycin biosynthesis cluster: A structural base for the macrocyclization of a non-ribosomal lipopeptide. *J. Mol. Biol.* **2006**, *359*, 876-889.

Sang-Cheol, L.; Kim, S.H.; Park, I.H.; Chung, S.Y.; Chandra, M.S.; Choi, Y.L. Isolation, purification, and characterization of novel fengycin S from *Bacillus amyloliquefaciens* LSC04 degrading-crude oil. *Biotechnol. Bioprocess Eng.* **2010**, *15*, 246-253.

Schneider, J.; Taraz, K.; Budzikiewicz, H.; Deleu, M.; Thonart, P.; Jacques, P. The structure of two fengycins from Bacillus subtilis S499. *Z. Naturforsch.* **1999**, *54c*, 859-866.

Schweizer, F. Cationic amphiphilic peptides with cancer-selective toxicity. *Eur. J. Pharmacol.* **2009**, *625*, 190-194.

Seo, H.; Lim, D.; Total synthesis of Halicylindramide A. *J. Org. Chem.* **2009**, *74*, 906-909.

Seydlová, G.; Svobodová, J. Review of surfactin chemical properties and the potential biomedical applications. *Cent. Eur. J. Med.* **2008**, *3(2)*, 123-133.

Shai, Y. Mode of action of membrane active antimicrobial peptides. *Biopolymers. Pept. Sci.* **2002**, *66*, 236-248.

Shin, S.Y.; Lee, S.H.; Yang, S.T.; Park, E.J.; Lee, D.G.; Lee, M.K.; Eom, S.H.; Song, W.K., Kim, Y.; Hahm, K.S.; Kim, J.I. Antibacterial, antitumor and hemolytic activities of α-helical antibiotic peptide, P18 and its analogs. *J. Peptide Res.* **2001**, *58*, 504-514.

Sieber, S. A.; Marahiel, M. A. Learning from Nature's Drug Factories: Nonribosomal Synthesis of Macrocyclic Peptides. *J. Bacteriol.* **2003**, *185 (4)*, 7036-7043.

Sieber, S.A.; Tao, J.; Walsh, C.T.; Marahiel, M.A. Peptidyl Thiophenols as substrates for nonribosomal peptide cyclases. *Angew. Chem. Int. Ed.* **2004**, *43*, 493-498.

Sieber, S.A.; Walsh, C.T.; Marahiel, M.A. Loading peptidyl-coenzyme A onto peptidyl carrier proteins: A novel approach in characterizing macrocyclization by thioesterase domains. *J. Am. Chem. Soc.* **2003**, *125*, 10862-10866.

Sivapathasekaran, C.; Das, P.; Mukherjee, S.; Saravanakumar, J.; Mandal, M.; Sen, R. Marine bacterium derived lipopeptides: Characteritzation and cytotoxic activity against cancer cell lines. *Int. J. Pept. Res. Ther.* **2010**, *16*, 215-222.

Stawikowski, M.; Cudic, P. A novel strategy for the solid-phase synthesis of cyclic lipodepsipeptides. *Tetrahedron Lett.* **2006**, *47*, 8587-8590.

Stein, T. *Bacillus subtilis* antibiotics: structures, syntheses and specific functions. *Mol. Microbiol.* **2005**, *56(4)*, 845-857.

Steiner, H.; Hultmark, D.; Engström, A.; Bennich, H.; Boman, H.G. Sequence and specificity of two antibacterial proteins involved in insect immunity. *Nature* **1981**, *292*, 246-248.

Stewart, K.M.; Horton, K.L.; Kelley, S.O. Cell-penetrating peptides as delivery vehicles for biology and medicine. *Org. Biomol. Chem.* **2008**, *6*, 2242-2255.

Subirós-Funosas, R.; Prohens, R.; Barbas, R.; El-Faham, A.; Albericio, F. Oxyma: An efficient additive for peptide synthesis to replace the benzotriazole-based HOBt and HOAt with lower risk of explosion. *Chem. Eur. J.* **2009**, *15*, 9394-9403.

Terwilliger, T.C.; Eisenberg, D. The structure of melittin. I. Structure determination and partial refinement. *J. Biol. Chem.* **1982a**, *257(11)*, 6010-6016.

Terwilliger, T.C.; Eisenberg, D. The structure of melittin. II. Interpretation of the structure. *J. Biol. Chem.* **1982b**, *257(11)*, 6016-6022.

Terwilliger, T.C.; Weissman, L.; Eisenberg, D. The structure of melittin in the form I crustals and its implication for melittin's lytic and surface activities. *Biophys. J.* **1982**, *37(1)*, 353-361.

Tossi, A.; Sandri, L.; Giangaspero, A. Amphipathic, α-helical antimicrobial peptides. *Biopolymers: Pept. Sci.* **2000**, *55*, 4-30.

Touré, Y.; Ongena, M.; Jacques, P.; Guiro, A.; Thonart, P. Role of lipopeptides produced by *Bacillus subtilis* GA1 in the reduction of grey mould disease caused by Botrytis cinerea on apple. *J. Appl. Microbiol.* **2004**, *96*, 1151-1160.

Vanittanakom, N.; Loeffler, W.; Koch, U.; Jung, G. Fengycin - A novel antifungal lipopeptide antibiotic produced by *Bacillus subtilis* F-29-3. *J. Antibiot.* **1986**, *39*, 888-901.

Villegas-Escobar, V.; Ceballos, I.; Mira, J.J.; Argel, L.E.; Peralta, S.O.; Romero-Tabarez, M. Fengycin C produced by *Bacillus subtilis* EA-CB0015. *J. Nat. Prod.* **2013**, *76*, 503-509.

Volpon, L.; Besson, F.; Lancelin, J.M. NMR structure of antibiotics plipastatins A and B from *Bacillus subtilis* inhibitors of phospholipase A_2. *FEBS Lett.* **2000**, *485*, 76-80.

Waghu, F. H.; Gopi, L.; Barai, R. S.; Ramteke, P.; Nizami, B.; Indicula-Thomas, S. CAMP: Collection of sequences and structures of antimicrobial peptides. *Nucleic Acids Res.* **2014**, *42*, D1154-D1158.

Wang, G.; Li, X.; Wang, Z. APD2: the updated antimicrobial peptide database and its application in peptide design. *Nucleic Acids Res.* **2009**, *37*, D933-D937.

Wang, J.; Liu, J.; Chen, H.; Yao, J. Characterization of *Fusarium graminearum* inhibitory lipopeptide from *Bacillus subtilis* IB. *Appl. Microbiol. Biotechnol.* **2007**, *76(4)*, 889-894.

Wang, J.; Liu, J.; Wang, X.; Yao, J.; Yu, Z. Application of electrospray ionization mass spectrometry in rapid typing of fengycin homologues produced by *Bacillus subtilis*. *Lett. Appl. Microbiol.* **2004**, *39*, 98-102.

Wang, S.S. *p*-Alkoxybenzyl alcohol resin and *p*-alkoxybenzylcarbonylhydrazide resin for solid phase synthesis of protected peptide fragments. *J. Am. Chem. Soc.* **1973**, *95(4)*, 1328-1333.

Wehrstedt, K.D.; Wandrey, P.A.; Heitkamp, D. Explosive properties of 1-hydroxybenzotriazoles. *J. Hazard. Mater.* **2005**, A*126*, 1-7.

Werle, M.; Bernkop-Schnürch, A. Strategies to improve plasma half life time of peptide and protein drugs. *Amino Acids*, **2006**, *30*, 351-367.

Whitmore, L.; Wallace, B. A. The Peptaibol Database: a database for sequences and structures of naturally occurring peptaibols. *Nucleic Acids Res.* **2004**, *32*, D593-D594.

Wu, W.K.K.; Wang, G.; Coffelt, S.B.; Betancourt, A.M.; Lee, C.W.; Fan, D.; Wu, K.; Yu, J.; Sung, J.J.Y., Cho, C.H. Emerging roles of the host defense peptide LL-37 in human cancer and its potential therapeutic applications. *Int. J. Cancer.* **2010**, *127*, 1741-1747.

Wu, D.; Gao, Y.; Qi, Y.; Chen, L.; Ma, Y.; Li, Y. Peptide-based cancer therapy: Opportunity and challenge. *Cancer Lett.* **2014**, *351*, 13-22.

Zakeri, B.; Lu, T.K. Synthetic Biology of Antimicrobial Discovery. *ACS Synth. Biol.* **2013**, *2*, 358-372.

Zasloff, M. Antimicrobial peptides of multicellular organisms. *Nature* **2002**, *415*, 389-395.

Zasloff, M. Magainins, a class of antimicrobial peptides from *Xenopus* skin: Isolation, characteritzation of two active forms, and partial cDNA sequence of a precursor. *Proc. Natl. Acad. Sci. USA* **1987**, *84*, 5449-5453.

Zhang, X.X.; Eden, H.S.; Chen, X. Peptides in cancer nanomedicine: Drugs carriers, targeting ligands and protease substrates. *J. Control. Release* **2012**, *159*, 2-13.

CHAPTER 2.

Main Objectives

The main objectives of this PhD thesis can be summarized as follows:

The first objective was the identification of sequences with anticancer activity from the CECMEL11 library of antimicrobial peptides and to study their conjugation to the cell-penetrating γ-peptide **PEG-1** in order to improve their activity. The achievement of this objective involves:

a) Solid-phase synthesis and evaluation of the anticancer activity of the selected peptides from the CECMEL11 library.

b) Solid-phase synthesis of antimicrobial undecapeptide/ γ-peptide **PEG-1** conjugates.

c) Evaluation of the activity of the conjugates against cancer cells and non-malignant cells.

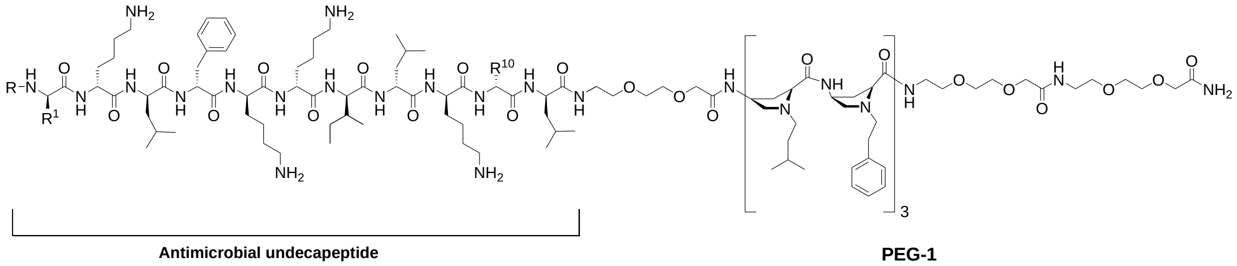
Antimicrobial undecapeptide
PEG-1
R^1
R^{10}
3

The second objective was the development of a suitable solid-phase strategy for the synthesis of fengycin derivatives. Towards this aim, we planned to study:

a) A feasible approach to obtain analogues of the macrolactone of eight amino acids present in fengycins.

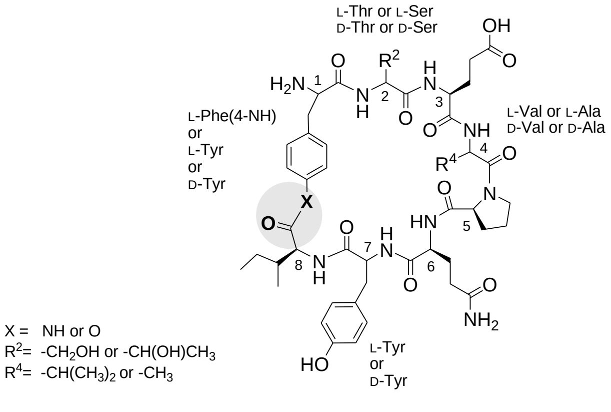
L-Thr or L-Ser
D-Thr or D-Ser
L-Val or L-Ala
D-Val or D-Ala
L-Phe(4-NH)
or
L-Tyr
or
D-Tyr
L-Tyr
or
D-Tyr
X = NH or O
R^2= -CH$_2$OH or -CH(OH)CH$_3$
R^4= -CH(CH$_3$)$_2$ or -CH$_3$

b) A methodology for the preparation of dehydroxy fengycin A, B and S derivatives.

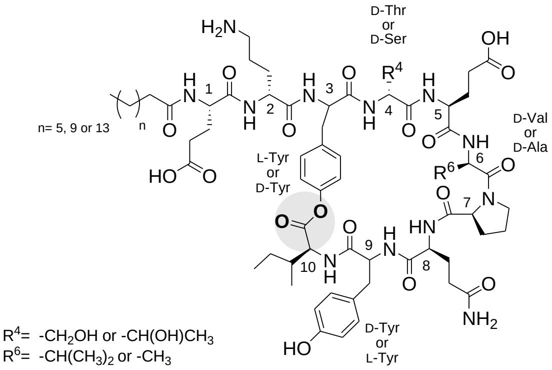
H₂N
D-Thr or D-Ser
OH
R4
n= 5, 9 or 13
n
L-Tyr or D-Tyr
D-Val or D-Ala
HO
O
1 2 3 4 5 6 7 8 9 10
NH₂
HO
D-Tyr or L-Tyr
R4= -CH2OH or -CH(OH)CH3
R6= -CH(CH3)2 or -CH3

CHAPTER 3.

Cell-penetrating γ-peptide/antimicrobial undecapeptide conjugates with anticancer activity

This chapter corresponds to the following publication:

Cristina Rosés[†], Daniel Carbajo[†], Glòria Sanclimens, Josep Farrera-Sinfreu, Adriana Blancafort, Glòria Oliveras, Anna Díaz-Cirac, Eduard Bardají, Teresa Puig[*], Marta Planas, Lidia Feliu[*], Fernando Albericio and Miriam Royo[*]. Cell-penetrating γ-peptide/antimicrobial undecapeptide conjugates with anticancer activity. *Tetrahedron* **2012**, *68*, 4406-4412.

[†] Authors contributed equally to this work

For this publication C.R. contributed to the design of the peptide conjugates and synthesized all these compounds. Moreover, C.R. carried out the cytotoxic assays. C.R. was also involved in argumentations and discussions, and wrote the manuscript draft.

In this study, we combined a cell-penetrating γ-peptide, **PEG-1**, with antimicrobial undecapeptides in order to provide compounds with anticancer properties against MDA-MB-231 human breast cancer cells. We demonstrated that the conjugates were more cytotoxic than **Ac-PEG-1** and the parent undecapeptides. We also evaluated the toxicity of the conjugates against non-malignant cells. The peptide conjugate with the best biological profile was **BP77-PEG-1**, which, at 10 µM, showed a 71% growth inhibition in MDA-MB-231 cells and only a 17% inhibition in non-malignant cells. Therefore, this study suggests that **PEG-1** mediated the undecapeptide delivery into cancer cells and that these conjugates are the proof-of-concept of this strategy to generate improved anticancer drugs based on peptides.

3.1. INTRODUCTION

In spite of great advances in cancer therapy, there is considerable current interest in developing anticancer agents with a new mode of action due to the development of resistance by cancer cells toward current anticancer drugs (Naumov et al., 2003; Mader and Hoskin, 2006; Lage, 2009). A growing number of studies have shown that some antimicrobial peptides, which are toxic to bacteria but not to normal mammalian cells, exhibit a broad spectrum of cytotoxic activity against cancer cells (Jenssen et al., 2006; Eckert, 2011; Mangoni, 2011; Yeung et al., 2011).

Although antimicrobial peptides display a wide structural diversity, many of them are short, cationically charged, and able to form amphipathic secondary structures (Leuschner and Hansel, 2004; Papo and Shai, 2005; Hancock and Sahl, 2006; Hoskin and Ramamoorthy, 2008; Baltzer and Brown, 2011; Brogden and Brogden, 2011; Mohd and Gupta, 2011). Their exact mode of action is not completely understood. However, there is a consensus that antimicrobial peptides act by disrupting negatively charged bacterial and cancer cell membranes to which they are electrostatically attracted, leading to cell lysis and death (Mader and Hoskin, 2006; Hoskin and Ramamoorthy, 2008), unlike currently available conventional drugs, which typically interact with a specific target protein. Upon binding, they disrupt cell membranes, possibly by transient pore formation or disruption of lipid packing (Mader and Hoskin, 2006; Hoskin and Ramamoorthy, 2008). Based on this mode of action, these peptides are unlikely to cause rapid emergence of resistance because it would require significant alteration of membrane composition, which is difficult to occur (Yeaman and Yount, 2003; Peschel and Sahl, 2006; Baltzer and Brown, 2011). In addition, there is increasing evidence that apart from membrane damage, other mechanisms may be involved including intracellular targets (Papo and Shai, 2005; Mader and Hoskin, 2006; Hoskin and Ramamoorthy, 2008; Yeung et al., 2011). Some of these AMPs showed remarkable selectivity to cancer cells versus untransformed proliferating cells (Leuschner and Hansel, 2004; Papo and Shai, 2005; Mader and Hoskin, 2006; Hoskin and Ramamoorthy, 2008).

Despite the excellent properties displayed by antimicrobial peptides, the development of peptide-based drugs is hampered by their limited access to the intracellular space. This obstacle has been tried to overcome by using diverse methods to promote the cellular uptake of exogenous molecules. Cell-penetrating peptides (CPPs) have become one of the most efficient and explored transporters for achieving intracellular access (Stewart et al., 2008; Fonseca et al., 2009). CPPs are usually short cationic sequences and may be derived from [i.e., TAT peptide (Vivès et al., 1997)] or be de novo designed peptides [polyarginine (Mitchell et al., 2000) or transportan (Pooga et al., 1998)]. The conjugation of biologically active peptides to CPPs offers advantages, such as low toxicity and selective and controlled cell delivery compared with other administration vectors (Stewart et al., 2008; Fonseca et al., 2009), being considered a promising strategy for the design of anticancer agents. A drawback of this strategy is the low stability of these CPPs to proteases that it can prevent the drug to reach its target, forcing an increment of the doses to keep the activity and consequently generating an increase in the toxicity. Some alternatives with good protease stability have been described keeping internalizing properties, like diverse oligomers with foldamer properties, such as peptoids (Simon et al., 1992; Wender et al., 2000), arylamide oligomers (Iriondo-Alberdi et al., 2010; Som et al., 2012), β- (Rueping et al., 2002; Umezawa et al., 2002; Potocky et al., 2003, 2005, 2007) and γ-peptides (Farrera-Sinfreu et al., 2004, 2005). Some of these foldamers have not only been explored as potential CPPs, but also as antimicrobial compounds with highly remarkable results (Hamuro et al., 1999; Porter et al., 2000, 2005; Tew et al., 2002, 2010; Liu et al., 2004; Schmitt et al., 2004; Chongsiriwatana et al., 2008; Claudon et al., 2010). Generally both applications derived in similar sequence pattern that combine hydrophobic/aromatic residues with cationic groups. In 2004, Farrera-Sinfreu and co-workers described a new family of γ-peptides hexamers based on the trifunctional amino acid *cis* 4-aminoproline that adopt a C9 ribbon in H_2O (Farrera-Sinfreu et al., 2004). This adopted secondary structure gives to these peptides a tridimensional pattern with high amphipaticity character that contribute to their internalization properties. Series of these γ-peptide diversely functionalized on the N^{α} of *cis* 4-aminoproline were synthesized and have proven capacity for cellular uptake (Farrera-Sinfreu et al., 2005). These peptides also showed low cytotoxicity and high resistance to proteases, properties that convert them in a promising class of CPPs, specially peptide **1** that showed a 40% of internalization capacity compared to TAT peptide (*Figure 3.1*) considered a gold standard in the field.

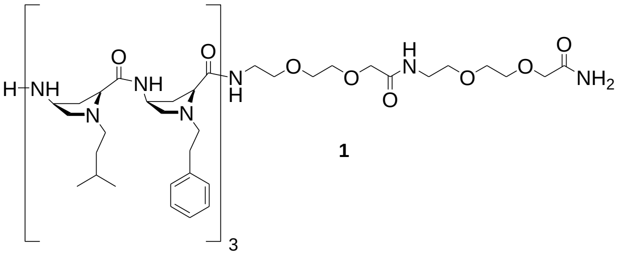

1

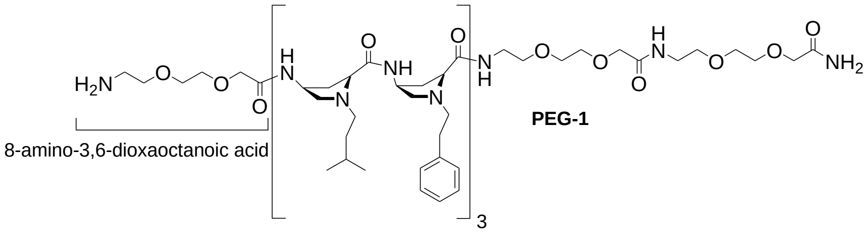

PEG-1

	Peptide:	Conjugate:
BP15	**K**KLFKKILK**V**L	**BP15-PEG-1**
BP33	**L**KLFKKILK**V**L	**BP33-PEG-1**
BP76	**K**KLFKKILK**F**L	**BP76-PEG-1**
BP77	**Ac-K**KLFKKILK**F**L	**BP77-PEG-1**
BP101	**Ac**-**K**KLFKKILK**Y**L	**BP101-PEG-1**
BP125	**Ts**-**K**KLFKKILK**K**L	**BP125-PEG-1**
BP126	**Bz**-**K**KLFKKILK**K**L	**BP126-PEG-1**

Figure 3.1. *Structures of the peptide conjugates.*

Recently, Badosa and co-workers designed linear undecapeptides (CECMEL11) to be used in plant protection (Ferre et al., 2006; Badosa et al., 2007). The general structure of this library was R-X^1KLFKKILKX^{10}L-NH_2, where X^1 and X^{10} corresponded to amino acids with various degrees of hydrophobicity and hydrophilicity (Leu, Lys, Phe, Trp, Tyr, Val) and R included different N-terminal derivatizations (H, Ac, Ts, Bz, Bn). The antimicrobial evaluation of the CECMEL11 library led to the identification of peptides with high antibacterial activity (MIC<7.5 µM) and with low hemolysis (2-6% at 50 µM and 8-40% at 150 µM). Based on these properties, these peptides can be considered as good candidates to explore its anticancer activity. Moreover, taking profit of the celluptake properties offered by γ-peptide **1** (see *Figure 3.1*), we decided to design new γ-peptide **1**/CECMEL11 undecapeptide conjugates. The conjugation of these antimicrobial peptides to **1** can promote its internalization, which can interact with intracellular targets increasing the cytotoxic effect, i.e., by disruption of mitochondrial membranes (Horton and Kelley, 2009).

As a linker between the CECMEL11 undecapeptides and γ-peptide **1**, it was decided to use a short monodisperse bifunctional polyethylene glycol (PEG) unit (8-

amino-3,6-dioxaoctanoic acid), generating the peptide **PEG-1**. Polyethylene glycol has many properties that make it an ideal carrier for peptides, such as high water solubility, high mobility in solution and low immunogenicity. PEG is often attached to the N or C termini of peptides (Jain and Jain, 2008). Besides increasing overall size, this modification also protects peptides from exopeptidases and therefore increases their overall stability in vivo.

In this report, we describe the design and synthesis of **PEG-1**/ antimicrobial undecapeptide conjugates. The influence of the γ-peptide on the anticancer activity is also discussed.

3.2. RESULTS AND DISCUSSION

3.2.1. Design and synthesis

The undecapeptides were representative examples of the 125-member CECMEL11 library (Ferre et al., 2006; Badosa et al., 2007). The selected peptides showed a good balance between antimicrobial and hemolytic activities. Their sequences differ from the N-terminal derivatization (H, Ac, Ts or Bz) and the residues at positions 1 (Lys or Leu) and 10 (Val, Phe, Tyr or Lys). Peptide conjugates were designed by linking the corresponding antimicrobial undecapeptide to the cell-penetrating peptide **PEG-1** (*Figure 3.1*).

The parent CECMEL11 undecapeptides **BP15**, **BP33**, **BP76**, **BP77**, **BP101**, **BP125**, and **BP126** were prepared using a Fmoc-Rink-MBHA resin following a standard Fmoc/^{t}Bu strategy (Ferre et al., 2006; Badosa et al., 2007). After the synthesis, peptides were cleaved from the resin by treatment with TFA/triisopropylsilane (TIS)/H_2O. HPLC and ESI-MS analysis of the crude reaction mixtures showed the formation of the expected peptides in good purities (>75%).

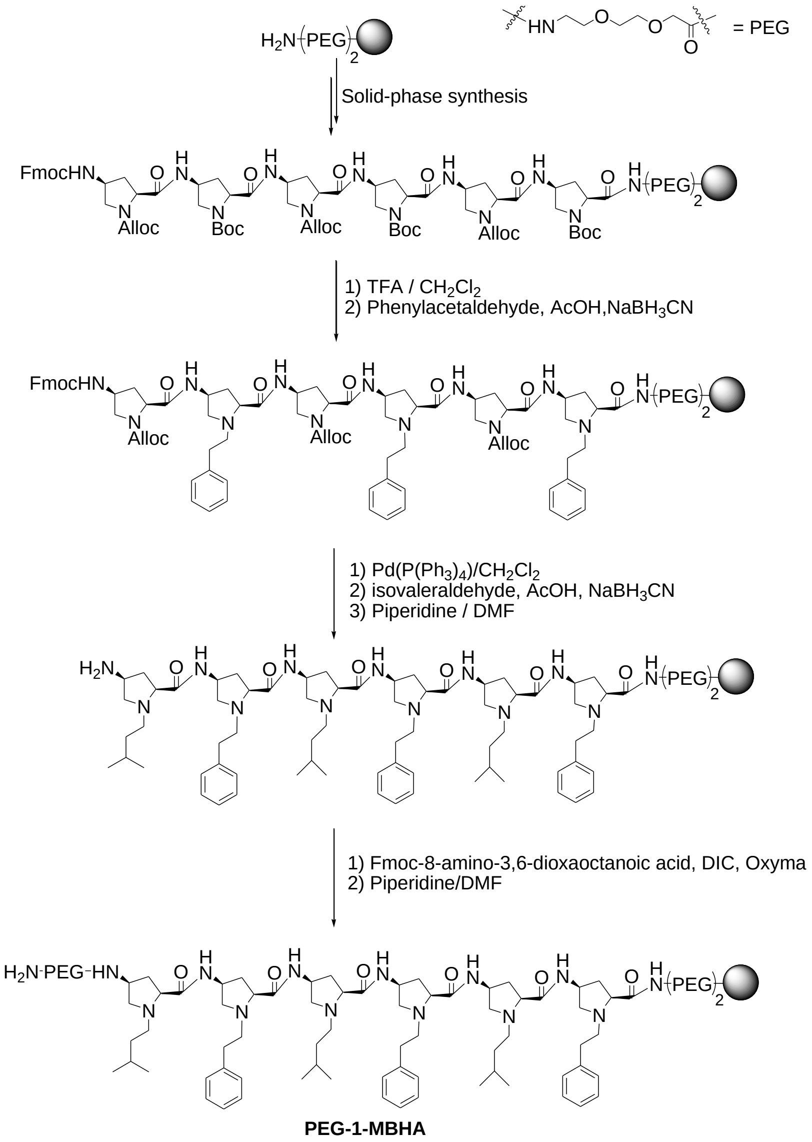
H2N(PEG)2
= PEG
Solid-phase synthesis
FmocHN
Alloc
Boc
1) TFA / CH2Cl2
2) Phenylacetaldehyde, AcOH,NaBH3CN
1) Pd(P(Ph3)4)/CH2Cl2
2) isovaleraldehyde, AcOH, NaBH3CN
3) Piperidine / DMF
1) Fmoc-8-amino-3,6-dioxaoctanoic acid, DIC, Oxyma
2) Piperidine/DMF
H2N-PEG-HN
PEG-1-MBHA

Scheme 3.1. *Solid phase synthesis of* ***PEG-1-MBHA.***

The cell-penetrating peptide **PEG-1** was synthesized on a 4-methylbenzhydrylamine (MBHA) resin following an Fmoc/Alloc/Boc combined solid-phase strategy, a modified version of the previously described (*Scheme 3.1*) (Farrera-Sinfreu et al., 2004, 2005). Instead of the sequential introduction of the alkylation moiety after each monomer coupling, this new strategy allows the simultaneous introduction of the same type of alkylation moiety once the backbone synthesis is finished. This results in a protocol with fewer synthetic steps and cleaner final peptide crudes. The seven conjugates were obtained by stepwise coupling of the corresponding Fmoc-amino acids to the growing peptide chain on the **PEG-1-MBHA** resin (*Scheme 3.2*). The couplings were mediated by ethyl cyanoglyoxylate-2-oxime (Oxyma) and

N,N'-diisopropylcarbodiimide (DIPCDI) in *N*-methylpyrrolidinone (NMP) (Subirós-Funosas et al., 2009). Once the chain assembly was completed, the N-terminal Fmoc group was removed by exposure to piperidine-NMP. **BP15-PEG-1**, **BP33-PEG-1**, and **BP76-PEG-1** were cleaved from the resin by treatment with HF. In the case of N-terminal derivatized conjugates, after removal of the Fmoc group, the resulting peptidyl resins were treated with acetic anhydride (Ac_2O)-pyridine-CH_2Cl_2 (**BP77-PEG-1** and **BP101-PEG-1**), with *p*-toluenesulfonyl chloride (*p*-TsCl), and *N,N'*-diisopropylethylamine (DIEA) (**BP125-PEG-1**) or with benzoyl chloride (BzCl) and DIEA (**BP126-PEG-1**), and then cleaved with HF. The crude peptides were purified by preparative reversed-phase HPLC. The purified peptide conjugates were analyzed by HPLC (≥95% purity) and their structures were confirmed by MALDI-TOF (*Table 3.1*).

For comparison purposes, **Ac-PEG-1** was prepared by acetylation of the **PEG-1-MBHA** resin with Ac_2O-pyridine-CH_2Cl_2 followed by acidolytic cleavage. RP-HPLC purification afforded the pure compound.

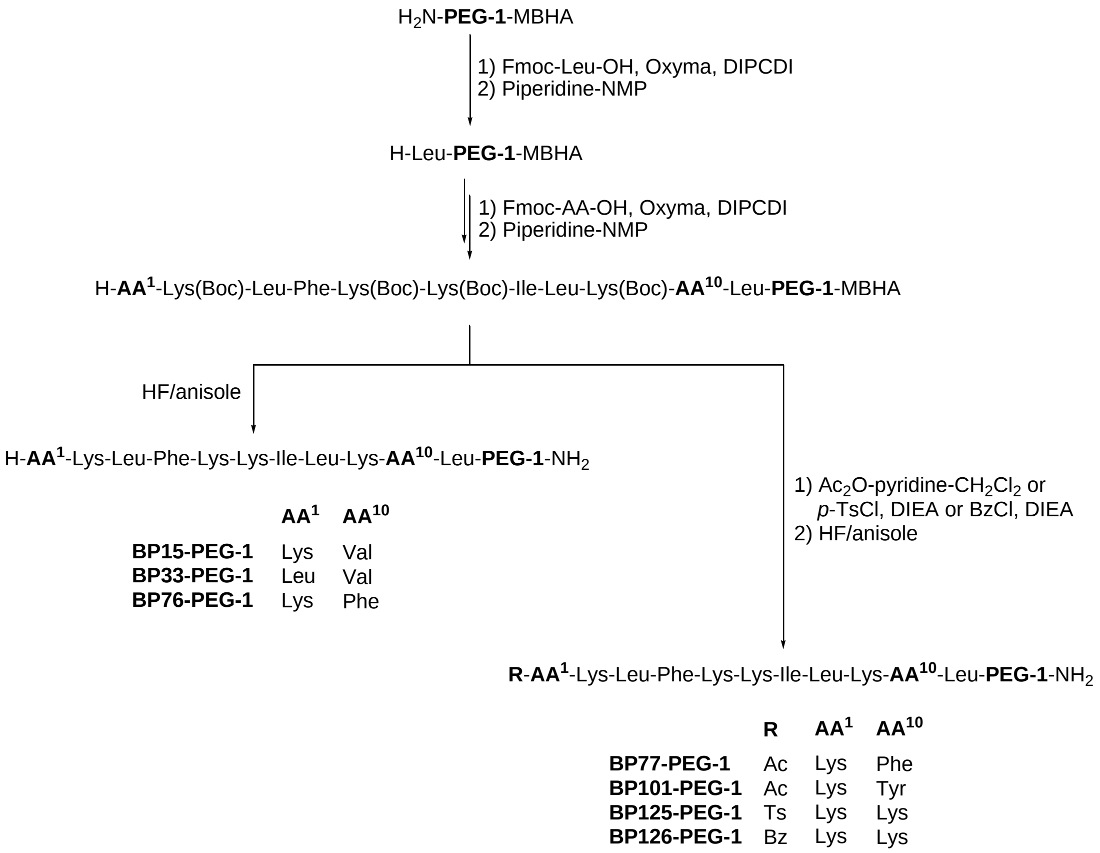
H2N-PEG-1-MBHA
1) Fmoc-Leu-OH, Oxyma, DIPCDI
2) Piperidine-NMP
H-Leu-PEG-1-MBHA
1) Fmoc-AA-OH, Oxyma, DIPCDI
2) Piperidine-NMP
H-AA1-Lys(Boc)-Leu-Phe-Lys(Boc)-Lys(Boc)-Ile-Leu-Lys(Boc)-AA10-Leu-PEG-1-MBHA
HF/anisole
H-AA1-Lys-Leu-Phe-Lys-Lys-Ile-Leu-Lys-AA10-Leu-PEG-1-NH2
AA1 AA10
BP15-PEG-1 Lys Val
BP33-PEG-1 Leu Val
BP76-PEG-1 Lys Phe
1) Ac2O-pyridine-CH2Cl2 or p-TsCl, DIEA or BzCl, DIEA
2) HF/anisole
R-AA1-Lys-Leu-Phe-Lys-Lys-Ile-Leu-Lys-AA10-Leu-PEG-1-NH2
R AA1 AA10
BP77-PEG-1 Ac Lys Phe
BP101-PEG-1 Ac Lys Tyr
BP125-PEG-1 Ts Lys Lys
BP126-PEG-1 Bz Lys Lys

Scheme 3.2. *Solid-phase synthesis of peptide conjugates.*

Table 3.1. *Characterization of peptide conjugates.*

Peptide conjugate	t_R[a] (min)	Purity[b] (%)	ESI
BP15-PEG-1	5.35	93	747.95 $[M+4H]^{4+}$ 996.51 $[M+3H]^{3+}$
BP33-PEG-1	7.43	95	744.11 $[M+4H]^{4+}$ 991.84 $[M+3H]^{3+}$
BP76-PEG-1	7.05	96	759.92 $[M+4H]^{4+}$ 1012.82 $[M+3H]^{3+}$
BP77-PEG-1	7.20	99	770.40 $[M+4H]^{4+}$ 1026.96 $[M+3H]^{3+}$
BP101-PEG-1	7.62	95	774.29 $[M+4H]^{4+}$ 1032.29 $[M+3H]^{3+}$
BP125-PEG-1	7.60	98	793.70 $[M+4H]^{4+}$ 1057.99 $[M+3H]^{3+}$
BP126-PEG-1	7.73	98	781.22 $[M+4H]^{4+}$ 1041.24 $[M+3H]^{3+}$

[a] RP-HPLC retention time. [b] Percentage determined by RP-HPLC at 210 nm of pure compounds.

3.2.2. Cytotoxicity

The anticancer activity of the CECMEL11 undecapeptides and that of the undecapeptides/**PEG-1** conjugates was screened in MDA-MB-231 human breast adenocarcinoma cells by determining the growth inhibition percentage at 10 and 30 µM peptide concentration using the standard 3-(4,5-dimethylthiazol-2-yl)-2,5-diphenyltetrazolium bromide (MTT) assay (Liu et al., 1997; Celis, 1998). MTT is a fast, sensitive, and economical assay that allows to evaluate the antiproliferation properties of different compounds. Growth inhibition values are summarized in *Table 3.2*.

The CECMEL11 undecapeptides showed low activity against breast carcinoma cells at 10 µM. They produced an inhibition percentage of cell growth between 5 and 39%, being the most active compounds **BP76** and the N-terminal derivatized peptides **BP77**, **BP125**, and **BP126** (24-39%). The inhibition percentage of these four peptides increased up to 51-81% at 30 µM. The highest activity was observed for **BP77** (81%). These results pointed out that, in general, N-terminal derivatization seems to be important for the anticancer activity of these peptides.

The **PEG-1**/undecapeptide conjugates were much more effective in inhibiting the growth of MDA-MB-231 adenocarcinoma cells than the CECMEL11 peptides. At 30 µM, the activity of the seven conjugates did not differ from that of **Ac-PEG-1** (>90% inhibition). In contrast, at 10 µM, whereas **Ac-PEG-1** only caused 3% inhibition, peptide conjugates were 10-20 times more active, with inhibition percentages between 34 and 71%. This result indicates that the peptide moiety is responsible for the anticancer activity. The peptide conjugate with the highest cytotoxic activity was **BP77-PEG-1**. As compared with the CECMEL11 parent peptides at 10 µM, conjugation to **PEG-1** increased the activity from 1.2 up to 10-fold. We speculate that the superior cytotoxicity of the peptide conjugates could be attributed to the cell-internalization efficiency of **PEG-1**, which enables the transport of the antimicrobial peptides over the cell membrane, enhancing their activity.

The activity on non-malignant human cells (fibroblasts N1) was also assessed for all the compounds at 10 and 30 µM. CECMEL11 peptides were non toxic, and only **BP77** caused significant growth inhibition at 30 µM (73%). These values correlate with the low hemolytic activity found for these peptides in previous studies (0-6% at 50 µM; 8-40% at 150 µM) (Ferre et al., 2006; Badosa et al., 2007). Modification of the peptides with **PEG-1** resulted in an increase of the cytotoxicity against N1 cells. The percentage of growth inhibition at 30 µM was of 79% for **Ac-PEG-1** and of >90% for all peptide conjugates, pointing out that the toxicity could be mainly attributed to **PEG-1**. Interestingly, at 10 µM the peptide conjugates were not significantly cytotoxic against non-malignant cells. A growth inhibition <10% was observed for four sequences and only two conjugates displayed an inhibition percentage >20%. Notably, **BP77-PEG-1** only produced a 17% of growth inhibition. This low toxicity together with the marked anticancer activity displayed by this peptide conjugate, suggest that **BP77-PEG-1** can be considered a proof-of-concept for future studies that will explore the use of these strategy to produce new anticancer conjugates that combine other anticancer peptides with peptide **1** or related γ-peptides with CPPs properties.

Table 3.2. *Cytotoxicity against MDA-MB-231 cells and non-malignan fibroblast (N1).*

Peptide	**MDA-MB-231 growth inhibition[a] (%)**		**N1 growth inhibition[a] (%)**		**Peptide conjugate**	**MDA-MB-231 growth inhibition[a] (%)**		**N1 growth inhibition[a] (%)**	
	10 μM	**30 μM**	**10 μM**	**30 μM**		**10 μM**	**30 μM**	**10 μM**	**30 μM**
					Ac-PEG-1	3±0.06	93±0.01	na[c]	79±0.08
BP15	5±0.04	12±0.03	na[c]	2±0.14	**BP15-PEG-1**	34±0.06	93±0.01	16±0.01	92±0.01
BP33	5±0.02	16±0.01	na[c]	na[c]	**BP33-PEG-1**	49±0.06	92±0.01	9±0.05	93±0.01
BP76	39±0.09	51±0.03	na[c]	na[c]	**BP76-PEG-1**	49±0.04	92±0.01	9±0.09	93±0.01
BP77	32±0.03	81±0.02	na[c]	73±0.07	**BP77-PEG-1**	71±0.02	92±0.01	17±0.14	93±0.01
BP101	-[b]	-	-	-	**BP101-PEG-1**	49±0.09	92±0.01	28±0.10	93±0.01
BP125	28±0.02	62±0.02	na[c]	5±0.16	**BP125-PEG-1**	59±0.06	92±0.01	25±0.07	93±0.01
BP126	24±0.05	61±0.05	na[c]	16±0.10	**BP126-PEG-1**	47±0.13	92±0.01	na[c]	93±0.01

[a] Percentage of cell growth inhibition plus standard deviation. Values were obtained from duplicate experiments performed in triplicate. [b] Not determined. [c] na: non active.

3.3. CONCLUSIONS

In summary, we have showed that by combining an antimicrobial peptide and a cell-penetrating γ-peptide effective anticancer agents are obtained. The efficacy of CECMEL11 undecapeptides toward breast cancers cells was several folds higher when conjugated to **PEG-1** as compared to treatment with antimicrobial peptides alone. This result suggests that the covalent linking to **PEG-1** was able to successfully deliver peptides into the cancer cells, enhancing their efficiency. Moreover, the most active peptide conjugate **BP77-PEG-1** also showed low toxicity against normal cells. These results constitute a proof of the usefulness of these γ-peptides as cellular transporters and open the possibility to conjugate them to other therapeutic peptides with the aim to improve their action.

3.4. EXPERIMENTAL SECTION

3.4.1. General methods

Commercially available reagents were used throughout without purification. **PEG-1**, **Ac-PEG-1**, and peptide conjugates were analyzed under standard analytical RP-HPLC conditions with a Waters liquid chromatography instrument equipped with a UV/vis detector. Analysis was carried out with a Symmetry C_{18} (150 mm×4.6 mm, 5µm) column using a 0-100% B linear gradient over 15 min at a flow rate of 1 ml/min. Solvent A was 0.1% aq TFA, and solvent B was 0.1% TFA in CH_3CN. Detection was performed at 210 nm.

Undecapeptides were analyzed under standard analytical HPLC conditions with a Dionex liquid chromatography instrument composed of a UV/vis Dionex UVD170U detector, a P680 Dionex bomb, an ASI-100 Dionex automatic injector, and CHROMELEON 6.60 software. Detectionwas performed at 220 nm. Analysis was carried out with a Kromasil 100 C_{18} (40 mm×4.6 mm, 3.5 µm) column with a 2-100% B linear gradient over 7 min at a flow rate of 1 ml/min. Solvent A was 0.1% aq TFA, and solvent B was 0.1% TFA in CH_3CN.

Undecapeptides ESI-MS analyses were performed with an Esquire 6000 ESI ion Trap LC/MS (Bruker Daltonics) instrument equipped with an electrospray ion source. The instrument was operated in the positive ESI(+) ion mode. Samples (5 µl) were introduced into the mass spectrometer ion source directly through an HPLC autosampler. The mobile phase (80:20 CH_3CN/H_2O at a flow rate of 100 µl/min) was delivered by a 1100 Series HPLC pump (Agilent). Nitrogen was employed as both the drying and nebulizing gas.

PEG-1 and the conjugates HPLC-ESI analyses were performed on Waters Alliance 2695 chromatography system equipped with Waters 995 photodiode array detector and ESI-MS Waters Micromass ZQ on a Symmetry column with linear gradients of B: CH_3CN (with 0.1% TFA) in A: H_2O (with 0.1% TFA) at a flow rate of 1ml/min.

Mass spectra were recorded on a MALDI Voyager DE RP time-of-flight (TOF) spectrometer (Applied Biosystems, Framingham). 2,5-Dihydroxybenzoic acid (DHB) was used as a matrix and was purchased from Aldrich.

3.4.1.1. General method for solid-phase synthesis of CECMEL11 undecapeptides

Peptides were synthesized manually by the solid-phase method using standard Fmoc chemistry. Fmoc-Rink-MBHA resin (0.56 mmol/g) was used as solid support. Couplings of the corresponding amino acids Fmoc-Leu-OH, Fmoc-Phe-OH, Fmoc-Lys(Boc)-OH, Fmoc-Ile-OH, Fmoc-Val-OH, and Fmoc-Tyr(^{t}Bu)-OH (4 equiv) were performed using ethyl cyanoglyoxylate-2-oxime (4 equiv), *N,N'*-diisopropylcarbodiimide (DIPCDI) (4 equiv) in DMF at room temperature for 1 h. The completion of the reactions was monitored by the Kaiser test (Kaiser et al., 1970). Fmoc group removal was achieved with piperidine/DMF (3:7, 1×2 min+1x10 min). After each coupling and deprotection step, the resin was washed with DMF (6×1 min) and CH_2Cl_2 (3×1 min) and air-dried. Once the peptide sequence was completed, the Fmoc group was removed and, when required, the resulting peptidyl resin was derivatized. Acidolytic cleavage was performed by treatment of the resin with

TFA/H_2O/triisopropylsilane (TIS) (95:2.5:2.5) for 2 h at room temperature. Following TFA evaporation and Et_2O extraction, the crude peptide was dissolved in H_2O/CH_3CN, lyophilized, analyzed by HPLC, and characterized by MS-ESI.

KKLFKKILKVL-NH_2 (BP15). Starting from resin Fmoc-Rink-MBHA (50 mg), sequential couplings of the corresponding Fmoc-protected amino acids and removal of the Fmoc group, followed by acidolytic cleavage afforded **BP15** (24 mg, 89% purity). t_R=4.39 min. MS (ESI): m/z=1356.83 $[M + H]^+$.

LKLFKKILKVL-NH_2 (BP33). Starting from resin Fmoc-Rink-MBHA (50 mg), sequential couplings of the corresponding Fmoc-protected amino acids and removal of the Fmoc group, followed by acidolytic cleavage afforded **BP33** (26 mg, 92% purity). t_R=4.46 min. MS (ESI): m/z=1341.81 $[M + H]^+$.

KKLFKKILKFL-NH_2 (BP76). Starting from resin Fmoc-Rink-MBHA (50 mg), sequential couplings of the corresponding Fmoc-protected amino acids and removal of the Fmoc group, followed by acidolytic cleavage afforded **BP76** (20 mg, 82% purity). t_R=4.20 min. MS (ESI): m/z=1404.87 $[M + H]^+$.

Ac-KKLFKKILKFL-NH_2 (BP77). Synthesis started from resin Fmoc-Rink-MBHA (50 mg) and after sequential couplings of the corresponding Fmoc-protected amino acids and removal of the Fmoc group, the resulting resin was treated with acetic anhydride–pyridine–CH_2Cl_2 (1:1:1, 2×30 min) and then washed with CH_2Cl_2 (3×2 min), NMP (3×2 min) and CH_2Cl_2 (6×1 min). Acidolytic cleavage afforded **BP77** (19 mg, 75% purity). t_R=4.72 min. MS (ESI): m/z=1446.91 $[M+H]^+$.

Ac-KKLFKKILKYL-NH_2 (BP101). Synthesis started from resin Fmoc-Rink-MBHA (50 mg) and after sequential couplings of the corresponding Fmoc-protected amino acids and removal of the Fmoc group, the resulting resin was treated with acetic anhydride–pyridine–CH_2Cl_2 (1:1:1, 2×30 min) and then washed with CH_2Cl_2 (3×2 min), NMP (3×2 min) and CH_2Cl_2 (6×1 min). Acidolytic cleavage afforded **BP101** (22 mg, 82% purity). t_R=4.56 min. MS (ESI): m/z=1462.91 $[M+H]^+$.

Ts-KKLFKKILKKL-NH_2 (BP125). Synthesis started from resin Fmoc-Rink-MBHA (50 mg) and after sequential couplings of the corresponding Fmoc-protected amino acids and removal of the Fmoc group, the resulting resin was treated with *p*-

toluenesulphonyl chloride (40 equiv) and DIEA (80 equiv) in CH_2Cl_2−NMP (9:1) for 1h and then washed with CH_2Cl_2 (3×2 min), NMP (3×2 min) and CH_2Cl_2 (6×1 min). Acidolytic cleavage afforded **BP125** (18 mg, 76% purity). t_R=4.53 min. MS (ESI): *m/z*=1540.06 $[M+H]^+$.

Bz-KKLFKKILKKL-NH$_2$ (BP126). Synthesis started from resin Fmoc-Rink-MBHA (50 mg) and after sequential couplings of the corresponding Fmoc-protected amino acids and removal of the Fmoc group, the resulting resin was treated with benzoyl chloride (40 equiv) and DIEA (80 equiv) in CH_2Cl_2−NMP (9:1) for 1 h and then washed with CH_2Cl_2 (3×2 min), NMP (3×2 min) and CH_2Cl_2 (6×1 min). Acidolytic cleavage afforded **BP126** (19 mg, 77% purity). t_R=4.63 min. MS (ESI): *m/z*=1489.98 $[M+H]^+$.

3.4.1.2. PEG-1-MBHA resin synthesis

PEG-1 peptidyl resin was synthesized manually by the solid-phase method using MBHA resin (500 mg, 0.63 mmol/g) as solid support following a combined Fmoc/Boc/Alloc strategy. Peptide synthesis was performed manually in a polypropylene syringe fitted with a polyethylene porous disc. Solvents and soluble reagents were removed by suction. Washings between deprotection, coupling, and subsequent deprotection steps were carried out with DMF (5×1 min) and CH_2Cl_2 (5×1 min) using 10 mL solvent/g resin for each wash.

Two units of Fmoc-8-amine-3,6-dioxaoctanoic acid were coupled consecutively to the resin using standard DIPCDI/HOBt coupling system (3 equiv). Then, alternate incorporations of Fmoc-Amp(Boc)- OH (3 equiv) and Fmoc-Amp(Alloc)-OH (3 equiv) were carried out with DIPCDI (3 equiv) and ethyl cyanoglyoxyl-2-oxime (3 equiv) in DMF for 2 h. The resin was washed with DMF (5×1 min) and CH_2Cl_2 (5×1 min) after each coupling. Couplings were monitored by the Kaiser test (Kaiser et al., 1970). Once the alternate Boc/Alloc α-amino protected skeleton had been built, the N^{α}-Boc protecting group was removed, alkylation of the amino group was performed by on-resin reductive amination using phenylacetaldehyde (5 equiv for each amine) in 1% HOAc in DMF for 30 min and then treating the resin with $NaBH_3CN$ (5 equiv for each amine) in CH_3OH for 2 h. After that, the resin was washed with DMF (5×1 min) and CH_2Cl_2 (5×1 min). Alkylation was monitored by chloranil test (Christensen, 1979). Then, N^{α}-Alloc protecting group was removed with $Pd(PPh_3)_3$/PhSiH (0.1:10) (2×10min in CH_2Cl_2) and alkylation with isovaleraldehyde was performed as above. After removal of last Fmoc protecting group (which provided **1-MBHA**) an aliquot of **PEG-1-MBHA** was cleaved to check the peptidyl resin quality by acidolytic cleavage with HF and **PEG-1** was obtained, which was dissolved in H_2O/CH_3CN, lyophilized and analyzed by HPLC (88% purity). t_R=6.28 min. MS (MALDI-TOF): *m/z*=1503.85 $[M+H]^+$, 1525.85 $[M+Na]^+$. ESI found: 752.8; 502.3.

Finally, an additional unit of Fmoc-8-amine-3,6-dioxaoctanoic acid was ad added to the 1-MBHA resin as described above rendering **PEG-1-MBHA**-resin.

Part of the **PEG-1-MBHA** resin (100 mg) was treated with acetic anhydride-pyridine-CH_2Cl_2 (1:1:1, 2×30 min) and then washed with CH_2Cl_2 (3×2 min), NMP (3×2 min), and CH_2Cl_2 (6×1 min). Acidolytic cleavage of the resulting resin afforded **Ac-PEG-1**.

3.4.1.3. General method for solid-phase synthesis of peptide conjugates

PEG-1-MBHA resin was divided on seven parts and on each one was built one of the antimicrobial peptides selected following an Fmoc/^{t}Bu strategy on a standard solid-phase peptide synthesis. Couplings of the corresponding amino acids Fmoc-Leu-OH, Fmoc-Phe-OH, Fmoc-Lys(Boc)-OH, Fmoc-Ile-OH, Fmoc-Val-OH, and Fmoc-Tyr(^{t}Bu)-OH (4 equiv) were performed using ethyl cyanoglyoxylate-2-oxime (4 equiv), DIPCDI (4 equiv) in NMP at room temperature for 3 h. The completion of the reactions was monitored by the Kaiser test (Kaiser et al., 1970). Fmoc group removal was achieved with piperidine/NMP (3:7, 1×2+2×10 min). After each coupling and deprotection step, the resin was washed with NMP (6×1 min) and CH_2Cl_2 (3×1 min) and air-dried. Once the peptide sequence was completed, the N-terminal Fmoc group was removed and, when required, the resulting peptidyl resin was derivatized.

Acidolytic cleavage was performed by treating the resin with HF in the presence of 10% anisole for 1 h at 0 ºC. Peptides were precipitated with cold anhydrous TMBE, dissolved in HOAc, and then lyophilized. Crude peptides were purified by preparative HPLC using a linear gradient of CH_3CN (containing 1% of TFA) and H_2O (containing 1% of TFA). The purity of each fraction was verified by analytical HPLC, HPLC-MS, and MALDI-TOF.

KKLFKKILKVL-PEG-1 (BP15-PEG-1). Starting from resin **PEG-1-MBHA** (100 mg), sequential couplings of the corresponding Fmoc-protected amino acids and removal of the Fmoc group, followed by acidolytic cleavage afforded **BP15-PEG-1**, which was purified by preparative HPLC (8 mg, 93% purity). MS (MALDI-TOF): m/z=747.95 $[M+4H]^{4+}$, 996.51 $[M+3H]^{3+}$.

LKLFKKILKVL-PEG-1 (BP33-PEG-1). Starting from resin **PEG-1-MBHA** (100 mg), sequential couplings of the corresponding Fmoc-protected amino acids and removal of the Fmoc group, followed by acidolytic cleavage afforded **BP33-PEG-1**, which was purified by preparative HPLC (16 mg, 95% purity). MS (MALDI-TOF): m/z=744.11 $[M+4H]^{4+}$, 991.84 $[M+3H]^{3+}$.

KKLFKKILKFL-PEG-1 (BP76-PEG-1). Starting from resin **PEG-1-MBHA** (100 mg), sequential couplings of the corresponding Fmoc-protected amino acids and removal of the Fmoc group, followed by acidolytic cleavage afforded **BP76-PEG-1**, which was purified by preparative HPLC (12 mg, 96% purity). MS (MALDI-TOF): m/z=759.92 $[M+4H]^{4+}$, 1012.82 $[M+3H]^{3+}$.

Ac-KKLFKKILKFL-PEG-1 (BP77-PEG-1). Synthesis started from resin **PEG-1-MBHA** (100 mg) and after sequential couplings of the corresponding Fmoc-protected amino acids and removal of the Fmoc group, the resulting resin was treated with acetic anhydride-pyridine-CH_2Cl_2 (1:1:1, 2×30 min) and then washed with CH_2Cl_2 (3×2 min), NMP (3×2 min) and CH_2Cl_2 (6×1 min). Acidolytic cleavage afforded **BP77-PEG-1**, which was purified by preparative HPLC (18 mg, 99% purity). MS (MALDI-TOF): m/z=770.40 $[M+4H]^{4+}$, 1026.96 $[M+3H]^{3+}$.

Ac-KKLFKKILKYL-PEG-1 (BP101-PEG-1). Synthesis started from resin **PEG-1-MBHA** (100 mg) and after sequential couplings of the corresponding Fmoc-protected amino acids and removal of the Fmoc group, the resulting resin was treated with acetic anhydride-pyridine-CH_2Cl_2 (1:1:1, 2×30 min) and then washed with CH_2Cl_2 (3×2 min), NMP (3×2 min) and CH_2Cl_2 (6×1 min). Acidolytic cleavage afforded **BP101-PEG-1**, which was purified by preparative HPLC (2 mg, 95% purity). MS (MALDI-TOF): m/z=774.29 $[M+4H]^{4+}$, 1032.29 $[M+3H]^{3+}$.

Ts-KKLFKKILKKL-PEG-1 (BP125-PEG-1). Synthesis started from resin **PEG-1-MBHA** (100 mg) and after sequential couplings of the corresponding Fmoc-protected amino acids and removal of the Fmoc group, the resulting resin was treated with *p*-toluenesulfonyl chloride (40 equiv) and DIEA (80 equiv) in CH_2Cl_2-NMP (9:1) for 1 h and then washed with CH_2Cl_2 (3×2 min), NMP (3×2 min), and CH_2Cl_2 (6×1 min). Acidolytic cleavage afforded **BP125-PEG-1**, which was purified by preparative HPLC (17 mg, 98% purity). MS (MALDI-TOF): m/z=793.70 $[M+4H]^{4+}$, 1057.99 $[M+3H]^{3+}$.

Bz-KKLFKKILKKL-PEG-1 (BP126-PEG-1). Synthesis started from resin **PEG-1-MBHA** (100 mg) and after sequential couplings of the corresponding Fmoc-protected amino acids and removal of the Fmoc group, the resulting resin was treated with benzoyl chloride (40 equiv) and DIEA (80 equiv) in CH_2Cl_2-NMP (9:1) for 1 h and then washed with CH_2Cl_2 (3×2 min), NMP (3×2 min), and CH_2Cl_2 (6×1 min). Acidolytic cleavage afforded **BP126-PEG-1**, which was purified by preparative HPLC (18 mg, 98% purity). MS (MALDI-TOF): m/z=781.22 $[M+4H]^{4+}$, 1041.24 $[M+3H]^{3+}$.

3.4.2. Cell lines and cell culture

MDA-MB-231 human breast Caucasian adenocarcinoma cells were obtained from the ATCC (American Type Culture Collection Rockville, MD, USA). Cells were routinely grown in Dulbecco's modified Eagle's medium (DMEM, Gibco, Berlin, Germany) containing 10% fetal bovine serum (FBS, Bio-Whittaker, Walkersville, MD, USA), 1% L-glutamine, 1% sodium pyruvate, 50 U/ml penicillin, and 50 µg/ml streptomycin (Gibco). The cells remained free of *Mycoplasma* and were propagated in adherent culture according to established protocols. Cells were maintained at 37 ºC in a humidified atmosphere of 95% air and 5% CO_2.

3.4.3. Cell growth inhibition assay

Peptides were dissolved in sterile Phosphate Saline Buffer (PBS) to get a final stock solution of 3200 µM. Sensitivity was determined using a standard colorimetric MTT assay. Briefly, MDA-MB-231 cells were plated out at a density of 7×10^3 cells/100 µl/well in 96-well microtiter plates and allowed an overnight period for attachment. Then, the medium was removed and fresh medium along with the corresponding peptide concentration (10 or 30 µM) were added to the cultures. Agents were not renewed during the 48 h of cell exposure, and control cells without agents were cultured under the same conditions. Following treatment, cells were fed with drug-free medium (100 µl/well) and MTT solution (10 µl, 5 mg/ml in PBS), and incubation was prolonged for 3 h at 37 ºC. After carefully removing the supernatants, the MTT-formazan crystals formed by metabolically viable cells were dissolved in dimethyl sulfoxide (DMSO,100 µl/well) and the absorbance was measured at 570 nm in a multi-well plate reader (Model SPECTRAmax 340 PC (380) reader). Using control optical density (OD) values©, test OD values (T), and time zero OD values (T_0), the growth inhibition (IC value) at every concentration was calculated from the equation, $100\times[(T-T_0)/(C-T_0)]=IC$.

3.5. REFERENCES

Badosa, E.; Ferre, R.; Planas, M.; Feliu, L.; Besalú, E.; Cabrefiga, J.; Bardají, E.; Montesinos, E. A Library of Linear Undecapeptides with Bactericidal Activity against Phytopathogenic Bacteria. *Peptides* **2007**, *28*, 2276–2285.

Baltzer, S. a; Brown, M. H. Antimicrobial Peptides: Promising Alternatives to Conventional Antibiotics. *J. Mol. Microbiol. Biotechnol.* **2011**, *20*, 228–235.

Brogden, N. K.; Brogden, K. A. Will New Generations of Modified Antimicrobial Peptides Improve Their Potential as Pharmaceuticals? *Int. J. Antimicrob. Agents* **2011**, *38*, 217–225.

Celis, J. E. *MTT-Cell Proliferation Assay; in Cell Biology: A Laboratory Handbook*; 2nd Editio.; Academic Press: London, 1998; Vol. 1, pp. 16–18.

Chongsiriwatana, N. P.; Patch, J. A.; Czyzewski, A. M.; Dohm, M. T.; Ivankin, A.; Gidalevitz, D.; Zuckermann, R. N.; Barron, A. E. Peptoids That Mimic the Structure, Function, and Mechanism of Helical Antimicrobial Peptides. *Proc. Natl. Acad. Sci. U. S. A.* **2008**, *105*, 2794–2799.

Christensen, T. A Qualitative Test for Monitoring Coupling Completeness in Solid Phase Peptide Synthesis Using Chloranil. *Acta Chemica Scandinavica*, 1979, *33b*, 763–766.

Claudon, P.; Violette, A.; Lamour, K.; Decossas, M.; Fournel, S.; Heurtault, B.; Godet, J.; Mély, Y.; Jamart-Grégoire, B.; Averlant-Petit, M. C.; et al. Consequences of Isostructural Main-Chain Modifications for the Design of Antimicrobial Foldamers: Helical Mimics of Host-Defense Peptides Based on a Heterogeneous Amide/urea Backbone. *Angew. Chemie - Int. Ed.* **2010**, *49*, 333–336.

Eckert, R. Road to Clinical Efficacy: Challenges and Novel Strategies for Antimicrobial Peptide Development. *Future Microbiol.* **2011**, *6*, 635–651.

Farrera-Sinfreu, J.; Zaccaro, L.; Vidal, D.; Salvatella, X.; Giralt, E.; Pons, M.; Albericio, F.; Royo, M. A New Class of Foldamers Based on Cis-γ-Amino-L-Proline. *J. Am. Chem. Soc.* **2004**, *126*, 6048–6057.

Farrera-Sinfreu, J.; Giralt, E.; Castel, S.; Albericio, F.; Royo, M. Cell-Penetrating Cis-γ-Amino-L-Proline-Derived Peptides. *J. Am. Chem. Soc.* **2005**, *127*, 9459–9468.

Ferre, R.; Badosa, E.; Feliu, L.; Planas, M.; Montesinos, E.; Bardajı, E. Inhibition of Plant-Pathogenic Bacteria by Short Synthetic Cecropin A-Melittin Hybrid Peptides. *Appl. evironmental Microbiol.* **2006**, *72*, 3302–3308.

Fonseca, S. B.; Pereira, M. P.; Kelley, S. O. Recent Advances in the Use of Cell-Penetrating Peptides for Medical and Biological Applications. *Adv. Drug Deliv. Rev.* **2009**, *61*, 953–964.

Hamuro, Y.; Schneider, J. P.; DeGrado, W. F. De Novo Design of Antibacterial *β*-Peptides. *J. Am. Chem. Soc.* **1999**, *121*, 12200–12201.

Hancock, R. E. W.; Sahl, H.-G. Antimicrobial and Host-Defense Peptides as New Anti-Infective Therapeutic Strategies. *Nat. Biotechnol.* **2006**, *24*, 1551–1557.

Horton, K. L.; Kelley, S. O. Engineered Apoptosis-Inducing Peptides with Enhanced Mitochondrial Localization and Potency. *J. Med. Chem.* **2009**, *52*, 3293–3299.

Hoskin, D. W.; Ramamoorthy, A. Studies on Anticancer Activities of Antimicrobial Peptides. *Biochim. Biophys. Acta* **2008**, *1778*, 357–375.

Iriondo-Alberdi, J.; Laxmi-Reddy, K.; Bouguerne, B.; Staedel, C.; Huc, I. Cellular Internalization of Water-Soluble Helical Aromatic Amide Foldamers. *ChemBioChem* **2010**, *11*, 1679–1685.

Jain, A.; Jain, S. K. PEGylation: An Approach for Drug Delivery. A Review. *Crit. Rev. Ther. Drug Carr. Syst.* **2008**, *25*, 403–447.

Jenssen, H.; Hamill, P.; Hancock, R. E. W. Peptide Antimicrobial Agents. *Clin. Microbiol. Rev.* **2006**, *19*, 491–511.

Kaiser, E.; Colescott, R. L.; Bossinger, C. D.; Cook, P. Color Test for Detection of Free Terminal Amino Groups in the Solid-Phase Synthesis of Peptides. *Anal. Biochem.* **1970**, 595–598.

Lage, H. Proteomic Approaches for Investigation of Therapy Resistance in Cancer. *Proteomics - Clin. Appl.* **2009**, *3*, 883–911.

Leuschner, C.; Hansel, W. Membrane Disrupting Lytic Peptides for Cancer Treatments. *Curr. Pharm. Des.* **2004**, *10*, 2299–2310.

Liu, D.; Choi, S.; Chen, B.; Doerksen, R. J.; Clements, D. J.; Winkler, J. D.; Klein, M. L.; DeGrado, W. F. Nontoxic Membrane-Active Antimicrobial Arylamide Oligomers. *Angew. Chem. Int. Ed. Engl.* **2004**, *43*, 1158–1162.

Liu, Y.; Peterson, D. A.; Kimura, H.; Schubert, D. Mechanism of Cellular 3-(4,5-Dimethylthiazol-2-yl)-2,5-Diphenyltetrazolium Bromide (MTT) Reduction. *J. Neurochem.* **1997**, *69*, 581–593.

Mader, J. S.; Hoskin, D. W. Cationic Antimicrobial Peptides as Novel Cytotoxic Agents for Cancer Treatment. *Expert Opin. Investig. Drugs* **2006**, *15*, 933–946.

Mangoni, M. L. Host-Defense Peptides: From Biology to Therapeutic Strategies. *Cell. Mol. Life Sci.* **2011**, *68*, 2157–2159.

Mitchell, D. J.; Kim, D.; Steinman, L. A.; Fathman, C. G.; Rothbard, J. B. Polyarginine Enters Cells More Efficiently than Other Polycationic Homopolymers. *J. Pept. Res.* **2000**, *56*, 318–325.

Mohd, A.; Gupta, U. S. Antimicrobial Peptides and Their Mechanism of Action. *Res. J. Biotechnol.* **2011**, *6*, 71–79.

Naumov, G. N.; Townson, J. L.; MacDonald, I. C.; Wilson, S. M.; Bramwell, V. H. C.; Groom, A. C.; Chambers, A. F. Ineffectiveness of Doxorubicin Treatment on Solitary Dormant Mammary Carcinoma Cells or Late-Developing Metastases. *Breast Cancer Res. Treat.* **2003**, *82*, 199–206.

Papo, N.; Shai, Y. Host Defense Peptides as New Weapons in Cancer Treatment. *Cell. Mol. Life Sci.* **2005**, *62*, 784–790.

Peschel, A.; Sahl, H.-G. The Co-Evolution of Host Cationic Antimicrobial Peptides and Microbial Resistance. *Nat. Rev. Microbiol.* **2006**, *4*, 529–536.

Pooga, M.; Hällbrink, M.; Zorko, M.; Langel, U. Cell Penetration by Transportan. *FASEB J.* **1998**, *12*, 67–77.

Porter, E. A.; Wang, X.; Lee, H.-S.; Weisblum, B.; Gellman, S. H. Non-Haemolytic *β*-Amino-Acid Oligomers. *Nature* **2000**, *404*, 565.

Porter, E. A.; Weisblum, B.; Gellman, S. H. Use of Parallel Synthesis to Probe Structure-Activity Relationships among 12-Helical *β*-Peptides: Evidence of a Limit on Antimicrobial Activity. *J. Am. Chem. Soc.* **2005**, *127*, 11516–11529.

Potocky, T. B.; Menon, A. K.; Gellman, S. H. Cytoplasmic and Nuclear Delivery of a TAT-Derived Peptide and a *β*-Peptide after Endocytic Uptake into HeLa Cells. *J. Biol. Chem.* **2003**, *278*, 50188–50194.

Potocky, T. B.; Menon, A. K.; Gellman, S. H. Effects of Conformational Stability and Geometry of Guanidinium Display on Cell Entry by *β*-Peptides. *J. Am. Chem. Soc.* **2005**, *127*, 3686–3687.

Potocky, T. B.; Silvius, J.; Menon, A. K.; Gellman, S. H. HeLa Cell Entry by Guanidinium-Rich *β*-Peptides: Importance of Specific Cation– Cell Surface Interactions. *ChemBioChem* **2007**, *8*, 917–926.

Rueping, M.; Mahajan, Y.; Sauer, M.; Seebach, D. Cellular Uptake Studies with *β*-Peptides. *ChemBioChem* **2002**, *3*, 257–259.

Schmitt, M. A.; Weisblum, B.; Gellman, S. H. Unexpected Relationships between Structure and Function in *α,β*-Peptides: Antimicrobial Foldamers with Heterogeneous Backbones. *J. Am. Chem. Soc.* **2004**, *126*, 6848–6849.

Simon, R. J.; Kania, R. S.; Zuckermann, R. N.; Huebner, V. D.; Jewell, D. A.; Banville, S.; Ng, S.; Wang, L.; Rosenberg, S.; Marlowe, C. K.; et al. Peptoids: A Modular Approach to Drug Discovery. *Proc. Natl. Acad. Sci. U. S. A.* **1992**, *89*, 9367–9371.

Som, A.; Xu, Y.; Scott, R. W.; Tew, G. N. Anion Mediated Activation of Guanidine Rich Small Molecules. *Org. Biomol. Chem.* **2012**, *10*, 40–42.

Stewart, K. M.; Horton, K. L.; Kelley, S. O. Cell-Penetrating Peptides as Delivery Vehicles for Biology and Medicine. *Org. Biomol. Chem.* **2008**, *6*, 2242–2255.

Subirós-Funosas, R.; Prohens, R.; Barbas, R.; El-Faham, A.; Albericio, F. Oxyma: An Efficient Additive for Peptide Synthesis to Replace the Benzotriazole-Based HOBt and HOAt with a Lower Risk of Explosion. *Chem. a Eur. J.* **2009**, *15*, 9394–9403.

Tew, G. N.; Liu, D.; Chen, B.; Doerksen, R. J.; Kaplan, J.; Carroll, P. J.; Klein, M. L.; DeGrado, W. F. De Novo Design of Biomimetic Antimicrobial Polymers. *Proc. Natl. Acad. Sci. U.S.A.* **2002**, *99*, 5110–5114.

Tew, G. N.; Scott, R. W.; Klein, M. L.; Degrado, W. F. De Novo Design of Antimicrobial Polymers, Foldamers, and Small Molecules: From Discovery to Practical Applications. *Acc. Chem. Res.* **2010**, *43*, 30–39.

Umezawa, N.; Gelman, M. A.; Haigis, M. C.; Raines, R. T.; Gellman, S. H. Translocation of a *β*-Peptide across Cell Membranes. *J. Am. Chem. Soc.* **2002**, *124*, 368–369.

Vivès, E.; Brodin, P.; Lebleu, B. A Truncated HIV-1 Tat Protein Basic Domain Rapidly Translocates through the Plasma Membrane and Accumulates in the Cell Nucleus. *J. Biol. Chem.* **1997**, *272*, 16010–16017.

Wender, P. A.; Mitchell, D. J.; Pattabiraman, K.; Pelkey, E. T.; Steinman, L.; Rothbard, J. B. The Design, Synthesis, and Evaluation of Molecules That Enable or Enhance Cellular Uptake: Peptoid Molecular Transporters. *Proc. Natl. Acad. Sci. U.S.A.* **2000**, *97*, 13003–13008.

Yeaman, M. R.; Yount, N. Y. Mechanisms of Antimicrobial Peptide Action and Resistance. *Pharmacol. Rev.* **2003**, *55,* 27–55.

Yeung, A. T. Y.; Gellatly, S. L.; Hancock, R. E. W. Multifunctional Cationic Host Defence Peptides and Their Clinical Applications. *Cell. Mol. Life Sci.* **2011**, *68,* 2161–2176.

CHAPTER 4.

Solid-phase synthesis of cyclic depsipeptides containing a phenyl ester bond

This chapter corresponds to a manuscript in preparation:

Cristina Rosés, Cristina Camó, Marta Planas, Lidia Feliu. Solid-phase synthesis of cyclic depsipeptides containing a phenyl ester bond. *In preparation*.

For this work, C.R. designed the cyclic depsipeptides and performed the synthesis and characterization of all the compounds. Moreover, C.R. was also involved in argumentations and discussions of the results, and wrote the manuscript draft.

An efficient solid-phase strategy for the synthesis of cyclic depsipeptides containing a phenyl ester linkage in their structure is described. Two different routes were studied that differed on the site of resin attachment and on the bond involved in the cyclization step. The key steps of these approaches were the formation of the phenyl ester bond and the on-resin head-to-side-chain cyclization. It was observed that the amino acid composition as well as its configuration significantly influenced the formation and the stability of the cyclic depsipeptides. The presence of a L-Tyr^1 and of a D-Tyr^7 led to the most stable sequences. This work constitutes the first report on the synthesis of cyclic depsipeptides containing a phenyl ester bond.

4.1 INTRODUCTION

Fengycins are cyclic lipodepsipeptides isolated from several *Bacillus* spp. that were first described in 1986 (Vanittanakom et al., 1986). These cyclic compounds show interesting antifungal activity mainly against filamentous fungi and, unlike other lipopeptides produced by *Bacillus* spp., they are low hemolytic (Vanittanakom et al., 1986; Deleu et al., 2008). Moreover, they have been described as elicitors of defence responses in plants, being a promising alternative for the protection of crops against phytopathogens (Ongena et al., 2005, 2007).

The fengycin family includes related compounds that share a common cyclic structure with exceptional features (Vanittanakom et al., 1986; Wang et al., 2004; Chen et al., 2008; Bie et al., 2009; Pueyo et al., 2009; Pecci et al., 2010; Pathak et al., 2012; Villegas-Escobar et al., 2013). They are decapeptides acylated at the *N*-terminus with a *β*-hydroxy fatty acid tail (*Figure 4.1*). Eight of the amino acids form a macrolactone in which the ester bond occurs between the phenol group of a tyrosine (Tyr) and the *α*-carboxylic group of an isoleucine (Ile). According to the amino acid sequences, fengycins A and B are the two major isoforms of this family. The former contains a D-alanine (D-Ala) at position 6 whereas the latter possess a D-valine (D-Val) at this position. Fengycin S is another isoform that was isolated by Sang-Cheol and co-workers from *Bacillus amyloliquefaciens* (Sang-Cheol et al., 2010). This isoform is analogous to fengycin B, but it bears a D-serine (D-Ser) at position 4 instead of an D-*allo*-threonine (D-*allo*-Thr). Concerning the Tyr residues at positions 3 and 9, it has to be mentioned that there has been some confusion over their configuration. Initially, fengycins were reported to have a D-Tyr^3/L-Tyr^9 configuration (Vanittanakom et al., 1986; Schneider et al., 1999), whereas a L-Tyr^3/D-Tyr^9 configuration was assigned to another family of related lipopeptides named plipastatins (Nishikiori et al., 1986a, 1986b; Volpon et al., 2000). Nevertheless, a recent study has shown that fengycins and plipastatins have the same primary structure, that is a L-Tyr^3/D-Tyr^9 configuration (Honma et al., 2012). Similarly to Nasir et al., we decided to name the peptides of this study as fengycins and to use the correct configuration, because this term is more widely employed than plipastatins (Nasir et al., 2013) (*Figure 4.1)*.

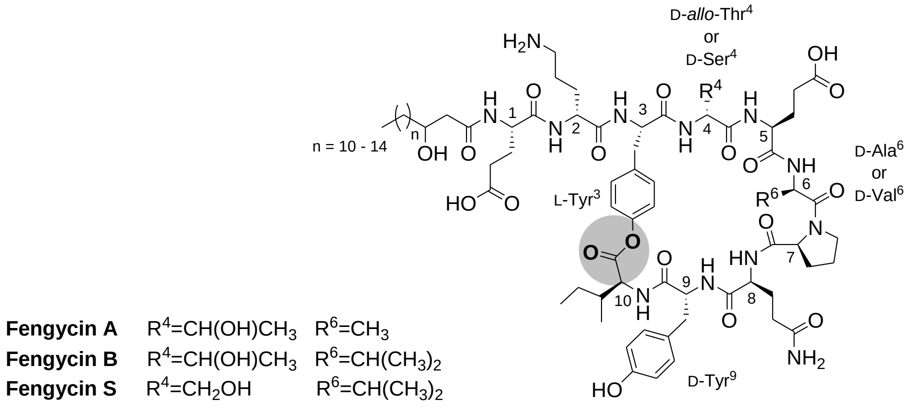
D-*allo*-Thr^4
or
D-Ser^4
H_2N
OH
R^4
D-Ala^6
or
D-Val^6
n = 10 - 14
L-Tyr^3
R^6
NH_2
HO
D-Tyr^9
1
2
3
4
5
6
7
8
9
10
Fengycin A $R^4=CH(OH)CH_3$ $R^6=CH_3$
Fengycin B $R^4=CH(OH)CH_3$ $R^6=CH(CH_3)_2$
Fengycin S $R^4=CH_2OH$ $R^6=CH(CH_3)_2$

Figure 4.1. *Structure of fengycins A, B and S.*

Most *Bacillus* cyclic depsipeptides are mainly extracted from the microorganism that produce them (Jacques et al., 1999; Chtioui et al., 2012; Ceballos et al., 2014; Rangarajan et al., 2015). However, fermentation has the disadvantage to simultaneously produce a range of analogues, which limits its application in industry. Therefore, the development of a general approach for the chemical synthesis of these cyclic depsipeptides has attracted interest because it would allow the preparation of specific analogues. The synthesis of these compounds encounters two main issues, i.e. the cyclization step and the formation of the ester bond. Solid-phase synthesis has been established as a good strategy for the obtention of cyclic depsipeptides because this strategy benefits from the avoidance of tedious work-up procedures, the possibility to employ an excess of reagents and the facile access to a range of analogues. Although several cyclic depsipeptides have been prepared on solid support (Krishnamoorthy et al., 2006; Cruz et al., 2007; Seo and Lim, 2009; Stolze et al., 2010; Hall et al., 2012), to the best of our knowledge, the solid-phase synthesis of fengycins has not yet been described. Moreover, it has to be taken into account that cyclic depsipeptides that have been synthesized on solid-phase bear an ester bond involving the β-hydroxyl group of a Thr or a Ser residue. No general examples have been reported on the formation of ester bonds involving the phenol group of a Tyr, which can be attributed to the high lability of phenyl esters. In fact, the formation of such ester bond has only been described by the group of Tam through a ligation protocol that yields depsipeptides as secondary products (Zhang and Tam, 1997, 1999). Moreover, up to now, the preparation of fengycins has only been addressed by the group of Marahiel and Essen, and it involves the solid-phase synthesis of the linear precursor followed by chemoenzymatic cyclization in solution (Sieber et al., 2003, 2004; Samel et al., 2006). Due to the structural requirements of this last step, this approach is restricted to the obtention of a limited number of analogues. Based on these considerations, the synthesis of fengycins constitutes an attractive synthetic challenge, not only for being constrained cyclic peptides, but also for containing a phenyl ester in their structure.

Herein, we explore a suitable solid-phase approach for the preparation of the macrolactone of eight amino acids present in fengycins (*Figure 4.1*). In particular, we focused our attention on the synthesis of compounds **I**, **II** and **III** (*Figure 4.2*). The structure of **I** consists of all L-amino acids; **II** contains amino acids with the configuration described for fengycins; and **III** are analogues of **II**, but with D-Tyr^1 and L-Tyr^7. All these compounds are cyclic depsipeptides except for **Ia** and **IIa** that only contain amide bonds and that were used as model systems.

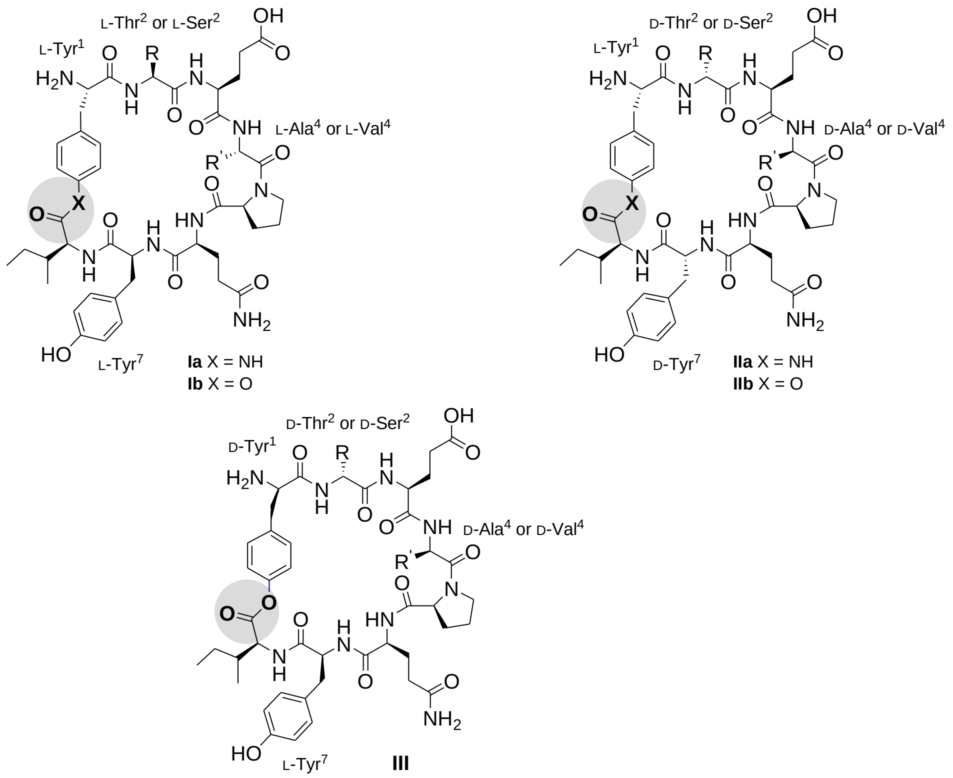
L-Thr^2 or L-Ser^2
L-Tyr^1
L-Ala^4 or L-Val^4
L-Tyr^7
Ia X = NH
Ib X = O
D-Thr^2 or D-Ser^2
L-Tyr^1
D-Ala^4 or D-Val^4
D-Tyr^7
IIa X = NH
IIb X = O
D-Thr^2 or D-Ser^2
D-Tyr^1
D-Ala^4 or D-Val^4
L-Tyr^7
III

Figure 4.2. *General structure of fengycin analogues* ***I***, ***II*** *and* ***III***.

4.2 RESULTS AND DISCUSSION

4.2.1 Retrosynthetic analysis

The main concerns when planning a retrosynthetic analysis for cyclic peptides **I-III** are the site of resin attachment and the point of cyclization. For cyclic depsipeptides, the selection of these issues is determined by the presence of the ester bond. Since esters are more labile and more difficult to form than amides, they are usually pre-formed in the linear precursor just before the cyclization step through an amide bond (Davies, 2003). Moreover, in the case of cyclic depsipeptides **Ib**, **IIb** and **III**, the formation of the phenyl ester bond is especially challenging due to its high reactivity (*Figure 4.2*).

Based on the above, we envisaged two retrosynthetic routes for the preparation of **I-III** (*Scheme 4.1*). In route A, we chose the side chain of Gln^6 as site of resin attachment, which would allow the formation of the cycle through an amide bond between the α-carboxylic acid of Gln^6 and the α-amino group of Tyr^7. In route B, the side chain of Tyr^7 would be the anchoring point to the resin and the cyclization would involve the formation of an amide bond between the α-carboxylic acid of Tyr^7 and the α-amino group of Ile^8. Therefore, both approaches would require (i) the anchoring of Gln^6 (route A) or Tyr^7 (route B) to the solid support, (ii) the preparation of the corresponding linear peptidyl resin, (iii) the ester or amide bond formation between the side chain of the amino acid at position 1 and the α-carboxylic acid of Ile^8, (iv) the deprotection of the carboxylic and amino groups involved in the cyclization step, and (v) the final on-resin cyclization and cleavage. Moreover, the N^α-amino group protection of Tyr^1 and Tyr^7 (route A), and of Tyr^1 and Ile^8 (route B) needed to be studied.

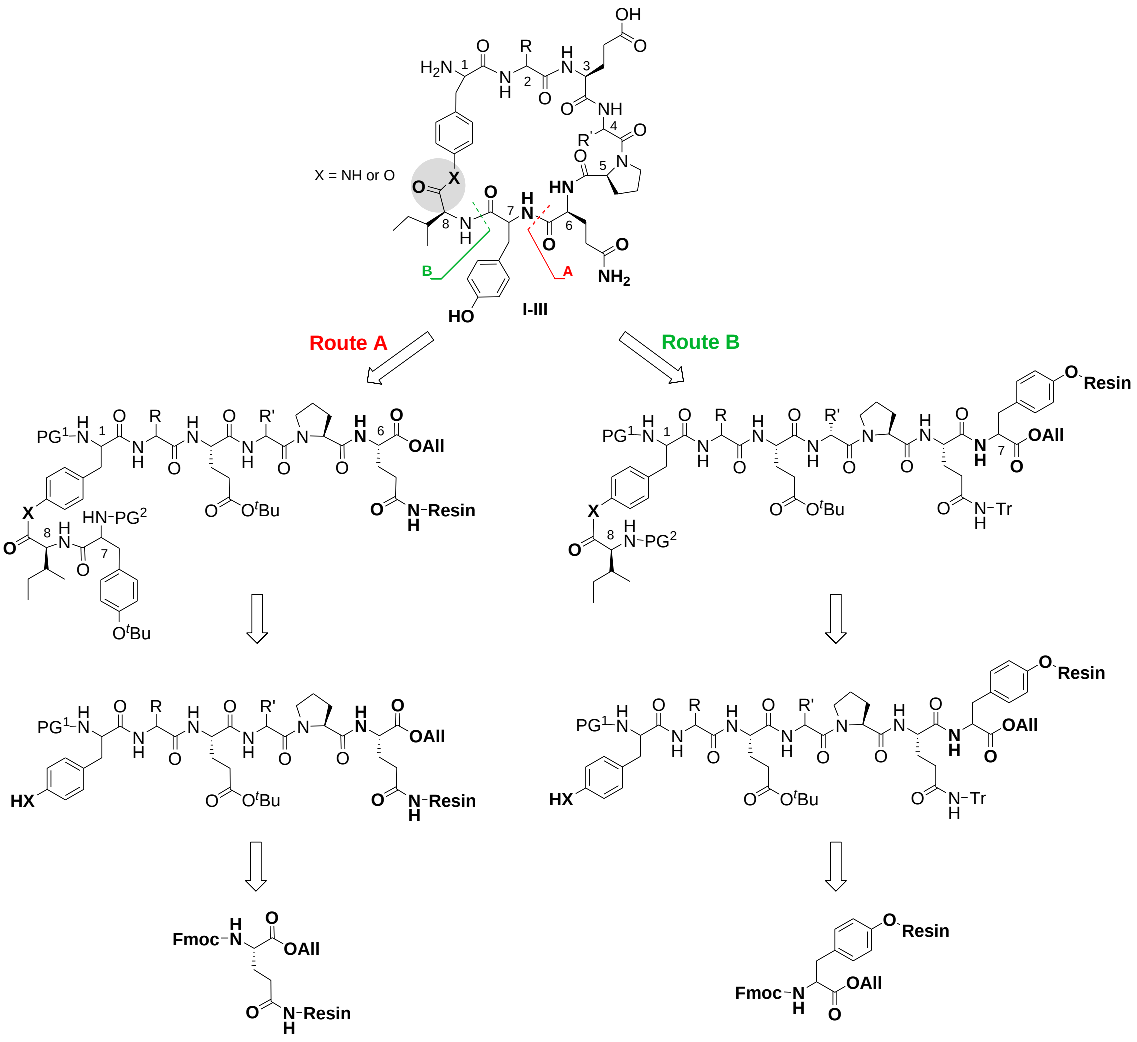

Scheme 4.1. *Retrosynthetic analysis of cyclic peptides* ***I-III****.*

4.2.2 Synthesis of cyclic octapeptides (route A)

Our investigations started with the solid-phase preparation of compounds **Ia** following route A, in particular of cyclic octapeptide **1** (L-Phe(4-NH$_2$)^1, L-Thr^2, L-Val^4, L-Tyr^7), which only contains L-amino acids and amide bonds (*Scheme 4.2*). This synthesis served as a model to check the feasibility of our approach. A three-dimensional orthogonal 9-fluorenylmethoxycarbonyl (Fmoc)/*tert*-butyl (^{t}Bu)/allyl (All) protecting strategy was selected. First, an Fmoc-Glu-OAll residue was anchored to an Fmoc-Rink-ChemMatrix (0.66 mmol/g) resin through its side chain. This trifunctional amino acid enables the cyclization onto solid support and results in a glutamine (Gln) residue after the peptide cleavage. For this purpose, first the Fmoc protecting group of

Fmoc-Rink-ChemMatrix was removed with piperidine/*N*,*N'*-dimethylformamide (DMF) (3:7) and then Fmoc-Glu-OAll was coupled in presence of *N*,*N'*-diisopropylcarbodiimide (DIPCDI) and ethyl 2-cyano-2-(hydroxyimino)acetate (Oxyma) in DMF for 1 h. Elongation of the peptide sequence was performed by sequential Fmoc removal and coupling steps leading to the pentapeptidyl resin Fmoc-Thr(^{t}Bu)-Glu(O^{t}Bu)-Val-Pro-Glu(Rink-ChemMatrix)-OAll. An aliquot of this resin was cleaved with trifluoroacetic acid (TFA)/H_2O/triisopropylsilane (TIS) (95:2.5:2.5) for 2 h affording the expected peptide in 93% HPLC purity. After Fmoc removal, Boc-Phe(4-NHFmoc)-OH was coupled using DIPCDI and Oxyma in DMF. The resulting resin was subjected to sequential Fmoc removal and coupling steps of Fmoc-Ile-OH and Fmoc-Tyr(^{t}Bu)-OH yielding the linear octapeptidyl resin Boc-Phe[4-NH-Ile-Tyr(^{t}Bu)-Fmoc]-Thr(^{t}Bu)-Glu(O^{t}Bu)-Val-Pro-Glu(Rink-ChemMatrix)-OAll. Acidolytic cleavage of an aliquot of this resin afforded the expected linear peptide in 93% HPLC purity, which was characterized by mass spectrometry. The *C*-terminal allyl ester was then removed by treatment with $Pd(PPh_3)_4$ in $CHCl_3$/AcOH/*N*-methylmorpholine (NMM) (3:2:1) for 3 h, and it was followed by Fmoc group removal. An aliquot of the resulting linear peptidyl resin Boc-Phe[4-NH-Ile-Tyr(^{t}Bu)-H]-Thr(^{t}Bu)-Glu(O^{t}Bu)-Val-Pro-Glu(Rink-ChemMatrix)-OH was acidolytically cleaved and the corresponding peptide was obtained in >99% HPLC purity, being characterized by mass spectrometry.

On-resin cyclization of this linear peptidyl resin was assayed using [ethyl cyano(hydroxyimino)acetato-O^2]tri-1-pyrrolidinylphosphonium hexafluorophosphate (PyOxim), Oxyma and *N*,*N'*-diisopropylethylamine (DIEA) in DMF for 24 h. After TFA cleavage, the HPLC chromatogram of the crude reaction mixture showed a broad band and mass spectrometry analysis revealed the presence of the expected cyclic octapeptide H-Phe(4-NH-&)-Thr-Glu-Val-Pro-Gln-Tyr-Ile-& (**1**) along with a substantial amount of a dimeric product (the "&" symbol is used to indicate the two residues that are linked through an amide bond). To try to avoid the formation of this dimeric compound, the synthesis of **1** was attempted starting with an Fmoc-Rink-ChemMatrix resin with lower loading (0.16 mmol/g). However, using this resin a significant amount of dimer was still detected.

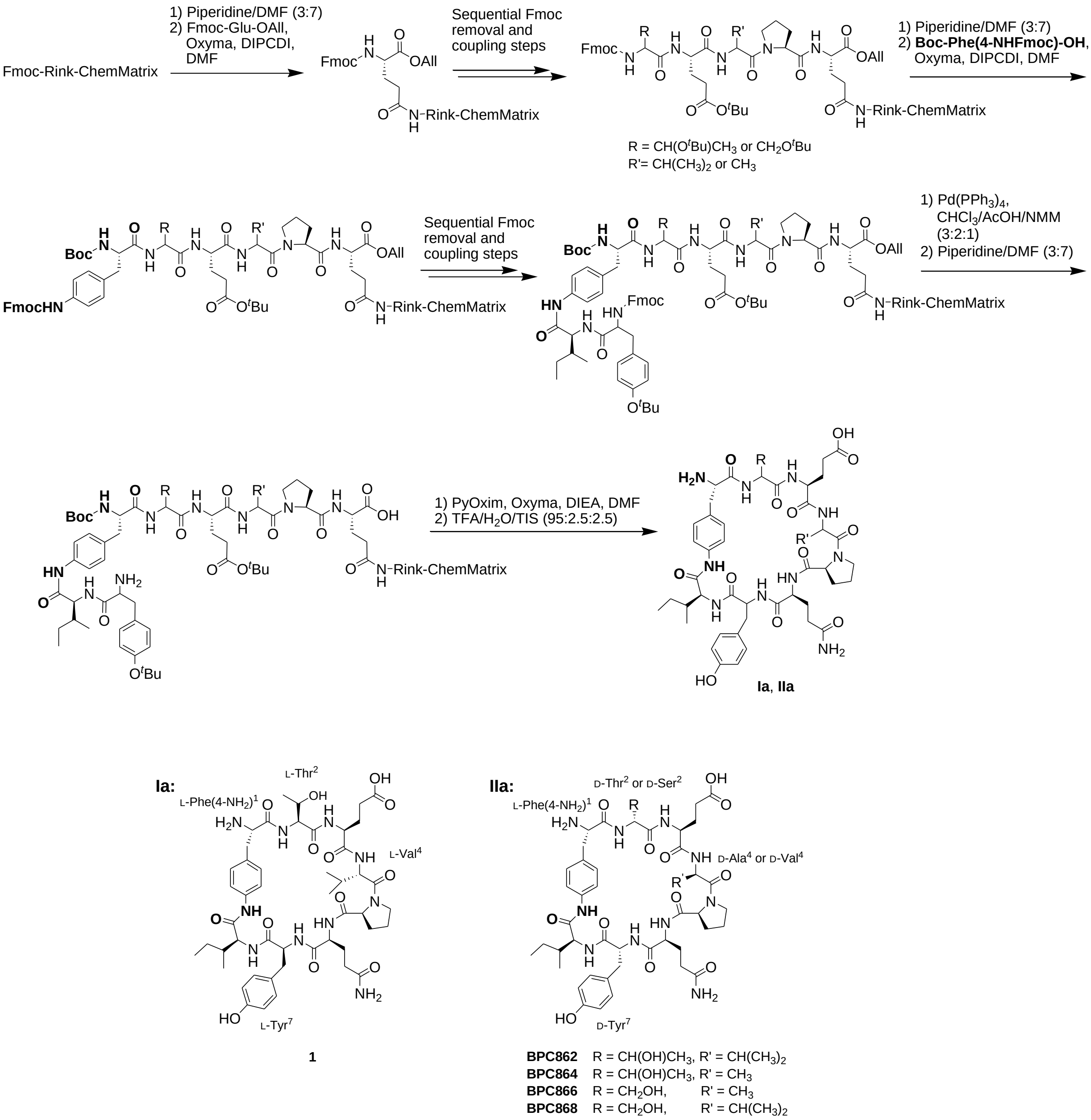
Fmoc-Rink-ChemMatrix
1) Piperidine/DMF (3:7)
2) Fmoc-Glu-OAll, Oxyma, DIPCDI, DMF
Sequential Fmoc removal and coupling steps
1) Piperidine/DMF (3:7)
2) Boc-Phe(4-NHFmoc)-OH, Oxyma, DIPCDI, DMF
R = CH(O^{t}Bu)CH$_3$ or CH$_2$O^{t}Bu
R'= CH(CH$_3$)$_2$ or CH$_3$
Sequential Fmoc removal and coupling steps
1) Pd(PPh$_3$)$_4$, CHCl$_3$/AcOH/NMM (3:2:1)
2) Piperidine/DMF (3:7)
1) PyOxim, Oxyma, DIEA, DMF
2) TFA/H$_2$O/TIS (95:2.5:2.5)
Ia, IIa
Ia:
IIa:
L-Phe(4-NH$_2$)^1
L-Thr^2
L-Val^4
L-Tyr^7
D-Thr^2 or D-Ser^2
D-Ala^4 or D-Val^4
D-Tyr^7
1
BPC862 R = CH(OH)CH$_3$, R' = CH(CH$_3$)$_2$
BPC864 R = CH(OH)CH$_3$, R' = CH$_3$
BPC866 R = CH$_2$OH, R' = CH$_3$
BPC868 R = CH$_2$OH, R' = CH(CH$_3$)$_2$

***Scheme 4.2.** Structure and general synthetic strategy of cyclic octapeptides **Ia** and **IIa** (route A).*

In view of these results, we decided to prepare cyclic octapeptides **IIa** incorporating D-amino acids to check if the presence of these residues would favour the cyclization step and would decrease the dimer formation. Therefore, following route A as described for compound **1**, we synthesized **BPC862** bearing D-Thr^2, D-Val^4 and D-Tyr^7. (*Scheme 4.2*). HPLC and mass spectrometry analysis of the crude peptide revealed the presence of **BPC862** in 39% purity together with the dimeric compound in 61%

purity. After purification by reverse-phase column chromatography the desired cyclic octapeptide **BPC862** was obtained in 98% of purity.

Similarly, we prepared cyclic octapeptides **BPC864** containing D-Thr^2, D-Ala^4 and D-Tyr^7; **BPC866** with D-Ser^2, D-Ala^4 and D-Tyr^7; and **BPC868** incorporating D-Ser^2, D-Val^4 and D-Tyr^7 (*Scheme 4.2*). These compounds were obtained in purities between 41-56% as shown by HPLC analysis of the corresponding crude reaction mixture. Dimeric compounds were also obtained in 44-57% HPLC purities. Reverse-phase column chromatography purification rendered the cyclic octapeptides in >99% HPLC purity, which were characterized by mass spectrometry.

4.2.3 Synthesis of cyclic octadepsipeptides (routes A and B)

According to our main objective of developing a solid-phase strategy for the preparation of cyclic depsipeptides, we evaluated the application of route A to the synthesis of cyclic depsipeptides **Ib**, containing all L-amino acids and a phenyl ester bond (*Figure 4.2, Scheme 4.3*). In particular, we assayed the synthesis of compound **2** (L-Tyr^1, L-Thr^2, L-Val^4, L-Tyr^7). Following a Fmoc/^{t}Bu/All strategy as described for **1**, the peptidyl resin Fmoc-Thr(^{t}Bu)-Glu(O^{t}Bu)-Val-Pro-Glu(Rink-MBHA)-OAll was prepared. After Fmoc group removal, Boc-Tyr-OH was incorporated using DIPCDI and Oxyma in DMF (*Scheme 4.3, route A1*). An aliquot of the resulting resin Boc-Tyr-Thr(^{t}Bu)-Glu(O^{t}Bu)-Val-Pro-Glu(Rink-MBHA)-OAll (**3a**) was acidolytically cleaved and H-Tyr-Thr-Glu-Val-Pro-Gln-OAll was obtained in >99% purity (*Scheme 4.3, route A1*). Then, the unprotected phenol group of Tyr was esterified with the α-carboxylic group of Fmoc-Ile-OH employing DIPCDI, *N,N'*-dimethylaminopyridine (DMAP) and DIEA in DMF for 24 h (Gracia et al., 2006). This reaction was repeated twice to obtain the linear depsipeptidyl resin Boc-Tyr^1(O-Ile^8-Fmoc)-Thr(^{t}Bu)-Glu(O^{t}Bu)-Val-Pro-Glu(Rink-MBHA)-OAll (**4a**). An aliquot of this resin was treated with TFA/H_2O/TIS and the expected depsipeptide was obtained in >99% HPLC purity, which was characterized by mass spectrometry. Unfortunately, when resin **4a** was subjected to the Fmoc group removal conditions, piperidine/DMF (3:7), HPLC and mass spectrometry analysis of the crude reaction mixture after acidolytic cleavage revealed the presence of H-Tyr-Thr-Glu-Val-Pro-Gln-OAll as major product (83% purity). This result pointed out that the basic conditions used for the α-amino group deprotection caused the aminolysis of the ester bond.

An alternative protecting group strategy was planned to avoid this side-reaction. Thus, route A2 involved the use of *p*-nitrobenzyloxycarbonyl (*p*NZ) and Boc groups for the α-amino protection of Tyr^1 and Ile^8, respectively (*Scheme 4.3, route A2*). The Boc group was chosen because it can be selectively removed under mild basic conditions (Zhang et al., 1998). The *p*NZ group has been reported to be orthogonal to Fmoc as well as to *tert*-butyl and allyl-based protecting groups, and its removal can be achieved under neutral conditions using $SnCl_2$ in presence of catalytic amounts of acid (Isidro-Llobet et al., 2005). *p*NZ-Tyr-OH was prepared from commercially available H-Tyr(O^{t}Bu)-OH by treatment with *p*NZ-N_3 (Isidro-Llobet et al., 2005), followed by side-chain deprotection under acidic conditions (68% overall yield). After Fmoc removal, this amino acid was coupled to the *N*-terminus of the previously prepared resin Fmoc-Thr(^{t}Bu)-Glu(O^{t}Bu)-Val-Pro-Glu(Rink-MBHA)-OAll leading to *p*NZ-Tyr-Thr(^{t}Bu)-Glu(O^{t}Bu)-Val-Pro-Glu(Rink-MBHA)-OAll (**3b)** (74% purity after cleavage). Subsequent esterification of the Tyr residue with Boc-Ile-OH under the conditions described above for **4a** afforded *p*NZ-Tyr^1(O-Ile^8-Boc)-Thr(^{t}Bu)-Glu(O^{t}Bu)-Val-Pro-Glu(Rink-MBHA)-OAll (**4b**). An aliquot of this resin was cleaved, and HPLC and mass spectrometry analysis of the crude revealed the formation of the ester bond, the expected depsipeptide was obtained in 80% purity. Selective Boc removal of **4b** was carried out under mild basic conditions using trimethylsilyl trifluoromethanesulfonate (TMSOTf) (2 M) and 2,6-lutidine (3 M) in CH_2Cl_2 (2×1 h) (Zhang et al., 1998). Subsequent incorporation of Boc-Tyr(^{t}Bu)-OH provided the linear depsipeptidyl resin *p*NZ-Tyr^1[O-Ile^8-Tyr^7(^{t}Bu)-Boc]-Thr(^{t}Bu)-Glu(O^{t}Bu)-Val-Pro-Glu(Rink-MBHA)-OAll. Unfortunately, when this resin was treated with TFA/H_2O/TIS the free amino group of Tyr^7 prompted the cleavage of the ester bond through the formation of a diketopiperazine leading to *p*NZ-Tyr-Thr-Glu-Val-Pro-Gln-OAll (19% purity), as observed by HPLC and mass spectrometry. Due to this result, this route was not further pursued, because the next synthetic step would involve the selective on-resin removal of the Boc group of Tyr^7 which would also result in diketopiperazine formation.

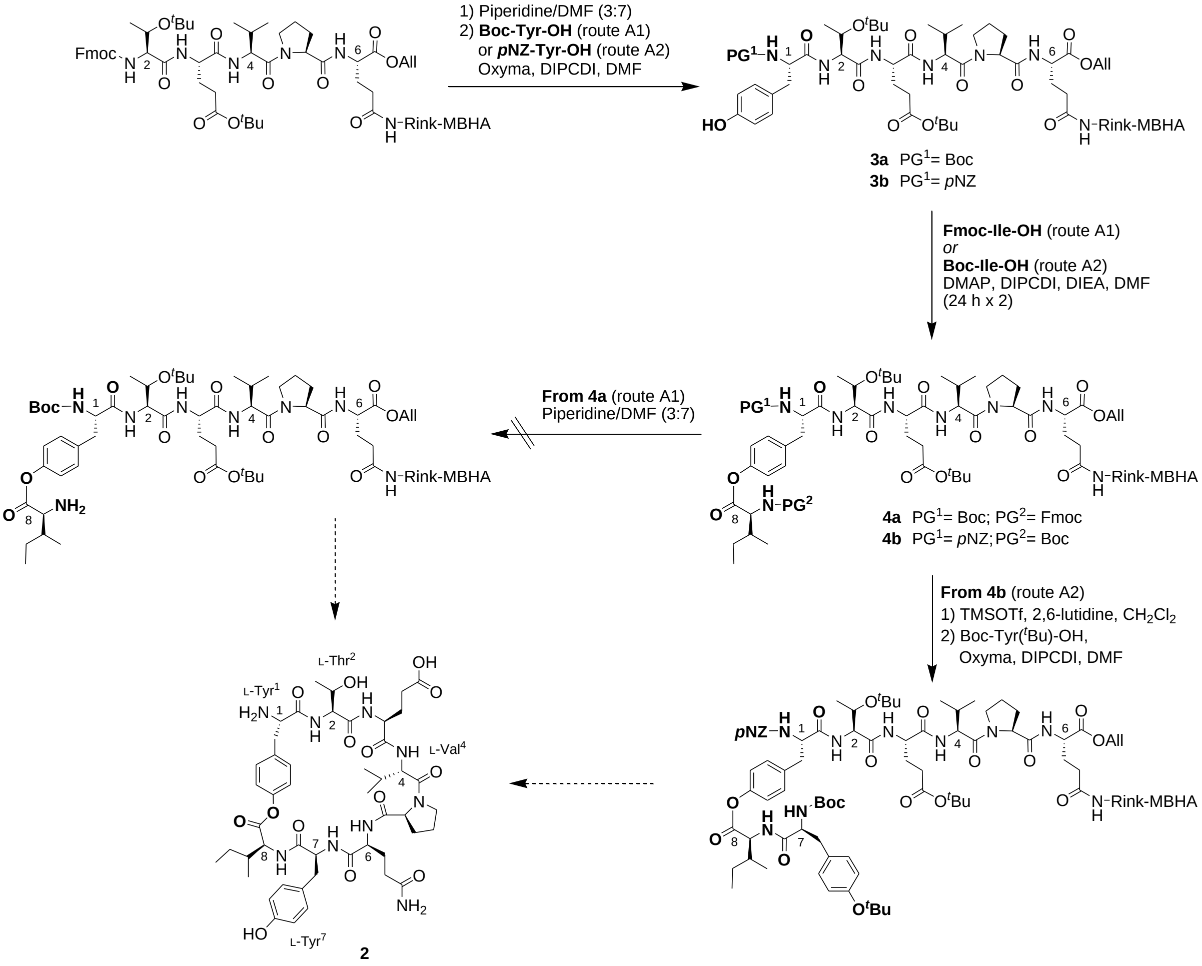
1) Piperidine/DMF (3:7)
2) Boc-Tyr-OH (route A1)
or pNZ-Tyr-OH (route A2)
Oxyma, DIPCDI, DMF
3a PG1= Boc
3b PG1= pNZ
Fmoc-Ile-OH (route A1)
or
Boc-Ile-OH (route A2)
DMAP, DIPCDI, DIEA, DMF
(24 h x 2)
From 4a (route A1)
Piperidine/DMF (3:7)
4a PG1= Boc; PG2= Fmoc
4b PG1= pNZ; PG2= Boc
From 4b (route A2)
1) TMSOTf, 2,6-lutidine, CH2Cl2
2) Boc-Tyr(tBu)-OH,
Oxyma, DIPCDI, DMF
N-Rink-MBHA
L-Tyr1
L-Thr2
L-Val4
L-Tyr7
2

Scheme 4.3. *Synthetic approaches for the synthesis of cyclic depsipeptide* ***2*** *(routes A1 and A2).*

These results prompted us to assay the synthesis of cyclic depsipeptide **2** following route B (*Scheme 4.4*). This strategy would avoid the formation of a diketopiperazine between Tyr^7 and Ile^8 because the linkage between these two amino acids would occur during the cyclization step. Accordingly, this route involved the attachment of Tyr^7 to the solid support through its phenol group. For this purpose, Wang resin was selected because it would enable the incorporation of this residue using a Mitsunobu reaction (Cabrele et al., 1999; Thutewohl and Waldmann, 2003; Kumar et al., 2006). The allyloxycarbonyl (Alloc) group was chosen for the protection of the *α*-amino group of Ile^8, because it has been demonstrated that the conditions for the selective Boc removal (TMSOTf and 2,6-lutidine) could lead to a high percentage of peptide cleavage when using a Wang resin (Lejeune et al., 2003). Moreover, the *α*-

carboxylic group of Tyr^7 was protected as allyl ester because Alloc/All groups could be simultaneously removed before the cyclization step using Pd(0) (Thieriet et al., 1997; Guibé, 1998). Similarly to route A, Tyr^1 was incorporated as *p*NZ-Tyr-OH. Therefore, this route involved the preparation of the linear peptidyl resin *p*NZ-Tyr^1(O-Ile^8-Alloc)-Thr(^{t}Bu)-Glu(O^{t}Bu)-Val-Pro-Gln(Tr)-Tyr^7(Wang)-OAll as precursor of cyclic depsipeptide **2**.

Towards this aim, Fmoc-Tyr-OAll was first prepared from Fmoc-Tyr(^{t}Bu)-OH by treatment with allyl bromide (Alsina et al., 1998) followed by acidolytic removal of the *tert*-butyl group. This amino acid was then anchored to the Wang resin by treatment with PPh_3 and diisopropylazodicarboxylate (DIAD) in anhydrous tetrahydrofuran (THF) under stirring at room temperature for 24 h (Cabrele et al., 1999; Thutewohl and Waldmann, 2003) (*Scheme 4.4*). As determined with the Fmoc method, resin Fmoc-Tyr(Wang)-OAll was obtained with a loading of 0.22 mmol/g (Grant, 1992). Moreover, according to the Marfey's test, the Tyr residue did not racemise under these conditions (Adamson et al., 1992). To reduce the reaction time, the use of microwave irradiation was evaluated. Resin Fmoc-Tyr(Wang)-OAll was obtained in a similar loading after only 30 min irradiation at 60º C. These conditions neither promoted the racemization of the Tyr. To the best of our knowledge, this is the first example of a microwave-assisted Mitsunobu reaction for the anchoring of a Tyr onto a solid support. Then, the peptidyl resin *p*NZ-Tyr^1-Thr(^{t}Bu)-Glu(O^{t}Bu)-Val-Pro-Gln(Tr)-Tyr^7(Wang)-OAll (**5**) was prepared through sequential Fmoc removal and coupling steps as previously described. Acidolytic cleavage of an aliquot of this resin afforded the expected peptide in 82% HPLC purity. Then, Alloc-Ile-OH, prepared from H-Ile-OH by treatment with Alloc-N_3 (Cruz et al., 2004), was incorporated using the conditions described for the ester formation in route A, i.e. DIPCDI, DMAP and DIEA in DMF (2×24 h). An aliquot of the resulting resin *p*NZ-Tyr^1(O-Ile^8-Alloc)-Thr(^{t}Bu)-Glu(O^{t}Bu)-Val-Pro-Gln(Tr)-Tyr^7(Wang)-OAll (**6**) was treated under acidolytic conditions yielding the expected linear peptide in 70% HPLC purity. Next, the Alloc and allyl protecting groups were simultaneously removed using a catalytic amount of $Pd(PPh_3)_4$ in presence of $PhSiH_3$ in CH_2Cl_2 for 4 h. After acidolytic cleavage of an aliquot of *p*NZ-Tyr^1(O-Ile^8-H)-Thr(^{t}Bu)-Glu(O^{t}Bu)-Val-Pro-Gln(Tr)-Tyr^7(Wang)-OH, the corresponding peptide was obtained in 57% HPLC purity. Subsequent on-resin cyclization was assayed using PyOxim, Oxyma and DIEA. However, the expected cyclic depsipeptide *p*NZ-Tyr^1(&)-Thr-Glu-

Val-Pro-Gln-Tyr^7-Ile^8-& (**7**) was not observed by ESI-MS analysis of the crude reaction mixture. The mass spectra showed a peak at $[M + H_2O]^+$ which was assigned to the linear peptide *p*NZ-Tyr^1-Thr-Glu-Val-Pro-Gln-Tyr^7-Ile^8-OH resulting from the hydrolysis of **7**. This result was confirmed because a sample of this crude reaction mixture coeluted with a sample of this linear peptide independently prepared on solid-phase. Therefore, we could conclude that the cyclic depsipeptide **7** was formed but that it hydrolysed during the cleavage step or during HPLC analysis.

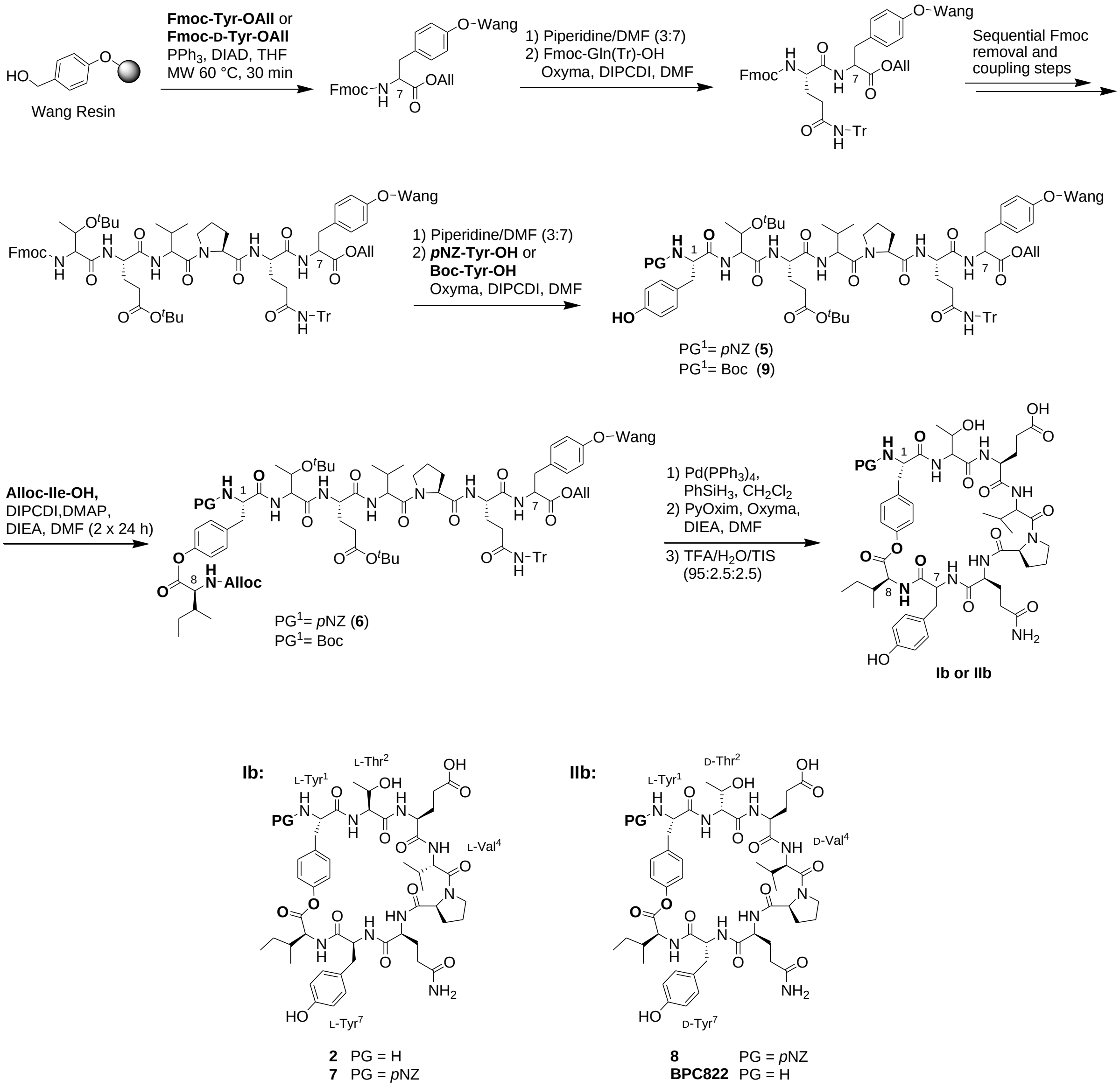
Wang Resin
Fmoc-Tyr-OAll or
Fmoc-D-Tyr-OAll
PPh3, DIAD, THF
MW 60 °C, 30 min
1) Piperidine/DMF (3:7)
2) Fmoc-Gln(Tr)-OH
Oxyma, DIPCDI, DMF
Sequential Fmoc removal and coupling steps
1) Piperidine/DMF (3:7)
2) pNZ-Tyr-OH or
Boc-Tyr-OH
Oxyma, DIPCDI, DMF
PG1= pNZ (5)
PG1= Boc (9)
Alloc-Ile-OH,
DIPCDI,DMAP,
DIEA, DMF (2 x 24 h)
PG1= pNZ (6)
PG1= Boc
1) Pd(PPh3)4,
PhSiH3, CH2Cl2
2) PyOxim, Oxyma,
DIEA, DMF
3) TFA/H2O/TIS
(95:2.5:2.5)
Ib or IIb
Ib:
L-Tyr1
L-Thr2
L-Val4
L-Tyr7
IIb:
L-Tyr1
D-Thr2
D-Val4
D-Tyr7
2 PG = H
7 PG = pNZ
8 PG = pNZ
BPC822 PG = H

Scheme 4.4. *Structure and general synthetic strategy of cyclic depsipeptides **2**, **7**, **8** and **BPC822** (route B).*

This methodology was then applied to the preparation of cyclic depsipeptides **IIb** containing D-amino acids. In particular, it was studied the synthesis of **BPC822** containing D-Thr^{2}, D-Val^{4} and D-Tyr^{7} (*Scheme 4.4*). In this case, Fmoc-D-Tyr-OAll was prepared and anchored to the Wang resin through a microwave-assisted Mitsunobu reaction under the conditions described above for its enantiomer, affording Fmoc-D-Tyr(Wang)-OAll in a 0.33 mmol/g loading. Peptide elongation and esterification with Alloc-Ile-OH led to the linear peptidyl resin *p*NZ-Tyr^{1}(O-Ile^{8}-Alloc)-D-Thr^{2}(^{t}Bu)-Glu(O^{t}Bu)-D-Val^{4}-Pro-Gln(Tr)-D-Tyr^{7}(Wang)-OAll. Subsequent Alloc and allyl group removal and on-resin cyclization yielded the cyclic depsipeptide *p*NZ-Tyr^{1}(&)-D-Thr^{2}-Glu-D-Val^{4}-Pro-Gln-D-Tyr^{7}-Ile^{8}-& (**8**) in 31% HPLC purity, as shown by ESI-MS where a peak at *m/z* 1195.5 corresponding to $[M + Na]^{+}$ was observed. The linear peptide precursor was not detected either by HPLC or mass spectrometry. To confirm the structure of **8**, the crude reaction mixture resulting from acidolytic cleavage was treated with $CH_3OH/H_2O/NH_3$ (4:1:1), conditions that are known to hydrolyse ester bonds (Kuroda et al., 2001; Stawikowski and Cudic, 2006; Cochrane et al., 2012). HPLC and mass spectrometry analysis of the resulting crude revealed only the presence of the linear peptide resulting from the hydrolysis of the ester bond in **8**, *p*NZ-Tyr^{1}-D-Thr^{2}-Glu-D-Val^{4}-Pro-Gln-D-Tyr^{7}-Ile^{8}-OH, and of the corresponding methyl ester *p*NZ-Tyr^{1}-D-Thr^{2}-Glu-D-Val^{4}-Pro-Gln-D-Tyr^{7}-Ile^{8}-OMe (*Scheme 4.5*). Therefore, this result demonstrated the formation of the cyclic depsipeptide **8** and that the presence of D-amino acids is crucial for the stability of this cyclic structure.

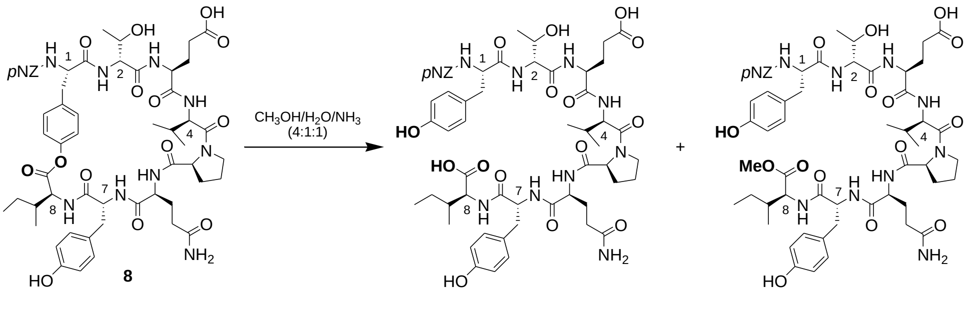

Scheme 4.5. *Hydrolysis of the ester bond of cyclic depsipeptide* ***8****.*

Next, to obtain **BPC822** we attempted the *p*NZ group removal using $SnCl_2$ (6 M) in HCl/dioxane (1.6 mM) and DMF. This deprotection resulted to be more troublesome than expected. After several treatments, an important amount of the *p*NZ-protected cyclic depsipeptide was still observed by mass spectrometry.

To overcome this limitation, synthesis of **BPC822** was planned starting from the linear peptidyl resin Boc-Tyr^1-D-Thr^2(^{t}Bu)-Glu(O^{t}Bu)-D-Val^4-Pro-Gln(Tr)-D-Tyr^7(Wang)-OAll (**9**), bearing a Boc group at Tyr^1 (*Scheme 4.4*). Incorporation of Alloc-Ile-OH through ester bond formation with Tyr^1 was followed by Alloc and allyl group removal, and cyclization. Acidolytic cleavage of the resulting resin yielded the cyclic depsipeptide **BPC822**. Mass spectrometry analysis showed only a major peak at *m/z* 994.5 corresponding to $[M + H]^+$ of **BPC822**, together with a small peak at *m/z* 1012.5. After treating the crude reaction mixture with $CH_3OH/H_2O/NH_3$ (4:1:1), the latter peak could be attributed to the linear peptide H-Tyr^1-D-Thr^2-Glu-D-Val^4-Pro-Gln-D-Tyr^7-Ile^8-OH, resulting from the hydrolysis of the ester function of **BPC822**. The corresponding linear *C*-terminal methylated peptide H-Tyr^1-D-Thr^2-Glu-D-Val^4-Pro-Gln-D-Tyr^7-Ile^8-OMe was also detected after this treatment.

Since the use of Boc allowed the preparation of **BPC822**, this synthetic methodology was extended to the preparation of the cyclic depsipeptides **IIb**: **BPC824** (D-Ser^2, D-Val^4 and D-Tyr^7), **BPC826** (D-Thr^2, D-Ala^4 and D-Tyr^7) and **BPC828** (D-Ser^2, D-Ala^4 and D-Tyr^7) (*Figure 4.3*). Mass spectrometry analysis showed that these cyclic depsipeptides were the only products of the synthesis. Similarly to **BPC822**, hydrolysis of the crude reaction mixtures confirmed the cyclic structure of these compounds. Cyclic depsipeptides **BPC822**, **BPC824**, **BPC826** and **BPC828** were purified by column chromatography and obtained in purities ranging from 88 to >99%.

Finally, the synthesis of cyclic depsipeptides **III** bearing a D-Tyr^1 and an L-Tyr^7 was also attempted following the above methodology. This set included **BPC830** (D-Tyr^1, D-Thr^2, D-Val^4), **BPC832** (D-Tyr^1, D-Ser^2, D-Val^4), **BPC834** (D-Tyr^1, D-Thr^2, D-Ala^4) and **BPC836** (D-Tyr^1, D-Ser^2, D-Ala^4). Contrary to our expectations, the cyclic depsipeptides were obtained together with a high amount of the corresponding dimeric product and a linear peptide that did not contain Ile^8. The formation of the latter product revealed that the cyclization was not complete and that the ester bond of the linear precursor hydrolysed prompting the release of the Ile residue. This result demonstrated that the cyclization of cyclic depsipeptides with a D-Tyr^1 and a L-Tyr^7 is difficult and that they are not stable, reinforcing the hypothesis by Honma and co-workers that postulated a L and D configuration for these residues in natural fengycins (Honma et al., 2012).

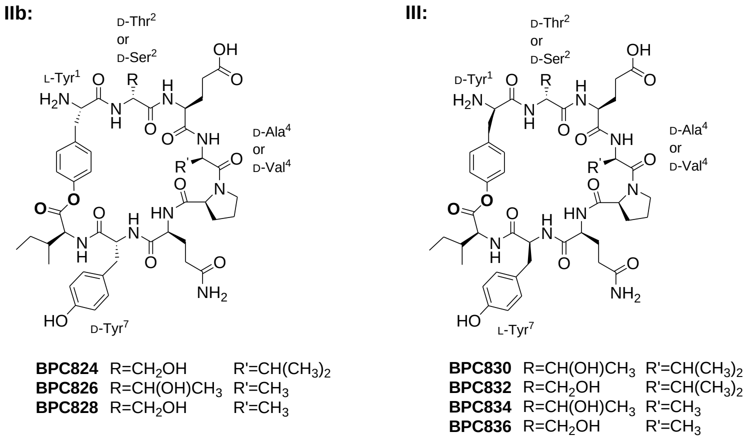
IIb:
D-Thr^2 or D-Ser^2
L-Tyr^1
D-Ala^4 or D-Val^4
D-Tyr^7
BPC824 R=CH$_2$OH R'=CH(CH$_3$)$_2$
BPC826 R=CH(OH)CH$_3$ R'=CH$_3$
BPC828 R=CH$_2$OH R'=CH$_3$
III:
D-Thr^2 or D-Ser^2
D-Tyr^1
D-Ala^4 or D-Val^4
L-Tyr^7
BPC830 R=CH(OH)CH$_3$ R'=CH(CH$_3$)$_2$
BPC832 R=CH$_2$OH R'=CH(CH$_3$)$_2$
BPC834 R=CH(OH)CH$_3$ R'=CH$_3$
BPC836 R=CH$_2$OH R'=CH$_3$

Figure 4.3. *Structure of cyclic depsipeptides* ***IIb*** *and* ***III****.*

4.3 CONCLUSIONS

Herein, we established a suitable strategy for the solid-phase synthesis of head-to-side-chain cyclic depsipeptides containing a phenyl ester linkage. Using a Fmoc/^{t}Bu/Alloc/allyl strategy, a set of cyclic octadepsipeptides derived from fengycins was successfully prepared. Our studies revealed the significance of the amino acid configuration on the stability of the cyclic depsipeptides, being those containing a L-Tyr^1 and a D-Tyr^7 the most stable. This study is the first example on the synthesis of cyclic depsipeptides incorporating a phenyl ester bond and represents a promising approach for the total synthesis of fengycins in future studies.

4.4 EXPERIMENTAL SECTION

4.4.1 General methods

Amino acid derivatives and resins were purchased from IrisBiotech, NovaBiochem or Sigma-Aldrich, except for ChemMatrix resin that was obtained from PCAS Biomatrix INC (USA). General reagents were purchased from Sigma-Aldrich, Fluka, Bachem, Panreac, Merk or IrisBiotech, and were used without further purification unless otherwise noted. Solvents were purchased from Sigma-Aldrich, Scharlau, SDS or VWR international. The organic solvents were synthesis grade, except for CH_3CN which was HPLC grade. Solvents were purified and dried using an activated alumina purification system (mBraun SPS-800) or by conventional distillation techniques. H_2O was deionised and filtered with a COT Millipore Q-gradient system (COT < 3ppb) with a resistivity of 18 $M\Omega \cdot cm^{-1}$.

Microwave-assisted reactions were carried out on a Discover® S-Class microwave from CEM Corporation, equipped with an Explorer autosampler. Time, temperature and power of the experiments were controlled with the Synergy^{TM} software. The equipment was supplied with a multispeed magnetic stirring system with adjustable speed and an automated power control system based on temperature feedback through a volume-independent non-invasive infrared sensor control (from 0 to 300 W). The operating temperature range is from 40 to 300 °C with a heating rate of 2-6 °C/second. Reactions were performed in a 10 or 35 mL reaction vessel.

All peptides were analysed under standard analytical HPLC conditions. Solvent A was 0.1% aq. TFA and solvent B was 0.1% TFA in CH_3CN. Detection was performed at 220 nm. Purity was estimated with the integrated area under the peaks. ***Method A***: Samples were analysed using a Dionex liquid chromatography instrument composed of an UV/Vis Dionex UVD170U detector, a P680 Dionex bomb, an ASI-100 Dionex automatic injector and CHROMELEON 6.60 software. Analyses were carried out with a Kromasil 100 C_{18} (4.6 mm × 40 mm, 3.5 µm) column with a 2-100% B linear gradient over 7 min at a flow rate of 1 mL/min. ***Method B***: An Agilent Technologies 1200 Series instrument was used. Analyses were carried out with a Kromasil 100 C_{18} (4.6 mm × 40 mm, 3.5 µm) column with a 2-100% B linear gradient over 6 min at a flow rate of 1 mL/min. ***Method C***: An Agilent Technologies 1200 Series instrument was used. Analyses were carried out with a Kromasil 100 C_{18} (4.6 mm × 40 mm, 3.5 µm) column with a 2-100% B linear gradient over 15.5 min at a flow rate of 1 mL/min. Peptide purifications were carried on a reverse-phase column chromatography CombiFlash Rf200.

MS (ESI) analyses were performed with an Esquire 6000 ESI Bruker ion Trap LC/MS instrument equipped with an electrospray ion source (Serveis Tècnics de

Recerca, University of Girona). The instrument was operated in both positive ESI *m/z*(+) and negative ESI *m/z*(-) ion modes. Samples (5 μL) were introduced into the mass spectrometer ion source directly through a 1200 Series Agilent HPLC autosampler. The mobile phase (80:20 CH_3CN/H_2O at a flow rate of 100 μL/min) was delivered by an Agilent 1200 Series HPLC pump. Nitrogen was employed as both drying and nebulizing gas.

HRMS were recorded under conditions of ESI with a Bruker MicroTOF-Q II instrument using a hybrid quadrupole time-of-flight mass spectrometer (Serveis Tècnics de Recerca, University of Girona). Samples were introduced into the mass spectrometer ion source by direct infusion through a syringe pump and were externally calibrated using sodium formate. The instrument was operated in the positive ESI *m/z*(+) ion mode.

^{1}H- and ^{13}C-NMR spectra were recorded on a Bruker Ultrashield Avance 300 or 400 MHz instrument. Chemical shifts were reported as δ values (ppm) directly referenced to the undeuterated residual solvent signal (i.e. $CHCl_3$ δ = 7.26 ppm). The following multiplicity abbreviations are used: (s) singlet, (d) doublet, (dd) double doublet, (t) triplet, (td) triple doublet, (tt) triple triplet, (m) multiplet and (br) broad peak.

IR spectra were recorded on a Bruker Alpha FT-IR spectrometer equipped with a Bruker Platinum ATR accessory. Wavenumbers (ν) are expressed in cm^{-1}.

The "&" symbol was used on the one-line formula of cyclic octapeptides and cyclic depsipeptides to indicate two residues that are linked through an amide or ester bond. The "&" symbol in a given position indicates the location of one end of the chemical bond and the point to which it is attached (Gracia et al., 2006).

4.4.2 Synthesis of Amino Acids

Allyl *N*$^{\alpha}$-(9-fluorenylmethyloxycarbonyl)-O-*tert*-butyl-L-tyrosinate (Alsina et al., 1998): To a solution of commercially available Fmoc-L-Tyr(^{t}Bu)-OH (2 g, 4.35 mmol) and allyl bromide (20 mL, 231.11 mmol) in CH_3CN (60 mL), *N,N'*-

diisopropylethylamine (DIEA) (0.76 mL, 4.35 mmol) was added dropwise. The mixture was stirred at room temperature for 24 h and the reaction was monitored by TLC. The solvent was then removed under reduced pressure and the resulting residue was taken up in AcOEt (150 mL). The organic layer was washed with 0.1 N HCl (3×75 mL), 10% $NaHCO_3$ (3×75 mL) and brine (3×75 mL), and it was then dried over anhydrous $MgSO_4$ and filtered. The solvent was removed under reduced pressure and the crude was purified by flash chromatography. Elution with *n*-hexane/AcOEt (13:1) yielded quantitatively Fmoc-L-Tyr(^{t}Bu)-OAll as a white solid (2.11 g, 97% yield). R_f (AcOEt/CH_3OH/H_2O, 5:1:1) = 0.90; IR (neat): 3500-3250 (NH_{st}), 2976 (CH_{st}), 1721 ($C{=}O_{st}$), 1505 (NH_{δ}), 1449 ($CH_{3\ \delta as}$), 1365, 1236, 1159 ($CO\text{-}O_{st\ as}$), 1103, 1048 ($N\text{-}CO\text{-}O_{st\ sim}$), 896 ($={CH}_{\delta oop}$), 758, 739 cm^{-1}; ^{1}H-NMR (400 MHz, $CDCl_3$) δ (ppm): 1.32 (s, 9H, $(CH_3)_3$), 3.07 (dd, *J* = 6.2, 14.0 Hz, 1H, CH_2-β), 3.11 (dd, *J* = 6.0, 14.0 Hz, 1H, CH_2-β), 4.21 (t, 1H, *J* = 7.0 Hz, 1H, CH-Fmoc), 4.35 (dd, *J* = 7.0, 10.8 Hz, 1H, OCH_2-Fmoc), 4.43 (dd, *J* = 7.2, 10.8 Hz, 1H, OCH_2-Fmoc), 4.61 (d, *J* = 5.6 Hz, 2H, OCH_2-All), 4.64-4.69 (m, 1H, CH-α), 5.24-5.33 (m, 3H, $=CH_2$, NH), 5.81-5.91 (m, 1H, =CH), 6.90 (d, *J* = 8.4 Hz, 2H, CH_{Arom9}-Tyr), 7.00 (d, *J* = 8.4 Hz, 2H, CH_{Arom8}-Tyr), 7.32 (tt, *J* = 1.2, 7.6 Hz, 2H, CH_{Arom18}-Fmoc), 7.41 (t, *J* = 7.6 Hz, 2H, CH_{Arom19}-Fmoc), 7.58 (dd, *J* = 3.2, 7.6 Hz, 2H, CH_{Arom17}-Fmoc), 7.77 (d, *J* = 7.6 Hz, 2H, CH_{Arom20}-Fmoc); ^{13}C-NMR (75 MHz, $CDCl_3$) δ (ppm): 28.95 ($(CH_3)_3$), 37.82 (CH_2-β), 47.30 (CH-Fmoc), 55.00 (CH-α), 66.20, 67.09 (OCH_2-Fmoc, OCH_2-All), 78.57 ($C(CH_3)_3$), 119.23, 120.12 (CH_{Arom9}-Tyr, $=CH_2$) 124.32, 125.20, 127.20, 127.85, 129.95 (CH_{Arom8}-Tyr, CH_{Arom17}-Fmoc, CH_{Arom18}-Fmoc, CH_{Arom19}-Fmoc, CH_{Arom20}-Fmoc), 130.52, 131.51 (C_{Arom}-Tyr, =CH), 141.44, 143.87 (C_{Arom16}-Fmoc, C_{Arom21}-Fmoc), 154.66, 155.67 (OC_{Arom}-Tyr, HN-C=O), 171.48 (O-C=O); MS (ESI) *m/z*: 500.1 $[M+H]^+$, 522.2 $[M+Na]^+$.

Allyl N^{α}-(9-fluorenylmethyloxycarbonyl)-O-*tert*-butyl-D-tyrosinate: This compound was prepared following the procedure described above for Fmoc-L-Tyr(^{t}Bu)-OAll, starting from commercially available Fmoc-D-Tyr(^{t}Bu)-OH (3 g, 6.53 mmol). Elution with *n*-hexane/AcOEt (12:1) yielded Fmoc-D-Tyr(^{t}Bu)-OAll as a white solid (3.10 g, 95% yield). R_f (AcOEt/CH_3OH/H_2O, 5:1:1) = 0.91; IR (neat): 3500-3250 (NH_{st}), 2976 (CH_{st}), 1721 ($C{=}O_{st}$), 1505 (NH_{δ}), 1449 ($CH_{3\ \delta as}$), 1365, 1236, 1159 ($CO\text{-}O_{st\ as}$), 1103, 1048 ($N\text{-}CO\text{-}O_{st\ sim}$), 896 ($={CH}_{\delta oop}$), 758, 739 cm^{-1}; ^{1}H-NMR (400 MHz, $CDCl_3$) δ (ppm): 1.32 (s, 9H, $(CH_3)_3$), 3.06 (dd, *J* = 5.6, 13.6 Hz, 1H, CH_2-β), 3.11 (dd, *J* = 5.6, 13.6 Hz, 1H, CH_2-β), 4.21 (t, 1H, *J* = 7.0 Hz, 1H, CH-Fmoc), 4.35 (dd, *J* = 7.0, 10.4 Hz, 1H, OCH_2-Fmoc), 4.43 (dd, *J* = 7.0, 10.4 Hz, 1H, OCH_2-Fmoc), 4.61 (d, *J* = 5.6 Hz, 2H, OCH_2-All), 4.64-4.69 (m, 1H, CH-α), 5.23-5.32 (m, 3H, $=CH_2$, NH), 5.81-5.91 (m, 1H, =CH), 6.90 (d, *J* = 8.4 Hz, 2H, CH_{Arom9}-Tyr), 7.01 (d, *J* = 8.4 Hz, 2H, CH_{Arom8}-Tyr), 7.31 (tt, *J* = 1.2, 7.6 Hz, 2H, CH_{Arom18}-Fmoc), 7.40 (td, *J* = 0.8, 7.6 Hz, 2H, CH_{Arom19}-Fmoc), 7.58 (dd, *J* = 3.2, 7.6 Hz, 2H, CH_{Arom17}-Fmoc), 7.77 (d, *J* = 7.6 Hz, 2H, CH_{Arom20}-Fmoc); ^{13}C-NMR (100 MHz, $CDCl_3$) δ (ppm): 28.94 ($(CH_3)_3$), 37.80 (CH_2-β), 47.28 (CH-Fmoc), 55.00 (CH-α), 66.18 (OCH_2-All), 67.08 (OCH_2-Fmoc), 78.56 ($C(CH_3)_3$), 119.21, 120.11 (CH_{Arom9}-Tyr, $=CH_2$), 124.31, 125.19, 127.19, 127.84, 129.94 (CH_{Arom8}-Tyr, CH_{Arom17}-Fmoc, CH_{Arom18}-Fmoc, CH_{Arom19}-Fmoc, CH_{Arom20}-Fmoc), 130.53, 131.48 (C_{Arom7}-Tyr, =CH), 141.43, 143.86 (C_{Arom16}-Fmoc, C_{Arom21}-Fmoc), 154.61, 155.66 (OC_{Arom}-Tyr, HN-C=O), 171.38 (O-C=O); MS (ESI) *m/z*: 500.1 $[M+H]^+$, 522.2 $[M+Na]^+$, 538.2 $[M+K]^+$.

Allyl *N*$^{\alpha}$-(9-fluorenylmethyloxycarbonyl)-L-tyrosinate: Fmoc-L-Tyr(^{t}Bu)-OAll (1.71 g, 3.43 mmol) was dissolved in TFA/CH_2Cl_2 (1:1) and the mixture was stirred at room temperature for 3 h. After this time, the solution was concentrated to dryness in vacuo, followed by repeated washings and evaporations with diethyl ether. Digestion of the resulting residue with pentane yielded Fmoc-L-Tyr-OAll as a white solid (1.39 g, 91% yield). IR (neat): 3311 (OH_{st}), 1717 ($C=O_{st}$), 1685 ($NH(C=O)-O_{st}$), 1514 (NH_{δ}), 1449 ($CH_{2\delta}$), 1311, 1254, 1218 ($C-O_{st}$, $arC-OH_{st}$), 1087, 1031, 933, 825, 757, 733 cm^{-1}; ^{1}H-NMR (400 MHz, $CDCl_3$) δ (ppm): 3.02 (dd, *J* = 6.0, 14.0 Hz, 1H, CH_2-β), 3.09 (dd, *J* = 6.0, 14.0 Hz, 1H, CH_2-β), 4.20 (t, 1H, *J* = 7.2 Hz, 1H, CH-Fmoc), 4.35 (dd, *J* = 7.2, 10.4 Hz, 1H, OCH_2-Fmoc), 4.44 (dd, *J* = 7.2, 10.4 Hz, 1H, OCH_2-Fmoc), 4.63 (d, *J* = 6.0 Hz, 2H, OCH_2-All), 4.65-4.68 (m, 1H, CH-α), 5.25-5.35 (m, 3H, $=CH_2$, NH), 5.84-5.93 (m, 1H, =CH), 6.72 (d, *J* = 8.4 Hz, 2H, CH_{Arom9}-Tyr), 6.95 (d, *J* = 8.4 Hz, 2H, CH_{Arom8}-Tyr), 7.31 (td, *J* = 1.2, 7.2 Hz, 2H, CH_{Arom16}-Fmoc), 7.40 (t, *J* = 7.2 Hz, 2H, CH_{Arom17}-Fmoc), 7.56 (dd, *J* = 3.6, 7.2 Hz, 2H, CH_{Arom15}-Fmoc), 7.76 (d, *J* = 7.6 Hz, 2H, CH_{Arom18}-Fmoc); ^{13}C-NMR (100 MHz, $CDCl_3$) δ (ppm): 37.55 (CH_2-β), 47.21 (CH-Fmoc), 55.08 (CH-α), 66.32 (OCH_2-All), 67.19 (OCH_2-Fmoc), 115.63 (CH_{Arom9}-Tyr), 119.38 ($=CH_2$), 120.11 (CH_{Arom18}-Fmoc), 125.16 (CH_{Arom15}-Fmoc), 127,19 (CH_{Arom16}-Fmoc), 127.45 (C_{Arom7}-Tyr), 127.86 (CH_{Arom17}-Fmoc), 130.62 (CH_{Arom8}-Tyr), 131.40 (=CH), 141.41, 143.74 (C_{Arom14}-Fmoc, C_{Arom19}-Fmoc), 155.11 ($OC_{q-Arom-}$Tyr), 155.89 (HN-C=O), 171.55 (O-C=O); MS (ESI) *m/z*: 222.0 $[M+2H]^{2+}$, 444.0 $[M+H]^+$, 466.1 $[M+Na]^+$.

Allyl N^{α}-(9-fluorenylmethyloxycarbonyl)-D-tyrosinate: This compound was prepared following the procedure described for Fmoc-L-Tyr-OAll starting from Fmoc-D-Tyr(^{t}Bu)-OAll (2.49 g, 4.99 mmol). Fmoc-D-Tyr-OAll was obtained quantitatively as a white solid (2.21 g, 99% yield). IR (neat): 3311 (OH_{st}), 1717 ($C=O_{st}$), 1685 ($NH(C=O)-O_{st}$), 1514 (NH_{δ}), 1449 ($CH_{2\delta}$), 1311, 1254 ($C-O_{st}$, $arC-OH_{st}$), 1087, 1031, 933, 825, 757, 733 cm^{-1}; ^{1}H-NMR (400 MHz, $CDCl_3$) δ (ppm): 3.02 (dd, *J* = 6.0, 14.0 Hz, 1H, CH_2-β), 3.09 (dd, *J* = 5.6, 14.0 Hz, 1H, CH_2-β), 4.20 (t, 1H, *J* = 7.2 Hz, 1H, CH-Fmoc), 4.36 (dd, *J* = 7.2, 10.4 Hz, 1H, OCH_2-Fmoc), 4.43 (dd, *J* = 7.2, 10.4 Hz, 1H, OCH_2-Fmoc), 4.63 (d, *J* = 6.0 Hz, 2H, OCH_2-All), 4.65-4.69 (m, 1H, CH-α), 5.26-5.35 (m, 3H, $=CH_2$, NH), 5.84-5.92 (m, 1H, =CH), 6.72 (d, *J* = 8.4 Hz, 2H, CH_{Arom9}-Tyr), 6.95 (d, *J* = 8.4 Hz, 2H, CH_{Arom8}-Tyr), 7.31 (td, *J* = 1.2, 7.6 Hz, 2H, CH_{Arom16}-Fmoc), 7.40 (t, *J* = 7.6 Hz, 2H, CH_{Arom17}-Fmoc), 7.56 (dd, *J* = 3.2, 7.6 Hz, 2H, CH_{Arom15}-Fmoc), 7.76 (d, *J* = 7.6 Hz, 2H, CH_{Arom18}-Fmoc); ^{13}C-NMR (100 MHz, $CDCl_3$) δ (ppm): 37.56 (CH_2-β), 47.23 (CH-Fmoc), 55.08 (CH-α), 66.34 (OCH_2-Al), 67.18 (OCH_2-Fmoc), 115.63 (CH_{Arom9}-Tyr), 119.40 ($=CH_2$-Al), 120.14 (CH_{Arom18}-Tyr), 125.25 (CH_{Arom15}-Fmoc), 127,21 (CH_{Arom16}-Fmoc), 127.51 (C_{Arom7}-Tyr), 127.87 (CH_{Arom17}-Tyr), 130.66 (CH_{Arom8}-Tyr), 131.44 (=CH), 141.43, 143.77 (C_{Arom14}-Fmoc, C_{Arom19}-Fmoc), 155.09 ($OC_{q\ Arom}$-Tyr), 155.86 (NH-C=O), 171.56 (O-C=O); MS (ESI) *m/z*: 222.0 $[M+2H]^{2+}$, 444.0 $[M+H]^+$, 466.1 $[M+Na]^+$.

N^{α}-(*p*-Nitrobenzyloxycarbonyl)-O-*tert*-butyl-L-tyrosine (Isidro-Llobet et al., 2005): NaN_3 (164.37 mg, 2.53 mmol) was dissolved in H_2O (0.66 mL) and the mixture was added to a solution of *p*Nz-Cl (468.3 mL, 2.11 mmol) in 1,4-dioxane (0.92 mL). The mixture was stirred at room temperature for 2 h until the formation of *p*-nitrobenzylazidoformate (*p*Nz-N_3). Next, a solution of H-L-Tyr(^{t}Bu)-OH (500 mg, 2.11 mmols) in 1% Na_2CO_3/1,4-dioxane (1:1, 2.63 mL) was added dropwise. The resulting white suspension was stirred for 48 h at room temperature keeping the pH between 8 and 10 by addition of 10% Na_2CO_3. The progress of the reaction was monitored by TLC. Once the reaction was completed, H_2O (30 mL) was added and the resulting suspension was washed with *tert*-butyl methyl ether (3×15 mL). The aqueous portion was acidified to pH 2 with 3 N HCl and a precipitate appeared, which was filtered off and dried to yield *p*Nz-L-Tyr(^{t}Bu)-OH as a white solid (653.3 mg, 75% yield). ^{1}H-NMR (400 MHz, CD_3OD) δ (ppm): 1.31 (s, 9H, $(CH_3)_3$), 2.87 (dd, *J* = 9.6, 14.0 Hz, 1H, CH_2-β), 3.20 (dd, *J* = 4.6, 14.0 Hz, 1H, CH_2-β), 4.39 (dd, *J* = 4.6, 9.6 Hz, 1H, CH-α), 5.09 (d,

J = 13.8 Hz, 1H, OCH_2), 5.19 (d, J = 13.8 Hz, 1H, OCH_2), 6.88 (d, J = 8.6 Hz, 2H, CH_{Arom3}-Tyr), 7.14 (d, J = 8.6 Hz, 2H, CH_{Arom2}-Tyr), 7.45 (d, J = 8.8 Hz, 2H, CH_{Arom2}-*p*Nz), 8.20 (d, J = 8.8 Hz, 2H, CH_{Arom3}-*p*Nz); ^{13}C-NMR (100 MHz, CD_3OD) δ (ppm): 29.18 ($(CH_3)_3$), 38.26 (CH_2-β), 57.30 (CH-α), 65.92 (OCH_2), 79.45 ($C(CH_3)_3$), 124.54, 125.07 (CH_{Arom3}-Tyr, CH_{Arom3}-*p*Nz), 128.87, 130.87 (CH_{Arom2}-Tyr, CH_{Arom2}-*p*Nz), 133.92 (C_{Arom1}-Tyr), 146.11, 148.84 (C_{Arom1}-*p*Nz, C_{Arom4}-*p*Nz), 155.27 (OC_{Arom4}-Tyr), 157.82 (HN-C=O), 175.70 (COOH).

N^{α}-(*p*-Nitrobenzyloxycarbonyl)-L-tyrosine: This compound was prepared following the procedure described for Fmoc-L-Tyr-OAll starting from *p*Nz-L-Tyr(^{t}Bu)-OH (613.3 mg, 1.47 mmol). *p*Nz-L-Tyr-OH was obtained quantitatively as a white solid (478.1 mg, 90% yield). IR (neat): 3325 (COO-H_{st}), 1697 (C=O_{st}), 1608, 1512 ($NO_{2\ st\ as}$), 1441, 1343 ($NO_{2\ st\ sim}$), 1201, 1105, 1059 cm^{-1}; ^{1}H-NMR (400 MHz, CD_3OD) δ (ppm): 2.82 (dd, J = 9.6, 14.0 Hz, 1H, CH_2-β), 3.13 (dd, J = 4.8, 14.0 Hz, 1H, CH_2-β), 4.38 (dd, J = 4.8, 9.6 Hz, 1H, CH-α), 5.11 (d, J = 14.0 Hz, 1H, OCH_2), 5.19 (d, J = 14.0 Hz, 1H, OCH_2), 6.70 (d, J = 8.4 Hz, 2H, CH_{Arom3}-Tyr), 7.05 (d, J = 8.4 Hz, 2H, CH_{Arom2}-Tyr), 7.45 (d, J = 8.8 Hz, 2H, CH_{Arom2}-*p*Nz), 8.19 (d, J = 8.8 Hz, 2H, CH_{Arom3}-*p*Nz); ^{13}C-NMR (100 MHz, CD_3OD) δ (ppm): 37.87 (CH_2-β), 57.03 (CH-α), 65.97 (OCH_2), 116.16 (CH_{Arom3}-Tyr), 124.50 (CH_{Arom3}-*p*Nz), 128.77, 129.16 (CH_{Arom2}-Tyr, CH_{Arom2}-*p*Nz), 131.31 (C_{Arom1}-Tyr), 146.06, 148.79 (C_{Arom1}-*p*Nz, C_{Arom4}-*p*Nz), 157.29, 157.94 (OC_{Arom4}-Tyr, HN-C=O), 175.17 (COOH); MS (ESI) *m/z* : 361.0 $[M+H]^+$, 383.0 $[M+Na]^+$.

N^{α}-Allyloxycarbonyl-L-isoleucine (Cruz et al., 2004): NaN_3 (1.49 g, 22.89 mmol) was dissolved in H_2O (4 mL) and the mixture was added to a solution of Alloc-Cl (2 mL, 18.31 mmol) in 1,4-dioxane (5 mL). The mixture was stirred at room temperature for 1 h until the formation of allylazidoformate (Alloc-N_3). Afterwards, a solution of H-L-Ile-OH (2 g, 15.26 mmols) in 1% Na_2CO_3/1,4-dioxane (1:1, 44.5 mL) was added dropwise and the mixture was stirred for 48 h at room temperature. The progress of the reaction was monitored by TLC and the pH was kept between 8 and 10 by addition of 10% Na_2CO_3. Once the reaction was completed, H_2O (44 mL) was added keeping the pH between 9 and 10 by addition of 10% Na_2CO_3. The resulting suspension was washed with *tert*-butyl methyl ether (3×60 mL), the aqueous layer was acidified to pH 2 with 2 N HCl and extracted with AcOEt (3×60 mL). The combined organic layers were dried over anhydrous $MgSO_4$ and filtered. The solvent was removed under reduced pressure to afford Alloc-L-Ile-OH as a colorless oil (3.25 g, 99% yield), which was immediately used without purification. R_f (AcOEt/CH_3OH/NH_3, 5:1:1) = 0.27; IR (neat): 3500-3250 (NH_{st}), 2965 (COO-H_{st}), 1703 (C=O_{st}), 1520 (NH_{δ}), 1407, 1209 (CO-O_{st}), 1120, 1041 cm^{-1}; ^{1}H-NMR (400 MHz, $CDCl_3$) δ (ppm): 0.93 (t, *J* = 7.2 Hz, 3H, CH_3), 0.97 (d, *J* = 6.8 Hz, 3H, CH_3), 1.16-1.28 (m, 1H, CH_2-Ile), 1.42-1.50 (m, 1H, CH_2-Ile), 1.93-1.95 (m, 1H, CH-β), 4.36 (dd, *J* = 4.8, 9.2 Hz, 1H, CH-α), 4.57 (d, *J* = 5.6 Hz, 2H, OCH_2-Alloc), 5.22 (dd, *J* = 1.2, 10.4 Hz, 1H, =CH_2), 5.31 (dd, *J* = 1.2, 13.2 Hz, 1H, =CH_2), 5.86-5.96 (m, 1H, =CH), 6.21 (d, *J* = 7.6 Hz, 1H, NH), 9.02 (br, 1H, COOH); ^{13}C-NMR (75 MHz, $CDCl_3$) δ (ppm): 11.60 (CH_3), 15.51 (CH_3), 24.82 (CH_2-Ile), 37.72 (CH-β), 58.23 (CH-α), 66.01 (OCH_2-Alloc), 118.01 (=CH_2), 132.52 (=CH), 156.14 (HN-C=O), 176.71 (O-C=O); MS (ESI) *m/z*: 216.0 $[M+H]^+$, 238.0 $[M+Na]^+$.

4.4.3 Solid-Phase Synthesis of cyclic octapeptides

4.4.3.1 General method for the synthesis of linear peptidyl resins

Peptides were synthesized manually by the solid-phase method starting from Fmoc-Rink-ChemMatrix (0.66 mmol/g) resin. Peptide synthesis was performed in a polypropylene syringe fitted with a polyethylene porous disc. Solvents and soluble reagents were removed by filtration. Sequential Fmoc group removal and couplings steps were carried out. The Fmoc group was removed using piperidine/DMF (3:7, 1×2 + 3×10 min). Couplings of the corresponding Fmoc- or Boc-amino acids (4 equiv) were carried out with ethyl 2-cyano-2-(hydroxyimino)acetate (Oxyma) (4 equiv) and *N,N'*-diisopropylcarbodiimide (DIPCDI) (4 equiv) in *N,N*'-dimethylformamide (DMF) at room temperature for 3 h. The completion of the reactions was checked by the Kaiser (Kaiser et al., 1970) or the chloranil test (Adamson et al., 1992). After each coupling and deprotection step, the resin was washed with DMF (6×1 min) and CH_2Cl_2 (3×1 min), and air-dried. An aliquot of the resulting peptidyl resin was treated with trifluoroacetic acid (TFA)/H_2O/triisopropylsilane (TIS) (95:2.5:2.5) for 2 h at room temperature. Following TFA evaporation and diethyl ether extraction, the crude peptide was dissolved in H_2O/CH_3CN, lyophilized, analyzed by HPLC and characterized by mass spectrometry.

Boc-Phe[4-NH-Ile-Tyr(^{t}Bu)-Fmoc]-Thr(^{t}Bu)-Glu(O^{t}Bu)-Val-Pro-Glu(Rink-ChemMatrix)-OAll. Starting from Fmoc-Rink-ChemMatrix resin (0.66 mmol/g), the peptidyl resin Fmoc-Thr(^{t}Bu)-Glu(O^{t}Bu)-Val-Pro-Glu(Rink-ChemMatrix)-OAll was prepared following the procedure described above. Acidolytic cleavage of an aliquot of this peptidyl resin afforded Fmoc-Thr-Glu-Val-Pro-Gln-OAll in 93% purity. HPLC (*λ = 220 nm, Method A*) t_R = 7.55 min. Further elongation of the peptide sequence provided the peptidyl resin Boc-Phe[4-NH-Ile-Tyr(^{t}Bu)-Fmoc]-Thr(^{t}Bu)-Glu(O^{t}Bu)-Val-Pro-Glu(Rink-ChemMatrix)-OAll. Acidolytic cleavage of an aliquot of this peptidyl resin afforded H-Phe(4-NH-Ile-Tyr-Fmoc)-Thr-Glu-Val-Pro-Gln-OAll in 93% purity. HPLC (*λ = 220 nm, Method A*) t_R = 7.68 min; MS (ESI) *m/z*(+): 1273.7 $[M+H]^+$, 1295.7 $[M+Na]^+$, 1311.7 $[M+K]^+$.

Boc-Phe[4-NH-Ile-D-Tyr(^{t}Bu)-Fmoc]-D-Thr(^{t}Bu)-Glu(O^{t}Bu)-D-Val-Pro-Glu(Rink-ChemMatrix)-OAll. Starting from Fmoc-Rink-ChemMatrix resin (0.66 mmol/g), this peptidyl resin was prepared following the general procedure described above. Acidolytic cleavage of an aliquot of this peptidyl resin afforded H-Phe(4-NH-Ile-D-Tyr-Fmoc)-D-Thr-Glu-D-Val-Pro-Gln-OAll in 94% purity. HPLC (*λ = 220 nm, Method A*) t_R = 7.66 min.

Boc-Phe[4-NH-Ile-D-Tyr(^{t}Bu)-Fmoc]-D-Thr(^{t}Bu)-Glu(O^{t}Bu)-D-Ala-Pro-Glu(Rink-ChemMatrix)-OAll. Starting from Fmoc-Rink-ChemMatrix resin (0.66 mmol/g), this peptidyl resin was prepared following the general procedure described above. Acidolytic cleavage of an aliquot of this peptidyl resin afforded H-Phe(4-NH-Ile-D-Tyr-Fmoc)-D-Thr-Glu-D-Ala-Pro-Gln-OAll in 96% purity. HPLC (*λ = 220 nm, Method A*) t_R = 7.51 min.

Boc-Phe[4-NH-Ile-D-Tyr(^{t}Bu)-Fmoc]-D-Ser(^{t}Bu)-Glu(O^{t}Bu)-D-Ala-Pro-Glu(Rink-ChemMatrix)-OAll. Starting from Fmoc-Rink-ChemMatrix resin (0.66 mmol/g), this peptidyl resin was prepared following the general procedure described above. Acidolytic cleavage of an aliquot of this peptidyl resin afforded H-Phe(4-NH-Ile-D-Tyr-Fmoc)-D-Ser-Glu-D-Ala-Pro-Gln-OAll in 95% purity. HPLC (*λ = 220 nm, Method A*) t_R = 7.52 min.

Boc-Phe[4-NH-Ile-D-Tyr(^{t}Bu)-Fmoc]-D-Ser(^{t}Bu)-Glu(O^{t}Bu)-D-Val-Pro-Glu(Rink-ChemMatrix)-OAll. Starting from Fmoc-Rink-ChemMatrix resin (0.66 mmol/g), this peptidyl resin was prepared following the general procedure described above. Acidolytic cleavage of an aliquot of this peptidyl resin afforded H-Phe(4-NH-Ile-D-Tyr-Fmoc)-D-Ser-Glu-D-Val-Pro-Gln-OAll in 96% purity. HPLC (λ = *220 nm, Method A*) t_R = 7.64 min.

4.4.3.2 General method for the allyl and Fmoc group removal from linear peptidyl resins

The corresponding linear peptidyl resin was treated with $Pd(PPh_3)_4$ (5 equiv) in $CHCl_3$/AcOH/*N*-methylmorpholine (NMM) (3:2:1) under nitrogen for 3 h. Then, the resin was washed with tetrahydrofuran (THF) (3×2 min), DMF (3×2 min), DIEA/CH_2Cl_2 (1:19, 3×2 min), sodium *N,N'*-diethyldithiocarbamate (0.03 M in DMF, 3×15 min), DMF (1×10 min) and CH_2Cl_2 (3×2 min). Next, the Fmoc group was removed with piperidine/DMF (3:7, 1×2 + 2×10 min) followed by washes with DMF (6×1 min) and CH_2Cl_2 (3×1 min). An aliquot of the resulting resin was exposed to TFA/H_2O/TIS (95:2.5:2.5) for 2 h at room temperature. The resulting crude peptide was analized by HPLC and characterized by mass spectrometry.

Boc-Phe[4-NH-Ile-Tyr(^{t}Bu)-H]-Thr(^{t}Bu)-Glu(O^{t}Bu)-Val-Pro-Glu(Rink-ChemMatrix)-OH. Starting from Boc-Phe[4-NH-Ile-Tyr(^{t}Bu)-Fmoc]-Thr(^{t}Bu)-Glu(O^{t}Bu)-Val-Pro-Glu(Rink-ChemMatrix)-OAll resin, the allyl and Fmoc groups were cleaved following the general procedure described above. Acidolytic cleavage of an aliquot of the resulting peptidyl resin afforded H-Phe(4-NH-Ile-Tyr-H)-Thr-Glu-Val-Pro-Gln-OH in >99% purity. HPLC (λ = *220 nm, Method A*) t_R = 5.70 min; MS (ESI) *m/z*(+): 506.2 $[M+2H]^{+2}$, 1011.6 $[M+H]^+$, 1033.6 $[M+Na]^+$, 1049.5 $[M+K]^+$.

Boc-Phe[4-NH-Ile-D-Tyr(^{t}Bu)-H]-D-Thr(^{t}Bu)-Glu(O^{t}Bu)-D-Val-Pro-Glu(Rink-ChemMatrix)-OH. Starting from Boc-Phe[4-NH-Ile-D-Tyr(^{t}Bu)-Fmoc]-D-Thr(^{t}Bu)-Glu(O^{t}Bu)-D-Val-Pro-Glu(Rink-ChemMatrix)-OAll, the allyl and Fmoc groups were cleaved following the general procedure described above. Acidolytic cleavage of an aliquot of the resulting peptidyl resin afforded H-Phe(4-NH-Ile-D-Tyr-H)-D-Thr-Glu-D-

Val-Pro-Gln-OH in 94% purity. HPLC (λ = *220 nm*, *Method A*) t_R = 6.03 min; MS (ESI) *m/z*(+): 506.2 $[M+2H]^{+2}$, 1011.6 $[M+H]^+$, 1033.6 $[M+Na]^+$.

Boc-Phe[4-NH-Ile-D-Tyr(^{t}Bu)-H]-D-Thr(^{t}Bu)-Glu(O^{t}Bu)-D-Ala-Pro-Glu(Rink-ChemMatrix)-OH. Starting from Boc-Phe[4-NH-Ile-D-Tyr(^{t}Bu)-Fmoc]-D-Thr(^{t}Bu)-Glu(O^{t}Bu)-D-Ala-Pro-Glu(Rink-ChemMatrix)-OAll, the allyl and Fmoc groups were cleaved following the general procedure described above. Acidolytic cleavage of an aliquot of the resulting peptidyl resin afforded H-Phe(4-NH-Ile-D-Tyr-H)-D-Thr-Glu-D-Ala-Pro-Gln-OH in 91% purity. HPLC (λ = *220 nm*, *Method A*) t_R = 5.86 min; MS (ESI) *m/z*(+): 983.6 $[M+H]^+$, 1005.5 $[M+Na]^+$.

Boc-Phe[4-NH-Ile-D-Tyr(^{t}Bu)-H]-D-Ser(^{t}Bu)-Glu(O^{t}Bu)-D-Ala-Pro-Glu(Rink-ChemMatrix)-OH. Starting from Boc-Phe[4-NH-Ile-D-Tyr(^{t}Bu)-Fmoc]-D-Ser(^{t}Bu)-Glu(O^{t}Bu)-D-Ala-Pro-Glu(Rink-ChemMatrix)-OAll the allyl and Fmoc groups were cleaved following the general procedure described above. Acidolytic cleavage of an aliquot of the resulting peptidyl resin afforded H-Phe(4-NH-Ile-D-Tyr-H)-D-Ser-Glu-D-Ala-Pro-Gln-OH in >99% purity. HPLC (λ = *220 nm*, *Method A*) t_R = 5.86 min; MS (ESI) *m/z*(+): 485.1 $[M+2H]^{2+}$, 969.5 $[M+H]^+$, 991.5 $[M+Na]^+$.

Boc-Phe[4-NH-Ile-D-Tyr(^{t}Bu)-H]-D-Ser(^{t}Bu)-Glu(O^{t}Bu)-D-Val-Pro-Glu(Rink-ChemMatrix)-OH. Starting from Boc-Phe[4-NH-Ile-D-Tyr(^{t}Bu)-Fmoc]-D-Ser(^{t}Bu)-Glu(O^{t}Bu)-D-Val-Pro-Glu(Rink-ChemMatrix)-OAll, the allyl and Fmoc groups were cleaved following the general procedure described above. Acidolytic cleavage of an aliquot of the resulting peptidyl resin afforded H-Phe(4-NH-Ile-D-Tyr-H)-D-Ser-Glu-D-Val-Pro-Gln-OH in 99% purity. HPLC (λ = *220 nm*, *Method A*) t_R = 6.02 min; MS (ESI) *m/z*(+): 499.1 $[M+2H]^{2+}$, 997.5 $[M+H]^+$, 1019.5 $[M+Na]^+$.

4.4.3.3 General method for the synthesis of cyclic peptides

The corresponding linear peptidyl resin was treated with [ethyl cyano(hydroxyimino)acetato-O^2]tri-(1-pyrrolidinyl)-phosphonium hexafluorophosphate (PyOxim) (5 equiv), Oxyma (5 equiv) and DIEA (10 equiv) in DMF under stirring for 24 h. Afterwards, the resin was washed with DMF (6×1 min) and CH_2Cl_2 (3×1 min). The completion of the cyclization was checked with the Kaiser test (Kaiser et al., 1970).

The resulting peptidyl resin was treated with TFA/H_2O/TIS (95:2.5:2.5) for 2 h at room temperature, followed by TFA evaporation and diethyl ether extraction. The resulting crude peptide was dissolved in H_2O/CH_3CN, lyophilized, analyzed by HPLC and characterized by mass spectrometry.

H-Phe(4-NH-&)-Thr-Glu-Val-Pro-Gln-Tyr-Ile-& (1). Starting from Boc-Phe[4-NH-Ile-Tyr(^{t}Bu)-H]-Thr(^{t}Bu)-Glu(O^{t}Bu)-Val-Pro-Glu(Rink-ChemMatrix)-OH resin, this cyclic octapeptide was prepared following the general procedure described above. Acidolytic cleavage of the resulting peptidyl resin afforded H-Phe(4-NH-&)-Thr-Glu-Val-Pro-Gln-Tyr-Ile-& (**1**) as a broad peak by HPLC (λ = *220 nm, Method A,* t_R = 6.66 min). MS (ESI) *m/z*(+): 993.6 $[M+H]^+$+$[M_{Dimer}+2H]^{2+}$, 1015.6 $[M+Na]^+$, 1031.6 $[M+K]^+$, 1987.2 $[M_{Dimer}+H]^+$.

H-Phe(4-NH-&)-D-Thr-Glu-D-Val-Pro-Gln-D-Tyr-Ile-& (BPC862). Starting from Boc-Phe[4-NH-Ile-D-Tyr(^{t}Bu)-H]-D-Thr(^{t}Bu)-Glu(O^{t}Bu)-D-Val-Pro-Glu(Rink-ChemMatrix)-OH, this cyclic octapeptide was prepared following the general procedure described above. Acidolytic cleavage of the resulting peptidyl resin afforded H-Phe(4-NH-&)-D-Thr-Glu-D-Val-Pro-Gln-D-Tyr-Ile-& (**BPC862**) (39% purity) together with the dimeric compound (61% purity). Reverse-phase column chromatography eluting with H_2O/CH_3CN (65:35) afforded the expected cyclic octapeptide **BPC862** in >99% purity. HPLC (λ = *220 nm, Method A*) t_R = 6.34 min. MS (ESI) *m/z*(+): 993.6 $[M+H]^+$, 1015.6 $[M+Na]^+$.

H-Phe(4-NH-&)-D-Thr-Glu-D-Ala-Pro-Gln-D-Tyr-Ile-& (BPC864). Starting from Boc-Phe[4-NH-Ile-D-Tyr(^{t}Bu)-H]-D-Thr(^{t}Bu)-Glu(O^{t}Bu)-D-Ala-Pro-Glu(Rink-ChemMatrix)-OH, this cyclic octapeptide was prepared following the general procedure described above. Acidolytic cleavage of the resulting peptidyl resin afforded H-Phe(4-NH-&)-D-Thr-Glu-D-Ala-Pro-Gln-D-Tyr-Ile-& (**BPC864**) (41% purity) together with the dimeric compound (57% purity). Reverse-phase column chromatography eluting with H_2O/CH_3CN (68:32) afforded the expected cyclic octapeptide **BPC864** in >99% purity. HPLC (λ = *220 nm, Method A*) t_R = 6.24 min. MS (ESI) *m/z*(+): 965.5 $[M+H]^+$, 987.4 $[M+Na]^+$.

H-Phe(4-NH-&)-D-Ser-Glu-D-Ala-Pro-Gln-D-Tyr-Ile-& (BPC866). Starting from Boc-Phe[4-NH-Ile-D-Tyr(^{t}Bu)-H]-D-Ser(^{t}Bu)-Glu(O^{t}Bu)-D-Ala-Pro-Glu(Rink-

ChemMatrix)-OH, this cyclic octapeptide was prepared following the general procedure described above. Acidolytic cleavage of the resulting peptidyl resin afforded H-Phe(4-NH-&)-D-Ser-Glu-D-Ala-Pro-Gln-D-Tyr-Ile-& (**BPC866**) (53% purity) together with the dimeric compound (47% purity). Reverse-phase column chromatography eluting with H_2O/CH_3CN (68:32) afforded the expected cyclic octapeptide **BPC866** in >99% purity. HPLC (λ = *220 nm, Method A*) t_R = 6.11 min. MS (ESI) *m/z*(+): 951.6 $[M+H]^+$, 973.6 $[M+Na]^+$.

H-Phe(4-NH-&)-D-Ser-Glu-D-Val-Pro-Gln-D-Tyr-Ile-& (BPC868). Starting from Boc-Phe[4-NH-Ile-D-Tyr(^{t}Bu)-H]-D-Ser(^{t}Bu)-Glu(O^{t}Bu)-D-Val-Pro-Glu(Rink-ChemMatrix)-OH, this cyclic octapeptide was prepared following the general procedure described above. Acidolytic cleavage of the resulting peptidyl resin afforded H-Phe(4-NH-&)-D-Ser-Glu-D-Val-Pro-Gln-D-Tyr-Ile-& (**BPC868**) (56% purity) together with the dimeric compound (44% purity). Reverse-phase column chromatography eluting with H_2O/CH_3CN (66:34) afforded the expected cyclic octapeptide **BPC868** in >99% purity. HPLC (λ = *220 nm, Method A*) t_R = 6.29 min. MS (ESI) *m/z*(+): 979.6 $[M+H]^+$, 1001.6 $[M+Na]^+$.

4.4.4 Solid-Phase Synthesis of cyclic octadepsipeptides

4.4.4.1 Synthesis of Fmoc-L-Tyr(Wang)-OAll or Fmoc-D-Tyr(Wang)-OAll

Wang resin (450 mg, 1.1 mmol/g) was placed on a 35 mL reaction vessel and swollen in dry THF for 30 min. Fmoc-L-Tyr-OAll or Fmoc-D-Tyr-OAll (878.11 mg, 1.98 mmol) and PPh_3 (519.35 mg, 1.98 mmol) were dissolved in dry THF (3 mL), and added to the resin. The resulting mixture was cooled at 0 ºC and a solution of diisopropyl azodicarboxylate (DIAD) (410 µL, 1.98 mmol) in dry THF (0.5 mL) was then added dropwise. After 1 h at 0 ºC, the mixture was left to warm to room temperature and either shaken for 24 h (Cabrele et al., 1999; Thutewohl and Waldmann, 2003) (conditions A) or heated in a microwave reactor at 60 °C for 30 min (conditions B). Next, the reaction mixture was transferred to a polypropylene syringe and filtered off. The resulting resin was washed with THF (3×2 min), CH_2Cl_2 (3×2 min), DMF/H_2O (1:1, 3×2 min), DMF (3×2 min), CH_3OH (3x2 min), CH_2Cl_2 (3x2 min) and diethyl ether (3×2 min), and dried in vacuo. The loading of the resulting resin was determined by the Fmoc test (Grant, 1992), being 0.22 mmol/g for Fmoc-L-Tyr(Wang)-OAll and 0.33 mmol/g for Fmoc-D-Tyr(Wang)-OAll. The racemization of the anchored amino acid was evaluated using the Marfey's reagent (Adamson et al., 1992). Finally, the resin was acetylated with acetic anhydride/pyridine/CH_2Cl_2 (86:7:7, 2×30 min), washed with CH_2Cl_2 (3×2 min), DMF (3×2 min), CH_3OH (3×1 min), CH_2Cl_2 (3×2 min) and diethyl ether (3 × 2 min), and dried in vacuo (Thutewohl and Waldmann, 2003).

4.4.4.2 Synthesis of the linear peptidyl resins

Starting from resins Fmoc-Rink-MBHA resin, Fmoc-L-Tyr(Wang)-OAll or Fmoc-D-Tyr(Wang)-OAll, the following peptidyl resins were synthesized according to the general solid-phase procedure described in *section 4.4.3.1*.

Boc-Tyr-Thr(^{t}Bu)-Glu(O^{t}Bu)-Val-Pro-Glu(Rink-MBHA)-OAll (3a). This peptidyl resin was prepared starting from Fmoc-Rink-MBHA resin (0.40 mmol/g). Acidolytic cleavage of an aliquot of this peptidyl resin afforded H-Tyr-Thr-Glu-Val-Pro-Gln-OAll in >99% purity. HPLC (λ *= 220 nm, Method A*) t_R = 6.33 min.

***p*NZ-Tyr-Thr(^{t}Bu)-Glu(O^{t}Bu)-Val-Pro-Glu(Rink-MBHA)-OAll (3b).** This peptidyl resin was prepared starting from Fmoc-Rink-MBHA resin (0.40 mmol/g). Acidolytic cleavage of an aliquot of this peptidyl resin afforded *p*Nz-Tyr-Thr-Glu-Val-Pro-Gln-OAll in 74% purity. HPLC (λ *= 220 nm, Method B*) t_R*:* = 3.51 min. MS (ESI) *m/z*(+): 955.4 $[M+H]^+$, 977.5 $[M+Na]^+$, 993.4 $[M+K]^+$.

***p*NZ-Tyr-Thr(^{t}Bu)-Glu(O^{t}Bu)-Val-Pro-Gln(Tr)-Tyr(Wang)-Oall (5).** This peptidyl resin was prepared starting from Fmoc-L-Tyr(Wang)-OAll (0.22 mmol/g). Acidolytic cleavage of an aliquot of the resulting resin afforded *p*NZ-Tyr-Thr-Glu-Val-Pro-Gln-Tyr-OAll in 82% purity. HPLC (λ *= 220 nm, Method B*) t_R = 3.97 min; MS (ESI) *m/z*(+): 1118.6 $[M+H]^+$, 1140.6 $[M+Na]^+$, 1156.5 $[M+K]^+$.

pNZ-Tyr-D-Thr(^{t}Bu)-Glu(O^{t}Bu)-D-Val-Pro-Gln(Tr)-D-Tyr(Wang)-OAll. This peptidyl resin was prepared starting from Fmoc-D-Tyr(Wang)-OAll (0.33 mmol/g). Acidolytic cleavage of an aliquot of the resulting resin afforded pNZ-Tyr-D-Thr-Glu-D-Val-Pro-Gln-D-Tyr-OAll in 65% purity. HPLC (λ = *220 nm, Method A*) t_R = 7.28 min; MS (ESI) *m/z*(+): 1118.5 [M+H]$^+$, 1140.4 [M+Na]$^+$, 1156.4 [M+K]$^+$.

Boc-Tyr-D-Thr(^{t}Bu)-Glu(O^{t}Bu)-D-Val-Pro-Gln(Tr)-D-Tyr(Wang)-OAll (9). This peptidyl resin was prepared starting from Fmoc-D-Tyr(Wang)-OAll (0.33 mmol/g). Acidolytic cleavage of an aliquot of the resulting resin afforded H-Tyr-D-Thr-Glu-D-Val-Pro-Gln-D-Tyr-OAll in 77% purity. HPLC (λ = *220 nm, Method A*) t_R = 6.60 min; MS (ESI) *m/z*(+): 939.5 [M+H]$^+$; MS (ESI) *m/z*(-): 937.4 [M-H]$^-$, 959.4 [M+Na-2H]$^-$.

Boc-Tyr-D-Ser(^{t}Bu)-Glu(O^{t}Bu)-D-Val-Pro-Gln(Tr)-D-Tyr(Wang)-OAll. This peptidyl resin was prepared starting from Fmoc-D-Tyr(Wang)-OAll (0.33 mmol/g). Acidolytic cleavage of an aliquot of the resulting resin afforded H-Tyr-D-Ser-Glu-D-Val-Pro-Gln-D-Tyr-OAll in 87% purity. HPLC (λ = *220 nm, Method A*) t_R = 6.58 min; MS (ESI) *m/z*(+): 925.5 [M+H]$^+$, 947.5 [M+Na]$^+$; MS (ESI) *m/z*(-): 923.4 [M-H]$^-$, 945.3 [M+Na-2H]$^-$.

Boc-Tyr-D-Thr(^{t}Bu)-Glu(O^{t}Bu)-D-Ala-Pro-Gln(Tr)-D-Tyr(Wang)-OAll. This peptidyl resin was prepared starting from Fmoc-D-Tyr(Wang)-OAll (0.33 mmol/g). Acidolytic cleavage of an aliquot of the resulting resin afforded H-Tyr-D-Thr-Glu-D-Ala-Pro-Gln-D-Tyr-OAll in 77% purity. HPLC (λ = *220 nm, Method A*) t_R = 6.38 min; MS (ESI) *m/z*(+): 911.5 [M+H]$^+$, 933.4 [M+Na]$^+$; MS (ESI) *m/z*(-): 909.4 [M-H]$^-$, 931.3 [M+Na-2H]$^-$.

Boc-Tyr-D-Ser(^{t}Bu)-Glu(O^{t}Bu)-D-Ala-Pro-Gln(Tr)-D-Tyr(Wang)-OAll. This peptidyl resin was prepared starting from Fmoc-D-Tyr(Wang)-OAll (0.33 mmol/g). Acidolytic cleavage of an aliquot of the resulting resin afforded H-Tyr-D-Ser-Glu-D-Ala-Pro-Gln-D-Tyr-OAll in 83% purity. HPLC *(λ = 220 nm, Method A)* t_R = 6.28 min; MS (ESI) *m/z*(+): 897.4 [M+H]$^+$, 919.4 [M+Na]$^+$; MS (ESI) *m/z*(-): 895.3 [M-H]$^-$, 917.3 [M+Na-2H]$^-$.

Boc-D-Tyr-D-Thr(^{t}Bu)-Glu(O^{t}Bu)-D-Val-Pro-Gln(Tr)-Tyr(Wang)-OAll. This peptidyl resin was prepared starting from Fmoc-L-Tyr(Wang)-OAll (0.22 mmol/g). Acidolytic cleavage of an aliquot of the resulting resin afforded H-D-Tyr-D-Thr-Glu-D-

Val-Pro-Gln-Tyr-OAll in 68% purity. HPLC (*λ = 220 nm, Method C*) t_R = 4.33 min; MS (ESI) *m/z*(+): 939.5 $[M+H]^+$, 961.5 $[M+Na]^+$; MS (ESI) *m/z*(-): 937.4 $[M-H]^-$, 959.3 $[M+Na-2H]^-$.

Boc-D-Tyr-D-Ser(^{t}Bu)-Glu(O^{t}Bu)-D-Val-Pro-Gln(Tr)-Tyr(Wang)-OAll. This peptidyl resin was prepared starting from Fmoc-L-Tyr(Wang)-OAll (0.22 mmol/g). Acidolytic cleavage of an aliquot of the resulting resin afforded H-D-Tyr-D-Ser-Glu-D-Val-Pro-Gln-Tyr-OAll in 64% purity. HPLC (*λ = 220 nm, Method C*) t_R = 4.33 min; MS (ESI) *m/z*(+): 925.5 $[M+H]^+$, 947.4 $[M+Na]^+$; MS (ESI) *m/z*(-): 923.4 $[M-H]^-$, 945.3 $[M+Na-2H]^-$.

Boc-D-Tyr-D-Thr(^{t}Bu)-Glu(O^{t}Bu)-D-Ala-Pro-Gln(Tr)-Tyr(Wang)-OAll. This peptidyl resin was prepared starting from Fmoc-L-Tyr(Wang)-OAll (0.22 mmol/g). Acidolytic cleavage of an aliquot of the resulting resin afforded H-D-Tyr-D-Thr-Glu-D-Ala-Pro-Gln-Tyr-OAll in 82% purity. HPLC (*λ = 220 nm, Method A*) t_R = 6.17 min; MS (ESI) *m/z*(+): 911.4 $[M+H]^+$, 933.4 $[M+Na]^+$; MS (ESI) *m/z*(-): 909.4 $[M-H]^-$, 931.3 $[M+Na-2H]^-$.

Boc-D-Tyr-D-Ser(^{t}Bu)-Glu(O^{t}Bu)-D-Ala-Pro-Gln(Tr)-Tyr(Wang)-OAll. This peptidyl resin was prepared starting from Fmoc-L-Tyr(Wang)-OAll (0.22 mmol/g). Acidolytic cleavage of an aliquot of the resulting resin afforded H-D-Tyr-D-Ser-Glu-D-Ala-Pro-Gln-Tyr-OAll in 66% purity. HPLC (*λ = 220 nm, Method C*) t_R = 3.95 min; MS (ESI) *m/z*(+): 897.4 $[M+H]^+$, 919.4 $[M+Na]^+$; MS (ESI) *m/z*(-): 895.3 $[M-H]^-$, 917.3 $[M+Na-2H]^-$.

4.4.4.3 General method for the solid-phase synthesis of the linear depsipeptidyl resins

Each peptidyl resin was treated with the corresponding protected isoleucine residue Fmoc-Ile-OH, Alloc-Ile-OH or Boc-Ile-OH (7 equiv), DIEA (1.4 equiv), DIPCDI (7 equiv) and DMAP (0.7 equiv) in DMF for 24 h. The treatment was repeated twice. After each treatment the resin was washed with DMF (6×1 min), CH_2Cl_2 (3×1 min) and air-dried. An aliquot of the resulting peptidyl resin was exposed to TFA/H_2O/TIS (95:2.5:2.5) for 2 h at room temperature. Following TFA evaporation and diethyl ether extraction, the crude peptide was dissolved in H_2O/CH_3CN, lyophilized, analyzed by HPLC and characterized by mass spectrometry.

Boc-Tyr(O-Ile-Fmoc)-Thr(^{t}Bu)-Glu(O^{t}Bu)-Val-Pro-Glu(Rink-MBHA)-OAll (4a). Starting from Boc-Tyr-Thr(^{t}Bu)-Glu(O^{t}Bu)-Val-Pro-Glu(Rink-MBHA)-OAll (**3a**), this peptidyl resin was prepared following the general procedure described above using Fmoc-Ile-OH. Acidolytic cleavage of an aliquot of this peptidyl resin afforded H-Tyr(O-Ile-Fmoc)-Thr-Glu-Val-Pro-Gln-OAll in >99% purity. HPLC (λ = *220 nm, Method A*) t_R = 7.93 min. MS (ESI) *m/z*(+): 1111.6 [M+H]$^+$, 1133.5 [M+Na]$^+$; MS (ESI) *m/z*(-): 1109.5 [M-H]$^-$.

***p*NZ-Tyr(O-Ile-Boc)-Thr(^{t}Bu)-Glu(O^{t}Bu)-Val-Pro-Glu(Rink-MBHA)-OAll (4b).** Starting from *p*NZ-Tyr-Thr(^{t}Bu)-Glu(O^{t}Bu)-Val-Pro-Glu(Rink-MBHA)-OAll (**3b**), this peptidyl resin was prepared following the general procedure described above using Boc-Ile-OH. Acidolytic cleavage of an aliquot of this peptidyl resin afforded *p*NZ-Tyr(O-Ile-H)-Thr-Glu-Val-Pro-Gln-OAll in 80% purity. HPLC (λ = *220 nm, Method B*) t_R = 3.45 min. MS (ESI) *m/z*(+): 1068.6 [M+H]$^+$, 1090.5 [M+Na]$^+$.

***p*NZ-Tyr(O-Ile-Alloc)-Thr(^{t}Bu)-Glu(O^{t}Bu)-Val-Pro-Gln(Tr)-Tyr(Wang)-OAll (6).** Starting from *p*NZ-Tyr-Thr(^{t}Bu)-Glu(O^{t}Bu)-Val-Pro-Gln(Tr)-Tyr(Wang)-OAll (**5**), this peptidyl resin was prepared following the general procedure described above using Alloc-Ile-OH. Acidolytic cleavage of an aliquot of the resulting resin afforded *p*NZ-Tyr(O-Ile-Alloc)-Thr-Glu-Val-Pro-Gln-Tyr-OAll in 70% purity. HPLC (λ = *220 nm, Method A*) t_R = 8.10 min; MS (ESI) *m/z*(+): 677.3 [M+H+K]$^{+2}$, 1315.6 [M+H]$^+$, 1337.6 [M+Na]$^+$, 1353.5 [M+K]$^+$.

***p*NZ-Tyr(O-Ile-Alloc)-D-Thr(^{t}Bu)-Glu(O^{t}Bu)-D-Val-Pro-Gln(Tr)-D-Tyr(Wang)-OAll.** Starting from *p*NZ-Tyr-D-Thr(^{t}Bu)-Glu(O^{t}Bu)-D-Val-Pro-Gln(Tr)-D-Tyr(Wang)-OAll, this peptidyl resin was prepared following the general procedure described above using Alloc-Ile-OH. Acidolytic cleavage of an aliquot of the resulting resin afforded *p*NZ-Tyr(O-Ile-Alloc)-D-Thr-Glu-D-Val-Pro-Gln-D-Tyr-OAll in 87% purity. HPLC (λ = *220 nm, Method A*) t_R = 8.21 min; MS (ESI) *m/z*(+): 1315.6 [M+H]$^+$, 1337.6 [M+Na]$^+$ 1353.5 [M+K]$^+$.

Boc-Tyr(O-Ile-Alloc)-D-Thr(^{t}Bu)-Glu(O^{t}Bu)-D-Val-Pro-Gln(Tr)-D-Tyr(Wang)-OAll. Starting from Boc-Tyr-D-Thr(^{t}Bu)-Glu(O^{t}Bu)-D-Val-Pro-Gln(Tr)-D-Tyr(Wang)-

OAll (**9**), this peptidyl resin was prepared following the general procedure described above using Alloc-Ile-OH. Acidolytic cleavage of an aliquot of the resulting resin afforded H-Tyr(O-Ile-Alloc)-D-Thr-Glu-D-Val-Pro-Gln-D-Tyr-OAll in 64% purity. HPLC (λ = *220 nm, Method A*) t_R = 7.48 min; MS (ESI) *m/z*(+): 1136.6 [M+H]$^+$, 1158.6 [M+Na]$^+$; MS (ESI) *m/z*(-): 1134.5 [M-H]$^-$.

Boc-Tyr(O-Ile-Alloc)-D-Ser(^{t}Bu)-Glu(O^{t}Bu)-D-Val-Pro-Gln(Tr)-D-Tyr(Wang)-OAll. Starting from Boc-Tyr-D-Ser(^{t}Bu)-Glu(O^{t}Bu)-D-Val-Pro-Gln(Tr)-D-Tyr(Wang)-OAll, this peptidyl resin was prepared following the general procedure described above using Alloc-Ile-OH. Acidolytic cleavage of an aliquot of the resulting resin afforded H-Tyr(O-Ile-Alloc)-D-Ser-Glu-D-Val-Pro-Gln-D-Tyr-OAll in 80% purity. HPLC (λ = *220 nm, Method A*) t_R = 7.55 min; MS (ESI) *m/z*(+): 1122.6 [M+H]$^+$, 1144.5 [M+Na]$^+$; MS (ESI) *m/z*(-): 1120.5 [M-H]$^-$.

Boc-Tyr(O-Ile-Alloc)-D-Thr(^{t}Bu)-Glu(O^{t}Bu)-D-Ala-Pro-Gln(Tr)-D-Tyr(Wang)-OAll. Starting from Boc-Tyr-D-Thr(^{t}Bu)-Glu(O^{t}Bu)-D-Ala-Pro-Gln(Tr)-D-Tyr(Wang)-OAll, this peptidyl resin was prepared following the general procedure described above using Alloc-Ile-OH. Acidolytic cleavage of an aliquot of the resulting resin afforded H-Tyr(O-Ile-Alloc)-D-Thr-Glu-D-Ala-Pro-Gln-D-Tyr-OAll in 77% purity. HPLC (λ = *220 nm, Method A*) t_R = 7.43 min; MS (ESI) *m/z*(+): 1108.6 [M+H]$^+$, 1130.5 [M+Na]$^+$; MS (ESI) *m/z*(-): 1106.5 [M-H]$^-$.

Boc-Tyr(O-Ile-Alloc)-D-Ser(^{t}Bu)-Glu(O^{t}Bu)-D-Ala-Pro-Gln(Tr)-D-Tyr(Wang)-OAll. Starting from Boc-Tyr-D-Ser(^{t}Bu)-Glu(O^{t}Bu)-D-Ala-Pro-Gln(Tr)-D-Tyr(Wang)-OAll, this peptidyl resin was prepared following the general procedure described above using Alloc-Ile-OH. Acidolytic cleavage of an aliquot of the resulting resin afforded H-Tyr(O-Ile-Alloc)-D-Ser-Glu-D-Ala-Pro-Gln-D-Tyr-OAll in 75% purity. HPLC (λ = *220 nm, Method A*) t_R = 7.27 min; MS (ESI) *m/z*(+): 1094.5 [M+H]$^+$, 1116.5 [M+Na]$^+$; MS (ESI) *m/z*(-): 1092.4 [M-H]$^-$.

Boc-D-Tyr(O-Ile-Alloc)-D-Thr(^{t}Bu)-Glu(O^{t}Bu)-D-Val-Pro-Gln(Tr)-Tyr(Wang)-OAll. Starting from Boc-D-Tyr-D-Thr(^{t}Bu)-Glu(O^{t}Bu)-D-Val-Pro-Gln(Tr)-Tyr(Wang)-OAll, this peptidyl resin was prepared following the general procedure described above using Alloc-Ile-OH. Acidolytic cleavage of an aliquot of the resulting resin afforded H-D-Tyr(O-Ile-Alloc)-D-Thr-Glu-D-Val-Pro-Gln-Tyr-OAll in 52% purity. HPLC (λ = *220* *nm, Method C*) t_R = 5.57 min; MS (ESI) *m/z*(+): 1136.6 $[M+H]^+$, 1158.6 $[M+Na]^+$; MS (ESI) *m/z*(-): 1134.5 $[M-H]^-$.

Boc-D-Tyr(O-Ile-Alloc)-D-Ser(*^t*Bu)-Glu(O*^t*Bu)-D-Val-Pro-Gln(Tr)-Tyr(Wang)-OAll. Starting from Boc-D-Tyr-D-Ser(^{t}Bu)-Glu(O^{t}Bu)-D-Val-Pro-Gln(Tr)-Tyr(Wang)-OAll, this peptidyl resin was prepared following the general procedure described above using Alloc-Ile-OH. Acidolytic cleavage of an aliquot of the resulting resin afforded H-D-Tyr(O-Ile-Alloc)-D-Ser-Glu-D-Val-Pro-Gln-Tyr-OAll in 56% purity. HPLC (λ = *220 nm, Method C*) t_R = 5.55 min; MS (ESI) *m/z*(+): 1122.6 $[M+H]^+$, 1144.5 $[M+Na]^+$; MS (ESI) *m/z*(-): 1120.5 $[M-H]^-$.

Boc-D-Tyr(O-Ile-Alloc)-D-Thr(*^t*Bu)-Glu(O*^t*Bu)-D-Ala-Pro-Gln(Tr)-Tyr(Wang)-OAll. Starting from Boc-D-Tyr-D-Thr(^{t}Bu)-Glu(O^{t}Bu)-D-Ala-Pro-Gln(Tr)-Tyr(Wang)-OAll, this peptidyl resin was prepared following the general procedure described above using Alloc-Ile-OH. Acidolytic cleavage of the resulting resin an aliquot of afforded H-D-Tyr(O-Ile-Alloc)-D-Thr-Glu-D-Ala-Pro-Gln-Tyr-OAll in 80% purity. HPLC (λ = *220 nm, Method A*) t_R = 7.17 min; MS (ESI) *m/z*(+): 1108.6 $[M+H]^+$, 1130.5 $[M+Na]^+$; MS (ESI) *m/z*(-): 1106.5 $[M-H]^-$.

Boc-D-Tyr(O-Ile-Alloc)-D-Ser(*^t*Bu)-Glu(O*^t*Bu)-D-Ala-Pro-Gln(Tr)-Tyr(Wang)-OAll. Starting from Boc-D-Tyr-D-Ser(^{t}Bu)-Glu(O^{t}Bu)-D-Ala-Pro-Gln(Tr)-Tyr(Wang)-OAll, this peptidyl resin was prepared following the general procedure described above using Alloc-Ile-OH. Acidolytic cleavage of an aliquot of the resulting resin afforded H-D-Tyr(O-Ile-Alloc)-D-Ser-Glu-D-Ala-Pro-Gln-Tyr-OAll in 62% purity. HPLC (λ = *220 nm, Method C*) t_R*:* 5.33 min; MS (ESI) *m/z*(+): 1094.5 $[M+H]^+$, 1116.5 $[M+Na]^+$; MS (ESI) *m/z*(-): 1092.4 $[M-H]^-$.

4.4.4.4 General method for the allyl and Alloc group removal from linear depsipeptidyl resins

The corresponding peptidyl resin was treated with $Pd(PPh_3)_3$ (0.1 equiv) and $PhSiH_3$ (10 equiv) in CH_2Cl_2 under nitrogen for 4 h. After this time, the resin was washed with THF (3×15 sec), CH_2Cl_2 (3×2 min), DMF (10×1 min) and CH_2Cl_2 (3×2 min). An aliquot of the resulting peptidyl resin was exposed to $TFA/H_2O/TIS$

(95:2.5:2.5) for 2 h at room temperature. Following TFA evaporation and diethyl ether extraction, the crude peptide was dissolved in H_2O/CH_3CN, lyophilized, analyzed by HPLC and characterized by mass spectrometry.

***p*NZ-Tyr(O-Ile-H)-Thr(^{t}Bu)-Glu(O^{t}Bu)-Val-Pro-Gln(Tr)-Tyr(Wang)-OH.** Starting from *p*NZ-Tyr(O-Ile-Alloc)-Thr(^{t}Bu)-Glu(O^{t}Bu)-Val-Pro-Gln(Tr)-Tyr(Wang)-OAll, this peptidyl resin was prepared following the general procedure described above. Acidolytic cleavage of an aliquot of the resulting resin afforded *p*NZ-Tyr(O-Ile-H)-Thr-Glu-Val-Pro-Gln-Tyr-OH in 57% purity. HPLC (λ = *220 nm, Method A*) t_R = 6.68 min; MS (ESI) *m/z*(+): 615.2 $[M+H+K]^{+2}$, 1191.5 $[M+H]^+$, 1213.5 $[M+Na]^+$, 1229.4 $[M+K]^+$.

***p*NZ-Tyr(O-Ile-H)-D-Thr(^{t}Bu)-Glu(O^{t}Bu)-D-Val-Pro-Gln(Tr)-D-Tyr(Wang)-OH.** Starting from *p*NZ-Tyr(O-Ile-Alloc)-D-Thr(^{t}Bu)-Glu(O^{t}Bu)-D-Val-Pro-Gln(Tr)-D-Tyr(Wang)-OAll, this peptidyl resin was prepared following the general procedure described above. Acidolytic cleavage of an aliquot of the resulting resin afforded *p*NZ-Tyr(O-Ile-H)-D-Thr-Glu-D-Val-Pro-Gln-D-Tyr-OH in 72% purity. HPLC (λ = *220 nm, Method A*) t_R = 6.77 min; MS (ESI) *m/z*(+): 615.2 $[M+H+K]^{+2}$, 1191.5 $[M+H]^+$, 1213.5 $[M+Na]^+$, 1229.5 $[M+K]^+$.

Boc-Tyr(O-Ile-H)-D-Thr(^{t}Bu)-Glu(O^{t}Bu)-D-Val-Pro-Gln(Tr)-D-Tyr(Wang)-OH. Starting from Boc-Tyr(O-Ile-Alloc)-D-Thr(^{t}Bu)-Glu(O^{t}Bu)-D-Val-Pro-Gln(Tr)-D-Tyr(Wang)-OAll, this peptidyl resin was prepared following the general procedure described above. Acidolytic cleavage of an aliquot of the resulting resin afforded H-Tyr(O-Ile-H)-D-Thr-Glu-D-Val-Pro-Gln-D-Tyr-OH (**BPC821**) in 75% purity. HPLC (λ *= 220 nm, Method A*) t_R = 6.01 min; MS (ESI) *m/z*(+): 506.7 $[M+2H]^{+2}$, 1012.5 $[M+H]^+$, 1034.5 $[M+Na]^+$; MS (ESI) *m/z*(-): 1010.4 $[M-H]^-$.

Boc-Tyr(O-Ile-H)-D-Ser(^{t}Bu)-Glu(O^{t}Bu)-D-Val-Pro-Gln(Tr)-D-Tyr(Wang)-OH. Starting from Boc-Tyr(O-Ile-Alloc)-D-Ser(^{t}Bu)-Glu(O^{t}Bu)-D-Val-Pro-Gln(Tr)-D-Tyr(Wang)-OAll, this peptidyl resin was prepared following the general procedure described above. Acidolytic cleavage of an aliquot of the resulting resin afforded H-Tyr(O-Ile-H)-D-Ser-Glu-D-Val-Pro-Gln-D-Tyr-OH (**BPC823**) in 76% purity. HPLC (λ *= 220 nm, Method A*) t_R = 5.96 min; MS (ESI) *m/z*(+): 499.7 $[M+2H]^{2+}$, 998.5 $[M+H]^+$, 1020.4 $[M+Na]^+$; MS (ESI) *m/z*(-): 996.4 $[M-H]^-$.

Boc-Tyr(O-Ile-H)-D-Thr(^{t}Bu)-Glu(O^{t}Bu)-D-Ala-Pro-Gln(Tr)-D-Tyr(Wang)-OH. Starting from Boc-Tyr(O-Ile-Alloc)-D-Thr(^{t}Bu)-Glu(O^{t}Bu)-D-Ala-Pro-Gln(Tr)-D-Tyr(Wang)-OAll, this peptidyl resin was prepared following the general procedure described above. Acidolytic cleavage of an aliquot of the resulting resin afforded H-Tyr(O-Ile-H)-D-Thr-Glu-D-Ala-Pro-Gln-D-Tyr-OH (**BPC825**) in 56% purity. HPLC (*λ = 220 nm, Method A*) t_R = 5.84 min; MS (ESI) *m/z*(+): 492.7 [M+2H]$^{2+}$, 984.5 [M+H]$^+$, 1007.4 [M+Na]$^+$; MS (ESI) *m/z*(-): 982.4 [M-H]$^-$.

Boc-Tyr(O-Ile-H)-D-Ser(^{t}Bu)-Glu(O^{t}Bu)-D-Ala-Pro-Gln(Tr)-D-Tyr(Wang)-OH. Starting from Boc-Tyr(O-Ile-Alloc)-D-Ser(^{t}Bu)-Glu(O^{t}Bu)-D-Ala-Pro-Gln(Tr)-D-Tyr(Wang)-OAll, this peptidyl resin was prepared following the general procedure described above. Acidolytic cleavage of an aliquot of the resulting resin afforded H-Tyr(O-Ile-H)-D-Ser-Glu-D-Ala-Pro-Gln-D-Tyr-OH (**BPC827**) in 62% of purity. HPLC (*λ = 220 nm, Method A*) t_R = 5.83 min; MS (ESI) *m/z*(+): 485.7 [M+2H]$^{2+}$, 970.5 [M+H]$^+$, 992.4 [M+Na]$^+$; MS (ESI) *m/z*(-): 968.4 [M-H]$^-$.

Boc-D-Tyr(O-Ile-H)-D-Thr(^{t}Bu)-Glu(O^{t}Bu)-D-Val-Pro-Gln(Tr)-Tyr(Wang)-OH. Starting from Boc-D-Tyr(O-Ile-Alloc)-D-Thr(^{t}Bu)-Glu(O^{t}Bu)-D-Val-Pro-Gln(Tr)-Tyr(Wang)-OAll, this peptidyl resin was prepared following the general procedure described above. Acidolytic cleavage of an aliquot of the resulting resin afforded H-D-Tyr(O-Ile-H)-D-Thr-Glu-D-Val-Pro-Gln-Tyr-OH (**BPC829**) in 69% purity. HPLC (*λ = 220 nm, Method A*) t_R = 5.98 min; MS (ESI) *m/z*(+): 506.7 [M+2H]$^{2+}$, 1012.5 [M+H]$^+$, 1034.5 [M+Na]$^+$; MS (ESI) *m/z*(-): 1010.5 [M-H]$^-$.

Boc-D-Tyr(O-Ile-H)-D-Ser(^{t}Bu)-Glu(O^{t}Bu)-D-Val-Pro-Gln(Tr)-Tyr(Wang)-OH. Starting from Boc-D-Tyr(O-Ile-Alloc)-D-Ser(^{t}Bu)-Glu(O^{t}Bu)-D-Val-Pro-Gln(Tr)-Tyr(Wang)-OAll, this peptidyl resin was prepared following the general procedure described above. Acidolytic cleavage of an aliquot of the resulting resin afforded H-D-Tyr(O-Ile-H)-D-Ser-Glu-D-Val-Pro-Gln-Tyr-OH (**BPC831**) in 66% purity. HPLC (*λ = 220 nm, Method A*) t_R = 5.96 min; MS (ESI) *m/z*(+): 499.7 [M+2H]$^{2+}$, 998.5 [M+H]$^+$, 1020.5 [M+Na]$^+$; MS (ESI) *m/z*(-): 996.4 [M-H]$^-$.

Boc-D-Tyr(O-Ile-H)-D-Thr(^{t}Bu)-Glu(O^{t}Bu)-D-Ala-Pro-Gln(Tr)-Tyr(Wang)-OH. Starting from Boc-D-Tyr(O-Ile-Alloc)-D-Thr(^{t}Bu)-Glu(O^{t}Bu)-D-Ala-Pro-Gln(Tr)-Tyr(Wang)-OAll, this peptidyl resin was prepared following the general procedure described above. Acidolytic cleavage of an aliquot of the resulting resin afforded H-D-Tyr(O-Ile-H)-D-Thr-Glu-D-Ala-Pro-Gln-Tyr-OH (**BPC833**) in 73% purity. HPLC (λ = *220 nm, Method A*) t_R = 5.80 min; MS (ESI) *m/z*(+): 492.7 [M+2H]$^{2+}$, 984.5 [M+H]$^{+}$, 1006.4 [M+Na]$^{+}$; MS (ESI) *m/z*(-): 982.4 [M-H]$^{-}$.

Boc-D-Tyr(O-Ile-H)-D-Ser(^{t}Bu)-Glu(O^{t}Bu)-D-Ala-Pro-Gln(Tr)-Tyr(Wang)-OH. From the peptidyl resin Boc-D-Tyr(O-Ile-Alloc)-D-Ser(^{t}Bu)-Glu(O^{t}Bu)-D-Ala-Pro-Gln(Tr)-Tyr(Wang)-OAll, this peptidyl resin was prepared following the general procedure described above. Acidolytic cleavage of an aliquot of the resulting resin afforded H-D-Tyr(O-Ile-H)-D-Ser-Glu-D-Ala-Pro-Gln-Tyr-OH (**BPC835**) in 61% purity. HPLC (λ = *220 nm, Method A*) t_R = 5.72 min; MS (ESI) *m/z*(+): 485.7 [M+2H]$^{2+}$, 970.5 [M+H]$^{+}$, 992.5 [M+Na]$^{+}$; MS (ESI) *m/z*(-): 968.4 [M-H]$^{-}$.

4.4.4.5 Synthesis of cyclic depsipeptides

***p*NZ-Tyr(&)-D-Thr-Glu-D-Val-Pro-Gln-D-Tyr-Ile-& (8).** Starting from *p*NZ-Tyr(O-Ile-H)-D-Thr(^{t}Bu)-Glu(O^{t}Bu)-D-Val-Pro-Gln(Tr)-D-Tyr(Wang)-OH, this cyclic depsipeptide was prepared following the general procedure described in *section 4.4.3.3*. Acidolytic cleavage afforded *p*NZ-Tyr(&)-D-Thr-Glu-D-Val-Pro-Gln-D-Tyr-Ile-& (**8**) in 31% purity. HPLC (λ = *220 nm, Method A*) t_R = 7.55 min; MS (ESI) *m/z*(+): 1195.5 [M+Na]$^{+}$, 1211.4 [M+K]$^{+}$; MS (ESI) *m/z*(-): 1171.5 [M-H]$^{-}$.

H-Tyr(&)-D-Thr-Glu-D-Val-Pro-Gln-D-Tyr-Ile-& (BPC822). Starting from Boc-Tyr(O-Ile-H)-D-Thr(^{t}Bu)-Glu(O^{t}Bu)-D-Val-Pro-Gln(Tr)-D-Tyr(Wang)-OH, this cyclic depsipeptide was prepared following the general procedure described in *section 4.4.3.3*. Acidolytic cleavage of the resulting peptidyl resin afforded H-Tyr(&)-D-Thr-Glu-D-Val-Pro-Gln-D-Tyr-Ile-& (**BPC822**) in 27% purity. Reverse-phase column chromatography eluting with H_2O/CH_3CN (67:33) afforded the expected cyclic depsipeptide **BPC822** in >99% purity. HPLC (λ = *220 nm, Method A*) t_R = 6.79 min; MS (ESI) *m/z*(+): 994.6 [M+H]$^{+}$, 1016.6 [M+Na]$^{+}$; MS (ESI) *m/z*(-): 992.5 [M+H]$^{+}$; HRMS (ESI) *m/z* (+): calcd. for $C_{48}H_{68}N_9O_{14}$ 994.4880, found 994.4867; calcd. for $C_{48}H_{67}N_9NaO_{14}$ 1016.4700, found 1016.4697.

H-Tyr(&)-D-Ser-Glu-D-Val-Pro-Gln-D-Tyr-Ile-& (BPC824). Starting from Boc-Tyr(O-Ile-H)-D-Ser(^{t}Bu)-Glu(O^{t}Bu)-D-Val-Pro-Gln(Tr)-D-Tyr(Wang)-OH, this cyclic depsipeptide was prepared following the general procedure described in *section 4.4.3.3*. Acidolytic cleavage of the resulting peptidyl resin afforded H-Tyr(&)-D-Ser-Glu-D-Val-Pro-Gln-D-Tyr-Ile-& (**BPC824**) in 43% purity. Reverse-phase column chromatography eluting with H_2O/CH_3CN (68:32) afforded the expected cyclic depsipeptide **BPC824** in >99% purity. HPLC (*λ = 220 nm, Method A*) t_R = 6.73 min; MS (ESI) *m/z*(+): 980.6 [M+H]$^+$, 1002.5 [M+Na]$^+$, 1018.5 [M+K]$^+$; HRMS (ESI) *m/z* (+): calcd. for $C_{47}H_{66}N_9O_{14}$ 980.4724, found 980.4740; calcd. for $C_{47}H_{65}N_9NaO_{14}$ 1002.4543, found 1002.4561.

H-Tyr(&)-D-Thr-Glu-D-Ala-Pro-Gln-D-Tyr-Ile-& (BPC826). Starting from Boc-Tyr(O-Ile-H)-D-Thr(^{t}Bu)-Glu(O^{t}Bu)-D-Ala-Pro-Gln(Tr)-D-Tyr(Wang)-OH, this cyclic depsipeptide was prepared following the general procedure described in *section 4.4.3.3*. Acidolytic cleavage of the resulting peptidyl resin afforded H-Tyr(&)-D-Thr-Glu-D-Ala-Pro-Gln-D-Tyr-Ile-& (**BPC826**) in 19% purity. Reverse-phase column chromatography eluting with H_2O/CH_3CN (68:32) afforded the expected cyclic depsipeptide **BPC826** in 93 % purity. HPLC (*λ = 220 nm, Method A*) t_R = 6.64 min; MS (ESI) *m/z*(+): 966.5 [M+H]$^+$, 988.5 [M+Na]$^+$, 1004. 5 [M+K]$^+$; HRMS (ESI) *m/z* (+): calcd. for $C_{46}H_{64}N_9O_{14}$ 966.4567, found 966.4549; calcd. for $C_{46}H_{63}N_9NaO_{14}$ 988.4387, found 988.4383.

H-Tyr(&)-D-Ser-Glu-D-Ala-Pro-Gln-D-Tyr-Ile-& (BPC828). Starting from Boc-Tyr(O-Ile-H)-D-Ser(^{t}Bu)-Glu(O^{t}Bu)-D-Ala-Pro-Gln(Tr)-D-Tyr(Wang)-OH, this cyclic depsipeptide was prepared following the general procedure described in *section 4.4.3.3*. Acidolytic cleavage of the resulting peptidyl resin afforded H-Tyr(&)-D-Ser-Glu-D-Ala-Pro-Gln-D-Tyr-Ile-& (**BPC828**) in 20% purity. Reverse-phase column chromatography eluting with H_2O/CH_3CN (70:30) afforded the expected cyclic depsipeptide **BPC828** in 88% purity. HPLC (*λ = 220 nm, Method A*) t_R = 6.56 min; MS (ESI) *m/z*(+): 476.7 [M+2H]$^{+2}$, 952.5 [M+H]$^+$, 974.5 [M+Na]$^+$, 990.5 [M+K]$^+$; MS (ESI) *m/z*(-): 950.4 [M-H]$^-$; HRMS (ESI) *m/z* (+): calcd. for $C_{45}H_{62}N_9O_{14}$ 952.4411, found 952.4419; calcd. for $C_{45}H_{61}N_9NaO_{14}$ 974.4248, found 974.4249.

H-D-Tyr(&)-D-Thr-Glu-D-Val-Pro-Gln-Tyr-Ile-& (BPC830). Starting from Boc-D-Tyr(O-Ile-H)-D-Thr(^{t}Bu)-Glu(O^{t}Bu)-D-Val-Pro-Gln(Tr)-Tyr(Wang)-OH, this cyclic depsipeptide was prepared following the general procedure described in *section 4.4.3.3*. Acidolytic cleavage afforded H-D-Tyr(&)-D-Thr-Glu-D-Val-Pro-Gln-Tyr-Ile-& (**BPC830**) as a broad peak by HPLC (λ = *220 nm, Method A*, t_R = 6.75 min). MS (ESI) *m/z*(+): 921.4 $[M_{Linear}\text{-Ile+Na}]^+$, 994.4 $[M+H]^+$+$[M_{Dimer}+2H]^{+2}$, 1012.5 $[M+H_2O+H]^+$, 1988.7 $[M_{Dimer}+H]^+$; MS (ESI) *m/z*(-): 919.3 $[M_{Linear}\text{-Ile-H}]^-$, 992.4 $[M-H]^-$, 1010.4 $[M+H_2O-H]^-$, 1985.7 $[M_{Dimer}-H]^-$.

H-D-Tyr(&)-D-Ser-Glu-D-Val-Pro-Gln-Tyr-Ile-& (BPC832). Starting from Boc-D-Tyr(O-Ile-H)-D-Ser(^{t}Bu)-Glu(O^{t}Bu)-D-Val-Pro-Gln(Tr)-Tyr(Wang)-OH, this cyclic depsipeptide was prepared following the general procedure described in *section 4.4.3.3*. Acidolytic cleavage afforded H-D-Tyr(&)-D-Ser-Glu-D-Val-Pro-Gln-Tyr-Ile-& (**BPC832**) as a broad peak by HPLC (λ = *220 nm, Method A*, t_R = 6.72 min). MS (ESI) *m/z*(+): 907.4 $[M_{Linear}\text{-Ile+Na}]^+$, 980.4 $[M+H]^+$+$[2M_{Dimer}+2H]^{+2}$, 998.4 $[M+H_2O+H]^+$, 1960.8 $[M_{Dimer}+H]^+$; MS (ESI) *m/z*(-): 905.3 $[M_{linear}\text{-Ile+Na-H}]^-$, 978.4 $[M-H]^-$, 996.3 $[M+H_2O-H]^-$, 1958.7 $[M_{Dimer}-H]^-$

H-D-Tyr(&)-D-Thr-Glu-D-Ala-Pro-Gln-Tyr-Ile-& (BPC834). Starting from Boc-D-Tyr(O-Ile-H)-D-Thr(^{t}Bu)-Glu(O^{t}Bu)-D-Ala-Pro-Gln(Tr)-Tyr(Wang)-OH, this cyclic depsipeptide was prepared following the general procedure described in *section 4.4.3.3*. Acidolytic cleavage afforded H-D-Tyr(&)-D-Thr-Glu-D-Ala-Pro-Gln-Tyr-Ile-& (**BPC834**) as a broad peak by HPLC (λ = *220 nm, Method A*, t_R = 6.55 min). MS (ESI) *m/z*(+): 966.50 $[M+H]^+$+$[M_{Dimer}+2H]^{+2}$, 984.47 $[M+H_2O+H]^+$, 1931.87 $[M_{Dimer}+H]^+$; MS (ESI) *m/z*(-): 964.40 $[M-H]^-$, 982.44 $[M+H_2O-H]^-$, 1930.79 $[M_{Dimer}-H]^-$.

H-D-Tyr(&)-D-Ser-Glu-D-Ala-Pro-Gln-Tyr-Ile-& (BPC836). Starting from Boc-D-Tyr(O-Ile-H)-D-Ser(^{t}Bu)-Glu(O^{t}Bu)-D-Ala-Pro-Gln(Tr)-Tyr(Wang)-OH, this cyclic depsipeptide was prepared following the general procedure described in *section 4.4.3.3*. Acidolytic cleavage afforded H-D-Tyr(&)-D-Ser-Glu-D-Ala-Pro-Gln-Tyr-Ile-& (**BPC836**) as a broad peak by HPLC (λ = *220 nm, Method A*, t_R = 6.45 min). MS (ESI) *m/z*(+): 879.4 $[M_{Linear}\text{-Ile+Na}]^+$, 952.4 $[M+H]^+$+$[M_{Dimer}+2H]^{+2}$, 970.4 $[M+H_2O+H]^+$, 1904.6 $[M_{Dimer}+H]^+$; MS (ESI) *m/z*(-): 877.3 $[M_{Linear}\text{-Ile+Na-H}]^-$, 950.3 $[M-H]^-$, 968.3 $[M+H_2O-H]^-$, 1901.6 $[M_{Dimer}-H]^-$.

4.4.4.6 General method for the hydrolysis of cyclic depsipeptides

Cyclic depsipeptides **8**, **BPC822**, **BPC824**, **BPC826** and **BPC828** were treated with a solution of $CH_3OH/H_2O/NH_3$ (4:1:1) for 24 h at room temperature (Cochrane et al., 2012). Next, the mixture was evaporated and the crude residue was dissolved in H_2O/CH_3CN, lyophilized, analyzed by HPLC and characterized by mass spectrometry.

***p*NZ-Tyr-D-Thr-Glu-D-Val-Pro-Gln-D-Tyr-Ile-OH.** The hydrolysis of the peptide **8** was perfomed following the methodology described above. *p*NZ-Tyr-D-Thr-Glu-D-Val-Pro-Gln-D-Tyr-Ile-OH (t_R = 7.34 min, 26% purity) together with the methyl ester derivative *p*NZ-Tyr-D-Thr-Glu-D-Val-Pro-Gln-D-Tyr-Ile-OMe (t_R = 7.49 min, 20% purity) were obtained; HPLC (λ = *220 nm, Method A*). MS (ESI) *m/z*(+): 1191.5 $[M+H]^+$, 1205.5 $[M(OMe)+H]^+$, 1213.5 $[M+Na]^+$, 1227.5 $[M(OMe)+Na]^+$; MS (ESI) *m/z*(-): 1189.5 $[M-H]^-$, 1203.5 $[M(OMe)-H]^-$.

H-Tyr-D-Thr-Glu-D-Val-Pro-Gln-D-Tyr-Ile-OH. The hydrolysis of the peptide **BPC822** was perfomed following the methodology described above. H-Tyr-D-Thr-Glu-D-Val-Pro-Gln-D-Tyr-Ile-OH (t_R = 6.65 min, 15% purity) together with the methyl ester derivative H-Tyr-D-Thr-Glu-D-Val-Pro-Gln-D-Tyr-Ile-OMe (t_R = 6.90 min, 34% purity) were obtained; HPLC (λ = *220 nm, Method A*). MS (ESI) *m/z*(+): 1012.5 $[M+H]^+$, 1026.5 $[M(OMe)+H]^+$, 1048.5 $[M(OMe)+Na]^+$; MS (ESI) *m/z*(-): 1010.5 $[M-H]^-$, 1024.5 $[M(OMe)-H]^-$.

H-Tyr-D-Ser-Glu-D-Val-Pro-Gln-D-Tyr-Ile-OH. The hydrolysis of the peptide **BPC824** was perfomed following the methodology described above. H-Tyr-D-Ser-Glu-D-Val-Pro-Gln-D-Tyr-Ile-OH (t_R = 6.63 min, 14% purity) together with the methyl ester derivative H-Tyr-D-Ser-Glu-D-Val-Pro-Gln-D-Tyr-Ile-OMe (t_R = 6.86 min, 37% purity) were obtained; HPLC (λ = *220 nm, Method A*). MS (ESI) *m/z*(+): 998.5 $[M+H]^+$, 1012.5 $[M(OMe)+H]^+$, 1034.5 $[M(OMe)+Na]^+$; MS (ESI) *m/z*(-): 996.4 $[M-H]^-$, 1010.4 $[M(OMe)-H]^-$.

H-Tyr-D-Thr-Glu-D-Ala-Pro-Gln-D-Tyr-Ile-OH. The hydrolysis of the peptide **BPC826** was perfomed following the methodology described above. H-Tyr-D-Thr-Glu-D-Ala-Pro-Gln-D-Tyr-Ile-OH (t_R = 6.40 min, 16% purity) together with the methyl ester derivative H-Tyr-D-Thr-Glu-D-Ala-Pro-Gln-D-Tyr-Ile-OMe (t_R = 6.66 min, 33% purity) were obtained; HPLC (λ = *220 nm, Method A*). MS (ESI) *m/z*(+): 984.48 $[M+H]^+$, 998.51 $[M(OMe)+H]^+$, 1020.45 $[M(OMe)+Na]^+$; MS (ESI) *m/z*(-): 982.42 $[M-H]^-$, 996.42 $[M(OMe)-H]^-$.

H-Tyr-D-Ser-Glu-D-Ala-Pro-Gln-D-Tyr-Ile-OH. The hydrolysis of the peptide **BPC828** was perfomed following the methodology described above. H-Tyr-D-Ser-Glu-D-Ala-Pro-Gln-D-Tyr-Ile-OH (t_R = 6.36 min, 16% purity) together with the methyl ester derivative H-Tyr-D-Ser-Glu-D-Ala-Pro-Gln-D-Tyr-Ile-OMe (t_R = 6.61 min, 31% purity) were obtained; HPLC (λ = *220 nm, Method A*). MS (ESI) *m/z*(+): 970.5 $[M+H]^+$, 984.5 $[M(OMe)+H]^+$; MS (ESI) *m/z*(-): 968.4 $[M-H]^-$, 982.4 $[M(OMe)-H]^-$.

4.5 REFERENCES

Adamson, J. G.; Hoang, T.; Crivici, A.; Lajoie, G. A. Use of Marfey's Reagent to Quantitate Racemization upon Anchoring of Amino Acids to Solid Supports for Peptide Synthesis. *Anal. Biochem.* **1992**, *202*, 210–214.

Alsina, J.; Rabanal, F.; Chiva, C.; Giralt, E.; Albericio, F. Active Carbonate Resins: Application to the Solid-Phase Synthesis of Alcohol, Carbamate and Cyclic Peptides. *Tetrahedron* **1998**, *54*, 10125–10152.

Bie, X.; Lu, Z.; Lu, F. Identification of Fengycin Homologues from *Bacillus Subtilis* with ESI-MS/CID. *J. Microbiol. Methods* **2009**, *79*, 272–278.

Cabrele, C.; Langer, M.; Beck-Sickinger, A. G. Amino Acid Side Chain Attachment Approach and Its Application to the Synthesis of Tyrosine-Containing Cyclic Peptides. *J. Org. Chem.* **1999**, *64*, 4353–4361.

Ceballos, I.; Villegas-Escobar, V.; Mosquera, S.; Mira, J. J.; Gutierrez, J. A.; Arroyave, J. J.; Posada, L. F. Production Process for Biomass and Metabolites of *Bacillus* Species and Compositions Thereof for Biological Pest Control, 2014.

Chen, H.; Wang, L.; Su, C. X.; Gong, G. H.; Wang, P.; Yu, Z. L. Isolation and Characterization of Lipopeptide Antibiotics Produced by *Bacillus Subtilis*. *Lett. Appl. Microbiol.* **2008**, *47,* 180–186.

Chtioui, O.; Dimitrov, K.; Gancel, F.; Dhulster, P.; Nikov, I. Rotating Discs Bioreactor, a New Tool for Lipopeptides Production. *Process Biochem.* **2012**, *47,* 2020–2024.

Cochrane, J. R.; Yoon, D. H.; McErlean, C. S. P.; Jolliffe, K. a. A Macrolactonization Approach to the Total Synthesis of the Antimicrobial Cyclic Depsipeptide LI-F04a and Diastereoisomeric Analogues. *Beilstein J. Org. Chem.* **2012**, *8*, 1344–1351.

Cruz, L. J.; Beteta, N. G.; Ewenson, A.; Albericio, F. " One-Pot " Preparation of N-Carbamate Protected Amino Acids via the Azide. *Org. Process Res. Dev.* **2004**, *8,* 920–924.

Cruz, L. J.; Francesch, A.; Cuevas, C.; Albericio, F. Synthesis and Structure-Activity Relationship of Cytotoxic Marine Cyclodepsipeptide IB-01212 Analogues. *ChemMedChem* **2007**, *2*, 1076–1084.

Davies, J. S. The Cyclization of Peptides and Depsipeptides. *J. Pept. Sci.* **2003**, *9*, 471–501.

Deleu, M.; Paquot, M.; Nylander, T. Effect of Fengycin, a Lipopeptide Produced by *Bacillus Subtilis*, on Model Biomembranes. *Biophys. J.* **2008**, *94*, 2667–2679.

Gracia, C.; Isidro-Llobet, A.; Cruz, L. J.; Acosta, G. a; Álvarez, M.; Cuevas, C.; Giralt, E.; Albericio, F. Convergent Approaches for the Synthesis of the Antitumoral Peptide, Kahalalide F. Study of Orthogonal Protecting Groups. *J. Org. Chem.* **2006**, *71*, 7196–7204.

Grant, G. A. *Synthetic Peptides. A User's Guide*; W. H. Freeman and Company: United States of America, 1992.

Guibé, F. Allylic Protecting Groups and Their Use in a Complex Environment Part II : Allylic Protecting Groups and Their Removal through Catalytic Palladium π-Allyl Methodology. *Tetrahedron* **1998**, *54*, 2967–3042.

Hall, E. A.; Kuru, E.; VanNieuwenhze, M. S. Solid-Phase Synthesis of Lysobactin (katanosin B): Insights into Structure and Function. *Org. Lett.* **2012**, *14,* 2730–2733.

Honma, M.; Tanaka, K.; Konno, K.; Tsuge, K.; Okuno, T.; Hashimoto, M. Termination of the Structural Confusion between Plipastatin A1 and Fengycin IX. *Bioorg. Med. Chem.* **2012**, *20*, 3793–3798.

Isidro-Llobet, A.; Guasch-Camell, J.; Álvarez, M.; Albericio, F. p-Nitrobenzyloxycarbonyl (pNZ) as a Temporary N$^{\alpha}$-Protecting Group in Orthogonal

Solid-Phase Peptide Synthesis - Avoiding Diketopiperazine and Aspartimide Formation. *Eur. J. Org. Chem.* **2005**, 3031–3039.

Jacques, P.; Hbid, C.; Destain, J.; Razafindralambo, H.; Paquot, M.; Pauw, E.; Thonart, P. Optimization of Biosurfactant Lipopeptide Production from *Bacillus Subtilis* S499 by Plackett-Burman Design. *Appl. Biochem. Biotechnol.* **1999**, *77-79*, 223–233.

Kaiser, E.; Colescott, R. L.; Bossinger, C. D.; Cook, P. Color Test for Detection of Free Terminal Amino Groups in the Solid-Phase Synthesis of Peptides. *Anal. Biochem.* **1970**, 595–598.

Krishnamoorthy, R.; Vazquez-Serrano, L. D.; Turk, J. A.; Kowalski, J. A.; Benson, A. G.; Breaux, N. T.; Lipton, M. a. Solid-Phase Total Synthesis and Structure Proof of Callipeltin B. *J. Am. Chem. Soc.* **2006**, *128*, 15392–15393.

Kumar, A.; Ye, G.; Wang, Y.; Lin, X.; Sun, G.; Parang, K. Synthesis and Structure - Activity Relationships of Linear and Conformationally Constrained Peptide Analogues of CIYKYY as Src Tyrosine Kinase Inhibitors. *J. Med. Chem.* **2006**, *49*, 3395–3401.

Kuroda, J.; Fukai, T.; Nomura, T. Collision-Induced Dissociation of Ring-Opened Cyclic Depsipeptides with a Guanidino Group by Electrospray Ionization/ion Trap Mass Spectrometry. *J. Mass Spectrom.* **2001**, *36*, 30–37.

Lejeune, V.; Martinez, J.; Cavelier, F. Towards a Selective Boc Deprotection on Acid Cleavable Wang Resin. *Tetrahedron Lett.* **2003**, *44*, 4757–4759.

Nasir, M. N.; Laurent, P.; Flore, C.; Lins, L.; Ongena, M.; Deleu, M. Analysis of Calcium-Induced Effects on the Conformation of Fengycin. *Spectrochim. Acta A Mol. Biomol. Spectrosc.* **2013**, *110*, 450–457.

Nishikiori, T.; Naganawa, H.; Muraoka, Y.; Aoyagi, T.; Umezawa, H. Plipastatins: New Inhibitors of Phospholipase A2, Produced by *Bacillus Cereus* BMG302-fF67. II. Structure of Fatty Acid Residue and Amino Acid Sequence. *J. Antibiot.* **1986a**, *XXXIX*, 745–754.

Nishikiori, T.; Naganawa, H.; Muraoka, Y.; Aoyagi, T.; Umezawa, H. Plipastatins: New Inhibitors of Phospholipase A2, Produced by *Bacillus Cereus* BMG302-fF67. III. Structural Elucidation of Plipastatins. *J. Antibiot.* **1986b**, *XXXIX*, 755–761.

Ongena, M.; Jacques, P.; Touré, Y.; Destain, J.; Jabrane, A.; Thonart, P. Involvement of Fengycin-Type Lipopeptides in the Multifaceted Biocontrol Potential of *Bacillus Subtilis*. *Appl. Microbiol. Biotechnol.* **2005**, *69*, 29–38.

Ongena, M.; Jourdan, E.; Adam, A.; Paquot, M.; Brans, A.; Joris, B.; Arpigny, J.-L.; Thonart, P. Surfactin and Fengycin Lipopeptides of *Bacillus Subtilis* as Elicitors of Induced Systemic Resistance in Plants. *Environ. Microbiol.* **2007**, *9*, 1084–1090.

Pathak, K. V; Keharia, H.; Gupta, K.; Thakur, S. S.; Balaram, P. Lipopeptides from the Banyan Endophyte, *Bacillus Subtilis* K1: Mass Spectrometric Characterization of a Library of Fengycins. *J. Am. Soc. Mass Spectrom.* **2012**, *23*, 1716–1728.

Pecci, Y.; Rivardo, F.; Martinotti, M. G.; Allegrone, G. LC/ESI-MS/MS Characterisation of Lipopeptide Biosurfactants Produced by the *Bacillus Licheniformis* V9T14 Strain. *J. Mass Spectrom.* **2010**, *45*, 772–778.

Pueyo, M. T.; Bloch, C.; Carmona-Ribeiro, A. M.; di Mascio, P. Lipopeptides Produced by a Soil *Bacillus Megaterium* Strain. *Microb. Ecol.* **2009**, *57*, 367–378.

Rangarajan, V.; Dhanarajan, G.; Sen, R. Bioprocess Design for Selective Enhancement of Fengycin Production by a Marine Isolate *Bacillus Megaterium*. *Biochem. Eng. J.* **2015**, *99*, 147–155.

Samel, S. A.; Wagner, B.; Marahiel, M. A.; Essen, L.-O. The Thioesterase Domain of the Fengycin Biosynthesis Cluster: A Structural Base for the Macrocyclization of a Non-Ribosomal Lipopeptide. *J. Mol. Biol.* **2006**, *359*, 876–889.

Sang-Cheol, L.; Kim, S.-H.; Park, I.-H.; Chung, S.-Y.; Chandra, M. S.; Yong-Lark, C. Isolation, Purification, and Characterization of Novel Fengycin S from *Bacillus Amyloliquefaciens* LSC04 Degrading-Crude Oil. *Biotechnol. Bioprocess Eng.* **2010**, *15*, 246–253.

Schneider, J.; Taraz, K.; Budzikiewicz, H.; Deleu, M.; Thonart, P.; Jacques, P. The Structure of Two Fengycins from *Bacillus Subtilis* S499. *Z. Naturforsch C* **1999**, *54*, 859–866.

Seo, H.; Lim, D. Total Synthesis of Halicylindramide A. *J. Org. Chem.* **2009**, *74*, 906–909.

Sieber, S. A.; Walsh, C. T.; Marahiel, M. A. Loading Peptidyl-Coenzyme A onto Peptidyl Carrier Proteins : A Novel Approach in Characterizing Macrocyclization by Thioesterase Domains. *J. Am. Chem. Soc.* **2003**, *125*, 10862–10866.

Sieber, S. A.; Tao, J.; Walsh, C. T.; Marahiel, M. A. Peptidyl Thiophenols as Substrates for Nonribosomal Peptide Cyclases. *Angew. Chem. Int. Ed. Engl.* **2004**, *43*, 493–498.

Stawikowski, M.; Cudic, P. A Novel Strategy for the Solid-Phase Synthesis of Cyclic Lipodepsipeptides. *Tetrahedron Lett.* **2006**, *47*, 8587–8590.

Stolze, S. C.; Meltzer, M.; Ehrmann, M.; Kaiser, M. Solid Phase Total Synthesis of the 3-Amino-6-Hydroxy-2-Piperidone (Ahp) Cyclodepsipeptide and Protease Inhibitor Symplocamide A. *Chem. Commun.* **2010**, *46*, 8857–8859.

Thieriet, N.; Alsina, J.; Giralt, E.; Guibé, F.; Albericio, F. Use of Alloc-Amino Acids in Solid-Phase Peptide Synthesis. Tandem Deprotection-Coupling Reactions Using Neutral Conditions . *Tetrahedron Lett.* **1997**, *38*, 7275–7278.

Thutewohl, M.; Waldmann, H. Solid-Phase Synthesis of a Pepticinnamin E Library. *Bioorg. Med. Chem.* **2003**, *11*, 2591–2615.

Vanittanakom, N.; Loeffler, W.; Koch, U.; Jung, G. Fengycin- A Novel Antifungal Lipopeptide Antibiotic Produced by *Bacillus Subtilis* F-29-3. *J. Antibiot.* **1986**, *XXXIX*, 888–901.

Villegas-Escobar, V.; Ceballos, I.; Mira, J. J.; Argel, L. E.; Peralta, S. O.; Romero-Tabarez, M. Fengycin C Produced by *Bacillus Subtilis* EA-CB0015. *J. Nat. Prod.* **2013**, *76*, 503–509.

Volpon, L.; Besson, F.; Lancelin, J. NMR Structure of Antibiotics Plipastatins A and B from *Bacillus Subtilis* Inhibitors of Phospholipase A2. *FEBS Lett.* **2000**, *485*, 76–80.

Wang, J.; Liu, J.; Wang, X.; Yao, J.; Yu, Z. Application of Electrospray Ionization Mass Spectrometry in Rapid Typing of Fengycin Homologues Produced by *Bacillus Subtilis*. *Lett. Appl. Microbiol.* **2004**, *39*, 98–102.

Zhang, A. J.; Russell, D. H.; Zhu, J.; Burgess, K. A Method for Removal of N-BOC Protecting Groups from Substrates on TFA-Sensitive Resins. *Tetrahedron Lett.* **1998**, *39*, 7439–7442.

Zhang, L.; Tam, J. P. Metal Ion-Assisted Peptide Cyclization. *Tetrahedron Lett.* **1997**, *38*, 4375–4378.

Zhang, L.; Tam, J. P. Lactone and Lactam Library Synthesis by Silver Ion-Assisted Orthogonal Cyclization of Unprotected Peptides. *J. Am. Chem. Soc.* **1999**, *121*, 3311–3320.

CHAPTER 5.

Total solid-phase synthesis of dehydroxy fengycin derivatives

This chapter corresponds to a manuscript in preparation:

Cristina Rosés, Nerea López, Àngel Oliveras, Lidia Feliu, Marta Planas. Total solid-phase synthesis of dehydroxy fengycin derivatives. *In preparation*.

For this work, C.R. designed the dehydroxy fengycin derivatives and performed the synthesis and characterization of all the compounds. Moreover, C.R. was also involved in argumentations and discussions of the results, and wrote the manuscript draft.

A rapid and efficient solid-phase strategy for the synthesis of dehydroxy fengycins derivatives is described. This synthetic approach involved the linkage of a Tyr to a Wang resin via a Mitsunobu reaction and the elongation of the peptide sequence followed by subsequent acylation of the N-terminus of the resulting linear peptidyl resin, esterification of the phenol group of a Tyr with an Ile, and final macrolactamization. The amino acid composition as well as the presence of the N-terminal acyl group significantly influenced the stability of the macrolactone. Cyclic lipodepsipeptides with a L-Tyr^3/D-Tyr^9 configuration were more stable than those containing the Tyr residues with an opposite configuration. This work constituted the first approach on the total solid-phase synthesis of dehydroxy fengycin derivatives.

5.1 INTRODUCTION

Cyclic lipodepsipeptides are a structurally diverse group of nonribosomal metabolites typically produced by bacterial and fungal species, such as *Pseudomonas* or *Bacillus* strains (Stein, 2005; Ongena and Jacques, 2008; Raaijmakers et al., 2010; Bionda and Cudic, 2011). This class of compounds have raised interest due to their wide range of biological activities and to their structural complexity. The main structural feature of these cyclic peptides is the occurrence of an ester bond between the side-chain of an amino acid and the C-terminal end of the sequence. The fatty acid moiety is commonly attached to the N-terminus of this macrolactone. Moreover, the complexity of the structure of these lipodepsipeptides is increased by the combination of L- and D-amino acids as well as of other unnatural residues present in their sequence (Sieber and Marahiel, 2003; Sarabia et al., 2004).

Fengycins are a family of natural cyclic lipodepsipeptides isolated from *Bacillus* strains (Vanittanakom et al., 1986). They consist of an eight-residue macrocycle with a phenyl ester linkage between the phenol group of a tyrosine (Tyr) and the α-carboxylic group of an isoleucine (Ile) (*Figure 5.1*). This cyclic depsipeptide bears at its N-terminus a dipeptidyl tail acylated with a β-hydroxy fatty acid. Different fengycin isoforms have been described, being fengycins A and B the most common (Vanittanakom et al., 1986; Chen et al., 2008; Bie et al., 2009; Pueyo et al., 2009; Pecci et al., 2010; Pathak et al., 2012; Villegas-Escobar et al., 2013). These two isoforms differ on the amino acid at position 6, which is a D-alanine (D-Ala) in fengycin A and a D-valine (D-Val) in the B isoform (*Figure 5.1*). Sang-Cheol et al. isolated from *Bacillus amyloliquefaciens* fengycin S (Sang-Cheol et al., 2010). Compared to fengycin B, this isoform bears a D-serine (D-Ser) at position 4 instead of a D-*allo*-threonine (D-*allo*-Thr). Concerning the configuration of Tyr residues at position 3 and 9, it was first reported to be D and L, respectively (Vanittanakom et al., 1986; Schneider et al., 1999). However, it has been recently confirmed that the configuration of these amino acids is L and D, respectively, and that this structure is the same than that of the previously isolated fengycin isoforms named as plipastatins (Nishikiori et al., 1986; Volpon et al., 2000; Honma et al., 2012). Since the term fengycins is most widely used than plipastatins, herein we employed the former term for the peptides of this study, but using the correct configuration.

CHAPTER 6.

General Discussion

Bioactive peptides have been an important focus of research over the last century due to their broad spectrum of activity (Jenssen et al., 2006; Bionda and Cudic, 2011; Henderson and Lee, 2013). Among them, antimicrobial peptides are considered as a promising alternative to traditional antibiotics. They can be found in numerous organisms, from vertebrate to bacteria, and are active towards a wide range of pathogens (Li et al., 2012; Pasupuleti et al., 2012). Their ability to interact with negatively charged membranes decreases the probability that microorganisms develop resistance mechanisms (Hancock, 2001; Baltzer and Brown, 2011). Although bacteria are the most studied targets, some of these peptides are also toxic against cancer cells, constituting interesting candidates as new anticancer agents (Papo and Shai, 2005; Mader and Hoskin, 2006; Hoskin and Ramamoorthy, 2008; Gaspar et al., 2013).

Despite the interest of antimicrobial peptides, several limitations must be overcome to be used in vivo, such as their high susceptibility to protease degradation. Several structural modifications have been described to prevent protease recognition, i.e. introduction of non-natural amino acids, modification of the peptide backbone or cyclization (Hancock and Sahl, 2006; Zakeri and Lu, 2013). Therefore, new synthetic strategies that allow the access to a wide range of analogues are required.

Solid-phase peptide synthesis (SPPS) has been established as the main methodology for the obtention of new peptide sequences (Coin et al., 2007; Pires et al., 2014). Through easy and low time-consuming sequential steps, SPPS allows the preparation of a large variety of analogues containing natural and non-natural amino acids as well as other moieties, such as fatty acids or nucleotides. This methodology can be applied to the preparation of short linear peptides as well as of large sequences with high structural complexity, such as cyclic or branched peptides.

This PhD thesis is focused on the development of new synthetic approaches to obtain bioactive peptides. With this objective in mind, the first part of this thesis deals with the synthesis of new anticancer agents by conjugating an antimicrobial undecapeptide with a cell-penetrating peptide (CPP) (Chapter 3). Next, our work was focused on devising a feasible strategy for the synthesis of bioactive cyclic lipodepsipeptides produced by *Bacillus* strains, useful for plant protection (Chapters 4 and 5).

CHAPTER 7.

General Conclusions

❖ Cell-penetrating γ-peptide/antimicrobial undecapeptide conjugates

- Antimicrobial undecapeptides from the CECMELL11 library showed an interesting anticancer activity against breast carcinoma cells while being non toxic against non-malignant cells. In particular, **BP76** and the N-terminal derivatized peptides **BP77**, **BP125**, **BP126** were identified as the most active undecapeptides. In general, these results suggested that the N-terminal derivatization is an important feature for the anticancer activity of these compounds.

- Seven antimicrobial undecapeptide/cell-penetrating *γ*-peptide **1** conjugates with general structure R-Aa^1-Lys-Leu-Phe-Lys-Lys-Ile-Leu-Lys-Aa^{10}-Leu-PEG-**1** (R = H, Ac, Ts or Bz; Aa^1 = Leu or Lys, Aa^{10} = Val, Phe, Tyr or Lys) were satisfactorily synthesized and obtained in 93-99% HPLC purity.

- The conjugation of the undecapeptides to **PEG-1** led to an improvement of their anticancer activity from 1.2 up to 10-fold. Results denoted that the peptide moiety is mostly responsible for this activity. Interestingly, at 10 µM the conjugates did not display significant cytotoxicity.

- **BP77-PEG-1** was the conjugate that displayed the best balance between toxicity and anticancer activity. **BP77-PEG-1** can be considered a proof of the usefulness of this strategy to design new anticancer drugs based on the conjugation between an antimicrobial peptide and a cell-penetrating *γ*-peptide.

❖ Cyclic lipodepsipeptides derived from fengycins

- Cyclic octapeptides analogous to the macrocycle of fengycins, with general structure H-Phe^1(4-NH-&)-Aa^2-Glu-Aa^4-Pro-Gln^6-D-Tyr^7-Ile-& (Aa^2 = D-Thr or D-Ser; Aa^4 = D-Ala or D-Val), were synthesized. The route devised involved the use of Gln^6 as site of resin attachment and the cyclization of the corresponding linear peptidyl resin Boc-Phe^1[4-NH-Ile-D-Tyr^7(^{t}Bu)-H]-Aa^2-Glu(O^{t}Bu)-Aa^4-Pro-Glu^6(Rink-MBHA)-OH through formation of an amide bond between Glu^6 and Tyr^7. Cyclic octapeptides **BPC862**, **BPC864**, **BPC866** and **BPC868** were obtained in >98% HPLC purity after purification. It was observed that when the sequence contained only L-amino acids, the cyclization step mainly led to a significant amount of a dimeric compound.

- The lability of the phenyl ester bond precluded the use of a similar route for the synthesis of cyclic octadepsipeptides. Aminolysis of the ester bond or the formation of diketopiperazines was observed.

- Cyclic octadepsipeptides with general structure H-Tyr^1(&)-Aa^2-Glu-Aa^4-Pro-Gln-D-Tyr^7-Ile-& (Aa^2 = D-Thr or D-Ser; Aa^4 = D-Ala or D-Val) were synthesized. In this case, Tyr^7 was linked to the support via a Mitsunobu reaction, the corresponding linear peptidyl resin Boc-Tyr^1-Aa^2-Glu(O^{t}Bu)-Aa^4-Pro-Gln(Tr)-D-Tyr^7(Wang)-OAll was prepared and esterified with Alloc-Ile-OH to yield Boc-Tyr^1(O-Ile-Alloc)-Aa^2-Glu(O^{t}Bu)-Aa^4-Pro-Gln(Tr)-D-Tyr^7(Wang)-OAll. Final allyl and Alloc group removal, and cyclization between Tyr^7 and Ile^8 provided the cyclic octadepsipeptides **BPC822**, **BPC824**, **BPC826** and **BPC828** from 88 to >99% HPLC purity after purification.

- The synthesis of cyclic octadepsipeptides containing an opposite configuration at the Tyr residues (D-Tyr^1/L-Tyr^7) was assayed following the above synthetic route. However, a high amount of a dimeric compound was formed together with a linear peptide resulting from the hydrolysis of the phenyl ester bond. These findings showed that the formation of this cyclic octadepsipeptides was more difficult than that of the ones bearing a L-Tyr^1/ D-Tyr^7 configuration.

- A straightforward strategy for the solid-phase synthesis of dehydroxy fengycin derivatives with the general formula Fatty acid-Glu^1-D-Orn-Tyr^3(&)-Aa^4-Glu-Aa^6-Pro-Gln-D-Tyr^9-Ile^{10}-& (Aa^4 = D-Thr or D-Ser; Aa^6 = D-Val or D-Ala) was developed. This strategy involved the anchoring of Tyr^9 through its side-chain phenol group to the solid support, followed by synthesis of the corresponding linear peptidyl resin and acylation of the N-terminus. The resulting resin Fatty acid-Glu^1(O^{t}Bu)-D-Orn(Boc)-Tyr^3-Aa^4-Glu(O^{t}Bu)-Aa^6-Pro-Gln(Tr)-D-Tyr^9(Wang)-OH was then esterified at Tyr^3 with Alloc-Ile-OH. Subsequent Alloc and allyl group removal, and final on-resin cyclization rendered the dehydroxy fengycin analogues **BPC838**, **BPC840**, **BPC842** and **BPC844**, bearing an octanoyl group, as major products. Derivatives **BPC854** and **BPC856** containing a lauroyl or a palmitoyl group, respectively, were also prepared and obtained in 89 and 92% of purity after RP-HPLC analysis.

- The synthesis of dehydroxy fengycin derivatives **BPC846**, **BPC848**, **BPC850**, **BPC852**, **BPC858** and **BPC860** bearing an opposite configuration at the Tyr residues (D-Tyr^3/L-Tyr^9) afforded the expected compound together with a substantial amount of a linear byproduct resulting from the hydrolysis of the macrolactone.

- Taking together the results obtained in the synthesis of the cyclic octadepsipeptides and those of the cyclic lipodepsipeptides, we concluded that the presence of the fatty acid tail favoured the cyclization of the sequences containing a D-Tyr^3/L-Tyr^9 configuration. Moreover, cyclic octadepsipeptides and cyclic lipdepsipeptides bearing a L-Tyr^3/D-Tyr^9 configuration were more stable than those with the opposite configuration. These findings strengthen the recently hypothesis of a L-Tyr^3/D-Tyr^9 configuration for natural fengycins.

APPENDIX

SUPPORTING INFORMATION OF DOCTORAL THESIS:

Solid-phase synthesis of cell-penetrating γ-peptide/antimicrobial peptide conjugates and of cyclic lipodepsipeptides derived from fengycins

Table of contents

- **Supporting Information Chapter 3:** Cell-penetrating γ-peptide/antimicrobial undecapeptide conjugates with anticancer activity S3

- **Supporting Information Chapter 4:** Solid-phase synthesis of cyclic depsipeptides containing a phenyl ester bond S9

- **Supporting Information Chapter 5:** Total solid-phase synthesis of dehydroxy fengycin derivatives S117

Supporting Information Chapter 3

Cell-penetrating γ-peptide/antimicrobial undecapeptide conjugates with anticancer activity

Cristina Rosés, Daniel Carbajo, Glòria Sanclimens, Josep Farrera-Sinfreu, Adriana Blancafort, Glòria Oliveras, Anna Díaz-Cirac, Eduard Bardají, Teresa Puig, Marta Planas, Lidia Feliu, Fernando Albericio and Miriam Royo

Table of contents

1. Synthesis of peptide conjugates....S5
    1.1. Lys-Lys-Leu-Phe-Lys-Lys-Ile-Leu-Lys-Val-Leu-PEG-1 (BP15-PEG-1)....S5
    1.2. Leu-Lys-Leu-Phe-Lys-Lys-Ile-Leu-Lys-Val-Leu-PEG-1 (BP33-PEG-1)....S6
    1.3. Lys-Lys-Leu-Phe-Lys-Lys-Ile-Leu-Lys-Phe-Leu-PEG-1 (BP76-PEG-1)....S6
    1.4. Ac-Lys-Lys-Leu-Phe-Lys-Lys-Ile-Leu-Lys-Phe-Leu-PEG-1 (BP77-PEG-1)....S7
    1.5. Ac-Lys-Lys-Leu-Phe-Lys-Lys-Ile-Leu-Lys-Tyr-Leu-PEG-1 (BP101-PEG-1)....S7
    1.6. Ts-Lys-Lys-Leu-Phe-Lys-Lys-Ile-Leu-Lys-Lys-Leu-PEG-1 (BP125-PEG-1)....S8
    1.7. Bz-Lys-Lys-Leu-Phe-Lys-Lys-Ile-Leu-Lys-Lys-Leu-PEG-1 (BP126-PEG-1)....S8

1. Synthesis of peptide conjugates

1.1. Lys-Lys-Leu-Phe-Lys-Lys-Ile-Leu-Lys-Val-Leu-PEG-1 (BP15-PEG-1)

HPLC (*λ = 220 nm*) / MS (MALDI-TOF)

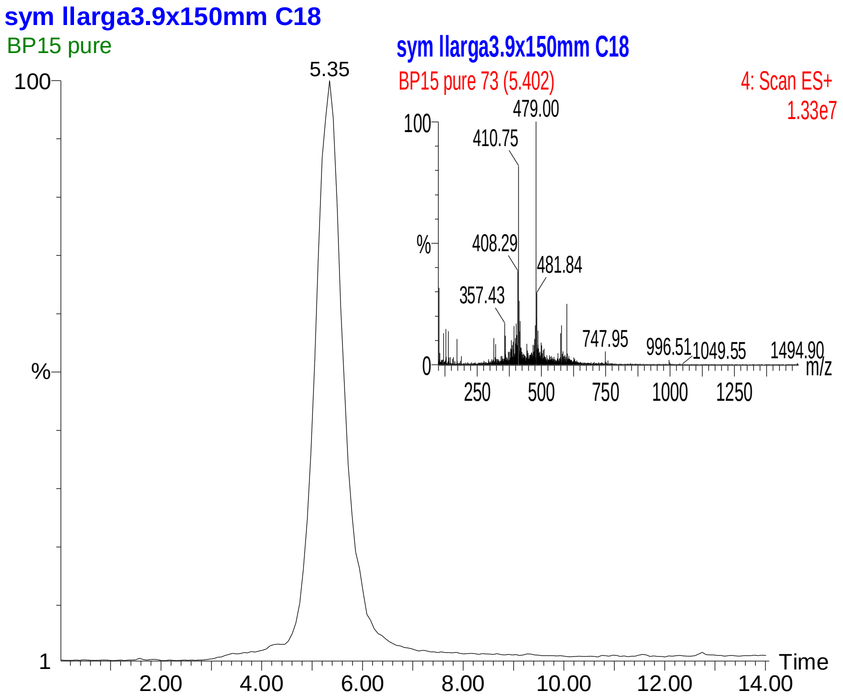

MS (ESI) *m/z* (+)

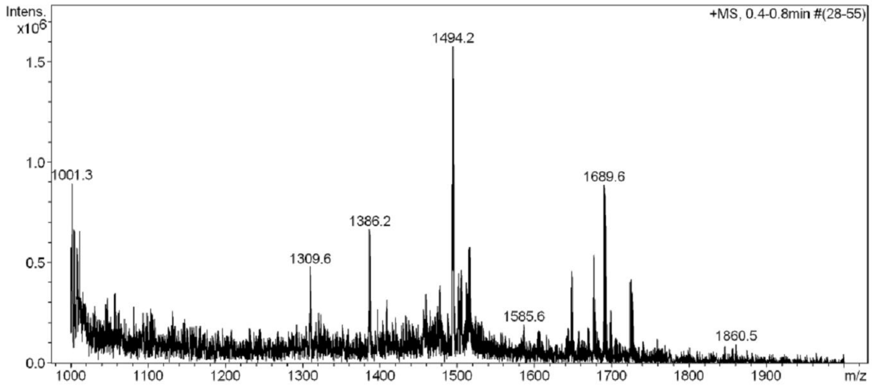

1.2. Leu-Lys-Leu-Phe-Lys-Lys-Ile-Leu-Lys-Val-Leu-PEG-1 (BP33-PEG-1)

HPLC (*λ = 220 nm*) / MS (MALDI-TOF)

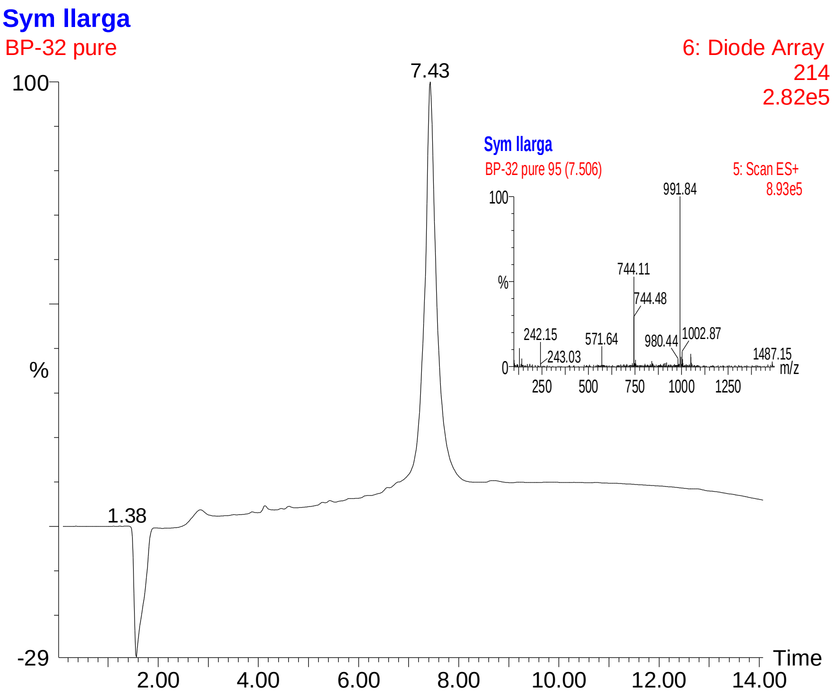

1.3. Lys-Lys-Leu-Phe-Lys-Lys-Ile-Leu-Lys-Phe-Leu-PEG-1 (BP76-PEG-1)

HPLC (*λ = 220 nm*) / MS (MALDI-TOF)

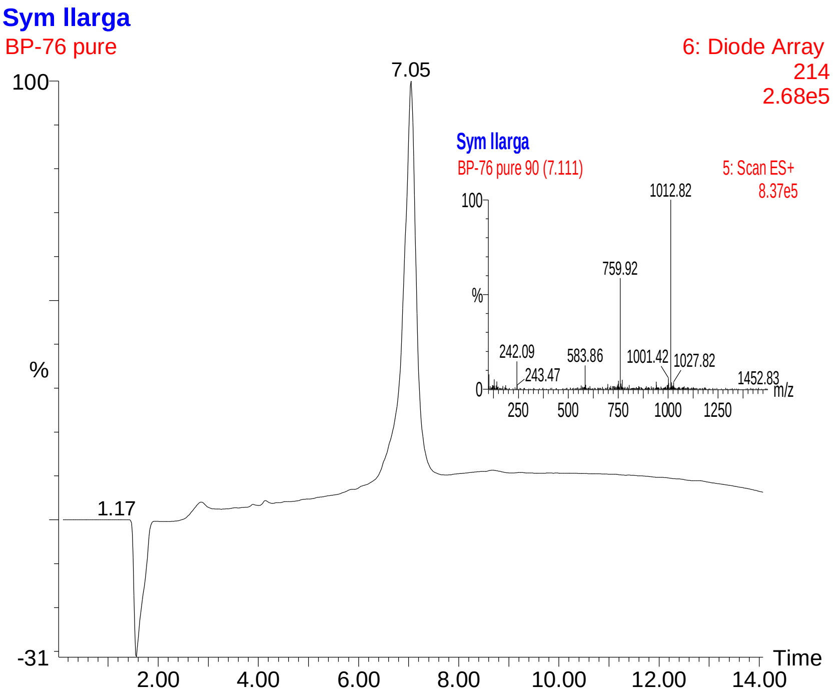

1.4. Ac-Lys-Lys-Leu-Phe-Lys-Lys-Ile-Leu-Lys-Phe-Leu-PEG-1 (BP77-PEG-1)

HPLC (*λ = 220 nm*) / MS (MALDI-TOF)

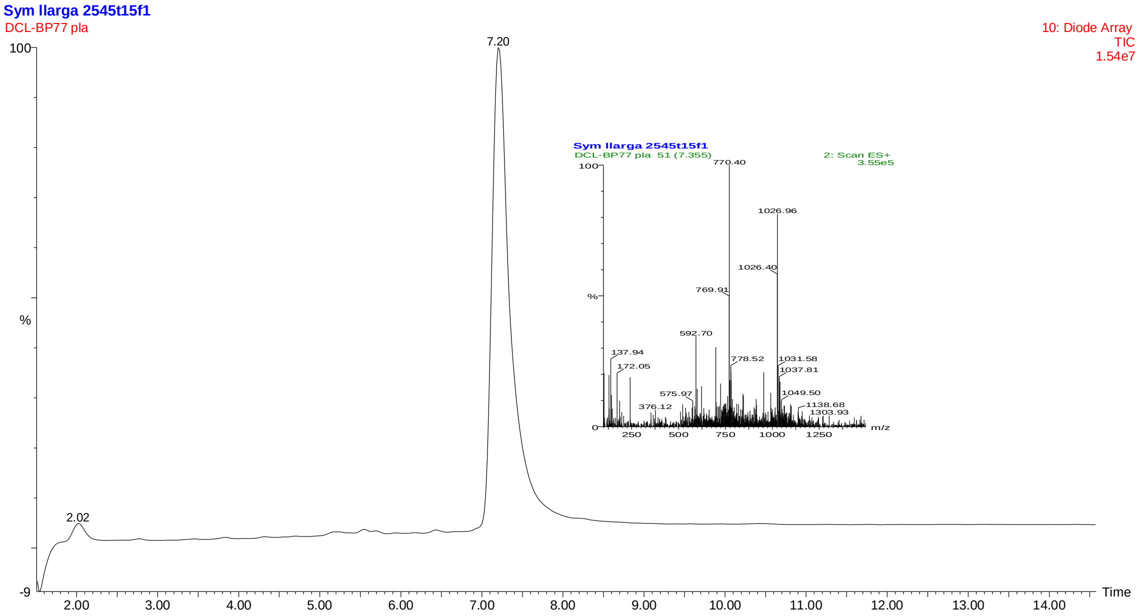

1.5. Ac-Lys-Lys-Leu-Phe-Lys-Lys-Ile-Leu-Lys-Tyr-Leu-PEG-1 (BP101-PEG-1)

HPLC (*λ = 220 nm*) / MS (MALDI-TOF)

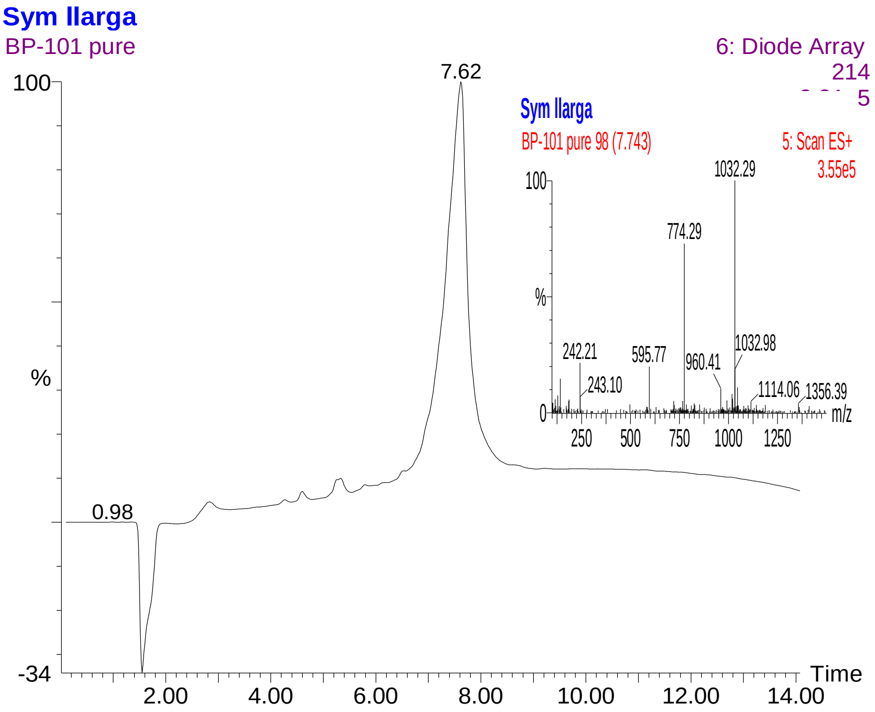

1.6. Ts-Lys-Lys-Leu-Phe-Lys-Lys-Ile-Leu-Lys-Lys-Leu-PEG-1 (BP125-PEG-1)

HPLC (*λ = 220 nm*) / MS (MALDI-TOF)

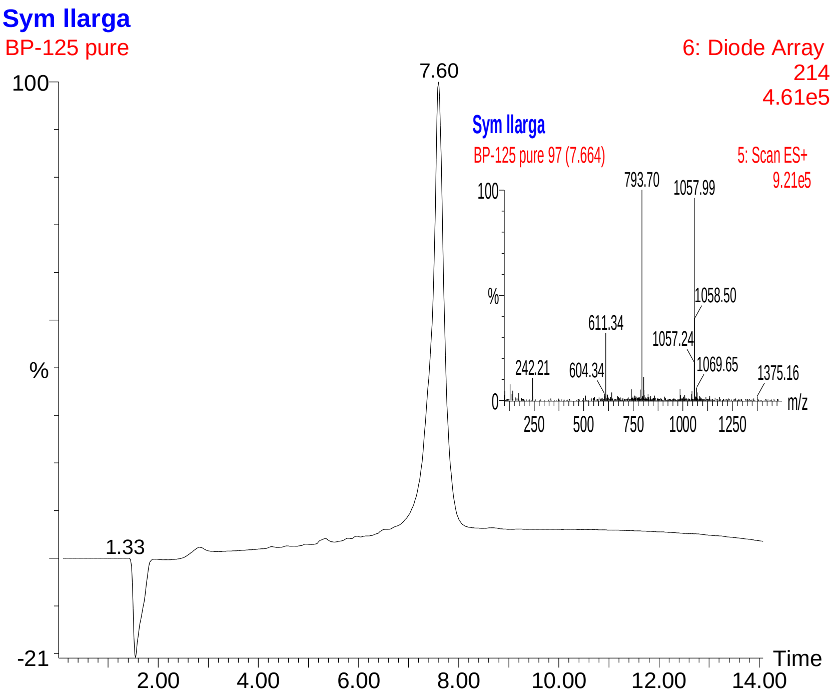

1.7. Bz-Lys-Lys-Leu-Phe-Lys-Lys-Ile-Leu-Lys-Lys-Leu-PEG-1 (BP126-PEG-1)

HPLC (*λ = 220 nm*) / MS (MALDI-TOF)

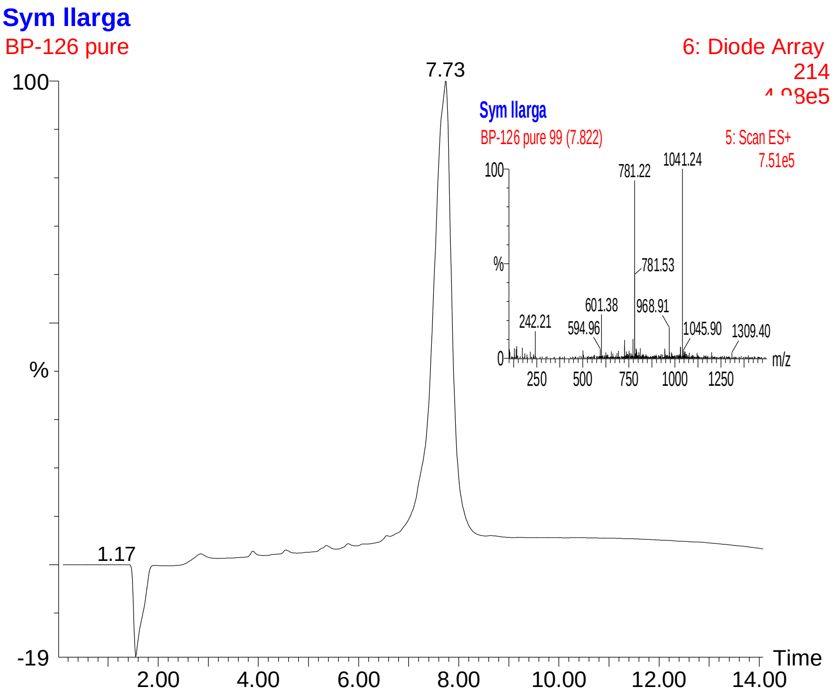

Supporting Information Chapter 4

Solid-phase synthesis of cyclic depsipeptides containing a phenyl ester bond

Cristina Rosés, Cristina Camó, Marta Planas and Lidia Feliu

Table of contents

1. Amino acids S13

2. Synthesis of cyclic octapeptides S28

  2.1. Linear peptides S28

    2.1.1. Fmoc-Thr-Glu-Val-Pro-Gln-OAll S28
    2.1.2. H-Phe(4-NH-Ile-Tyr-Fmoc)-Thr-Glu-Val-Pro-Gln-OAll S29
    2.1.3. H-Phe(4-NH-Ile-D-Tyr-Fmoc)-D-Thr-Glu-D-Val-Pro-Gln-OAll S30
    2.1.4. H-Phe(4-NH-Ile-D-Tyr-Fmoc)-D-Thr-Glu-D-Ala-Pro-Gln-OAll S31
    2.1.5. H-Phe(4-NH-Ile-D-Tyr-Fmoc)-D-Ser-Glu-D-Ala-Pro-Gln-OAll S32
    2.1.6. H-Phe(4-NH-Ile-D-Tyr-Fmoc)-D-Ser-Glu-D-Val-Pro-Gln-OAll S33
    2.1.7. H-Phe(4-NH-Ile-Tyr-H)-Thr-Glu-Val-Pro-Gln-OH S34
    2.1.8. H-Phe(4-NH-Ile-D-Tyr-H)-D-Thr-Glu-D-Val-Pro-Gln-OH S35
    2.1.9. H-Phe(4-NH-Ile-D-Tyr-H)-D-Thr-Glu-D-Ala-Pro-Gln-OH S36
    2.1.10. H-Phe(4-NH-Ile-D-Tyr-H)-D-Ser-Glu-D-Ala-Pro-Gln-OH S37
    2.1.11. H-Phe(4-NH-Ile-D-Tyr-H)-D-Ser-Glu-D-Val-Pro-Gln-OH S38

2.2. Cyclic octapeptides S39
2.2.1. H-Phe(4-NH-&)-Thr-Glu-Val-Pro-Gln-Tyr-Ile-& (1) S39
2.2.2. H-Phe(4-NH-&)-D-Thr-Glu-D-Val-Pro-Gln-D-Tyr-Ile-& (BPC862) S40
2.2.3. H-Phe(4-NH-&)-D-Thr-Glu-D-Ala-Pro-Gln-D-Tyr-Ile-& (BPC864) S42
2.2.4. H-Phe(4-NH-&)-D-Ser-Glu-D-Ala-Pro-Gln-D-Tyr-Ile-& (BPC866) S44
2.2.5. H-Phe(4-NH-&)-D-Ser-Glu-D-Val-Pro-Gln-D-Tyr-Ile-& (BPC868) S46

3. Synthesis of cyclic octadepsipeptides S48

3.1. Linear peptides S48
3.1.1. H-Tyr-Thr-Glu-Val-Pro-Gln-OAll S48
3.1.2. *p*NZ-Tyr-Thr-Glu-Val-Pro-Gln-OAll S49
3.1.3. *p*NZ-Tyr-Thr-Glu-Val-Pro-Gln-Tyr-OAll S50
3.1.4. *p*NZ-Tyr-D-Thr-Glu-D-Val-Pro-Gln-D-Tyr-OAll S51
3.1.5. H-Tyr-D-Thr-Glu-D-Val-Pro-Gln-D-Tyr-OAll S52
3.1.6. H-Tyr-D-Ser-Glu-D-Val-Pro-Gln-D-Tyr-OAll S53
3.1.7. H-Tyr-D-Thr-Glu-D-Ala-Pro-Gln-D-Tyr-OAll S54
3.1.8. H-Tyr-D-Ser-Glu-D-Ala-Pro-Gln-D-Tyr-OAll S55
3.1.9. H-D-Tyr-D-Thr-Glu-D-Val-Pro-Gln-Tyr-OAll S56
3.1.10. H-D-Tyr-D-Ser-Glu-D-Val-Pro-Gln-Tyr-OAll S57
3.1.11. H-D-Tyr-D-Thr-Glu-D-Ala-Pro-Gln-Tyr-OAll S58
3.1.12. H-D-Tyr-D-Ser-Glu-D-Ala-Pro-Gln-Tyr-OAll S59

3.2. Linear depsipeptides S60
3.2.1. H-Tyr(O-Ile-Fmoc)-Thr-Glu-Val-Pro-Gln-OAll S60
3.2.2. *p*NZ-Tyr(O-Ile-H)-Thr-Glu-Val-Pro-Gln-OAll S61
3.2.3. *p*NZ-Tyr(O-Ile-Alloc)-Thr-Glu-Val-Pro-Gln-Tyr-OAll S62
3.2.4. *p*NZ-Tyr(O-Ile-Alloc)-D-Thr-Glu-D-Val-Pro-Gln-D-Tyr-OAll S63
3.2.5. H-Tyr(O-Ile-Alloc)-D-Thr-Glu-D-Val-Pro-Gln-D-Tyr-OAll S64
3.2.6. H-Tyr(O-Ile-Alloc)-D-Ser-Glu-D-Val-Pro-Gln-D-Tyr-OAll S65
3.2.7. H-Tyr(O-Ile-Alloc)-D-Thr-Glu-D-Ala-Pro-Gln-D-Tyr-OAll S66
3.2.8. H-Tyr(O-Ile-Alloc)-D-Ser-Glu-D-Ala-Pro-Gln-D-Tyr-OAll S67
3.2.9. H-D-Tyr(O-Ile-Alloc)-D-Thr-Glu-D-Val-Pro-Gln-Tyr-OAll S68
3.2.10. H-D-Tyr(O-Ile-Alloc)-D-Ser-Glu-D-Val-Pro-Gln-Tyr-OAll S69
3.2.11. H-D-Tyr(O-Ile-Alloc)-D-Thr-Glu-D-Ala-Pro-Gln-Tyr-OAll S70
3.2.12. H-D-Tyr(O-Ile-Alloc)-D-Ser-Glu-D-Ala-Pro-Gln-Tyr-OAll S71

3.3. Deprotected linear depsipeptides S72
3.3.1. *p*NZ-Tyr(O-Ile-H)-Thr-Glu-Val-Pro-Gln-Tyr-OH S72
3.3.2. *p*NZ-Tyr(O-Ile-H)-D-Thr-Glu-D-Val-Pro-Gln-D-Tyr-OH S73
3.3.3. H-Tyr(O-Ile-H)-D-Thr-Glu-D-Val-Pro-Gln-D-Tyr-OH (BPC821) S74
3.3.4. H-Tyr(O-Ile-H)-D-Ser-Glu-D-Val-Pro-Gln-D-Tyr-OH (BPC823) S75

3.3.5. H-Tyr(O-Ile-H)-D-Thr-Glu-D-Ala-Pro-Gln-D-Tyr-OH (BPC825) S76
3.3.6. H-Tyr(O-Ile-H)-D-Ser-Glu-D-Ala-Pro-Gln-D-Tyr-OH (BPC827) S77
3.3.7. H-D-Tyr(O-Ile-H)-D-Thr-Glu-D-Val-Pro-Gln-Tyr-OH (BPC829) S78
3.3.8. H-D-Tyr(O-Ile-H)-D-Ser-Glu-D-Val-Pro-Gln-Tyr-OH (BPC831) S79
3.3.9. H-D-Tyr(O-Ile-H)-D-Thr-Glu-D-Ala-Pro-Gln-Tyr-OH (BPC833) S80
3.3.10. H-D-Tyr(O-Ile-H)-D-Ser-Glu-D-Ala-Pro-Gln-Tyr-OH (BPC835) S81

3.4. Cyclic depsipeptides S82

3.4.1. *p*NZ-Tyr(&)-D-Thr-Glu-D-Val-Pro-Gln-D-Tyr-Ile-& (8) S82
3.4.2. H-Tyr(&)-D-Thr-Glu-D-Val-Pro-Gln-D-Tyr-Ile-& (BPC822) S85
3.4.3. H-Tyr(&)-D-Ser-Glu-D-Val-Pro-Gln-D-Tyr-Ile-& (BPC824) S90
3.4.4. H-Tyr(&)-D-Thr-Glu-D-Ala-Pro-Gln-D-Tyr-Ile-& (BPC826) S95
3.4.5. H-Tyr(&)-D-Ser-Glu-D-Ala-Pro-Gln-D-Tyr-Ile-& (BPC828) S101
3.4.6. H-D-Tyr(&)-D-Thr-Glu-D-Val-Pro-Gln-Tyr-Ile-& (BPC830) S107
3.4.7. H-D-Tyr(&)-D-Ser-Glu-D-Val-Pro-Gln-Tyr-Ile-& (BPC832) S109
3.4.8. H-D-Tyr(&)-D-Thr-Glu-D-Ala-Pro-Gln-Tyr-Ile-& (BPC834) S111
3.4.9. H-D-Tyr(&)-D-Ser-Glu-D-Ala-Pro-Gln-Tyr-Ile-& (BPC836) S113

1. Amino acids

Fmoc-L-Tyr(^{t}Bu)-OAll

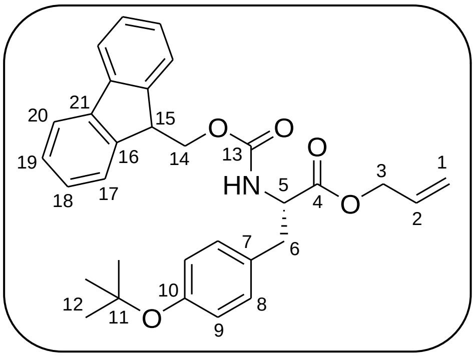

20
21
15
O
O
19
16
14
13
O
HN
5
3
1
18
17
4
O
2
7
6
10
12
8
11
O
9

MS (ESI) *m/z* (+)

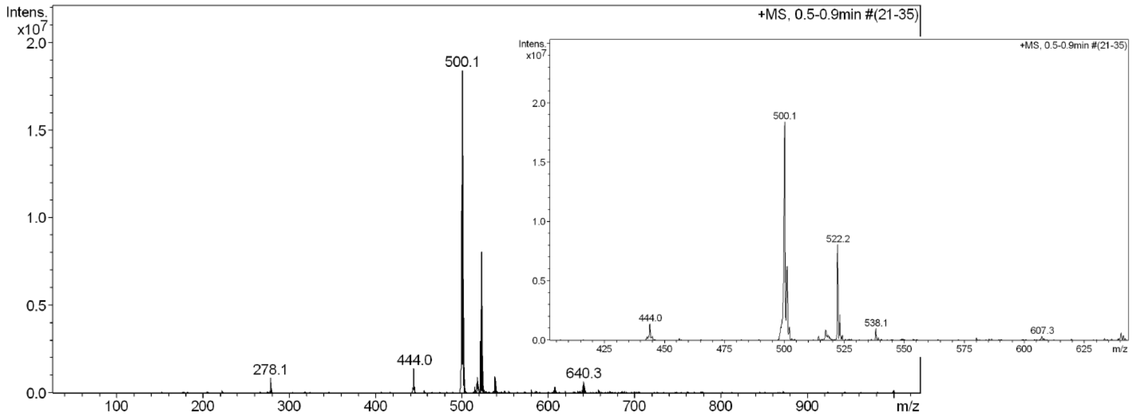

^{1}H-NMR (400 MHz), CDCl$_3$

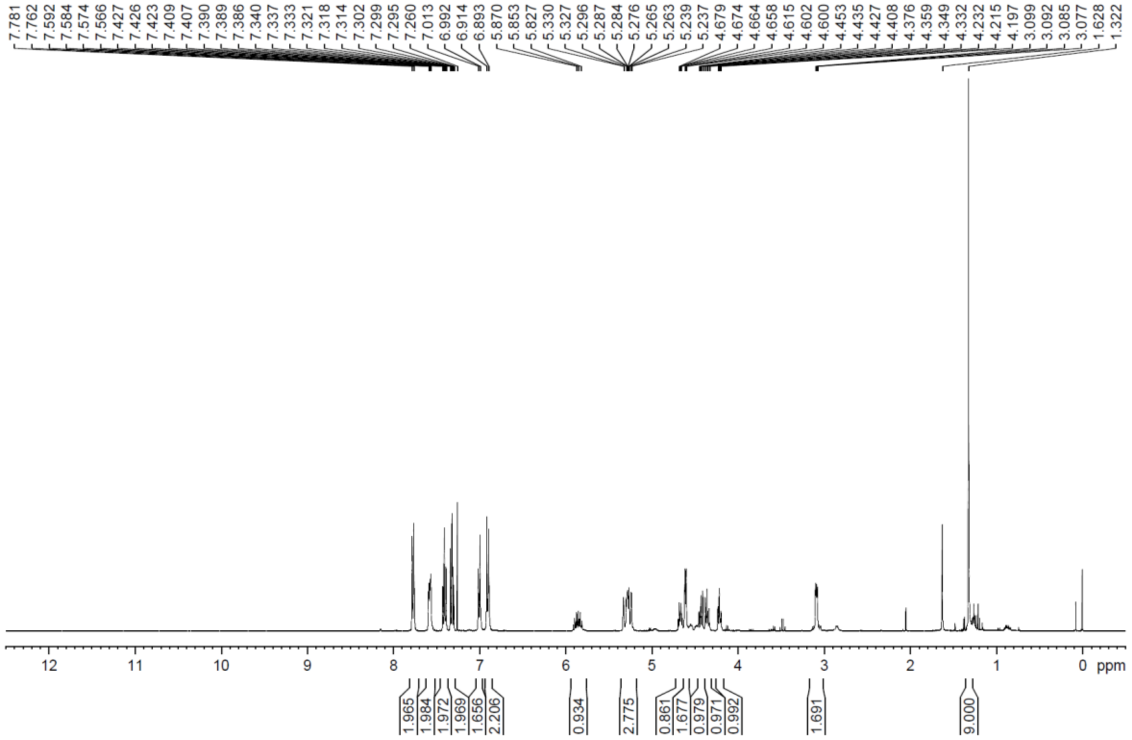

^{13}C-NMR (300 MHz), CDCl$_3$

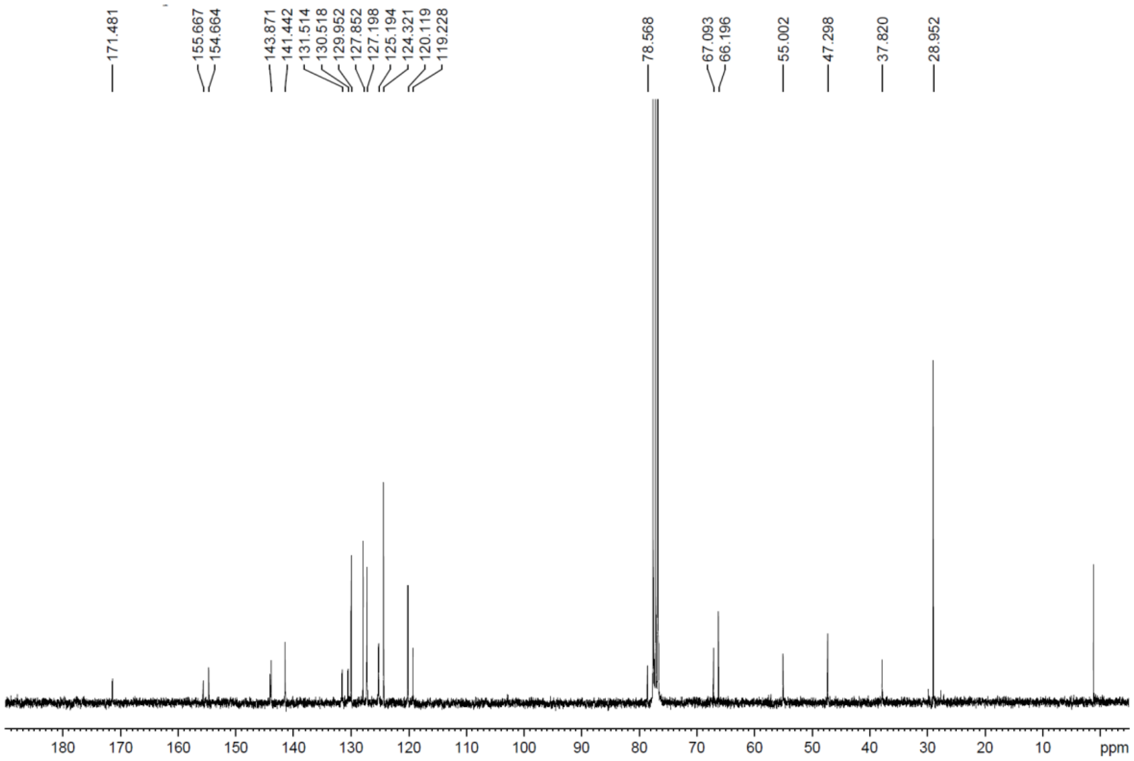

IR

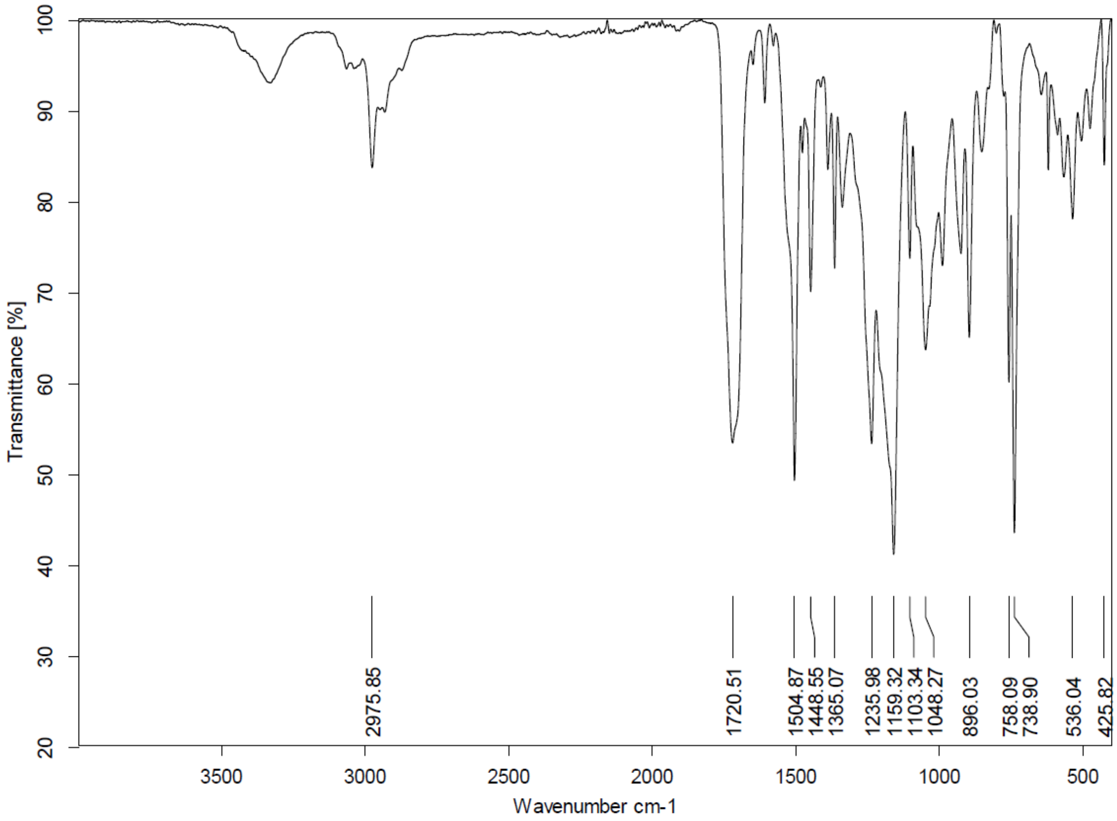

Fmoc-D-Tyr(^{t}Bu)-OAll

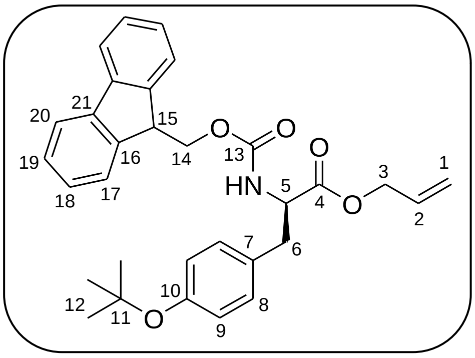
1
2
3
4
5
6
7
8
9
10
11
12
13
14
15
16
17
18
19
20
21
HN
O
O
O
O
O

MS (ESI) ***m/z*** **(+)**

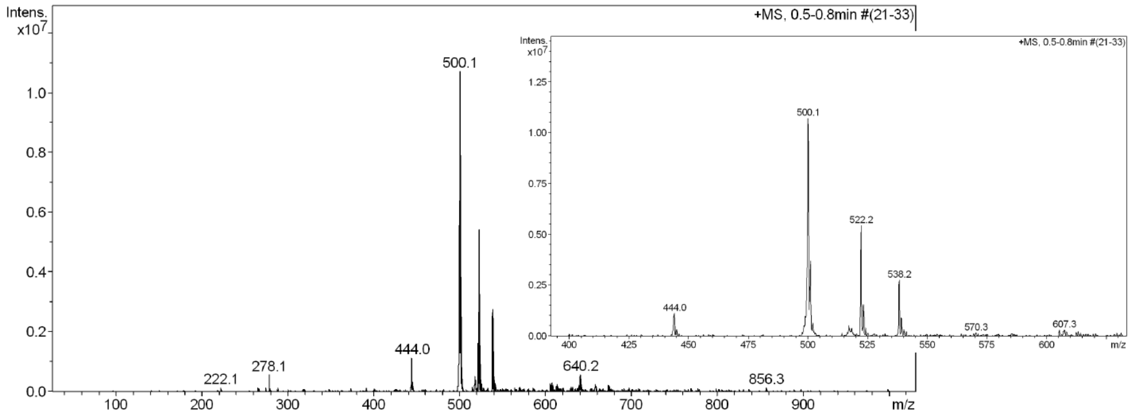

^{1}H-NMR (400 MHz), CDCl$_3$

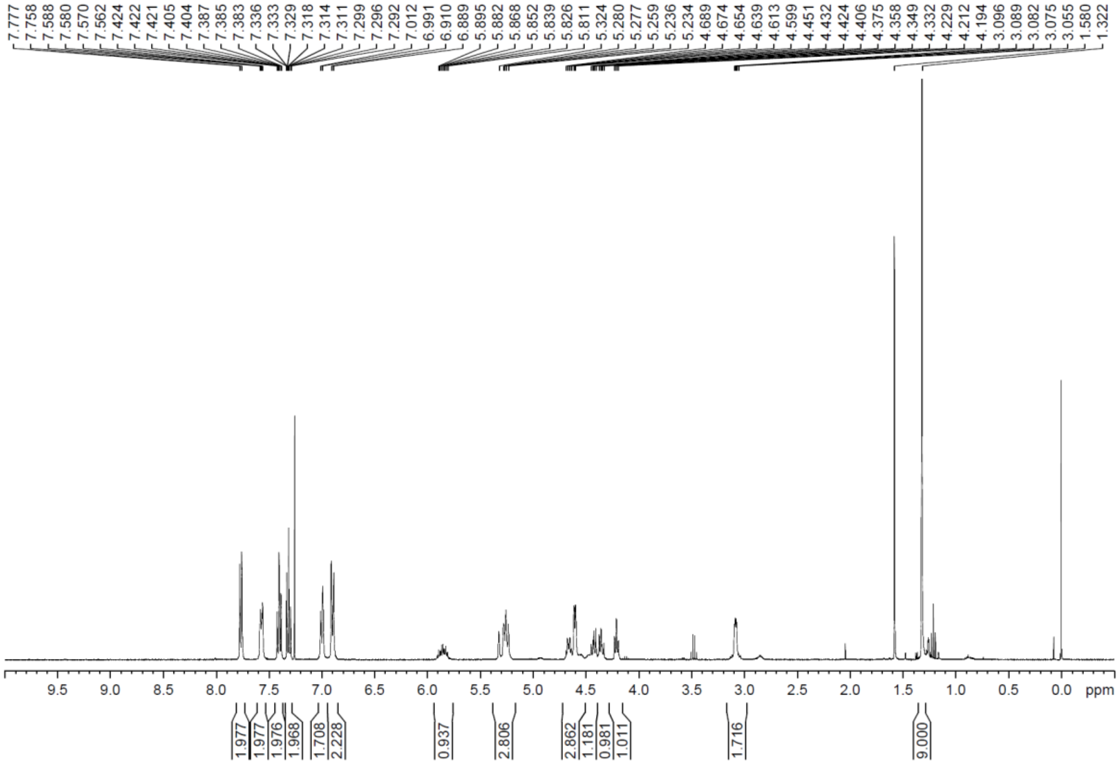

^{13}C-NMR (400 MHz), $CDCl_3$

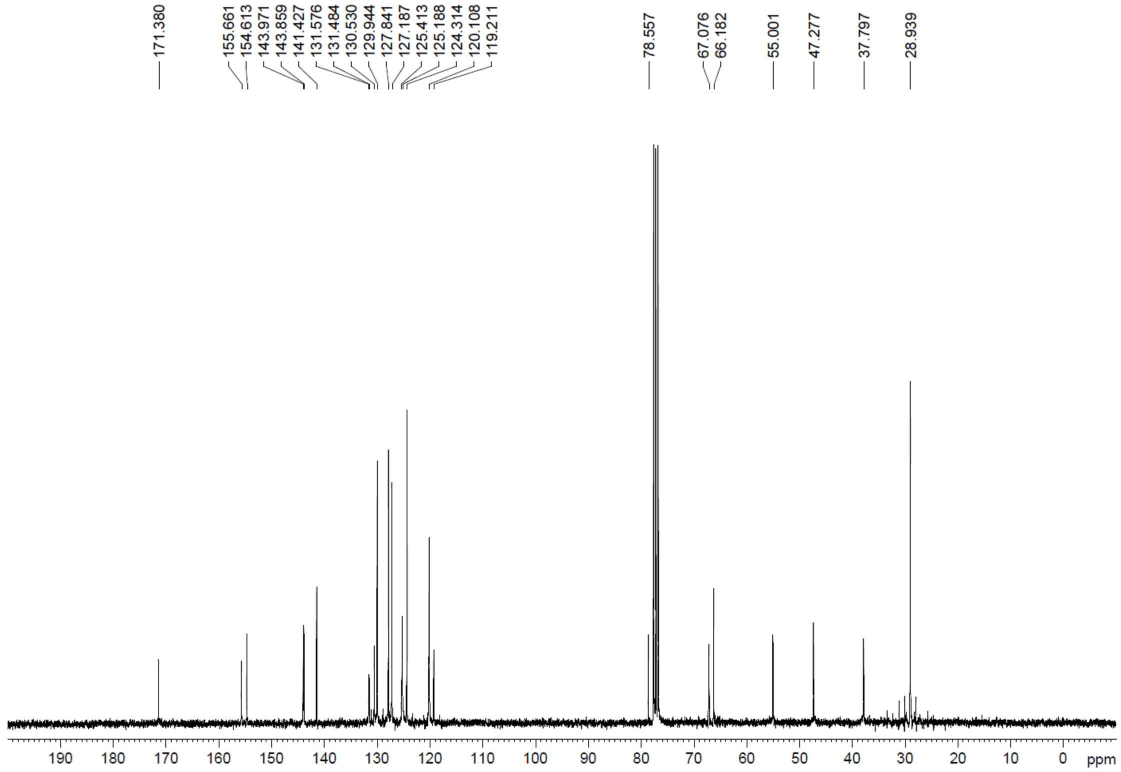

IR

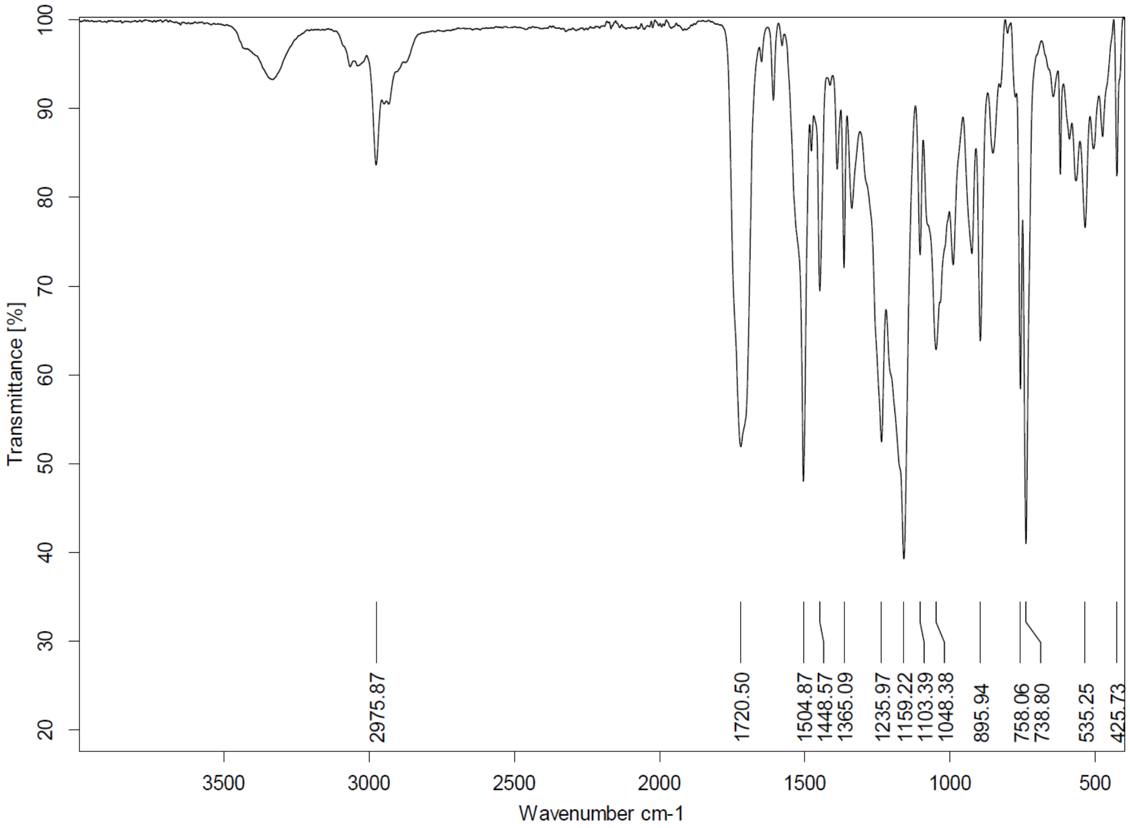

Fmoc-L-Tyr-OAll

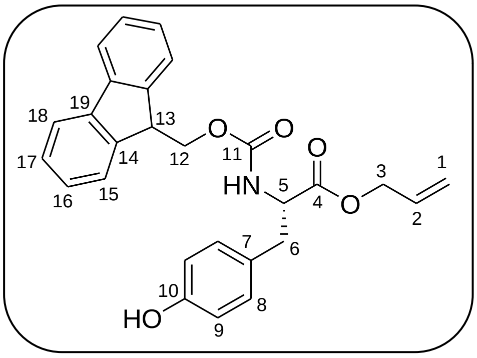
19
18
13
O
O
17
14
12
11
O
3
1
HN
5
4
O
2
16
15
7
6
10
8
HO
9

MS (ESI) *m/z* (+)

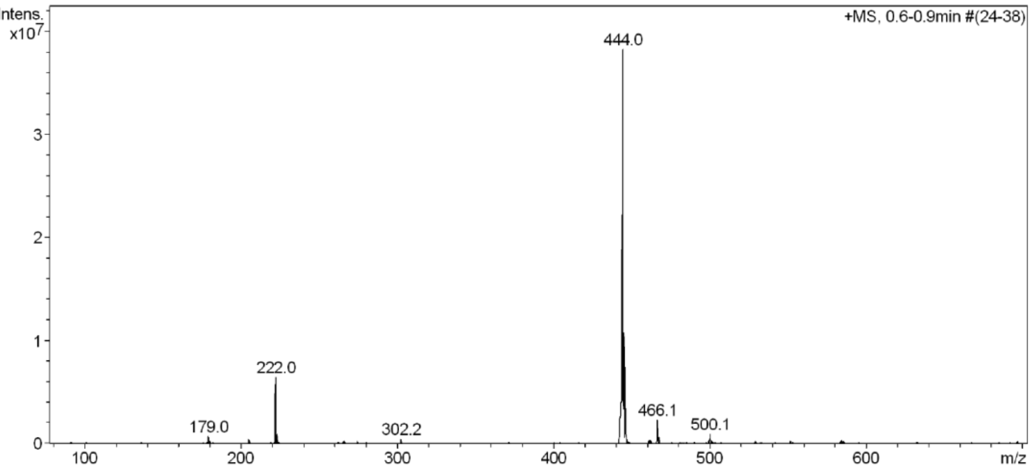

^{1}H-NMR (400 MHz), $CDCl_3$

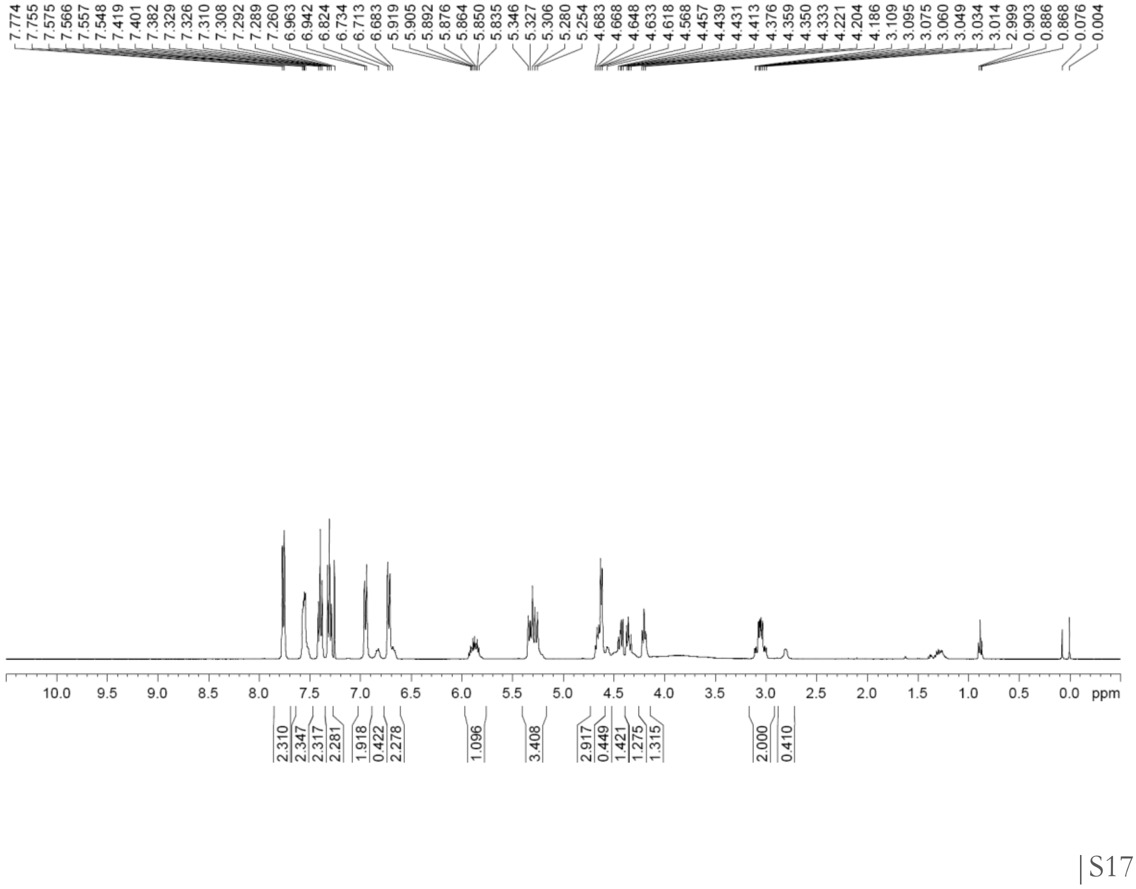

^{13}C-NMR (400 MHz), CDCl$_3$

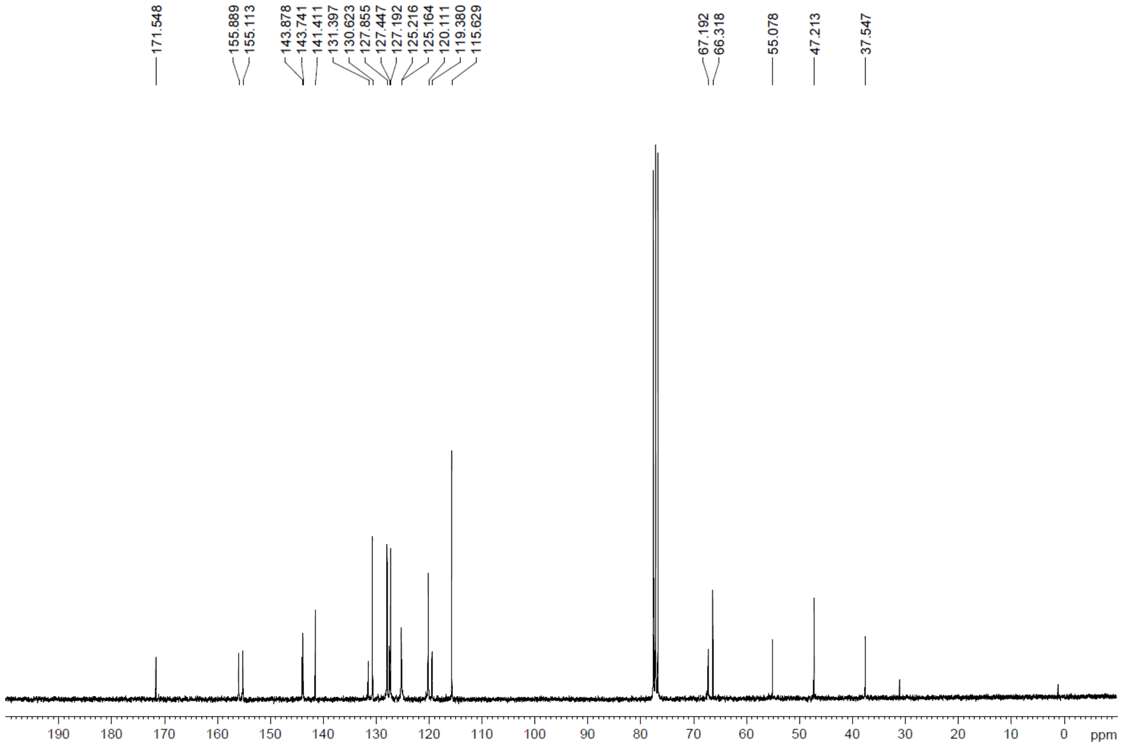

IR

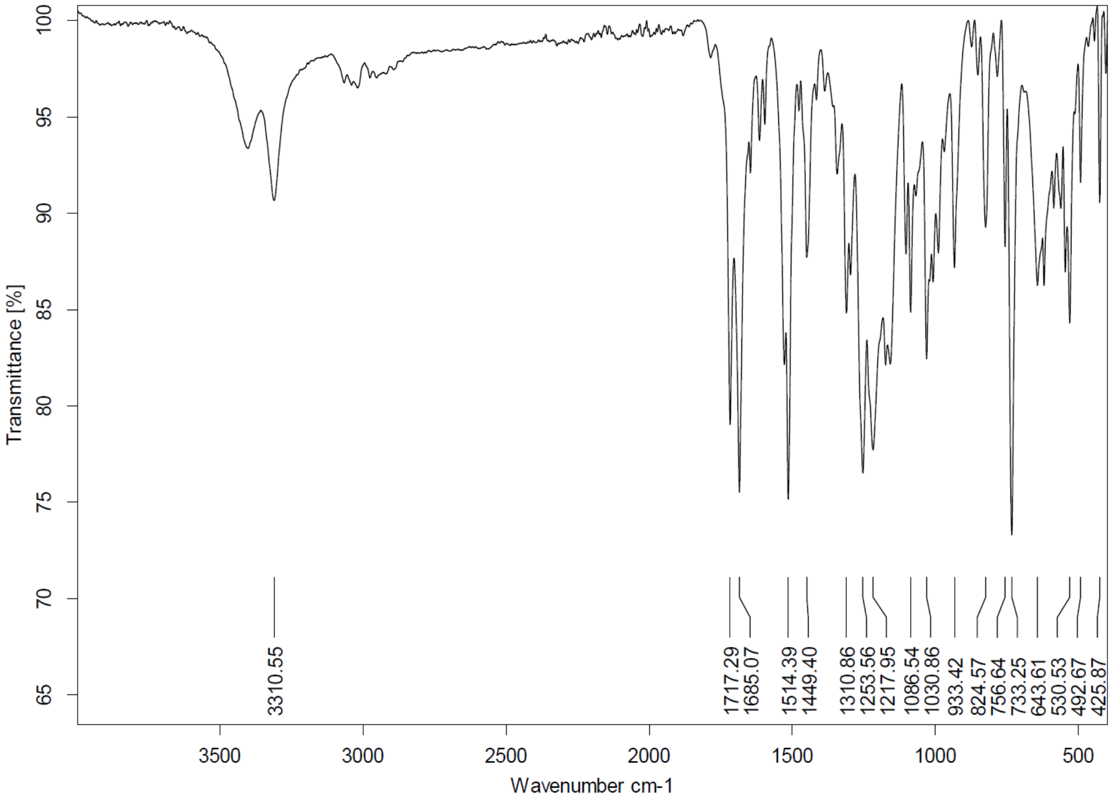

Fmoc-D-Tyr-OAll

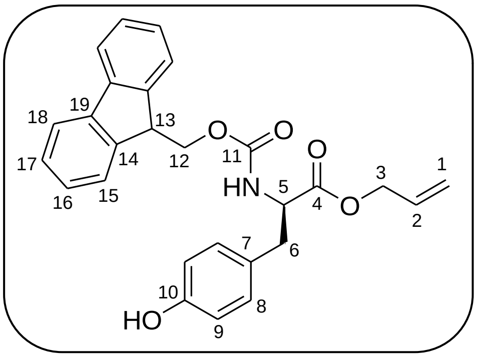

18
19
13
O
O
17
14
12
11
O
3
1
HN
5
16
15
4
O
2
7
6
10
8
HO
9

MS (ESI) *m/z* (+)

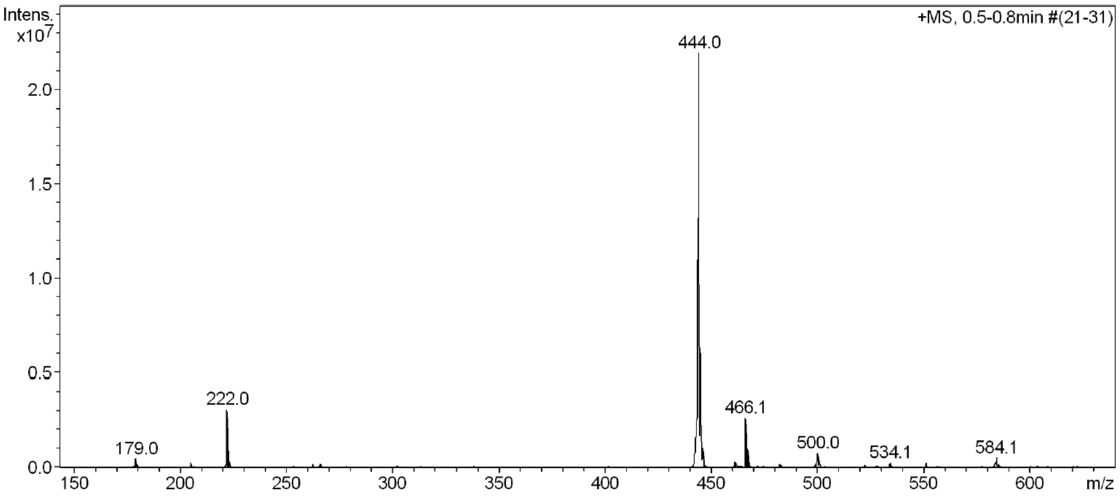

^{1}H-NMR (400 MHz), CDCl$_3$

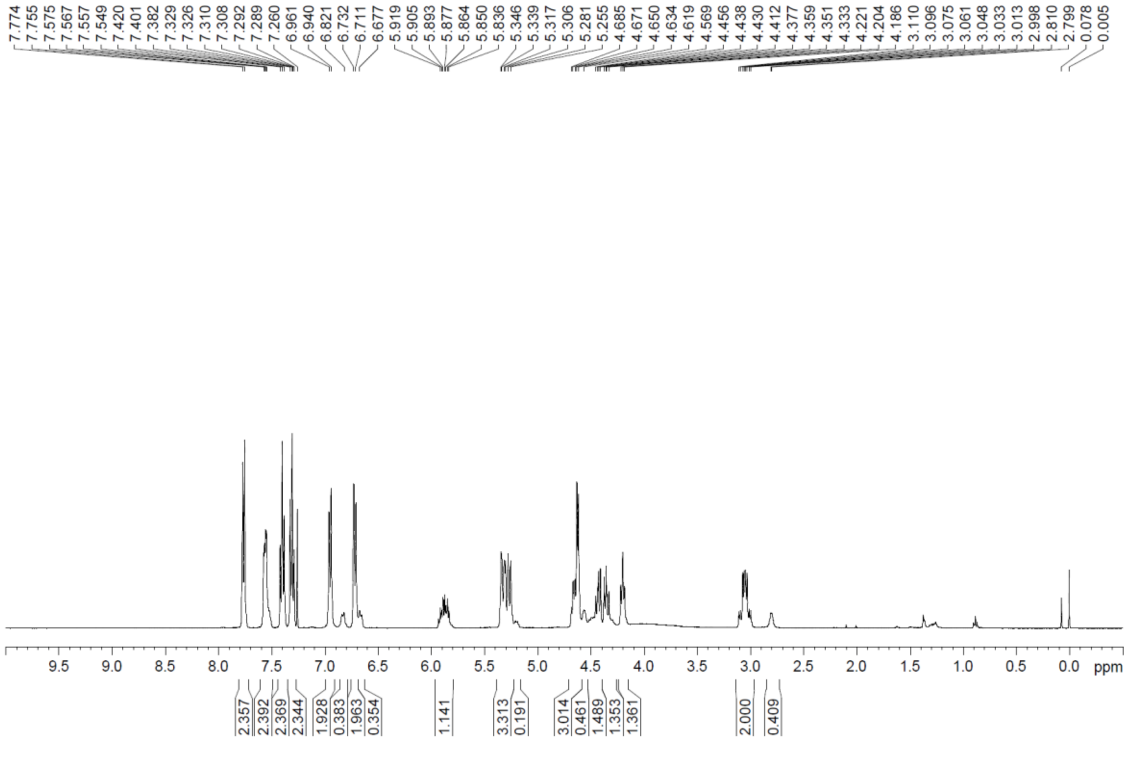

^{13}C-NMR (400 MHz), CDCl$_3$

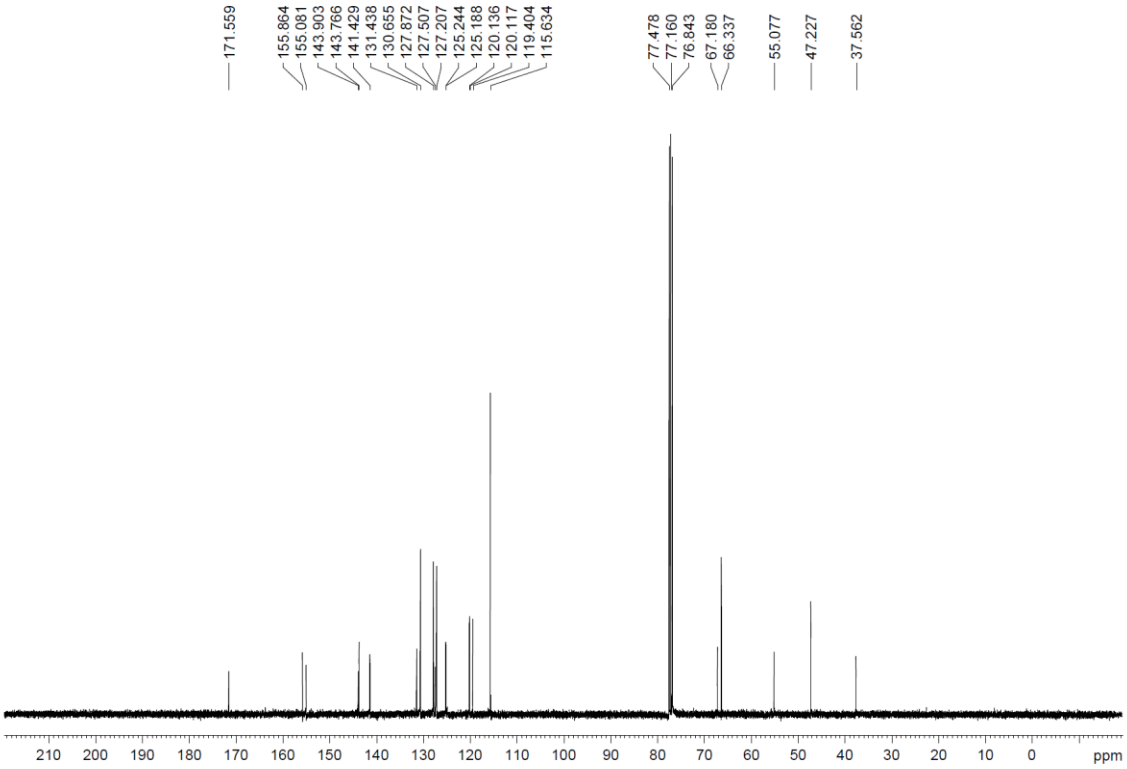

HSQC-NMR (400 MHz), CDCl$_3$

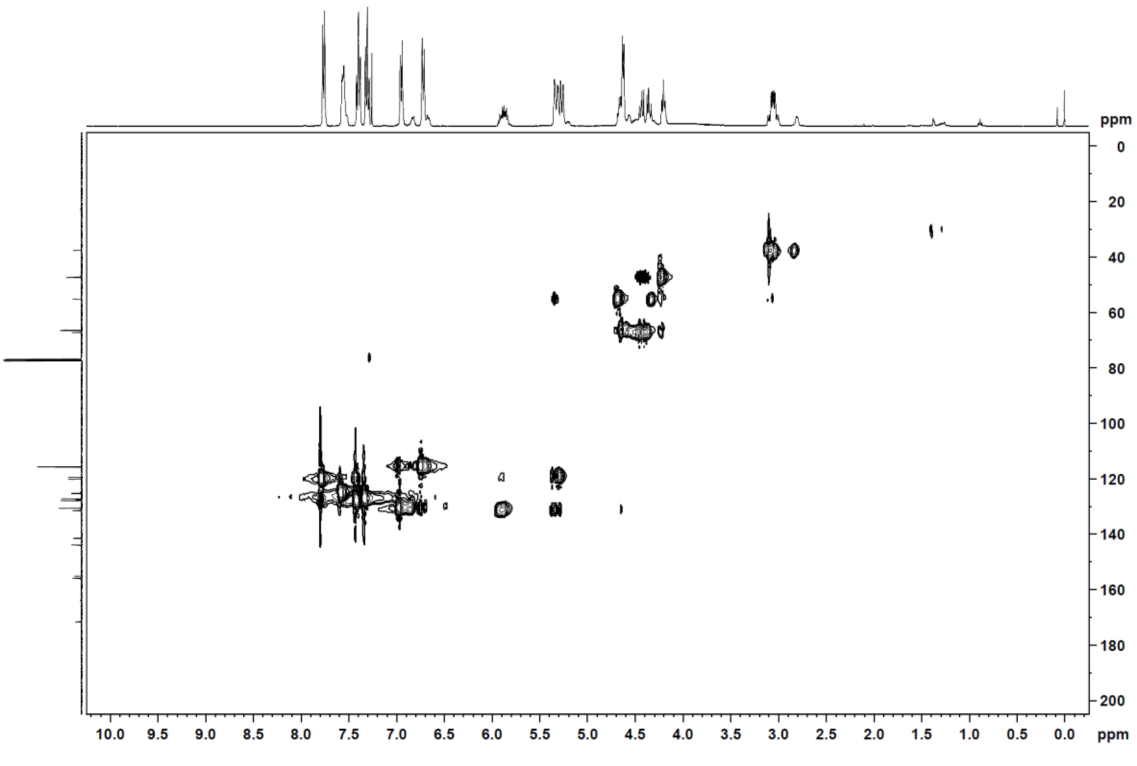

IR

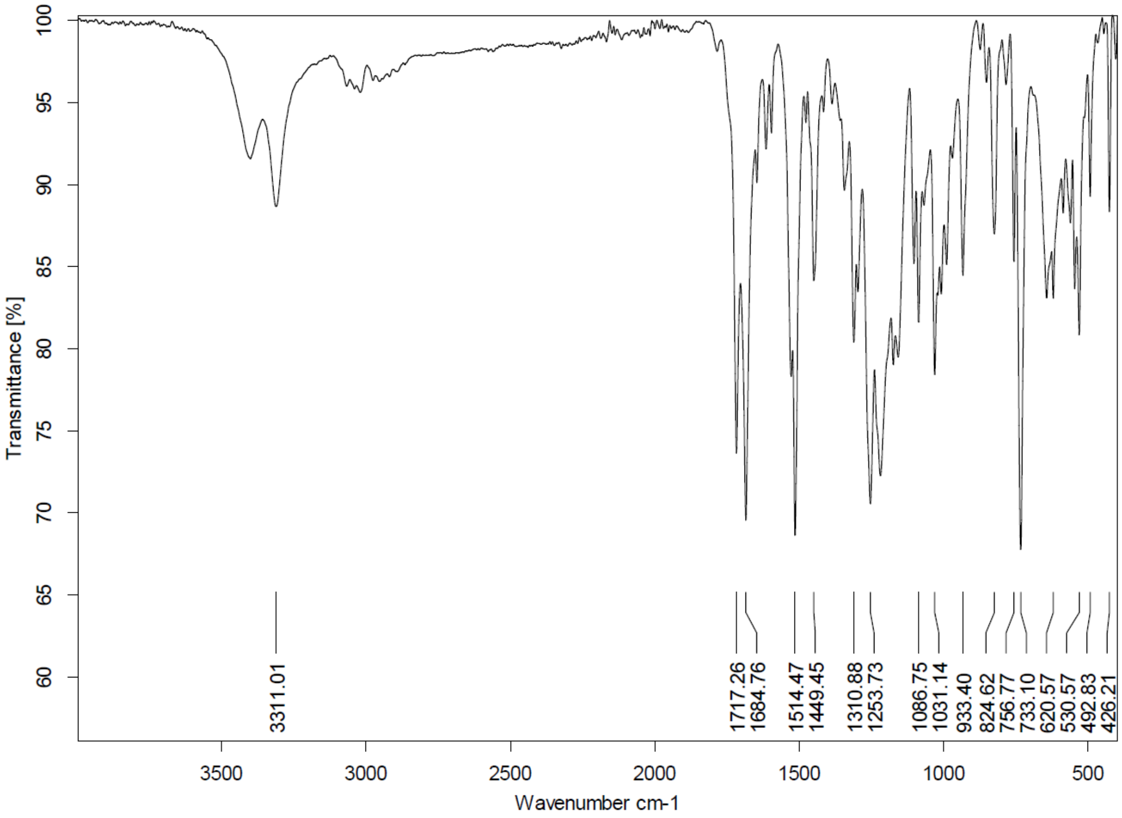
Transmittance [%]
100
95
90
85
80
75
70
65
60
3311.01
1717.26
1684.76
1514.47
1449.45
1310.88
1253.73
1086.75
1031.14
933.40
824.62
756.77
733.10
620.57
530.57
492.83
426.21
3500
3000
2500
2000
1500
1000
500
Wavenumber cm-1

*p*NZ-L-Tyr(^{t}Bu)-OH

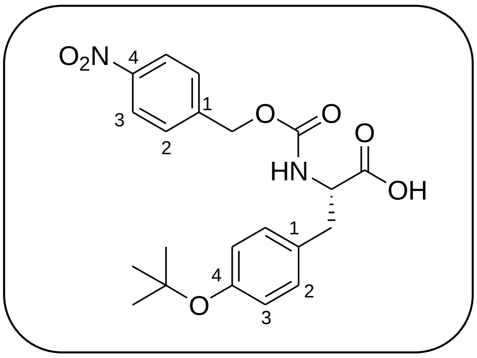
O2N
4
1
3
2
O
O
O
HN
OH
1
4
2
O
3

^{1}H-NMR (400 MHz), CD_3OD

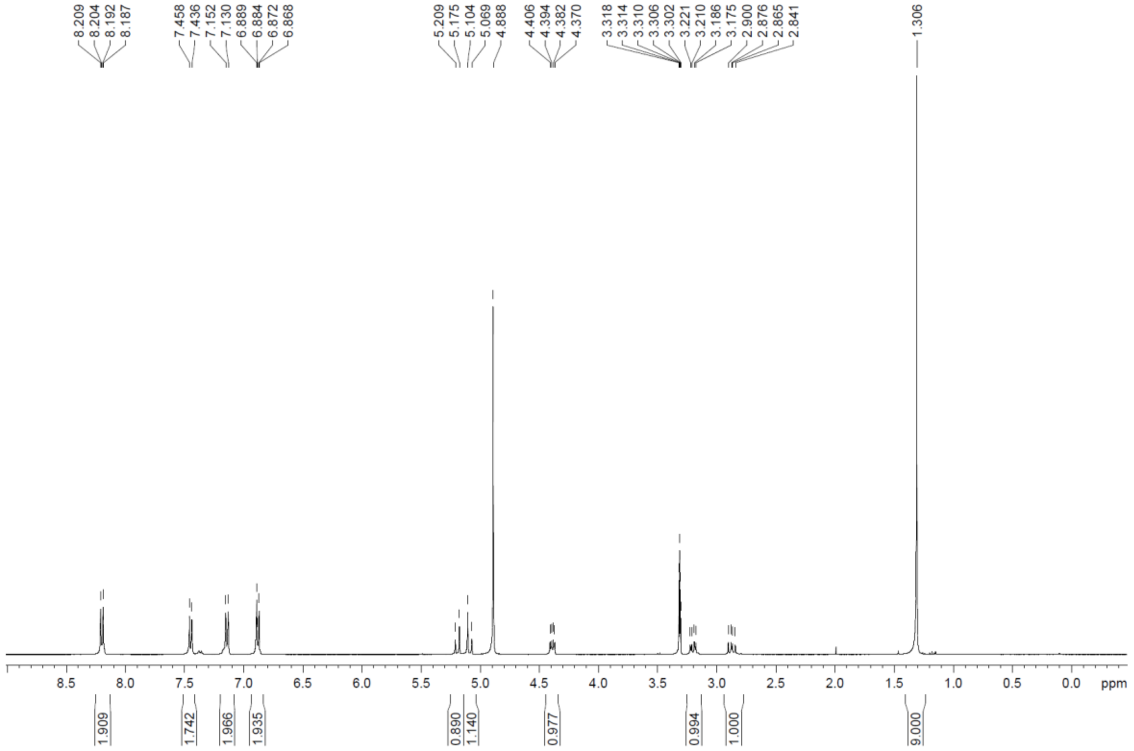

^{13}C-NMR (400 MHz), CD$_3$OD

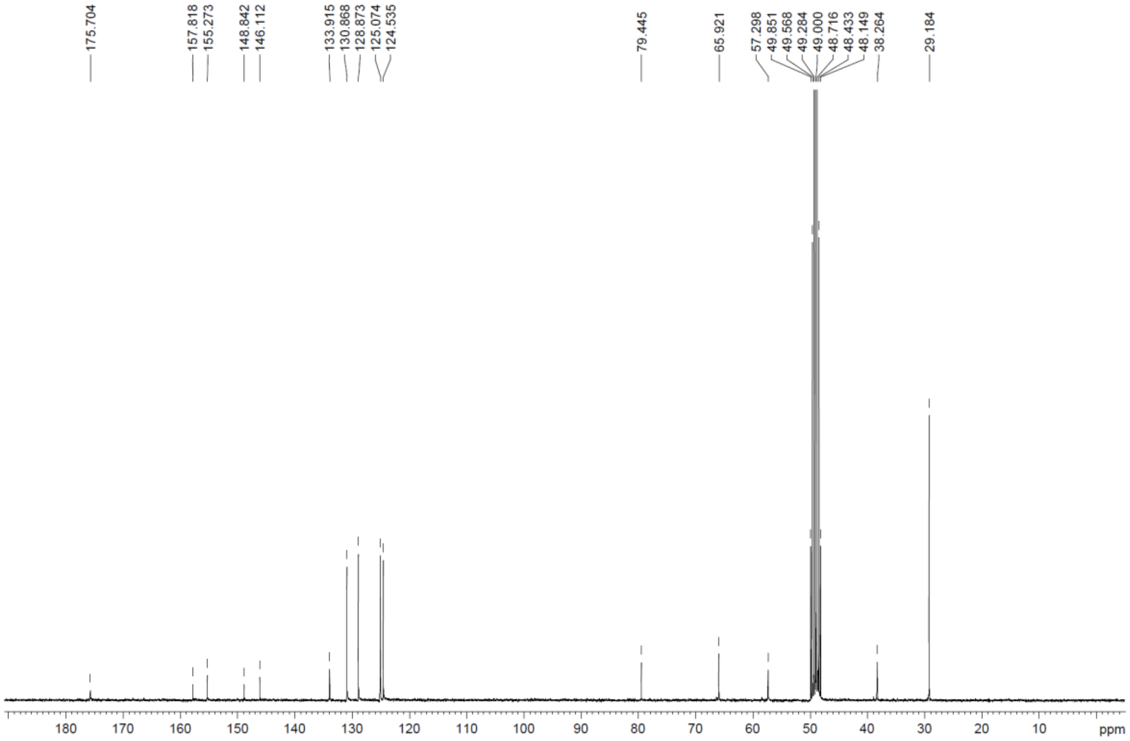

*p*NZ-L-Tyr-OH

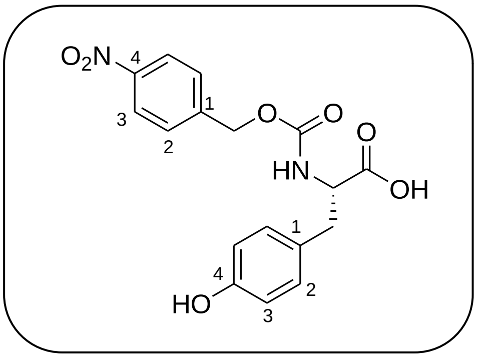
O_2N
4
1
3
2
O
O
O
HN
OH
1
4
2
HO
3

MS (ESI) *m/z* (+)

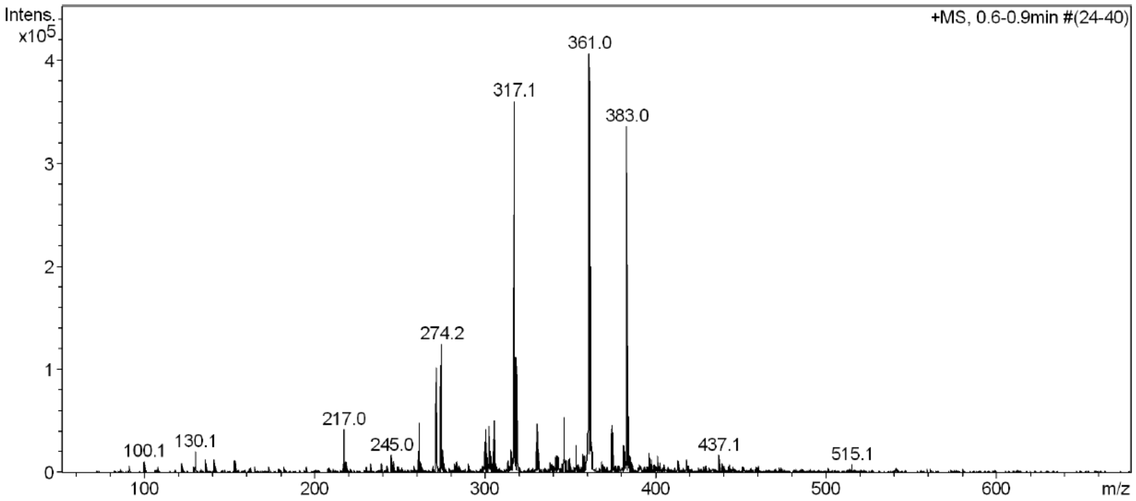

^{1}H-NMR (400 MHz), CD_3OD

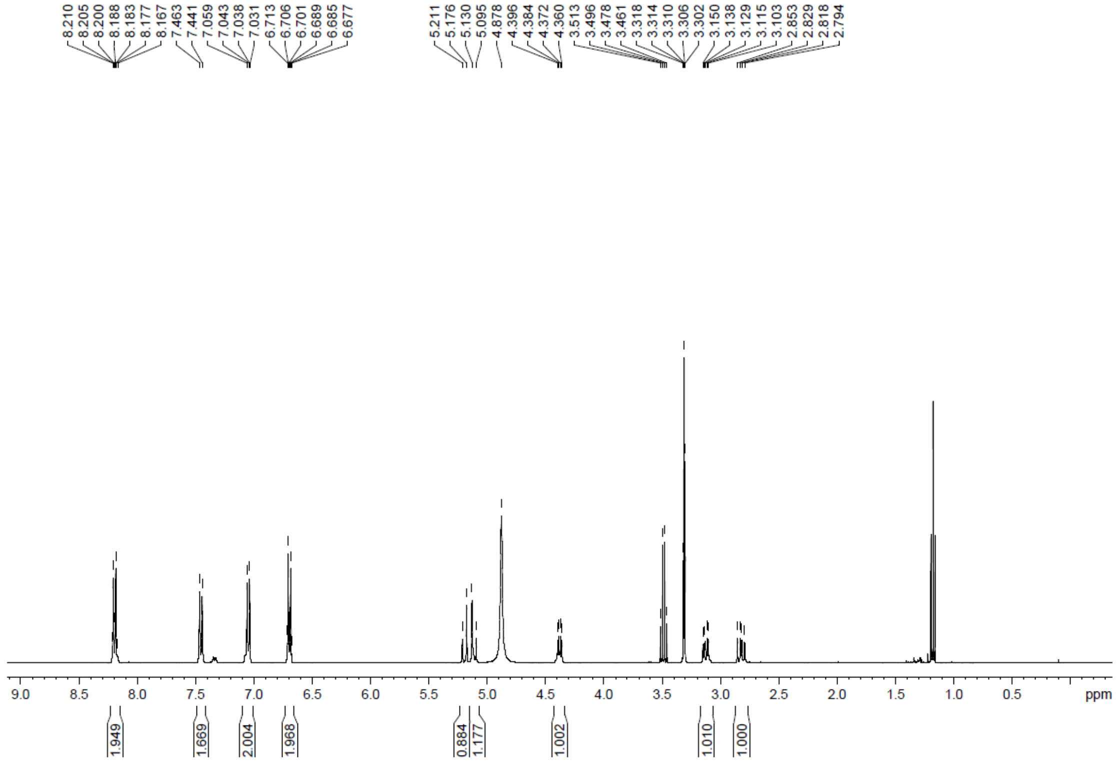

^{13}C-NMR (400 MHz), CDCl$_3$

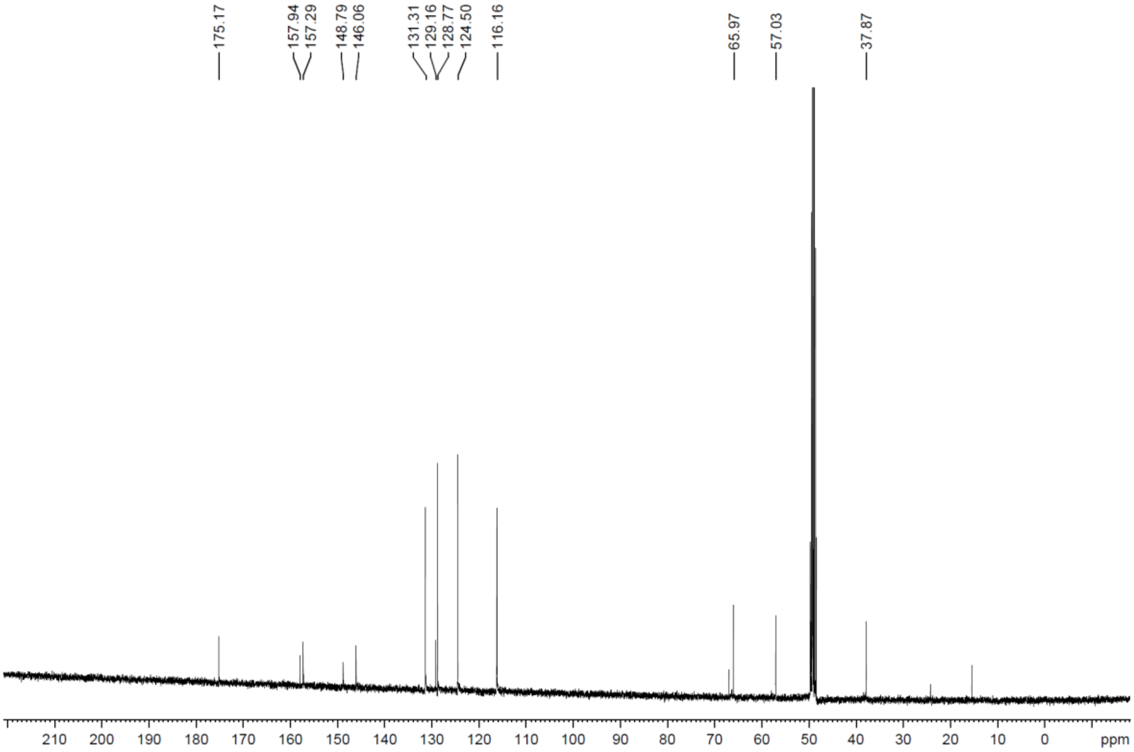

IR

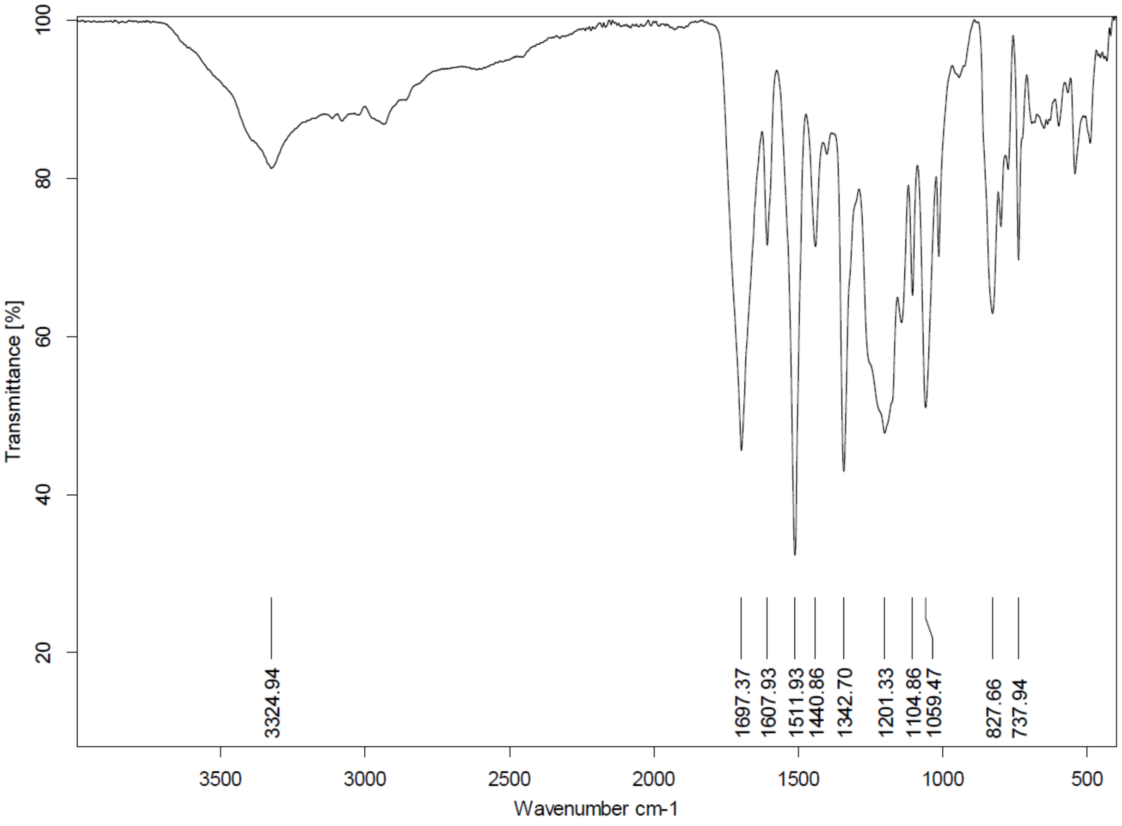

Alloc-L-Ile-OH

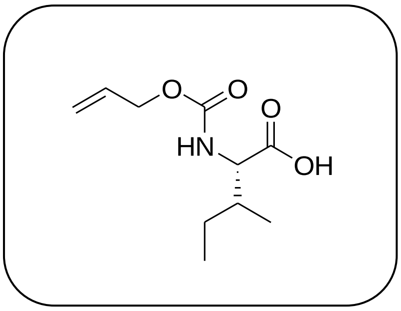

MS (ESI) *m/z* (+)

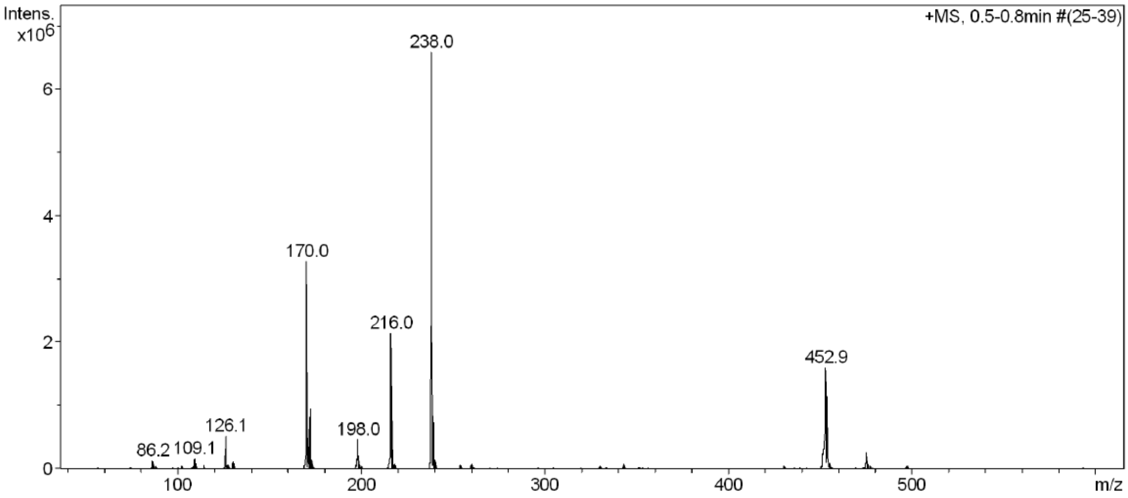

^{1}H-NMR (400 MHz), $CDCl_3$

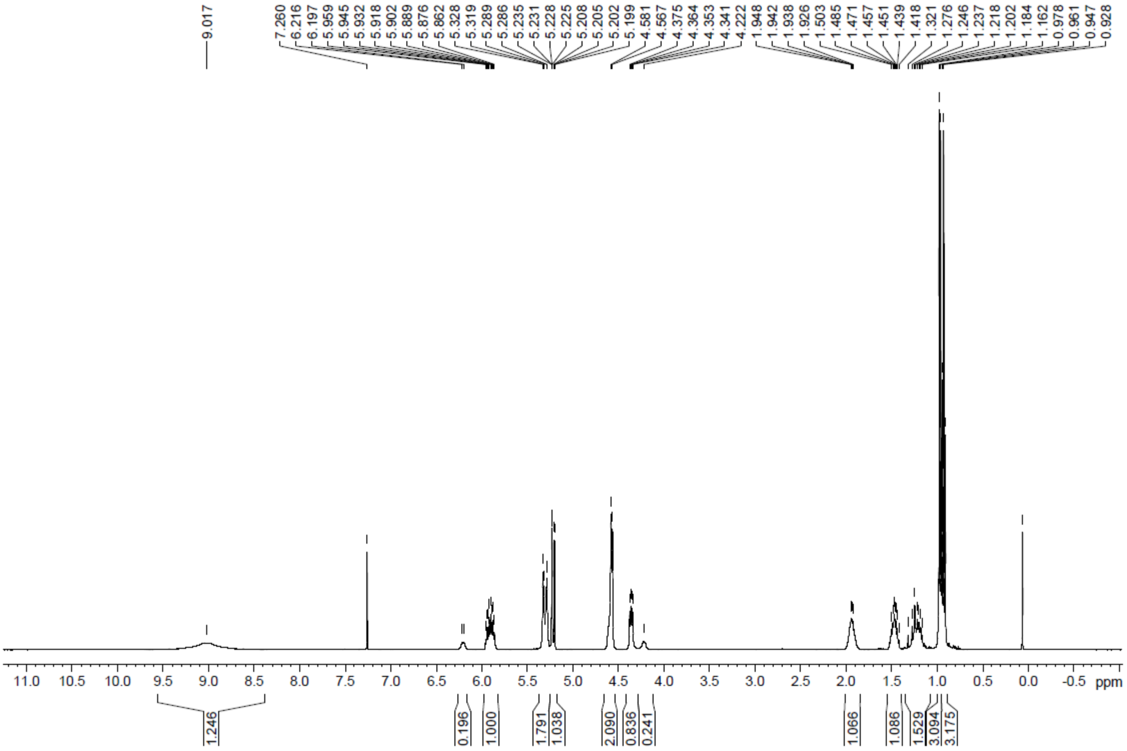

^{13}C-NMR (300 MHz), CDCl$_3$

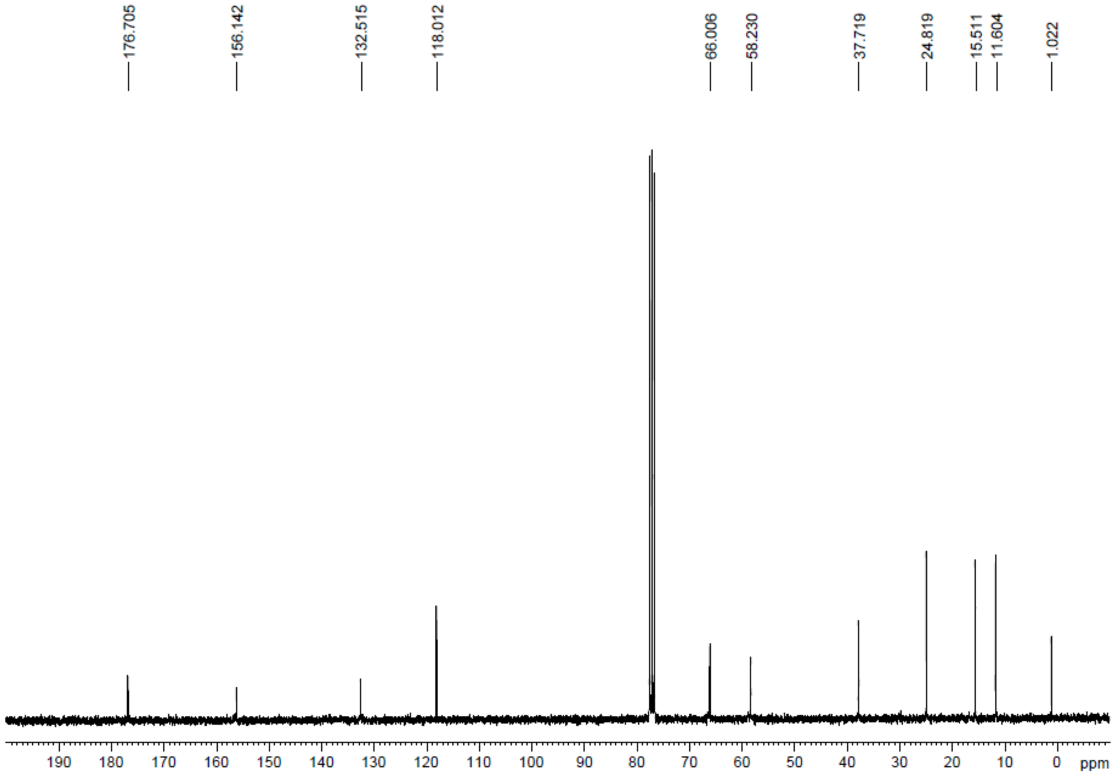

IR

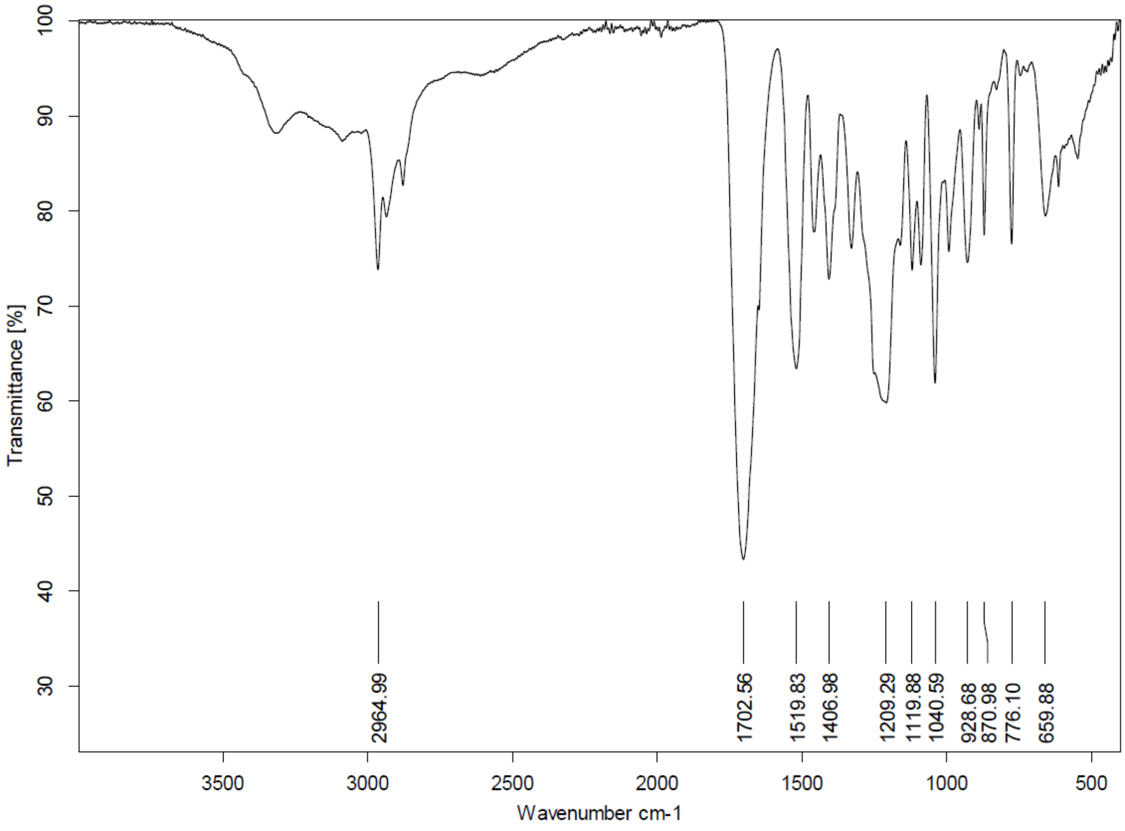

2. Synthesis of cyclic octapeptides

2.1. Linear peptides

2.1.1. Fmoc-Thr-Glu-Val-Pro-Gln-OAll

HPLC (λ = 220 nm) (*Method A*)

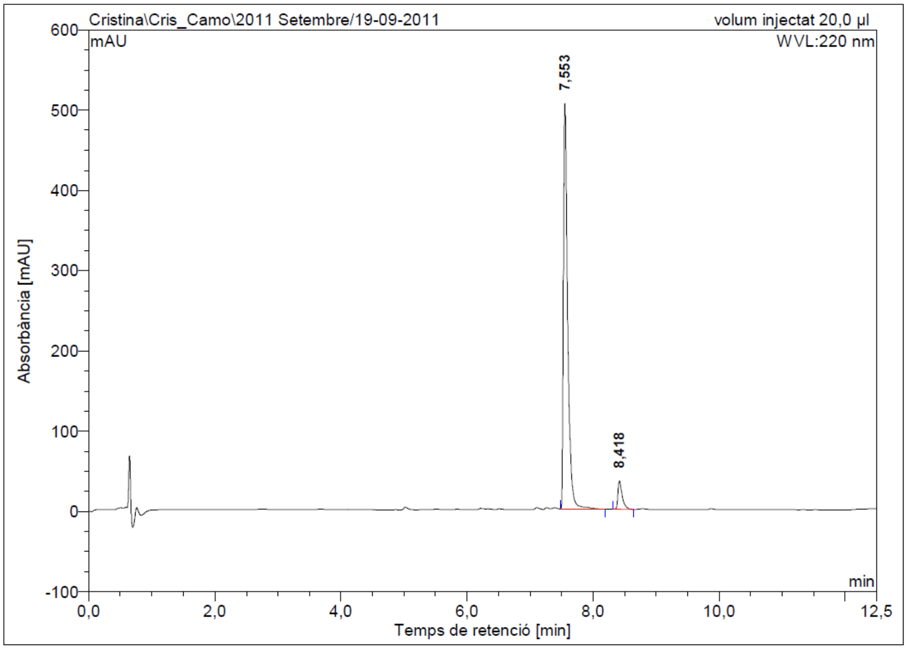

No.	Ret.Time (detected) min	Height mAU	Area mAU*min	Rel.Area %
1	7,55	505,273	39,414	93,46
2	8,42	35,434	2,758	6,54
Total:		540,706	42,172	100,00

2.1.2. H-Phe(4-NH-Ile-Tyr-Fmoc)-Thr-Glu-Val-Pro-Gln-OAll

HPLC (λ = 220 nm) (*Method A*)

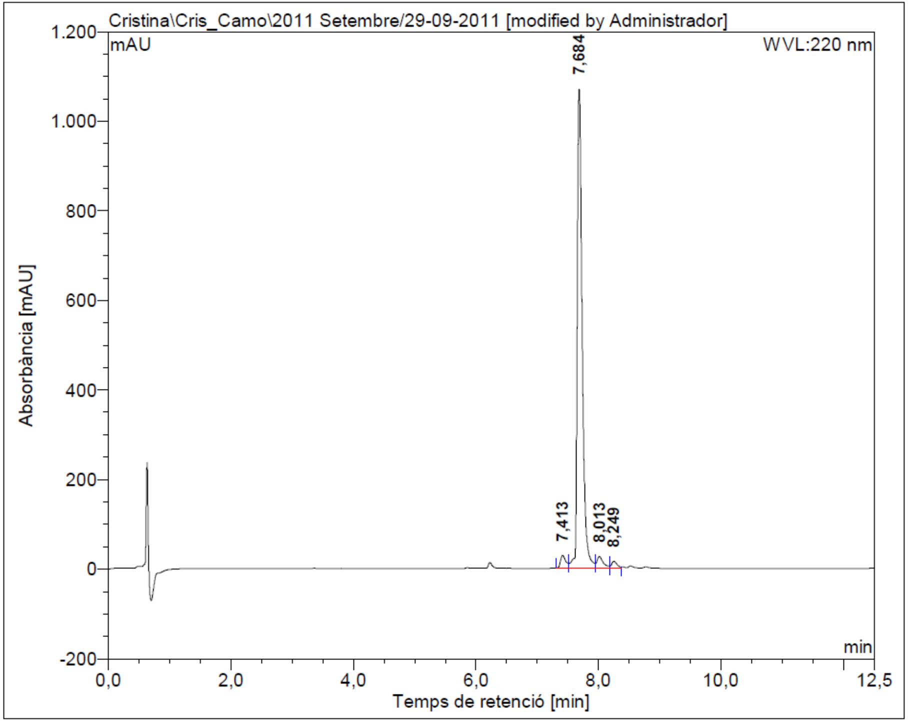

No.	Temps retenció min	alçada mAU	Area mAU*min	Area relativa %
1	7,41	28,118	2,834	2,64
2	7,68	1068,674	99,770	93,06
3	8,01	25,556	3,060	2,85
4	8,25	14,867	1,547	1,44
Total:		1137,215	107,211	100,00

MS (ESI) *m/z* (+)

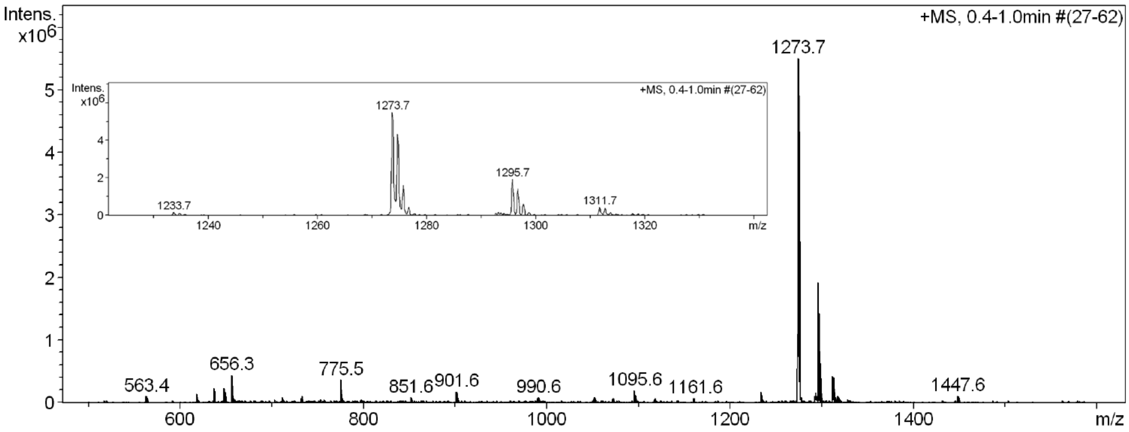

2.1.3. H-Phe(4-NH-Ile-D-Tyr-Fmoc)-D-Thr-Glu-D-Val-Pro-Gln-OAll

HPLC (*λ* = 220 nm) (*Method A*)

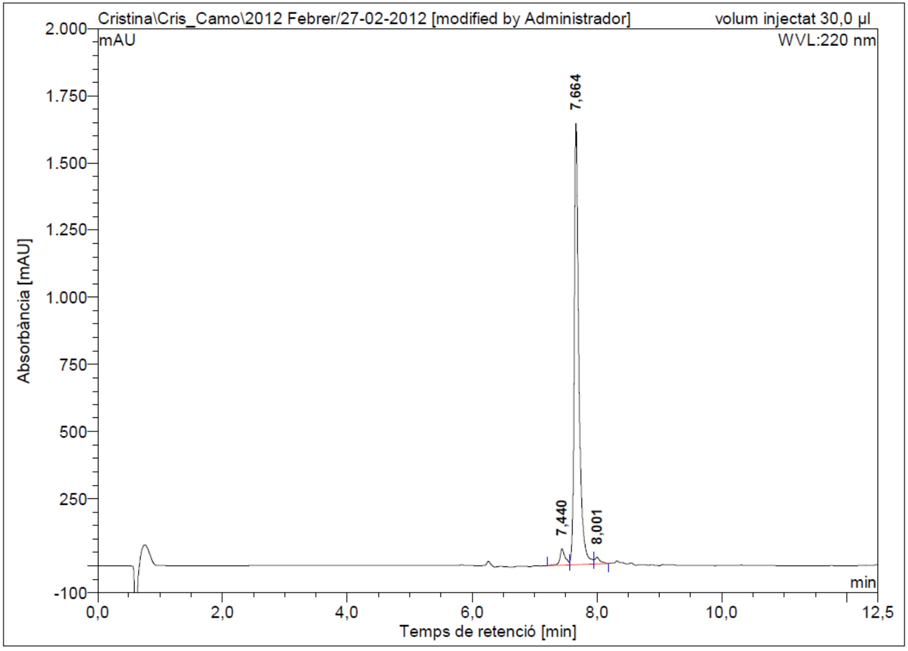

No.	Ret.Time (detected) min	Height mAU	Area mAU*min	Rel.Area %
1	7,44	60,573	5,864	3,92
2	7,66	1643,785	141,105	94,38
3	8,00	24,600	2,533	1,69
Total:		1728,959	149,502	100,00

2.1.4. H-Phe(4-NH-Ile-D-Tyr-Fmoc)-D-Thr-Glu-D-Ala-Pro-Gln-OAll

HPLC (λ = 220 nm) (*Method A*)

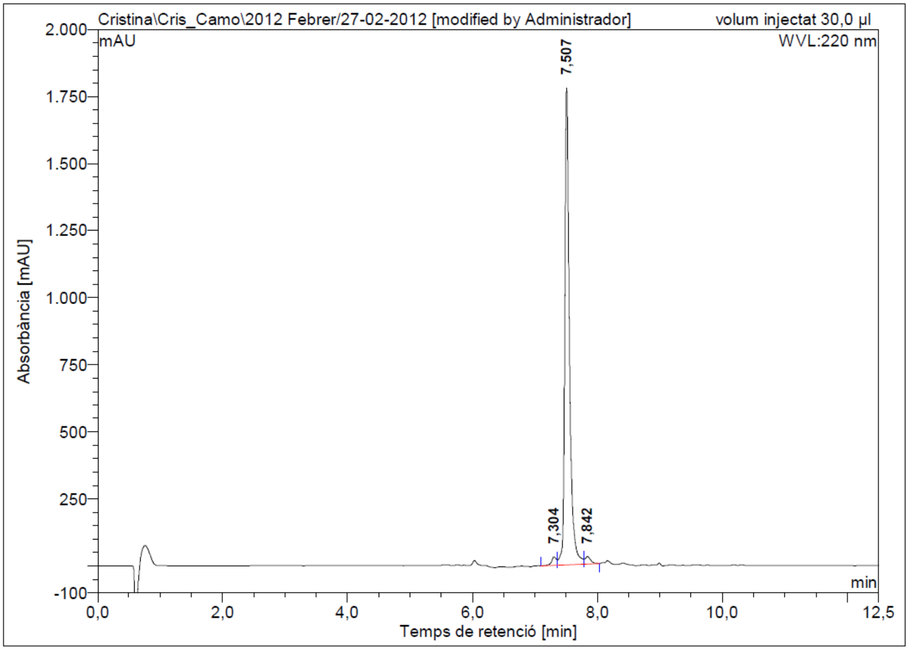

No.	Ret.Time (detected)	Height	Area	Rel.Area
	min	mAU	mAU*min	%
1	7,30	32,298	2,987	1,87
2	7,51	1778,110	154,244	96,31
3	7,84	28,078	2,923	1,83
Total:		1838,485	160,154	100,00

2.1.5. H-Phe(4-NH-Ile-D-Tyr-Fmoc)-D-Ser-Glu-D-Ala-Pro-Gln-OAll

HPLC (λ = 220 nm) (*Method A*)

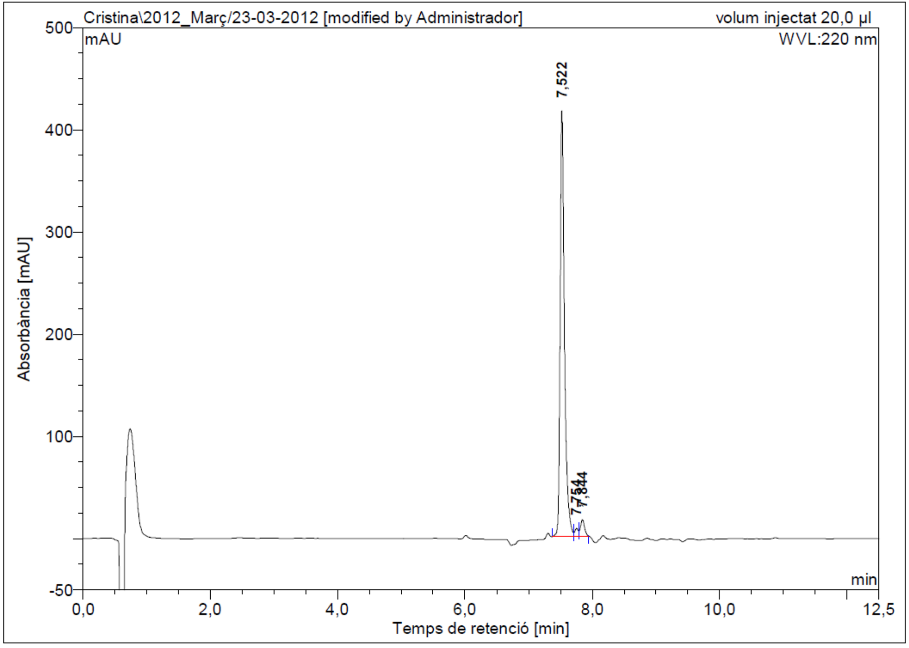

No.	Ret.Time (detected) min	Height mAU	Area mAU*min	Rel.Area %
1	7,52	416,578	32,825	94,84
2	7,75	8,038	0,530	1,53
3	7,84	16,729	1,256	3,63
Total:		441,345	34,611	100,00

2.1.6. H-Phe(4-NH-Ile-D-Tyr-Fmoc)-D-Ser-Glu-D-Val-Pro-Gln-OAll

HPLC (λ = 220 nm) (*Method A*)

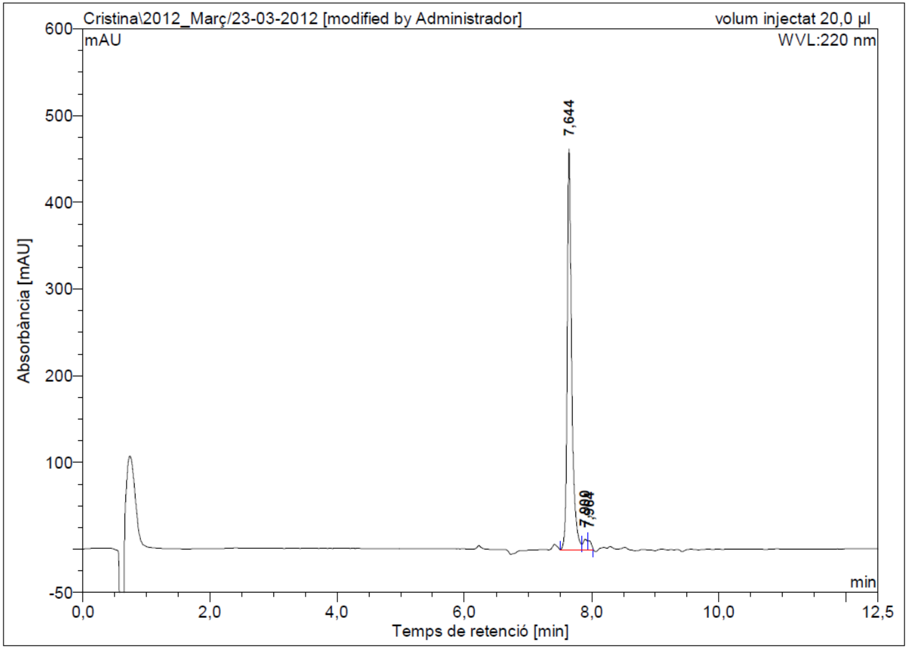

No.	Ret.Time (detected) min	Height mAU	Area mAU*min	Rel.Area %
1	7,64	462,039	37,713	96,09
2	7,90	11,878	0,878	2,24
3	7,96	10,169	0,657	1,67
Total:		484,086	39,249	100,00

2.1.7. H-Phe(4-NH-Ile-Tyr-H)-Thr-Glu-Val-Pro-Gln-OH

HPLC (λ = 220 nm) (*Method A*)

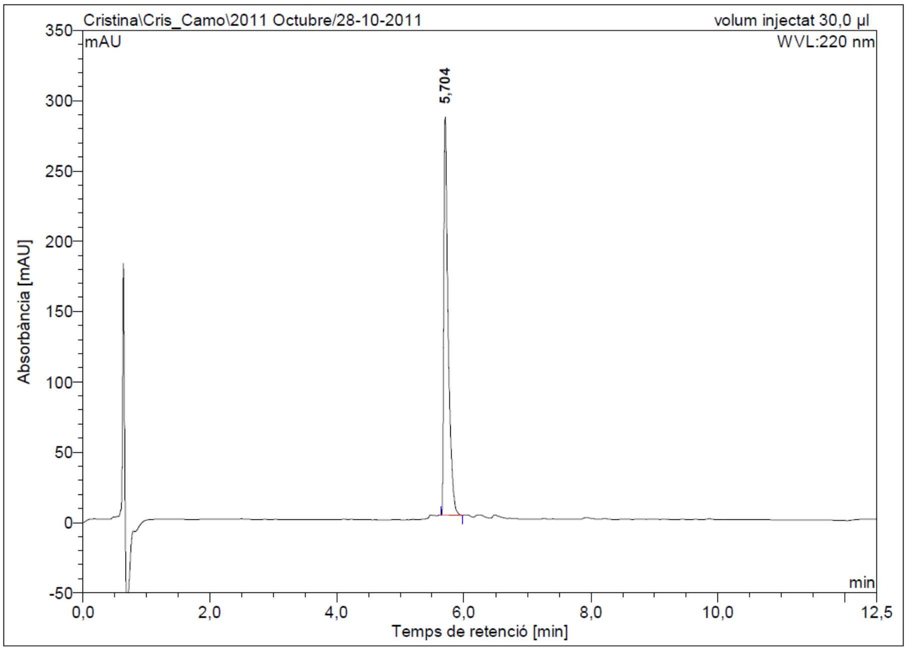

No.	Ret.Time (detected) min	Height mAU	Area mAU*min	Rel.Area %
1	5,70	283,187	22,562	100,00
Total:		283,187	22,562	100,00

MS (ESI) *m/z* (+)

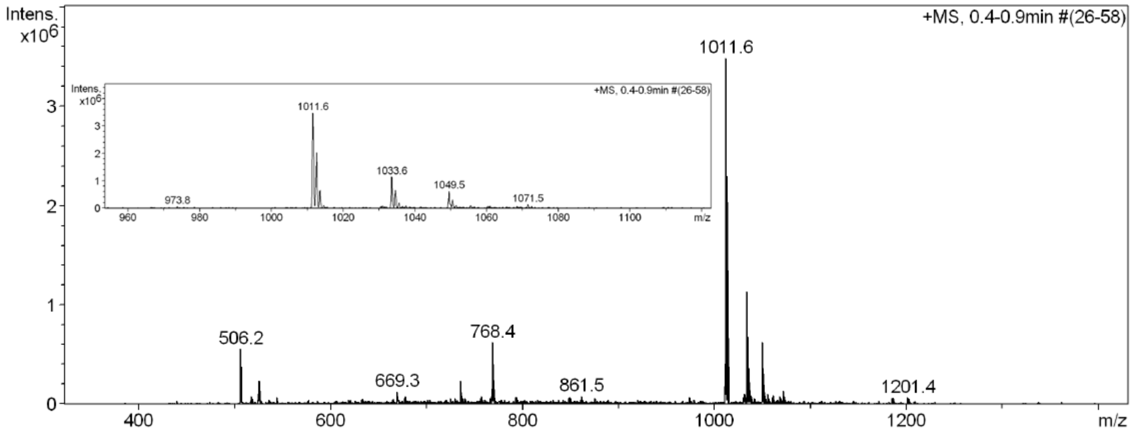

2.1.8. H-Phe(4-NH-Ile-D-Tyr-H)-D-Thr-Glu-D-Val-Pro-Gln-OH

HPLC (λ = 220 nm) (*Method A*)

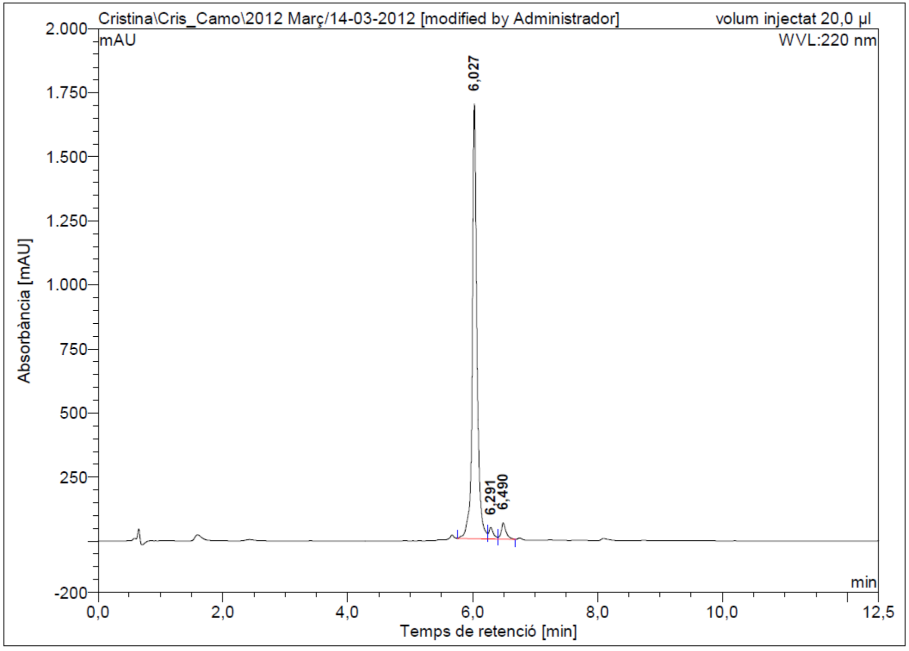

No.	Ret.Time (detected) min	Height mAU	Area mAU*min	Rel.Area %
1	6,03	1696,703	147,111	93,99
2	6,29	44,495	3,754	2,40
3	6,49	63,343	5,652	3,61
Total:		1804,541	156,516	100,00

MS (ESI) *m/z* (+)

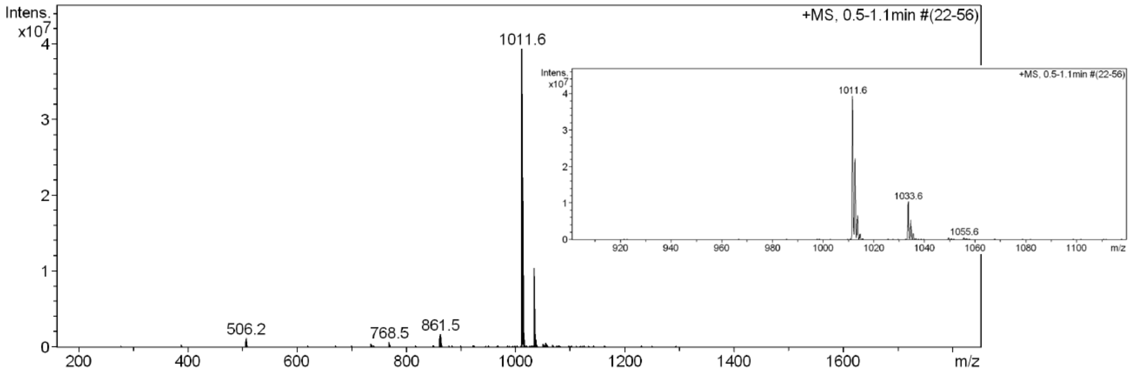

2.1.9. H-Phe(4-NH-Ile-D-Tyr-H)-D-Thr-Glu-D-Ala-Pro-Gln-OH

HPLC (λ = 220 nm) (*Method A*)

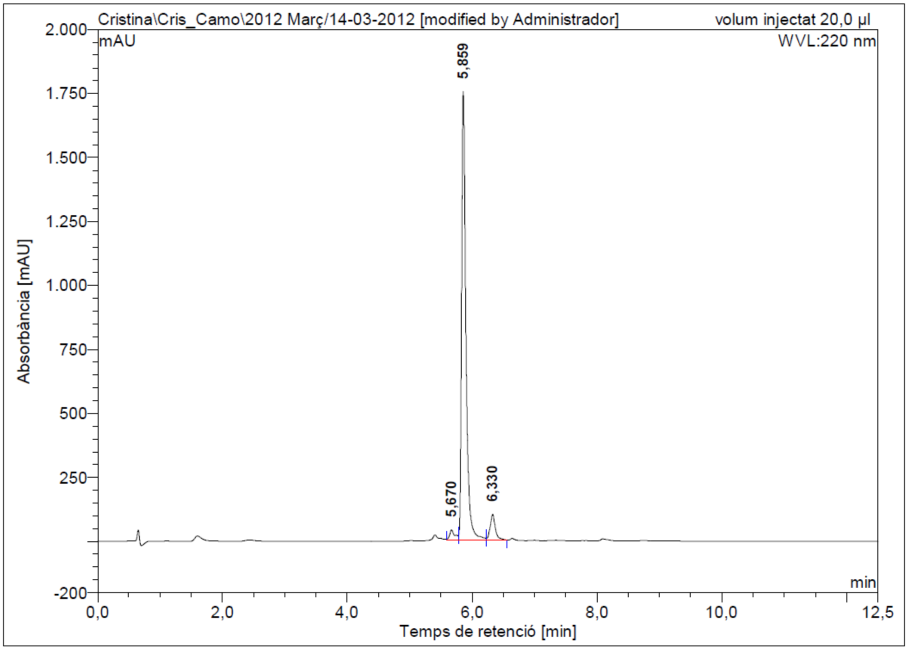

No.	Ret.Time (detected) min	Height mAU	Area mAU*min	Rel.Area %
1	5,67	39,807	3,937	2,56
2	5,86	1752,514	140,057	91,10
3	6,33	101,333	9,750	6,34
Total:		1893,654	153,744	100,00

MS (ESI) *m/z* (+)

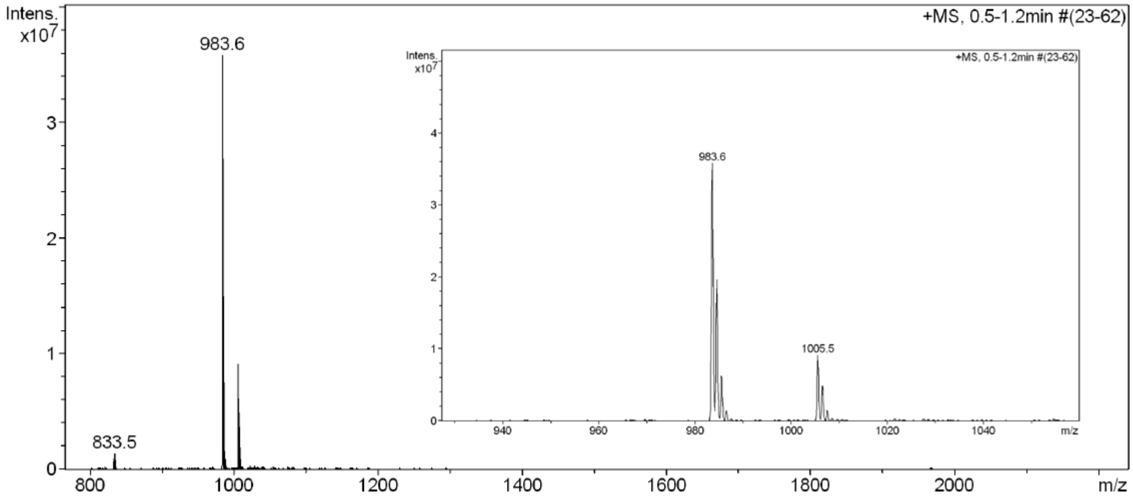

2.1.10. H-Phe(4-NH-Ile-D-Tyr-H)-D-Ser-Glu-D-Ala-Pro-Gln-OH

HPLC (*λ* = 220 nm) (*Method A*)

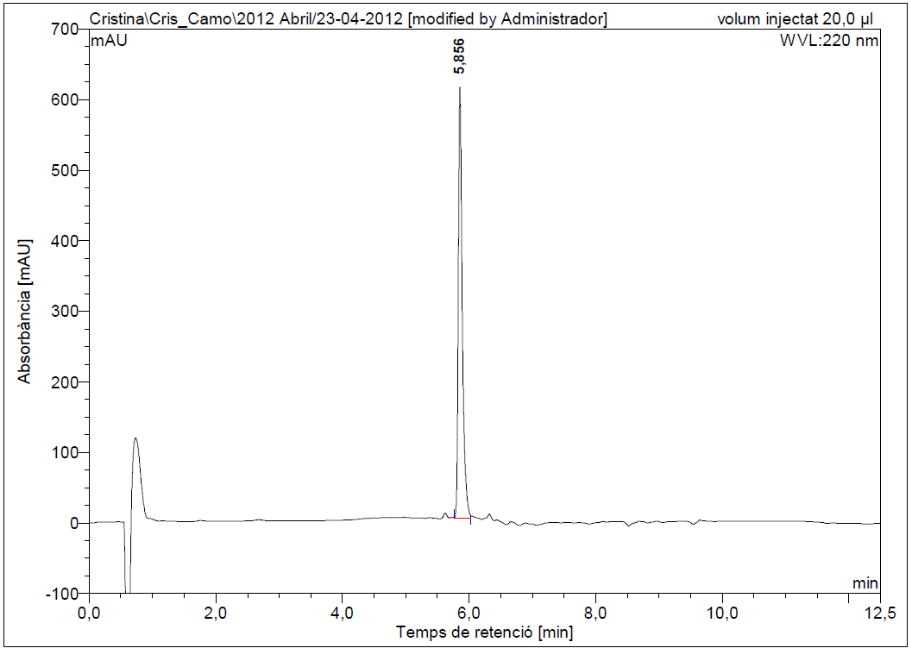

No.	Ret.Time (detected) min	Height mAU	Area mAU*min	Rel.Area %
1	5,86	610,972	44,579	100,00
Total:		610,972	44,579	100,00

MS (ESI) *m/z* (+)

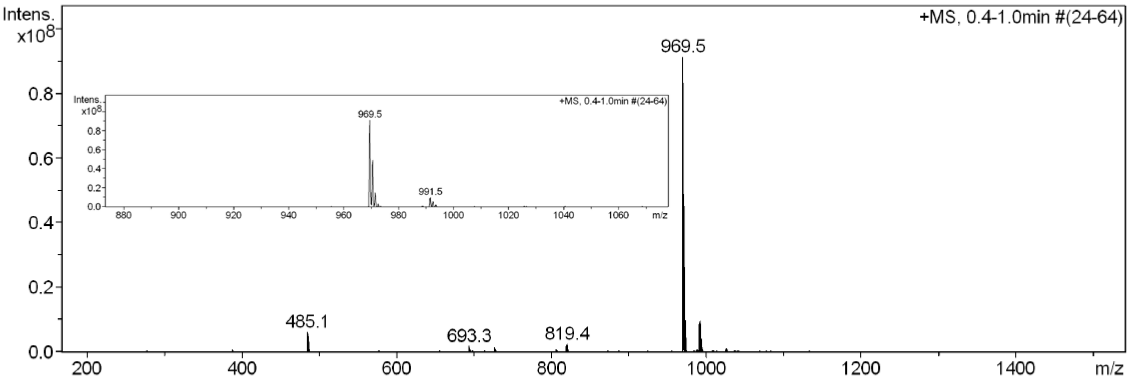

2.1.11. H-Phe(4-NH-Ile-D-Tyr-H)-D-Ser-Glu-D-Val-Pro-Gln-OH

HPLC (λ = 220 nm) (*Method A*)

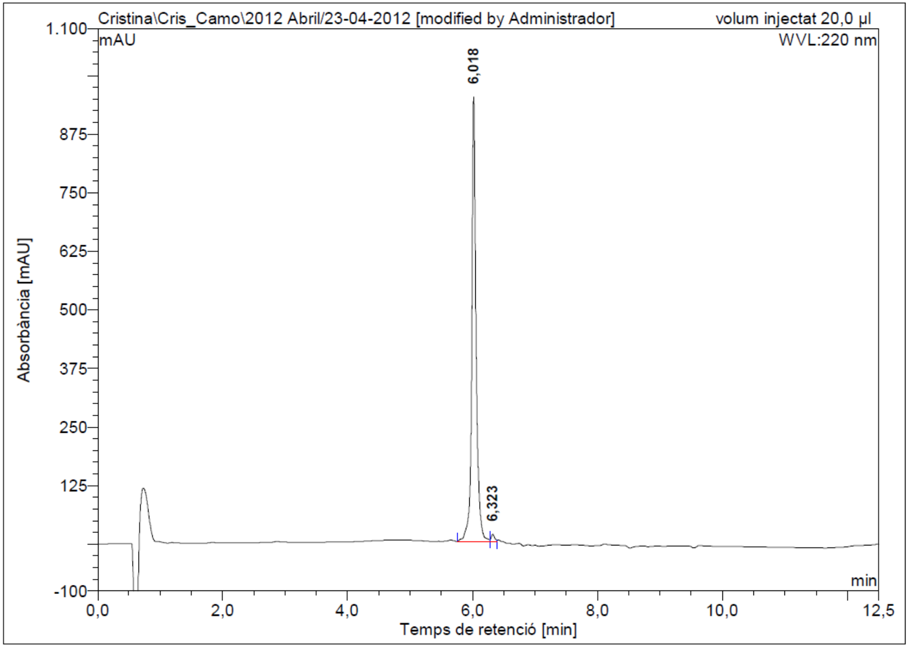

No.	Ret.Time (detected) min	Height mAU	Area mAU*min	Rel.Area %
1	6,02	948,898	76,119	98,73
2	6,32	15,080	0,981	1,27
Total:		963,978	77,100	100,00

MS (ESI) *m/z* (+)

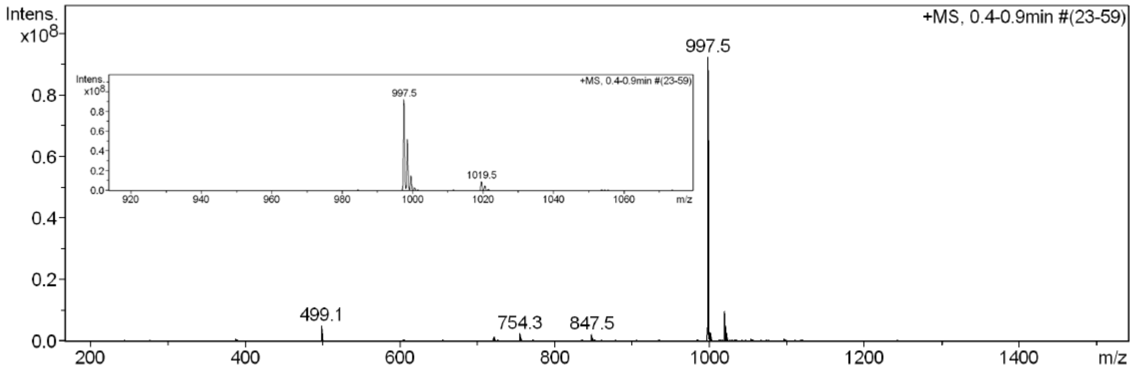

2.2. Cyclic octapeptides

2.2.1. H-Phe(4-NH-&)-Thr-Glu-Val-Pro-Gln-Tyr-Ile-& (1)

HPLC (λ = 220 nm) (*Method A*)

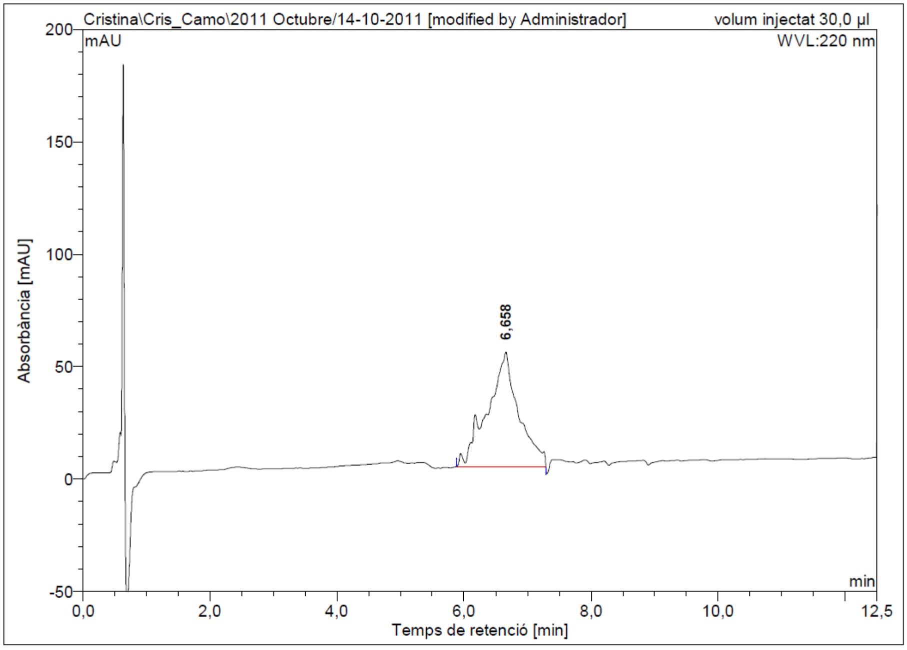

No.	Ret.Time (detected) min	Height mAU	Area mAU*min	Rel.Area %
1	6,66	50,874	28,613	100,00
Total:		50,874	28,613	100,00

MS (ESI) *m/z* (+)

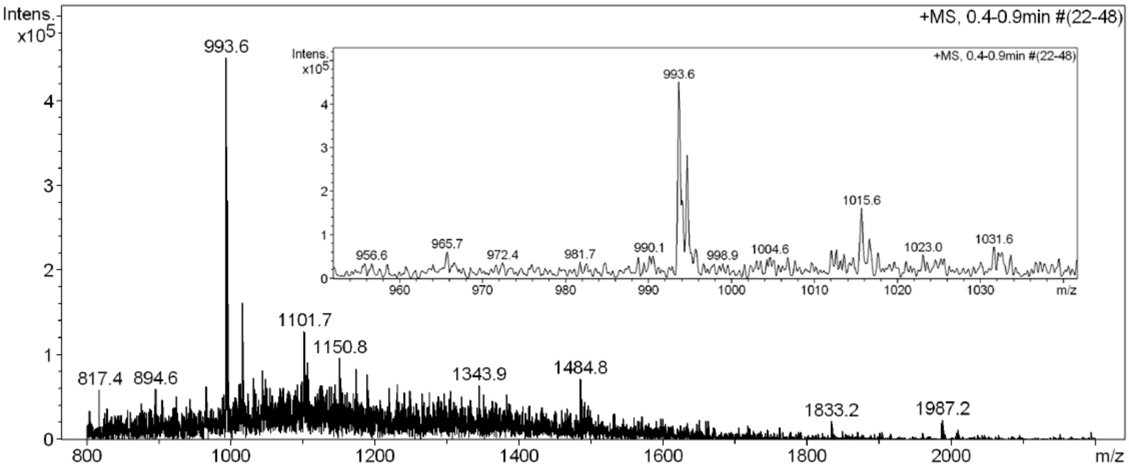

2.2.2. H-Phe(4-NH-&)-D-Thr-Glu-D-Val-Pro-Gln-D-Tyr-Ile-& (BPC862)

HPLC (λ = 220 nm) (*Method A*)

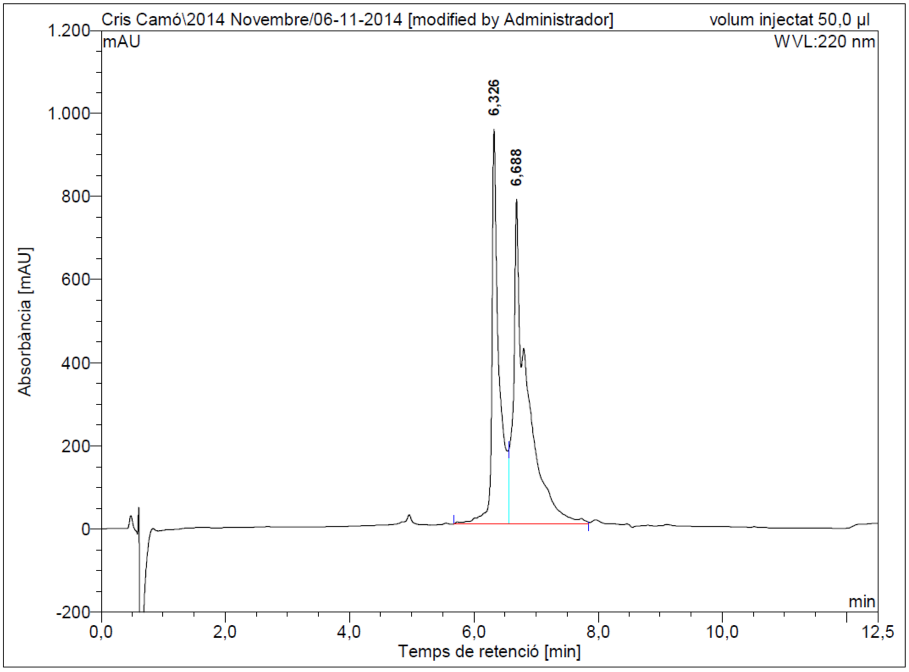

No.	Temps retenció min	alçada mAU	Area mAU*min	Area relativa %
1	6,33	949,433	126,534	39,28
2	6,69	781,668	195,595	60,72
Total:		1731,101	322,129	100,00

Purification of BPC862

HPLC (λ = 220 nm) (*Method A*)

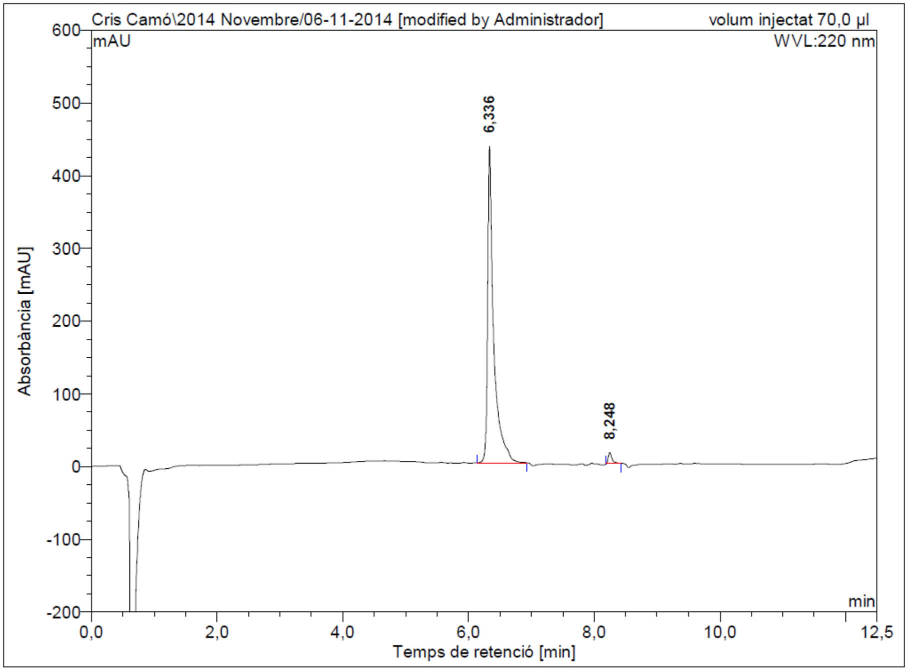

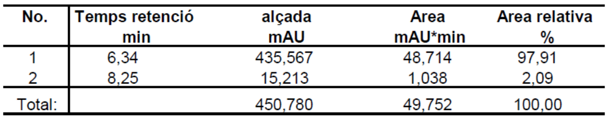

No.	Temps retenció min	alçada mAU	Area mAU*min	Area relativa %
1	6,34	435,567	48,714	97,91
2	8,25	15,213	1,038	2,09
Total:		450,780	49,752	100,00

MS (ESI) *m/z* (+)

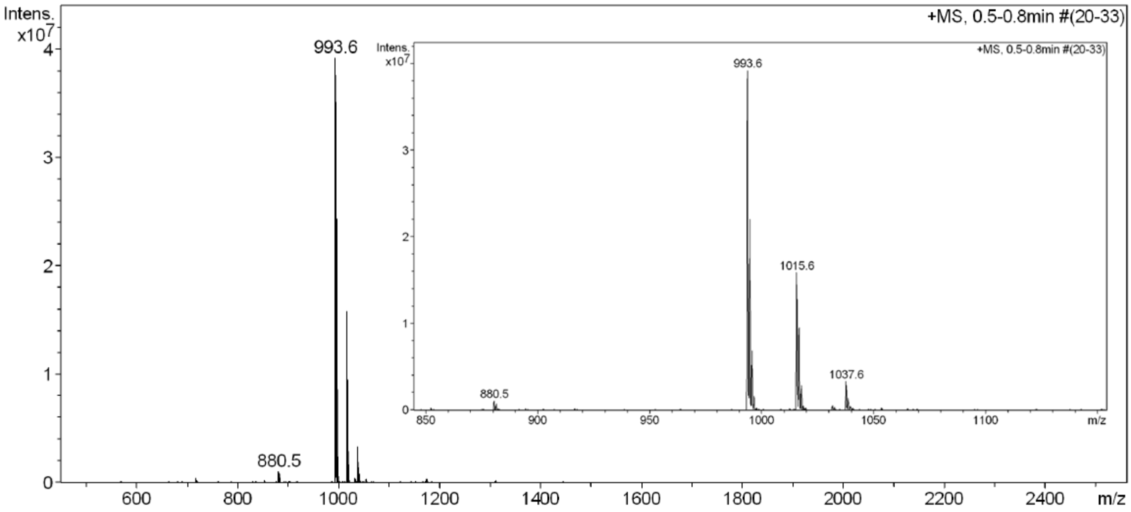

2.2.3. H-Phe(4-NH-&)-D-Thr-Glu-D-Ala-Pro-Gln-D-Tyr-Ile-& (BPC864)

HPLC (λ = 220 nm) (*Method A*)

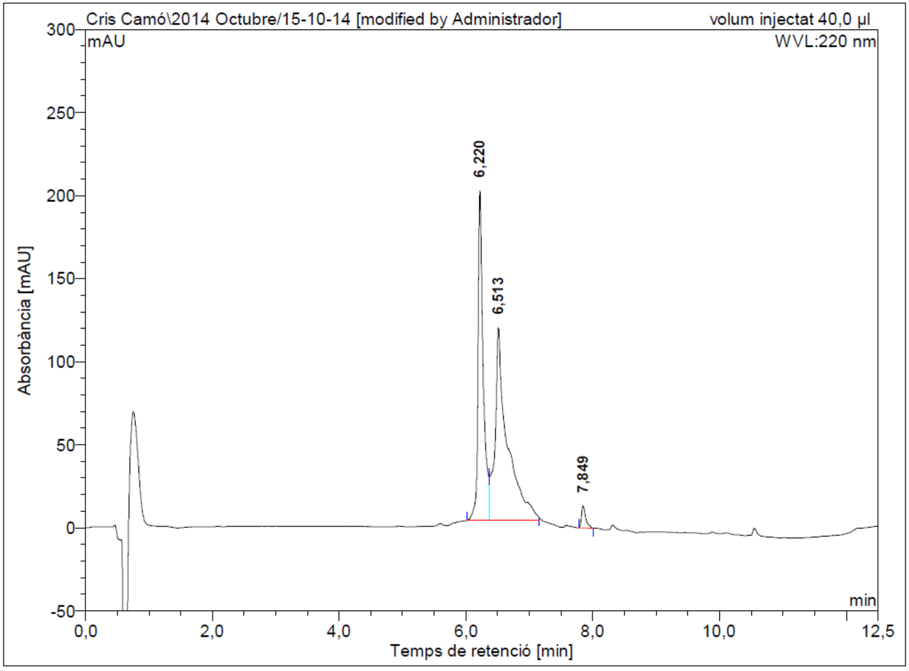

No.	Temps retenció min	alçada mAU	Area mAU*min	Area relativa %
1	6,22	198,688	18,870	40,96
2	6,51	116,123	26,173	56,81
3	7,85	13,321	1,026	2,23
Total:		328,131	46,069	100,00

Purification of BPC864

HPLC (λ = 220 nm) (*Method A*)

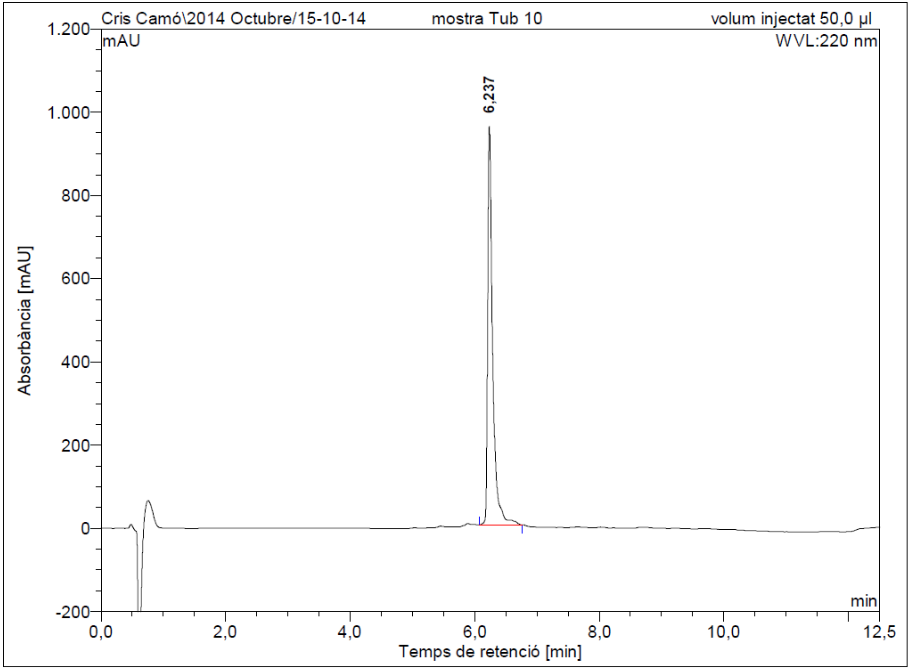

No.	Temps retenció min	alçada mAU	Area mAU*min	Area relativa %
1	6,24	958,853	89,274	100,00
Total:		958,853	89,274	100,00

MS (ESI) *m/z* (+)

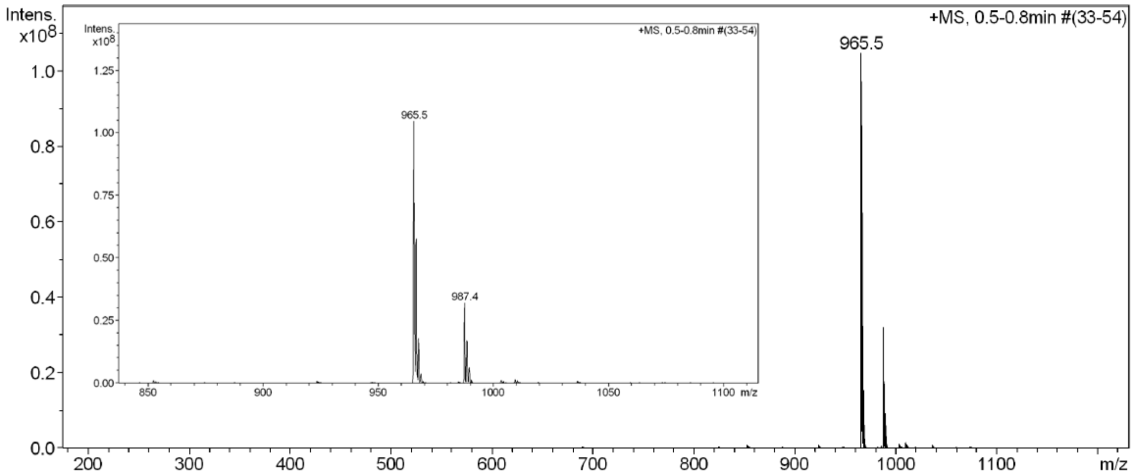

2.2.4. H-Phe(4-NH-&)-D-Ser-Glu-D-Ala-Pro-Gln-D-Tyr-Ile-& (BPC866)

HPLC (λ = 220 nm) (*Method A*)

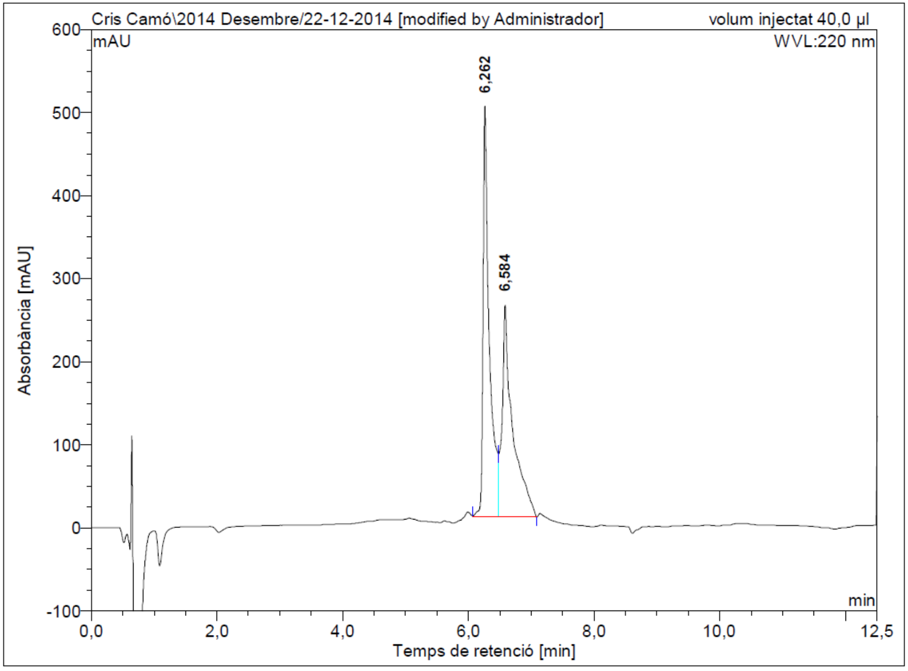

No.	Temps retenció min	alçada mAU	Area mAU*min	Area relativa %
1	6,26	494,820	57,207	53,18
2	6,58	255,478	50,365	46,82
Total:		750,299	107,572	100,00

Purification of BPC866

HPLC (λ = 220 nm) (*Method A*)

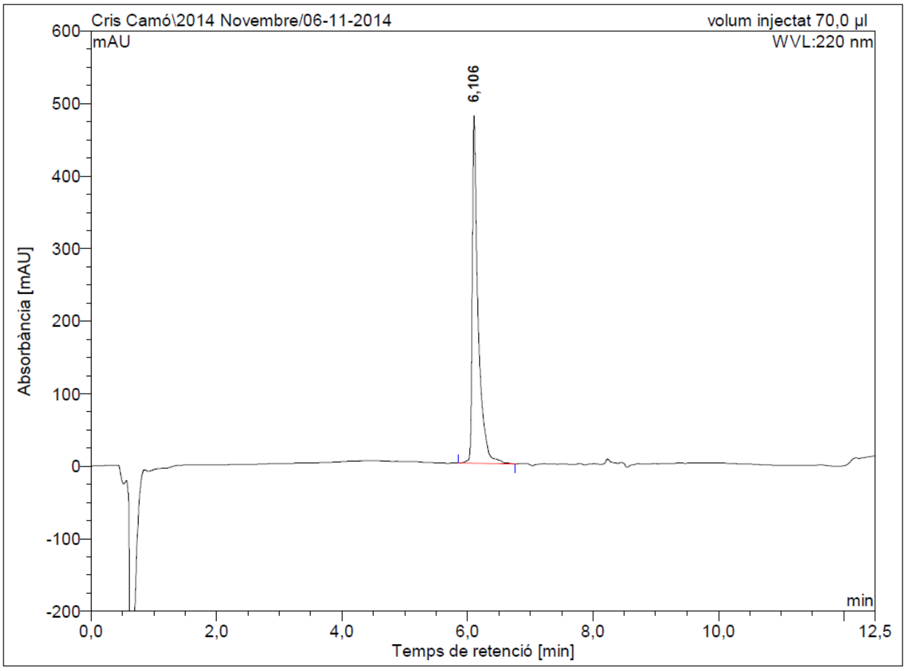

No.	Temps retenció min	alçada mAU	Area mAU*min	Area relativa %
1	6,11	479,275	51,685	100,00
Total:		479,275	51,685	100,00

MS (ESI) *m/z* (+)

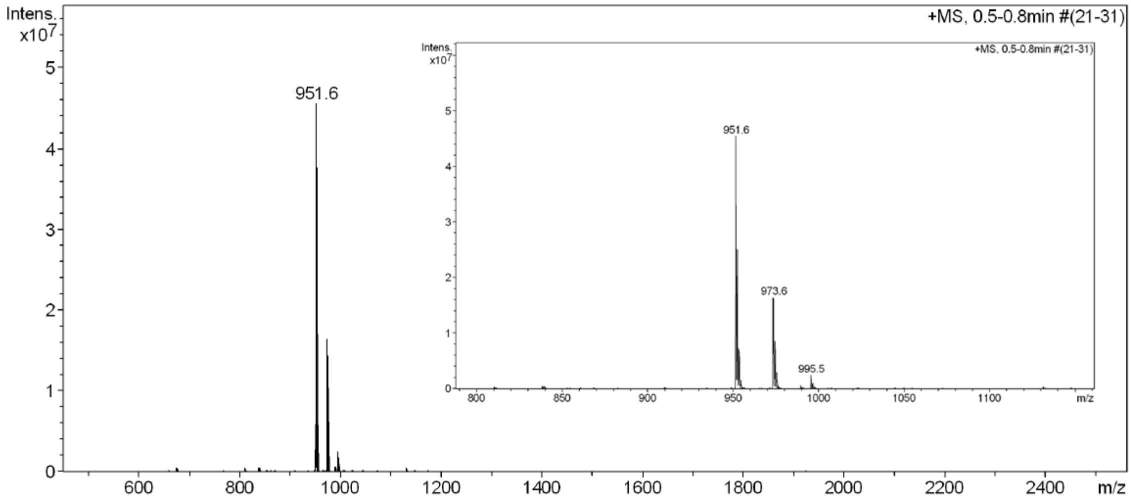

2.2.5. H-Phe(4-NH-&)-D-Ser-Glu-D-Val-Pro-Gln-D-Tyr-Ile-& (BPC868)

HPLC (λ = 220 nm) (*Method A*)

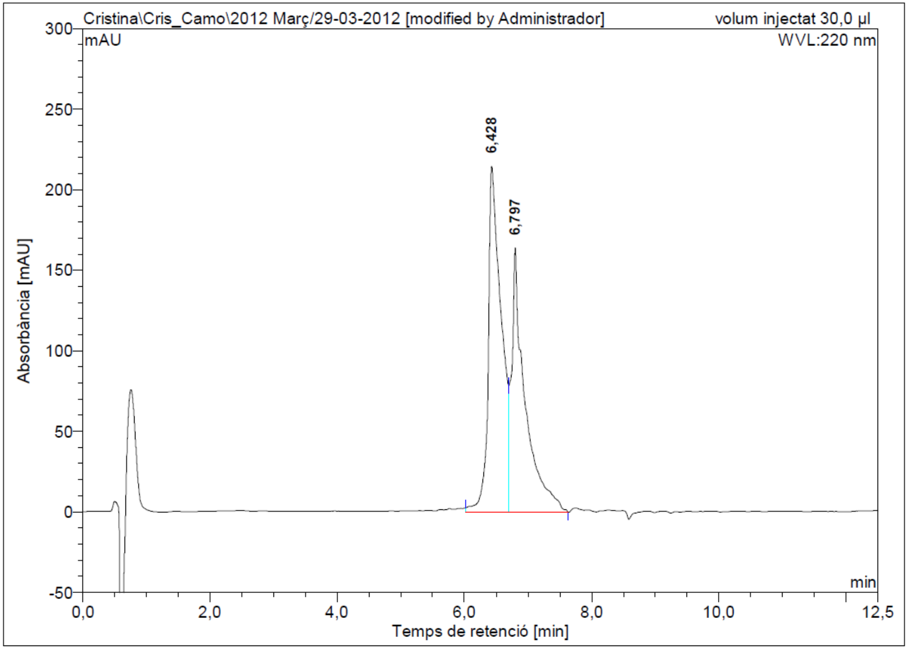

No.	Ret.Time (detected) min	Height mAU	Area mAU*min	Rel.Area %
1	6,43	214,938	51,287	56,07
2	6,80	164,084	40,180	43,93
Total:		379,022	91,467	100,00

Purification of BPC868

HPLC (λ = 220 nm) (*Method A*)

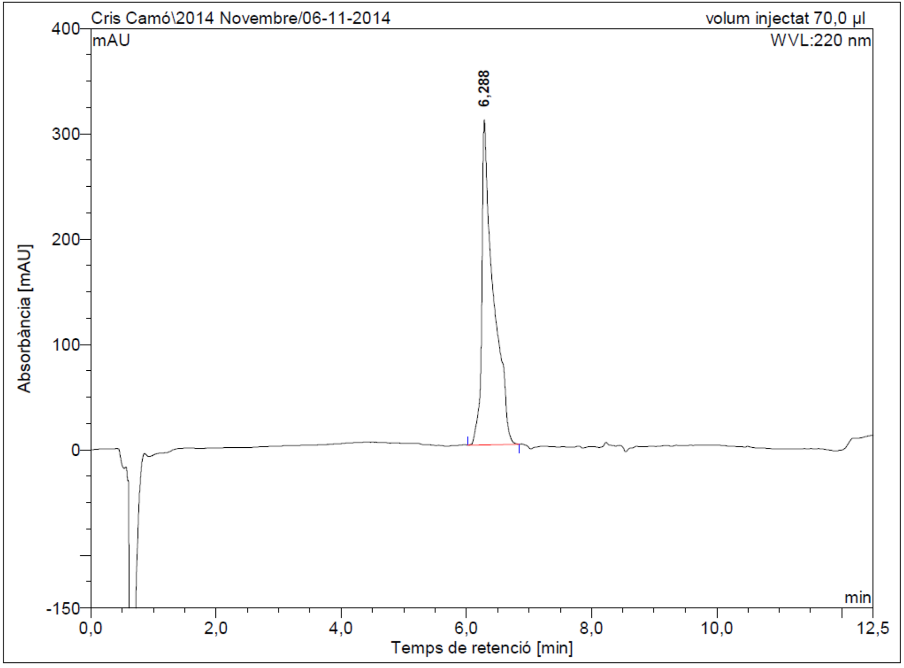

No.	Temps retenció min	alçada mAU	Area mAU*min	Area relativa %
1	6,29	308,375	66,111	100,00
Total:		308,375	66,111	100,00

MS (ESI) *m/z* (+)

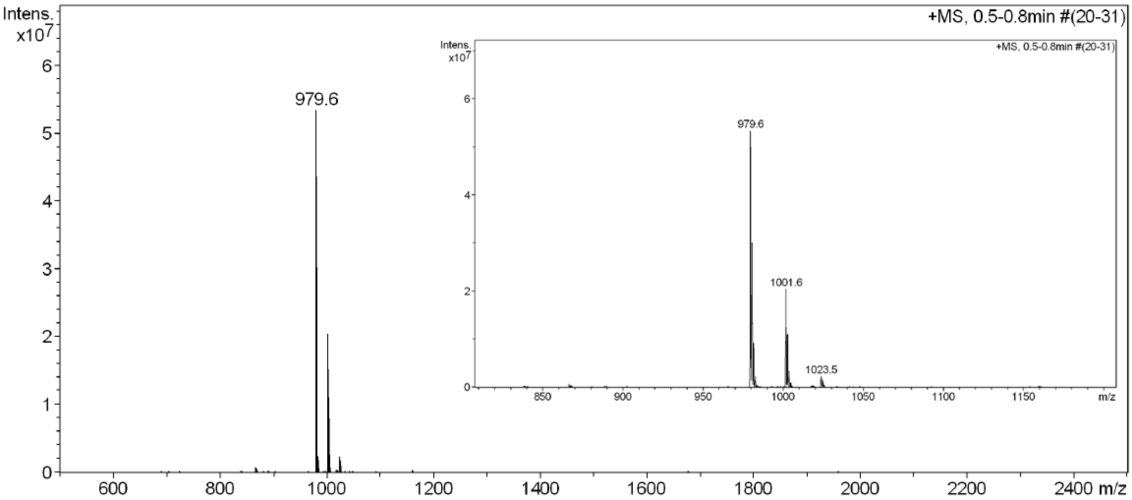

3. Synthesis of cyclic octadepsipeptides

3.1. Linear peptides

3.1.1. H-Tyr-Thr-Glu-Val-Pro-Gln-OAll

HPLC (λ = 220 nm) (*Method A*)

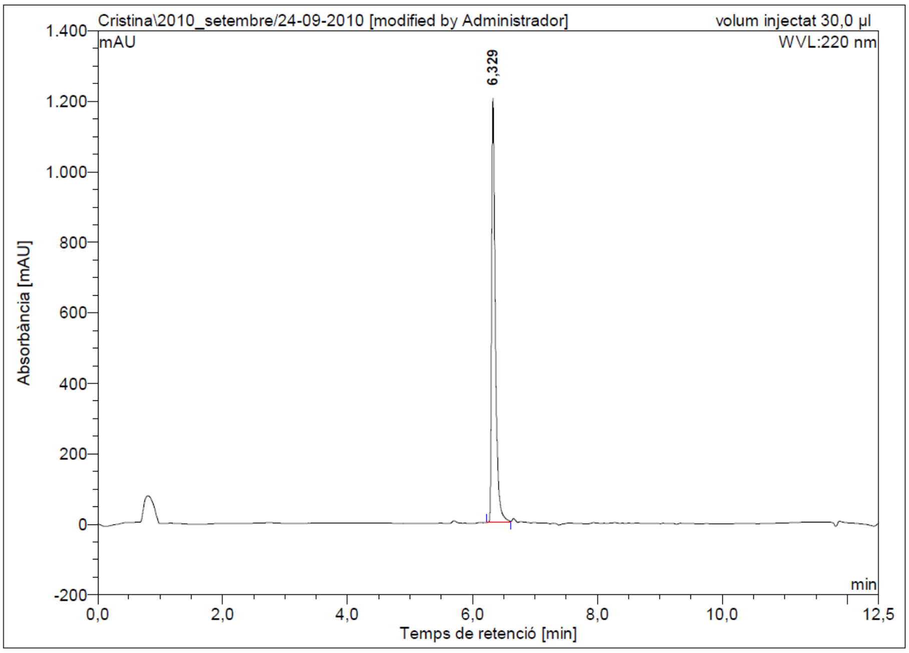

No.	Ret.Time (detected) min	Height mAU	Area mAU*min	Rel.Area %
1	6,33	1203,853	83,807	100,00
Total:		1203,853	83,807	100,00

3.1.2. *p*NZ-Tyr-Thr-Glu-Val-Pro-Gln-OAll

HPLC (λ = 220 nm) (*Method B*)

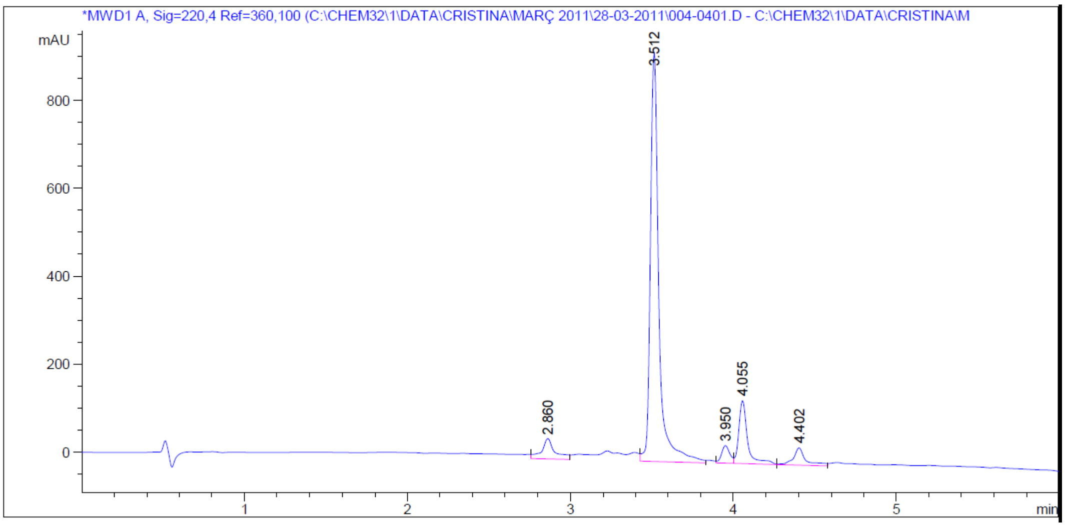

```
Peak RetTime Type  Width     Area      Height     Area
  #   [min]        [min]   [mAU*s]     [mAU]       %
----|-------|----|-------|----------|----------|--------|
   1   2.860 VV    0.0792  270.49011   46.94996   5.9663
   2   3.512 VV    0.0539 3361.18140  934.85895  74.1387
   3   3.950 VV    0.0555  145.12778   40.77485   3.2011
   4   4.055 VV    0.0580  543.85529  144.16953  11.9960
   5   4.402 VV    0.0767  212.98369   39.64968   4.6979
```

MS (ESI) *m/z* (+)

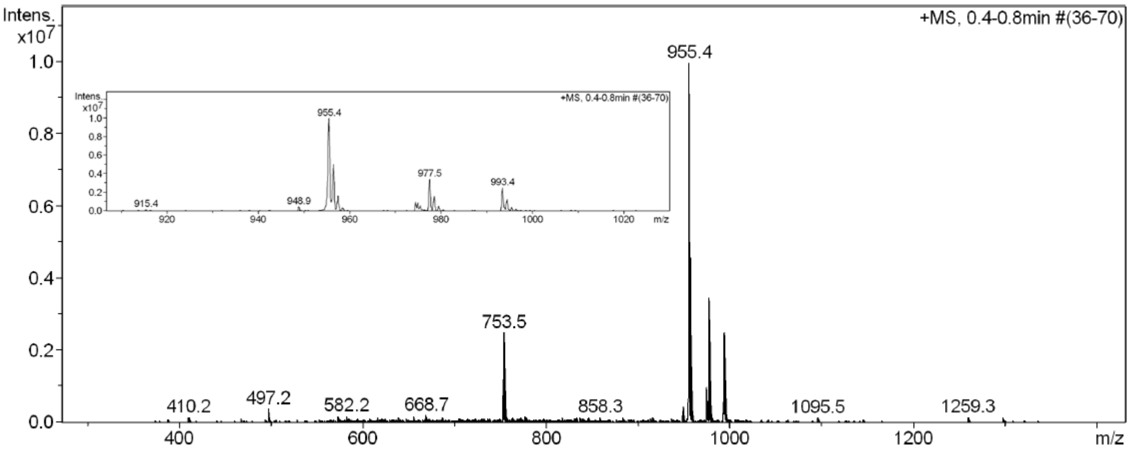

3.1.3. *p*NZ-Tyr-Thr-Glu-Val-Pro-Gln-Tyr-OAll

HPLC (λ = 220 nm) (*Method B*)

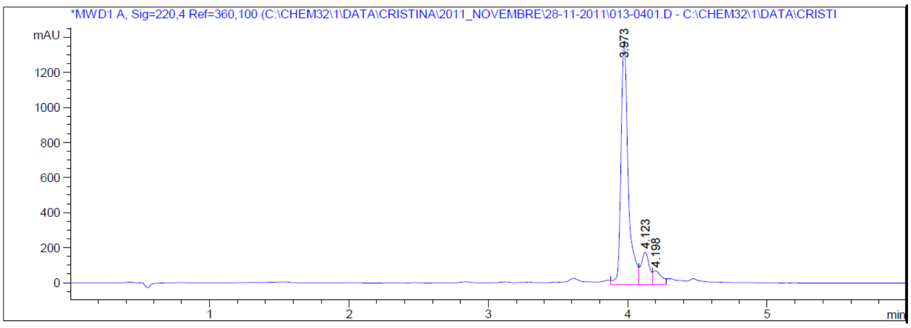

```
Peak RetTime Type  Width     Area      Height     Area
  #   [min]        [min]   [mAU*s]     [mAU]       %
----|-------|----|-------|----------|----------|--------|
   1   3.973 VV    0.0539 5012.18506 1395.41443  82.0916
   2   4.123 VV    0.0589  746.24805  185.55293  12.2224
   3   4.198 VV    0.0636  347.16812   78.45352   5.6861

Totals :                  6105.60123 1659.42088
```

MS (ESI) *m/z* (+)

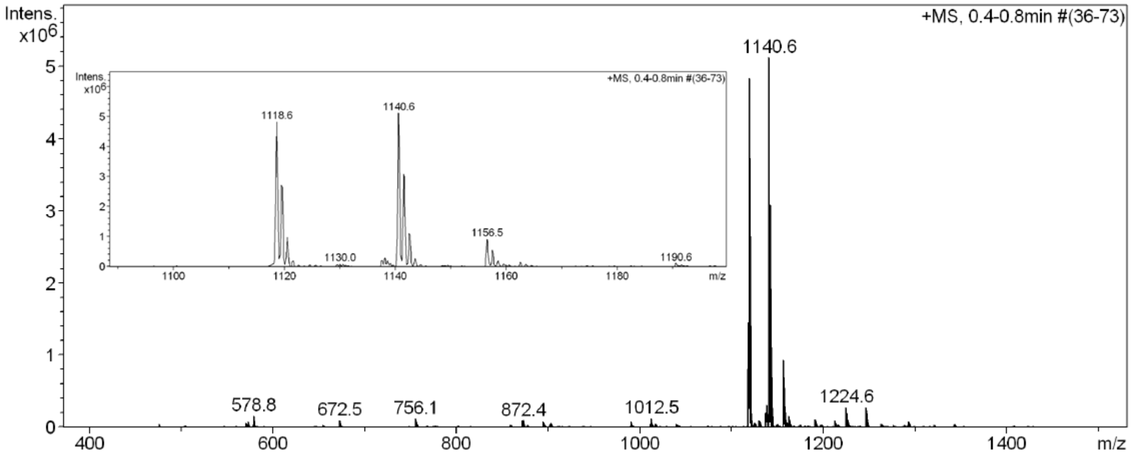

3.1.4. *p*NZ-Tyr-D-Thr-Glu-D-Val-Pro-Gln-D-Tyr-OAll

HPLC (λ = 220 nm) (*Method A*)

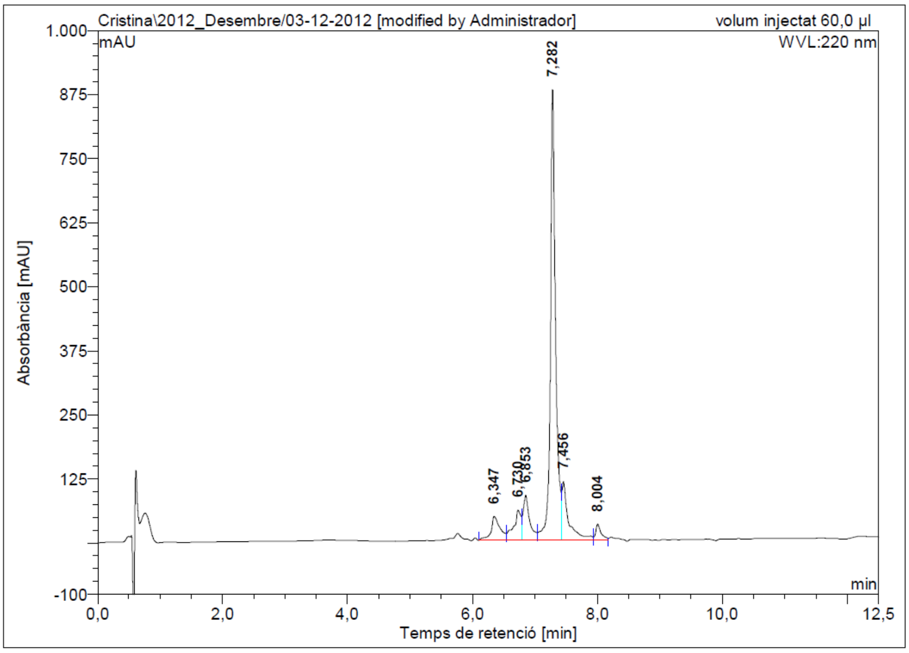

No.	Ret.Time (detected) min	Height mAU	Area mAU*min	Rel.Area %
1	6,35	46,923	7,996	6,15
2	6,73	59,082	8,098	6,23
3	6,85	88,136	10,904	8,39
4	7,28	879,556	84,335	64,90
5	7,46	114,568	15,302	11,78
6	8,00	31,665	3,304	2,54
Total:		1219,930	129,939	100,00

MS (ESI) *m/z* (+)

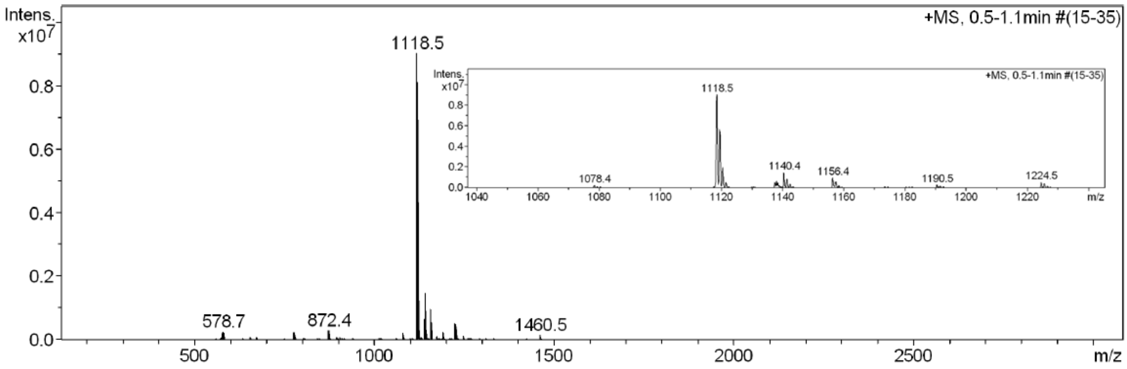

3.1.5. H-Tyr-D-Thr-Glu-D-Val-Pro-Gln-D-Tyr-OAll

HPLC (λ = 220 nm) (*Method A*)

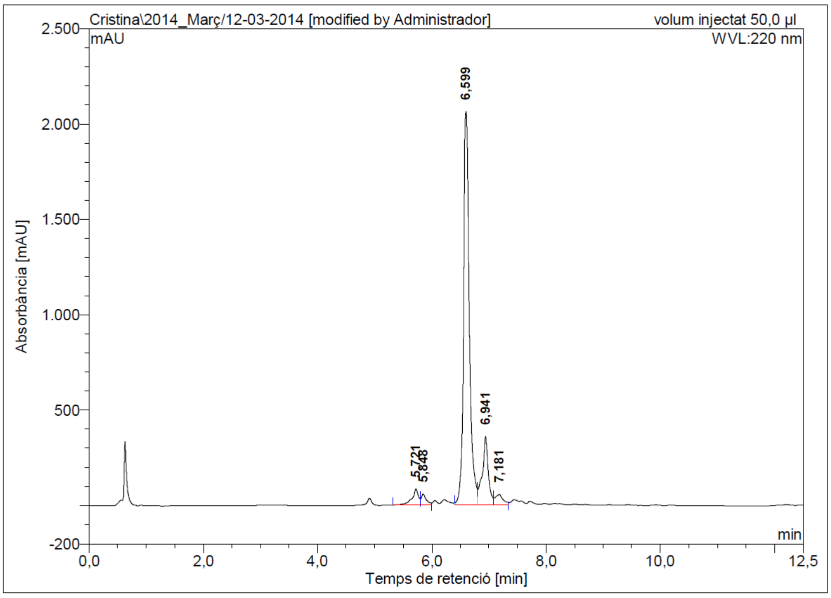

No.	Ret.Time (detected) min	Height mAU	Area mAU*min	Rel.Area %
1	5,72	85,425	11,264	3,58
2	5,85	57,902	6,182	1,97
3	6,60	2062,499	243,174	77,37
4	6,94	359,082	44,106	14,03
5	7,18	55,986	9,590	3,05
Total:		2620,895	314,316	100,00

MS (ESI) *m/z* (+)

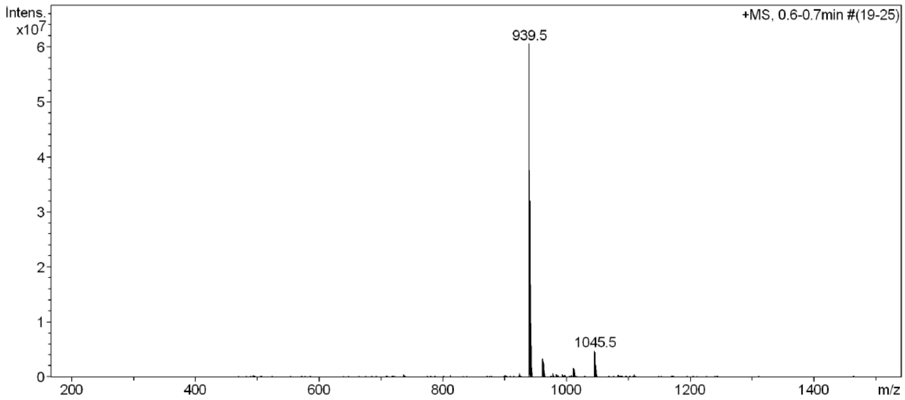

MS (ESI) *m/z* (-)

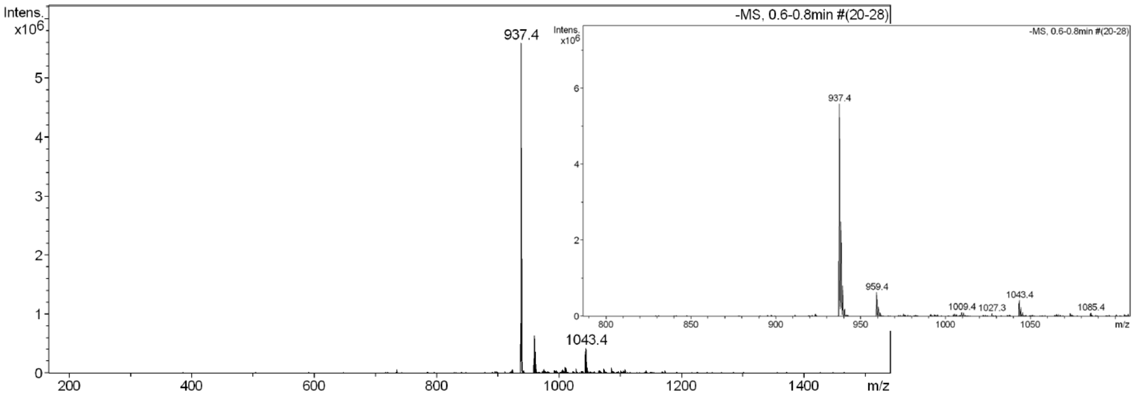

3.1.6. H-Tyr-D-Ser-Glu-D-Val-Pro-Gln-D-Tyr-OAll

HPLC (λ = 220 nm) (*Method A*)

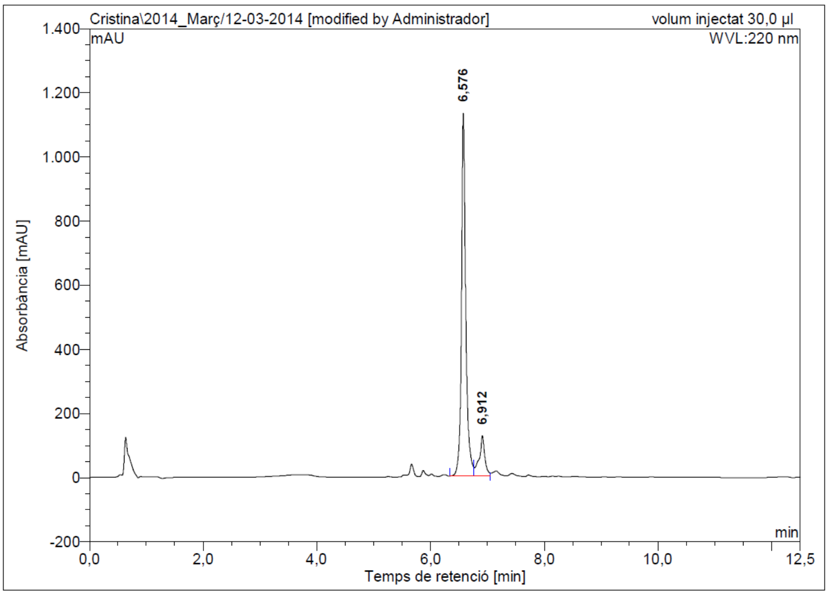

No.	Ret.Time (detected) min	Height mAU	Area mAU*min	Rel.Area %
1	6,58	1130,144	99,362	87,17
2	6,91	125,281	14,620	12,83
Total:		1255,425	113,982	100,00

MS (ESI) *m/z* (+)

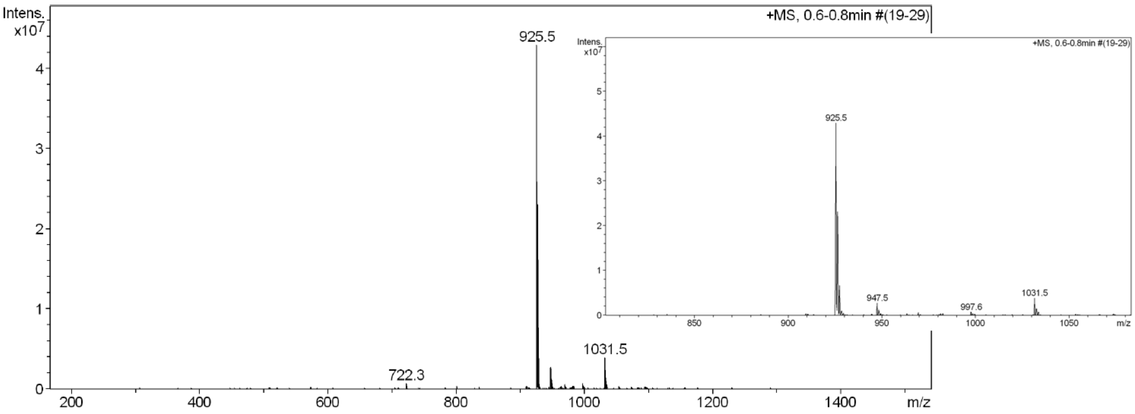

MS (ESI) *m/z* (-)

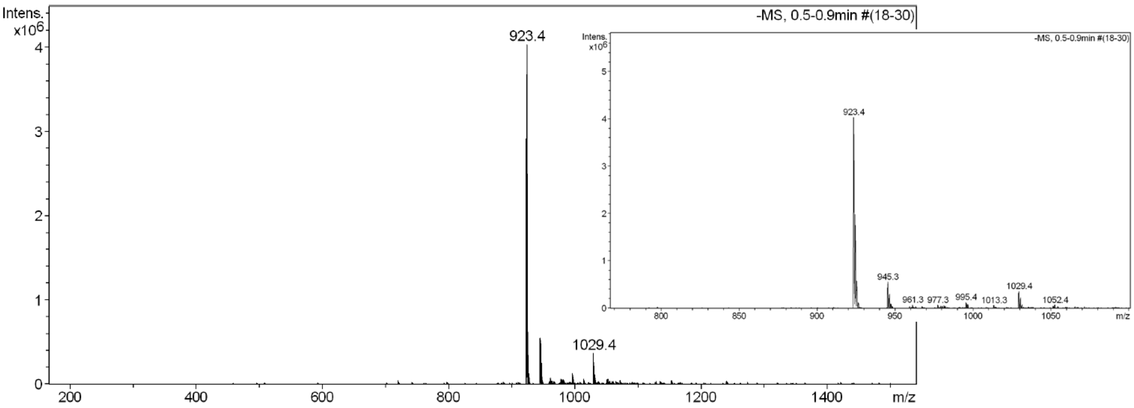

3.1.7. H-Tyr-D-Thr-Glu-D-Ala-Pro-Gln-D-Tyr-OAll

HPLC (λ = 220 nm) (*Method A*)

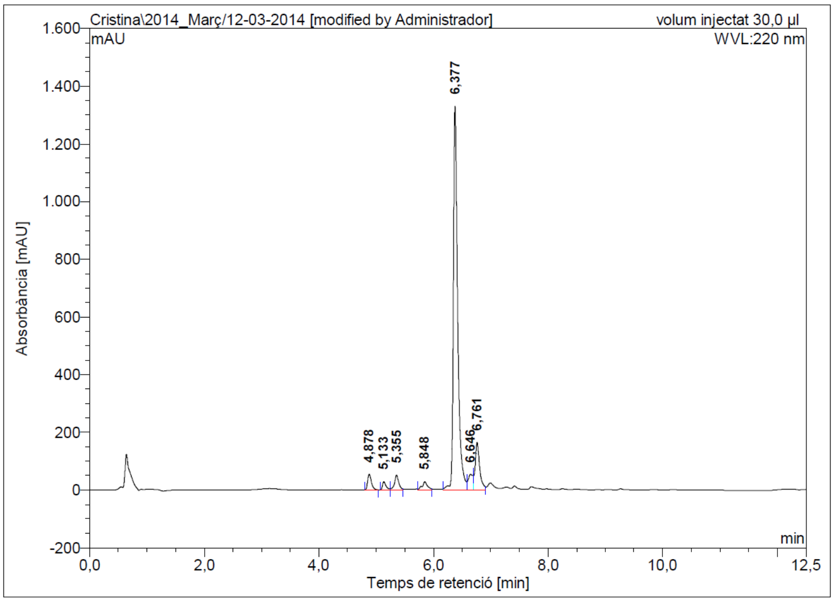

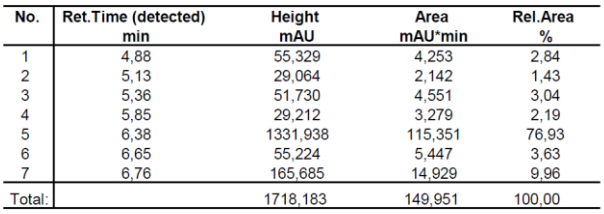

No.	Ret.Time (detected) min	Height mAU	Area mAU*min	Rel.Area %
1	4,88	55,329	4,253	2,84
2	5,13	29,064	2,142	1,43
3	5,36	51,730	4,551	3,04
4	5,85	29,212	3,279	2,19
5	6,38	1331,938	115,351	76,93
6	6,65	55,224	5,447	3,63
7	6,76	165,685	14,929	9,96
Total:		1718,183	149,951	100,00

MS (ESI) *m/z* (+)

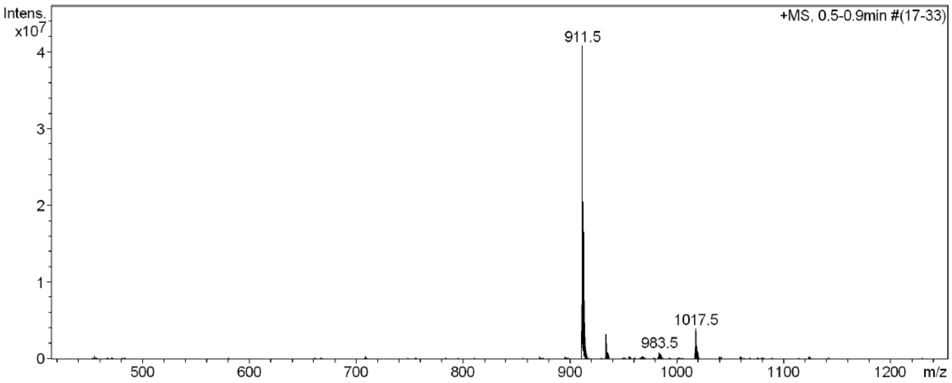

MS (ESI) *m/z* (-)

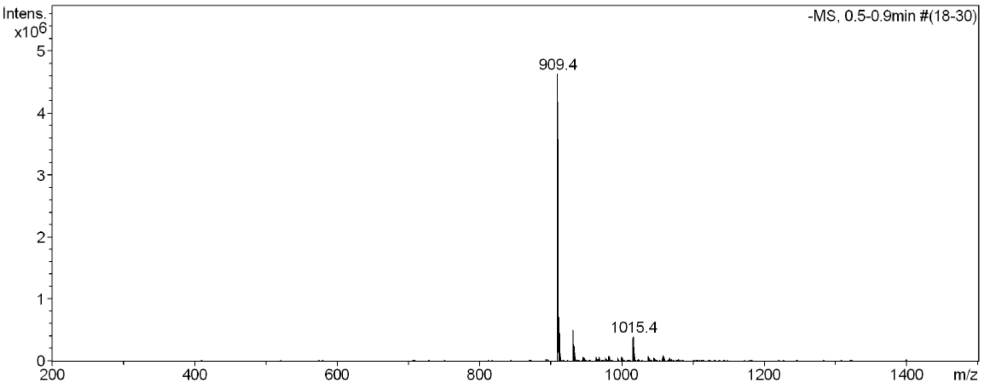

3.1.8. H-Tyr-D-Ser-Glu-D-Ala-Pro-Gln-D-Tyr-OAll

HPLC (*λ* = 220 nm) (*Method A*)

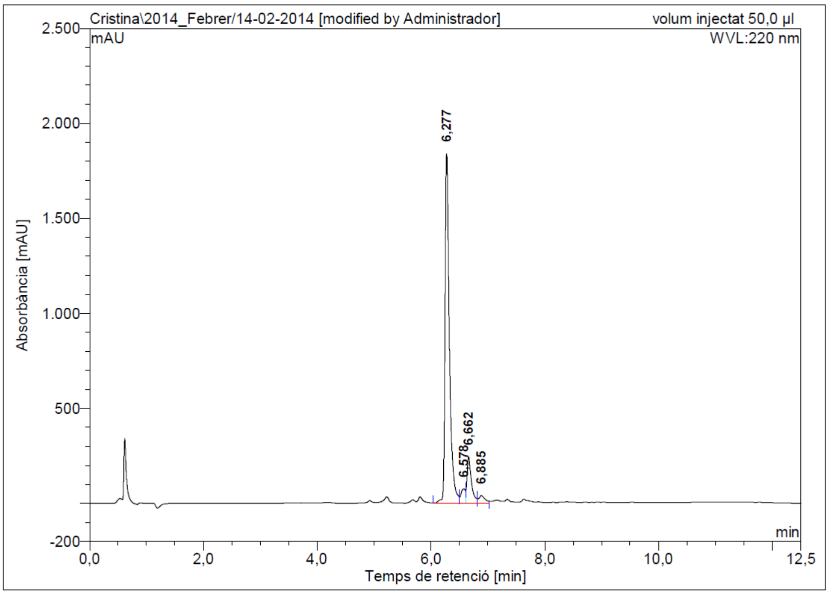

No.	Ret.Time (detected) min	Height mAU	Area mAU*min	Rel.Area %
1	6,28	1837,551	163,359	82,83
2	6,58	74,968	6,671	3,38
3	6,66	244,378	22,027	11,17
4	6,89	39,918	5,167	2,62
Total:		2196,816	197,224	100,00

MS (ESI) *m/z* (+)

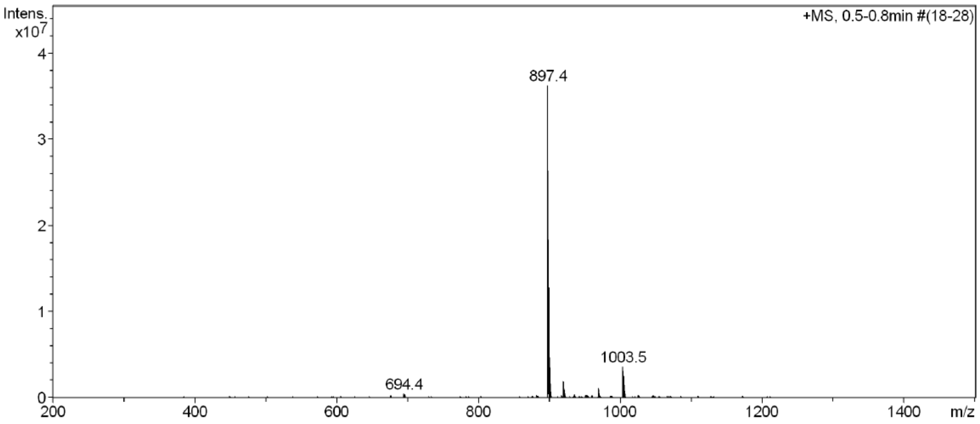

MS (ESI) *m/z* (-)

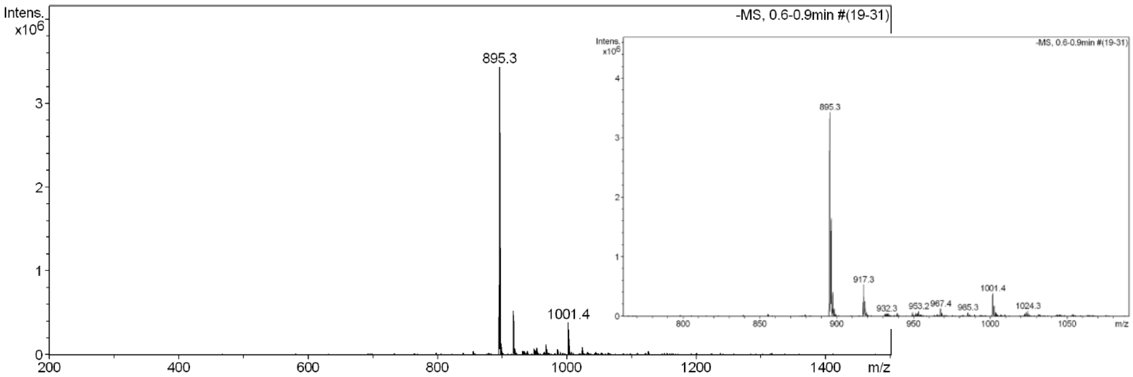

3.1.9. H-D-Tyr-D-Thr-Glu-D-Val-Pro-Gln-Tyr-OAll

HPLC (λ = 220 nm) (*Method C*)

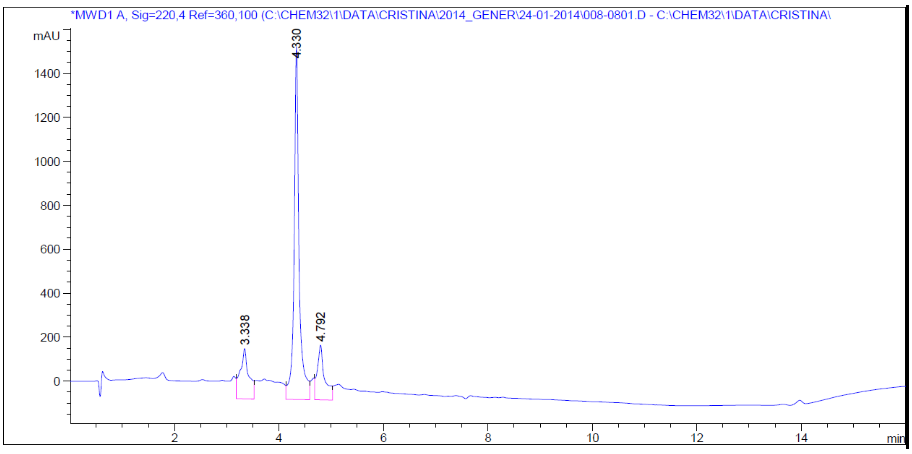

```
Peak RetTime Type  Width     Area      Height     Area
  #   [min]        [min]   [mAU*s]     [mAU]       %
----|-------|----|-------|----------|----------|--------|
  1   3.338 VV    0.1505 2649.76685  229.88855  16.7259
  2   4.330 VV    0.0957 1.07004e4  1607.08350  67.5432
  3   4.792 VV    0.1323 2492.12817  249.89232  15.7309

Totals :                 1.58423e4  2086.86436
```

MS (ESI) *m/z* (+)

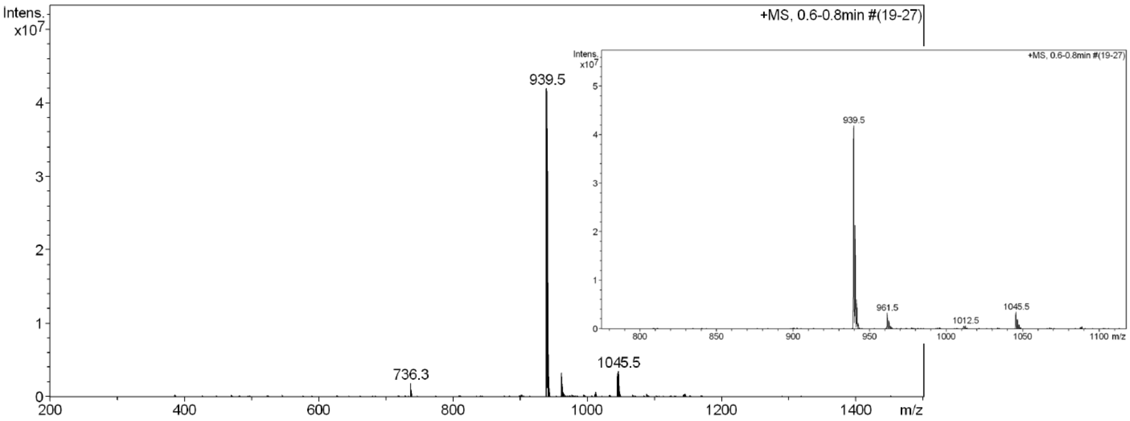

MS (ESI) *m/z* (-)

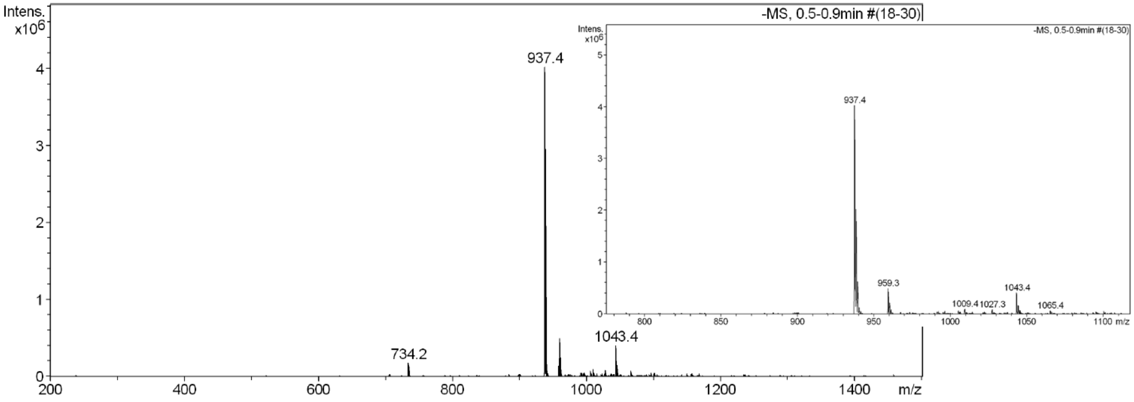

3.1.10. H-D-Tyr-D-Ser-Glu-D-Val-Pro-Gln-Tyr-OAll

HPLC (λ = 220 nm) (*Method C*)

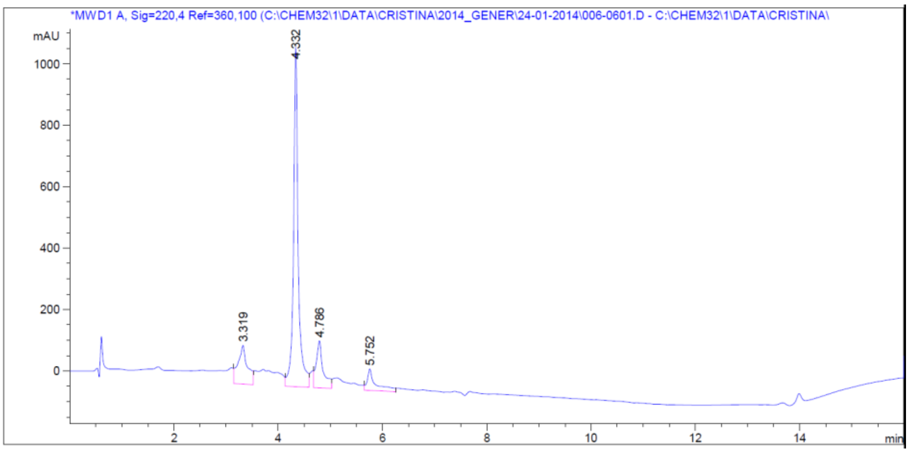

```
Peak RetTime Type  Width     Area      Height     Area
  #   [min]        [min]   [mAU*s]     [mAU]       %
----|-------|----|-------|----------|----------|--------|
   1   3.319 VV    0.1637 1603.37207  126.64928  14.8137
   2   4.332 VV    0.0871 6940.79883 1107.32080  64.1267
   3   4.786 VV    0.1271 1442.97803  154.30269  13.3318
   4   5.752 VV    0.1542  836.42023   70.59526   7.7278

Totals :                  1.08236e4  1458.86803
```

MS (ESI) *m/z* (+)

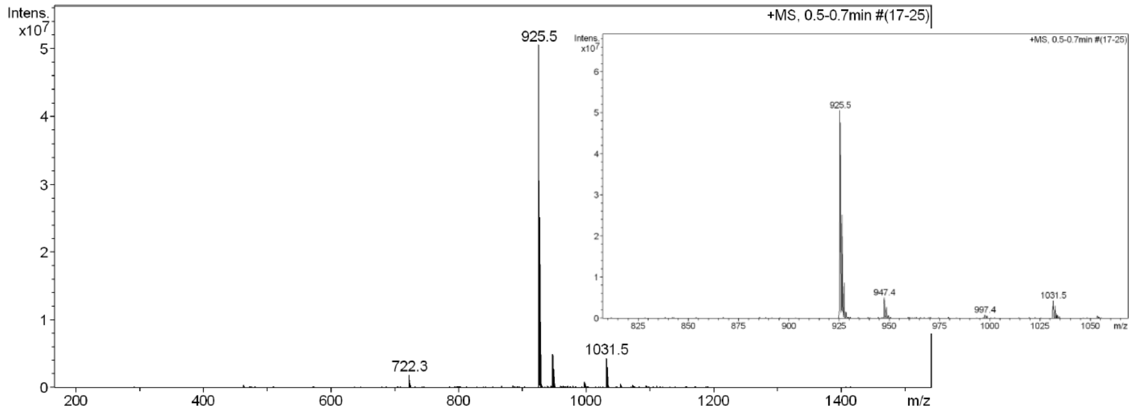

MS (ESI) *m/z* (-)

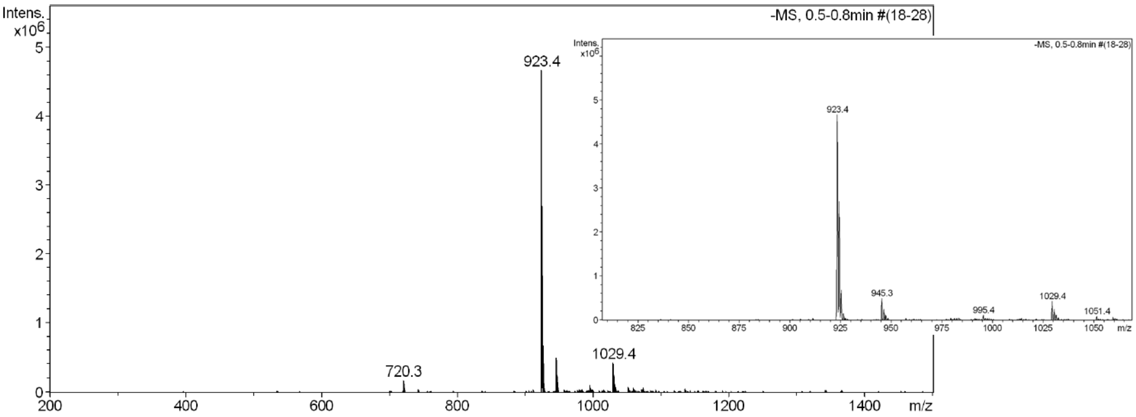

3.1.11. H-D-Tyr-D-Thr-Glu-D-Ala-Pro-Gln-Tyr-OAll

HPLC (λ = 220 nm) (*Method A*)

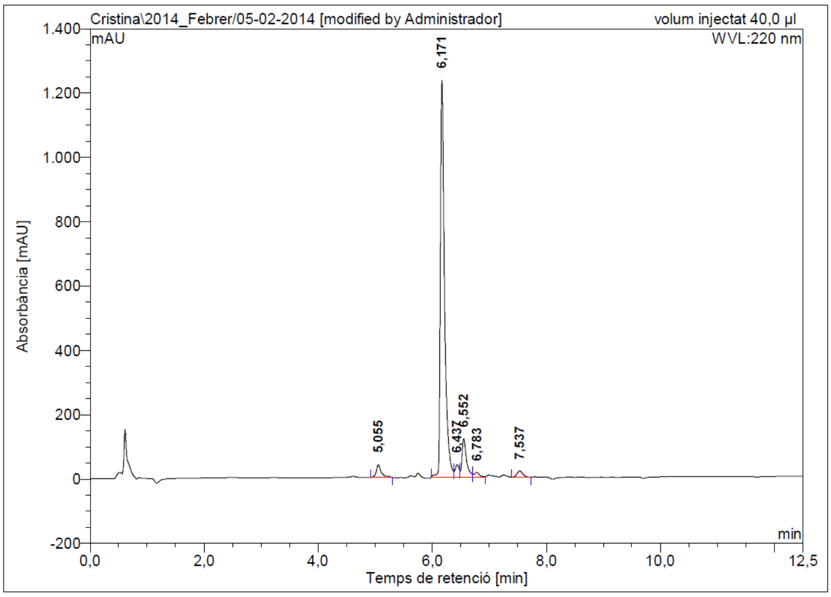

No.	Ret.Time (detected) min	Height mAU	Area mAU*min	Rel.Area %
1	5,06	39,438	4,072	3,17
2	6,17	1234,611	105,576	82,15
3	6,44	40,064	3,305	2,57
4	6,55	120,430	11,180	8,70
5	6,78	15,691	1,800	1,40
6	7,54	20,775	2,582	2,01
Total:		1471,008	128,515	100,00

MS (ESI) *m/z* (+)

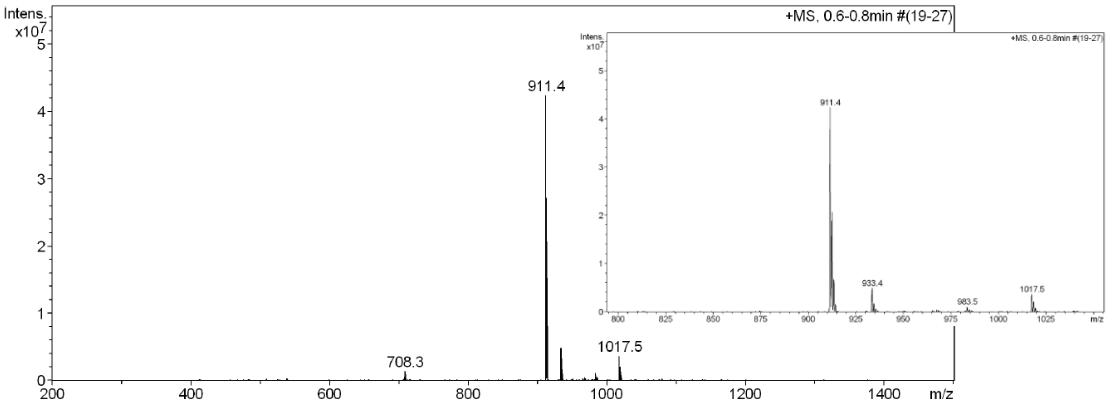

MS (ESI) *m/z* (-)

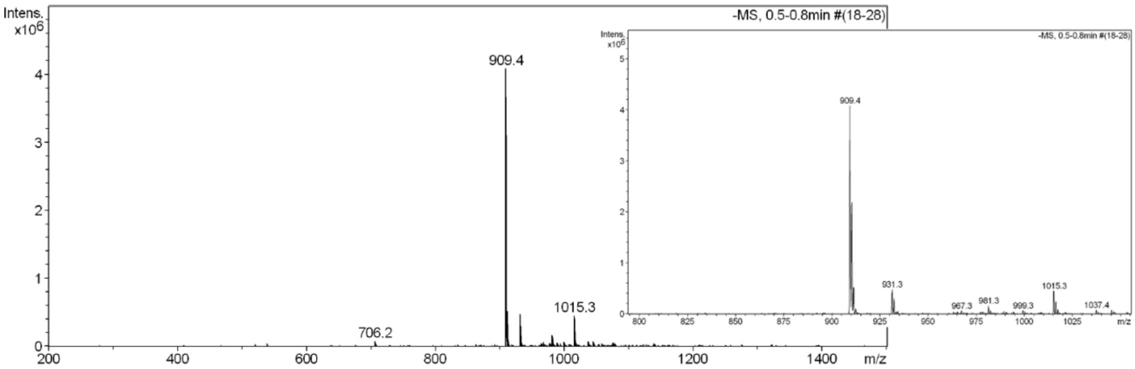

3.1.12. H-D-Tyr-D-Ser-Glu-D-Ala-Pro-Gln-Tyr-OAll

HPLC (λ = 220 nm) (*Method C*)

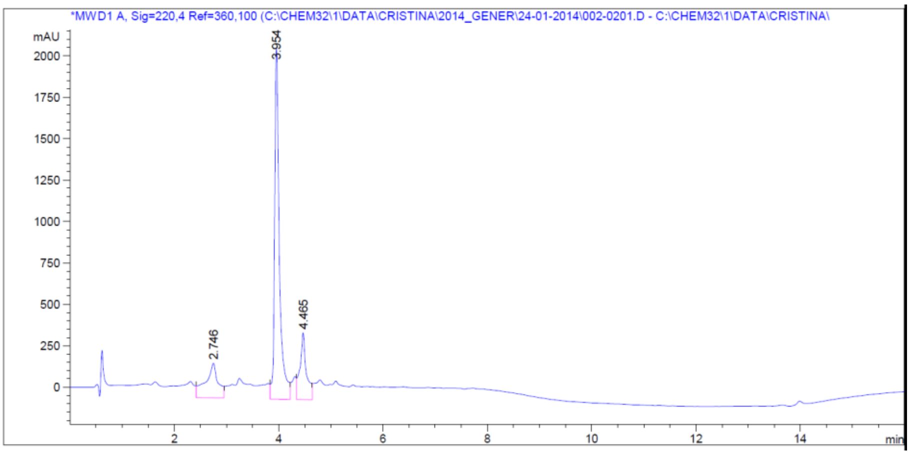

```
Peak RetTime Type  Width     Area      Height     Area
  #   [min]        [min]   [mAU*s]     [mAU]       %
----|-------|----|-------|----------|----------|--------|
   1   2.746 VV    0.2128 3476.40405  210.36153  17.0367
   2   3.954 VV    0.0939 1.34629e4  2124.78662  65.9770
   3   4.465 VV    0.1159 3466.12598  404.72244  16.9863

Totals :                  2.04054e4  2739.87059
```

MS (ESI) *m/z* (+)

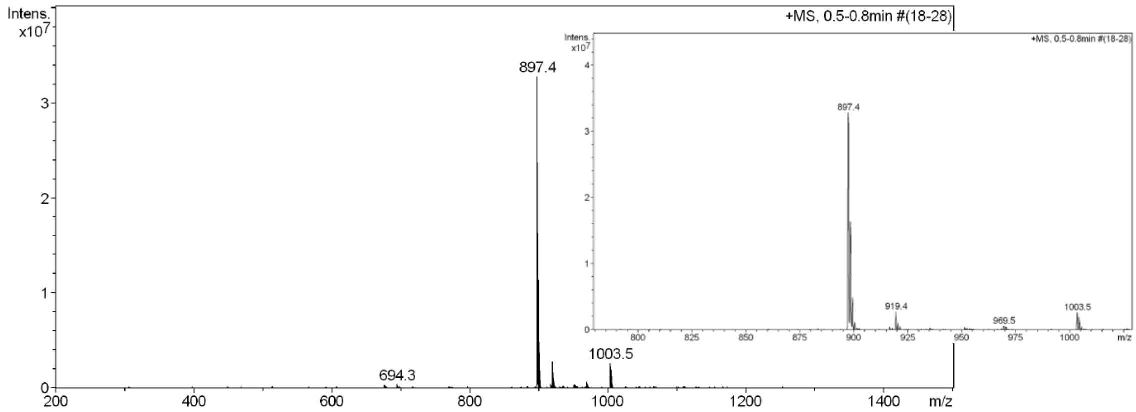

MS (ESI) *m/z* (-)

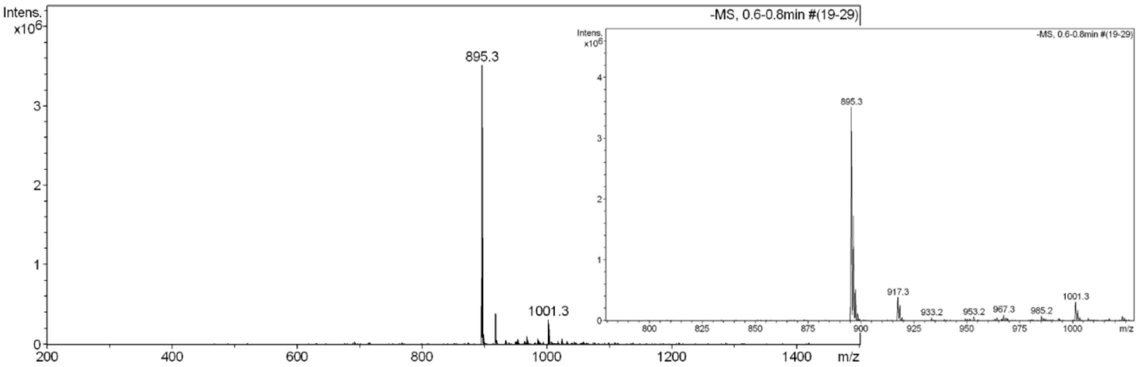

3.2. Linear depsipeptides

3.2.1. H-Tyr(O-Ile-Fmoc)-Thr-Glu-Val-Pro-Gln-OAll

HPLC (λ = 220 nm) (*Method A*)

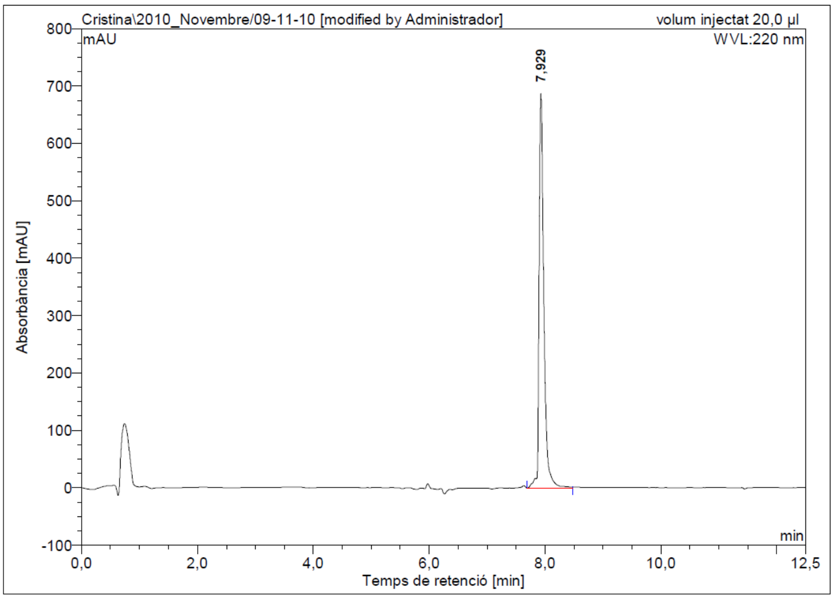

No.	Ret.Time (detected) min	Height mAU	Area mAU*min	Rel.Area %
1	7,93	687,951	66,204	100,00
Total:		687,951	66,204	100,00

MS (ESI) *m/z* (+)

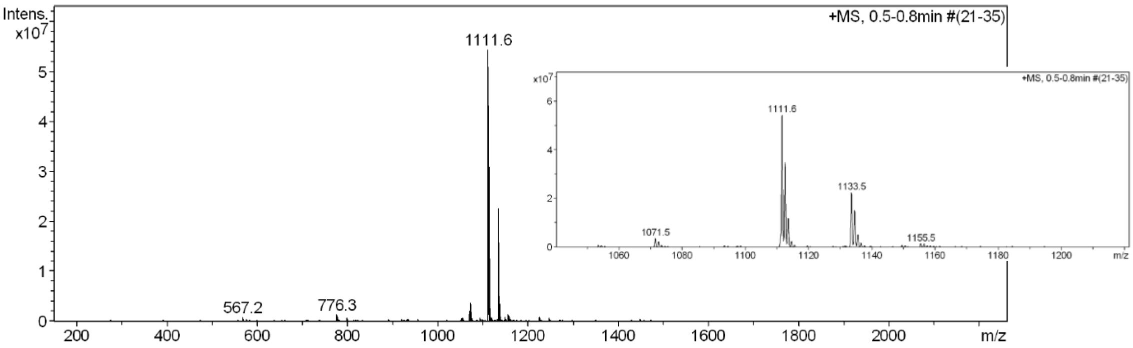

MS (ESI) *m/z* (+)

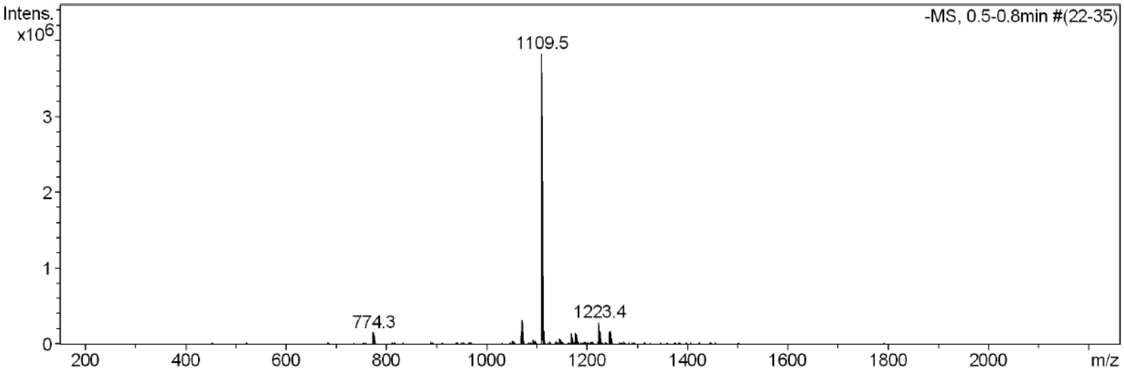

3.2.2. *p*NZ-Tyr(O-Ile-H)-Thr-Glu-Val-Pro-Gln-OAll

HPLC (λ = 220 nm) (*Method B*)

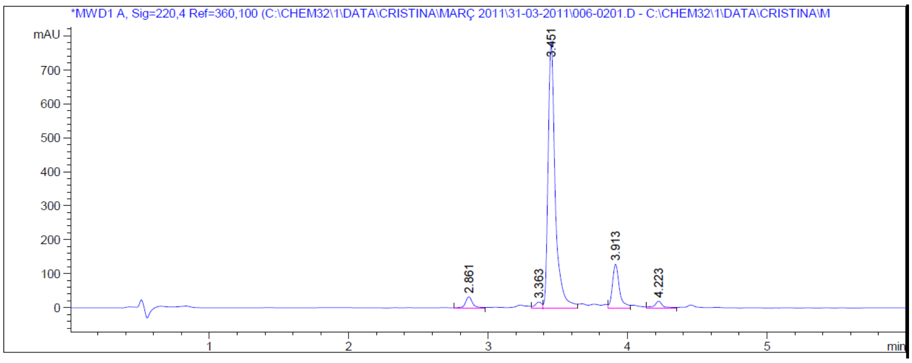

```
Peak RetTime Type  Width     Area      Height     Area
  #   [min]        [min]   [mAU*s]     [mAU]       %
----|-------|----|-------|----------|----------|--------|
   1   2.861 VV    0.0534  117.46292   33.08478   3.3609
   2   3.363 VV    0.0489   55.18627   17.43038   1.5790
   3   3.451 VV    0.0534 2788.41772  785.92554  79.7842
   4   3.913 VV    0.0527  450.95483  129.15253  12.9030
   5   4.223 VV    0.0599   82.92767   20.21841   2.3728

Totals :                  3494.94941  985.81163
```

MS (ESI) *m/z* (+)

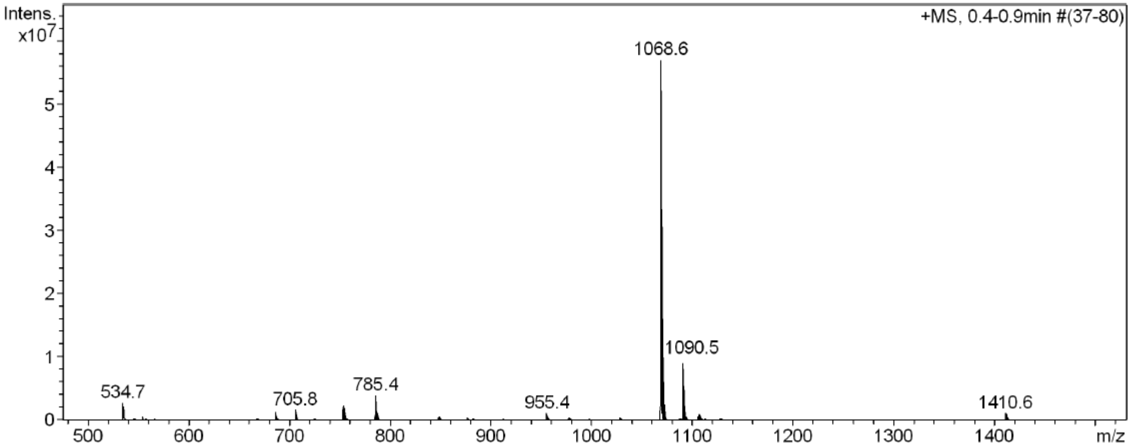

3.2.3. *p*NZ-Tyr(O-Ile-Alloc)-Thr-Glu-Val-Pro-Gln-Tyr-OAll

HPLC (*λ* = 220 nm) (*Method A*)

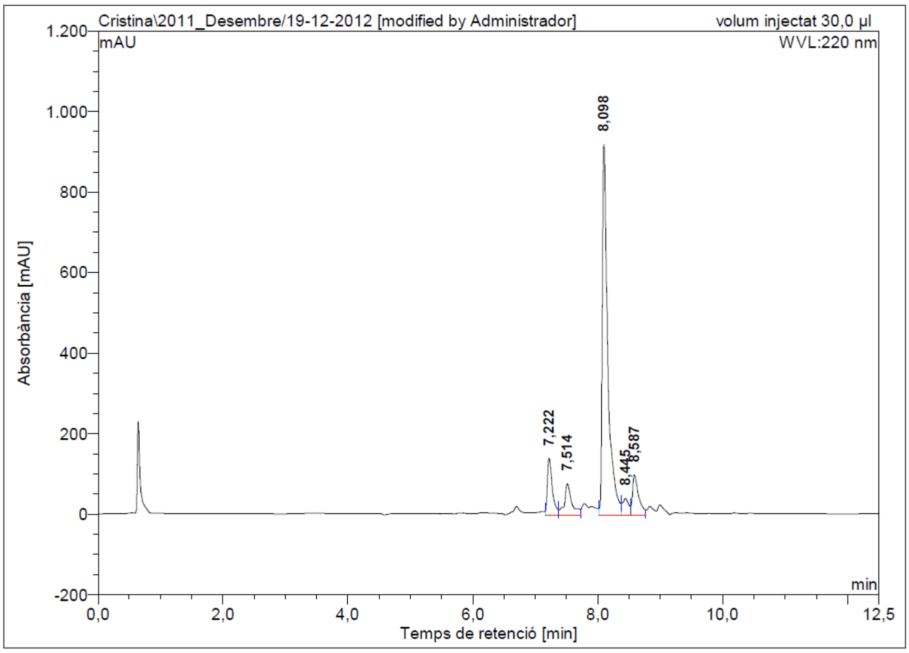

No.	Ret.Time (detected) min	Height mAU	Area mAU*min	Rel.Area %
1	7,22	139,804	12,919	9,63
2	7,51	77,363	10,507	7,83
3	8,10	919,575	94,438	70,41
4	8,44	40,821	4,807	3,58
5	8,59	99,138	11,446	8,53
Total:		1276,701	134,116	100,00

MS (ESI) *m/z* (+)

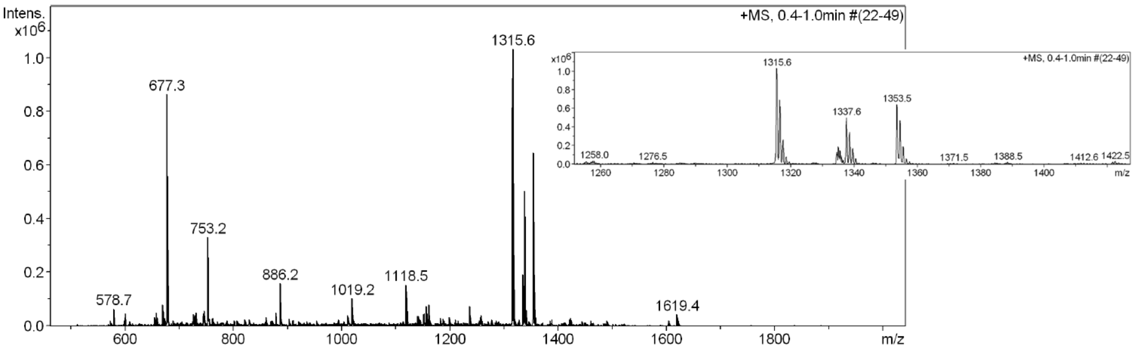

3.2.4. *p*NZ-Tyr(O-Ile-Alloc)-D-Thr-Glu-D-Val-Pro-Gln-D-Tyr-OAll

HPLC (λ = 220 nm) (*Method A*)

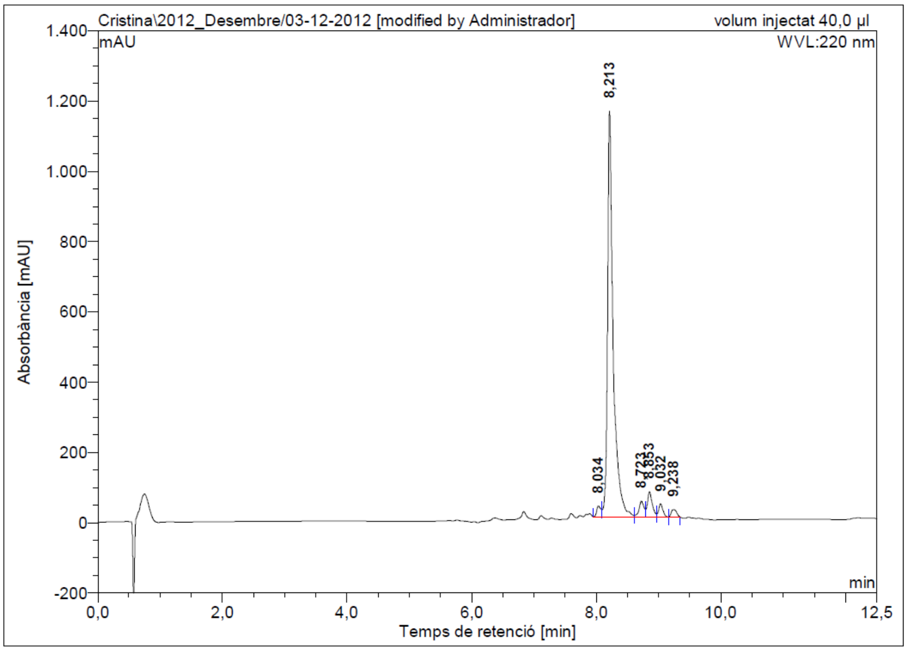

No.	Ret.Time (detected) min	Height mAU	Area mAU*min	Rel.Area %
1	8,03	31,452	2,514	1,80
2	8,21	1155,142	121,076	86,78
3	8,72	45,686	4,293	3,08
4	8,85	72,298	6,561	4,70
5	9,03	37,286	3,012	2,16
6	9,24	21,079	2,065	1,48
Total:		1362,943	139,521	100,00

MS (ESI) *m/z* (+)

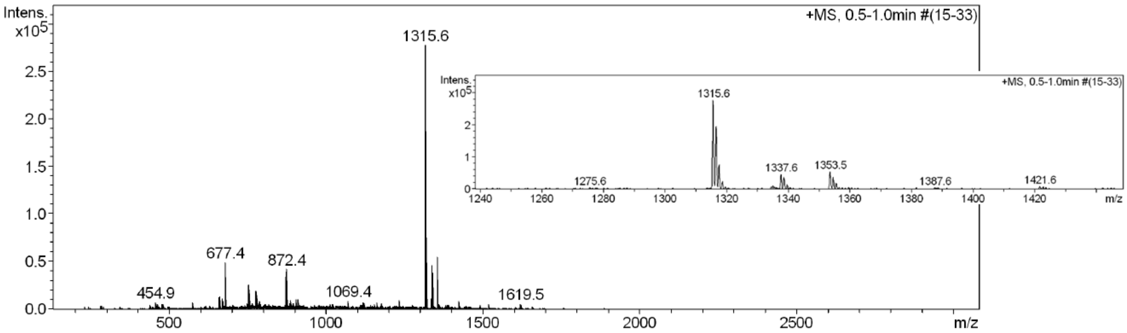

3.2.5. H-Tyr(O-Ile-Alloc)-D-Thr-Glu-D-Val-Pro-Gln-D-Tyr-OAll

HPLC (λ = 220 nm) (*Method A*)

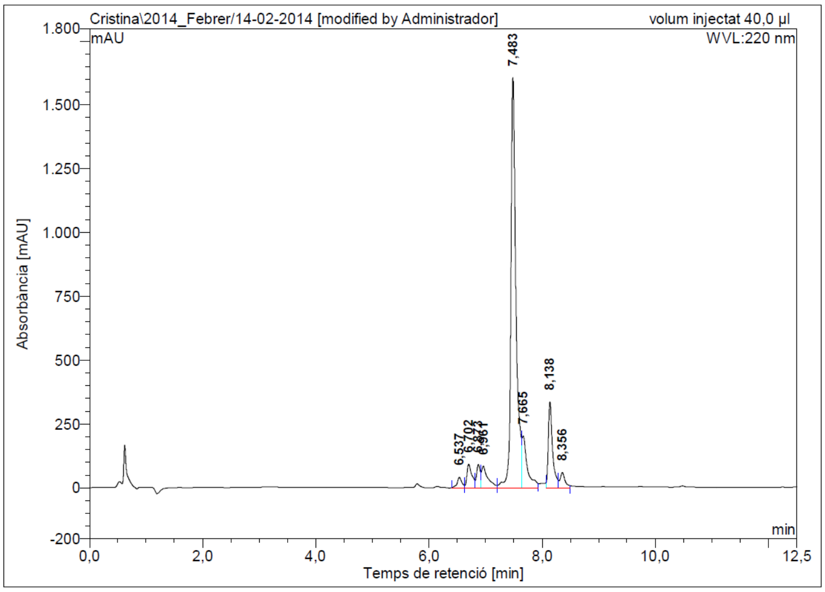

No.	Ret.Time (detected) min	Height mAU	Area mAU*min	Rel.Area %
1	6,54	42,279	4,200	1,61
2	6,70	93,735	9,778	3,75
3	6,87	92,699	6,953	2,67
4	6,96	85,783	11,277	4,33
5	7,48	1608,738	167,967	64,46
6	7,67	204,696	23,691	9,09
7	8,14	338,564	30,116	11,56
8	8,36	61,844	6,584	2,53
Total:		2528,338	260,566	100,00

MS (ESI) *m/z* (+)

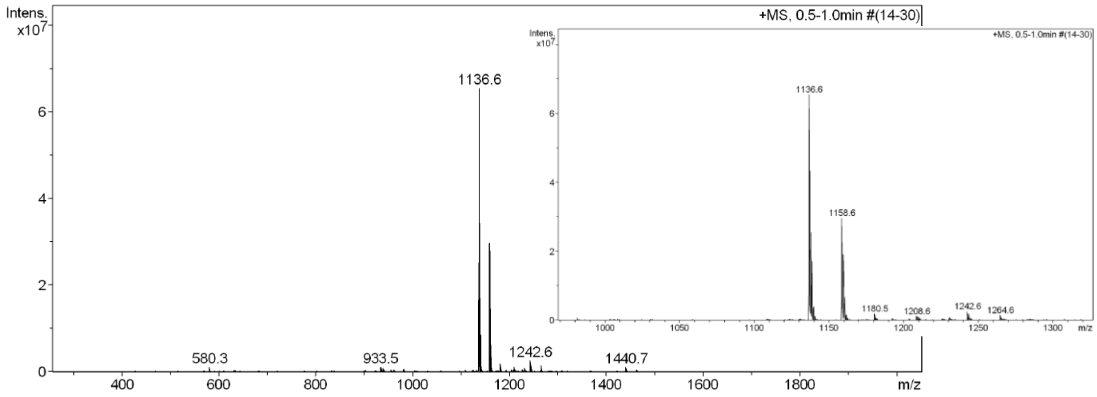

MS (ESI) *m/z* (-)

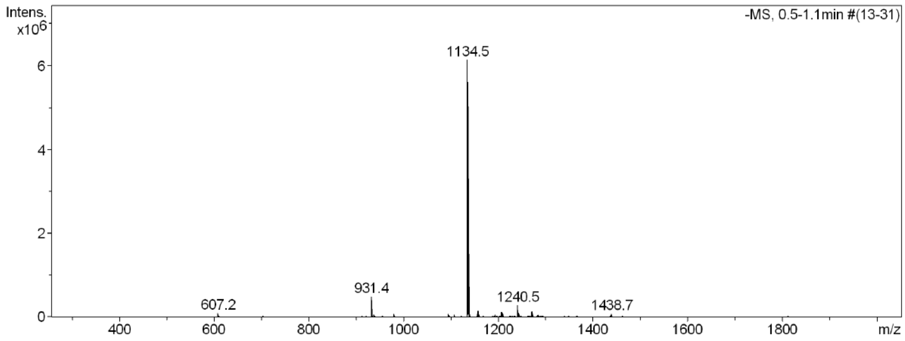

3.2.6. H-Tyr(O-Ile-Alloc)-D-Ser-Glu-D-Val-Pro-Gln-D-Tyr-OAll

HPLC (λ = 220 nm) (*Method A*)

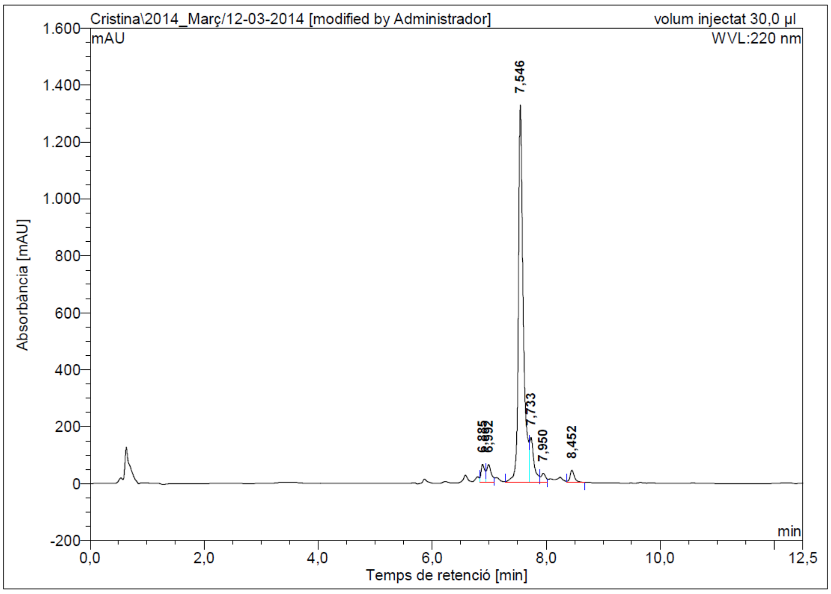

No.	Ret.Time (detected) min	Height mAU	Area mAU*min	Rel.Area %
1	6,89	63,968	4,779	2,92
2	6,99	63,144	6,017	3,68
3	7,55	1327,644	130,962	80,05
4	7,73	158,287	14,723	9,00
5	7,95	32,318	3,186	1,95
6	8,45	43,446	3,933	2,40
Total:		1688,807	163,600	100,00

MS (ESI) *m/z* (+)

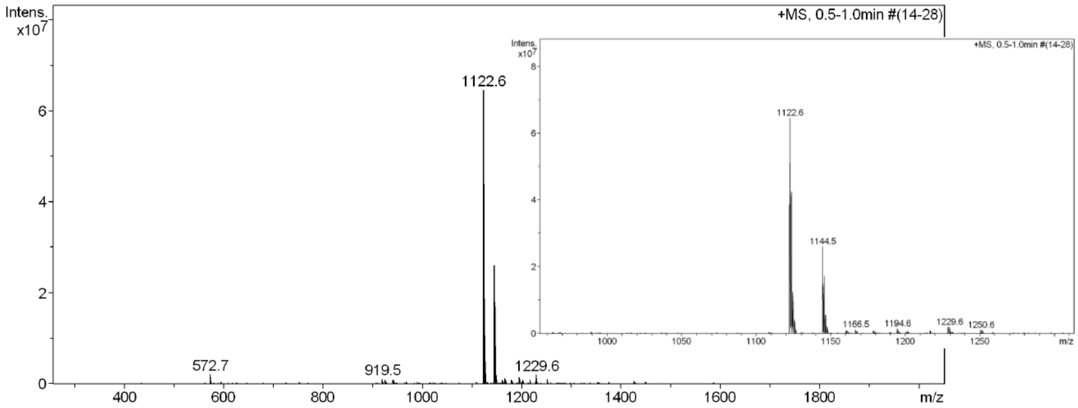

MS (ESI) *m/z* (-)

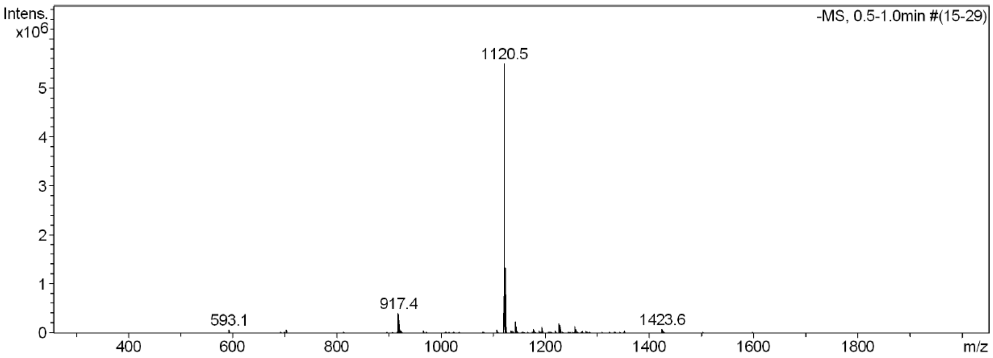

3.2.7. H-Tyr(O-Ile-Alloc)-D-Thr-Glu-D-Ala-Pro-Gln-D-Tyr-OAll

HPLC (*λ* = 220 nm) (*Method A*)

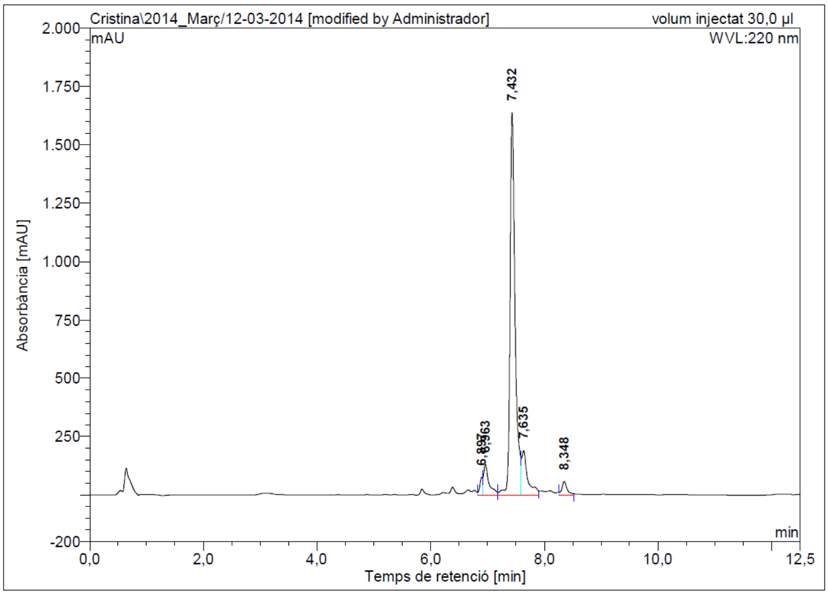

No.	Ret.Time (detected) min	Height mAU	Area mAU*min	Rel.Area %
1	6,90	77,653	4,411	2,00
2	6,96	131,989	14,867	6,74
3	7,43	1640,191	170,612	77,35
4	7,63	192,448	24,053	10,91
5	8,35	59,430	6,615	3,00
Total:		2101,711	220,558	100,00

MS (ESI) *m/z* (+)

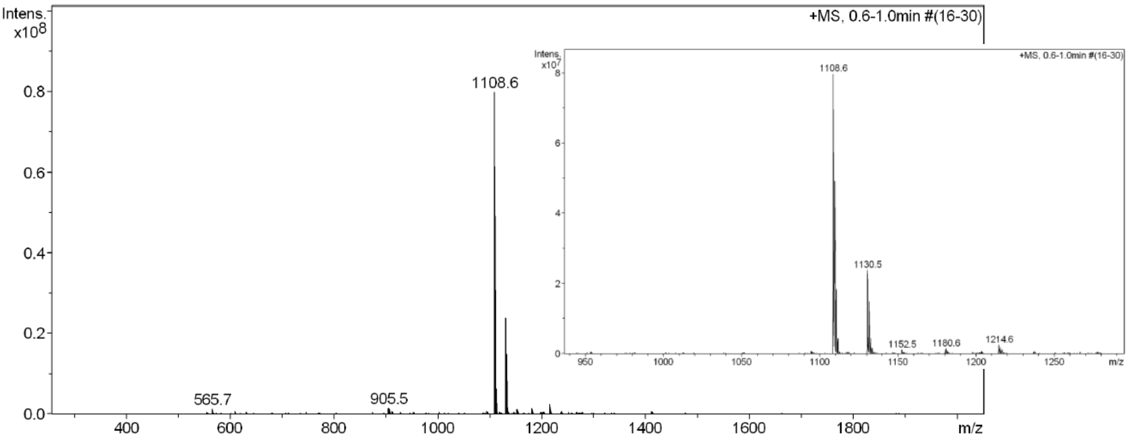

MS (ESI) *m/z* (-)

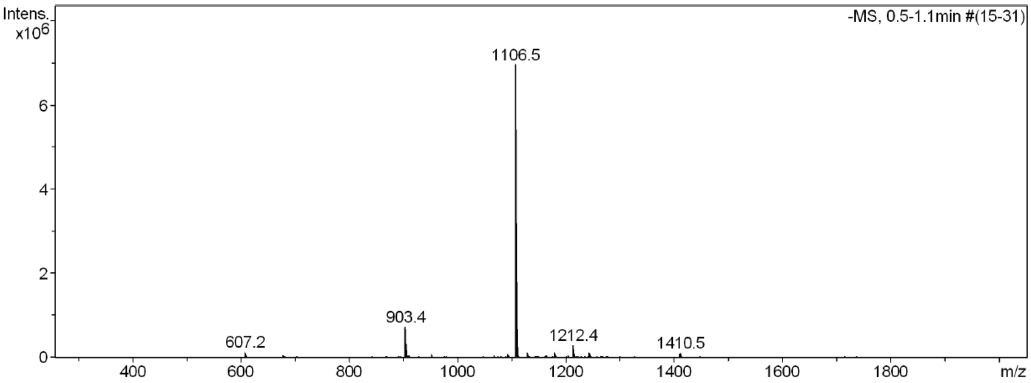

3.2.8. H-Tyr(O-Ile-Alloc)-D-Ser-Glu-D-Ala-Pro-Gln-D-Tyr-OAll

HPLC (λ = 220 nm) (*Method A*)

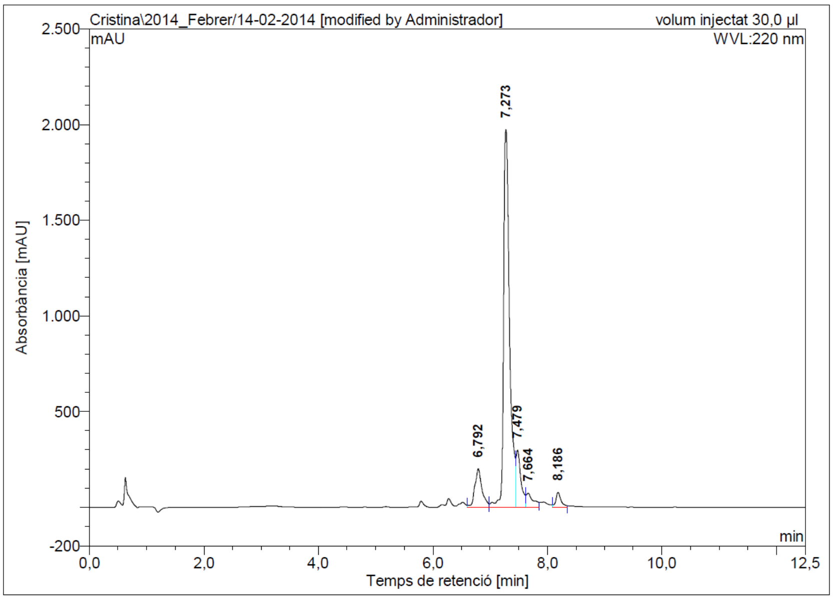

No.	Ret.Time (detected) min	Height mAU	Area mAU*min	Rel.Area %
1	6,79	201,893	29,512	9,28
2	7,27	1973,340	238,102	74,91
3	7,48	298,504	31,142	9,80
4	7,66	73,773	10,513	3,31
5	8,19	78,976	8,591	2,70
Total:		2626,485	317,859	100,00

MS (ESI) *m/z* (+)

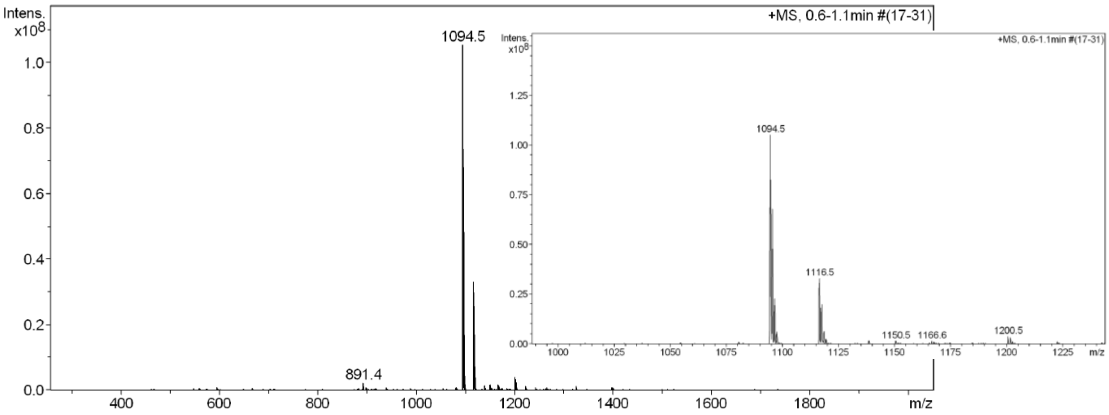

MS (ESI) *m/z* (-)

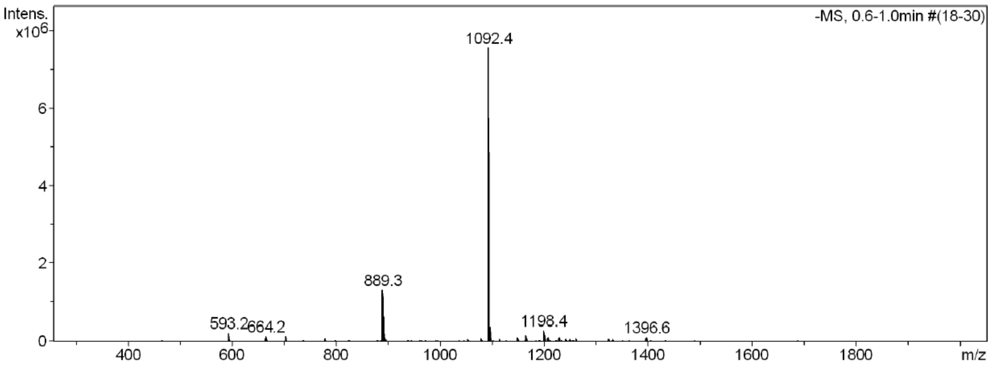

3.2.9. H-D-Tyr(O-Ile-Alloc)-D-Thr-Glu-D-Val-Pro-Gln-Tyr-OAll

HPLC (λ = 220 nm) (*Method C*)

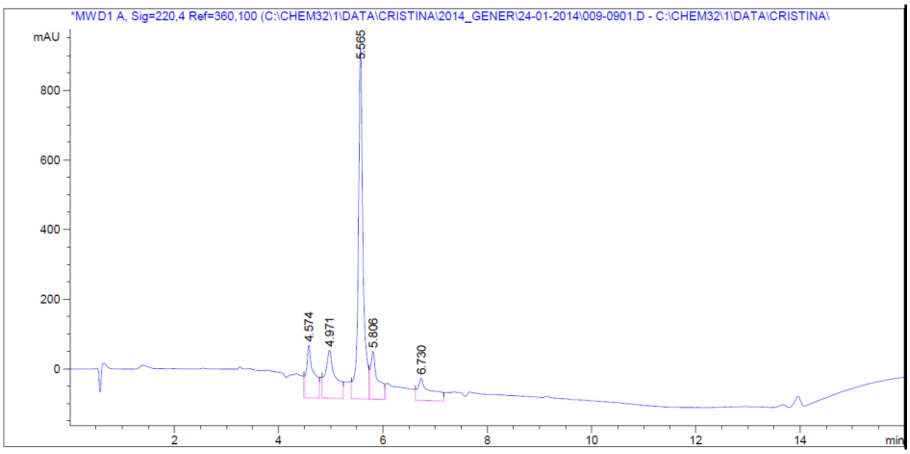

```
Peak RetTime Type  Width     Area      Height     Area
  #   [min]        [min]   [mAU*s]     [mAU]      %
----|-------|----|-------|----------|----------|--------|
   1   4.574 VV    0.1307 1507.73401  150.75711  12.3038
   2   4.971 VV    0.1777 1871.50659  138.47758  15.2724
   3   5.565 VV    0.0918 6389.54590 1010.26642  52.1418
   4   5.806 VV    0.1291 1341.04382  138.34393  10.9436
   5   6.730 VV    0.2256 1144.33667   64.32008   9.3383

Totals :                  1.22542e4  1502.16513
```

MS (ESI) *m/z* (+)

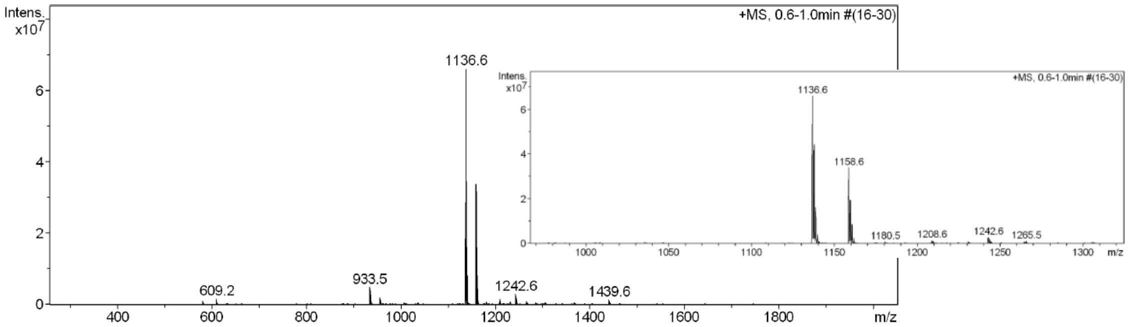

MS (ESI) *m/z* (-)

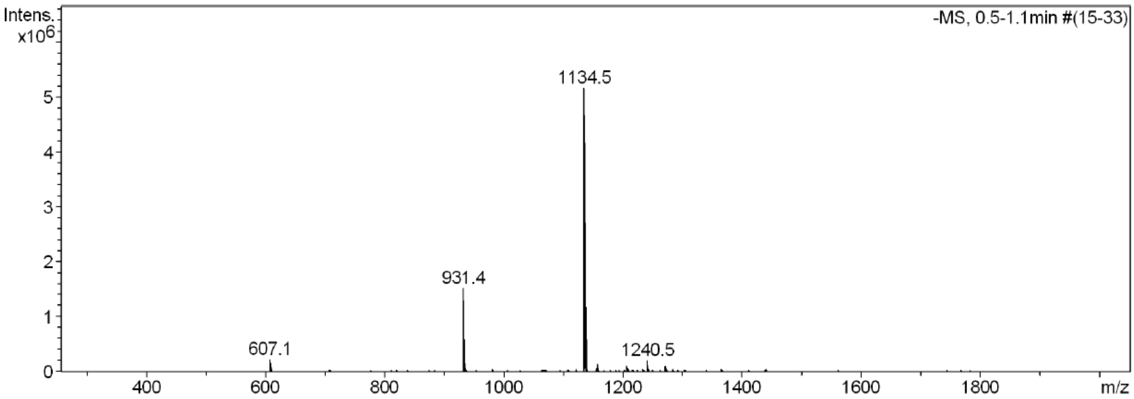

3.2.10. H-D-Tyr(O-Ile-Alloc)-D-Ser-Glu-D-Val-Pro-Gln-Tyr-OAll

HPLC (λ = 220 nm) (*Method C*)

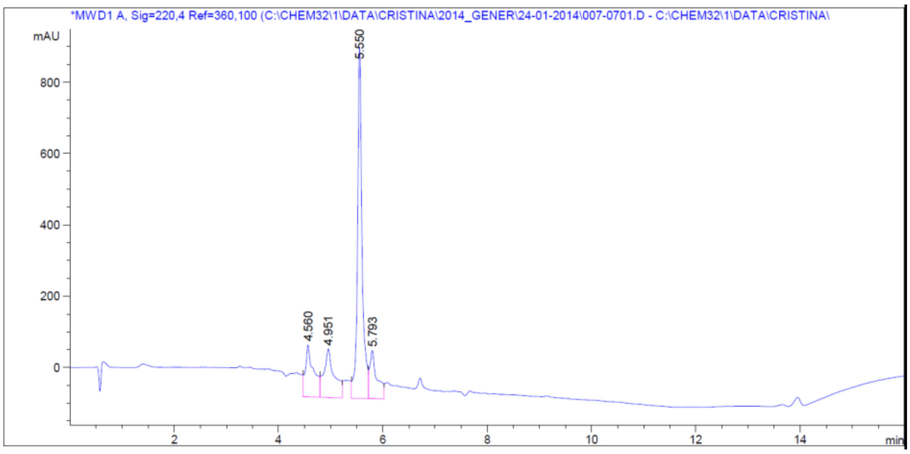

```
Peak RetTime Type  Width     Area      Height     Area
  #   [min]        [min]   [mAU*s]     [mAU]       %
----|-------|----|-------|----------|----------|--------|
   1   4.560 VV    0.1428 1617.77551  146.58409  14.8006
   2   4.951 VV    0.1803 1907.00049  137.11357  17.4466
   3   5.550 VV    0.0900 6084.38770  985.98712  55.6644
   4   5.793 VV    0.1294 1321.31250  135.99600  12.0883

Totals :                  1.09305e4  1405.68079
```

MS (ESI) *m/z* (+)

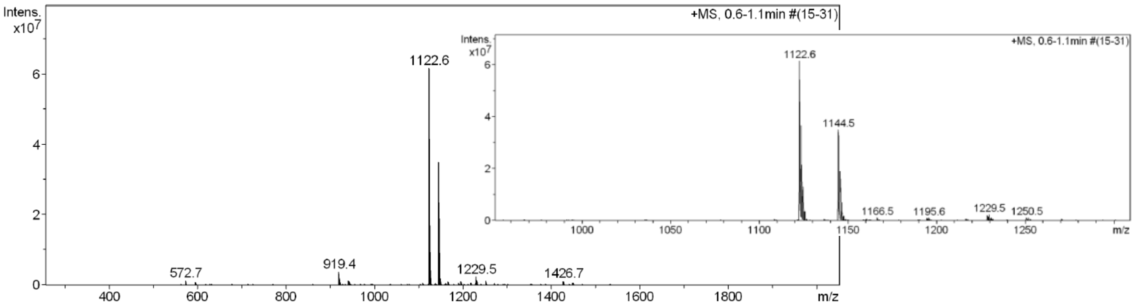

MS (ESI) *m/z* (-)

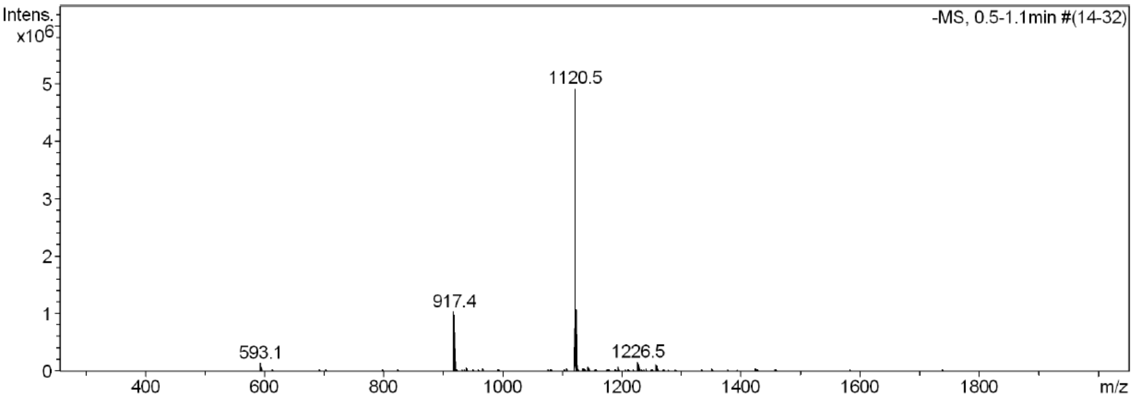

3.2.11. H-D-Tyr(O-Ile-Alloc)-D-Thr-Glu-D-Ala-Pro-Gln-Tyr-OAll

HPLC (λ = 220 nm) (*Method A*)

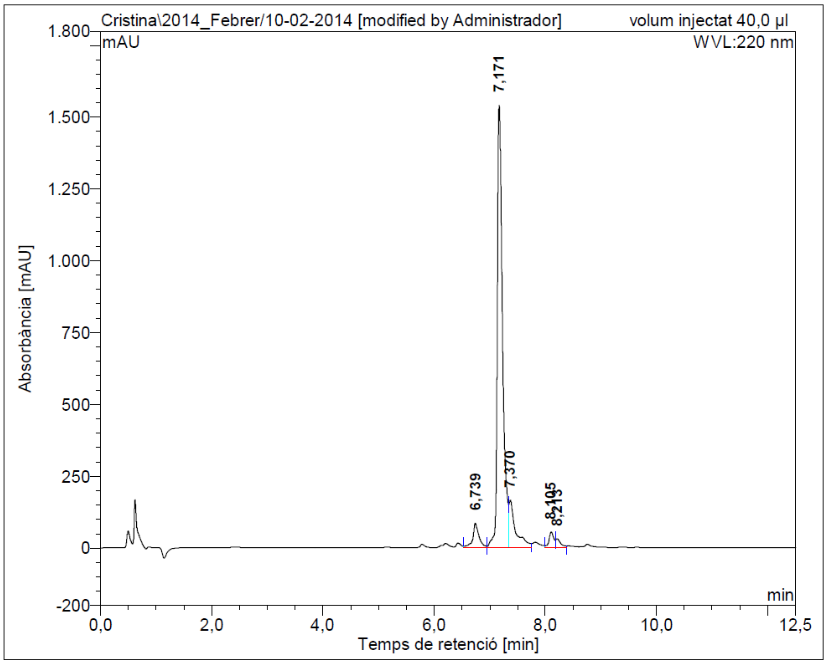

No.	mps retenc min	alçada mAU	Area mAU*min	Area relativa %
1	6,74	84,012	10,884	5,13
2	7,17	1539,938	169,632	80,02
3	7,37	165,108	22,865	10,79
4	8,11	54,340	5,345	2,52
5	8,21	30,609	3,254	1,53
Total:		1874,007	211,981	100,00

MS (ESI) *m/z* (+)

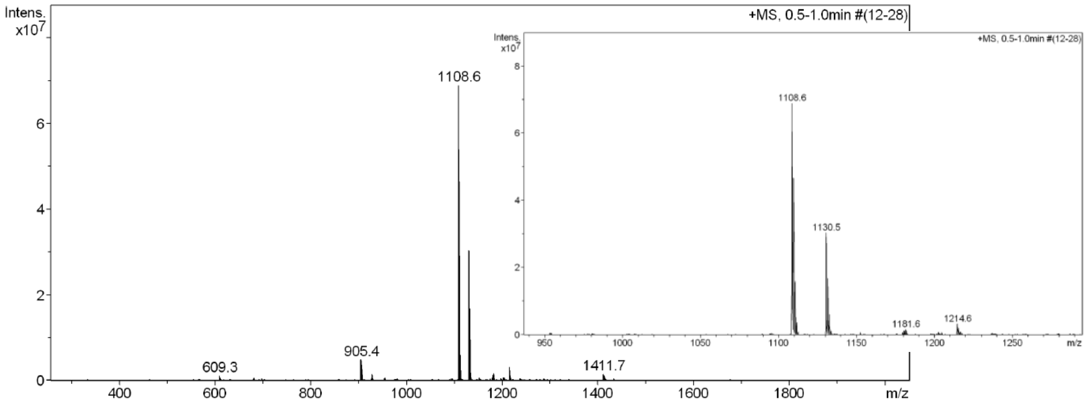

MS (ESI) *m/z* (-)

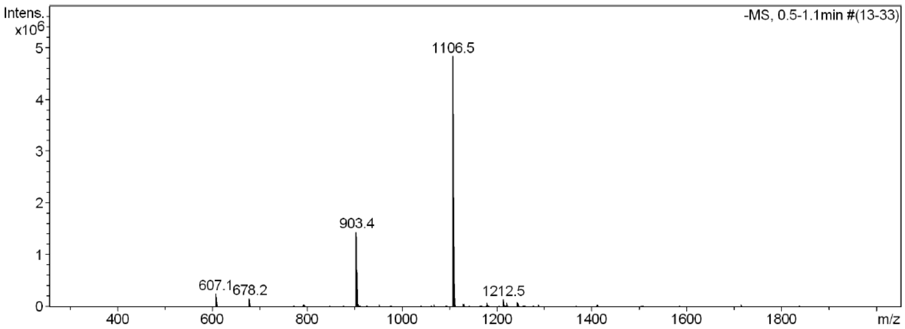

3.2.12. H-D-Tyr(O-Ile-Alloc)-D-Ser-Glu-D-Ala-Pro-Gln-Tyr-OAll

HPLC (λ = 220 nm) (*Method C*)

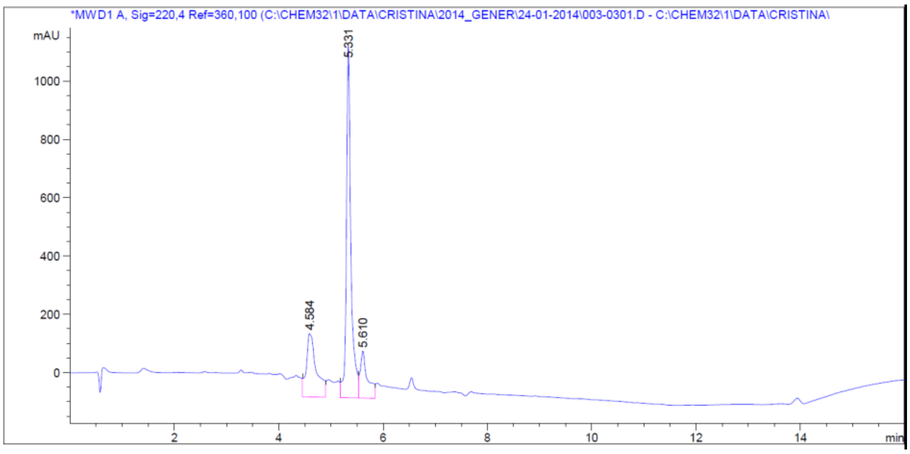

```
Peak RetTime Type  Width     Area      Height     Area
  #   [min]        [min]   [mAU*s]     [mAU]        %
----|-------|----|-------|----------|----------|--------|
   1   4.584 VV    0.1734 2945.10840  218.27769  24.9068
   2   5.331 VV    0.0860 7280.00732 1212.71277  61.5670
   3   5.610 VV    0.1329 1599.41956  162.34128  13.5263

Totals :                  1.18245e4  1593.33174
```

MS (ESI) *m/z* (+)

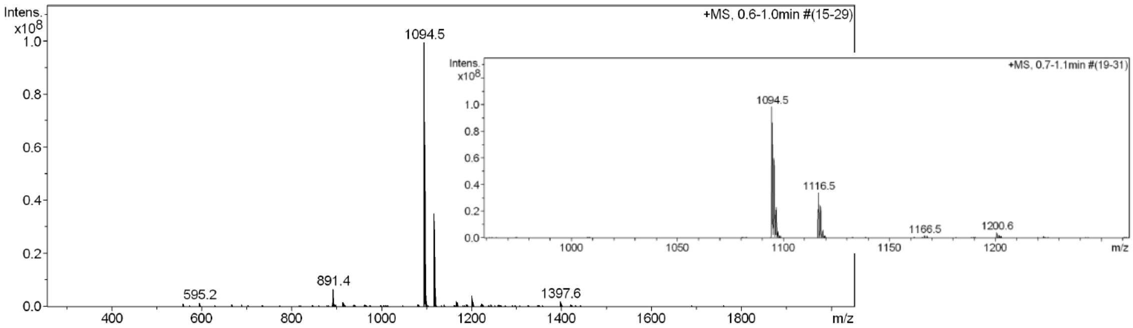

MS (ESI) *m/z* (-)

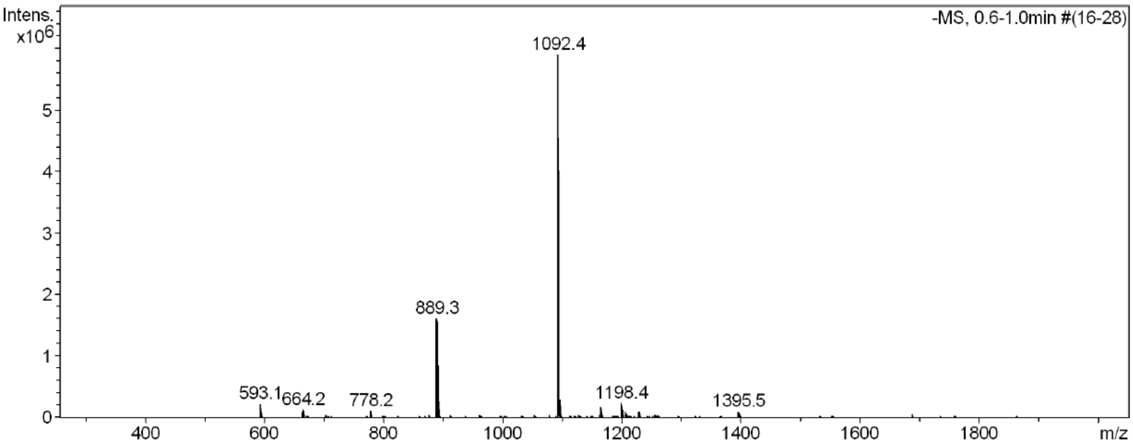

3.3. Deprotected linear depsipeptides

3.3.1. *p*NZ-Tyr(O-Ile-H)-Thr-Glu-Val-Pro-Gln-Tyr-OH

HPLC (λ = 220 nm) (*Method A*)

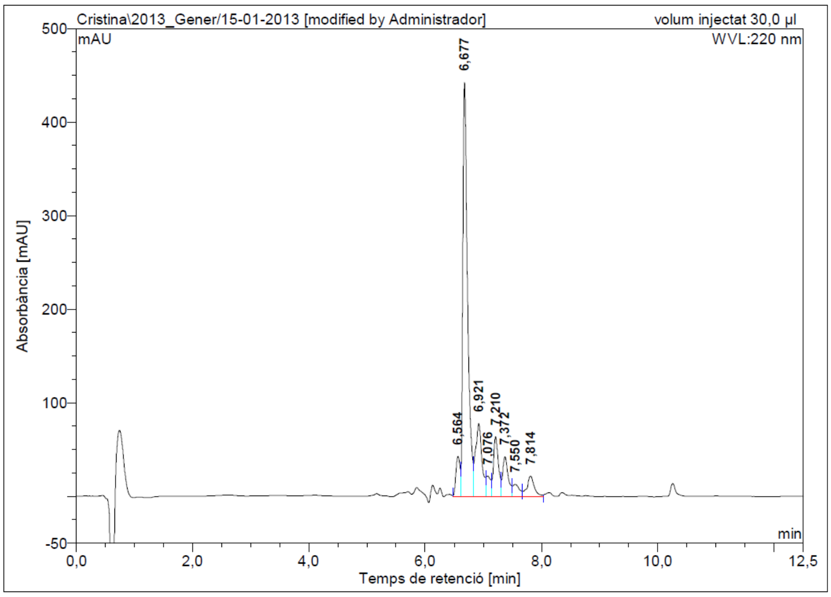

No.	Ret.Time (detected) min	Height mAU	Area mAU*min	Rel.Area %
1	6,56	43,170	3,506	4,73
2	6,68	443,047	42,103	56,83
3	6,92	78,349	10,061	13,58
4	7,08	21,983	2,105	2,84
5	7,21	64,306	6,457	8,72
6	7,37	42,638	4,721	6,37
7	7,55	13,390	1,846	2,49
8	7,81	22,000	3,280	4,43
Total:		728,885	74,079	100,00

MS (ESI) *m/z* (+)

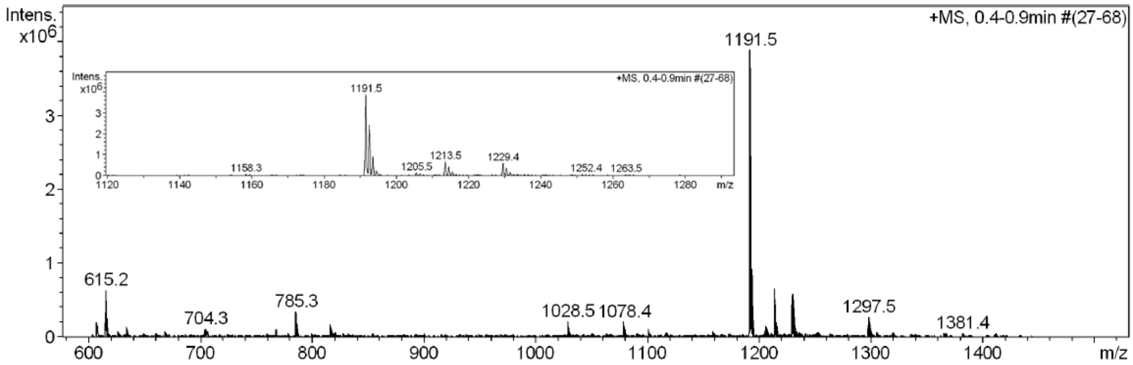

3.3.2. *p*NZ-Tyr(O-Ile-H)-D-Thr-Glu-D-Val-Pro-Gln-D-Tyr-OH

HPLC (λ = 220 nm) (*Method A*)

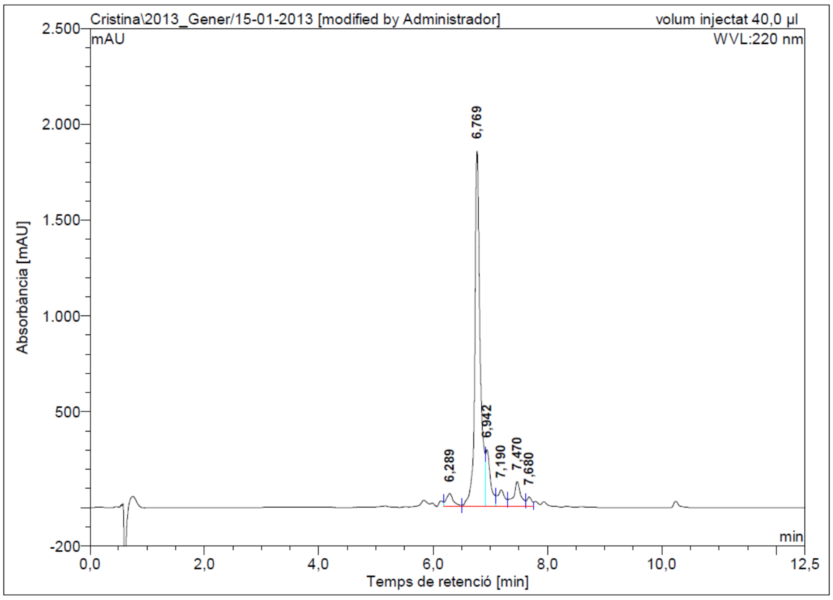

No.	Ret.Time (detected) min	Height mAU	Area mAU*min	Rel.Area %
1	6,29	67,793	9,703	3,50
2	6,77	1853,683	201,018	72,49
3	6,94	296,736	29,890	10,78
4	7,19	85,297	12,706	4,58
5	7,47	128,808	19,352	6,98
6	7,68	48,566	4,643	1,67
Total:		2480,883	277,312	100,00

MS (ESI) *m/z* (+)

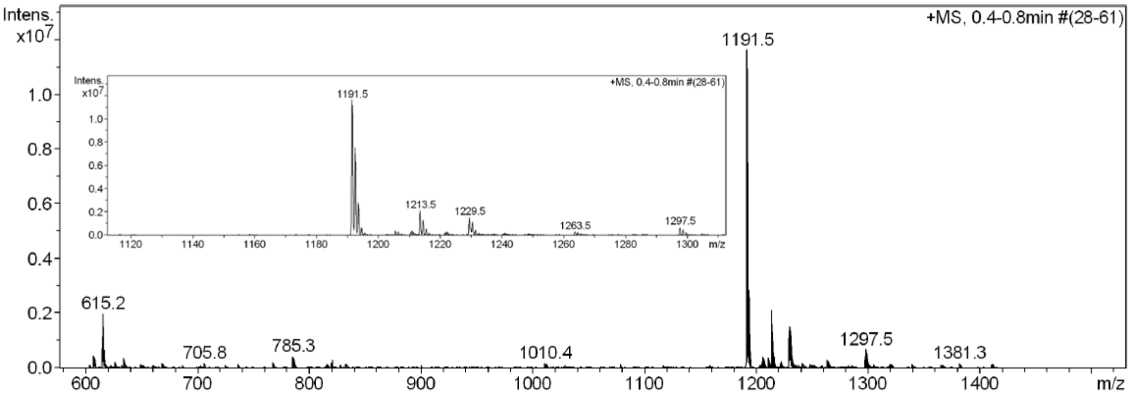

3.3.3. H-Tyr(O-Ile-H)-D-Thr-Glu-D-Val-Pro-Gln-D-Tyr-OH (BPC821)

HPLC (λ = 220 nm) (*Method A*)

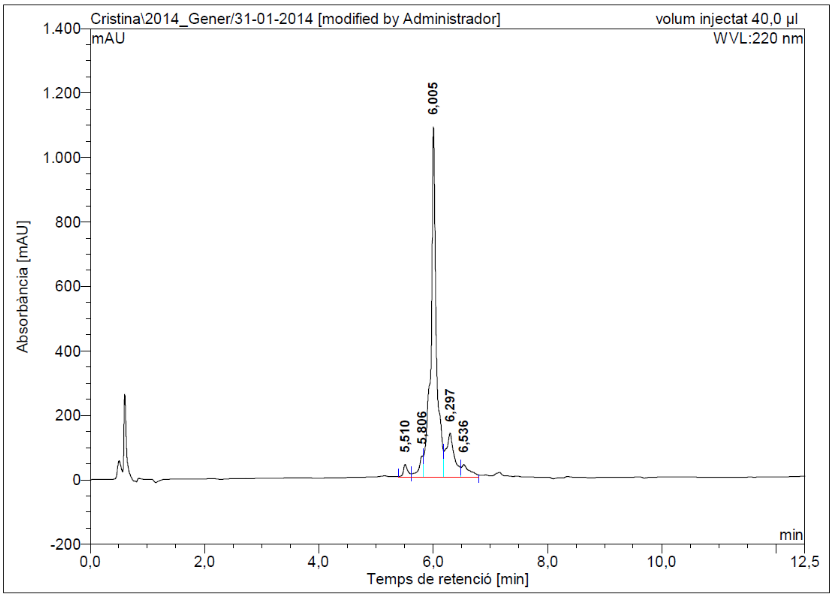

No.	Ret.Time (detected) min	Height mAU	Area mAU*min	Rel.Area %
1	5,51	40,488	3,823	2,39
2	5,81	66,347	6,357	3,97
3	6,01	1087,111	119,807	74,82
4	6,30	137,253	23,204	14,49
5	6,54	39,752	6,935	4,33
Total:		1370,951	160,127	100,00

MS (ESI) *m/z* (+)

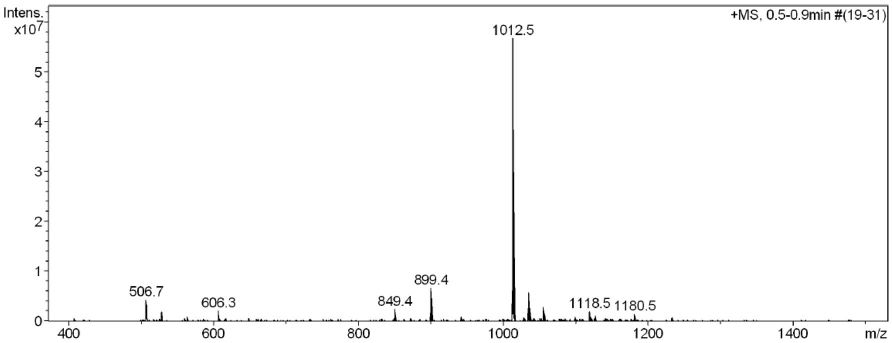

MS (ESI) *m/z* (-)

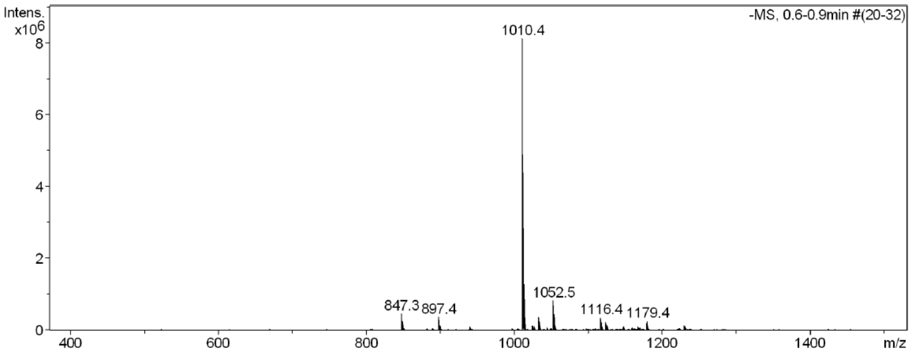

3.3.4. H-Tyr(O-Ile-H)-D-Ser-Glu-D-Val-Pro-Gln-D-Tyr-OH (BPC823)

HPLC (λ = 220 nm) (*Method A*)

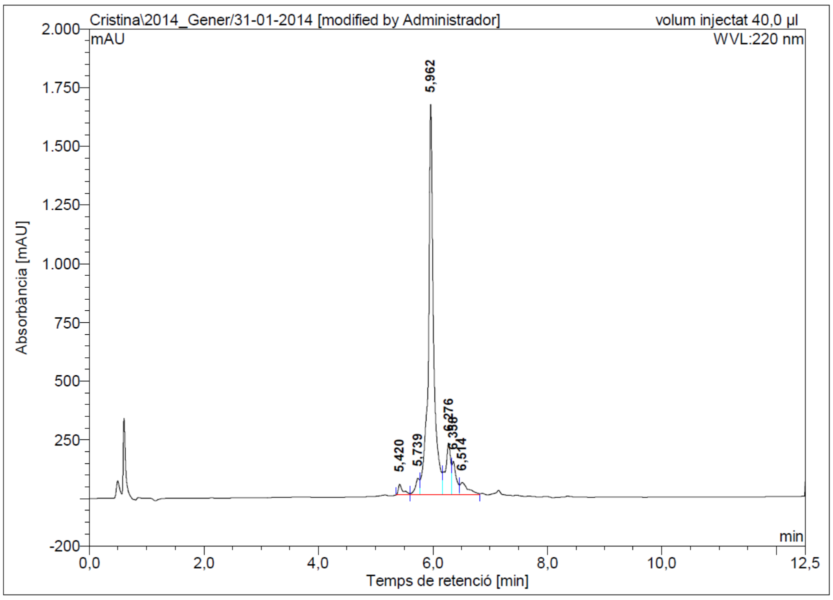

No.	Ret.Time (detected) min	Height mAU	Area mAU*min	Rel.Area %
1	5,42	45,393	4,455	1,91
2	5,74	71,417	5,937	2,55
3	5,96	1662,396	176,693	75,78
4	6,28	221,463	23,942	10,27
5	6,36	143,720	13,134	5,63
6	6,51	53,166	9,012	3,86
Total:		2197,555	233,173	100,00

MS (ESI) *m/z* (+)

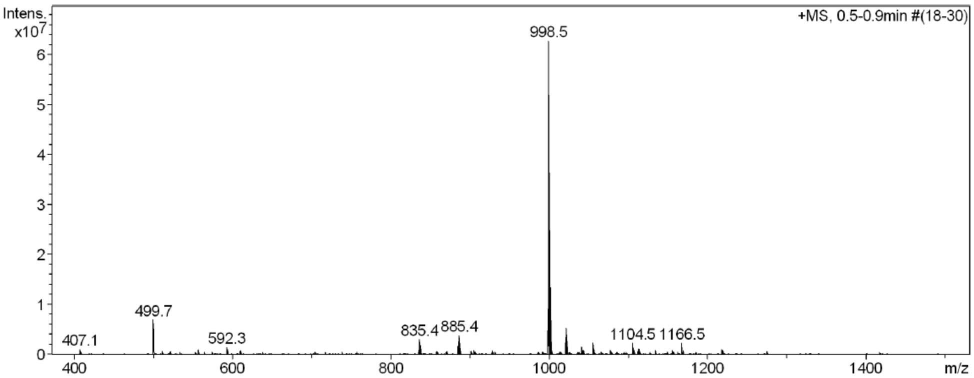

MS (ESI) *m/z* (-)

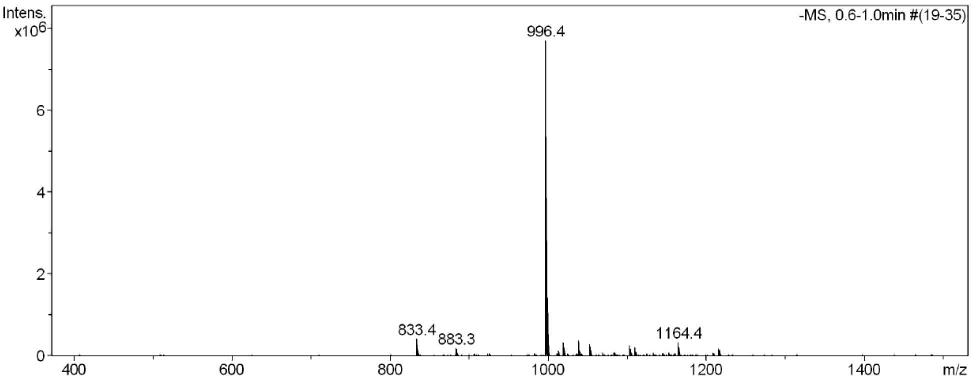

3.3.5. H-Tyr(O-Ile-H)-D-Thr-Glu-D-Ala-Pro-Gln-D-Tyr-OH (BPC825)

HPLC (*λ* = 220 nm) (*Method A*)

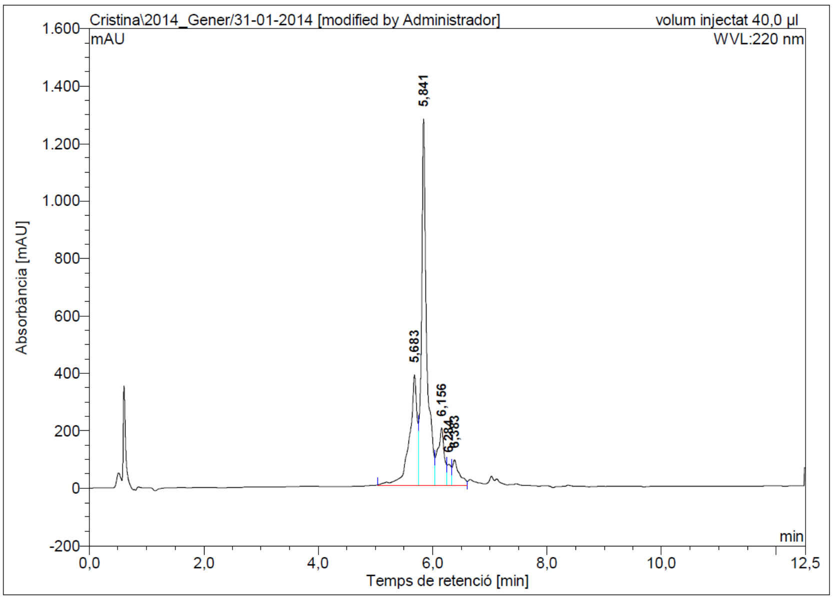

No.	Ret.Time (detected) min	Height mAU	Area mAU*min	Rel.Area %
1	5,68	384,217	59,682	25,06
2	5,84	1275,413	133,013	55,86
3	6,16	199,791	27,022	11,35
4	6,28	72,420	6,050	2,54
5	6,38	88,281	12,341	5,18
Total:		2020,121	238,108	100,00

MS (ESI) *m/z* (+)

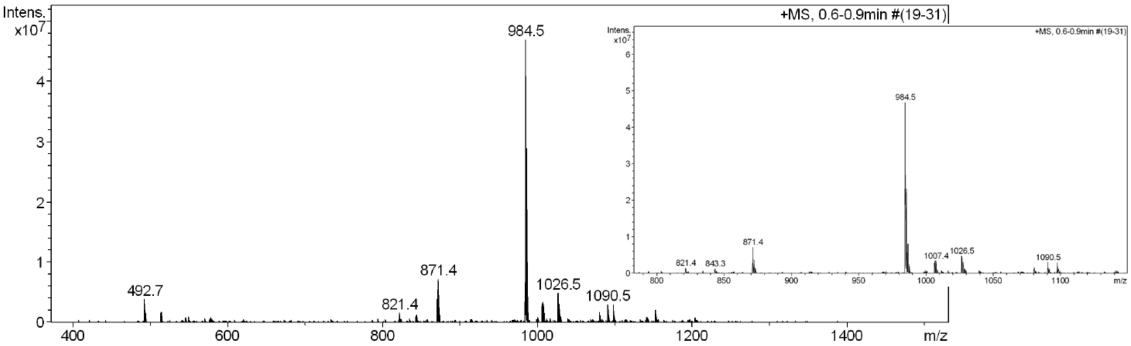

MS (ESI) *m/z* (-)

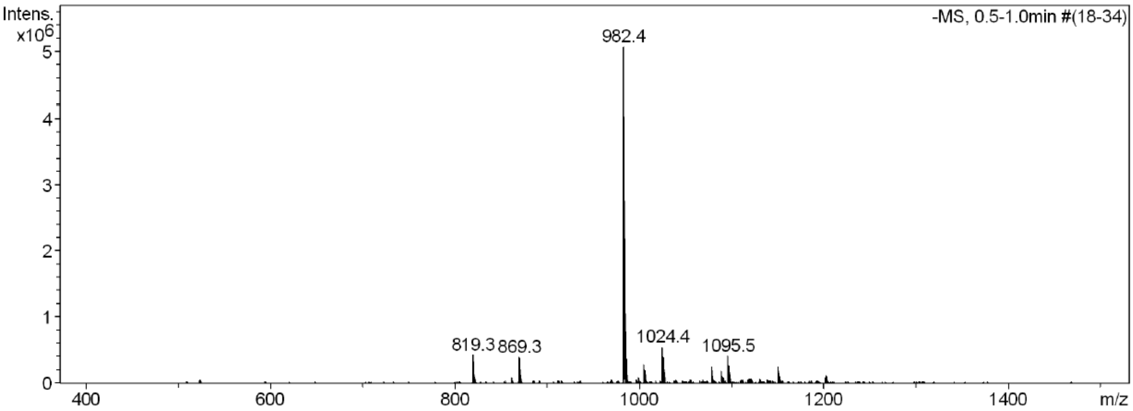

3.3.6. H-Tyr(O-Ile-H)-D-Ser-Glu-D-Ala-Pro-Gln-D-Tyr-OH (BPC827)

HPLC (λ = 220 nm) (*Method A*)

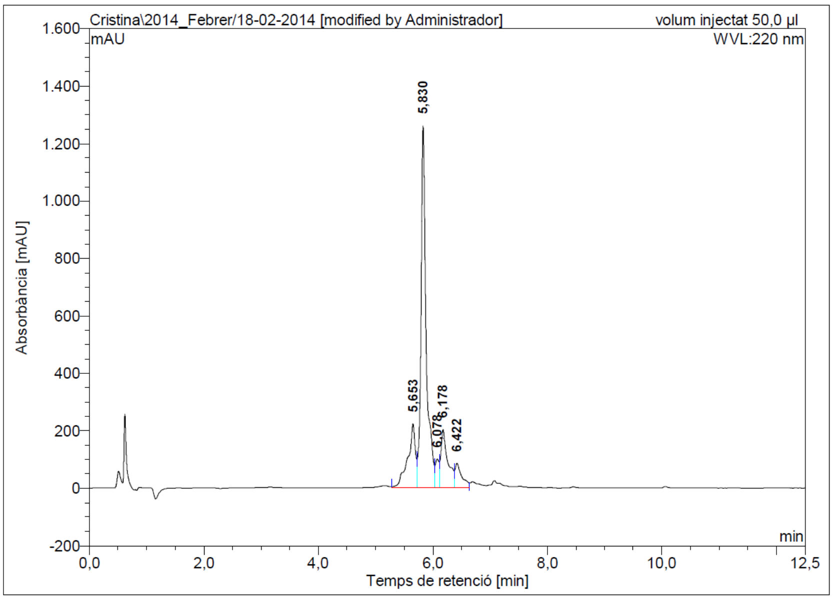

No.	Ret.Time (detected) min	Height mAU	Area mAU*min	Rel.Area %
1	5,65	222,387	33,838	15,86
2	5,83	1258,984	131,700	61,72
3	6,08	98,747	7,770	3,64
4	6,18	201,045	28,219	13,22
5	6,42	84,082	11,859	5,56
Total:		1865,244	213,386	100,00

MS (ESI) *m/z* (+)

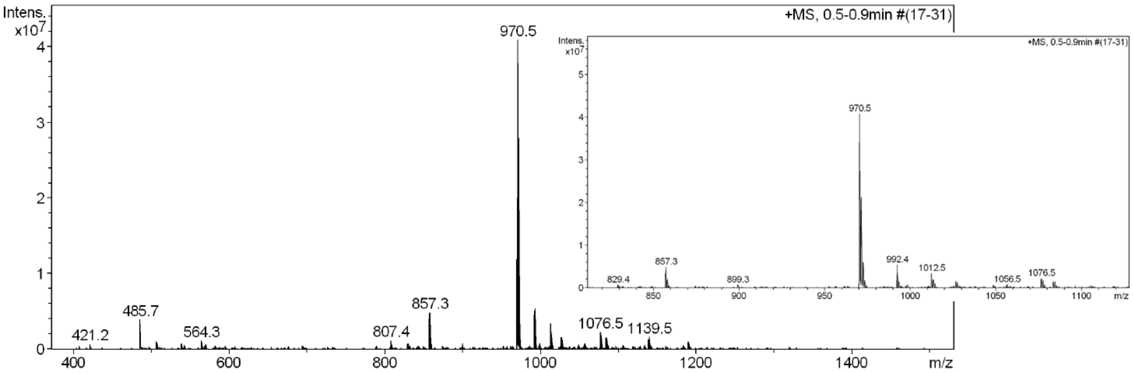

MS (ESI) *m/z* (-)

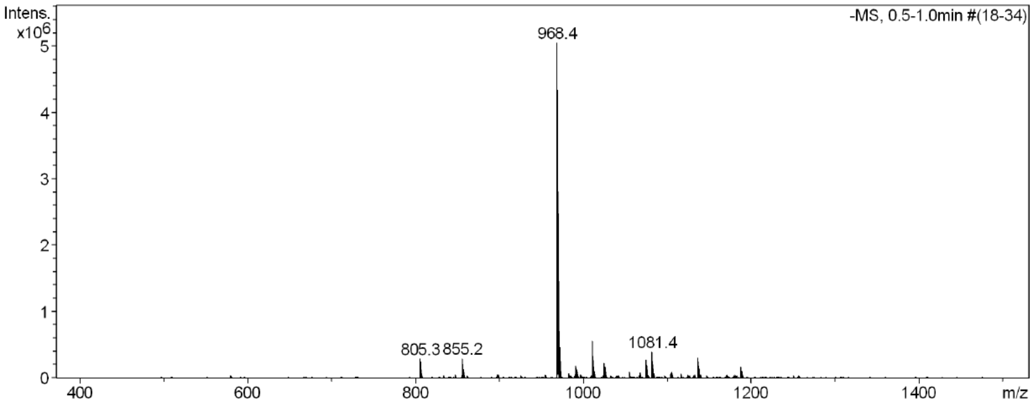

3.3.7. H-D-Tyr(O-Ile-H)-D-Thr-Glu-D-Val-Pro-Gln-Tyr-OH (BPC829)

HPLC (λ = 220 nm) (*Method A*)

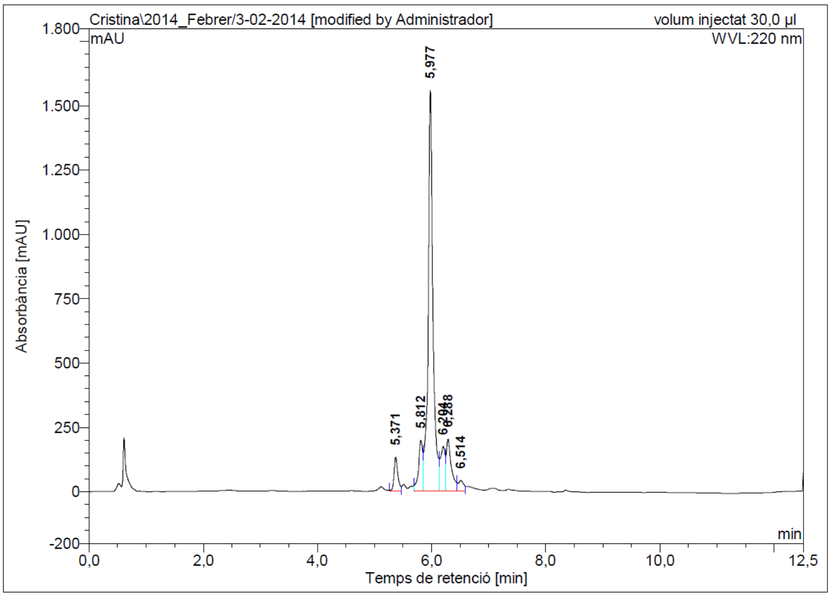

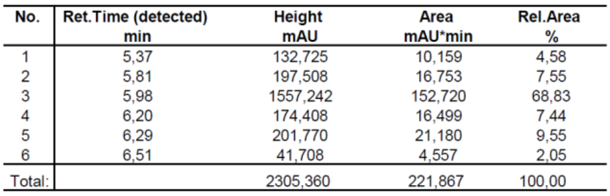

No.	Ret.Time (detected) min	Height mAU	Area mAU*min	Rel.Area %
1	5,37	132,725	10,159	4,58
2	5,81	197,508	16,753	7,55
3	5,98	1557,242	152,720	68,83
4	6,20	174,408	16,499	7,44
5	6,29	201,770	21,180	9,55
6	6,51	41,708	4,557	2,05
Total:		2305,360	221,867	100,00

MS (ESI) *m/z* (+)

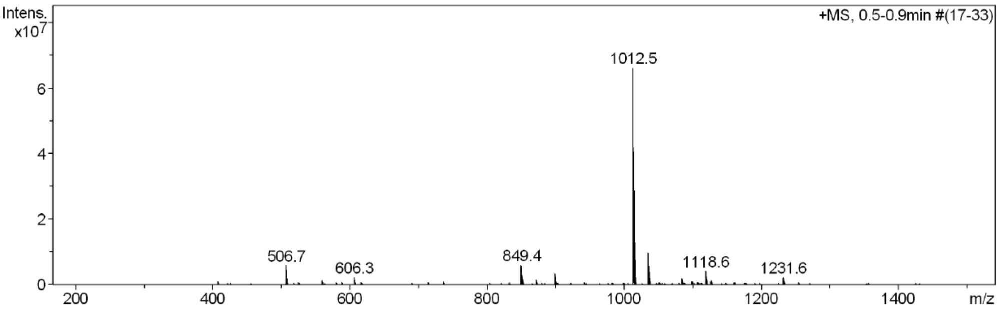

MS (ESI) *m/z* (-)

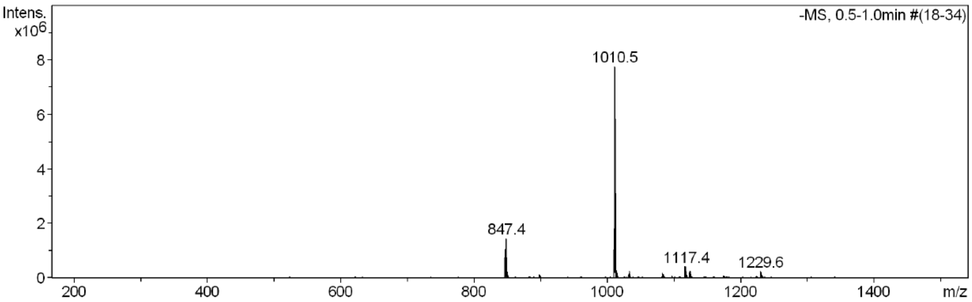

3.3.8. H-D-Tyr(O-Ile-H)-D-Ser-Glu-D-Val-Pro-Gln-Tyr-OH (BPC831)

HPLC (λ = 220 nm) (*Method A*)

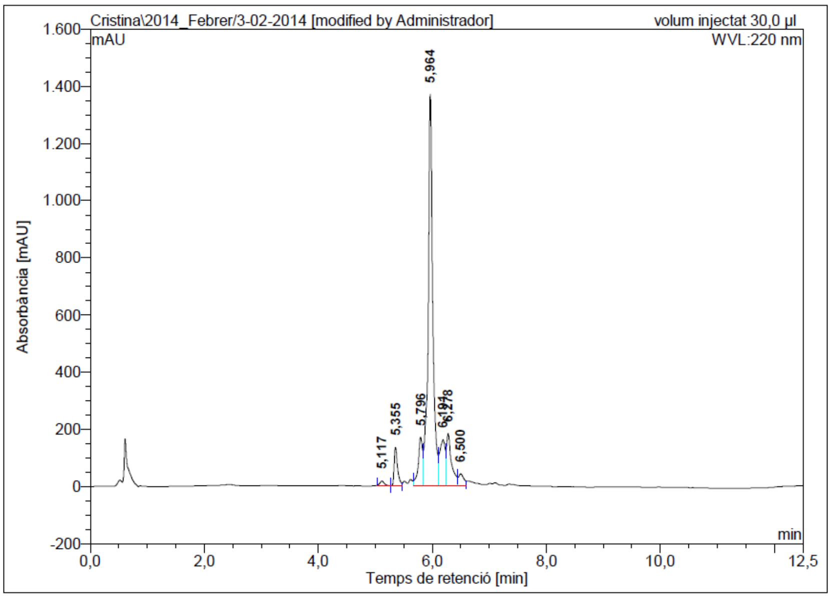

No.	Ret.Time (detected) min	Height mAU	Area mAU*min	Rel.Area %
1	5,12	17,498	1,772	0,89
2	5,35	135,511	9,626	4,83
3	5,80	170,962	14,785	7,42
4	5,96	1370,385	131,017	65,77
5	6,19	162,087	17,725	8,90
6	6,28	184,132	19,443	9,76
7	6,50	42,435	4,844	2,43
Total:		2083,009	199,210	100,00

MS (ESI) *m/z* (+)

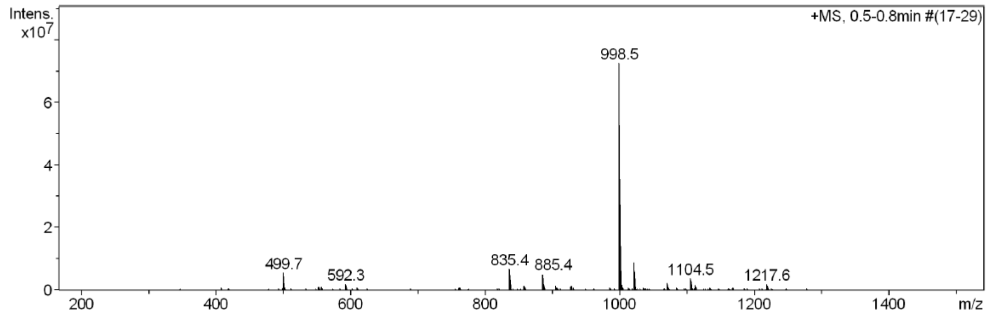

MS (ESI) *m/z* (-)

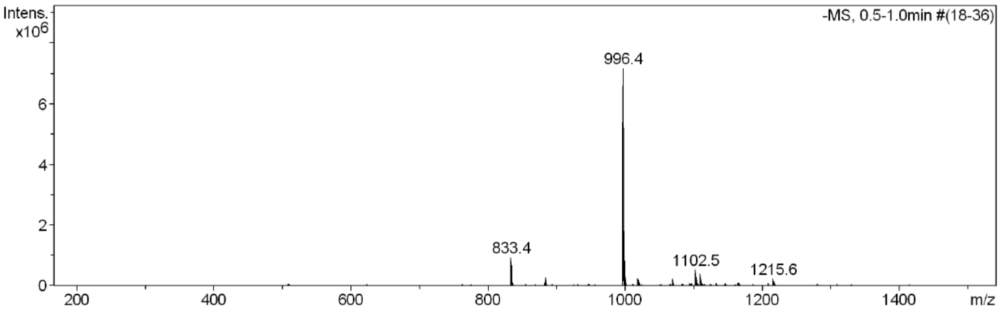

3.3.9. H-D-Tyr(O-Ile-H)-D-Thr-Glu-D-Ala-Pro-Gln-Tyr-OH (BPC833)

HPLC (λ = 220 nm) (*Method A*)

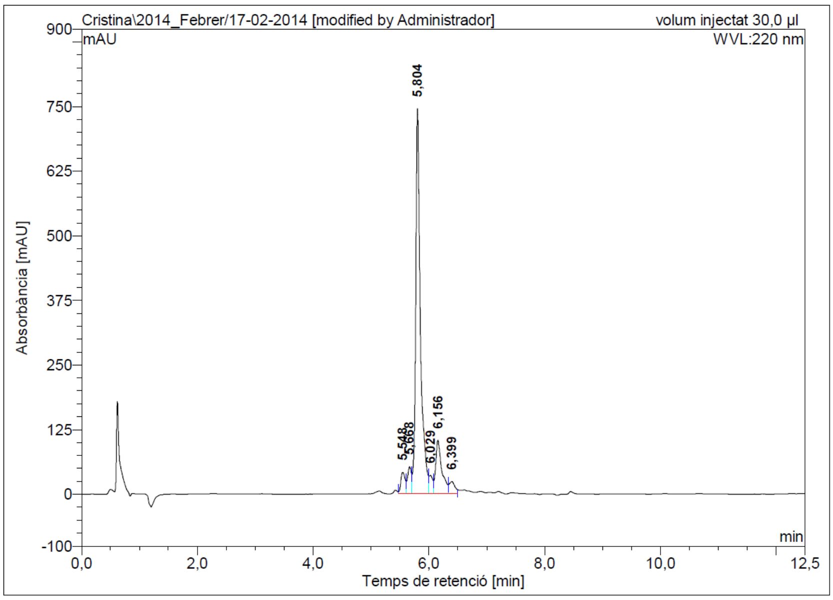

No.	Ret.Time (detected) min	Height mAU	Area mAU*min	Rel.Area %
1	5,55	41,298	3,611	3,76
2	5,67	51,879	3,933	4,09
3	5,80	744,776	70,344	73,21
4	6,03	35,097	2,709	2,82
5	6,16	103,135	12,609	13,12
6	6,40	23,494	2,876	2,99
Total:		999,679	96,081	100,00

MS (ESI) *m/z* (+)

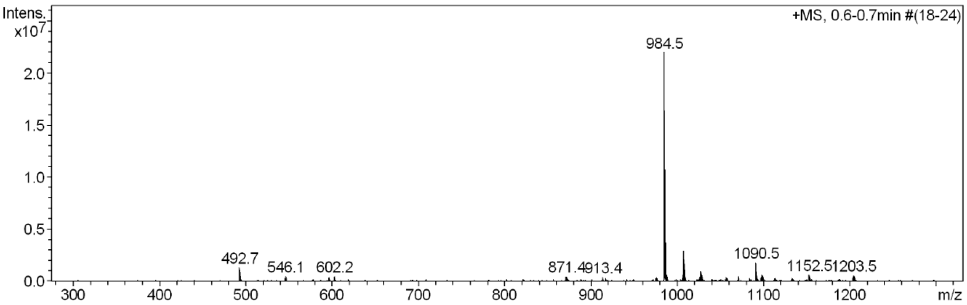

MS (ESI) *m/z* (-)

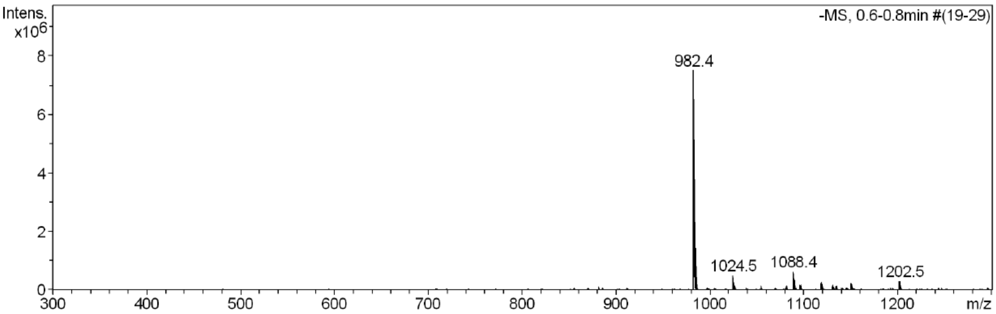

3.3.10. H-D-Tyr(O-Ile-H)-D-Ser-Glu-D-Ala-Pro-Gln-Tyr-OH (BPC835)

HPLC (λ = 220 nm) (*Method A*)

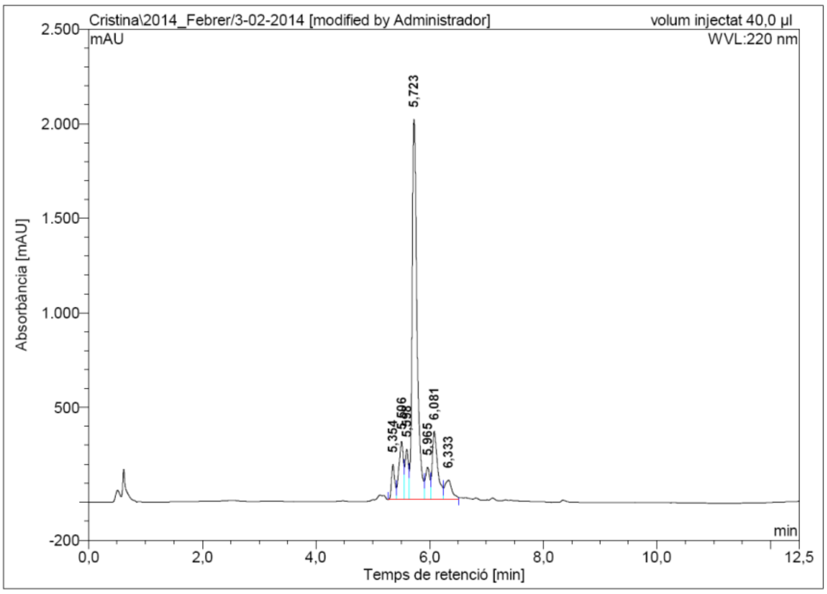

No.	Ret.Time (detected) min	Height mAU	Area mAU*min	Rel.Area %
1	5,35	184,948	12,292	3,73
2	5,51	307,449	28,659	8,69
3	5,60	264,955	18,315	5,55
4	5,72	2008,986	199,643	60,53
5	5,96	171,233	15,239	4,62
6	6,08	361,633	40,021	12,13
7	6,33	103,219	15,649	4,74
Total:		3402,424	329,819	100,00

MS (ESI) *m/z* (+)

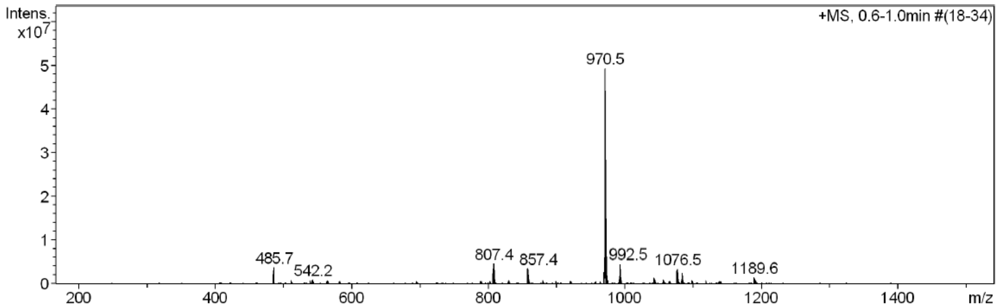

MS (ESI) *m/z* (-)

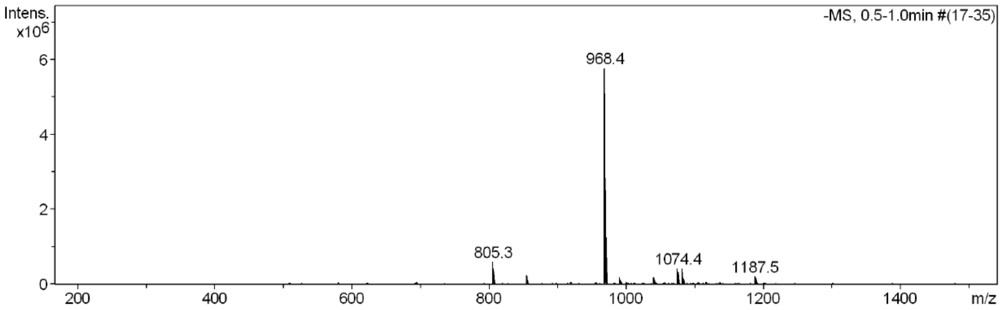

3.4. Cyclic depsipeptides

3.4.1. *p*NZ-Tyr(&)-D-Thr-Glu-D-Val-Pro-Gln-D-Tyr-Ile-& (8)

HPLC (λ = 220 nm) (*Method A*) (crude reaction)

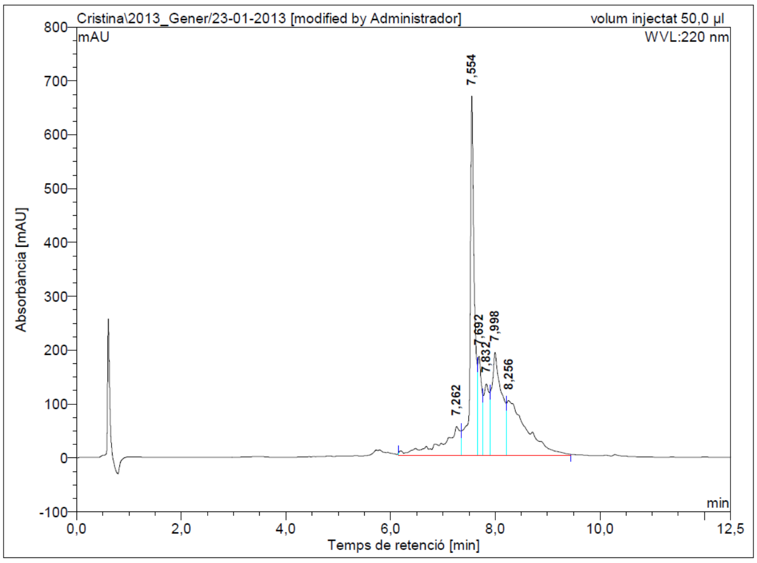

No.	Temps retenció min	alçada mAU	Area mAU*min	Area relativa %
1	7,26	53,443	22,905	11,07
2	7,55	667,242	63,462	30,66
3	7,69	184,172	16,607	8,02
4	7,83	132,609	15,890	7,68
5	8,00	191,299	41,801	20,19
6	8,26	101,703	46,336	22,38
Total:		1330,467	207,002	100,00

MS (ESI) *m/z* (+)

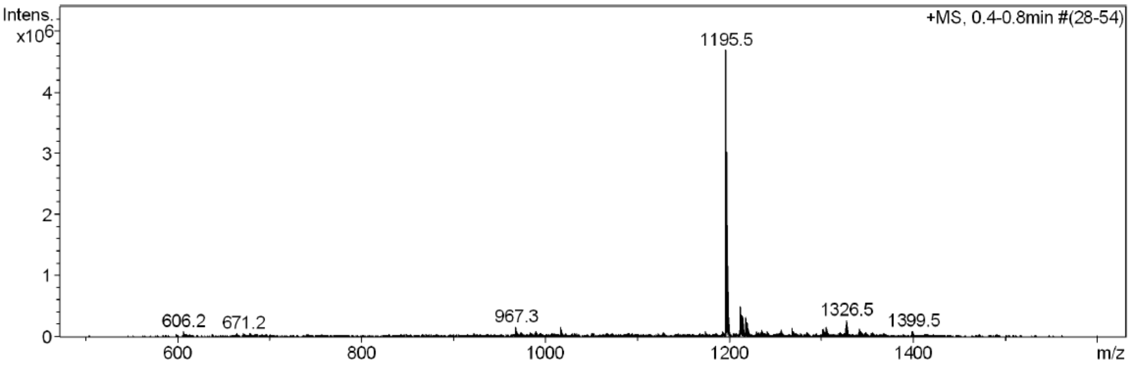

MS (ESI) *m/z* (-)

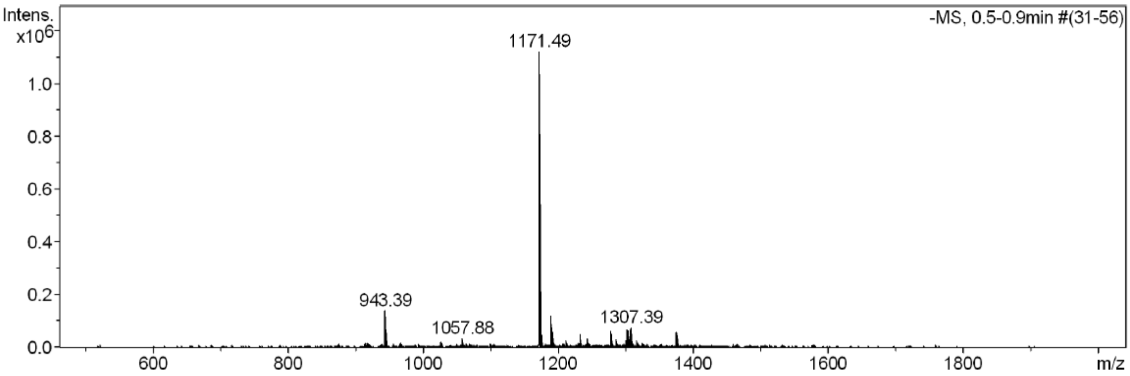

Hydrolysis of the crude reaction (8)

HPLC (λ = 220 nm) (*Method A*)

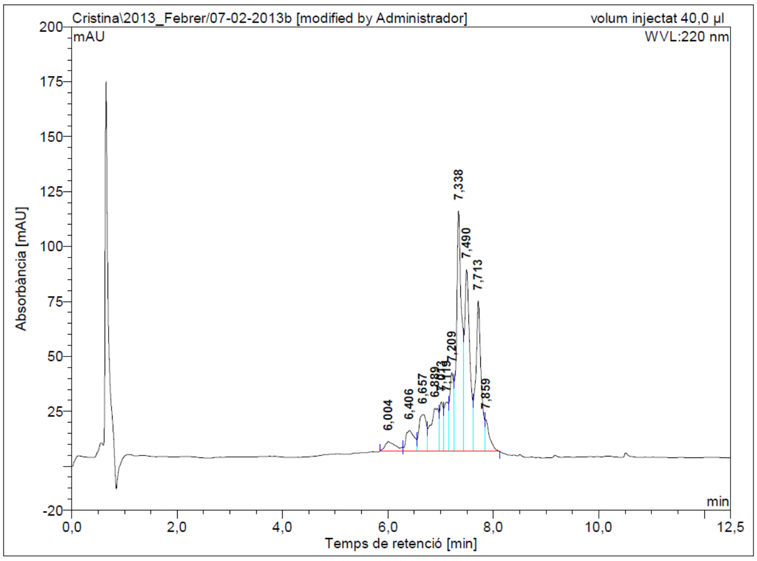

No.	Temps retenció min	alçada mAU	Area mAU*min	Area relativa %
1	6,00	4,393	1,054	2,23
2	6,41	9,344	1,778	3,75
3	6,66	16,673	2,666	5,63
4	6,89	19,524	3,489	7,37
5	7,01	22,424	1,641	3,47
6	7,12	22,431	2,146	4,53
7	7,21	35,707	3,209	6,78
8	7,34	109,389	12,452	26,29
9	7,49	82,490	9,251	19,54
10	7,71	68,423	8,146	17,20
11	7,86	14,308	1,523	3,22
Total:		405,106	47,357	100,00

MS (ESI) *m/z* (+)

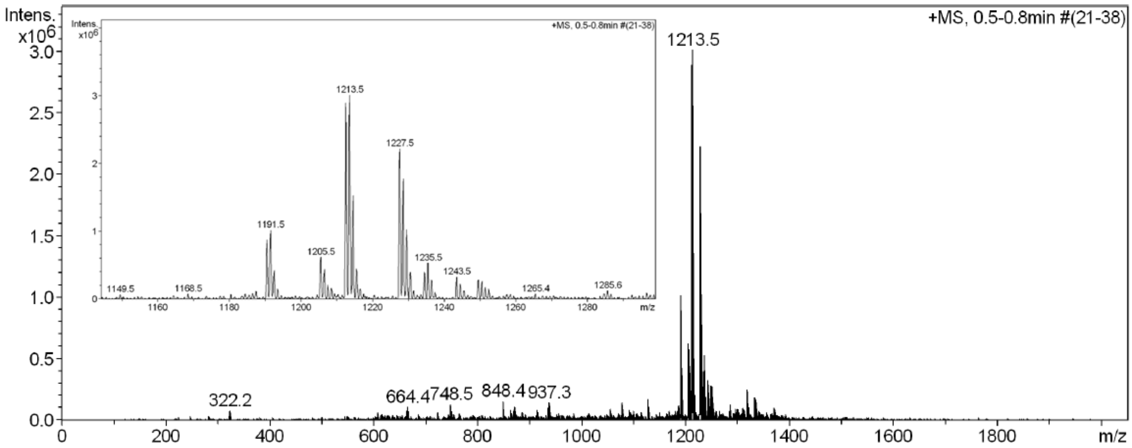

MS (ESI) *m/z* (-)

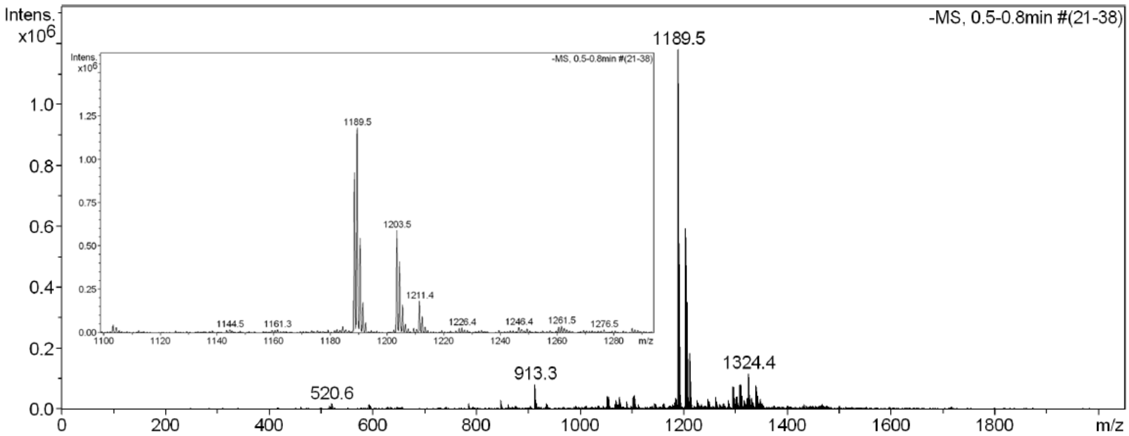

Intens.
x10^6
-MS, 0.5-0.8min #(21-38)
1189.5
1324.4
913.3
520.6
1.0
0.8
0.6
0.4
0.2
0.0
0
200
400
600
800
1000
1200
1400
1600
1800
m/z
Intens.
x10^6
-MS, 0.5-0.8min #(21-38)
1189.5
1203.5
1211.4
1144.5
1161.3
1226.4
1246.4
1261.5
1276.5
1.25
1.00
0.75
0.50
0.25
0.00
1100
1120
1140
1160
1180
1200
1220
1240
1260
1280
m/z

3.4.2. H-Tyr(&)-D-Thr-Glu-D-Val-Pro-Gln-D-Tyr-Ile-& (BPC822)

HPLC (λ = 220 nm) (*Method A*) (crude reaction)

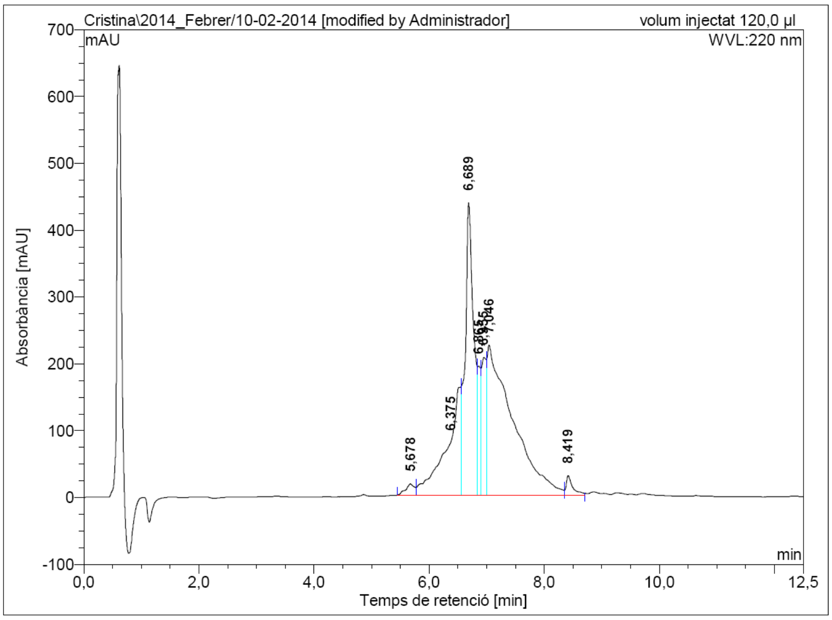

No.	Temps retenció min	alçada mAU	Area mAU*min	Area relativa %
1	5,68	16,890	3,104	1,12
2	6,38	78,309	46,306	16,69
3	6,69	437,766	75,491	27,20
4	6,87	193,057	12,380	4,46
5	6,95	206,197	19,096	6,88
6	7,05	224,806	117,166	42,22
7	8,42	29,566	3,947	1,42
Total:		1186,591	277,490	100,00

MS (ESI) *m/z* (+)

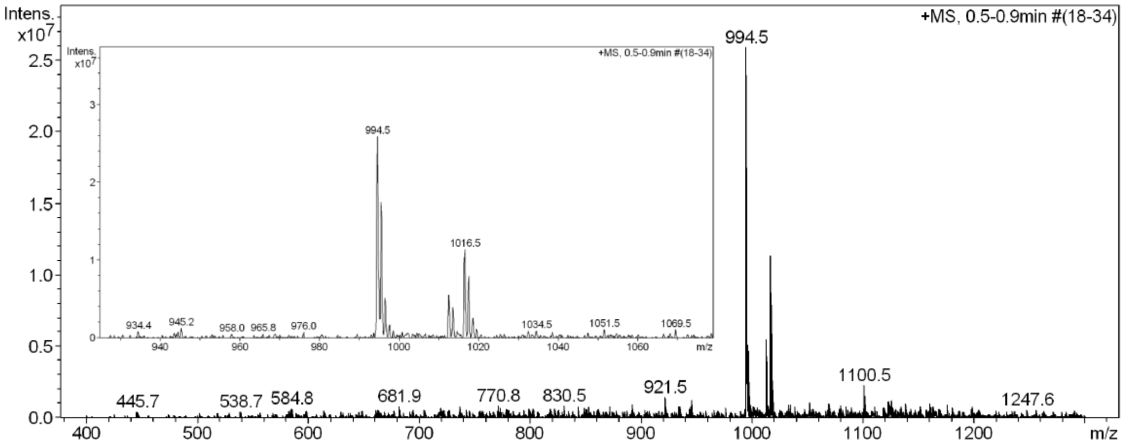

MS (ESI) *m/z* (-)

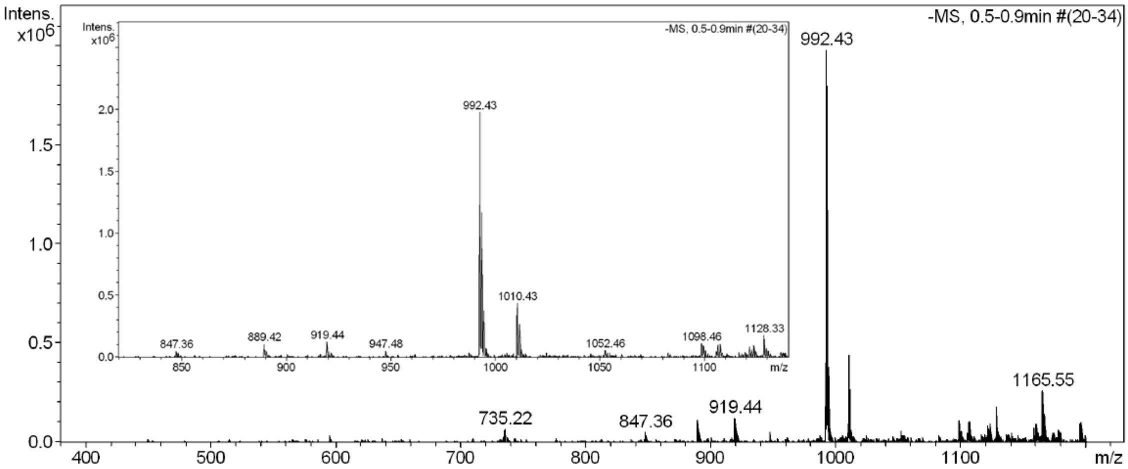
Intens.
x10^6
-MS, 0.5-0.9min #(20-34)
992.43
1165.55
919.44
847.36
735.22
0.0
0.5
1.0
1.5
400
500
600
700
800
900
1000
1100
m/z
Intens.
x10^6
-MS, 0.5-0.9min #(20-34)
992.43
1010.43
847.36
889.42
919.44
947.48
1052.46
1098.46
1128.33
0.0
0.5
1.0
1.5
2.0
850
900
950
1000
1050
1100
m/z

Purification of BPC822

HPLC (λ = 220 nm) (*Method A*)

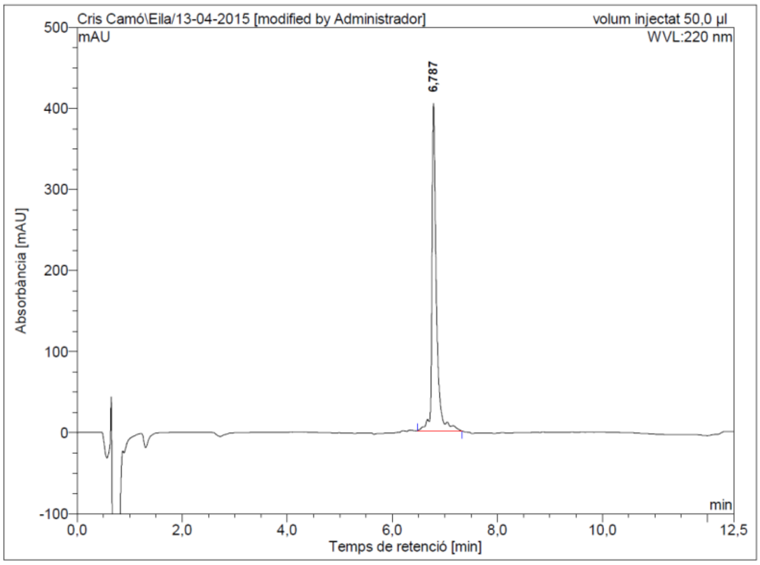

No.	Temps retenció min	alçada mAU	Area mAU*min	Area relativa %
1	6,79	403,598	39,182	100,00
Total:		403,598	39,182	100,00

MS (ESI) *m/z* (+)

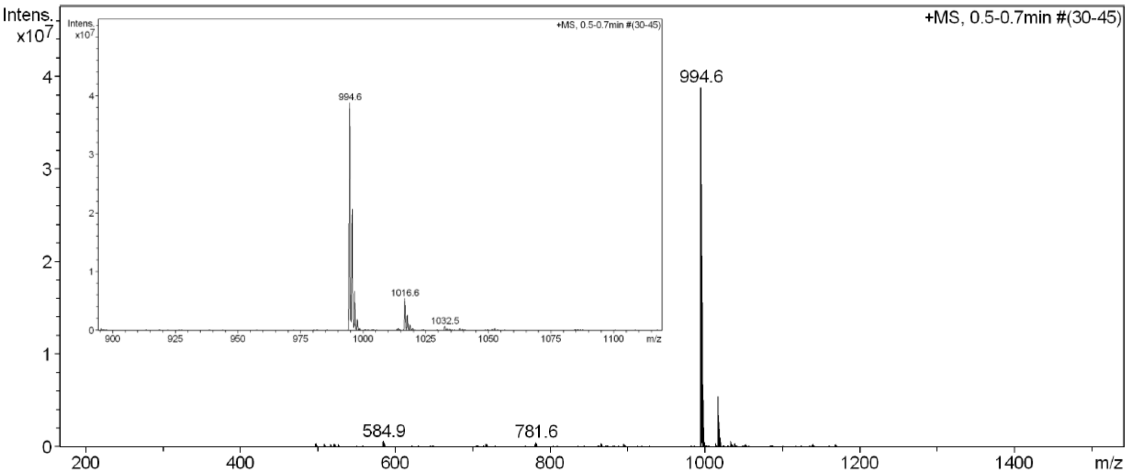

MS (ESI) *m/z* (-)

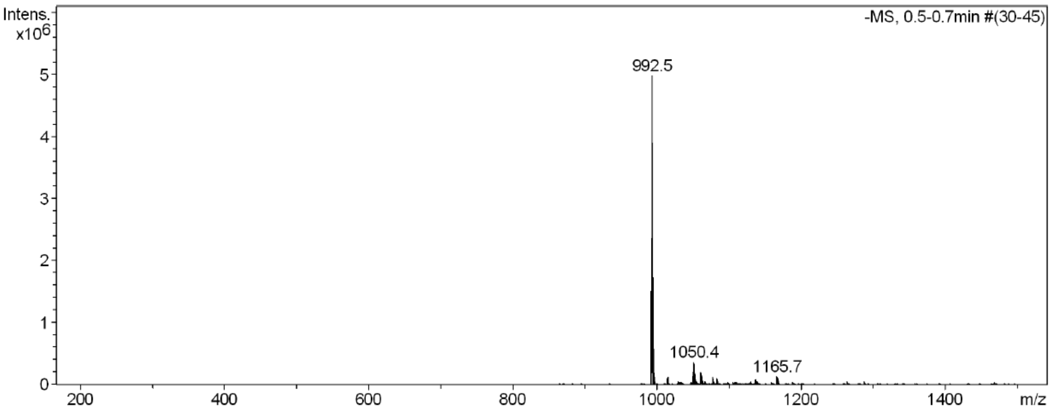

HRMS (ESI) *m/z* (+)

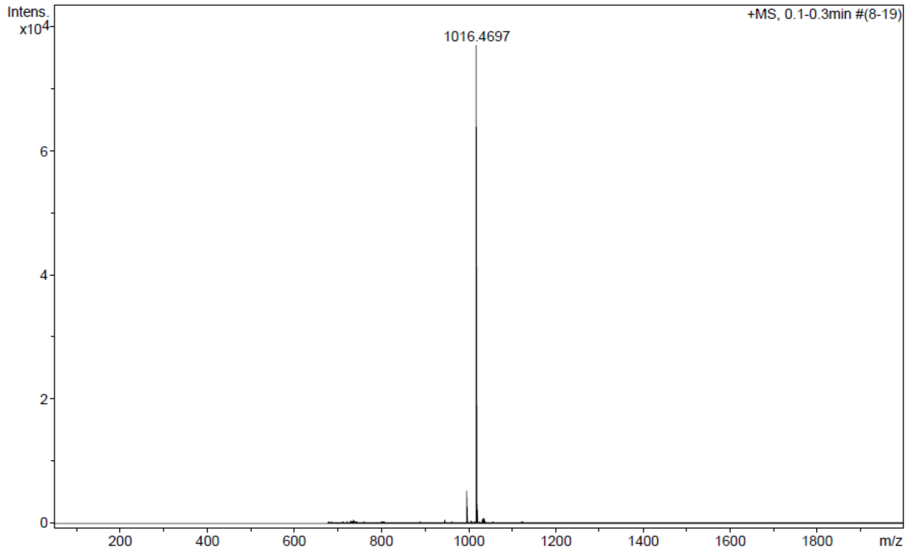

Intens.
x10^4
+MS, 0.1-0.3min #(8-19)
1016.4697
6
4
2
0
200
400
600
800
1000
1200
1400
1600
1800
m/z

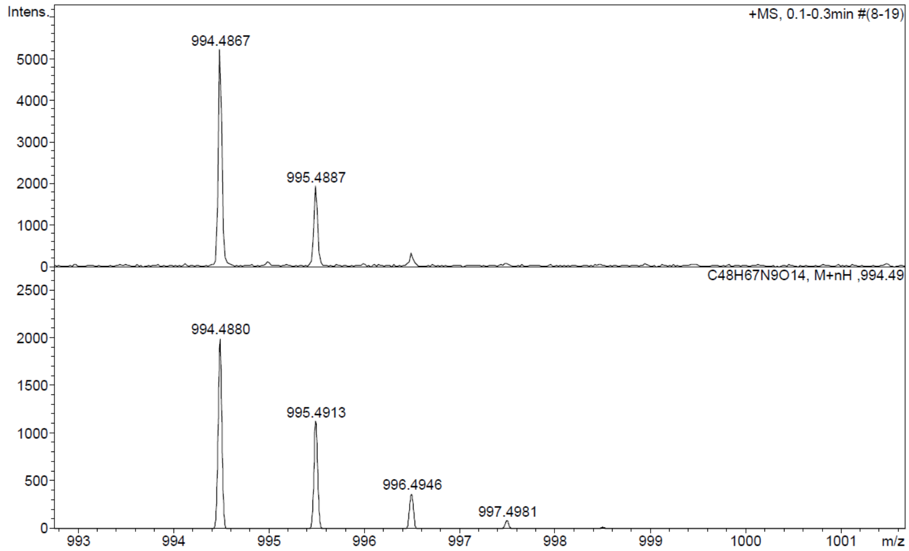

Intens.
+MS, 0.1-0.3min #(8-19)
994.4867
995.4887
5000
4000
3000
2000
1000
0
C48H67N9O14, M+nH ,994.49
2500
994.4880
995.4913
996.4946
997.4981
2000
1500
1000
500
0
993
994
995
996
997
998
999
1000
1001
m/z

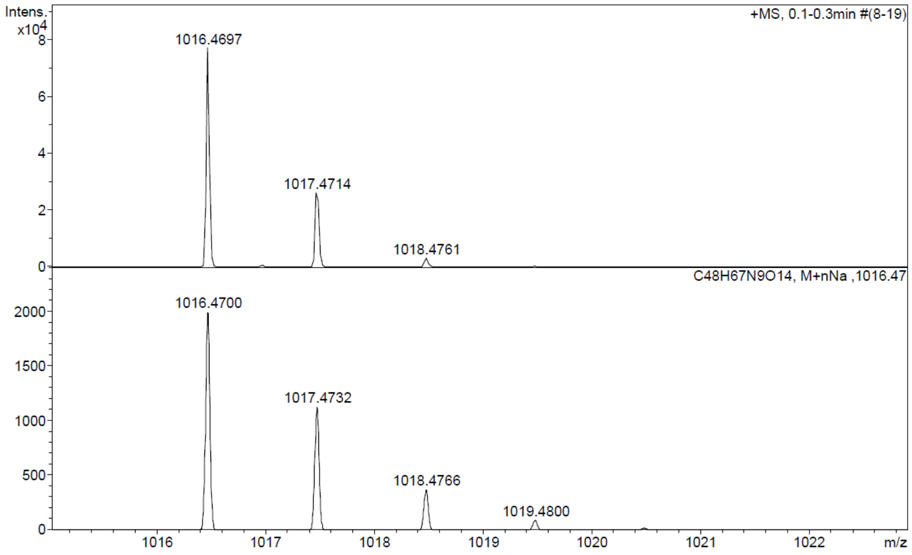

Intens.
x10^4
+MS, 0.1-0.3min #(8-19)
1016.4697
1017.4714
1018.4761
8
6
4
2
0
C48H67N9O14, M+nNa ,1016.47
1016.4700
1017.4732
1018.4766
1019.4800
2000
1500
1000
500
0
1016
1017
1018
1019
1020
1021
1022
m/z

Hydrolysis of the crude reaction (BPC822)

HPLC (λ = 220 nm) (*Method A*)

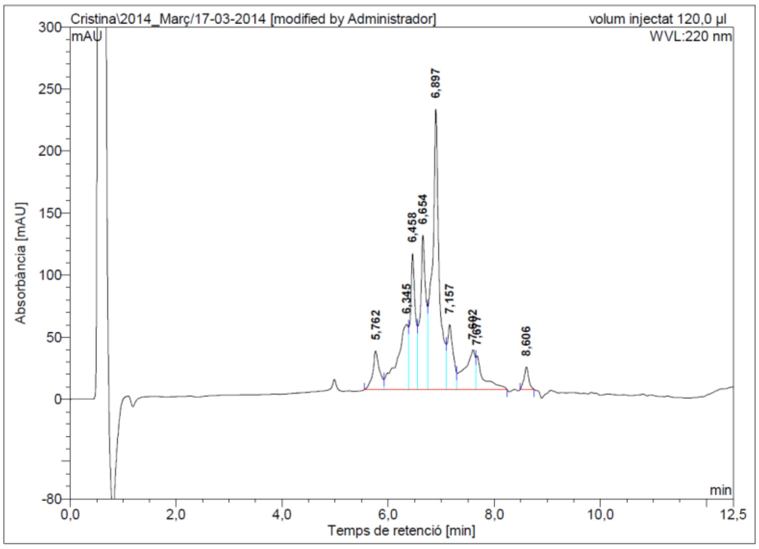

No.	Ret.Time (detected) min	Height mAU	Area mAU*min	Rel.Area %
1	5,76	31,293	4,724	4,70
2	6,35	52,495	12,663	12,60
3	6,46	109,586	12,476	12,41
4	6,65	124,601	15,516	15,44
5	6,90	226,093	34,091	33,92
6	7,16	52,342	7,171	7,14
7	7,60	32,119	7,265	7,23
8	7,68	27,253	4,722	4,70
9	8,61	18,344	1,868	1,86
Total:		674,126	100,496	100,00

MS (ESI) *m/z* (+)

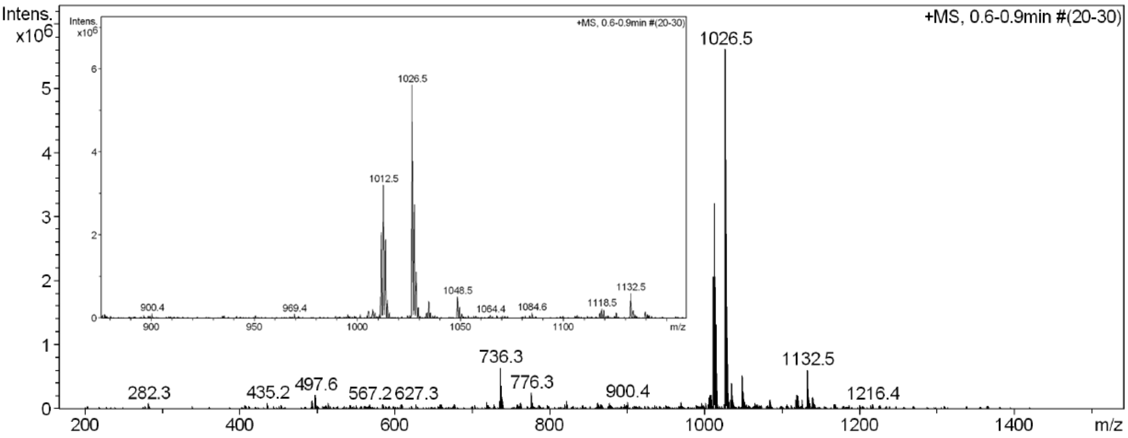

MS (ESI) *m/z* (-)

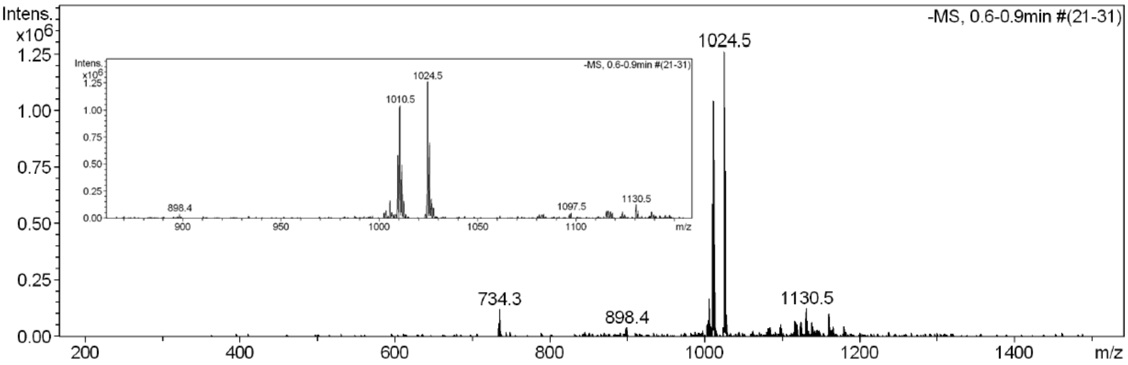

3.4.3. H-Tyr(&)-D-Ser-Glu-D-Val-Pro-Gln-D-Tyr-Ile-& (BPC824)

HPLC (λ = 220 nm) (*Method A*) (crude reaction)

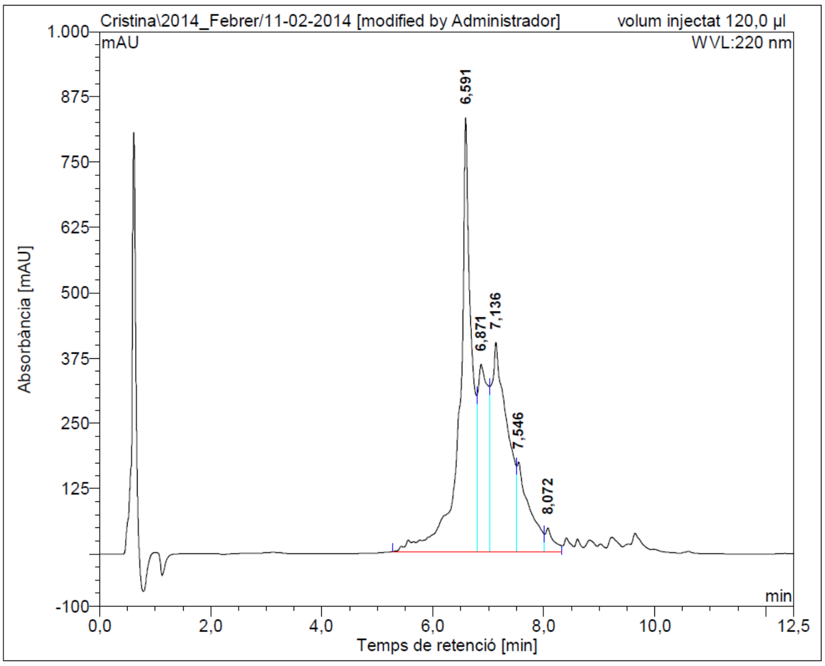

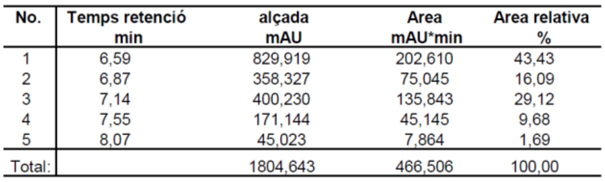

No.	Temps retenció min	alçada mAU	Area mAU*min	Area relativa %
1	6,59	829,919	202,610	43,43
2	6,87	358,327	75,045	16,09
3	7,14	400,230	135,843	29,12
4	7,55	171,144	45,145	9,68
5	8,07	45,023	7,864	1,69
Total:		1804,643	466,506	100,00

MS (ESI) *m/z* (+)

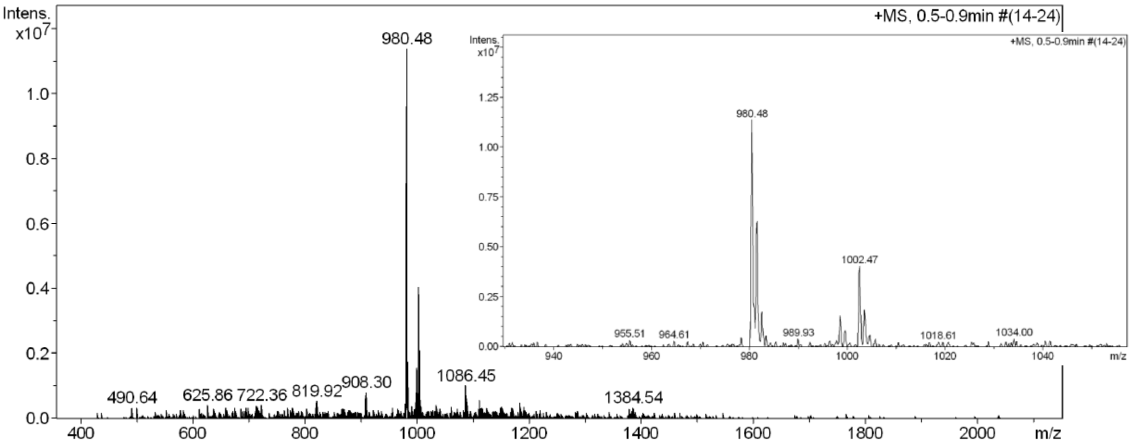

MS (ESI) *m/z* (-)

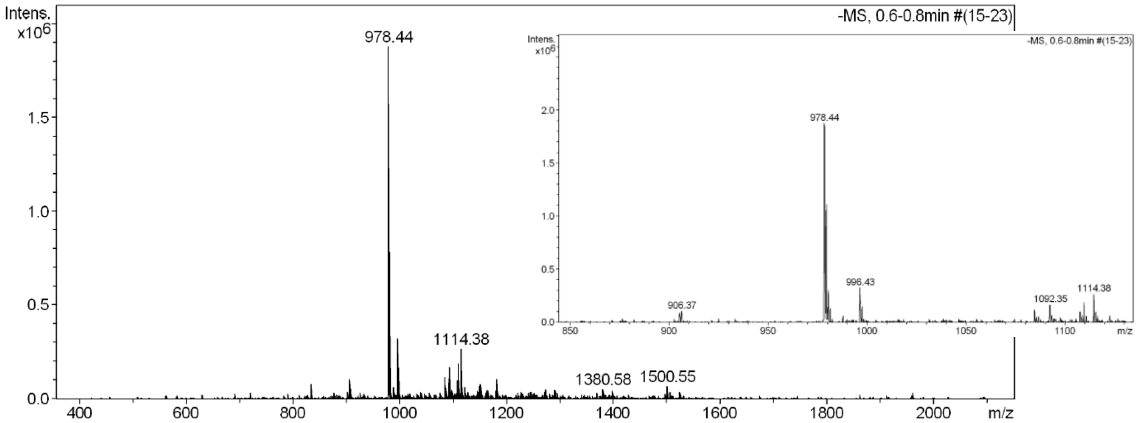

Intens.
x10^6
-MS, 0.6-0.8min #(15-23)
978.44
1114.38
1380.58
1500.55
1.5
1.0
0.5
0.0
400
600
800
1000
1200
1400
1600
1800
2000
m/z
Intens.
x10^6
-MS, 0.6-0.8min #(15-23)
978.44
996.43
906.37
1092.35
1114.38
2.0
1.5
1.0
0.5
0.0
850
900
950
1000
1050
1100
m/z

Purification of BPC824

HPLC (λ = 220 nm) (*Method A*)

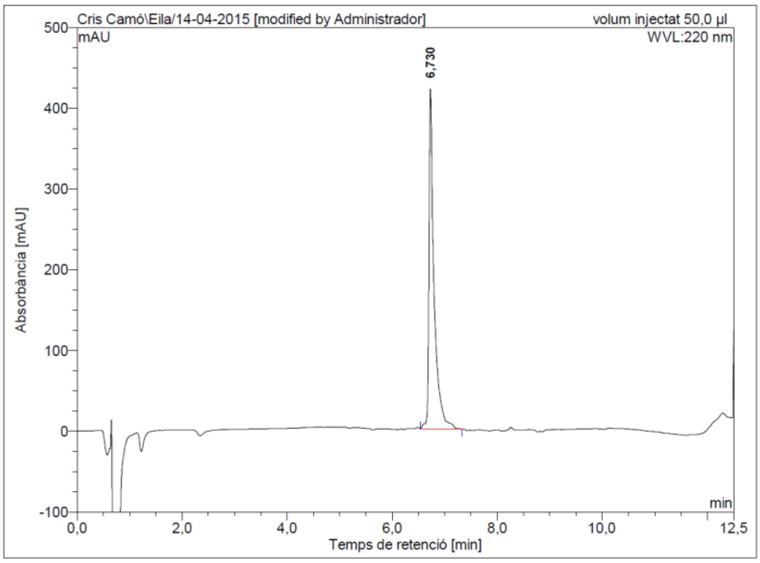

No.	Temps retenció min	alçada mAU	Area mAU*min	Area relativa %
1	6,73	421,544	47,069	100,00
Total:		421,544	47,069	100,00

MS (ESI) *m/z* (+)

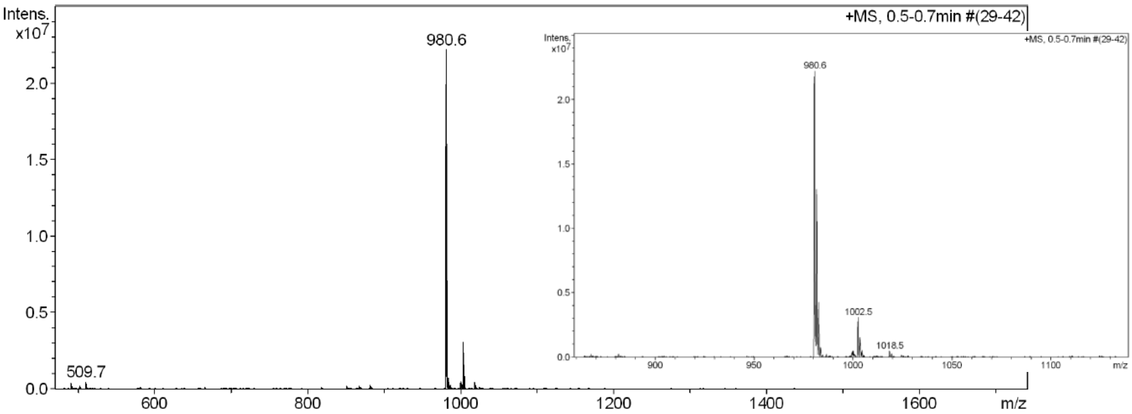

HRMS (ESI) *m/z* (+)

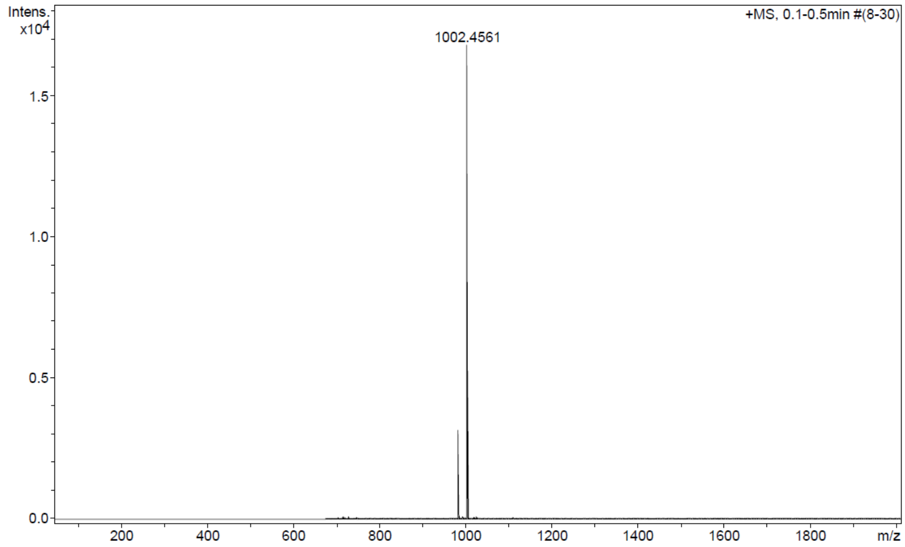
Intens.
x10^4
+MS, 0.1-0.5min #(8-30)
1002.4561
1.5
1.0
0.5
0.0
200
400
600
800
1000
1200
1400
1600
1800
m/z

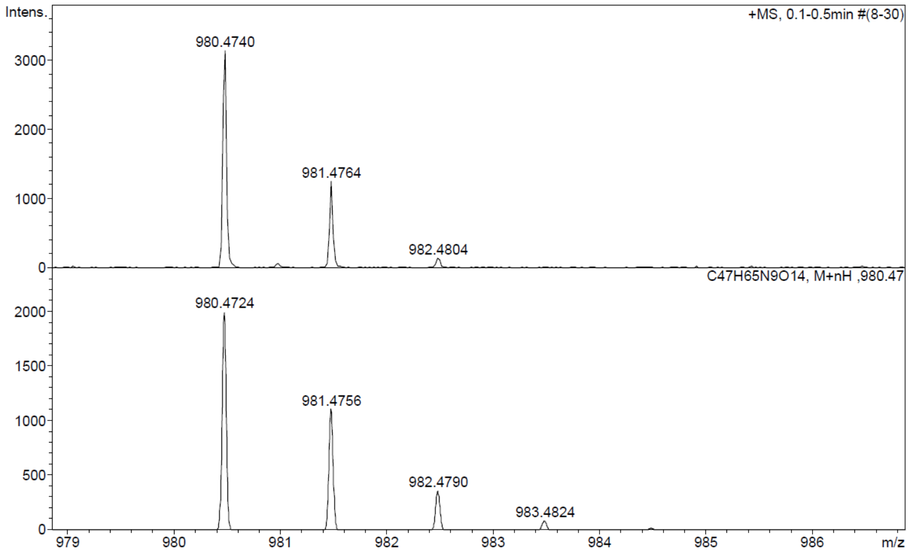
Intens.
+MS, 0.1-0.5min #(8-30)
980.4740
981.4764
982.4804
3000
2000
1000
0
C47H65N9O14, M+nH ,980.47
980.4724
981.4756
982.4790
983.4824
2000
1500
1000
500
0
979
980
981
982
983
984
985
986
m/z

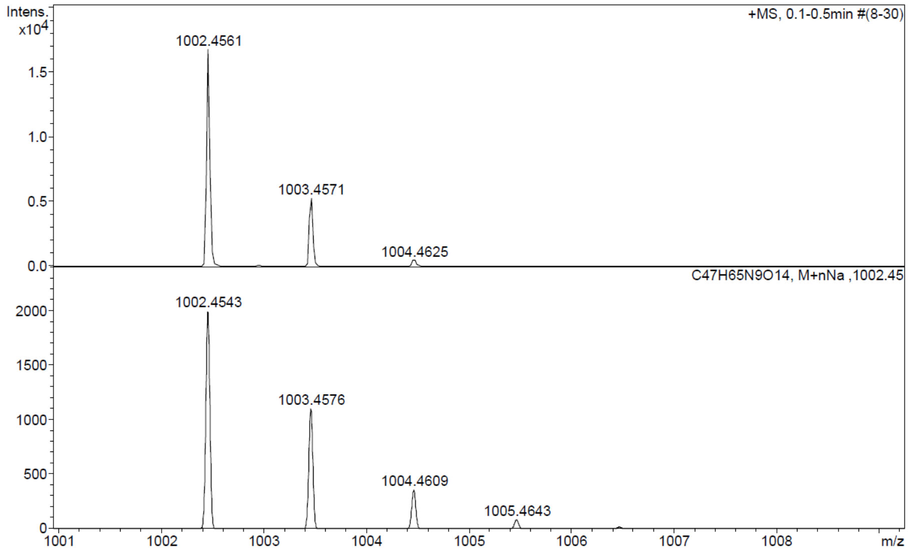
Intens.
x10^4
+MS, 0.1-0.5min #(8-30)
1002.4561
1003.4571
1004.4625
1.5
1.0
0.5
0.0
C47H65N9O14, M+nNa ,1002.45
1002.4543
1003.4576
1004.4609
1005.4643
2000
1500
1000
500
0
1001
1002
1003
1004
1005
1006
1007
1008
m/z

Hydrolysis of the crude reaction (BPC824)

HPLC (λ = 220 nm) (*Method A*)

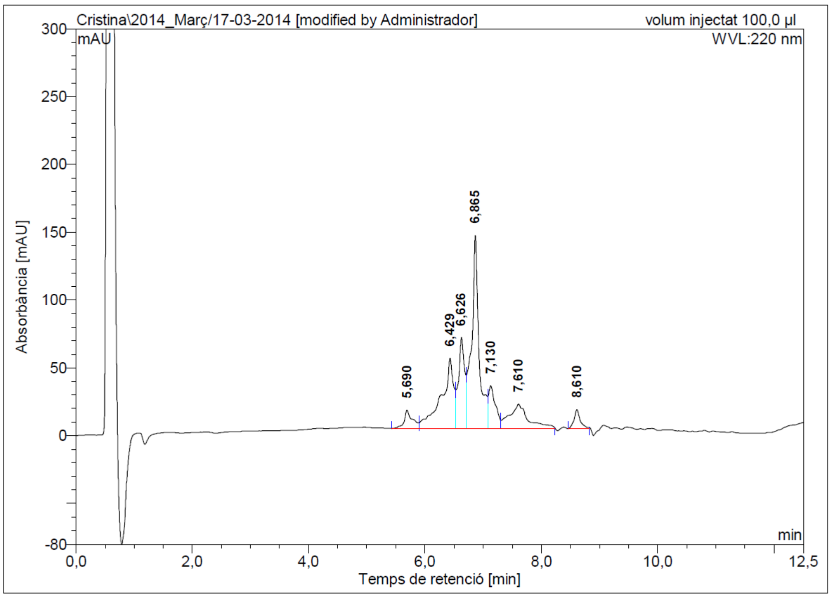

No.	Ret.Time (detected) min	Height mAU	Area mAU*min	Rel.Area %
1	5,69	13,511	2,226	3,87
2	6,43	51,922	12,711	22,08
3	6,63	67,142	8,300	14,42
4	6,86	142,212	21,434	37,23
5	7,13	31,610	4,427	7,69
6	7,61	17,990	6,794	11,80
7	8,61	13,959	1,682	2,92
Total:		338,346	57,574	100,00

MS (ESI) *m/z* (+)

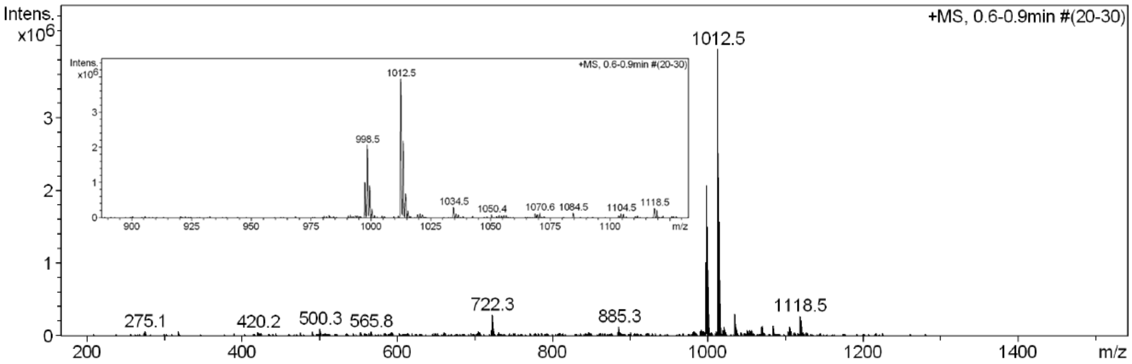

MS (ESI) *m/z* (-)

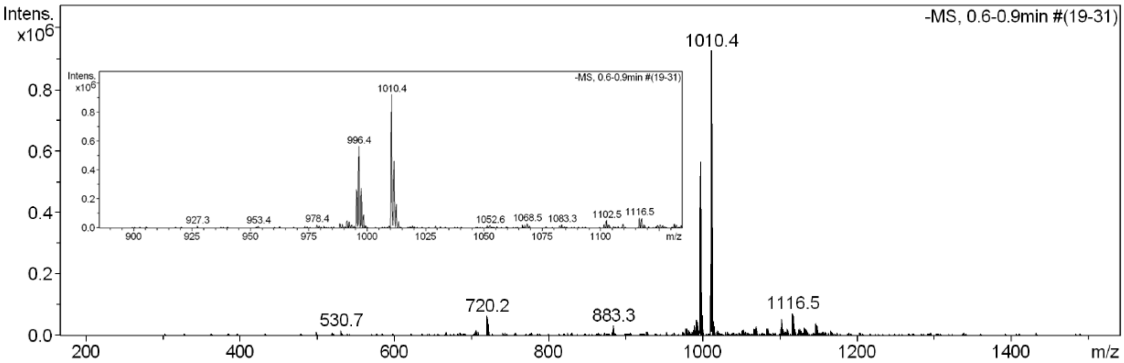

3.4.4. H-Tyr(&)-D-Thr-Glu-D-Ala-Pro-Gln-D-Tyr-Ile-& (BPC826)

HPLC (λ = 220 nm) (*Method A*) (crude reaction)

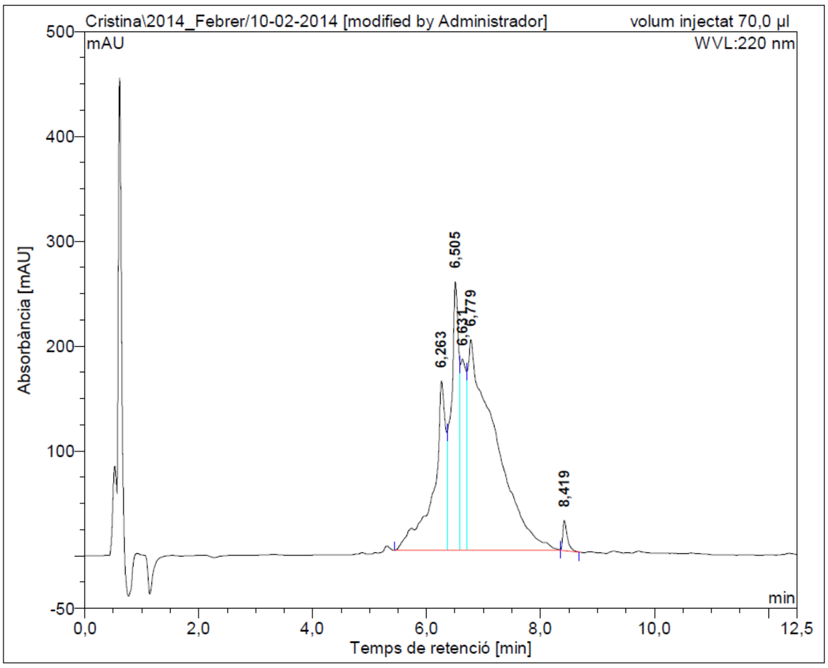

No.	Temps retenció min	alçada mAU	Area mAU*min	Area relativa %
1	6,26	161,266	40,568	18,47
2	6,50	255,866	42,285	19,25
3	6,63	182,297	20,363	9,27
4	6,78	200,723	113,801	51,81
5	8,42	28,692	2,616	1,19
Total:		828,845	219,633	100,00

MS (ESI) *m/z* (+)

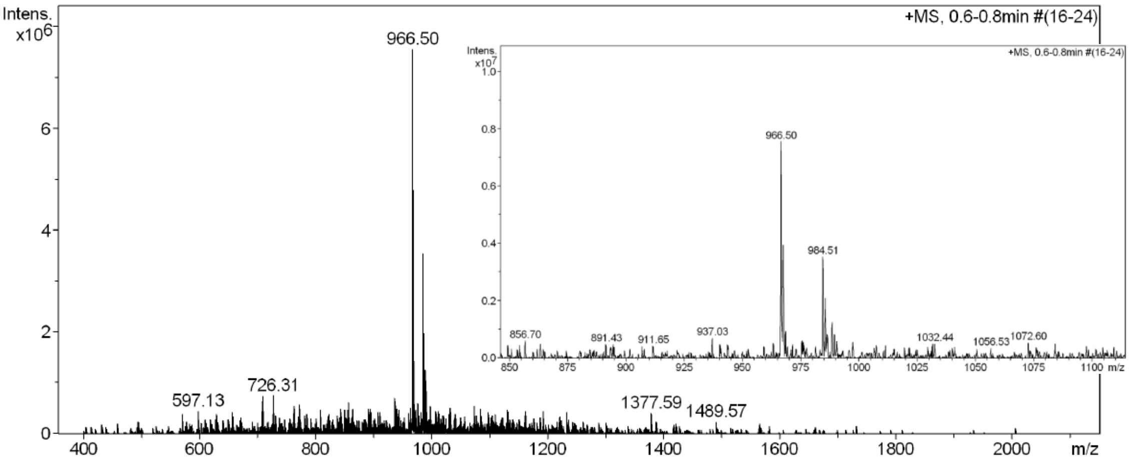

MS (ESI) *m/z* (-)

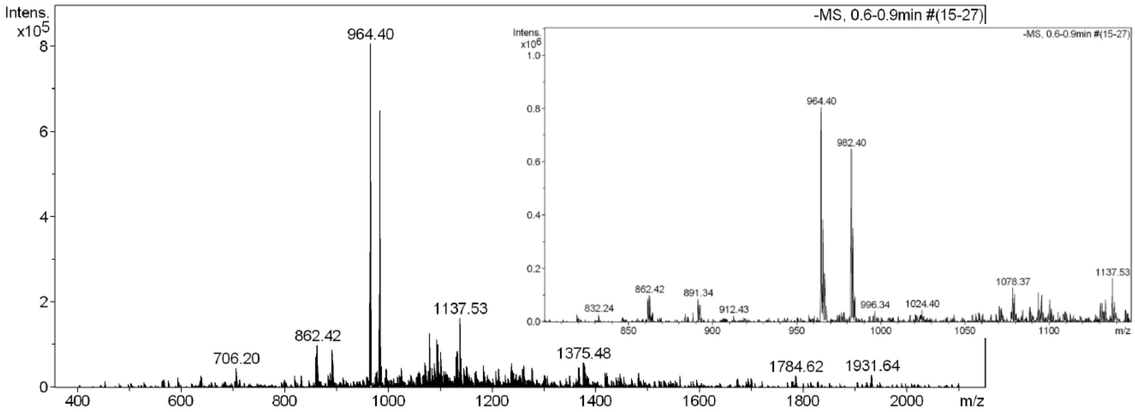

Intens.
x10^5
-MS, 0.6-0.9min #(15-27)
964.40
1137.53
862.42
706.20
1375.48
1784.62
1931.64
0
2
4
6
8
400
600
800
1000
1200
1400
1600
1800
2000
m/z
Intens.
x10^6
-MS, 0.6-0.9min #(15-27)
1.0
0.8
0.6
0.4
0.2
0.0
964.40
982.40
832.24
862.42
891.34
912.43
996.34
1024.40
1078.37
1137.53
850
900
950
1000
1050
1100
m/z

Purification of BPC826

HPLC (λ = 220 nm) (*Method A*)

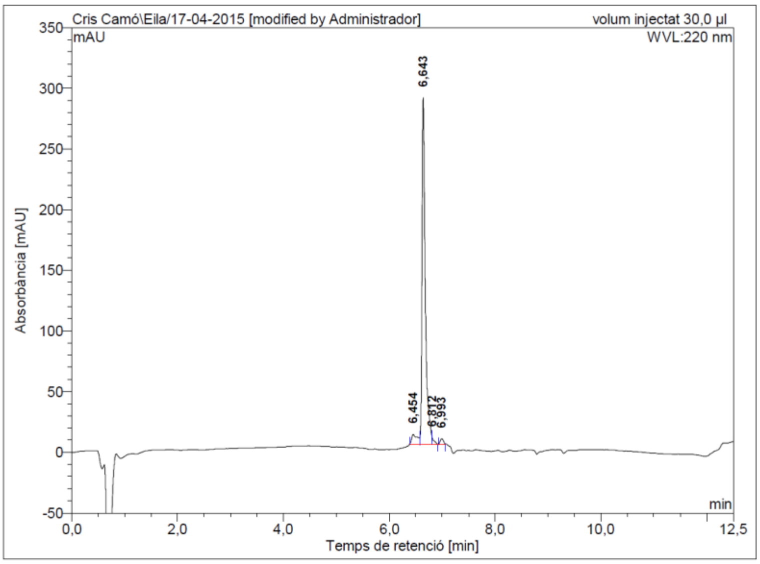

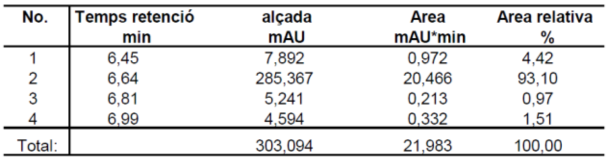

No.	Temps retenció min	alçada mAU	Area mAU*min	Area relativa %
1	6,45	7,892	0,972	4,42
2	6,64	285,367	20,466	93,10
3	6,81	5,241	0,213	0,97
4	6,99	4,594	0,332	1,51
Total:		303,094	21,983	100,00

MS (ESI) *m/z* (+)

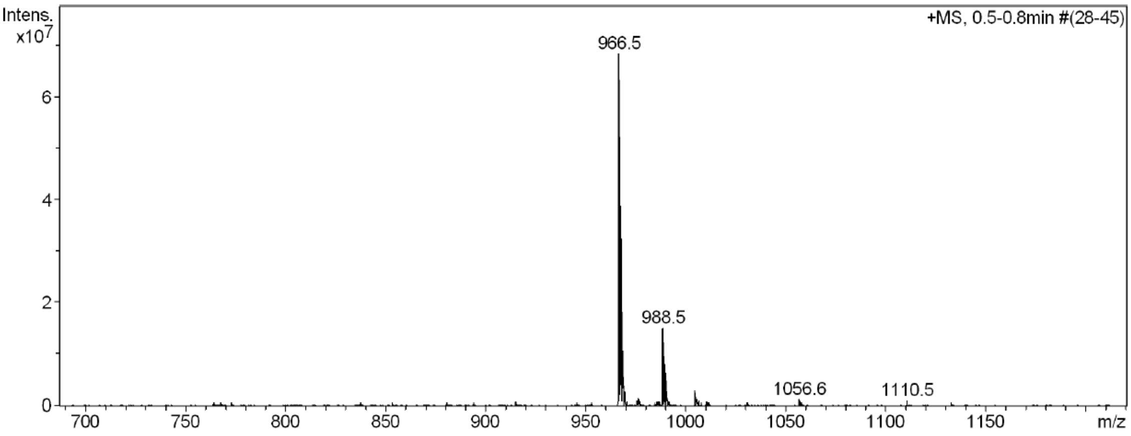

HRMS (ESI) *m/z* (+)

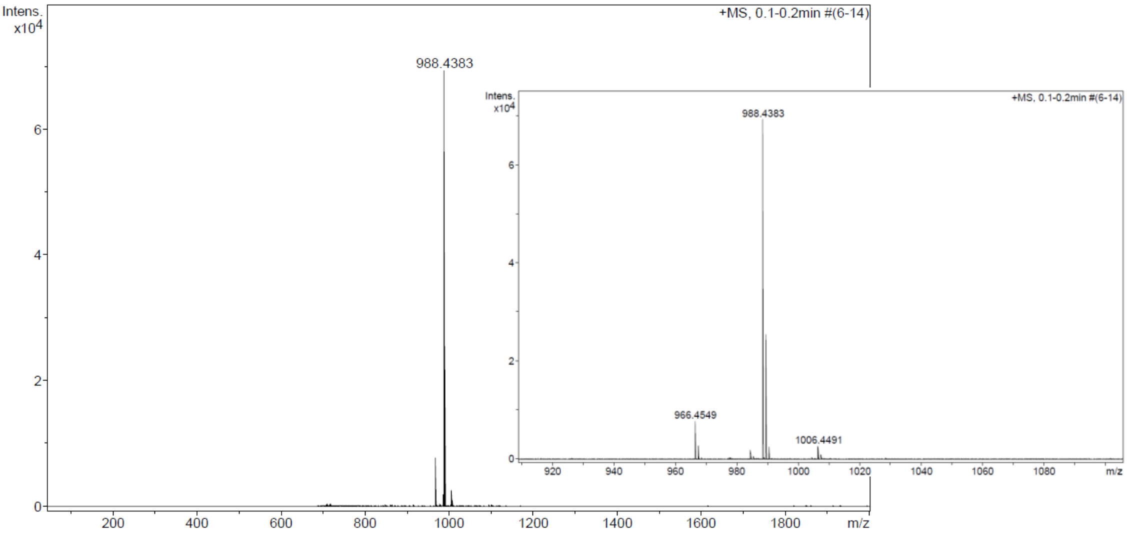
Intens.
x10^4
+MS, 0.1-0.2min #(6-14)
988.4383
6
4
2
0
200
400
600
800
1000
1200
1400
1600
1800
m/z
Intens.
x10^4
+MS, 0.1-0.2min #(6-14)
988.4383
966.4549
1006.4491
920
940
960
980
1000
1020
1040
1060
1080
m/z

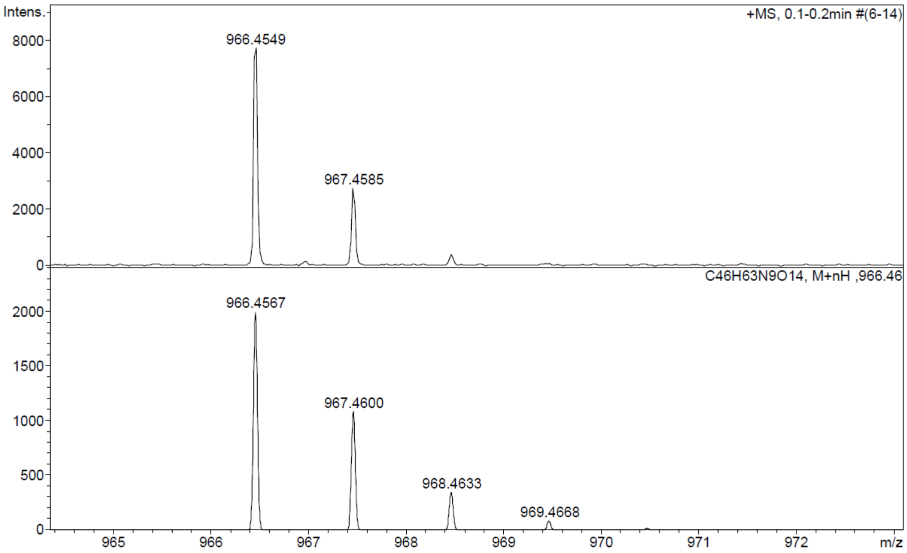
Intens.
+MS, 0.1-0.2min #(6-14)
8000
6000
4000
2000
0
966.4549
967.4585
C46H63N9O14, M+nH ,966.46
2000
1500
1000
500
0
966.4567
967.4600
968.4633
969.4668
965
966
967
968
969
970
971
972
m/z

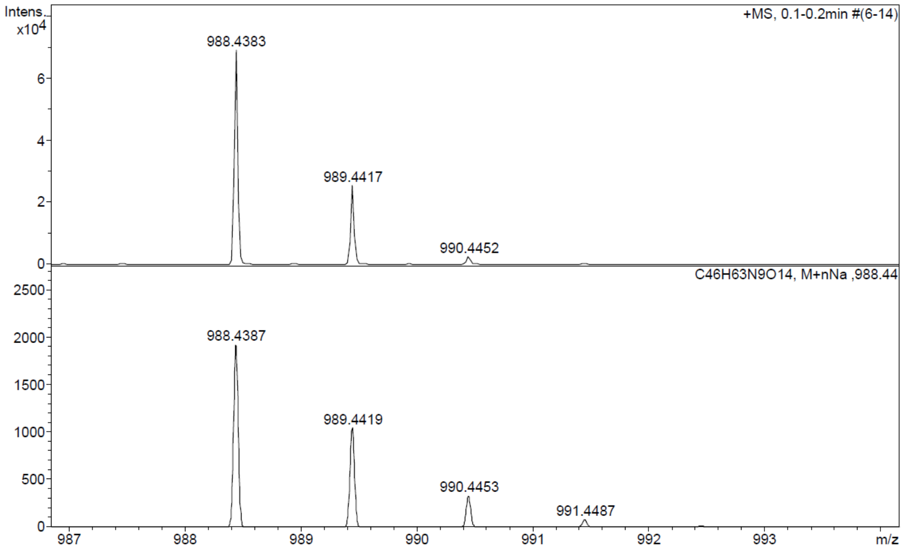
Intens.
x10^4
+MS, 0.1-0.2min #(6-14)
6
4
2
0
988.4383
989.4417
990.4452
C46H63N9O14, M+nNa ,988.44
2500
2000
1500
1000
500
0
988.4387
989.4419
990.4453
991.4487
987
988
989
990
991
992
993
m/z

Hydrolysis of the crude reaction (BPC826)

HPLC (λ = 220 nm) (*Method A*)

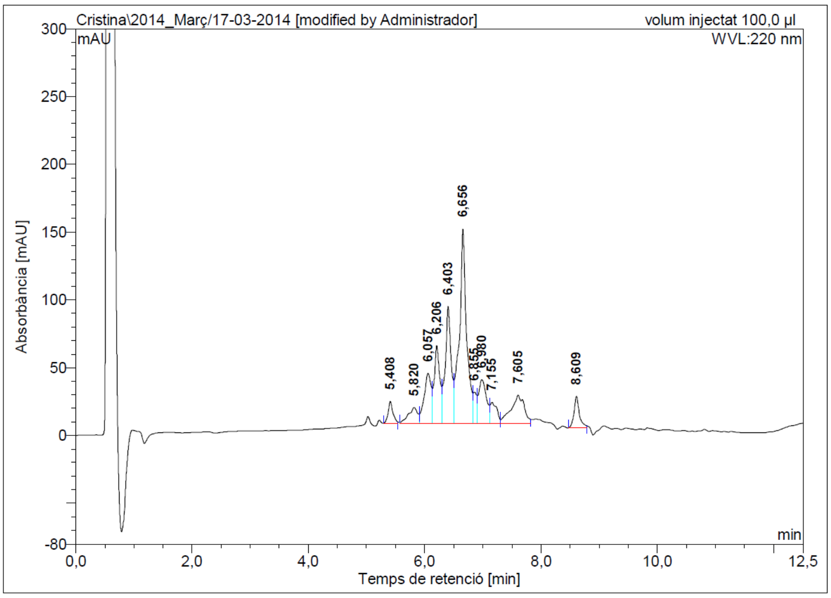

No.	Ret.Time (detected) min	Height mAU	Area mAU*min	Rel.Area %
1	5,41	16,050	1,525	2,42
2	5,82	11,665	2,087	3,31
3	6,06	36,765	5,286	8,39
4	6,21	57,396	6,368	10,10
5	6,40	86,116	10,264	16,29
6	6,66	143,101	20,796	33,00
7	6,86	22,976	1,832	2,91
8	6,98	32,082	4,876	7,74
9	7,16	15,310	2,115	3,36
10	7,61	20,712	5,415	8,59
11	8,61	23,119	2,456	3,90
Total:		465,291	63,020	100,00

MS (ESI) *m/z* (+)

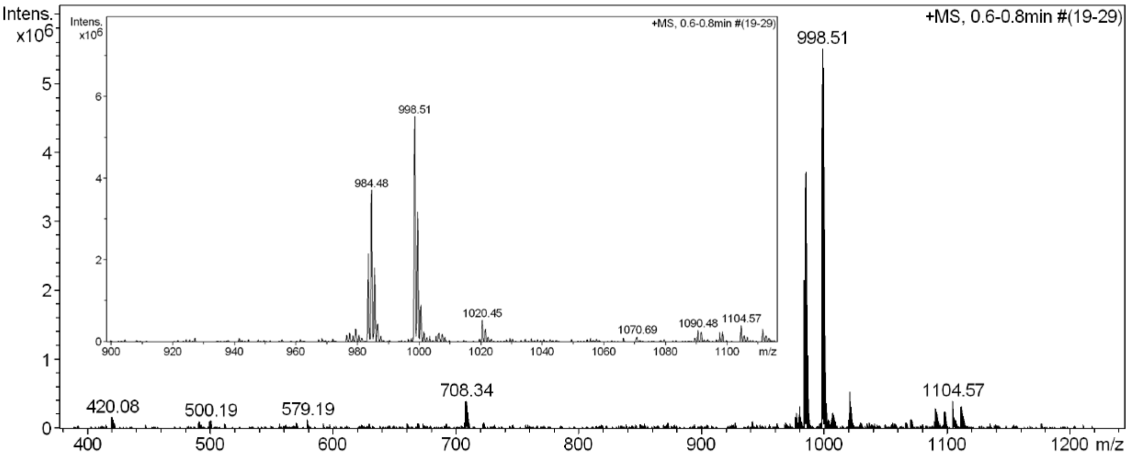

MS (ESI) *m/z* (-)

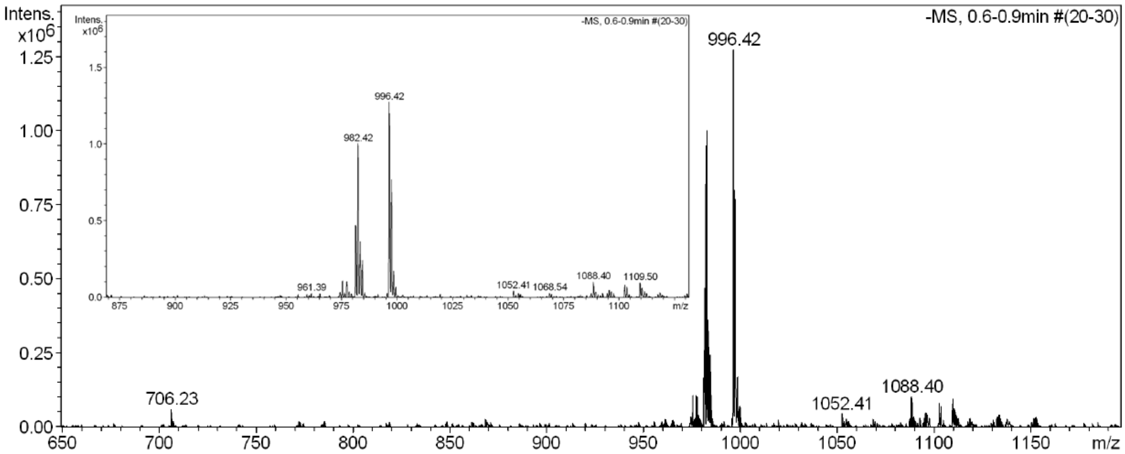
Intens.
x10^6
1.25
1.00
0.75
0.50
0.25
0.00
650
700
750
800
850
900
950
1000
1050
1100
1150
m/z
-MS, 0.6-0.9min #(20-30)
996.42
706.23
1052.41
1088.40
Intens.
x10^6
1.5
1.0
0.5
0.0
875
900
925
950
975
1000
1025
1050
1075
1100
m/z
-MS, 0.6-0.9min #(20-30)
996.42
982.42
961.39
1052.41
1068.54
1088.40
1109.50

3.4.5. H-Tyr(&)-D-Ser-Glu-D-Ala-Pro-Gln-D-Tyr-Ile-& (BPC828)

HPLC (λ = 220 nm) (*Method A*) (crude reaction)

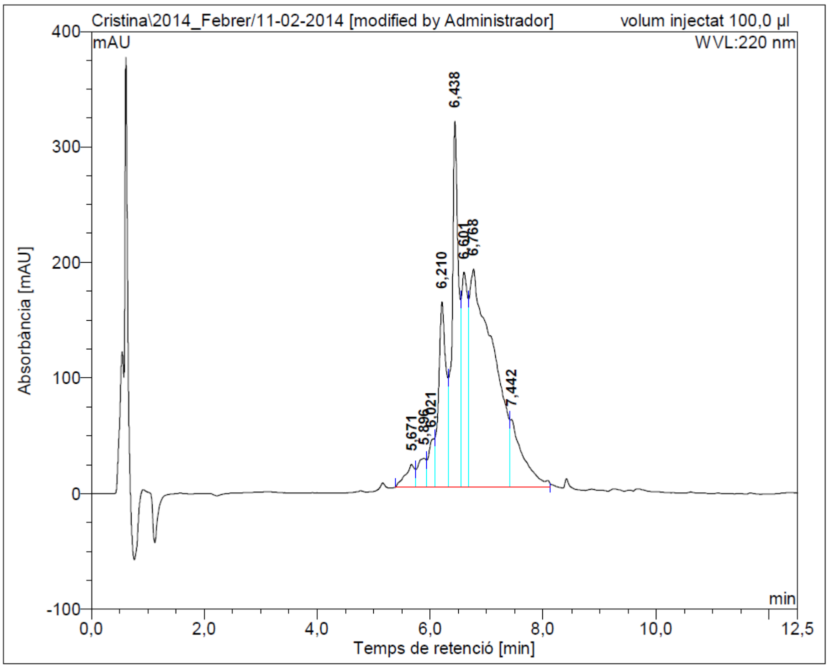

No.	Temps retenció min	alçada mAU	Area mAU*min	Area relativa %
1	5,67	19,359	3,752	1,77
2	5,90	24,518	4,262	2,01
3	6,02	39,874	4,991	2,35
4	6,21	159,871	24,963	11,78
5	6,44	316,413	41,696	19,67
6	6,60	185,722	24,461	11,54
7	6,77	188,356	92,255	43,52
8	7,44	58,197	15,595	7,36
Total:		992,310	211,975	100,00

MS (ESI) *m/z* (+)

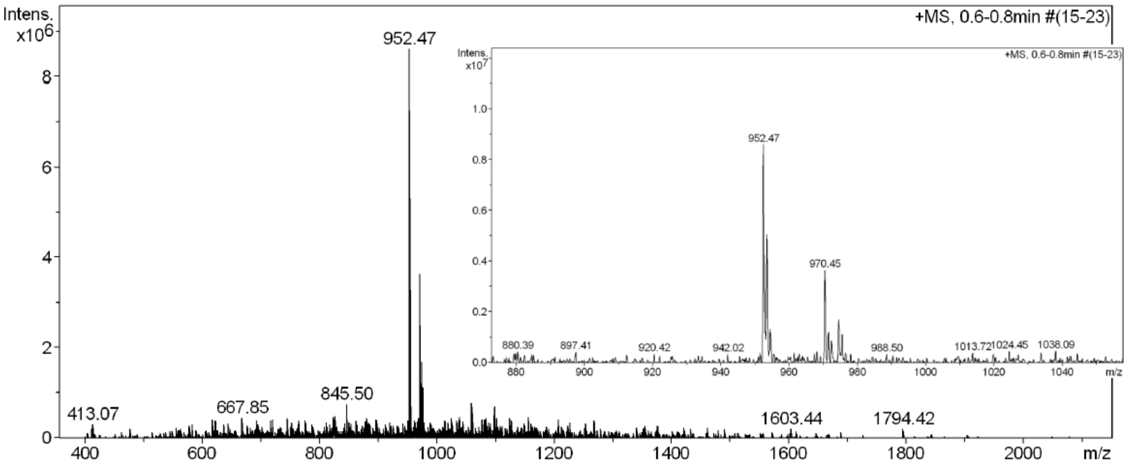

MS (ESI) *m/z* (-)

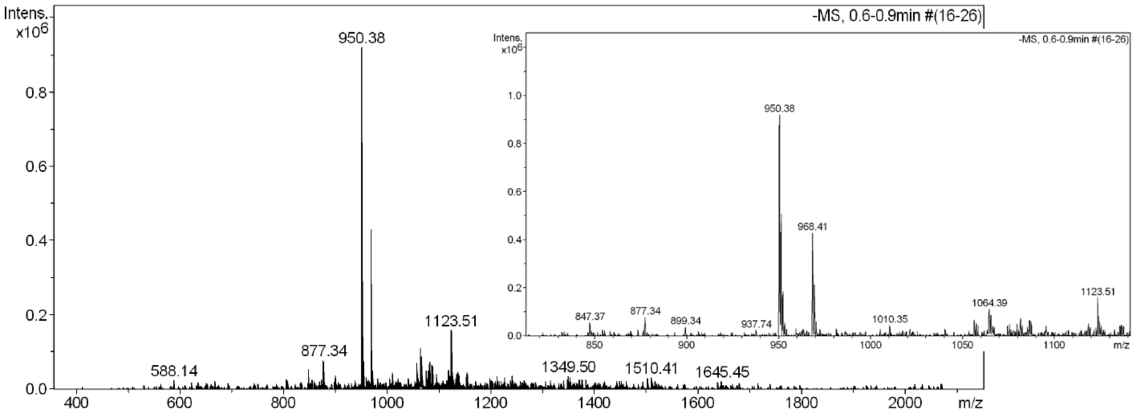
Intens.
x10^6
-MS, 0.6-0.9min #(16-26)
950.38
1123.51
877.34
588.14
1349.50
1510.41
1645.45
0.8
0.6
0.4
0.2
0.0
400
600
800
1000
1200
1400
1600
1800
2000
m/z
Intens.
x10^6
-MS, 0.6-0.9min #(16-26)
950.38
968.41
847.37
877.34
899.34
937.74
1010.35
1064.39
1123.51
1.0
0.8
0.6
0.4
0.2
0.0
850
900
950
1000
1050
1100
m/z

Purification of BPC828

HPLC (λ = 220 nm) (*Method A*)

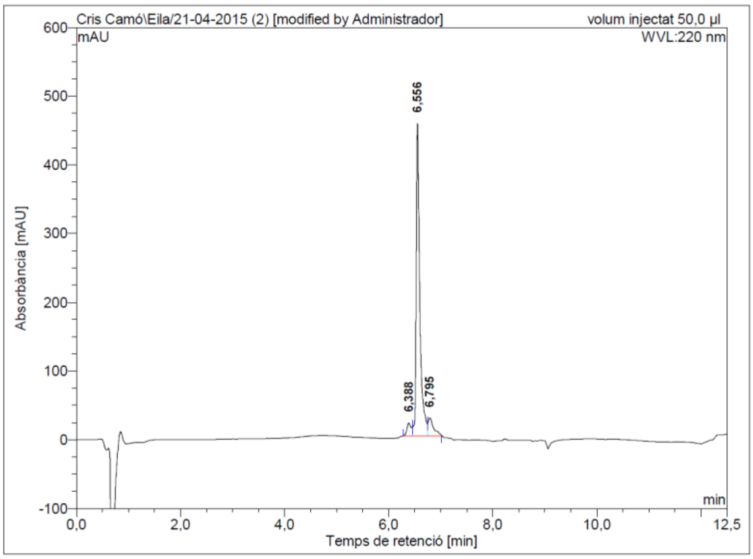

No.	Temps retenció min	alçada mAU	Area mAU*min	Area relativa %
1	6,39	18,560	1,752	4,21
2	6,56	454,770	36,583	87,84
3	6,80	26,199	3,312	7,95
Total:		499,529	41,646	100,00

MS (ESI) *m/z* (+)

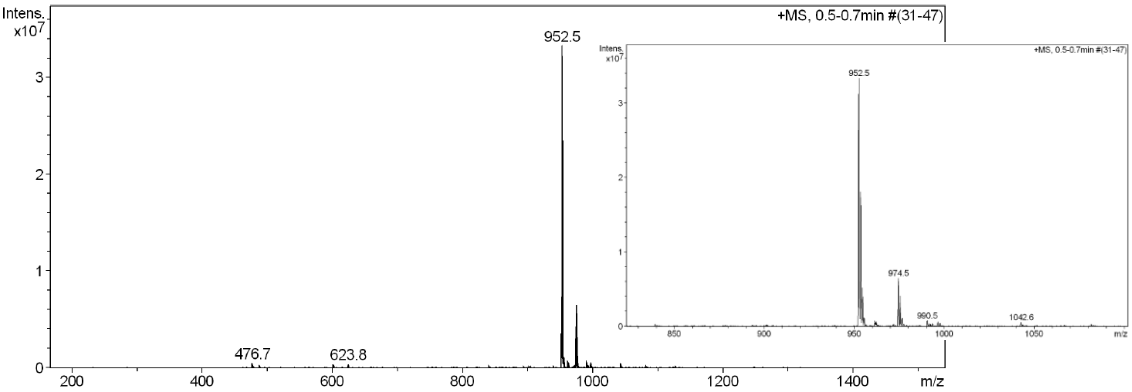

MS (ESI) *m/z* (-)

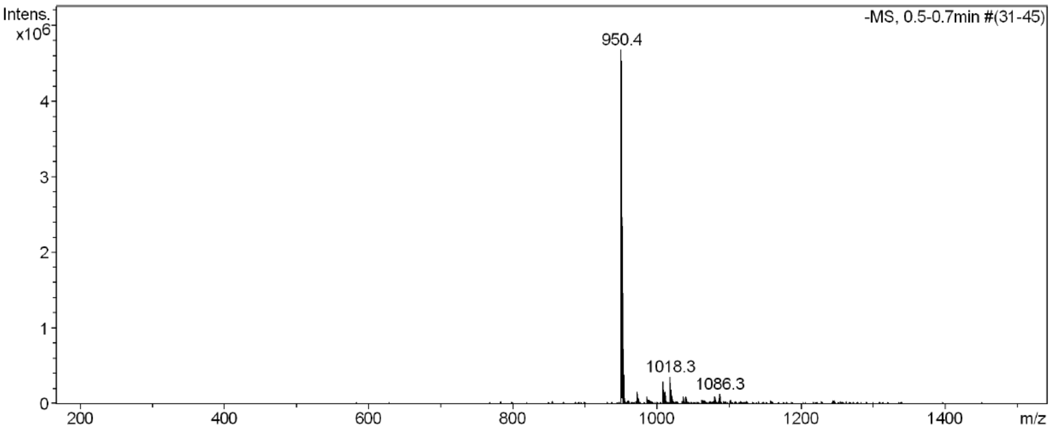

HRMS (ESI) *m/z* (+)

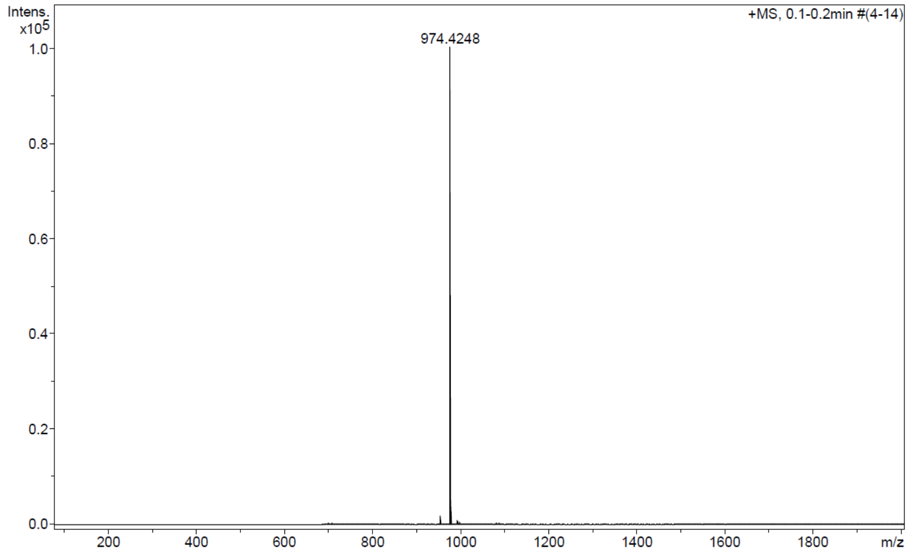
Intens.
x10^5
1.0
0.8
0.6
0.4
0.2
0.0
+MS, 0.1-0.2min #(4-14)
974.4248
200
400
600
800
1000
1200
1400
1600
1800
m/z

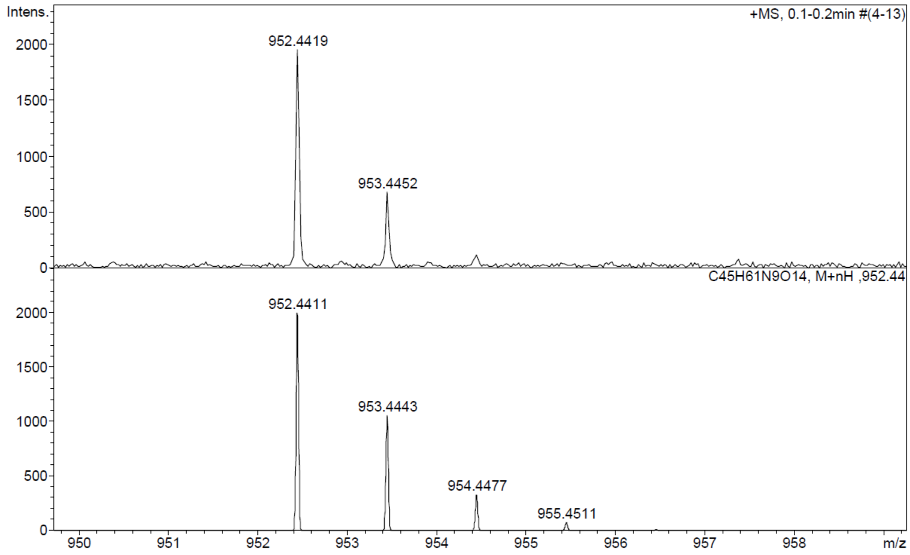
Intens.
2000
1500
1000
500
0
+MS, 0.1-0.2min #(4-13)
952.4419
953.4452
C45H61N9O14, M+nH ,952.44
952.4411
953.4443
954.4477
955.4511
950
951
952
953
954
955
956
957
958
m/z

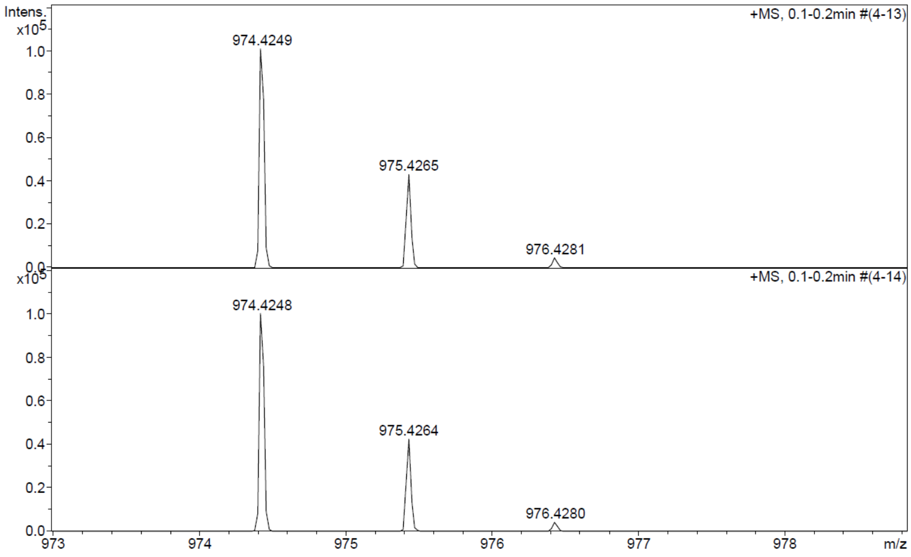
Intens.
x10^5
1.0
0.8
0.6
0.4
0.2
0.0
+MS, 0.1-0.2min #(4-13)
974.4249
975.4265
976.4281
x10^5
+MS, 0.1-0.2min #(4-14)
974.4248
975.4264
976.4280
973
974
975
976
977
978
m/z

Hydrolysis of the crude reaction (BPC828)

HPLC (λ = 220 nm) (*Method A*)

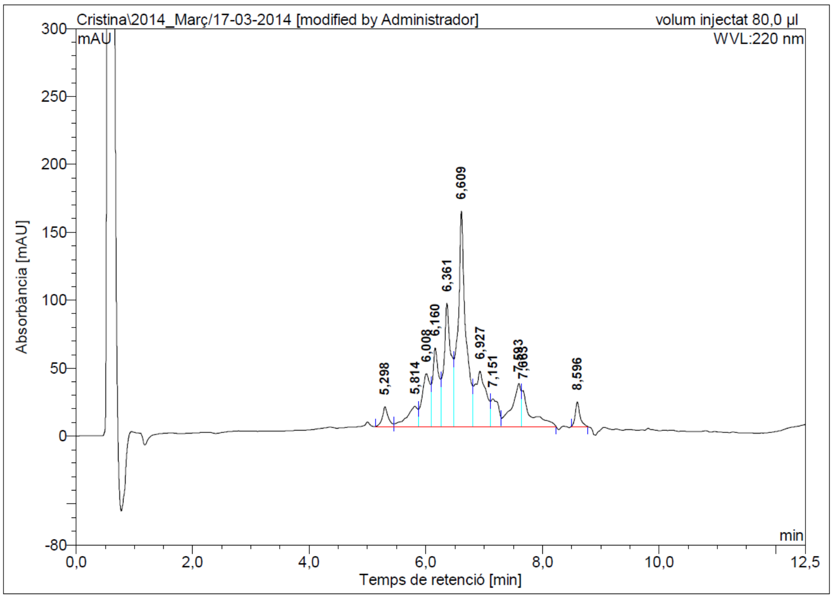

No.	Ret.Time (detected) min	Height mAU	Area mAU*min	Rel.Area %
1	5,30	14,576	1,703	2,12
2	5,81	14,867	3,211	4,01
3	6,01	39,003	5,981	7,46
4	6,16	57,849	7,316	9,13
5	6,36	90,741	13,126	16,38
6	6,61	158,435	24,640	30,74
7	6,93	40,723	8,943	11,16
8	7,15	20,247	3,053	3,81
9	7,59	31,505	5,708	7,12
10	7,66	26,536	4,800	5,99
11	8,60	18,062	1,667	2,08
Total:		512,545	80,145	100,00

MS (ESI) *m/z* (+)

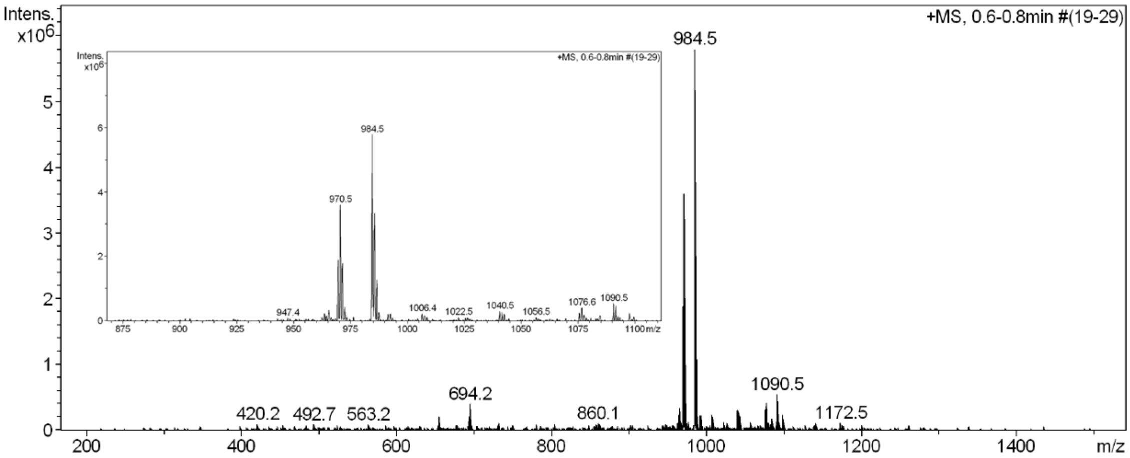

MS (ESI) *m/z* (-)

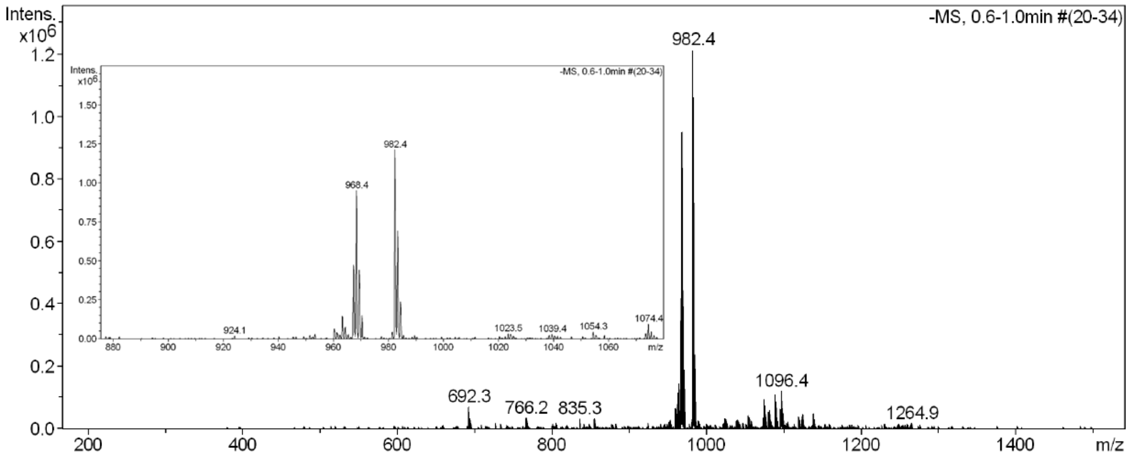
Intens.
x10^6
1.2
1.0
0.8
0.6
0.4
0.2
0.0
-MS, 0.6-1.0min #(20-34)
982.4
692.3
766.2
835.3
1096.4
1264.9
200
400
600
800
1000
1200
1400
m/z
Intens.
x10^6
1.50
1.25
1.00
0.75
0.50
0.25
0.00
-MS, 0.6-1.0min #(20-34)
982.4
968.4
924.1
1023.5
1039.4
1054.3
1074.4
880
900
920
940
960
980
1000
1020
1040
1060
m/z

3.4.6. H-D-Tyr(&)-D-Thr-Glu-D-Val-Pro-Gln-Tyr-Ile-& (BPC830)

HPLC (λ = 220 nm) (*Method A*) (crude reaction)

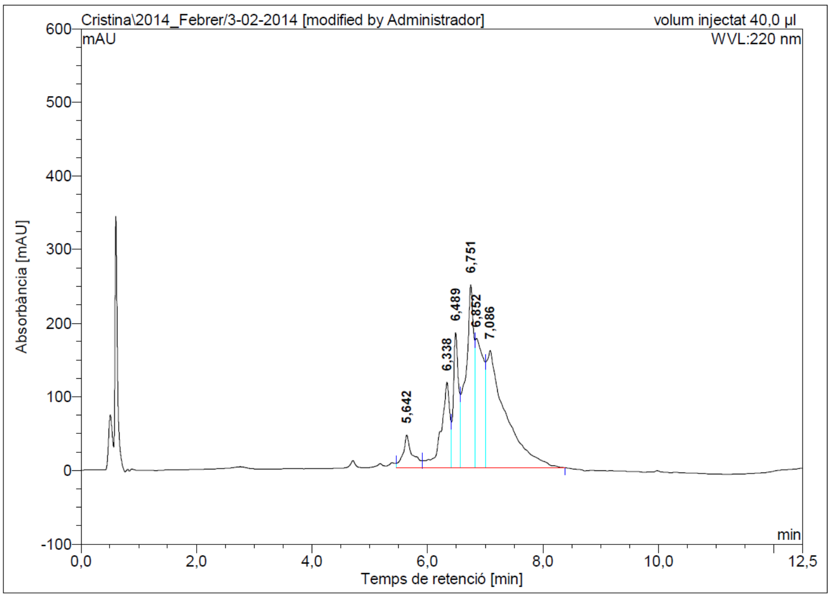

No.	Ret.Time (detected) min	Height mAU	Area mAU*min	Rel.Area %
1	5,64	44,707	8,472	4,64
2	6,34	116,545	21,102	11,55
3	6,49	183,864	19,283	10,56
4	6,75	248,757	40,561	22,21
5	6,85	175,866	29,321	16,06
6	7,09	159,359	63,885	34,98
Total:		929,098	182,623	100,00

MS (ESI) *m/z* (+)

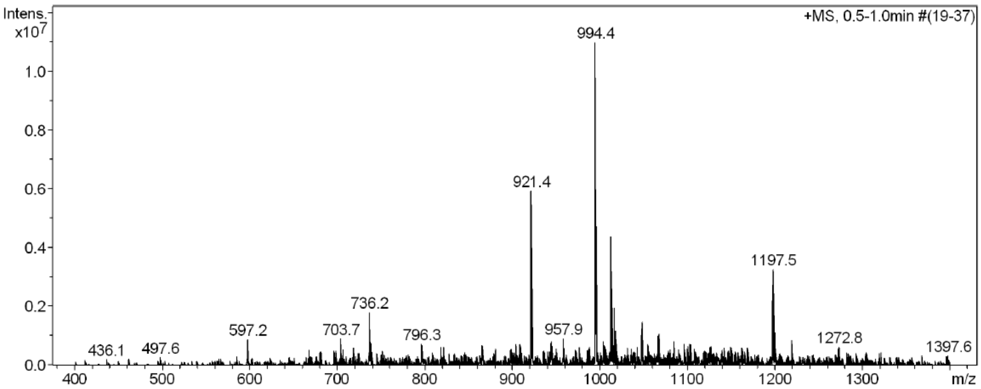

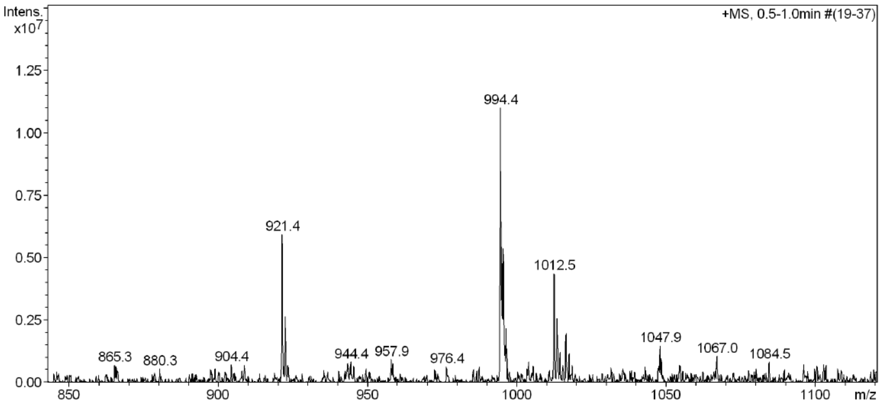

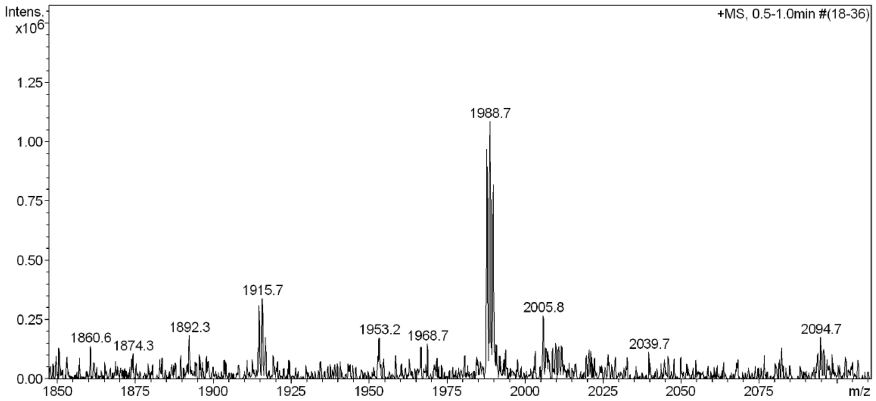
Intens.
x10^6
+MS, 0.5-1.0min #(18-36)
1.25
1.00
0.75
0.50
0.25
0.00
1988.7
1915.7
2005.8
1860.6
1874.3
1892.3
1953.2
1968.7
2039.7
2094.7
1850
1875
1900
1925
1950
1975
2000
2025
2050
2075
m/z

MS (ESI) *m/z* (-)

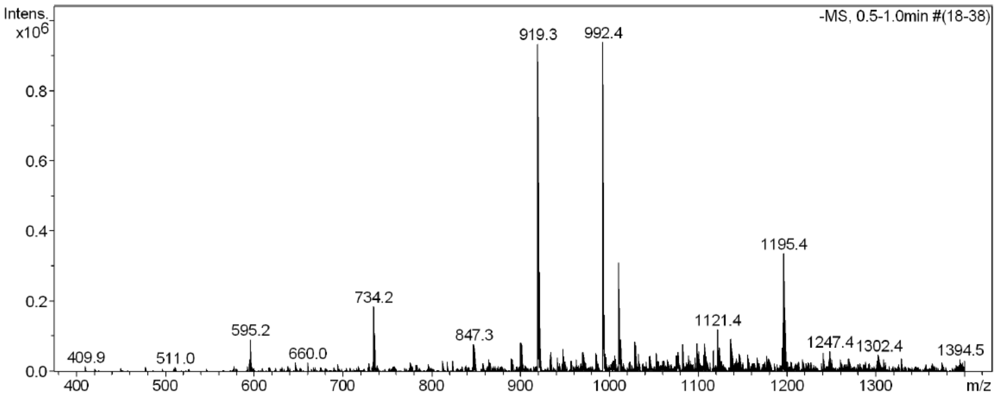
Intens.
x10^6
-MS, 0.5-1.0min #(18-38)
0.8
0.6
0.4
0.2
0.0
919.3
992.4
1195.4
734.2
1121.4
595.2
847.3
1247.4
1302.4
1394.5
409.9
511.0
660.0
400
500
600
700
800
900
1000
1100
1200
1300
m/z

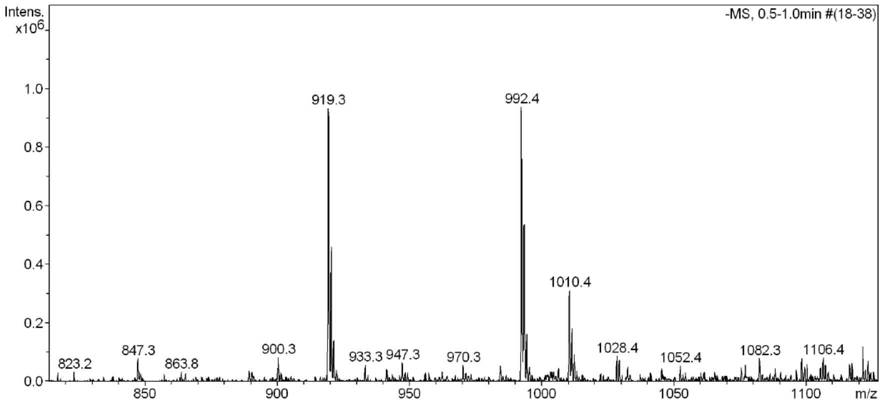
Intens.
x10^6
-MS, 0.5-1.0min #(18-38)
1.0
0.8
0.6
0.4
0.2
0.0
919.3
992.4
1010.4
823.2
847.3
863.8
900.3
933.3
947.3
970.3
1028.4
1052.4
1082.3
1106.4
850
900
950
1000
1050
1100
m/z

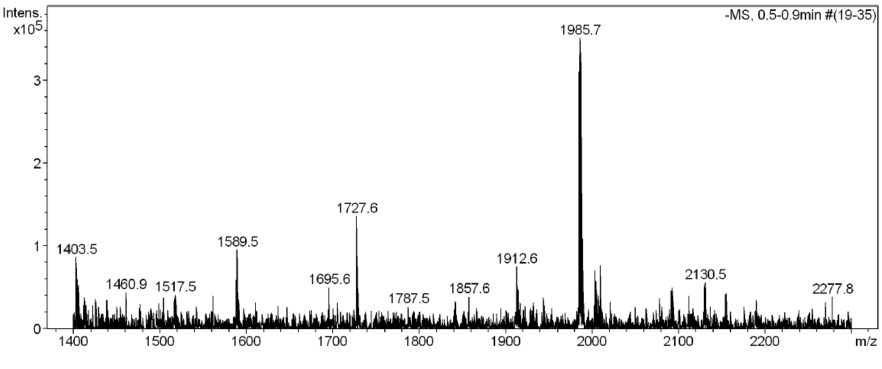
Intens.
x10^5
-MS, 0.5-0.9min #(19-35)
3
2
1
0
1985.7
1727.6
1589.5
1403.5
1912.6
1460.9
1517.5
1695.6
1787.5
1857.6
2130.5
2277.8
1400
1500
1600
1700
1800
1900
2000
2100
2200
m/z

3.4.7. H-D-Tyr(&)-D-Ser-Glu-D-Val-Pro-Gln-Tyr-Ile-& (BPC832)

HPLC (λ = 220 nm) (*Method A*) (crude reaction)

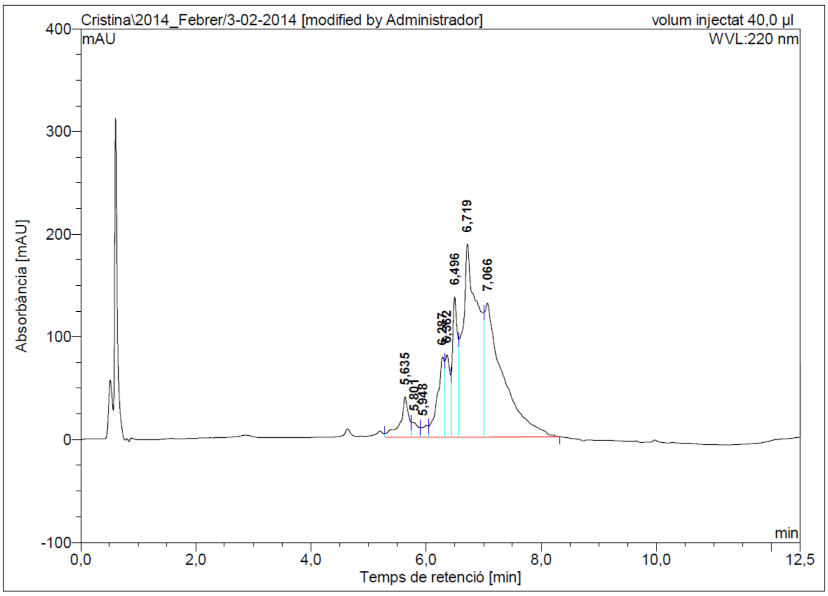

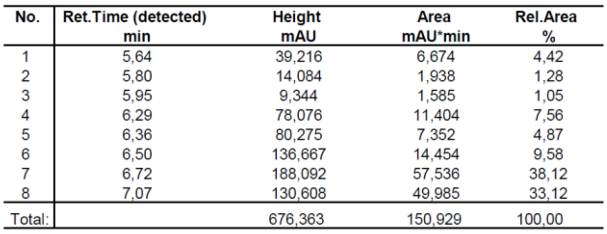

No.	Ret.Time (detected) min	Height mAU	Area mAU*min	Rel.Area %
1	5,64	39,216	6,674	4,42
2	5,80	14,084	1,938	1,28
3	5,95	9,344	1,585	1,05
4	6,29	78,076	11,404	7,56
5	6,36	80,275	7,352	4,87
6	6,50	136,667	14,454	9,58
7	6,72	188,092	57,536	38,12
8	7,07	130,608	49,985	33,12
Total:		676,363	150,929	100,00

MS (ESI) *m/z* (+)

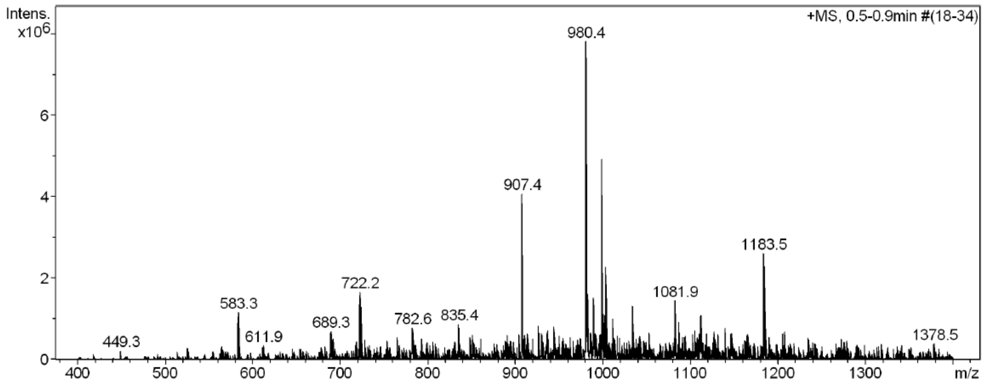

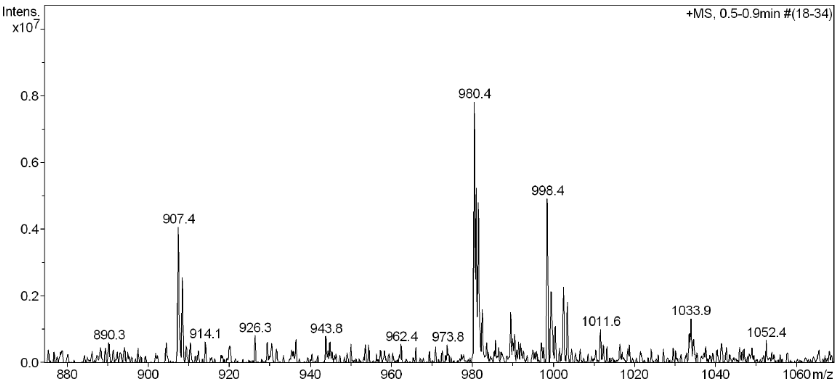

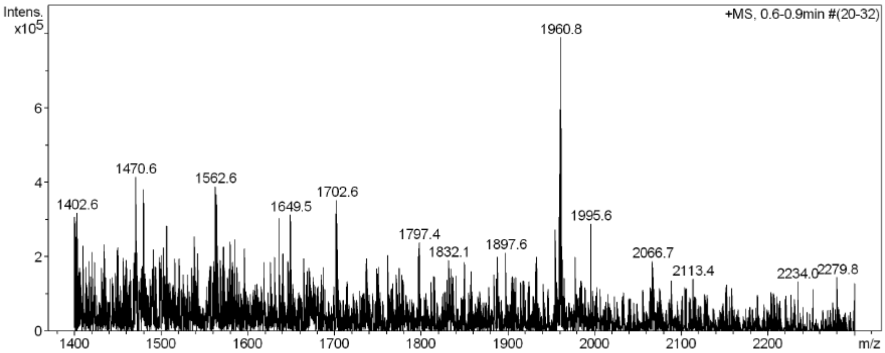
Intens.
x10^5
+MS, 0.6-0.9min #(20-32)
1960.8
1470.6
1562.6
1402.6
1649.5
1702.6
1995.6
1797.4
1832.1
1897.6
2066.7
2113.4
2234.0
2279.8
0
2
4
6
1400
1500
1600
1700
1800
1900
2000
2100
2200
m/z

MS (ESI) *m/z* (-)

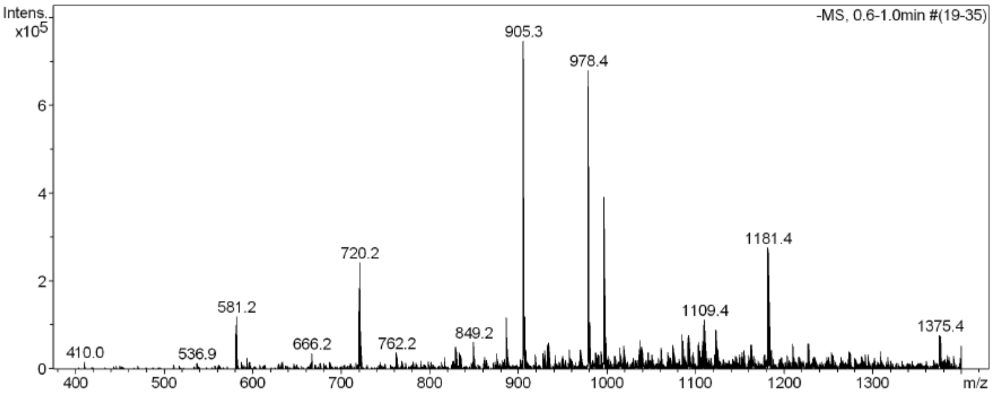
Intens.
x10^5
-MS, 0.6-1.0min #(19-35)
905.3
978.4
1181.4
720.2
581.2
1109.4
1375.4
410.0
536.9
666.2
762.2
849.2
0
2
4
6
400
500
600
700
800
900
1000
1100
1200
1300
m/z

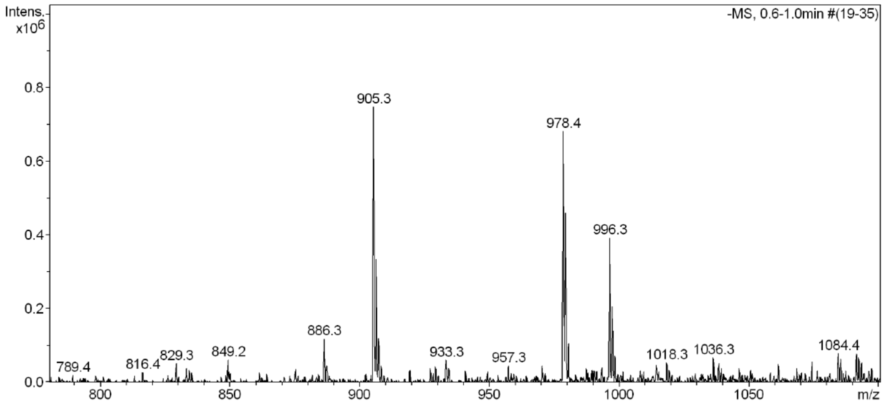
Intens.
x10^6
-MS, 0.6-1.0min #(19-35)
905.3
978.4
996.3
886.3
789.4
816.4
829.3
849.2
933.3
957.3
1018.3
1036.3
1084.4
0.0
0.2
0.4
0.6
0.8
800
850
900
950
1000
1050
m/z

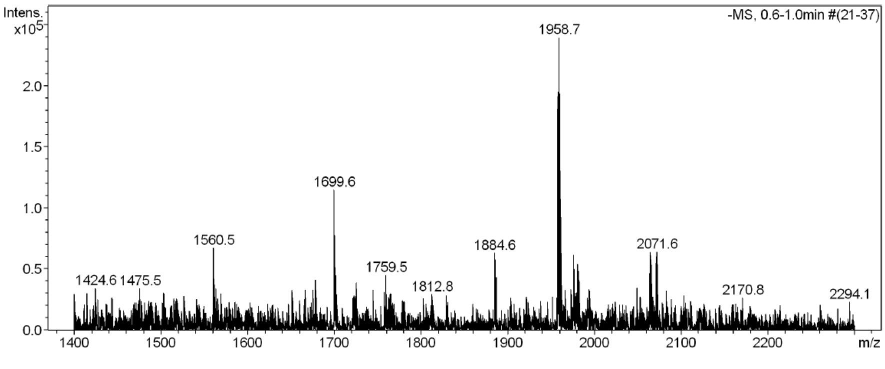
Intens.
x10^5
-MS, 0.6-1.0min #(21-37)
1958.7
1699.6
1560.5
1884.6
2071.6
1424.6
1475.5
1759.5
1812.8
2170.8
2294.1
0.0
0.5
1.0
1.5
2.0
1400
1500
1600
1700
1800
1900
2000
2100
2200
m/z

3.4.8. H-D-Tyr(&)-D-Thr-Glu-D-Ala-Pro-Gln-Tyr-Ile-& (BPC834)

HPLC (*λ* = 220 nm) (*Method A*) (crude reaction)

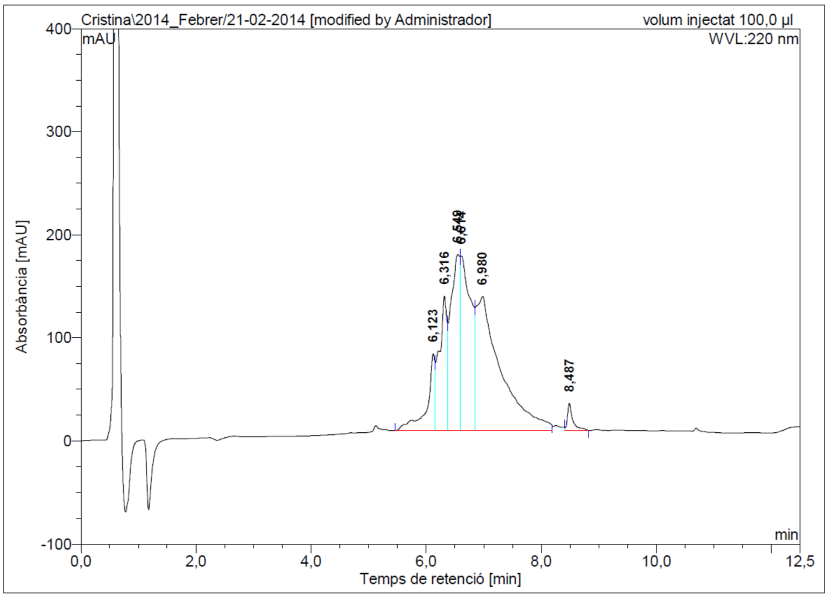

No.	Ret.Time (detected) min	Height mAU	Area mAU*min	Rel.Area %
1	6,12	74,415	12,192	7,27
2	6,32	130,338	20,483	12,21
3	6,55	170,545	30,090	17,94
4	6,61	169,352	36,142	21,54
5	6,98	130,220	65,977	39,33
6	8,49	26,214	2,872	1,71
Total:		701,085	167,757	100,00

MS (ESI) *m/z* (+)

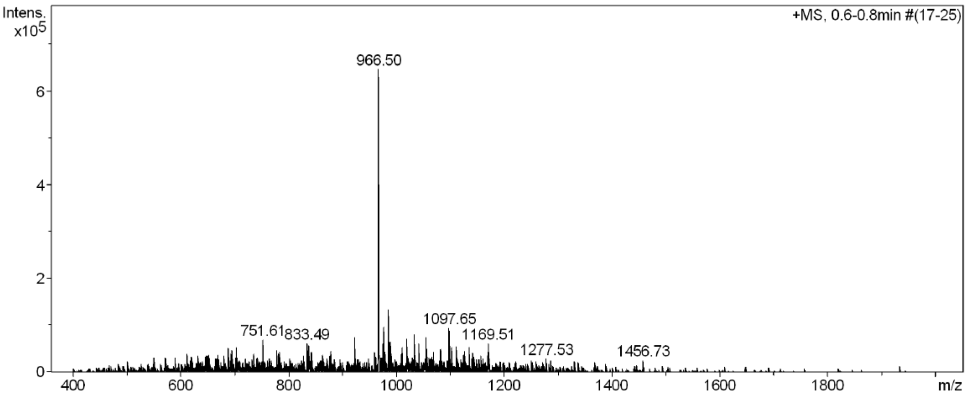

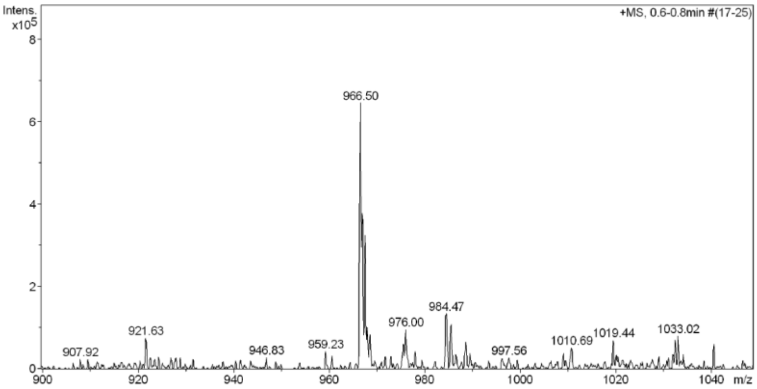

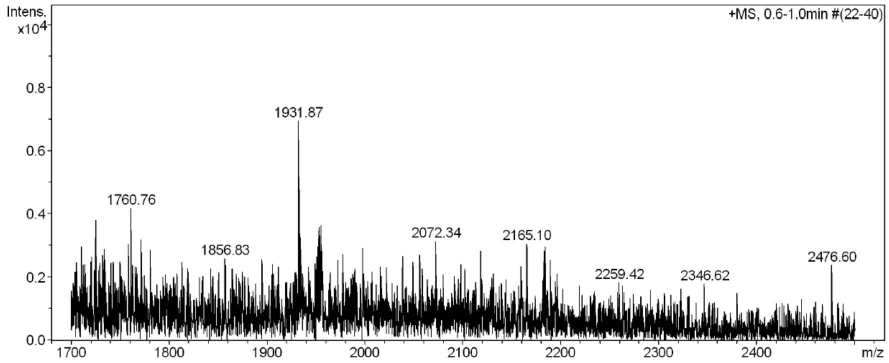
Intens.
x10^4
+MS, 0.6-1.0min #(22-40)
0.8
0.6
0.4
0.2
0.0
1931.87
1760.76
1856.83
2072.34
2165.10
2259.42
2346.62
2476.60
1700
1800
1900
2000
2100
2200
2300
2400
m/z

MS (ESI) *m/z* (-)

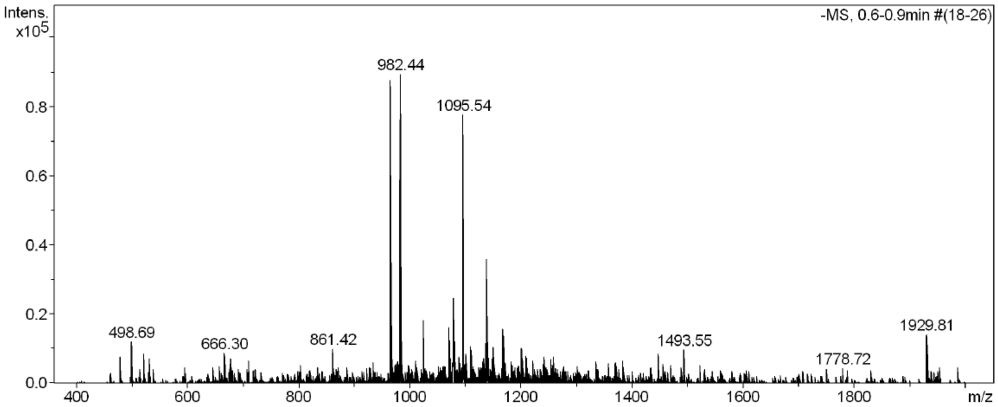
Intens.
x10^5
-MS, 0.6-0.9min #(18-26)
0.8
0.6
0.4
0.2
0.0
982.44
1095.54
498.69
666.30
861.42
1493.55
1778.72
1929.81
400
600
800
1000
1200
1400
1600
1800
m/z

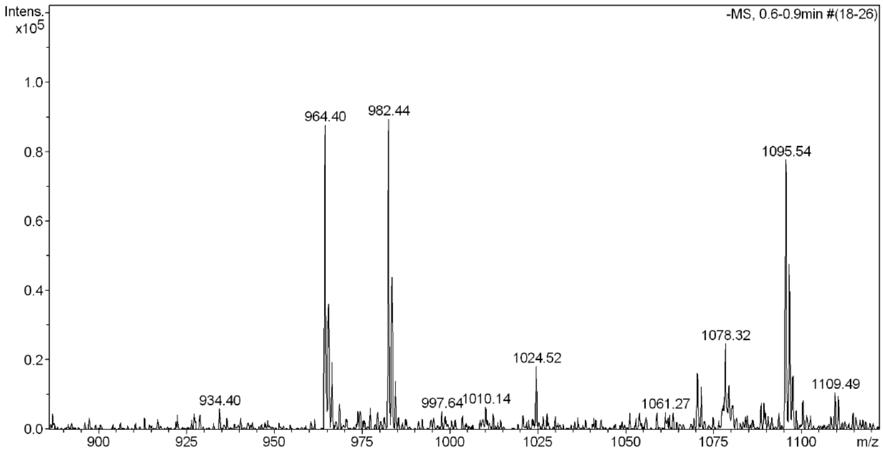
Intens.
x10^5
-MS, 0.6-0.9min #(18-26)
1.0
0.8
0.6
0.4
0.2
0.0
964.40
982.44
1095.54
1078.32
1024.52
934.40
997.64
1010.14
1061.27
1109.49
900
925
950
975
1000
1025
1050
1075
1100
m/z

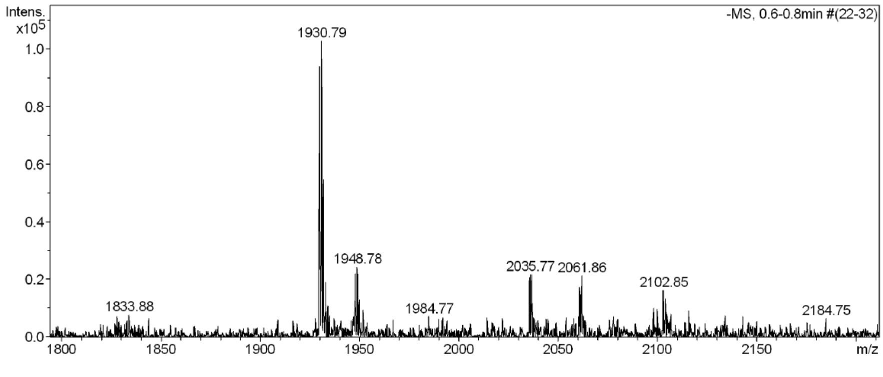
Intens.
x10^5
-MS, 0.6-0.8min #(22-32)
1.0
0.8
0.6
0.4
0.2
0.0
1930.79
1948.78
1833.88
1984.77
2035.77
2061.86
2102.85
2184.75
1800
1850
1900
1950
2000
2050
2100
2150
m/z

3.4.9. H-D-Tyr(&)-D-Ser-Glu-D-Ala-Pro-Gln-Tyr-Ile-& (BPC836)

HPLC (λ = 220 nm) (*Method A*) (crude reaction)

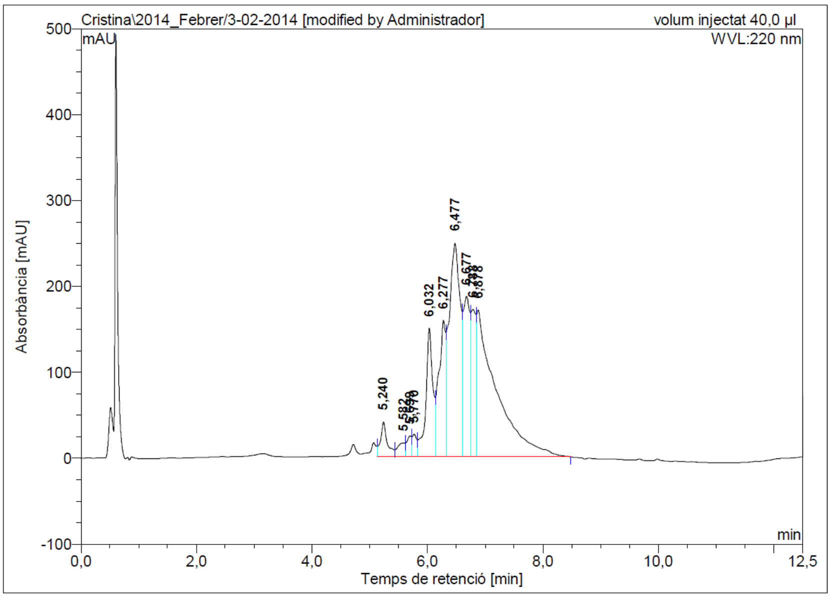

No.	Ret.Time (detected) min	Height mAU	Area mAU*min	Rel.Area %
1	5,24	40,206	5,450	2,46
2	5,58	15,896	2,448	1,11
3	5,70	24,131	2,388	1,08
4	5,77	26,002	2,231	1,01
5	6,03	149,687	20,911	9,44
6	6,28	158,655	21,849	9,87
7	6,48	248,345	56,170	25,36
8	6,68	186,696	24,049	10,86
9	6,79	171,507	17,088	7,72
10	6,88	170,863	68,867	31,10
Total:		1191,987	221,452	100,00

MS (ESI) *m/z* (+)

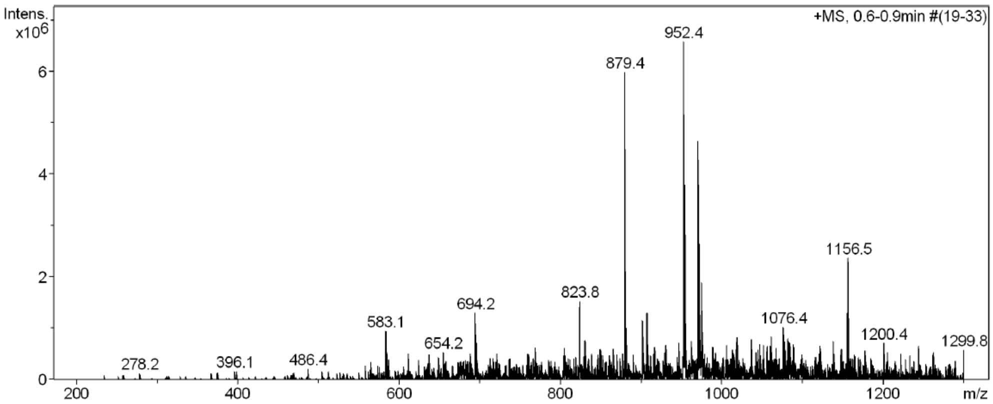

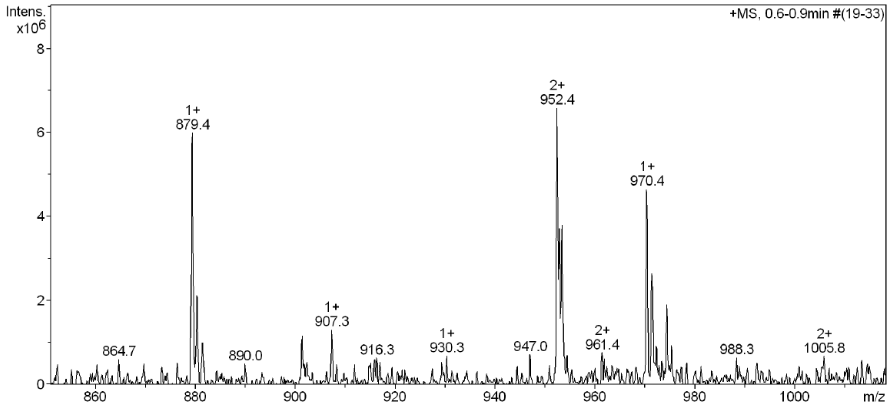
Intens.
x10^6
+MS, 0.6-0.9min #(19-33)
8
6
4
2
0
1+
879.4
2+
952.4
1+
970.4
1+
907.3
1+
930.3
2+
961.4
2+
1005.8
864.7
890.0
916.3
947.0
988.3
860
880
900
920
940
960
980
1000
m/z

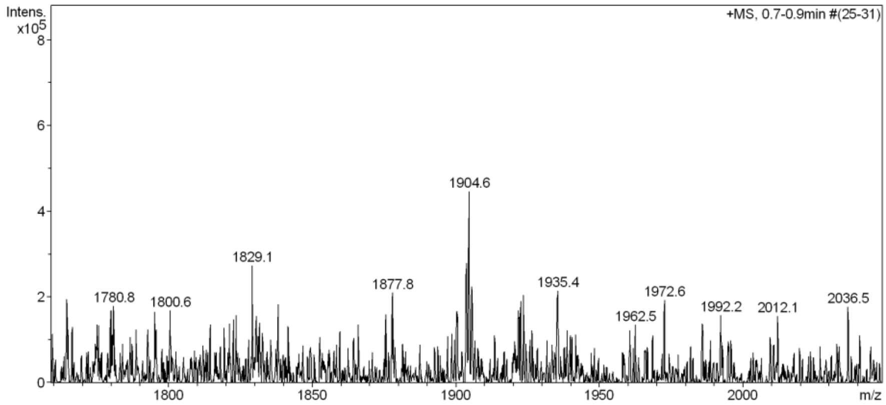
Intens.
x10^5
+MS, 0.7-0.9min #(25-31)
8
6
4
2
0
1904.6
1829.1
1877.8
1935.4
1780.8
1800.6
1972.6
1962.5
1992.2
2012.1
2036.5
1800
1850
1900
1950
2000
m/z

MS (ESI) *m/z* (-)

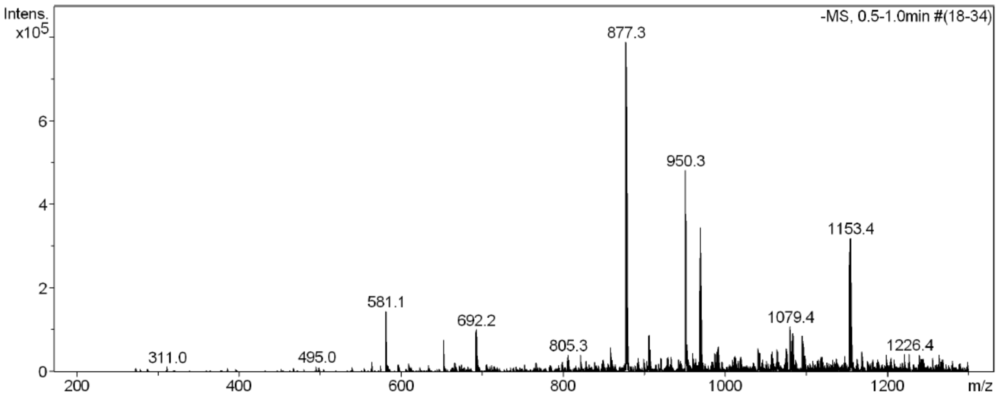
Intens.
x10^5
-MS, 0.5-1.0min #(18-34)
6
4
2
0
877.3
950.3
1153.4
581.1
692.2
1079.4
311.0
495.0
805.3
1226.4
200
400
600
800
1000
1200
m/z

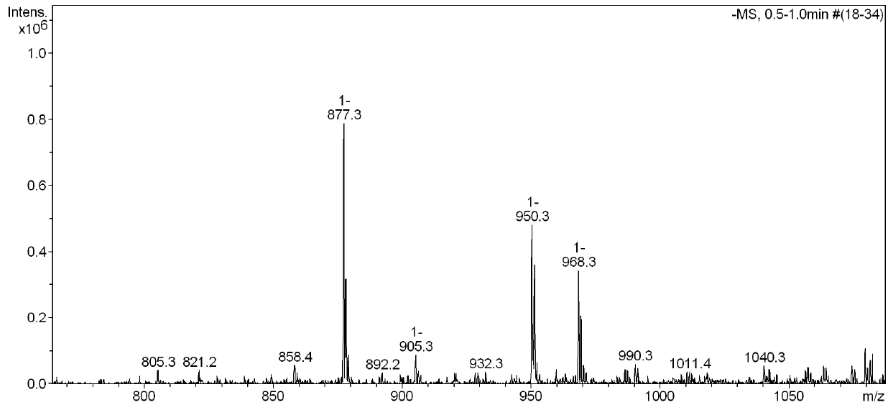
Intens.
x10^6
-MS, 0.5-1.0min #(18-34)
1.0
0.8
0.6
0.4
0.2
0.0
1-
877.3
1-
950.3
1-
968.3
1-
905.3
805.3
821.2
858.4
892.2
932.3
990.3
1011.4
1040.3
800
850
900
950
1000
1050
m/z

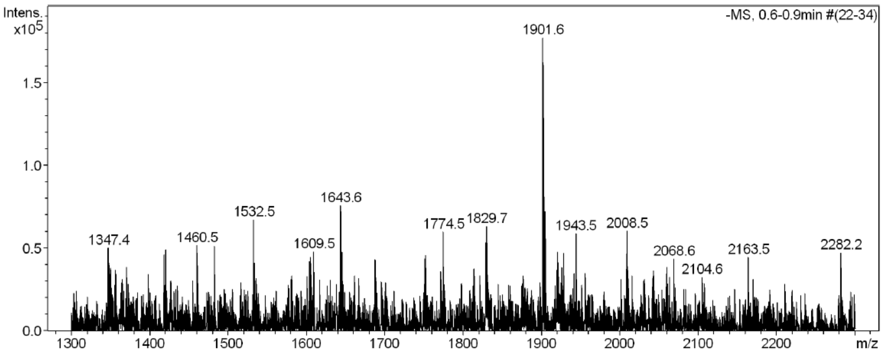
Intens.
x10^5
-MS, 0.6-0.9min #(22-34)
1.5
1.0
0.5
0.0
1901.6
1643.6
1532.5
1774.5
1829.7
1943.5
2008.5
1347.4
1460.5
1609.5
2068.6
2163.5
2282.2
2104.6
1300
1400
1500
1600
1700
1800
1900
2000
2100
2200
m/z